swiss medical weekly

A diamond open access online journal | established in 1871 | published by the SMW supporting association | www.smw.ch

Supplementum 287
ad Swiss Med Wkly 2025;155
May 28, 2025

Swiss Society of Cardiology
Swiss Society of Cardiac Surgery

Abstracts of the joint annual meeting 2025

Zurich (Switzerland), June 4–6, 2025

JOINT ANNUAL MEETING OF THE SWISS SOCIETY OF CARDIOLOGY AND THE SWISS SOCIETY OF CARDIAC SURGERY

ZURICH, JUNE 4–6, 2025

TABLE OF CONTENTS

Orals

Posters

RAPID FIRE ABSTRACT SESSION "HEART FAILURE"

O01

Undetected Heart Failure in Cardiology in Switzerland: Prevalence, Characteristics, Predictors and Outcomes - Phase II

Laureve Chollet[1], Klara Rumora, Ivo Strebel, Stefanie Aeschbacher[1], Desiree Wussler[1], Maria Belkin[1], Pedro Lopez Ayala, Gabrielle Hure, Michael Zellweger[1], Felix Mahfoud, Otmar Pfister[1], Tobias Reichlin[2], Stefan Osswald[1], Michael Kühne[1], Christian Müller

[1]Cardiovascular Research Institute Basel (CRIB), University Hospital Basel, University of Basel, Department of Cardiology, University Hospital Basel, University of Basel, Basel, Switzerland, [2]Cardiovascular Research Institute Basel (CRIB), University Hospital Basel, University of Basel, Department of Cardiology, University Hospital Bern, Inselspital, Bern, Switzerland

Introduction: Late diagnosis of heart failure (HF) is a missed opportunity for treatment and a contributor to high mortality and morbidity. Undetected HF is thought to be rare in cardiology. However, in the first phase of this study we observed an unexpectedly high prevalence of undetected HF even in tertiary care/cardiology. The second phase of the study aims to advance to knowledge regarding the Prevalence, Characteristics, Predictors and Outcomes of Undetected Heart Failure in Cardiology in Switzerland.

Material and Methods: We assessed the characteristics, prevalence, predictors, and outcome of undetected HF in one additional large prospective cohort study with central adjudication of HF according to clinical practice guidelines combining symptoms, elevated natriuretic peptides, and structural and/or functional cardiac abnormalities in cardiac imaging: 1715 patients referred for coronary artery disease (CAD) work-up with cardiac PET imaging. Cardiovascular death and acute HF (AHF) hospitalization during long-term follow-up were the prognostic endpoints.

Results: Among 1715 patients (median age 67 years, 31% women) undergoing PET work-up, 133 patients (7.8%) had known HF, and 487 patients (28.4%) were adjudicated to have undetected HF, resulting in a ratio of undetected to known HF of 3.7 (95%CI, 3.0-4.5)-to-1. Predictors of undetected HF included age, previous cardiac pacemaker implantation, atrial fibrillation, conduction and repolarization disorders. Patients with undetected HF were at significantly higher risk of cardiovascular death or hospitalization for acute heart failure during 2-year follow-up (adjusted HR 3.5 [95%CI, 1.9-6.4] versus no HF). In the first phase of this study, we observed similar results with a prevalence of 26% of undetected HF in the main cohort (362 patients undergoing CAD work-up).

Conclusion: One out of five patients in tertiary care/cardiology had undetected HF. They are many predictors of undetected HF and their presence should aim to unmask heart failure. Undetected HF was associated with increased risk of cardiovascular death or AHF hospitalization.

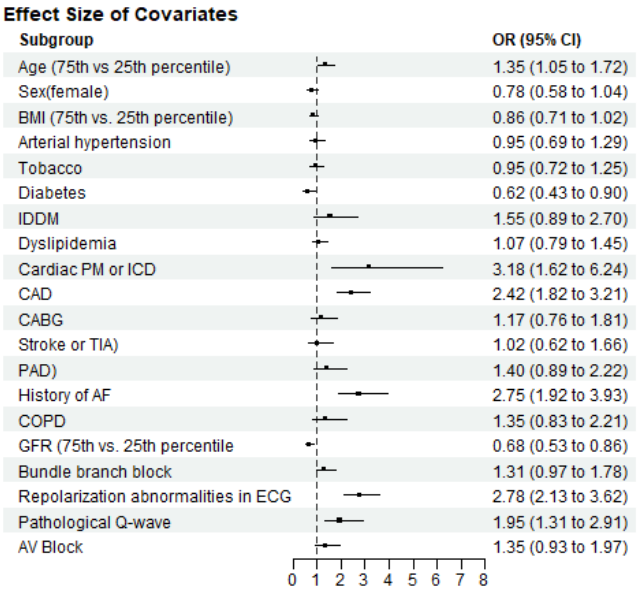

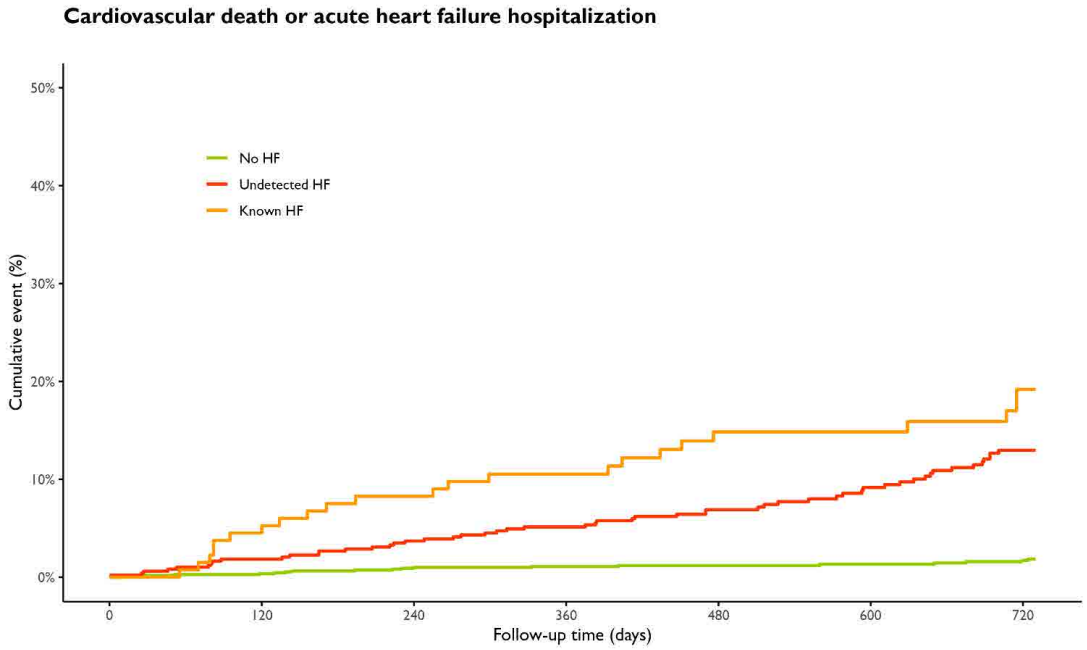

O02

Right ventricular outflow tract diameter for diagnosis of arrhythmogenic right ventricular cardiomyopathy

Thierry Donati[1], Francesca Ortelli[1], Alexandros Protonotarios[2], Qi Chen[1], Monika Hebeisen[1 3], Neria E. Winkler[1], Giulia Montrasio[2], Konstantinos Savvatis[4], Paul A.S. Olsen[4], Corinna Brunckhorst[1], Firat Duru[1], Ardan Saguner[1], Perry Elliott[2], Kristina H. Haugaa[4], Felix C. Tanner[1]

[1]Department of Cardiology, University Heart Center, University Hospital Zurich and University of Zurich, Zurich, Switzerland, [2]Inherited Cardiovascular Disease Unit, St Bartholomew's Hospital, London, United Kingdom, [3]Department of Biostatistics, Epidemiology, Biostatistics and Prevention Institute, University of Zurich, Zurich, Switzerland, [4]ProCardio Centre for Innovation, Department of Cardiology, Oslo University Hospital, Rikshospitalet, Oslo, Norway

Introduction: Enlargement of the right ventricular outflow tract (RVOT) is a key phenotypic feature of arrhythmogenic right ventricular cardiomyopathy (ARVC). Nevertheless, it is uncertain a) whether ARVC can cause isolated RVOT dilatation in general or in certain genotypes, b) which RVOT diameter shows the best properties for diagnosis of ARVC, and c) whether RVOT diameters exhibit added diagnostic value over the generally recommended basal right ventricular end-diastolic diameter (RVEDD).

Material and Methods: This study included patients with genetic testing and fulfilling the revised 2010 Task Force Criteria for definite ARVC. Participants were recruited from three prospective ARVC registries. Healthy asymptomatic subjects served as controls. Four RVOT diameters (Figure 1), RVEDD, and right ventricular end diastolic area (RVEDA) were measured offline and indexed to body surface area (BSA). Isolated RVOT dilatation was defined as RVOT diameter above the upper reference limit without concurrent RVEDA enlargement. Receiver operating characteristic (ROC) curves were used to compare the diagnostic properties of each diameter.

Results: A total of 370 ARVC patients and 100 healthy subjects were enrolled. All RVOT diameters were larger in ARVC patients compared to controls (mean (SD) RVOT2/BSA: 19.6 (4.0) mm/m2; control: 16.5 (2.4) mm/m2). A dilated RVOT occurred in 189 (51%) and an isolated dilatation in 66 (18%) of patients. The percentages of isolated dilatation within specific genotypes were as follows: 13% PKP2, 23% DSP, 12% DSG2, 26% others, and 20% gene-elusive. All RVOT diameters showed similar diagnostic performance [RVOT2/BSA: Area under the curve (AUC) 0.75 (95% CI: 0.7–0.8)] and were comparable to RVEDD/BSA [AUC 0.70 (95% CI: 0.65–0.75)], although RVEDD/BSA exhibited the lowest point estimate (Figure 2).

Conclusion: An isolated RVOT dilatation is observed in almost 20% of patients regardless of the genotype. All RVOT diameters showed similar diagnostic properties and were at least as useful as RVEDD.

Figure 1: Echocardiographic Right Ventricular Diameters

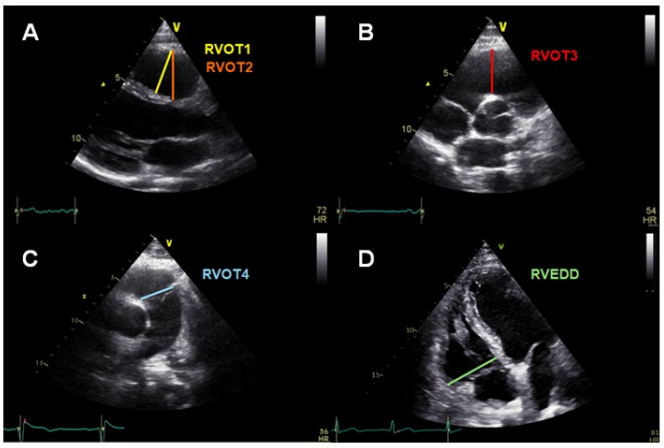

Figure 2: Diagnostic Proprieties of Right Ventricular Diameters in ARVC

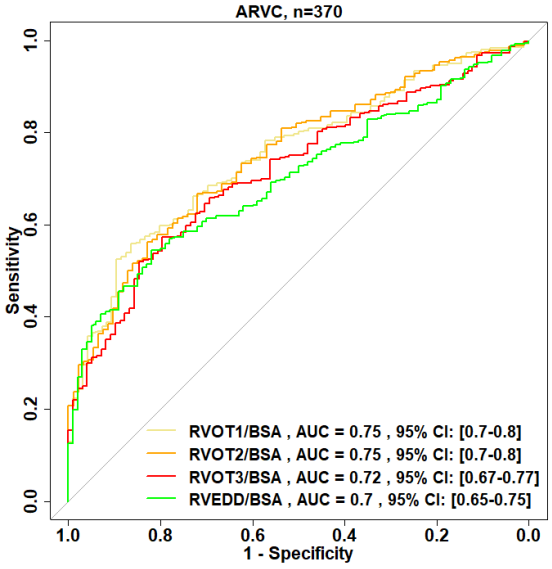

O03

Performance of the BNP and NTproBNP Triage Algorithm for Acute Heart Failure including the Effect of Renal Dysfunction

Desiree Wussler[1 2], Maria Belkin[1], Freya Jenkins[1], Samyut Shresta[1], Paolo Bima[1], Zaid Sabti[1], Eleni Michou[1], Androniki Papachristou[1], Ivo Strebel[1], Nikola Kozhuharov[3 4], Otmar Pfister[1], Felix Mahfoud[1], Tobias Breidthardt[5], Christian Mueller[1]

[1]Department of Cardiology and Cardiovascular Research Institute Basel (CRIB), University Hospital Basel, University of Basel, Basel, Switzerland, [2]Department of Cardiology, Vancouver General Hospital, University of British Columbia, Vancouver, Canada, [3]Department of Cardiology, Inselspital, Bern University Hospital, Bern, Switzerland, [4]Cardiovascular Research Institute Basel (CRIB), University Hospital Basel, University of Basel, Basel, Switzerland, [5]Department of Internal Medicine and Cardiovascular Research Institute Basel (CRIB), University Hospital Basel, University of Basel, Basel, Switzerland

Introduction: The European Society of Cardiology recommends natriuretic peptide testing for confirmation or rule-out of acute heart failure (AHF) in patients presenting with acute dyspnea irrespective of renal function. Higher BNP and NTproBNP levels can be found in patients with renal dysfunction, wherefore concern has been raised regarding the performance of natriuretic peptide triage algorithms in renal dysfunction (RD).

Material and Methods: This prospective diagnostic study enrolled unselected patients presenting with acute dyspnea. Their final diagnosis was centrally adjudicated by two independent cardiologists. BNP, NT-proBNP and eGFR measurements were obtained upon presentation. RD was defined as an eGFR<60ml/min/m2. Safety was quantified as sensitivity in the rule-out zone and accuracy as the specificity in the rule-in zone.

Results: Among 1579 eligible patients, RD was present in 658 (42%) patients. The prevalence of AHF was substantially increasing with worsening renal function (40, 71 and 82% for eGFR>60, 31-59 and <30ml/min/m2). Using BNP, patients with RD had a comparable sensitivity of rule-out (99% and 98% for eGFR<30 and 30-59ml/min/m2 versus 97% for eGFR >60ml/min/m2) and a lower specificity of rule-in (72% and 85% for eGFR <30 and 30-59ml/min/m2 versus 96% for eGFR >60ml/min/m2) compared to patients with normal renal function. Using NTproBNP, patients with RD had a comparable sensitivity of rule-out (100% and 99% for eGFR<30 and 30-59ml/min/m2 versus 97% for eGFR >60ml/min/m2) and a lower specificity of rule-in (46% and 68% for eGFR<30 and 30-59ml/min/m2 versus 91% for eGFR >60ml/min/m2) as compared to patients with normal renal function. When directly comparing BNP and NTproBNP, BNP was superior with regards to specificity for rule-in with even higher extent in patients with RD.

Conclusion: In patients with RD the safety of current BNP and NTproBNP triage algorithms for AHF is high. In contrast, overall specificity of rule-in is decreased with higher diagnostic accuracy of BNP compared to NTproBNP.

Performance of the BNP and NTproBNP triage algorithm for AHF in patients with renal dysfunction and normal renal function

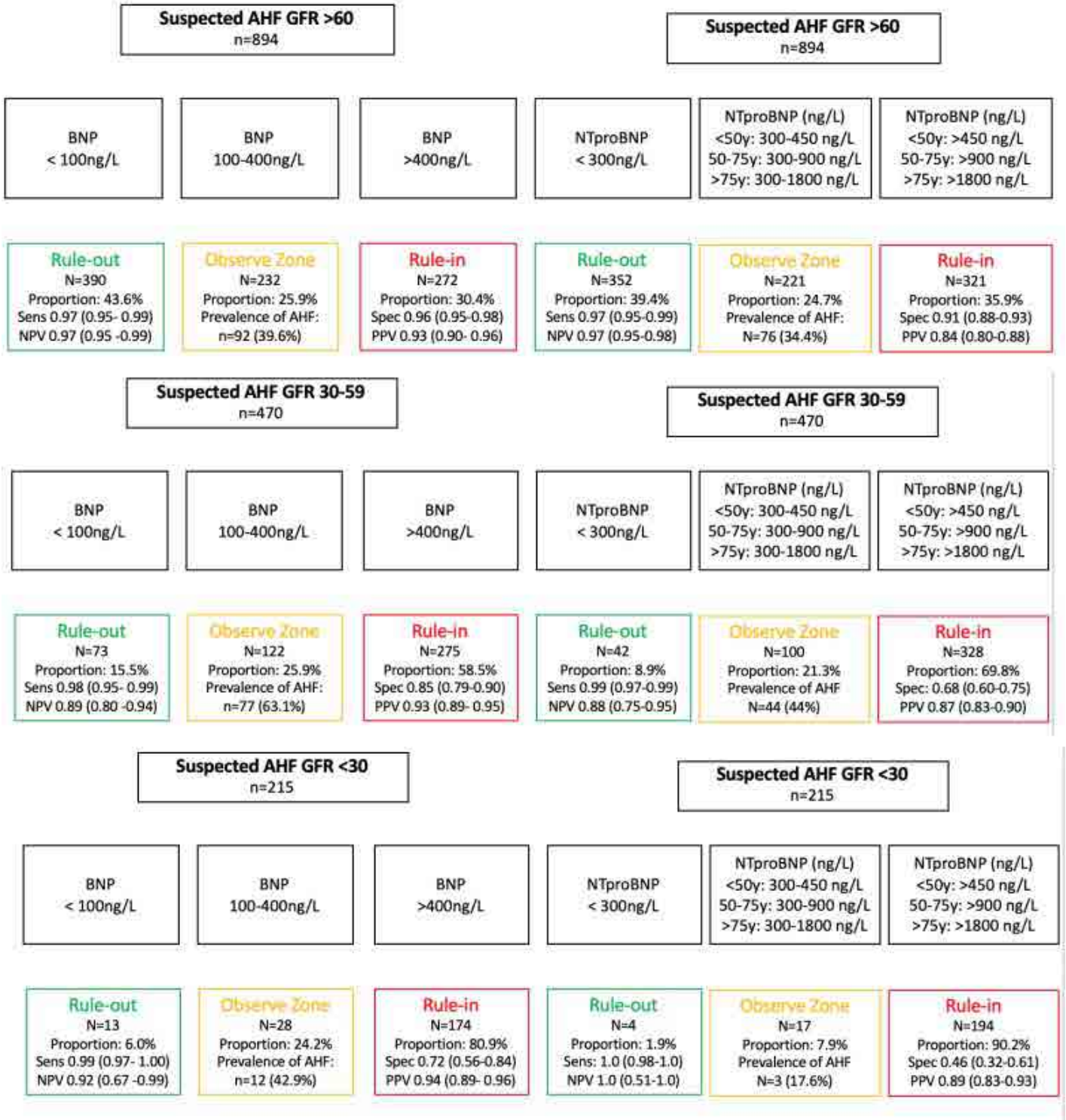

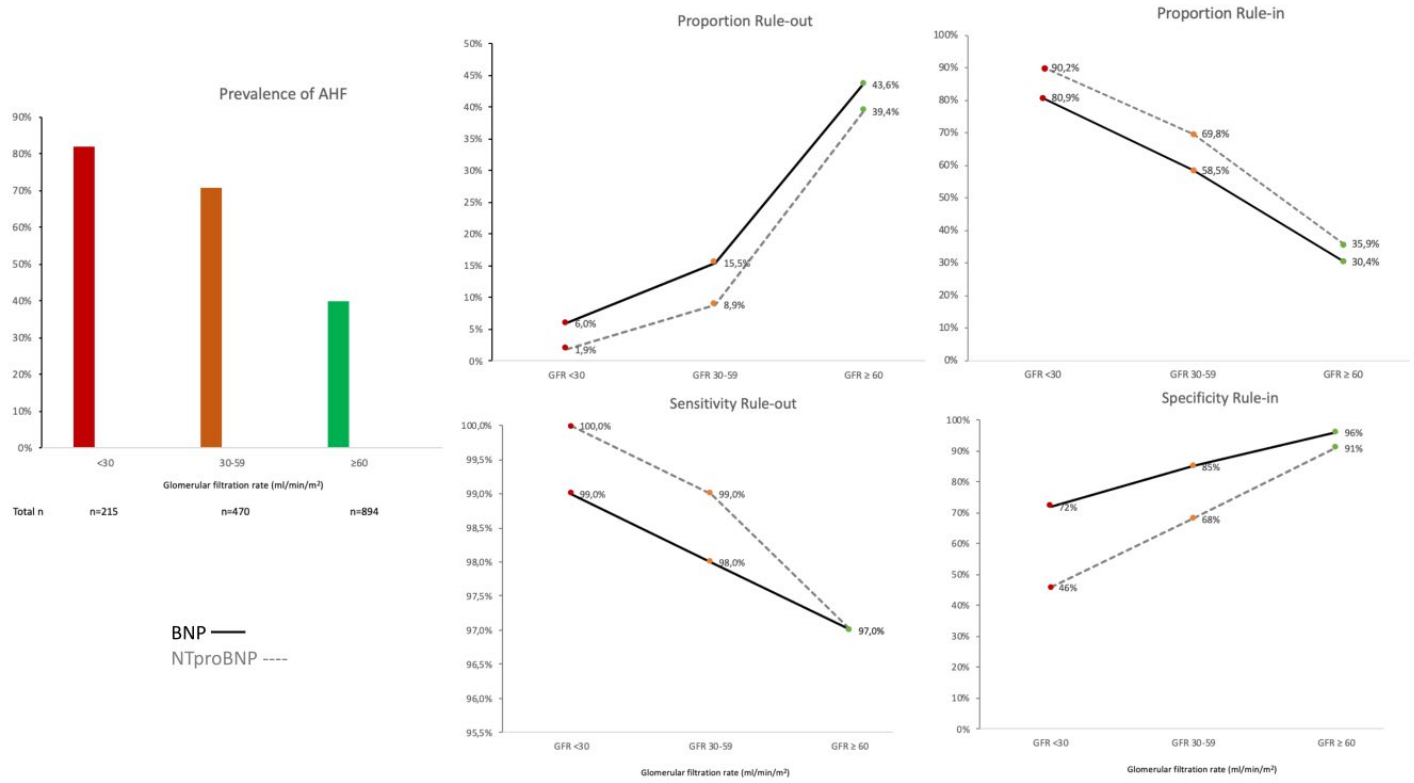

O04

Prognostic proprieties of echocardiographic right ventricular outflow tract diameter in arrhythmogenic right ventricular cardiomyopathy

Thierry Donati[1], Francesca Ortelli[1], Alexandros Protonotarios[2], Qi Chen[1], Monika Hebeisen[1 3], Neria E. Winkler[1], Denis Cener[1], Giulia Montrasio[2], Konstantinos Savvatis[4], Paul A.S. Olsen[4], Corinna Brunckhorst[1], Firat Duru[1], Ardan Saguner[1], Perry Elliott[2], Kristina H. Haugaa[4], Felix C. Tanner[1]

[1]Department of Cardiology, University Heart Center, University Hospital Zurich and University of Zurich, Zurich, Switzerland, [2]Inherited Cardiovascular Disease Unit, St Bartholomew's Hospital, London, United Kingdom, [3]Department of Biostatistics, Epidemiology, Biostatistics and Prevention Institute, University of Zurich, Zurich, Switzerland, [4]ProCardio Centre for Innovation, Department of Cardiology, Oslo University Hospital, Rikshospitalet, Oslo, Norway

Introduction: Right ventricular outflow tract (RVOT) dilatation is a key phenotypic feature of arrhythmogenic right ventricular cardiomyopathy (ARVC). It is not known whether the echocardiographic RVOT diameter predicts adverse cardiovascular events.

Material and Methods: This study included patients with genetic testing and fulfilling the revised 2010 Task Force Criteria for definite ARVC. Participants were recruited from three prospective ARVC registries and categorized according to a primary or secondary prevention situation. The outcome was defined as the first occurrence of sustained ventricular arrhythmia (VA) or death. The RVOT diameter was indexed to body surface area (BSA) and Cox regression models were used to evaluate its association with outcome.

Results: 331 ARVC patients with mean age 47 (16.2) years, 73% in primary prevention, and median follow-up of 6.8 [3.9-10.5] years were included. Mean RVOT/BSA diameter was 19.6 (4.1) mm/m2. Univariable regression revealed a strong association between RVOT/BSA and increased risk of VA (hazard ratio (HR) 1.07 [1.02-1.13], p-value 0.003) or death (HR 1.33 [1.24-1.42], p-value <0.001). Multivariable models demonstrated that the association with VA was independent of LVEF (HR 1.08 [1.03-1.14], p-value 0.003), but not RV fractional area change (FAC) (HR 1.02 [0.96-1.08], p-value 0.506) or RV basal end-diastolic diameter (EDD) (HR 1.03 [0.97-1.10], p-value 0.355), while the association with death was independent of LVEF, RVFAC, and RVEDD (all p-values <0.001). In primary prevention, RVOT/BSA was marginally associated with VA (HR 1.07 [1.00-1.16], p-value 0.050), but strongly with death (HR 1.34 [1.22-1.47], p-value <0.001). In secondary prevention, RVOT/BSA was not associated with VA (HR 1.00 [0.93-1.07], p-value 0.968) but with death (HR 1.29 [1.13-1.48], p-value <0.001).

Conclusion: Patients with definite ARVC and larger RVOT/BSA diameter are at increased risk of adverse events during follow-up. In patients with definite ARVC, RVOT/BSA diameter is useful for event prediction in both primary and secondary prevention.

Figure 1: Echocardiographic RVOT diameter and outcomes during follow-up in ARVC patients

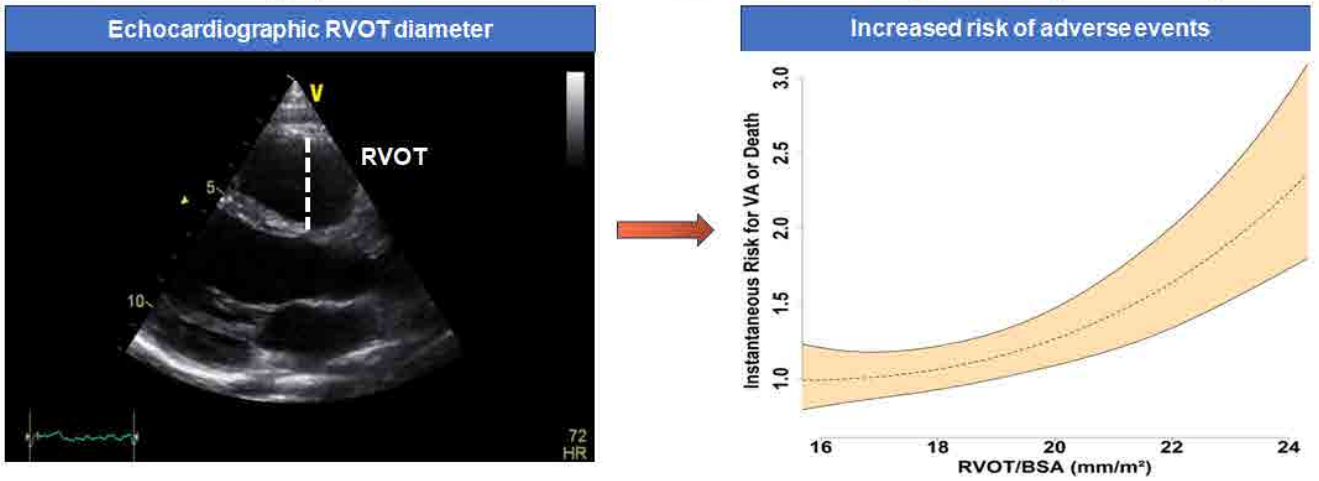

O05

Plasma Proteomics Identify Molecular Features and Biomarkers of Fulminant Myocarditis

Yuxiao Hu[1], Luqi Yang[2], Jinpu Cai[2], Yaxin Liu[3]

[1]University Hospital Zurich, University Heart Center, Zurich, Switzerland, [2]Global Institute of Future Technology, Shanghai Jiao Tong University, Shanghai, China, [3]Fuwai Hospital, National Center for Cardiovascular Diseases, Chinese Academy of Medical Sciences and Peking Union Medical College, Beijing, China

Introduction: Fulminant myocarditis (FM) is a most severe subtype of myocarditis, characterized by acute onset and high mortality. Limited data are available on potential non-invasive biomarkers for the differential diagnosis of diseases. We aim to investigate the plasma proteomic profile and identify biomarkers that can facilitate early diagnosis and treatment of FM.

Material and Methods: In this study, data-independent acquisition proteomic sequencing was performed on plasma samples obtained from eight FM patients, eight ST-segment elevation myocardial infarction (STEMI) patients and eight healthy controls (HCs). A larger cohort included 15 FM, 16 STEMI and 15 HCs was used to validate the proteomic signatures by enzyme-linked immunosorbent assay (ELISA).

Results: A total of 573 proteins were identified in all plasma samples. Functional enrichment analyses uncovered dysregulation of complement and coagulation-related pathways, inflammation, and immune cell degranulation, which were likely contribute to the pathogenesis of FM. We found that two processes, complement activation (classical pathway) and the complement and coagulation cascades, obtained the highest enrichment ratio scores in the GO and KEGG analyses, respectively. We also derived protein coexpression networks through weighted gene correlation network analysis (WGCNA), grouping proteins into five coexpression modules that were associated with clinical traits and enriched for complement activation (turquoise) and acute-phase proteins (blue) in FM. 51 proteins were confirmed able to distinguish FM and STEMI patients through a machine-learning pipeline. Furthermore, a unique biomarker panel comprising GPX3, C7, PGLYRP2, BCHE and ANPEP was established to differentiate FM from STEMI with high accuracy (auROC = 1.000). Some of these biomarkers were further validated by ELISA by the larger cohort.

Conclusion: Proteomic signatures developed in this study reflected the deficiency of key hematological functions in FM patients, and show potential for developing a valuable biomarker panel in complementary to current clinical parameters to aid in the early diagnosis of FM via plasma proteome.

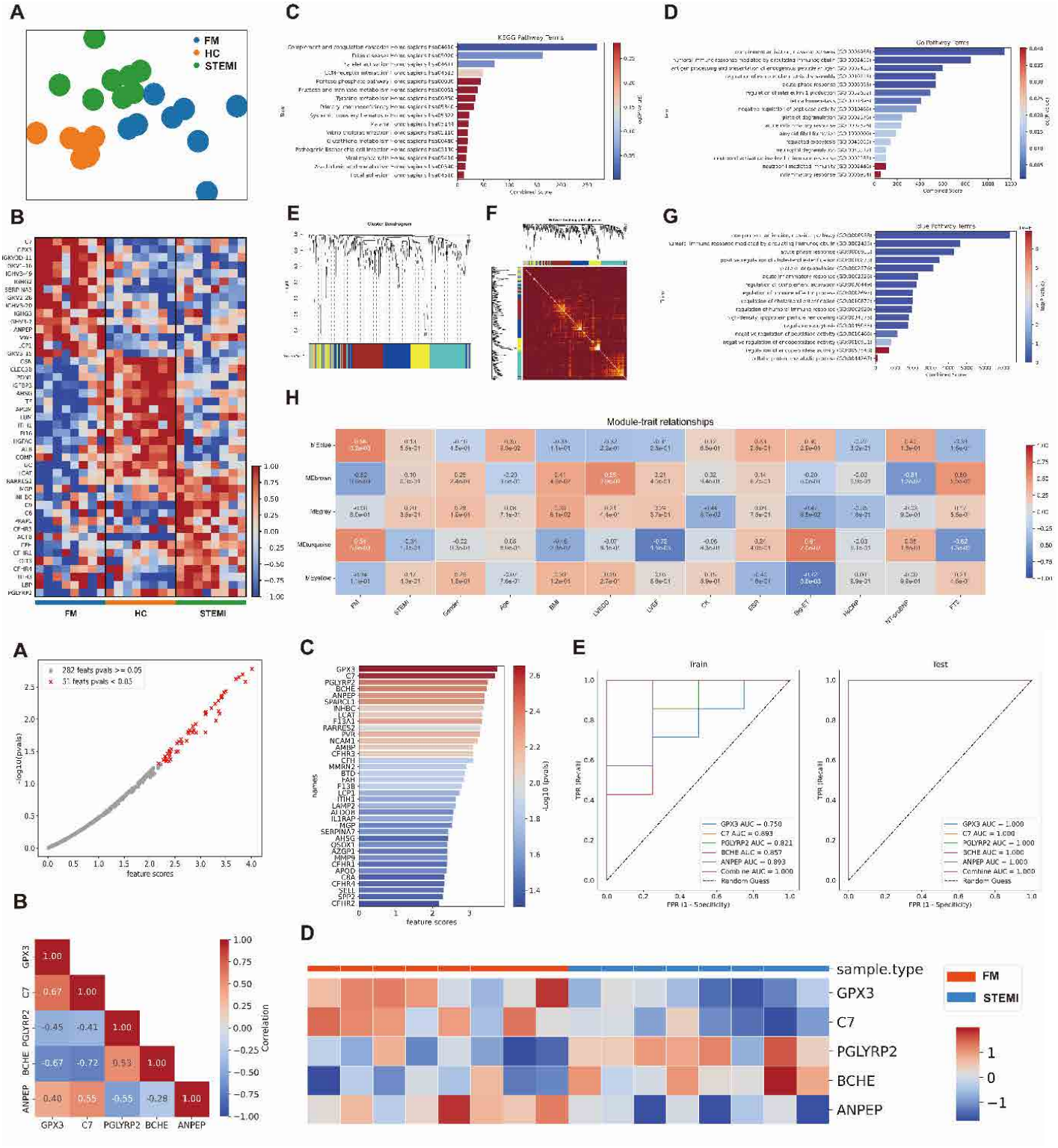

O06

Cardiac Shockwave Therapy Induces Long-term Myocardial Improvement in Ischemic Heart Failure – Results from a Prospective, Randomized Controlled Trial

Johannes Holfeld[1 2], Philipp Steiner[3], Felix Nägele[2], Leo Pölzl[2], Clemens Engler[2], Michael Graber[2], Jakob Hirsch[2], Sophia Schmidt[2], Agnes Mayr[4], Elfriede Ruttmann-Ulmer[2], Hanno Ulmer[5], Axel Bauer[6], Can Gollmann-Tepeköylü[2], Michael Grimm[2]

[1]Department of Cardiovascular Surgery German Heart Center Munich School of Medicine & Health Technical University of Munich, Munich, Germany, [2]University Clinic of Cardiac Surgery, Medical University of Innsbruck, Innsbruck, Austria, [3]Medical University of Innsbruck, Innsbruck, Austria, [4]Department of Radiology, Medical University of Innsbruck, Innsbruck, Austria, [5]Institute of Medical Statistics and Informatics, Medical University of Innsbruck, Innsbruck, Austria, [6]Department of Internal Medicine III, Medical University of Innsbruck, Innsbruck, Austria

Introduction: Chronic ischemic heart failure remains a significant clinical challenge, as revascularization strategies relieve symptoms but provide limited improvement in left ventricular ejection fraction (LVEF). The randomized controlled CAST-HF trial previously demonstrated that cardiac shockwave therapy (SWT) is both safe and effective. The current work focuses on the long-term follow-up results of the CAST-HF trial.

Material and Methods: This single-blind, sham-controlled trial, randomized patients with LVEF ≤40% undergoing surgical revascularization to receive cardiac SWT or sham treatment alongside coronary bypass surgery. Patients were then followed up to 4 years after surgery. The primary endpoint consists of the improvement of LVEF. Secondary endpoints include the improvement of 6-minute walking distance and quality of life (Minnesota Living with Heart Failure Questionnaire).

Results: Of the initial 63 patients, 41 completed long-term follow-up: 22 in the SWT group and 19 in the sham group. At the 1-year follow-up, the SWT group showed a greater improvement in the primary endpoint (Δ from baseline to 360 days: SWT 11.3%, SD 8.8; Sham 6.3%, SD 7.4, p = .0146). Comparing these results with the long-term follow-up, the SWT group showed an even more significant improvement in LVEF up to 4 years after treatment (Δ from baseline: SWT 11.5%, SD 10.1; Sham 2.8%, SD 8.3, p = .0009). Secondary endpoints also showed persistent improvements in the SWT group up to 4 years after treatment, including the 6-minute walking distance (Δ from baseline: SWT 62.6m, SD 114.9; Sham -1.5m, SD 147.0, p = .031) and quality of life (score at long-term follow-up: SWT 18.9, SD 17.5; Sham 28.5, SD 19.6, p = .046).

Conclusion: The long-term follow-up concludes that cardiac SWT is safe, effective on improvement of LVEF, and shows a stable long-term benefit.

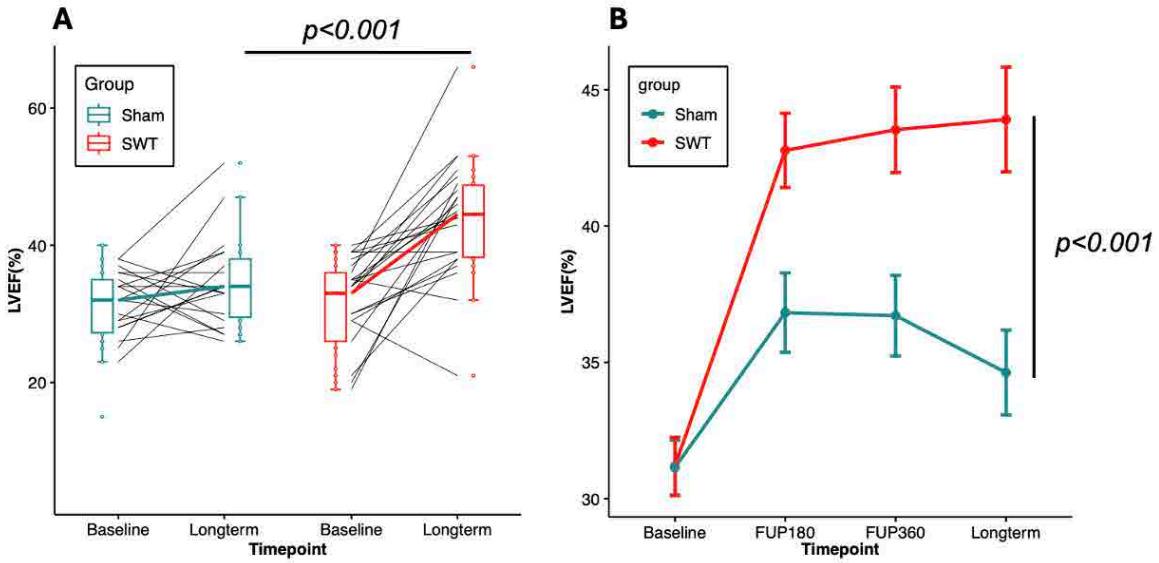

Figure 1 *(A) Improvement in left ventricular ejection fraction for each patient, from baseline to long-term follow-up. (B) Improvement in left ventricular ejection fraction from baseline to day 180, day 360 and long-term follow-up.*

O07

The prognostic role of left atrioventricular coupling index in patients with reduced ejection fraction

Anna Giulia Pavon[1], Damiano Fedele[2], Luca Bergamaschi[2], Matteo Armillotta[2], Marco Valgimigli[2], Giovanni Pedrazzini[1], Marco Guglielmo[3], Gianluca Pontone[4]

[1]Istituto Cardiocentro Ticino, EOC, Lugano, Switzerland, [2]Department of Medical and Surgical Sciences, DIMEC, Alma Mater Studiorum, University of Bologna, Bologna, Italy, [3]Department of Cardiology, Division of Heart and Lungs, Utrecht University, Utrecht University Medical Center, Utrecht, the Netherlands, Utrecht, Netherlands, [4]Department of Perioperative Cardiology and Cardiovascular Imaging,Centro Cardiologico Monzino IRCCS, Milano, Italy

Introduction: The left atrioventricular coupling index (LACI) has been recently introduced as a novel index exploring the intricate relationship among the left ventricle (LV) and left atrium (LA), known to be a key player in maintaining a normal global heart performance. To date the LACI was found providing incremental prognostic value to predict major adverse cardiovascular events (MACE) beyond common risk factors in patients without cardiovascular disease. Aim of the study is to investigate the long-term prognostic role of LACI measured in Cardiac magnetic resonance (CMR) in patients with reduced EF.

Material and Methods: 2170 patients with reduced EF in the DERIVATE registry were analysed. Demographical, echocardiography and CMR data have been collected. CMR datasets were evaluated by an international imaging core-laboratory that collected volumetric, functional parameters and myocardial fibrosis analysis. LACI was defined as LA end-diastolic volume/LV end-diastolic volume * 100. Primary endpoints were all-cause mortality (ACM), hospitalisation for heart failure (HF) and major adverse arrhythmic events (MAACE).

Results: Median LACI was 19.4% (13.3–28.8%). At a median follow up of 1016 days (25th-75th percentiles: 580.3–1609.5 days) HR with 95% CI for LACI in predicting, ACM or HF, and MAACE were 1.011 (1.002-1.021), 1.017 (1.012-1.023), and 1.015 (1.006-1.025) respectively. LACI ≥ 21% allowed the identification of patients at higher risk of ACM, ACM-HF and MAACE (log-rank test p-value <0.001 for all) (Fig.1). A multiparametric score considering LACI ≥ 21% proved to be a better prognosticator with respect to LVEF≤ 35% and previous published DERIVATE scores (Fig. 2)

Conclusion: LACI is an independent predictor of ACM, HF, and MAACE. A cut-off of 21% was associated with an increased risk of MACE. If included in multiparametric score has proven to add incremental prognostic value.

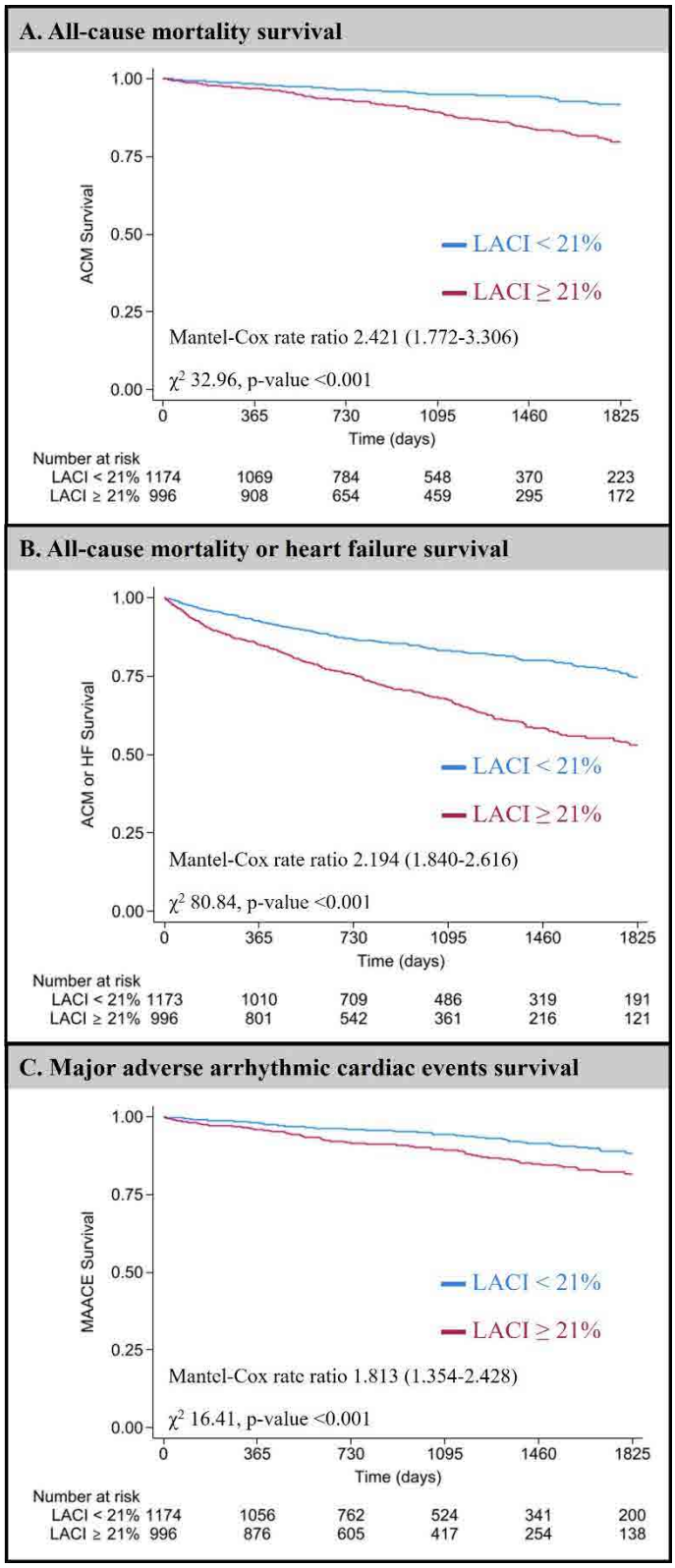

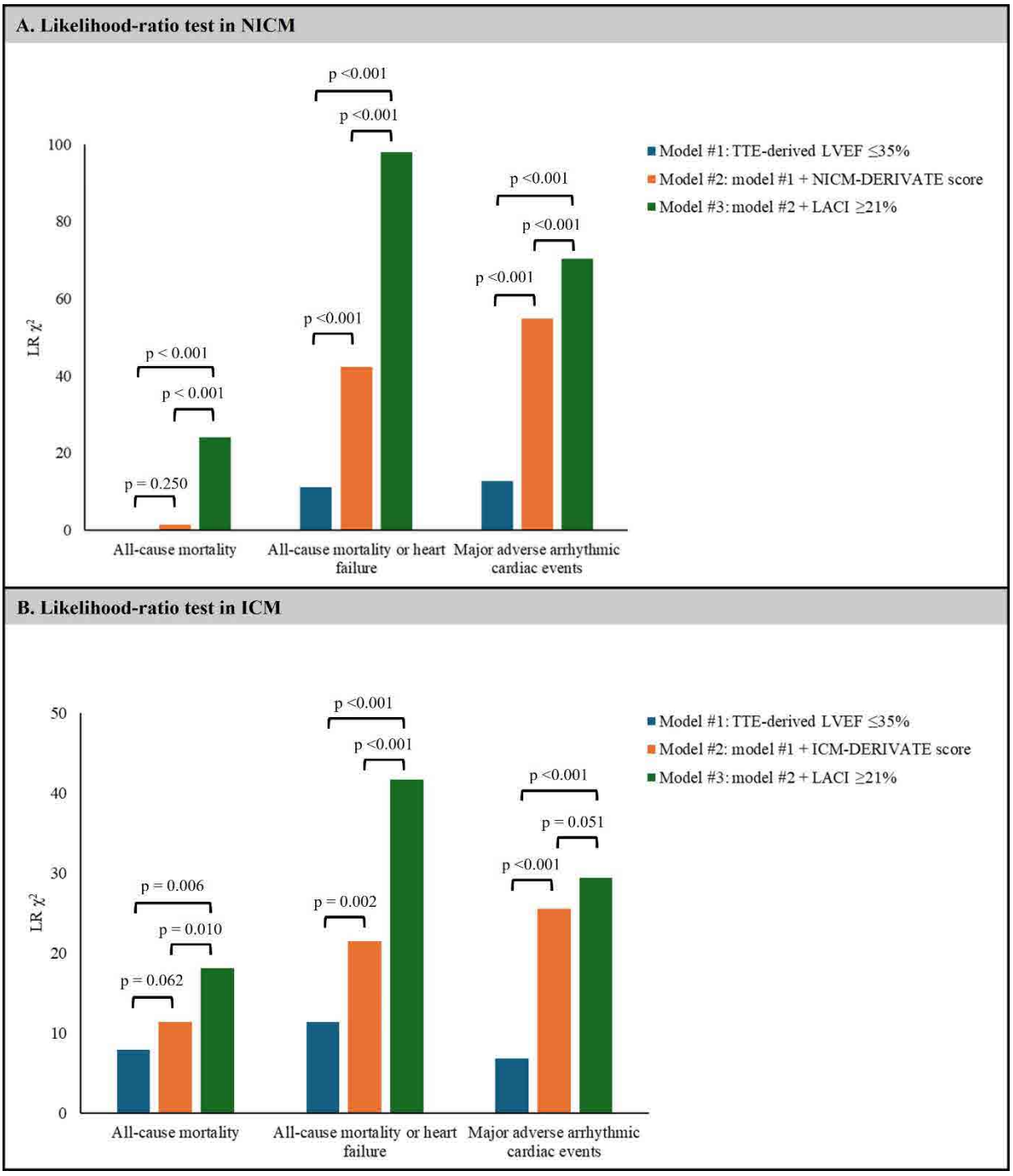

O08

Adherence to medication in patients with acutely decompensated heart failure: a cross-sectional study at the emergency department – The ADHF-ED Trial

Michael Kunz[1], Juel Maalouli Schaar[2], Katharina Welker[3], Lucas Lauder[1], Felix Götzinger[1], Martin Schulz[4 5], Michael Böhm[3], Markus Meyer[2], Felix Mahfoud

[1]Department of Cardiology, University Heart Center Basel, University Hospital Basel, Basel, Switzerland, [2]Department of Experimental and Clinical Toxicology, Institute of Experimental and Clinical Pharmacology and Toxicology, Center for Molecular Signaling (PZMS), Saarland University, Homburg (Saar), Germany, [3]Department of Internal Medicine III, Cardiology, Angiology and Intensive Care Medicine, University Hospital Saarland, Saarland University, Homburg (Saar), Germany, [4]German Institute for Drug Use Evaluation (DAPI) e.V., Berlin, Germany, [5]Institute of Pharmacy, Freie Universität Berlin, Berlin, Germany

Introduction: Non-adherence to guideline-directed medical therapy may cause worsening of chronic heart failure (CHF). However, adherence to medication in patients with acutely decompensated heart failure (ADHF) remains largely unknown.

Material and Methods: This cross-sectional study included patients with ADHF, who presented to the emergency department (ED). Adherence to medication was assessed using both indirect (questionnaires) and direct (qualitative toxicological analysis by liquid chromatography coupled to high-resolution mass spectrometry) methods. The trial is registered under clinicaltrials.gov (NCT06459115).

Results: A total of 100 patients were included in the final analysis, of which 61% were men, with a mean age of 77.9±10.1 years, and median NT-proBNP of 4,846 pg/ml (interquartile range 2,091-9,863). Of the cohort, 35% had HFrEF, 22% HFmrEF, and 43% HFpEF. According to the adherence definition used in this study, 39% of patients were adherent, 39% were partially adherent, and 22% were non-adherent. Adherence rates to different drug classes varied (figure 1). Interestingly, 41% of patients had drugs detected that were not on their medication plans and not given at the ED (mainly cardiovascular drugs and painkillers). Non-adherent patients had significantly more substances prescribed for the treatment of CHF than partially adherent (p = 0.0047) and adherent (p = 0.0002) patients and had a significantly higher pill burden for CHF treatment than adherent patients (p = 0.002, figure 2). Non-adherent patients were significantly younger than partially adherent (p = 0.0144) and adherent (p = 0.0054) patients. Adherent patients were significantly more likely to have an abnormal DemTect test result (p = 0.049). Having medication prepared by a third party significantly reduced the risk of non-adherence and partial adherence. Indirect adherence monitoring using questionnaires proved to be inaccurate.

Conclusion: Adherence rates in patients with ADHF were notably low. Non-adherence to medical therapy is a neglected contributor to the worsening of CHF, leading to hospitalization due to ADHF.

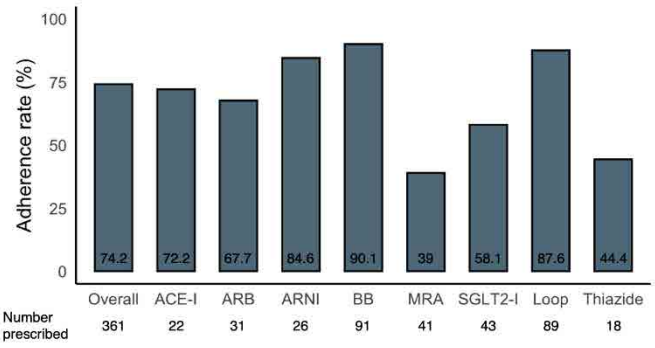

Figure 1: Adherence rates for different substance classes

Adherence rates were corrected for single-pill combinations. One patient was prescribed to ertugliflozin and two patients to indapamide, but these substances are not detectable in the analyses used, so these were excluded.

ACE-I= angiotensin-converting enzyme inhibitor, ARB= angiotensin II receptor blocker, ARNI= angiotensin receptor-neprilysin inhibitor, BB= β blocker, MRA= mineralocorticoid receptor antagonist, SGLT2-I= sodium-glucose co-transporter 2 inhibitor, Loop= loop diuretic

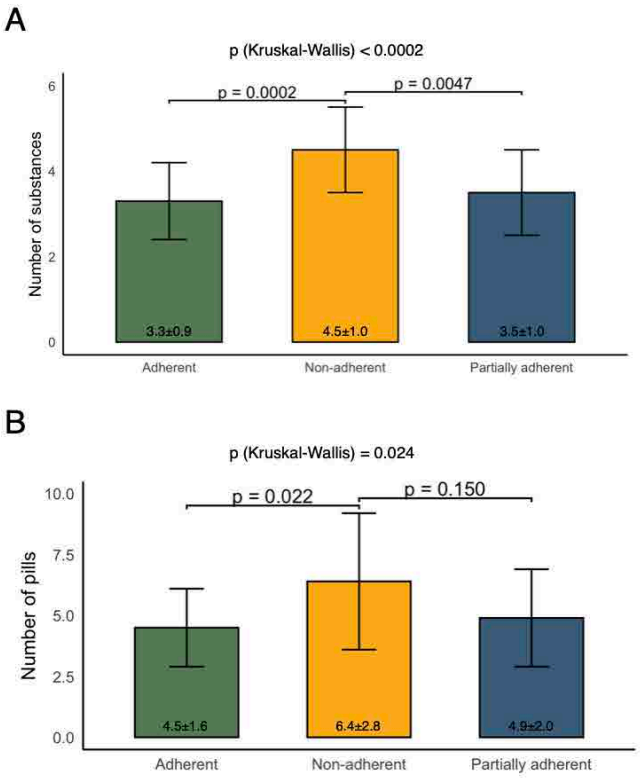

Figure 2: Impact of chronic heart failure therapy and dosing regimen on adherence

The impact of the total number of substances (A) and total number of pills for chronic heart failure treatment (B) on adherence.

Adherence rates were corrected for single-pill combinations. P values are given for between-group comparisons.

RAPID FIRE ABSTRACT SESSION "CORONARY ARTERY DISEASE AND ACUTE CARDIAC CARE"

O09

Enhanced coronary physiology assessment with endothelial shear stress predicts residual cardiovascular risk in older patients with myocardial infarction

Alessandro Candreva[1 2], Andrea Erriquez[3], Maurizio Lodi Rizzini[2], Frank Ruschitzka[1], Gianluca Campo[3], Umberto Morbiducci[2], Simone Biscaglia[3], Diego Gallo[2], Barbara Staehli

[1]University Hospital Zurich, Zurich, Switzerland, [2]Politecnico di Torino, Turin, Italy, [3]Ospedale Sant'Anna, Ferrara, Italy

Introduction: The interplay between traditional risk factors and anatomo-functional coronary lesion descriptors remains uncertain. In this study, we sought to evaluate the cross-talk of endothelial shear stress (ESS)-based metrics and traditional clinical and anatomical parameters for predicting cardiovascular risk.

Material and Methods: This post hoc analysis of the Functional Assessment in Elderly MI Patients with Multivessel Disease (FIRE) trial included older patients (≥75 years) with acute myocardial infarction (MI) and multivessel coronary artery disease (MVD) undergoing percutaneous coronary intervention (PCI). Time-averaged wall shear stress (TAWSS) and topological shear variation index (TSVI) were calculated using computational fluid dynamics simulations in non-culprit coronary lesions with negative functional assessment left untreated. Major adverse cardiovascular events (MACE) at 1 year were defined as composite of any-cause death, non-fatal MI, stroke and ischemia-driven revascularization. Multivariate models and causal inference analysis were used to assess the inter-relationship of anatomo-functional metrics alongside traditional risk factors.

Results: 335 patients from the FIRE trial were included. Percentage area stenosis (%AS), lesion length, TAWSS and TSVI averaged 57.2%, 12.3mm, 2.9 Pa, 59.2 m-1. Higher %AS in non-culprit lesions increased the residual MACE risk at one year (HR 1.024, 95%CI 1.002-1.046, p = 0.031), while longer lesion length of all-cause death (HR 1.042, 95%CI 1.009-1.077, p = 0.013) and higher TSVI of MI (HR 1.006, 95%CI 1.000-1.012, p = 0.021). %AS, lesion length and TSVI significantly improved the multivariate outcome prediction accuracy when associated with traditional risk factors. The causality analysis demonstrated the interaction between %AS, TSVI, and clinical factors, showing that the adverse effect of %AS on MI risk is mediated by TSVI.

Conclusion: Integrating TSVI with traditional clinical and anatomical parameters significantly enhances cardiovascular risk prediction in elderly patients with MVD.

O10

Association between inflammatory biomarkers, chronic stress, and pericoronary adipose tissue attenuation obtained with coronary CT

Tobia Albertini[1], Marc Dörner[2], Andreas A. Giannopoulos[1], Roland von Känel[2], Dominik C. Benz[1], Nidaa Mikail[1], Clarissa D. Voegel[3], Tina M. Binz[3], Philipp A. Kaufmann[1], Catherine Gebhard[1], Ronny R. Buechel[1], Aju P. Pazhenkottil[1]

[1]Cardiac Imaging, Department of Nuclear Medicine, University Hospital Zurich, University of Zurich, Zürich, Switzerland, [2]Department of Consultation-Liaison-Psychiatry and Psychosomatic Medicine, University Hospital Zurich, Zürich, Switzerland, [3]Center for Forensic Hair Analytics, Zurich Institute of Forensic Medicine, University of Zurich, Zürich, Switzerland

Introduction: Pericoronary adipose tissue (PCAT) attenuation is a novel imaging biomarker of coronary inflammation associated with an increased risk of coronary artery disease (CAD). However, no studies have examined the relationship between chronic stress and PCAT. This study aimed to evaluate the intersection between chronic stress, inflammatory biomarkers, coronary plaque features, and PCAT attenuation.

Material and Methods: A total of 98 participants with low-pretest probability of CAD were included. PCAT attenuation, total plaque volume (TPV) quantification, and vulnerable plaque features were assessed by coronary CT angiography and chronic stress was measured by hair cortisol concentration (HCC) and vital exhaustion questionnaire. Regression models were used to analyse associations of PCAT with the inflammatory biomarkers interleukin-6 (IL-6) and tumour necrosis factor-α (TNF-α), TPV, vulnerable plaque features, and coronary stenosis >50%. Moderating analyses were performed to test whether chronic stress modulated the association between inflammatory biomarkers and PCAT attenuation.

Results: PCAT attenuation was significantly associated with IL-6 (mean difference 1.11, 95% CI 0.29-1.94, p = 0.009), TNF-α (mean difference 0.62, 95% CI 0.08-1.15, p = 0.023), and a greater TPV (mean difference 3.51, 95% CI 0.04-6.98, p = 0.047), but not vulnerable plaque features or coronary stenosis >50%. HCC (interaction term -0.12, 95% CI -0.27 to -0.003, p = 0.019) and vital exhaustion (interaction term 0.13, 95% CI 0.01-0.34, p = 0.024) moderated the relationship between IL-6, but not TNF-α, and PCAT attenuation.

Conclusion: This study suggests that circulating inflammatory biomarkers are associated with PCAT attenuation, which was further correlated with TPV. Chronic stress might have synergistic effects on inflammation and PCAT.

CORONARY CT ANALYSIS

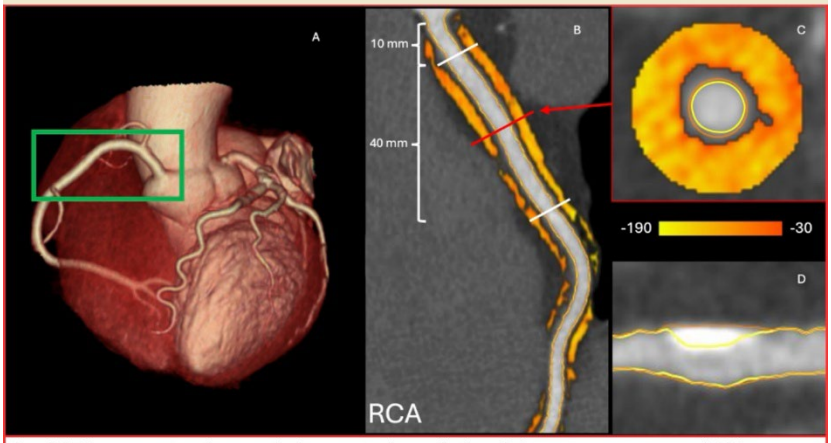

A: CCTA reconstruction and demonstration of the right coronary artery (RCA, green rectangle). **B** and **C**: The proximal 10-50 mm of the RCA were analysed, shown here in a curved multiplanar reconstruction (B) and axial section (C) with visualisation of pericoronary adipose tissue (PCAT) attenuation in the corresponding colour map (-190 to -30 Hounsfield units). **C** and **D** highlight the contour of the inner lumen (yellow circle (C) or line (D)) and outer vessel wall (orange circle (C) or line (D)). Total plaque volume was defined as volume between these two lines. **D** illustrates a calcified plaque.

CENTRAL ILLUSTRATION Association between inflammatory biomarkers, chronic stress and pericoronary adipose tissue attenuation

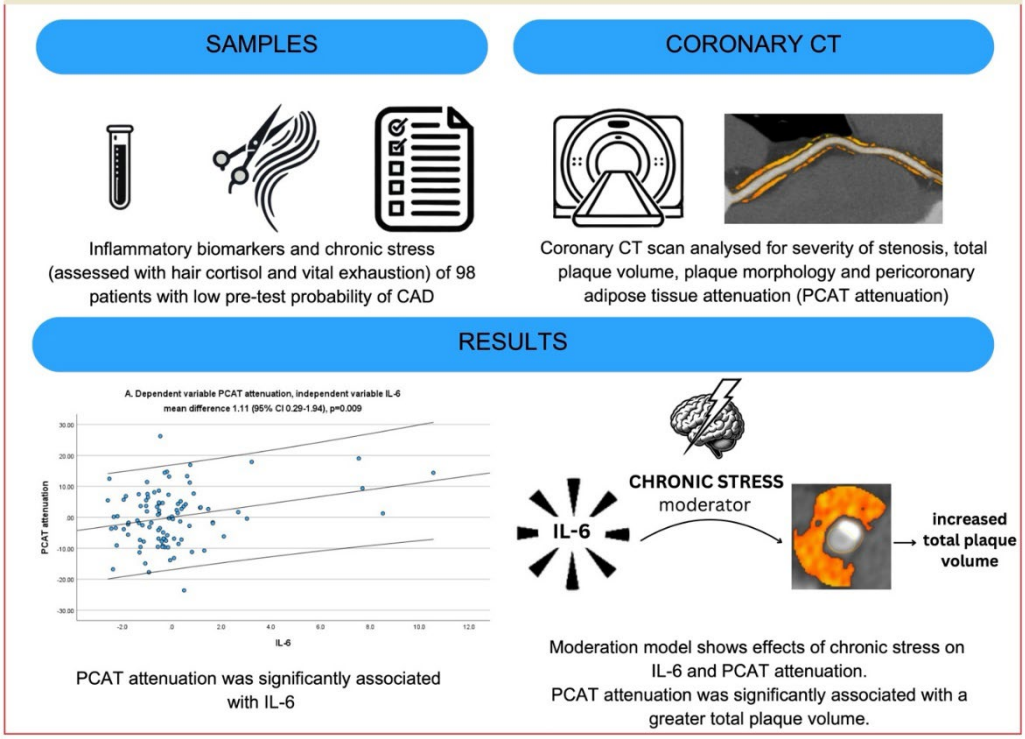

O11

Cangrelor in patients with myocardial infarction complicated by cardiogenic shock and/or cardiac arrest

Wesley Bennar[1], Yuan Zhi[2], Dorian Garin[1], Chiara Schaffner[2], Stéphane Cook[1], Matthias Bossard[2], Diego Arroyo[1]

[1]Hôpital Fribourgeois, Fribourg, Switzerland, [2]Lucerne Cantonal Hospital, Lucerne, Switzerland

Introduction: This study assesses the efficacy and safety of Cangrelor, an intravenous P2Y12 inhibitor, in patients with myocardial infarction complicated by cardiogenic shock and/or cardiac arrest, where delayed oral P2Y12 inhibitor absorption poses challenges. Key outcomes include early stent thrombosis rates, bleeding events, and cardiovascular mortality.

Material and Methods: A total of 168 patients treated with Cangrelor for myocardial infarction complicated by cardiogenic shock (SCAI stage C or higher) and/or cardiac arrest were retrospectively included. The mean age was 66.3 years, and 75.6% were male. Cardiac arrest occurred in 39.9%, and the mean return of spontaneous circulation time was 21.8 minutes. ST-elevation myocardial infarction was present in 85.1% of cases, with an average left ventricular ejection fraction of 33.2%. Femoral access was used in 73.8% of PCI procedures. Pre-procedural flow in culprit vessels were TIMI 0 in 62.3%, TIMI 1 in 15.5%, TIMI 2 in 13.7%, and TIMI 3 in 3.6%. Cangrelor administration protocol consisted in a 30 µg/kg bolus followed by a 4 µg/kg/min infusion for 2-4 hours. Most patients received intravenous aspirin (96.4%) and unfractionated heparin (98.8%) peri-procedurally. GPIIb/IIIa inhibitors were used in 4.8% of cases. Mechanical circulatory support included Impella (50.6%), intra-aortic balloon pumps (7.1%), and ECMO (3.0%).

Results: No acute stent thrombosis or reinfarction (<48 hours) were observed, indicating an adequate antiplatelet effect. Post-procedural TIMI 3 flow was achieved in 89%. Significant bleeding (BARC 3-5) occurred in 25.6%, primarily at puncture sites (62.8%). Mortality during index hospitalization occurred in 43 (25.6%) patients, with 30 (17.9%) deaths attributed to cardiovascular causes.

Conclusion: Cangrelor effectively prevents peri-intintervential and acute stent thrombosis in high-risk patients, despite frequent bleeding complications. The findings support the use of cangrelor as a valuable therapeutic option in acute coronary syndromes with cardiogenic shock and/or cardiac arrest. Further prospective randomized studies are warranted to establish a comparison with oral P2Y12 inhibitors.

O12

The impact of achieving guideline-endorsed low-density lipoprotein cholesterol target levels on neoatherosclerosis formation in patients with ST-segment myocardial infarction: a substudy of the international CONNECT trial

Jonas Häner[1], Ryota Kakizaki[1], Masanori Taniwaki[2], Yohei Ohno[3], Kazuyuki Yahagi[2], Yoshiharu Higuchi[4], Georgios Siontis[1], Kenji Ando[5], Naoki Watanabe[6], Jonas Lanz[1], Yasushi Ueki[7], Masami Sakurada[8], Konstantinos Koskinas[1], Sylvain Losdat[9], Lorenz Räber[1]

[1]Bern University Hospital, Inselspital, University of Bern, Bern, Switzerland, [2]Mitsui Memorial Hospital, Tokyo, Japan, [3]Tokai University Hospital, Kanagawa, Japan, [4]Osaka Police Hospital,, Osaka, Japan, [5]Kokura Memorial Hospital, Fukuoka, Japan, [6]Ogaki Municipal Hospital, Gifu, Japan, [7]Shinshu University School of Medicine, Nagano, Japan, [8]Tokorozawa Heart Center, Saitama, Japan, [9]Clinical Trials Unit Bern, University of Bern, Bern, Switzerland

Introduction: Secondary preventive lowering of low-density lipoprotein cholesterol (LDL-C) reduces cardiovascular event rates after ST-elevation myocardial infarction (STEMI). However, the impact of achieving guideline-endorsed LDL-C target levels on neoatherosclerosis formation after drug-eluting stent (DES) implantation remains uninvestigated.

Material and Methods: This is a post-hoc analysis of the CONNECT trial that randomized 239 patients with STEMI to percutaneous coronary intervention (PCI) with biodegradable polymer or durable polymer Everolimus-eluting stents in Switzerland and Japan. The frequency of neoatherosclerosis, determined by intracoronary optical coherence tomography (OCT) 3 years after primary PCI, was compared between patients with or without on-treatment LDL-C levels below guideline-endorsed thresholds. The LDL-C target was 1.4 mmol/l in European and 1.8 mmol/l in Japanese guidelines.

Results: Among 178 patients (91 Swiss, 87 Japanese) who underwent OCT at 3 years, 98 patients achieved target LDL-C levels, and 80 patients did not. On-treatment LDL-C level was 1.24±0.34 mmol/l and 2.25±0.96 mmol/l, respectively. The frequency of neoatherosclerosis was significantly lower in patients who achieved target LDL-C levels as compared to patients who did not (7.1 vs 18.8%, P = 0.023, Figure, Panel A). Furthermore, patients with high-intensity statin therapy (N = 142) as compared to patients with moderate, low or no statin therapy (N = 36) were less likely to develop neoatherosclerosis at 3 years (8.5 vs 27.8%, P = 0.004, Figure, Panel B).

Conclusion: This is the first multi-center study to compare the long-term formation of neoatherosclerosis in relation to whether or not patients achieved current guideline-endorsed LDL-C levels. Neoatherosclerosis occurred less frequently among patients achieving guideline-endorsed LDL-C levels 3 years after DES implantation for STEMI. Intensive lipid-lowering therapy may inhibit neoatherosclerosis formation and thus prevent late stent failure.

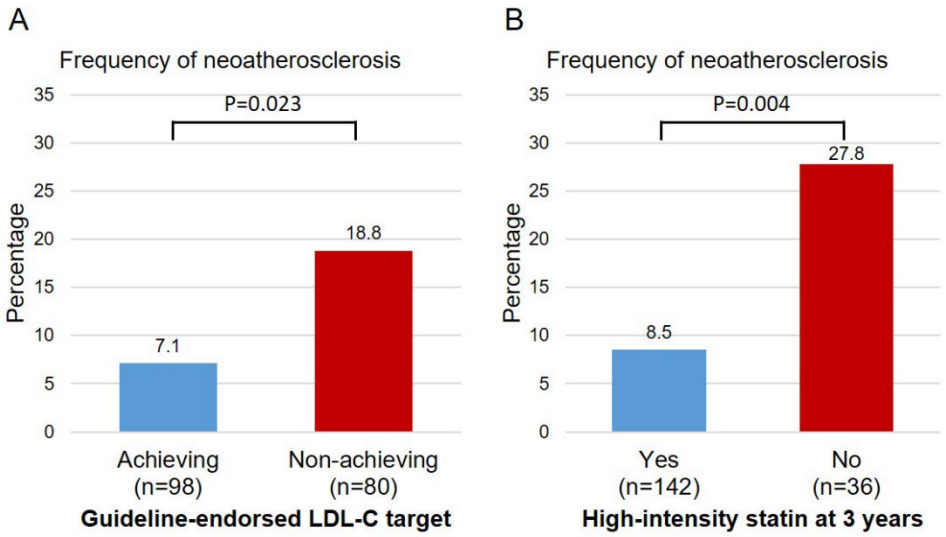

O13

Durable- versus Biodegradable Polymer Drug-Eluting Stents in All-Comers

Thierry Witzig*[1], Serban Puricel[1], Alain Witzig[1], Pascal Meier[1], Diego Arroyo[1], Mario Togni[1], Stéphane Cook[1]

[1]University and Hospital Fribourg, Fribourg, Switzerland

Introduction: Drug-eluting stents (DES) have become the gold standard of coronary angioplasty since their inception in 2002. Biodegradable polymer DES (BP-DES) have been postulated to be superior to durable polymer DES (DP-DES) due to their more biocompatible polymer. To date, no study has shown the superiority of one type of polymer compared to the other. We aimed to compare outcomes between a broad range of second-generation DP-DES and BP-DES in an allcomer population.

Material and Methods: We analyzed data from 2,824 patients who underwent percutaneous coronary intervention (PCI) with BP-DES or DP-DES in our database. Of these, 2,079 (1286 DP-DES and 793 BP-DES) met the inclusion and exclusion criteria and completed a two-year follow-up: The primary outcome was the device-oriented composite endpoint (DOCE) of cardiac death, non-fatal target vessel myocardial infarction (TVMI) and target lesion revascularization (TLR).

Results: Mean age was 67 years, with 75% male. Despite the DP-DES group exhibiting significantly higher rates of risk factors, such as arterial hypertension (63.1% vs 57.5%, p = 0.010), a greater average number of stents implanted per patient (1.72±0.92 vs 1.63±0.84, p = 0.040), more acute coronary syndrome (ACS) (55.1% vs 50.2%, p = 0.031), and a higher rate of post-dilatation (42.2% vs 35.2%, p<0.001), the rate of acute stent thrombosis was significantly lower than in the BP-DES group (HR 0.240, 95% CI: 0.075–0.766; p = 0.016). This difference remained significant after adjusting for covariates using a Cox proportional hazards model and performing a win ratio analysis (4.09, 95% CI: 1.28–13.09; p = 0.018). Despite this increased rate of acute ST, there was no difference in DOCE (12.1% vs 14.5%, OR 1.218, 95% CI: 0.926-1.600; p = 0.158) between the two groups up to 2 years.

Conclusion: Clinical follow-up up to two years shows similar outcomes between BP-DES and DP-DES. The rate of acute stent thrombosis is higher in patients with BP-DES.

O14

Temporal trends of normal scan results and pretest probability in myocardial perfusion imaging in a tertiary referral center in Switzerland between 2000 and 2023

Igor Schneider[1 2], Simon Frey[1 2], Ann-Sophie Otto[1 2], Florian Geiser[1 2], Damian Wild[3], Philip Haaf[1 2], Felix Mahfoud, Michael Zellweger[1 2]

[1]University Heart Center, University Hospital Basel, Basel, Switzerland, [2]Cardiovascular Research Institute Basel (CRIB), Basel, Switzerland, [3]Division of Nuclear Medicine, University Hospital Basel, Basel, Switzerland

Introduction: A high proportion of patients referred for coronary artery disease (CAD) testing with myocardial perfusion imaging (MPI) have normal test results. With decreasing prevalence of CAD and overestimation of pre-test probability (PTP) by existing models, normal tests results have continuously increased over time. This study aimed to evaluate temporal trends of normal scan results over 23 years in a large referral center in Switzerland.

Material and Methods: Data from all available MPI scans (Single Photon Emission Computed Tomography and Positron Emission Tomography) performed between 2000 and 2023 were extracted from the electronic medical record. An abnormal scan result was defined as Summed Stress Score (SSS) ≥4. PTP according to the 2019 ESC guidelines on chronic coronary syndromes was calculated. Temporal trends of Summed Rest Score (SRS), Summed Difference Score (SDS) and SSS were also analyzed.

Results: Overall, 45’113 patients were analyzed. The mean age was 66 ± 11 years, 35% were female. Typical and atypical angina were reported in 22% and 24%, respectively. Overall, MPI was abnormal in 44%. Small (SDS ≥2) and relevant (≥10% myocardium involved) ischemia was observed in 36% and 13%, respectively. The proportion of normal scan results increased from 53% in 2000 to 62% in 2023 (p <0.001) (figure 1). SRS and SSS, but not SDS decreased over time (figure 2). In multivariate regression analysis, the year of exam was a significant predictor for normal MPI (OR 1.026 (95% CI 1.023-1.029), p <0.001). PTP remained unchanged over time (20% in 2000 vs. 21% in 2023) (figure 1).

Conclusion: The proportion of normal scan results significantly increased over 23 years, whereas PTP remained unchanged. To counter this trend and reduce unnecessary diagnostic tests, patient preselection must further be optimized.

Figure 1: Absolute and relative numbers of normal scan results and mean pre-test probability between 2000 and 2023

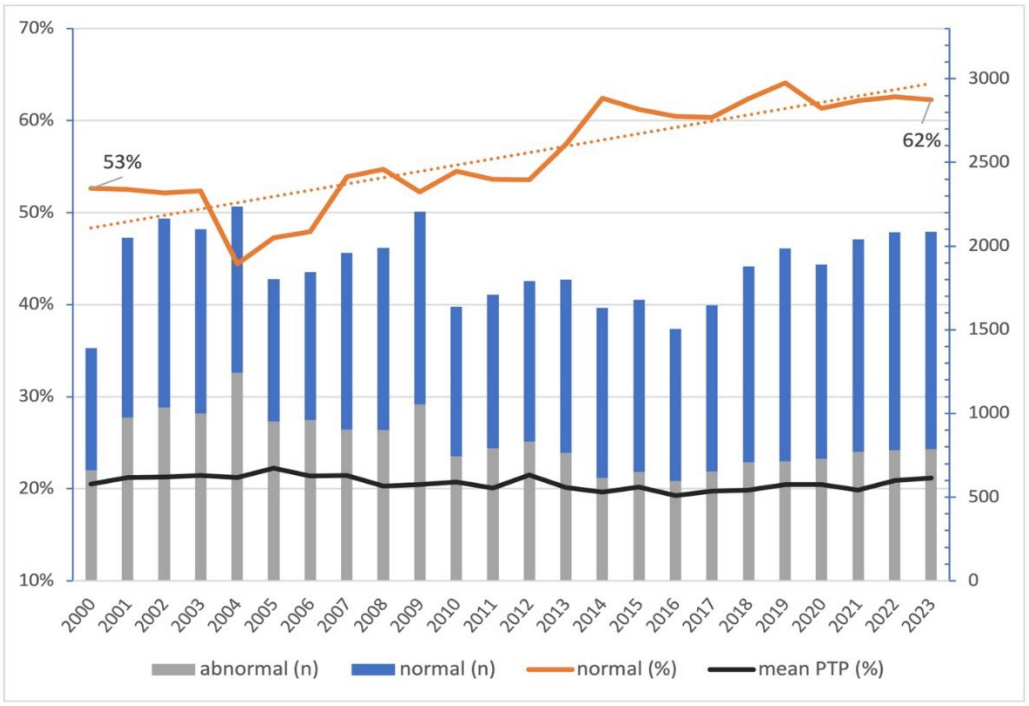

Left y-axis indicates percentages for proportion of normal scans and pre-test probability (PTP). Right y-axis indicates absolute number of patients with normal and abnormal scan results.

Figure 2: Temporal trend of semi-quantitative MPI results

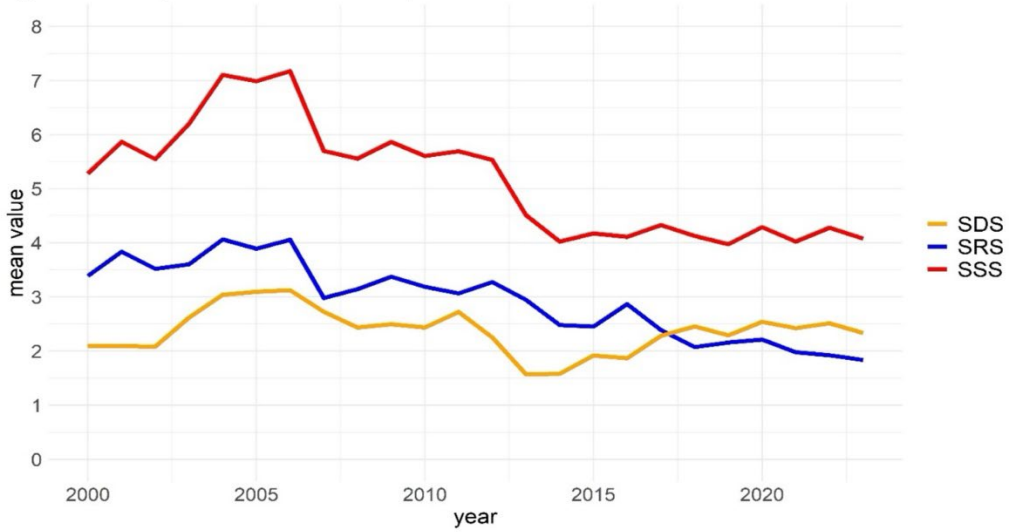

SDS: summed difference score; SRS: summed rest score; SSS: summed stress score.

O15

Temporal trends in management and outcomes of patients with myocardial infarction and concomitant moderate to severe renal failure – Insights from the Acute Myocardial Infarction in Switzerland (AMIS) Plus Registry 2002-2024

Erika Aagaard[1], Matthias Bossard[1], Fabienne Foster[2], Mehdi Madanchi[1], Dragana Radovanovic[2], Hans Rickli[3], Florim Cuculi[1]

[1]Luzerner Kantonsspital, Kardiologie, Luzern, Switzerland, [2]University of Zürich, Amis Plus Registry, Zürich, Switzerland, [3]Kantonsspital St. Gallen, Kardiologie, St. Gallen, Switzerland

Introduction: The prevalence of renal failure (RF) is expected to increase with the aging population, and myocardial infarction (MI) with concomitant moderate-severe RF has been associated with worse outcomes. Due to advances in medical treatment during the last decades, updated knowledge is needed regarding treatment and prognosis of these patients. We aimed to evaluate the trends in management and in-hospital mortality of patients with MI and moderate-severe RF in Switzerland since 2002.

Material and Methods: We used data from the Acute Myocardial Infarction in Switzerland (AMIS) Plus cohort between 2002 and 2024, according to 2-year periods, and defined RF (moderate-severe) based on the Charlson Comorbidity Score.

Results: Overall, 59,510 MI patients with available information on renal function were included in the analysis from the AMIS Registry. Of these patients, 4,083 (6.9%) had established RF. This group was significantly older with more comorbidities (including heart failure, cerebrovascular and peripheral vascular disease, p<0.001). They typically presented later to admission after symptom onset, more often had dyspnea, and less frequently had ST-elevation MI than the none-mild RF group. RF patients less frequently received guideline-recommended therapy during an MI, including percutaneous coronary intervention (PCI), P2Y12 inhibitors, angiotensin-converting enzyme inhibitors/angiotensin II receptor antagonists, and statins (p<0.001). However, they were more frequently already treated with these medications on admission. Between 2002 and 2024, the percentage of PCIs increased for MI patients with concomitant RF (Figure 1). During the same period, in-hospital mortality rate significantly decreased, and there is now no significant difference with the none-mild RF group (Figure 2).

Conclusion: Over the last two decades, significant improvements have been achieved in providing guideline-recommended therapy and reducing in-hospital mortality of MI patients with moderate to severe renal failure. These advancements have markedly enhanced the care and outcomes for this high-risk patient population.

Temporal trends in management and outcomes of patients with MI and concomitant moderate to severe renal failure – AMIS Plus Registry 2002-2024

Figure 1. Patients receiving PCI according to presence of RF between 2002 to 2024.

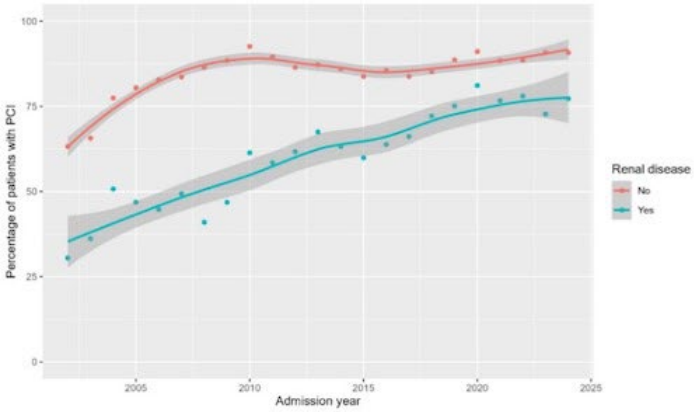

Figure 2. Temporal trends in in-hospital mortality after MI according to presence of RF

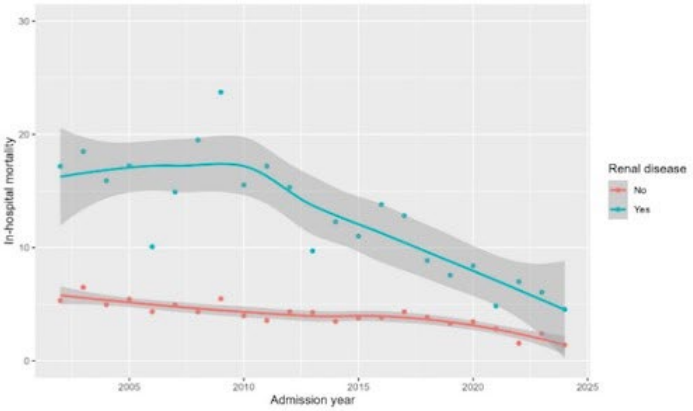

Abbreviations: MI = Myocardial infarction; PCI = Percutaneous coronary interventions;

O16

Angiographic types of spontaneous coronary artery dissection and their impact on long-term outcome

Desiree Wussler[1 2], Mehima Kang[1], Tejana Grewal[1], John Mancini[1], Jacqueline Saw[1]

[1]Department of Cardiology, Vancouver General Hospital, University of British Columbia, Vancouver, Canada, [2]Department of Cardiology and Cardiovascular Research Institute Basel (CRIB), University Hospital Basel, University of Basel, Basel, Switzerland

Introduction: Spontaneous coronary artery dissection (SCAD) is an increasingly recognized cause of myocardial infarction (MI). However, it remains unclear whether and in which extent the different angiographic types of SCAD (type 1-3) impact patients´ outcome.

Material and Methods: We analyzed data from all patients included in the Canadian SCAD Study. For this analysis, only patients with angiographically classified type of SCAD and complete follow-up were eligible. Patients with different types of SCAD during their index event were excluded. Cumulative rate of recurrent MI was the primary endpoint and assessed by Kaplan-Meier curves.

Results: Of 684 eligible patients, SCAD type 2 during index event was the most common diagnosis affecting 478 (69.8%) patients. SCAD type 1 was more common than SCAD type 3 (150 patients (22.0%) versus 56 patients (8.2%), respectively). Within the long-term follow-up of 1800 days, 57 patients (7.9%)

had a recurrent MI of which 22 patients (38.6%) had recurrent SCAD. Assessment of cumulative rate of recurrent MI showed a significant gradient within 1800 days of long-term follow-up over the 3 predefined types of SCAD (p = 0.04, Figure 1). Patients with type 1 SCAD during their index event had the highest rate of recurrent MI when compared to patients with type 2 and type 3 SCAD (12.0% versus 6.7% versus 5.3%, respectively). There was a statistically significant difference when comparing the cumulative rate of recurrent MI in patients with type 1 and type 2 SCAD during 1800 days of follow-up (p = 0.01).

Conclusion: The angiographic type of SCAD had a significant impact on the cumulative rate of recurrent MI during long-term follow-up. Patients with initial type 1 SCAD had the highest event rate when compared to patients with type 2 and 3 SCAD.

Figure 1: Cumulative event rate over 1800 days for the angiographic types of spontaneous coronary dissection

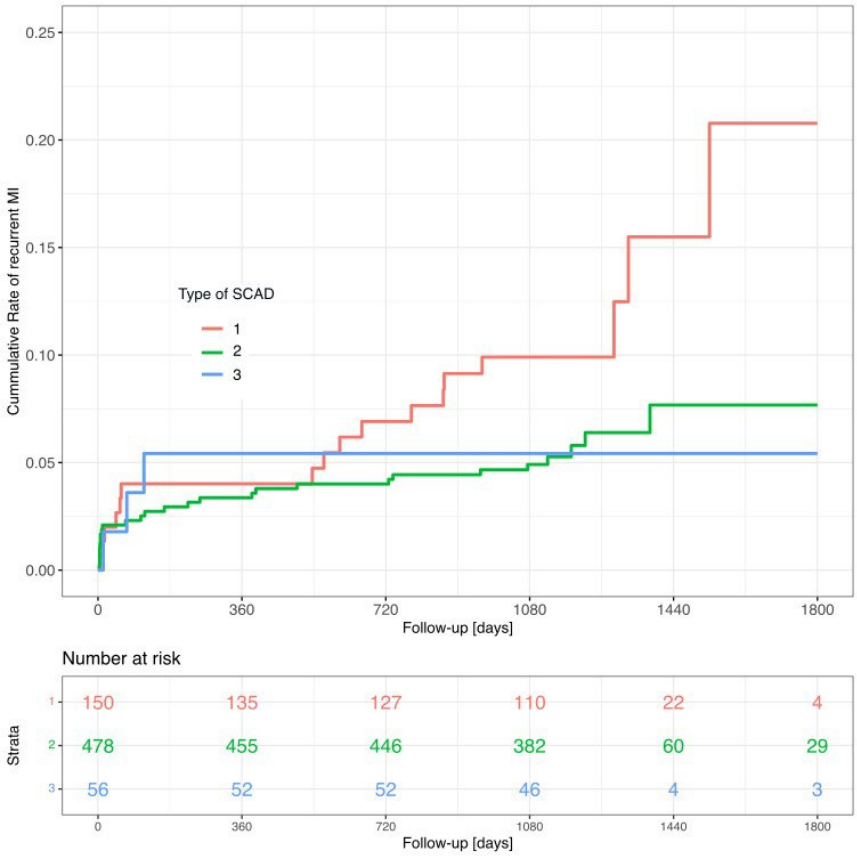

RAPID FIRE ABSTRACT SESSION "RHYTHM DISORDERS 1"

O17

Impact of alternative efficacy endpoint definitions on reported outcomes after ablation of paroxysmal atrial fibrillation – insights from the COMPARE-CRYO study using continuous rhythm monitoring

Salik Ur Rehman Iqbal[1], Thomas Kueffer[1], Sven Knecht[2], Patrick Badertscher[2], Jens Maurhofer[1], Philip Krisai[2], Corinne Jufer[1], Gregor Thalmann[1], Dik Heg[1], Helge Servatius[1], Hildegard Tanner[1], Micheal Kuhne[2], Laurent Roten[1], Christian Sticherling[2], Tobias Reichlin[1]

[1]Inselspital, University of Bern, Bern, Switzerland, [2]University of Basel Hospital, Basel, Switzerland

Introduction: Recurrence after atrial fibrillation (AF) ablation is currently defined as any atrial arrhythmia lasting >30s. While it is generally agreed that this definition has limited value from a disease burden and patient perspective, data on the impact of alternative endpoint definitions for AF ablation is scarce. The purpose of this study was to evaluate the impact of alternative endpoint definitions after AF ablation based on the arrhythmia duration, the number of episodes and AF burden using continuous rhythm monitoring by means of implantable cardiac monitors (ICM).

Material and Methods: This is a prespecified sub study of the COMPARE-CRYO study, which enrolled patients with paroxysmal atrial fibrillation undergoing cryoballoon ablation. All patients underwent ICM implantation and the blanking period duration was 90 days. The time and duration of every atrial arrhythmia episode were evaluated.

Results: For the 201 patients enrolled in the study, a total of 6104 arrhythmia episodes occurring between days 91 and 365 were analysed. The 1-year success rate increased with arrhythmia duration thresholds from 56% (≥30 sec) to 97% (≥24h, p<0.0001, Figure 1A). Similarly, the success rate increased with definitions based on the minimal number of episodes from 56% for a single episode of recurrence to 98% for at least 100 epi-

sodes of AF (p<0.001, Figure 1B). Definitions based on AF burden resulted in 1-year success rates from 56% for an AF-Burden >0% to 93% for an AF-Burden >2% (p<0.001, Figure 1C).

Conclusion: Alternative endpoint definitions based on arrhythmia duration, number of episodes or AF burden have a significant impact on the reported efficacy outcomes after AF ablation. Our findings are important when considering endpoint definitions other than the traditional 30 seconds in the design of future AF ablation trials.

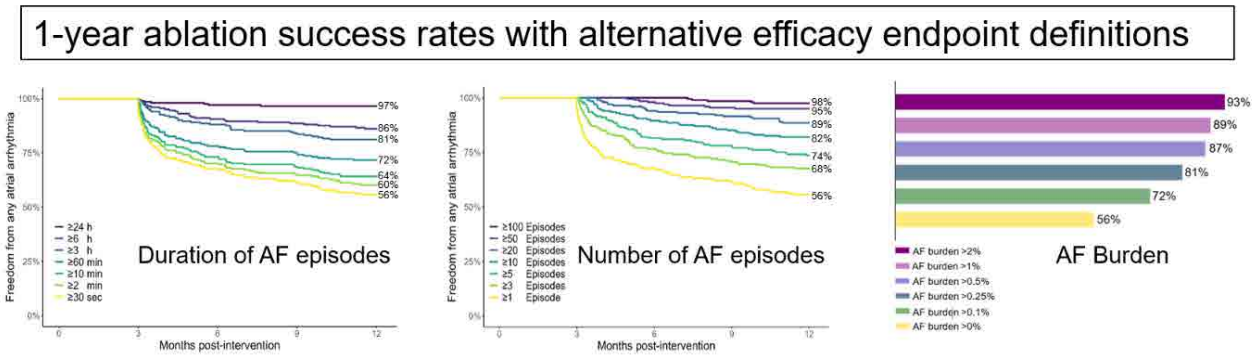

O18

Swiss National Strategy for Out-of-Hospital Cardiac Arrest: Impact on Survival Outcomes

Maria Luce Caputo[1], Roman Burkart[2], André Wilmes[2], Helge Regener[2], Ruggero Cresta[3], Claudio Benvenuti[3], Valentina Guerini Giusteri[1], Tardu Oezkartal[1], Marco Bergonti[1], Catherine Klersy[4], Giulio Conte[1]

[1]Cardiocentro Ticino Institute, Ente Ospedaliero Cantonale, Fondazione Ticino Cuore, Lugano, Switzerland, [2]Interassociation for Rescue Services (IVR-IAS), Bern, Switzerland, [3]Fondazione Ticino Cuore, Lugano, Switzerland, [4]Service of Biostatistics and Clinical Trial Center, Fondazione IRCCS Policlinico San Matteo, Pavia, Italy

Introduction: In 2019, the Swiss Resuscitation Council launched the "National Survival Strategy in the Event of Cardiac Arrest". The document is composed of eight key performance indicators (KPIs), each representing specific objectives intended to enhance patient outcomes following OHCA. Aims of this study were to evaluate the impact of the KPIs achievement on return of spontaneous circulation (ROSC) and 30-day survival with good neurological outcome (Cerebral Performance Category [CPC] 1-2) and, to assess the current state of implementation of the strategy.

Material and Methods: The study included all OHCAs occurred in Switzerland between 2019 and 2023. The Fisher exact test was applied to compare ROSC rates upon arrival at the emergency room and survival rates at discharge with good neurological outcomes across varying levels of KPI achievement. Odds ratios (OR) and 95% confidence intervals (95% CI) were estimated from the models and presented as Forest plots. Additionally, trends in KPI achievement over time were evaluated using trend analysis.

Results: 30,344 OHCAs occurred during the study period, with resuscitation attempted in 17,997 cases (59%). Among the eight KPIs, fast recognition of OHCA (≤3 min), bystander CPR within 3 minutes, ambulance arrival time ≤ 15 minutes, admission to a cardiac arrest center demonstrated the strongest associations with improved ROSC and survival with favourable neurological outcomes. Significant improvements in the achievement of KPIs were observed over the years for nearly all indicators. (Figure 1 illustrates the associations between KPIs and outcomes, while Figure 2 highlights trends in KPI achievement over time.)

Conclusion: The Swiss National Survival Strategy for OHCA demonstrated consistent implementation at the cantonal level, resulting in significant improvements in KPI achievement over the study period. Fast recognition of OHCA, bystander resuscitation, and rapid transfer to cardiac arrest centers had the most significant impact on survival rates and favourable neurological outcomes.

Figure 1. Odds ratios and 95% confidence intervals (CI) for survival following out-of-hospital cardiac arrest (OHCA) based on key performance indicators. The upper panel shows the probability of return of spontaneous circulation (ROSC), while the lower panel displays 30-day survival with a favorable neurological outcome (CPC 1-2). All models are adjusted for year.

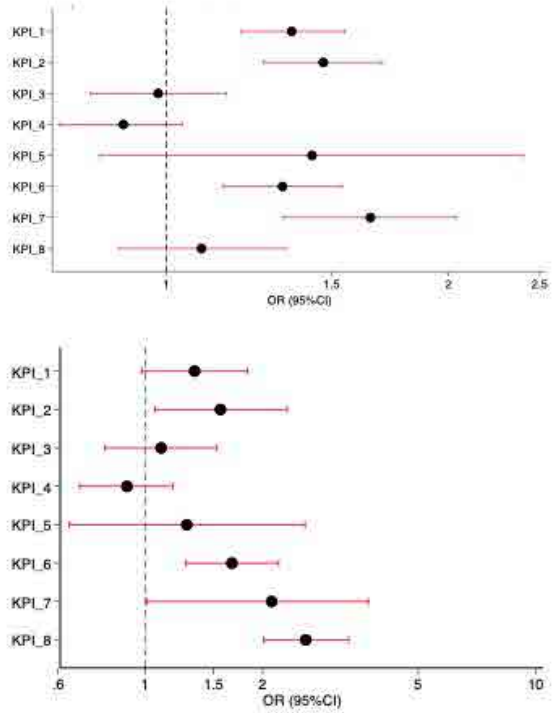

Figure 2. Trends of the Key Performance Indicators (KPIs) from 2019 to 2023. KPIs with statistically significant improvements (Test for trend p value < 0.05) are highlighted in bold lines, while others are represented by dashed lines. KP1: OHCA recognition≤3 min; KPI2: bystander CPR ≤3; KPI3: Telephone CPR≥90% OHCA; KPI4: First responder on site≥90% OHCA ; KPI5: AED use ≥90% OHCA; KPI6: ambulance arrival ≤10 min in ≥50% OHCA: KPI7: ambulance arrival ≤15 min in ≥50% OHCA; KPI8: patient admission TO OHCA specialized Hospital ≥90% OHCA.

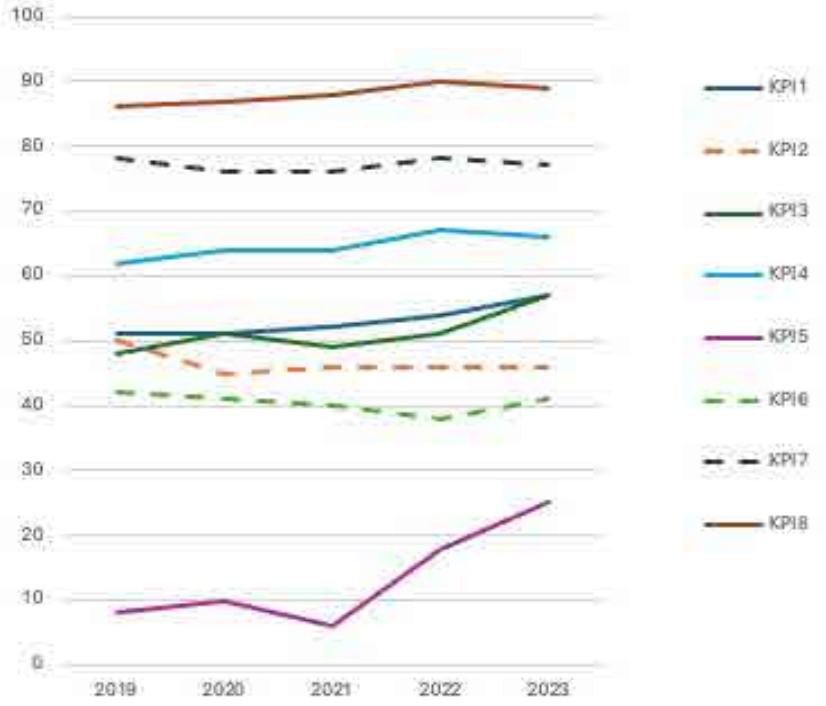

O19

Sex differences in electrophysiological characteristics of left bundle branch area pacing

Jeanne Pouly[1], Melina Krempke[1], David Spreen[1], Kseniya Bulatova[1], Sven Knecht[1], Behnam Subin[1], Nicolas Schärli[1], Beat Schär[1], Patrick Badertscher[1], Felix Mahfoud[1], Michael Kühne[1], Christian Sticherling[1], Philipp Krisai[1]

[1]Department of Cardiology and Cardiovascular Research Institute Basel, University Hospital Basel, University of Basel, Basel, Switzerland

Introduction: Conduction system pacing (CSP) with left bundle branch area pacing (LBBAP) is a novel and promising technique for pacemaker implantation. However, sex differences in the electrophysiological characteristics of LBBAP and its potential impact on CSP criteria have not yet been thoroughly studied.

Material and Methods: We prospectively included 218 consecutive patients, undergoing LBBAP at a tertiary center between 04/2022 and 10/2024, into our CSP-registry. LBBAP capture types included proximal left bundle pacing (LBP), left bundle fascicular pacing (LBFP), and left ventricular septal pacing (LVSP). Intracardiac and surface electrograms were recorded at 100 mm/s. We compared sex differences in pre- and intraprocedural electrophysiological parameters.

Results: Overall, median age was 76 (IQR 68-82) years, and 62 (28%) patients were female. The most frequent indications for pacemaker implantation were high-grade AV block (68%), sick-sinus-syndrome (6.5%) and atrial fibrillation (4.6%). Compared to men, female patients undergoing LBBAP were older (80 vs. 75 years, p = 0.011) and had lower BMI (25.2 vs. 26.7 kg/m2, p = 0.041). There was no sex difference in pacemaker indications, comorbidities, or procedural length. In the preprocedural ECG, women had shorter QRS durations than men (104 vs. 127 ms, p <0.001). After lead placement, the distribution of different LBBAP capture types was similar between sexes. However, women had shorter paced QRS durations (112 vs. 119 ms, p = 0.016) and a shorter V6 R-wave peak time (V6RWPT) (70 vs. 80 ms, p = 0.002), but similar V6-V1 interpeak interval (25 vs. 30 ms, p = 0.7). There were no differences in ventricular sensing (10.3 vs. 10.0 mV, p = 0.4), bipolar threshold (0.85 vs 0.80 V, p = 0.7), and bipolar impedance (767 vs. 741 Ohm, p = 0.4).

Conclusion: In patients undergoing LBBAP, women had shorter paced QRS durations and V6RWPT compared to men. Our findings indicate faster left ventricular activation with LBBAP in women and suggest, that different electrophysiological criteria for CSP may be needed for women.

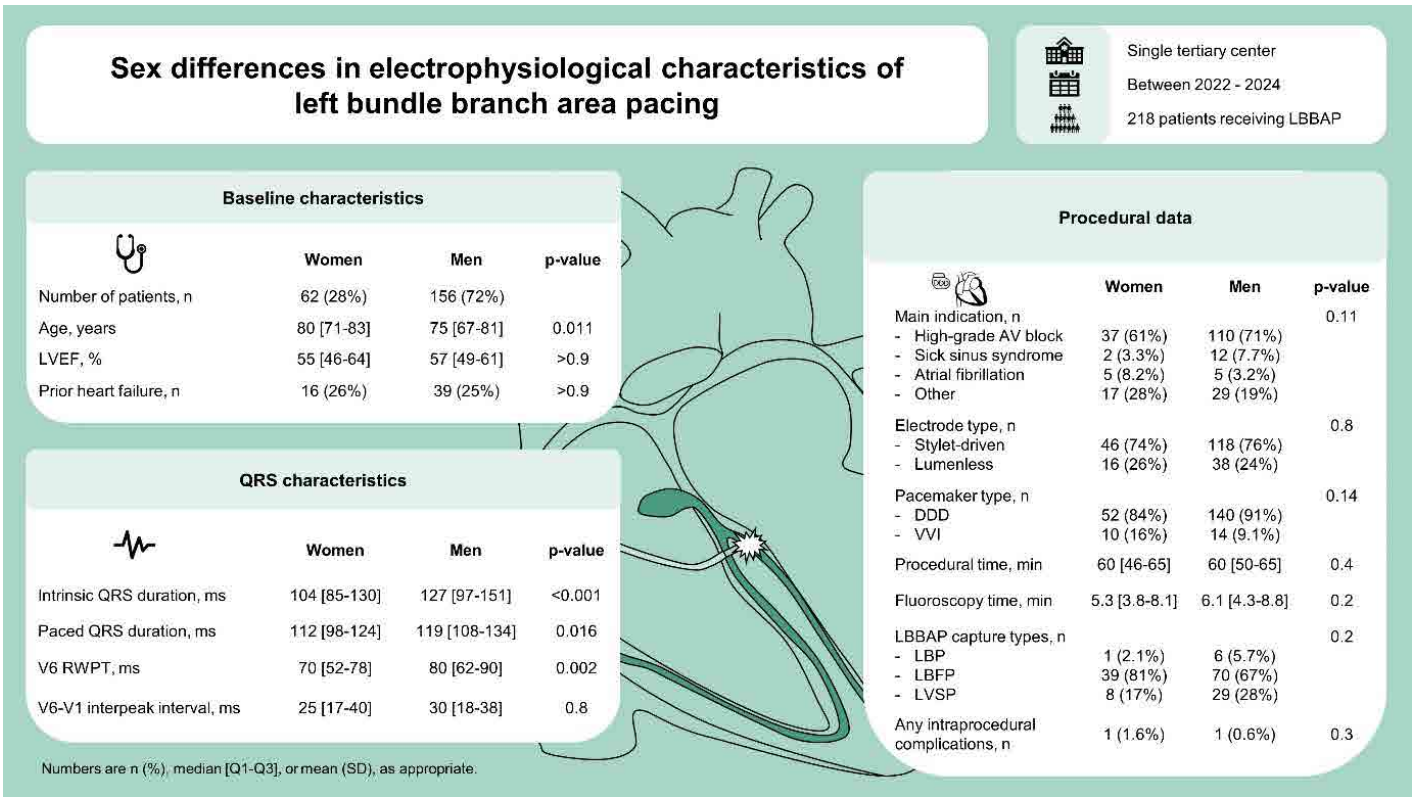

O20

Drug-drug interactions of NOACs with comedication: prevalence and implications for adverse events in patients with atrial fibrillation

Elisa Hennings[1], Stefanie Aeschbacher[1], Pia Neuschwander[2], Michael Coslovsky[2], Ioanna Istampoulouoglou[3], Anne Leuppi-Taegtmeyer[2 4], Philipp Krisai[1], Christine Meyer-Zürn[1], David Conen[5], Christian Sticherling[1], Stefan Osswald[1], Michael Kühne[1]

[1]Cardiology, Cardiovascular Research Institute Basel, University Hospital Basel, University of Basel, Basel, Switzerland, [2]Department of Clinical Research, University Hospital Basel, University of Basel, Basel, Switzerland, [3]Department of Clinical Pharmacology & Toxicology, University Hospital Basel, University of Basel, Basel, Switzerland, [4]Department of Patient Safety, Medical Directorate, University Hospital Basel, Basel, Switzerland, [5]Population Health Research Institute, McMaster University, Hamilton, Canada

Introduction: Non-vitamin K-antagonist oral anticoagulants (NOACs) are a cornerstone in the treatment of patients with atrial fibrillation (AF) to prevent stroke. The clinical relevance of drug-drug interactions associated with NOACs in AF patients remains poorly understood. We examined the prevalence of pharmacokinetic and/or pharmacodynamic drug-drug interactions and their association with adverse clinical outcomes in AF patients receiving NOACs.

Material and Methods: In this analysis, we included patients from the prospective, multicenter Swiss-AF cohort study. The drug-drug interactions of various comedications with NOACs were systematically categorized into 'potentially increased plasma levels of NOAC/higher bleeding risk' and 'potentially reduced plasma levels of NOAC/decreased oral anticoagulation effect'. We employed frailty survival models to investigate the association of the different potential interactions with the respective clinical adverse outcomes (major bleeding, clinically relevant non-major bleeding, any bleeding, ischemic stroke/systemic embolism).

Results: Our analysis comprised 1732 AF patients (mean age 73 ± 8 years, 501 [29%] females) with a median follow-up period of 6 years. For 683 (39%) of these patients, we recorded at least one potential drug-drug interaction (37% with potentially increased bleeding risk, 2% with potentially decreased oral anticoagulation effect). In the multivariable adjusted model, the HR of the respective drug-drug interaction was 1.21 (95% CI 0.84; 1.75, p = 0.31) for major bleeding, 1.22 (95% CI 0.92; 1.62, p = 0.17) for clinically relevant non-major bleeding, 1.22 (95% CI 0.97; 1.54, p = 0.09) for any bleeding, and 1.00 (95% CI 0.22; 4.53, p = 0.99) for ischemic stroke/systemic embolism.

Conclusion: In a large real-world cohort of AF patients, the prevalence of potential interactions of comedication with NOACs was high. We found no strong evidence supporting an association between such drug-drug interactions and an increased risk of major bleeding or ischemic stroke/systemic embolism, but there was a trend toward an increase in the risk of any bleeding.

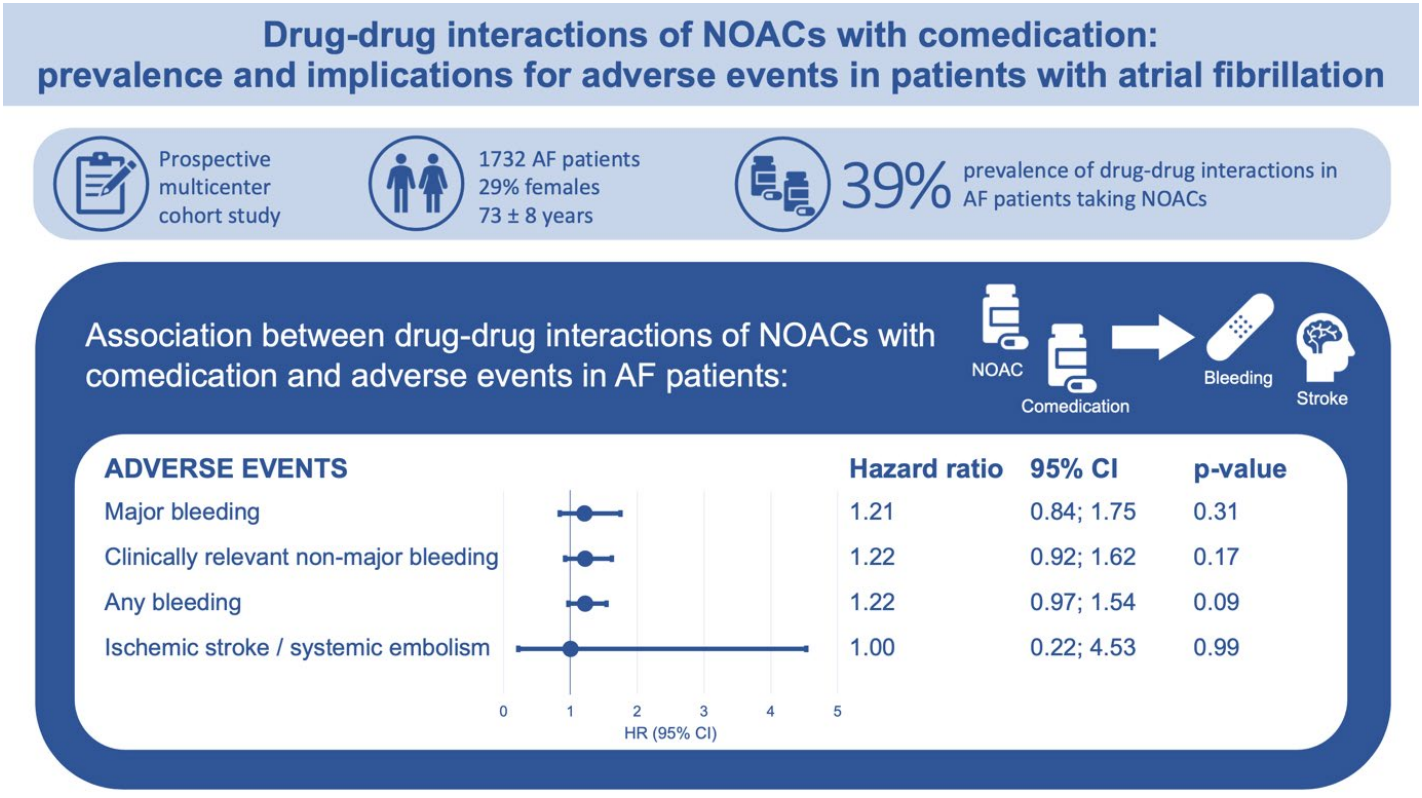

O21

Life-threatening arrhythmia in patients with suspected acute myocarditis

Melina Krempke[1], Jasmin Büchel[1], Kseniya Bulatova[1], Gianmarco Balestra[1], Philip Haaf[1], Jeanne Pouly[1], Mikko Mutti*[1], Paul Drews[1], Christian Mueller[1], Sven Knecht[1], Patrick Badertscher[1], Felix Mahfoud[1], Michael Kühne[1], Christian Sticherling[1], Philipp Krisai[1]

[1]Department of Cardiology and Cardiovascular Research Institute Basel, University Hospital Basel, University of Basel, Basel, Switzerland

Introduction: Patients with acute myocarditis (AM) often undergo prolonged rhythm monitoring due to the risk for life-threatening arrhythmia. We aimed to describe the occurrence, timing and potential early rule-out of life-threatening arrhythmia in patients with AM.

Material and Methods: We included consecutive patients with suspected AM admitted to the ICU/IMC for continuous rhythm monitoring into a cohort study. We assessed the incidence and timing of life-threatening arrhythmia (sustained ventricular tachycardia, ventricular fibrillation, cardiac arrest). To rule-out arrhythmia, we evaluated left ventricular ejection fraction (LVEF), maximal cardiac troponin-T (cTnT) levels and a multivariable model.

Results: Among 304 patients with AM (41±16.6 years, 27% female), 13 life-threatening arrhythmias occurred in 10 (3.3%) patients. Of these, 8 occurred within 24h, 2 between 24-48h and 3 after 72h of hospitalization. Patients with life-threatening arrhythmia had substantially higher mortality rates (40% vs. 0.3%, p<0.001). There was no binary cut-off for LVEF and cTnT to rule-out arrhythmia. The last life-threatening arrhythmia occurred before the cTnT-peak in 3 (42.9%), simultaneously with the peak in 1 (14.3%), and after the peak in 3 (42.9%) patients. The final multivariable model included female sex, cTnT, and LVEF and demonstrated an area under the curve of 0.98 (95% CI 0.96-1), with a sensitivity of 99% and specificity of 75% to rule-out life-threatening arrhythmia

Conclusion: In patients with suspected AM, life-threatening arrhythmias were rare but associated with a 40% mortality rate. A combined model including 3 clinical variables ruled-out lifethreatening arrhythmia with a high sensitivity and may help to guide the indication of rhythm monitoring.

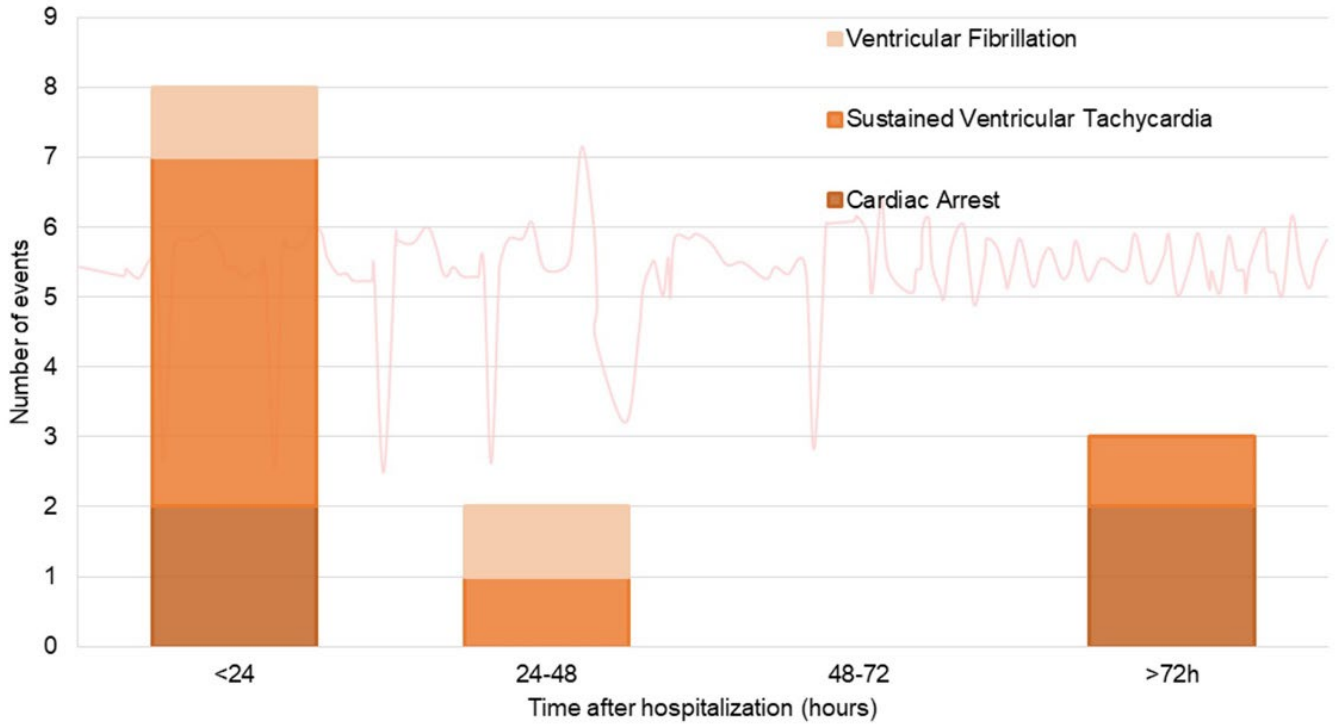

Fig. 1: Temporal occurrence of life-threatening arrhythmia during hospitalization

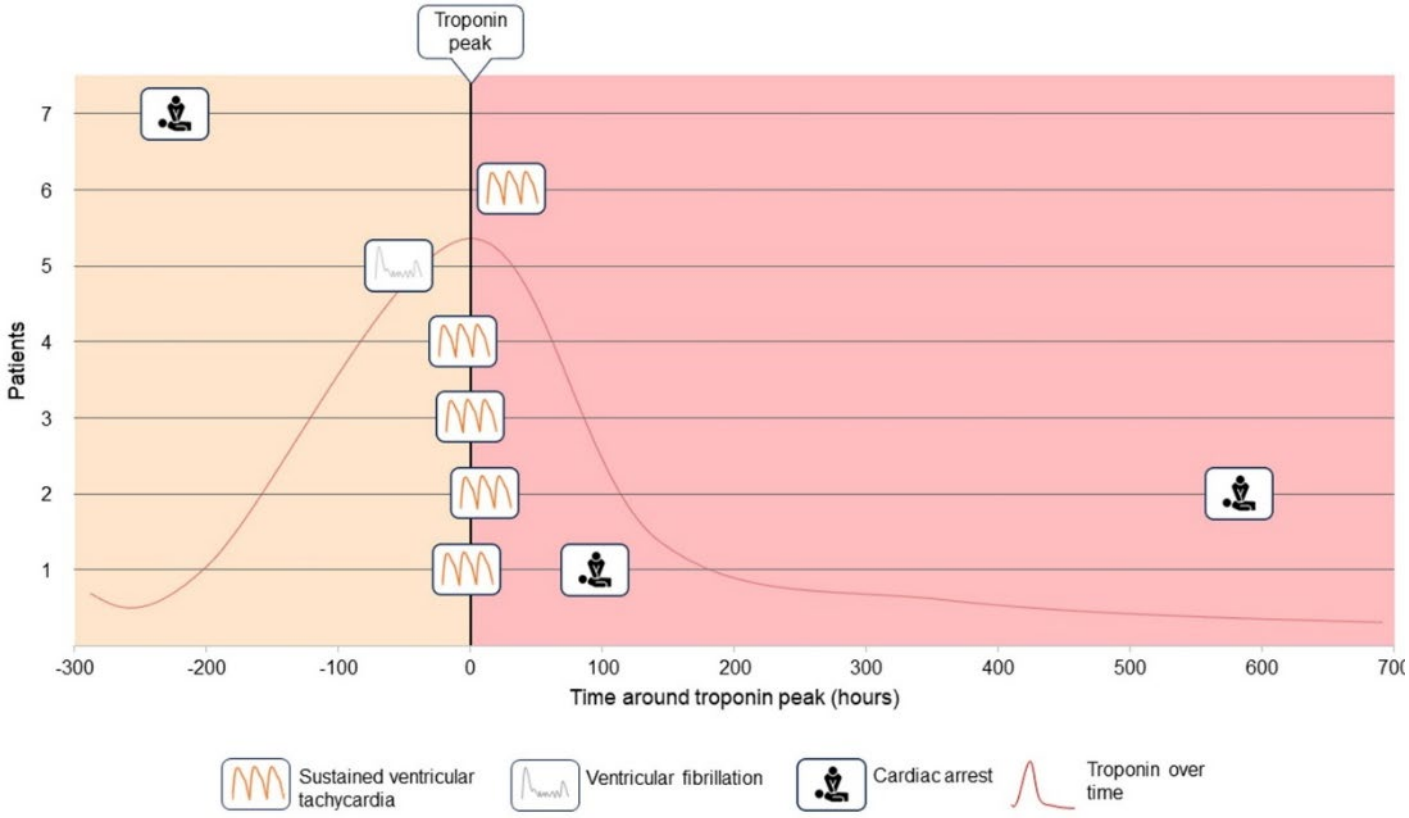

Fig. 2: Relationship between troponin peaks and life-threatening arrhythmia.

O22

Brugada Syndrome and Atrial Fibrillation: predisposing factors and clinical implications

Marco Bergonti[1], Daniele Faccenda[1], Giulio Conte[1]

[1]Cardiocentro Ticino Institute - Ente Ospedaliero Cantonale, Lugano, Switzerland

Introduction: Atrial fibrillation (AF) occurs in up to 20% of patients with Brugada Syndrome (BrS). Yet its predisposing factors and prognostic implications remain uncertain. We aimed to: 1) identify predisposing factors for AF in patients with BrS. 2) evaluate the prognostic impact of AF on ventricular arrhythmias (VAs), stroke, and sick sinus syndrome (SSS).

Material and Methods: This was a multicenter, retrospective study conducted across 24 international centers. Patients with BrS were stratified based on the presence or absence of AF. Patients with previous episodes of ventricular arrhythmias or ICD carriers were excluded. The primary endpoint was the occurrence of VAs, defined as sustained ventricular tachycardia, ventricular fibrillation, or arrhythmic sudden cardiac death. Secondary endpoints included stroke and the development of SSS.

Results: A total of 686 BrS patients were analyzed (39.3 years of age, 33.1% female, 31.8% spontaneous type I ECG, 36.0% P/LP SCN5A variant), including 280 with AF (40.8%). Predisposing factors for AF included proband status, older age, hypertension, and an enlarged left atrium. Over a median follow-up of 48.8 months, the incidence of VA was 0.26%/year, with no significant difference between patients with and without AF (OR 0.67, p = 0.58). AF occurring before age 20 significantly increased the risk of VAs (p <0.001). Sick sinus syndrome was twice as prevalent in patients with AF (10.0% vs. 6.2%), and stroke occurred exclusively in the AF group (2.5%), despite low CHA_2DS_2-VA.

Conclusion: AF in BrS is likely linked to a distinct atrial phenotype, marked by similar risk of ventricular arrhythmias to patients without AF, but significant risk of sick sinus syndrome and stroke. The predisposing factors for AF only marginal overlap with those associated with VAs. Early-onset AF identifies a specific subgroup of BrS patients with elevated VA risk.

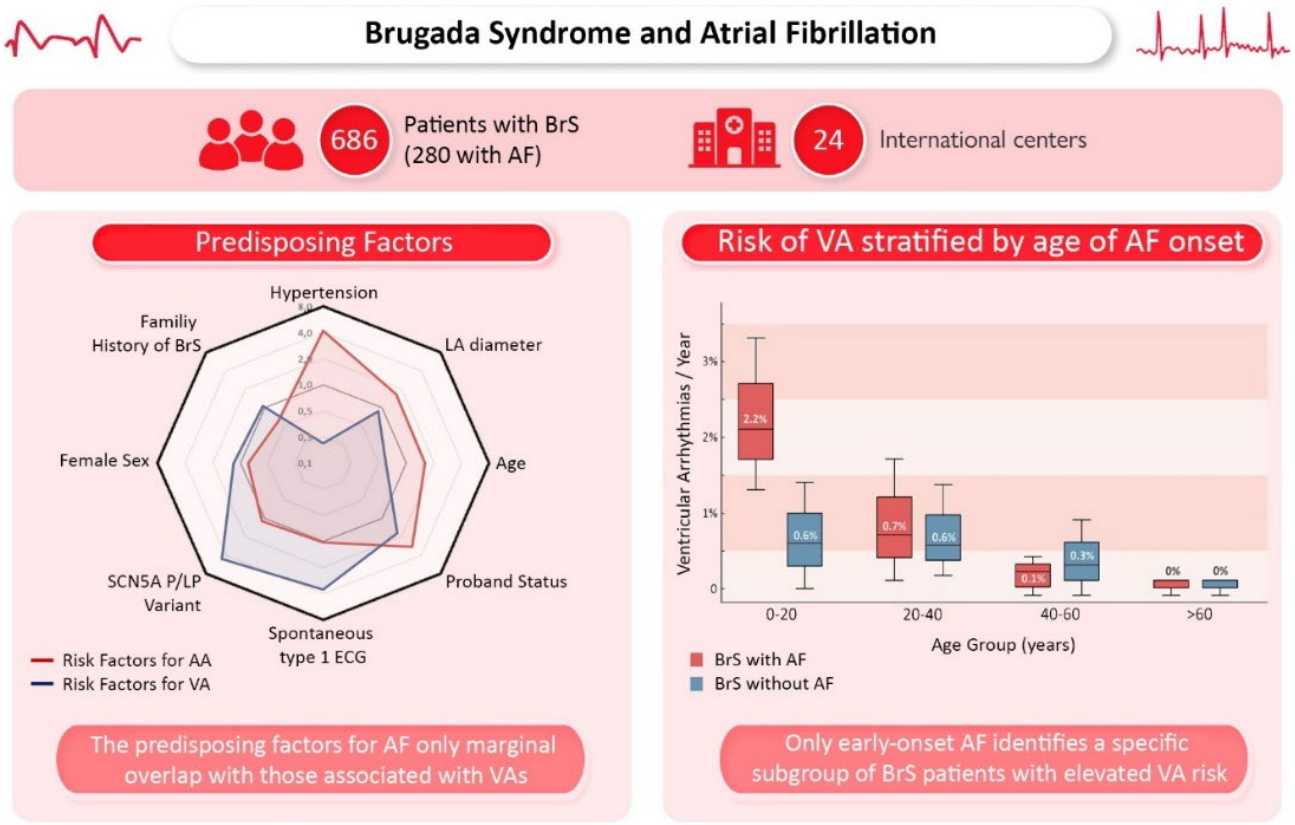

O23

3-Year Outcomes From the Comparison of Amulet and Watchman/FLX Device in Patients Undergoing Left Atrial Appendage Closure: The SWISS-APERO Randomized Clinical Trial

Roberto Galea[1], Federico De Marco[2], Adel Aminian[3], Nicolas Meneveau[4], Konstantina Chalkou[5], Frederic Anselme[6], Christoph Gräni[7], Anna Franzone[8], Pascal Vranckx[9], Urs Fischer[10], Marco Valgimigli[11], Lorenz Räber[7]

[1]Department of Cardiology, Inselspital, University Hospital of Bern, Hospital of Biel, Bern, Switzerland, [2]Department of Cardiology, Monzino Cardiology Center, Milan, Italy, Milan, Italy, [3]Department of Cardiology, Centre Hospitalier Universitaire de Charleroi, Charleroi, Belgium, Charleroi, Belgium, [4]Besancon University Hospital, EA3920, University of Burgundy Franche-Comté, Besancon, France, Besancon, France, [5]Department of Clinical Research, CTU Bern, University of Bern, Bern, Switzerland, Bern, Switzerland, [6]Department of Cardiology, University Hospital of Rouen, Rouen, France, Rouen, France, [7]Department of Cardiology, Bern University Hospital, University of Bern, Bern, Switzerland, Bern, Switzerland, [8]Department of Advanced Biomedical Sciences, University Federico II University, Naples, Italy, Naples, Italy, [9]Department of Cardiology and Critical Care Medicine, Hartcentrum Hasselt, Jessa Ziekenhuis, Hasselt, Belgium, Faculty of Medicine and Life Sciences, Hasselt University, Hasselt, Belgium, Hasselt, Belgium, [10]Department of Neurology, Bern University Hospital, University of Bern, Bern, Switzerland, Bern, Switzerland, [11]Cardiocentro Ticino Institute and Università della Svizzera Italiana (USI), Lugano, Switzerland, Lugano, Switzerland

Introduction: No study has so far compared Amulet with Watchman FLX for clinical outcomes beyond 1 year after percutaneous left atrial appendage closure (LAAC).

Material and Methods: In the investigator-initiated SWISS APERO trial, patients with atrial fibrillation and high bleeding risk undergoing LAAC were randomly assigned (1: 1) to receive Amulet or Watchman/FLX across 8 centers. Pre-specified analyses included the ischemic composite endpoint including cardiovascular death (CVD), stroke, transient ischemic attack (TIA) or systemic embolism (SE) at 3 years. Additional endpoints were major bleedings, device related thrombus (DRT), and peridevice leak (PDL). Analyses were repeated in the as-treated (AT) populations.

Results: Of the 221 randomized patients, 220 completed LAAC and 3 patients randomized to Amulet received Watchman FLX. Follow-up rate at three years was 96.4% in the Amulet and 97.3% in the Watchman group. The majority of patients were on single antiplatelet therapy (Amulet 59% vs. Watchman 49%, p = 0.26). The composite of CVD, stroke, TIA or SE occurred numerically less frequently in the Amulet as compared to Watchman group (18.2%vs. 31.0%; HR: 0.58; 95%CI: 0.33-1.03; p = 0.06). Major bleedings (16.5%vs.18.0%; HR: 1.03; 95%CI: 0.53-1.97; p = 0.94), DRT (3.6%vs.6.4%; RR: 0.57: 95%CI: 0.17-1.88; p = 0.35) and PDL (35.1%vs.42.7%; RR: 0.82; 95%CI: 0.59-1.15; p = 0.25) did not differ between groups. In the AT population, the composite of CVD, stroke, TIA or SE was significantly lower in the Amulet as compared to Watchman group (17.0%vs.31.1%; HR: 0.53; 95%CI: 0.30-0.96 ; p = 0.04). Major bleedings (16.2% vs.17.5%; HR: 1.03; 95%CI: 0.53-2.00; p = 0.93), DRT (2.8%vs.7.1%; RR: 0.40; 95%CI: 0.11-1.45; p = 0.15) and PDL (34.6%vs.43.4%; RR: 0.80; 95%CI: 0.57-1.11; p = 0.18) did not differ between groups.

Conclusion: At three years after LAAC, the primary analysis indicates a trend towards a lower ischemic risk in patients treated with Amulet as compared to Watchman FLX. This finding is corroborated by significantly lower occurrence of the ischemic composite endpoint in the AT analysis. Longer follow-up and more comparative studies are needed to confirm potential differences in ischemic outcomes between devices.

RAPID FIRE ABSTRACT SESSION "CLINICAL CASES 1"

O24

First in-man radiofrequency ablation of the cavo-tricuspid isthmus in an interventional MRI in Switzerland

Etienne Pruvot[1], Jorge Solana Muñoz[1], Hélène Leupi[1], Adrian Luca[1], Ambra Masi[1], Marta Cepeda[1], Kate Lindborg[2], Vjeran Karloci[2], Jennifer Sommerville[2], David Seraiva[1], Isabel Goetz[2], Carlo Marcucci[1], Lucie Vaudroz[1], Cheryl Teres-Castillo[1], Jürg Schwitter[1]

[1]Lausanne university hospital, CHUV, Lausanne, Switzerland, [2]IMRICOR, Burnsville, United States

Introduction: MRI is the gold standard to characterize cardiac function and scars. Atrial flutter has a class I indication for ablation. Recurrences, however, occur in <50% due to difficult anatomies and cavo-tricuspid isthmus (CTI) contractile motion. Herein, we report for the first time in Switzerland the ablation of the CTI in a patient with atrial flutter in an interventional MRI (iMRI) environment.

Material and Methods: A 80 yo male patient was hospitalized because of rapid heart rate (HR) and dyspnea. The ECG (panel A of the figure) revealed a typical atrial flutter, for which an electrical cardioversion was performed after unsuccessful control of the HR despite antiarrhythmic drugs. A month later, the patient underwent an ablation of the CTI in general anesthesia in the iMRI. Panel B shows the dedicated room with the operator, the nurse and the patient within the bore.

Results: Ablation was performed using the active tracking RF catheter (Vision-MR Ablation Catheter 2.0, Imricor, USA) and a 3D-MRI NORTHSTAR mapping system, with delivery of RF lesions along the CTI at 40-50 Watt (Panel C). Cumulated ablation time to achieve bidirectional CTI conduction block was 16 min, for an overall skin to skin procedure duration of 58 min. Following obtention of bidirectional block, T2 mapping revealed a continuous linear lesion along the CTI without gaps (arrows, panel D). ECG and EGM signals were hardly analyzable during active RF catheter tracking because of electromagnetic interferences but were readable in-between.

Conclusion: We report herein the first successful ablation of the CTI in an interventional MRI in Switzerland. The added value of this approach relies in its ability to visualize the contractile pattern of the target and to characterize the 3D distribution and continuity of RF lesions to ensure durable success. Further development is underway to improve ECG and EGM visualization during active catheter tracking.

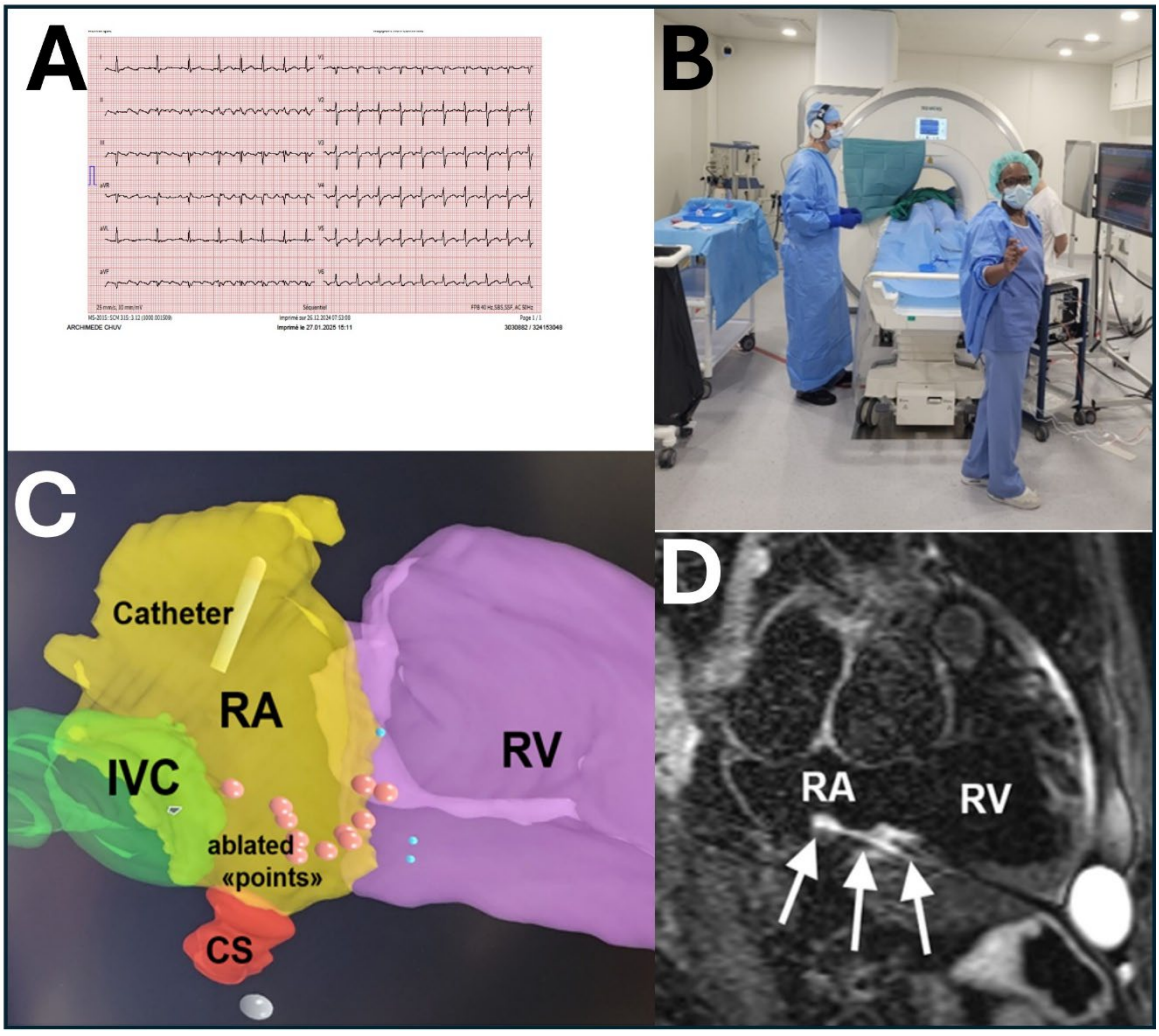

O25

Bridging cardiogenic shock secondary to severe tachycardia-induced cardiomyopathy with left ventricular unloading – A case report

Manuel Gschwend[1], Matthias Bossard[1], Florim Cuculi[1], Amir Jadidi[1]

[1]Luzerner Kantonsspital, Luzern, Switzerland

Introduction: Tachycardia-induced cardiomyopathy (TIC) is a rare but often underestimated, reversible condition caused by sustained arrhythmias with rapid ventricular response. TIC is a known cause of heart failure but can also lead to cardiogenic shock (CS) if undetected. This case highlights the presentation and management of TIC with profound CS (SCAI E).

Material and Methods: A 60-year-old male with hypertension first presented in July 2024 with asymptomatic tachycardia. Adenosine revealed tachycardic atrial flutter with 2: 1 conduction (ventricular rate 165/min). TEE showed mildly reduced EF. Successful cardioversion and RF ablation of the cavotricuspid isthmus were performed in August. During follow-up, the patient reported exertional dyspnea and exercise intolerance. The ECG now showed tachycardic atrial fibrillation at 150/min. Amiodarone was started but discontinued due to gastrointestinal side effects, and he refused another cardioversion. In September, the patient re-presented with worsening symptoms: severe reduction in performance, tachycardia, dyspnea, cold sweats, and dizziness. BNP was 15,000 ng/l, ECG showed tachycardic atrial fibrillation at 150/min, and signs of impending cardiogenic shock were present. Early shock management included inotropic support with norepinephrine and rate control with intravenous amiodarone. Multiple electrical cardioversions (ECV) were attempted. Due to persistent organ hypoperfusion, an Impella™ CP was inserted, upgraded to Impella™ 5.5 two days later, and led to hemodynamic stabilization.

Results: After successful ECV under amiodarone, pulmonary vein isolation was performed. The Impella™ 5.5 was removed after 10 days. The patient was discharged after 24 days. Following cardiac rehabilitation on optimal medical therapy, his LVEF was 45%. At 4-month follow-up, the patient had recovered normal heart function and regained daily activities.

Conclusion: This case shows that TIC can lead to profound CS if not recognized and managed timely. It highlights the utility of temporary mechanical circulatory support (MCS) devices in providing ventricular unloading. In TIC, MCS can facilitate hemodynamic stabilization and myocardial recovery.

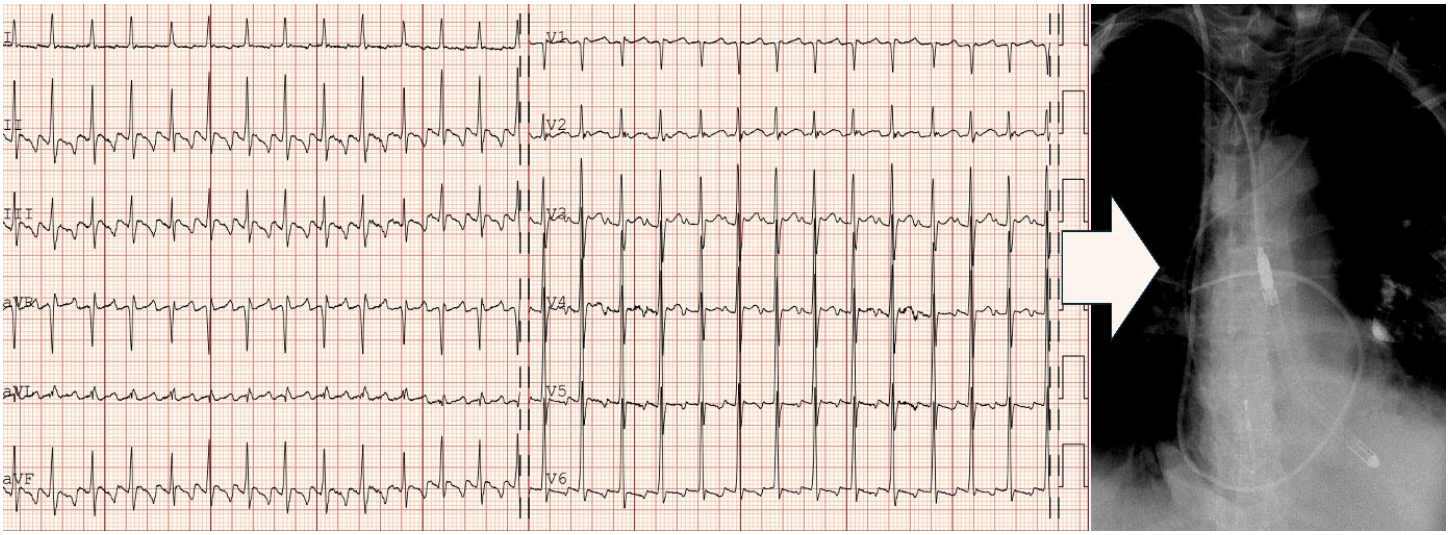

O26

Early fracture of a stylet-driven lead for left bundle branch area pacing

Reto Stump[1], Florian Franzeck[1], Sebastian Seidl[1], Roman Brenner[1], Peter Ammann[1]

[1]Klinik für Kardiologie, Kantonsspital St.Gallen, St. Gallen, Switzerland

Introduction: Left bundle branch area pacing (LBBAP) has quickly made its way into the daily business of the cardiac pacing community due to the opportunity of delivering physiological pacing without the need to implant an additional left ventricular lead. Compared to the earlier developed His-bundle pacing, it provides an easier implantation technique and simpler follow-up. As most of the stylet-driven (SDL) and lumen-less (LLL) pacing leads used for LBBAP have originally been engineered for other conventional pacing sites, there is concern regarding lead integrity performance. We present a case of a distal SDL fracture in LBBAP in a patient with complete atrioventricular block.

Results: A 56-year-old woman with syncope due to an intermittent complete atrioventricular block was implanted with a dual chamber pacemaker with an atrial lead positioned in the right atrial appendage and an SDL (Biotronik Solia) in the left bundle branch area position. Fourteen months post-implantation, the patient was referred again due to recurrent syncopes. Device interrogation revealed a uni- and bipolar impedance of >2500 Ω of the ventricular lead with a pacing threshold of 7.5 V/0.4 ms, suggestive of a lead fracture. The X-ray confirmed the suspected diagnosis, showing a fracture between the tip and the ring electrode (Figure 1). Consequently, a new lead was implanted in a right ventricular apical position.

Conclusion: Reviewing the literature, the incidence of early conductor failure in SDL used for LBBAP seems to be higher than placing those electrodes in the conventional right apical position. Compared to LLL used for LBBAP, SDL also seem to exhibit higher rates of fractures. Due to most SDL implantations up to now being performed using the Biotronik Solia lead, it remains unclear whether all SDL are prone to a higher incidence of fractures in LBBAP or if this is design-related.

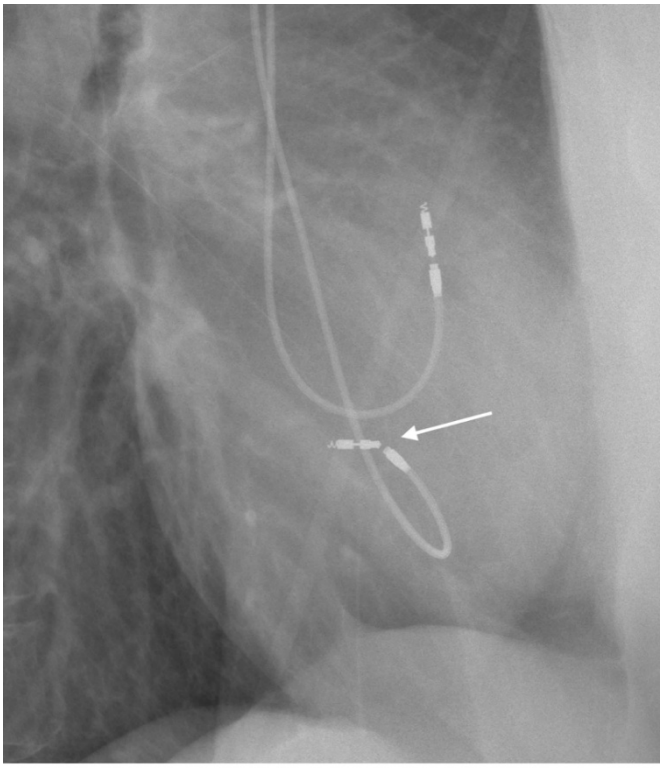

Figure 1: Lateral thoracic X-ray showing the fracture between tip and ring electrode (arrow)

O27

Late response to cardioneuroablation in a young patient with asymptomatic suprahisian atrioventricular block: a case report

Samaksha Pant[1], Nicolas Dayal[1], Patrizio Pascale[2], Aki Mizuno[1], Chan-Il Park[1]

[1]Hôpital de La Tour, Genève, Switzerland, [2]Centre Hospitalier Universitaire Vaudois, Lausanne, Switzerland

Introduction: Functional atrioventricular block (AVB) is a rare condition, which is typically managed by observation and pacemaker implantation in case of symptomatic bradycardia. Cardioneuroablation (CNA), initially developed for vagally mediated syncope, reduces excessive parasympathetic tone by ablating ganglionated plexi (GP). This interesting case shows a 32-year-old male diagnosed at the age of seven with second-degree Mobitz I AVB and paroxysmal complete asymptomatic AVB with junctional escape. Its echocardiography was normal. His peak exertional heart rate was 114 bpm (60% of predicted) with Mobitz I AVB. Despite his chronotropic incompetence, he experienced dyspnoea only during high levels of exertion.

Material and Methods: An electrophysiologic study revealed a suprahisian AVB (Wenckebach point at 109 bpm), which was corrected under isoproterenol. A cardiac CT was performed and fat pad segmentation with GP anatomy was noted using the InHeart software. CNA was performed after merging an electroanatomic CARTO map of both atria with cardiac-CT. Irrigated radiofrequency was applied at 35W in both atria using a QDot catheter.

Results: Immediate conduction improvement was very modest, with the increase of sinus rate from 45 to 53/' and shortening of PR interval from 450 ms to 420 ms and the patient remain in second-degree AVB. However, we observed at two months after the procedure, a significant clinical and electrocardiographic improvement during follow-up, with the PR interval further improving to 340–360 ms and complete AVB resolving. The patient achieved sinus-driven rates up to 140 bpm during exertion and reported a wonderful enhancement in exercise capacity, experiencing no more cardiopulmonary limitations during high-intensity activities.

Conclusion: This case confirms that CNA may be an effective treatment for improving AV conduction in patients with suprahisian AVB. It highlights the importance of advanced mapping systems like InHeart in optimizing GP localization and emphasizes the potential for delayed clinical improvement following the procedure.

Figure 1: ECG before cardioneuroablation and 3 months after the procedure of cardioneuroablation

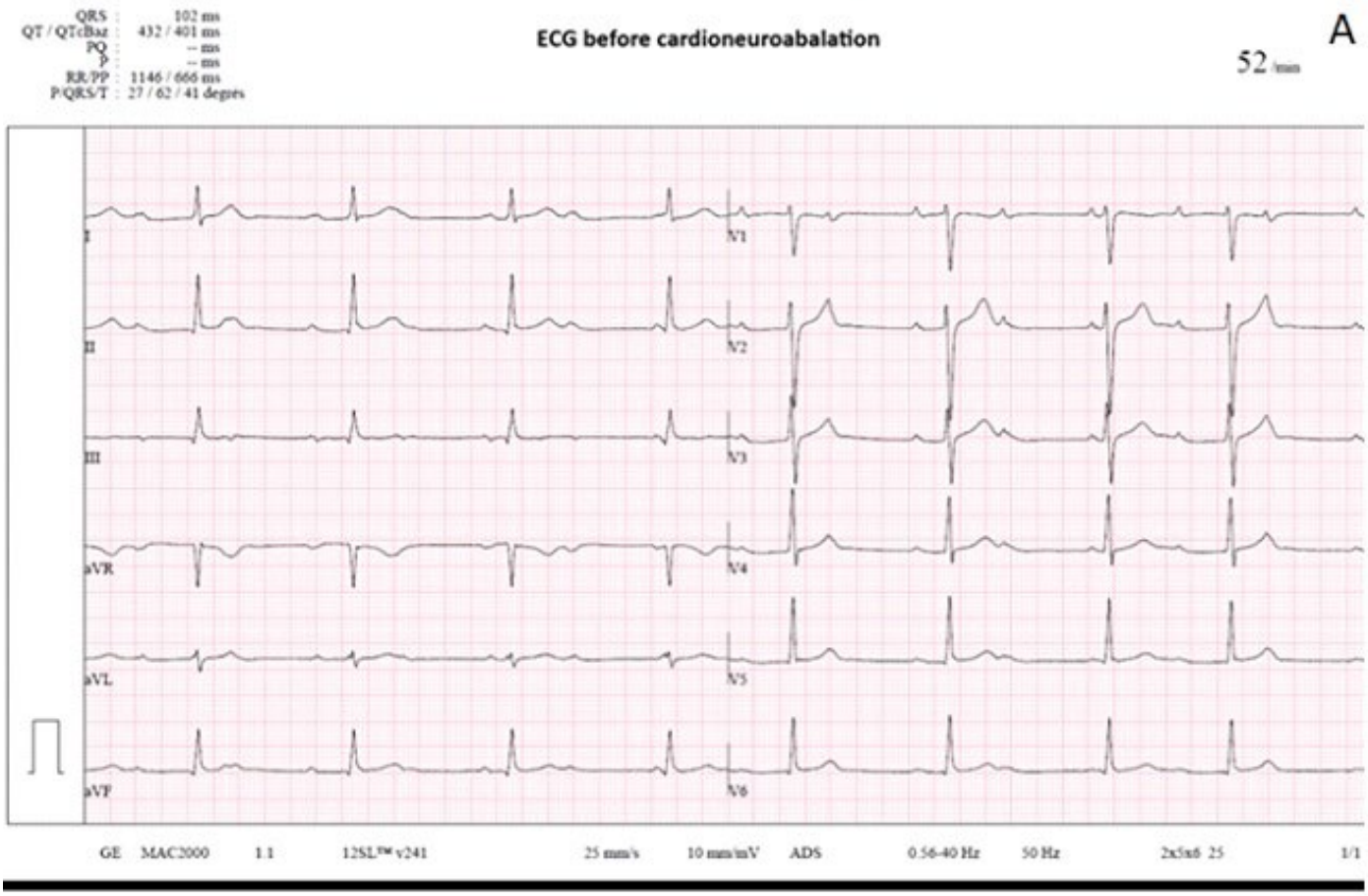

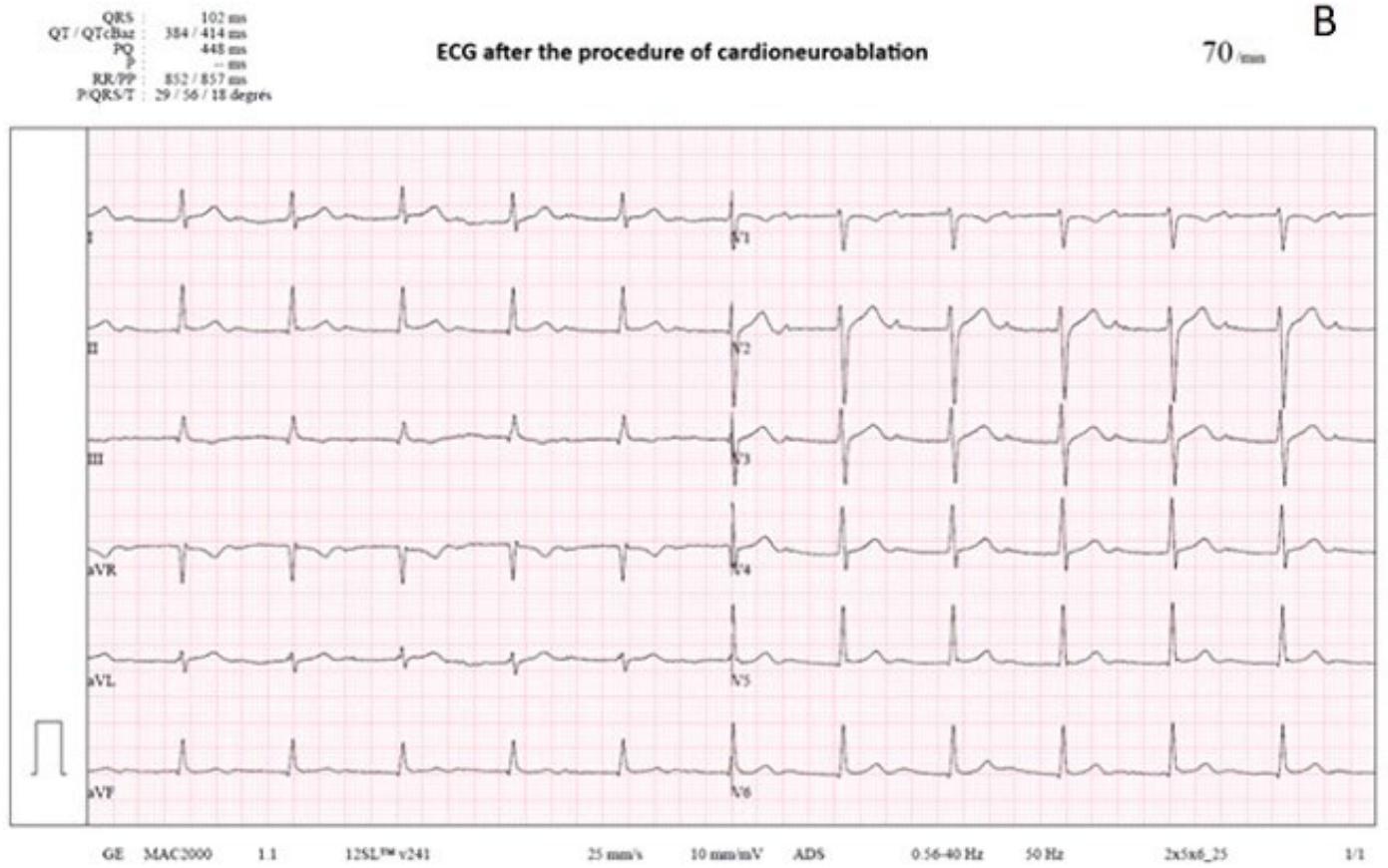

Figure 2: Integration of a cardiac CT scan with fat pad segmentation and GP anatomy, processed using InHeart software, combined with an electroanatomic CARTO map of the right atrium (A and B) and left atrium (C and D). The green line shows the right phrenic nerve, and the green dots indicate points of stimulation of this nerve by electrophysiology. The yellow dots represent the His bundle. The blue structures represent the venous coronary system. The red dots mark the ablation sites targeted by radiofrequency. The purple structures represent fat pads. CS= coronary sinus; OS = ostium; SVC = superior vena cava; lat = lateral; LSPV = left superior pulmonary vein; LA = left atrium; RSPV = right superior pulmonary vein.

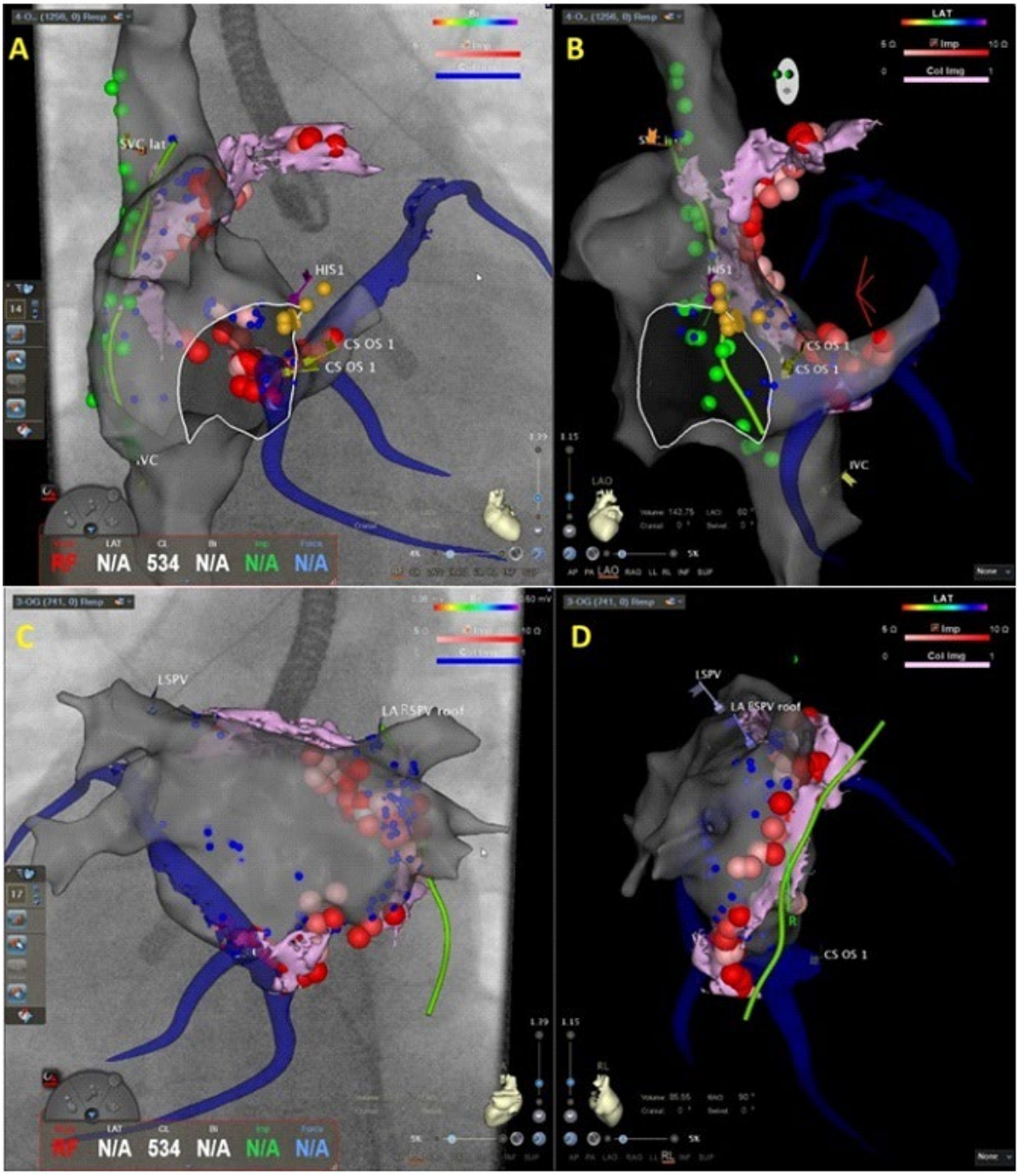

O28

First pediatric implantation of an extravascular implantable cardioverter-defibrillator (EV-ICD) in Switzerland

Florian Berger[1], Alexander Breitenstein[2], Christian Balmer[1], Matthias Gass[1], Martin Schweiger[1]

[1]University Children´s Hospital Zurich, Zurich, Switzerland, [2]University Hospital Zurich, Zurich, Switzerland

Introduction: Currently there are no implantable cardioverter-defibrillator (ICD) systems specifically designed for children and adolescents. We report on the implantation of the novel substernal extravascular ICD (Aurora EV-ICD, Medtronic) as an off label use in children. This is the first implantation of an EV-ICD in a child in Switzerland.

Material and Methods: The 11-year-old female patient (weight 35 kg, height 145 cm) had a history of dilated cardiomyopathy of unknown origin and experienced sudden cardiac arrest due to ventricular fibrillation, successfully resuscitated including external defibrillation. The patients intrinsic rhythm was adequate and pacemaker therapy was not indicated. The EV-ICD system was chosen for secondary prevention. This system consists of a combined sense/pace/shock electrode, implanted substernally via a subxyphoidal incision and advanced along the posterior sternal surface after blunt preparation with a specific tool under fluoroscopy guidance. The lead's proximal end was tunneled subcutaneously to the device, placed in a left thoracic subcutaneous pocket.

Results: The EV-ICD was successfully implanted under general anesthesia in a hybrid operating room (OR) suite. There were no procedural complications. Peri-procedural implant measurements showed optimal results for RV sensing (4.2 mV), capture threshold (1.5 V/2.0 ms) and defibrillation threshold (30 J). Procedure duration was 78 minutes with a fluoroscopy time of 2 minutes. The patient was extubated in the OR and transferred to intermediate care for monitoring. Chest x-ray confirmed correct lead and device positioning. RV sensing and lead impedance remained stable.

Conclusion: Although developed for adults, the EV-ICD was implanted safely and effectively in this pediatric patient. The extravascular system, comprising a compact device with long battery life, capable of defibrillation and antitachycardia pacing, and a substernal lead implanted via a minimally invasive technique, offers crucial advantages over previously available ICD systems. This case highlights the potential of EV-ICD systems to address unique pediatric and adolescent needs.

RAPID FIRE ABSTRACT SESSION "CABG & IMAGING OF CAD"

O29

Early CABG with Intraoperative Hemoadsorption in Patients on Ticagrelor

Omer Dzemali[1 2], Robert Storey[3], Steven Hunter[4], Kambiz Hassan[5], Anna Meyer[6], Thomas Eberle[7], Nikolaas Deneve[8], Matthias Thielmann[9], Marijana Matejic-Spasic[10], Daniel Wendt[10], Efythymios Deliargyris[11], Michael Schmoeckel[12]

[1]Department of Cardiac Surgery, University Hospital Zürich, Zurich, Switzerland, [2]Department of Cardiac Surgery, City Hospital Triemli, Zurich, Zurich, Switzerland, [3]Division of Clinical Medicine, Immunity and Cardiovascular Disease, Sheffield, United Kingdom, [4]Department of Cardiac Surgery, University of Sheffield, Sheffield, United Kingdom, [5]Department of Cardiac Surgery, Asklepios Hospital Hamburg, Hamburg, Germany, [6]Department of Cardiac Surgery, University of Heidelberg, Heidelberg, Germany, [7]Department of Anesthesia and Intensive Care Medicine, MediClin Heart Center Coswig, Coswig, Coswig, Germany, [8]Department of Intensive Care Medicine, OLV Hospital, Aalst, Belgium; Department of Anesthesiology, OLV Hospital, Aalst, Aalst, Belgium, [9]Westgerman Heart & Vascular Center, University Hospital Essen, Essen, Germany, [10]CytoSorbents Europe GmbH, Berlin, Germany, [11]CytoSorbents Inc., Princeton, United States, [12]Dept. of Cardiac Surgery, LMU Munich, Munich, Germany

Introduction: Severe perioperative bleeding occurs in over 30% of patients on ticagrelor undergoing isolated coronary artery bypass grafting (i-CABG) before completing the recommended 3-day washout. Intraoperative ticagrelor removal with a polymer bead hemoadsorption device is an approved therapy that may reduce perioperative bleeding

Material and Methods: The current analysis from the international Safe and Timely Antithrombotic Removal (STAR) registry reports outcomes with intraoperative hemoadsorption in patients on ticagrelor undergoing i-CABG before completing the recommended washout. Bleeding was assessed by the Universal Definition of Perioperative Bleeding (UDPB) definition.

Results: 102 patients (63.8±10.1 years, 81.2% male) underwent i-CABG at mean time from last dose (TLD) of 22.8±14.6h. Groups were created based on TLD to CABG: Group-1 (G1): <24h (n = 61; TLD 12.6±6.5h); Group-2 (G2): 24-72h (n = 41; 37.2±10.1h). G1 was higher risk than G2 based on EuroSCORE-II (median: 4.2% vs. 1.7%, p = 0.006) and emergency indication (66.1% vs. 12.2%, p<0.001). Operation and cardiopulmonary bypass durations were similar (G1: 4.3±1.5h and 94.9±37.1min vs. G2: 4.4±1h and 94.7±36.1min, p = ns). Severe bleeding (UDPB 3) and re-operations for bleeding were more frequent in G1 vs. G2 (14.8% vs. 2.4%, p = 0.047; and 8.2% vs. 0%, p = 0.08, respectively). One severe bleeding event was caused by a bleeding LIMA side branch. Any transfusion of red blood cells or platelets was also more frequent in G1 vs. G2 (45.9% vs. 26.8%, p = 0.05 and 59.0% vs. 34.1%, p = 0.014, respectively). There were 5 deaths overall (4 emergencies and one urgent ST-elevation myocardial infarction), all of them in G1 (overall 30-day mortality: 4.9%; mortality G1 vs. G2 p = 0.08). All deaths were cardiac-related and associated with low output states and multi-organ failure. There were no bleeding-related deaths.

Conclusion: Intraoperative ticagrelor removal may help reduce ticagrelor-related bleeding in patients undergoing i-CABG before completing the 3-day washout. High risk emergency procedures within the first 24 hours of last ticagrelor dose have an increased bleeding risk.

O30

Disparities in STEMI diagnosis and management among patients with mental health conditions

Dorian Garin[1], Wesley Bennar[1], Mario Togni[1], Pascal Meier[1], Peter Wenaweser[1], Puricel Serban[1], Diego Arroyo[1], Stéphane Cook[1], Sonja Lehmann[1]

[1]*University and Hospital Fribourg, Fribourg, Switzerland*

Introduction: Patients with mental health conditions often experience delayed diagnosis and treatment. This study evaluated whether such patients face longer delays and worse outcomes despite a dedicated STEMI fast-track protocol.

Material and Methods: We analyzed data from the prospective EVALFAST registry, which includes patients with suspected STEMI admitted directly to the catheterization lab at Fribourg Hospital since 2008. Patients were categorized into a mental health cohort if their electronic health record documented a mental health condition (mainly anxiety or depression) at diagnosis. The primary endpoint was time from first medical contact (FMC) to diagnosis, with secondary endpoints including FMC-to-balloon, door-to-balloon times, and peak CK-MB levels. Generalized linear models adjusted for confounders were built. Cox regression were used to assess 30-day and 5-year major adverse cardiac events (MACE).

Results: Among 1,330 patients in the EVALFAST registry, 122 (9.2%) were excluded because they presented in cardiac arrest. Of the remaining 1,208 patients, 147 (12.1%) had a documented mental health condition in their EHR at the time of diagnosis. Baseline characteristics were similar between groups, except for a higher proportion of women and a higher prevalence of hypertension in the mental health cohort. After adjustment these patients had longer FMC-to-diagnosis times (+16.43 minutes; p = 0.009) and FMC-to-balloon times (+18.63 minutes; p = 0.008) (Figure 1), particularly when self-presenting to the ER (+32.67 minutes; p = 0.041). They also had higher peak CK-MB levels (+71.3 U/L; p = 0.009). Despite greater participation in cardiac rehabilitation (43.5% vs. 30.5%; p = 0.002), they faced increased risks of 30-day (HR 1.77; p = 0.041) and 5-year MACE (HR 1.41; p = 0.036), driven by cardiovascular death (HR 2.06; p = 0.010) (Figure 2).

Conclusion: Mental health comorbidities in STEMI patients are linked to delays in treatment, elevated cardiac enzyme levels, and worse long-term outcomes, including cardiovascular death. Targeted interventions are needed to improve care for this high-risk group.

Figure 1

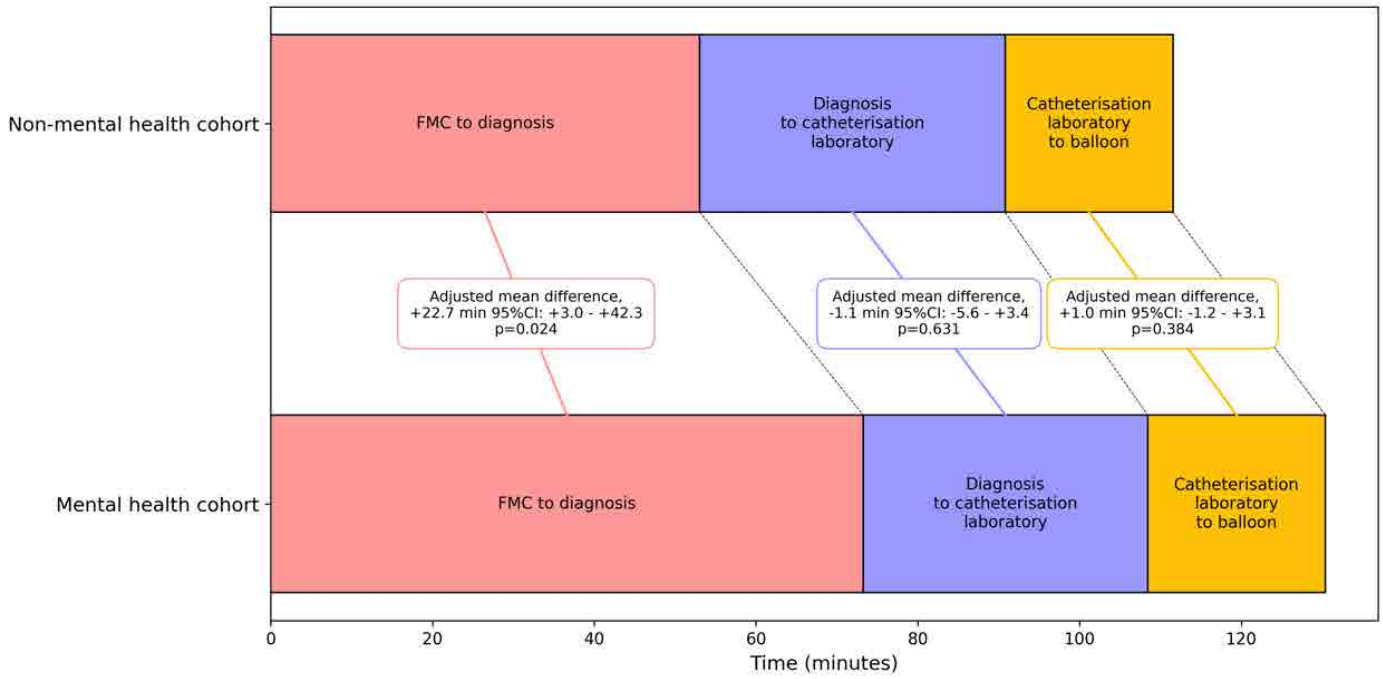

Figure 2

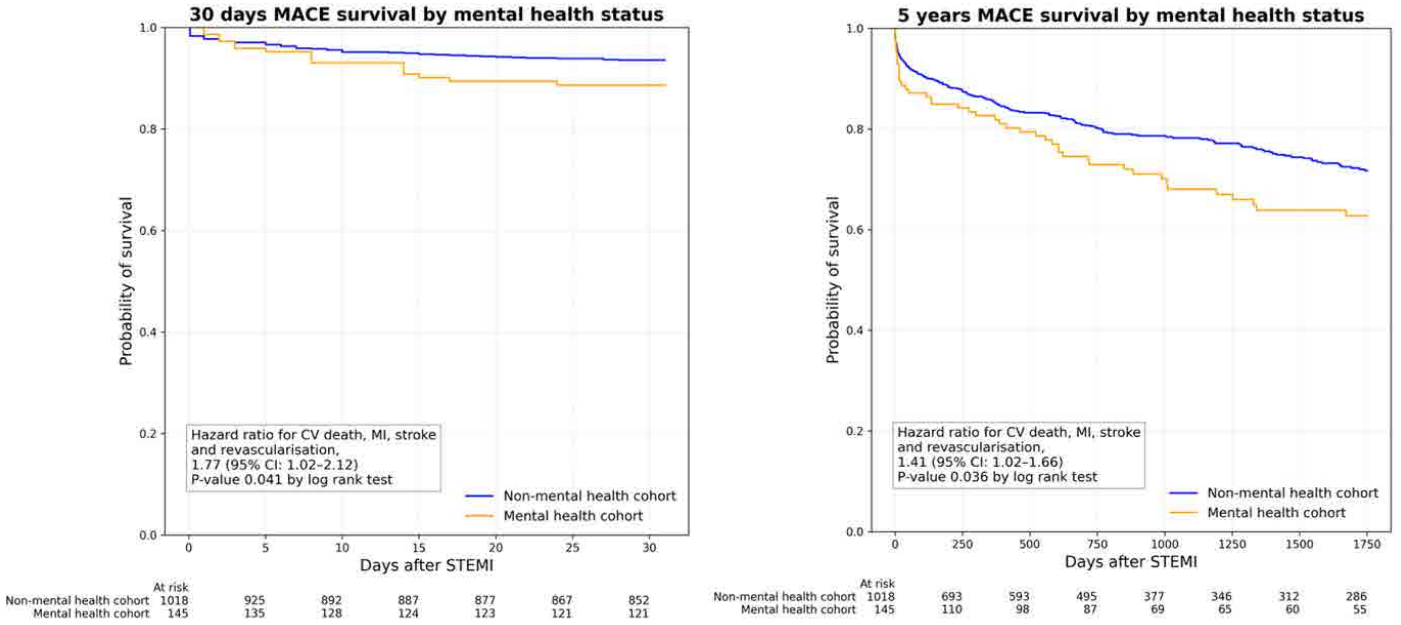

O32

Optimizing saphenous vein harvest site closure: A comparison of PRINEO and traditional staples in CABG patients

Elsa Hoti[1], Gabriella Giandotti-Gomar[1], Mario Verdugo-Marchese[1], Amir-Reza Hosseinpour[1], Matthias Kirsch[1], Ziyad Gunga[1]

[1]Centre Hospitalier Universitaire Vaudois - CHUV, Lausanne, Switzerland

Introduction: Complications at saphenous vein harvest sites, including infections and wound dehiscence, are often overlooked in cardiac surgery, despite their profound effects on patient recovery, hospital stays, and healthcare costs. Up to 25% of CABG patients experience such complications, highlighting the need for better management strategies. This study compares traditional staple closure with PRINEO, a method combining adhesive and mesh technology, to assess their effects on post-operative complications, infection rates, wound healing, and patient outcomes.

Material and Methods: This retrospective, single-center cohort study included adult CABG patients with vein grafts from January 2018 to October 2024, excluding those with arterial grafts only. Participants were grouped by harvest site closure method: staples versus PRINEO. Primary outcomes were incidence of infection, and wound dehiscence. Secondary outcomes included hospital stay duration, re-intervention, and 30-day mortality.

Results: A total of 748 patients were included. Of these, 83% were male, with a mean age of 67.3 ± 12 years. Both groups were comparable in terms of preoperative risk factors for surgical site infections (SSIs). The operative workload, as well as bypass and clamping times, showed no significant differences. The use of PRINEO was associated with a significant reduction in the incidence of SSIs (n = 24, 3.58% versus n = 9, 11.8%; *P*<0.005) and local wound dehiscence (n = 33,4.92% versus n = 15, 19.7%; *P*<0.001). Regarding secondary outcomes, while there was no observed difference in mortality, the PRINEO group demonstrated a significant reduction in hospital stay duration.

Conclusion: Our study highlights the safety and efficacy of PRINEO as a closure system for vein graft harvest sites. By significantly reducing the incidence of surgical site infections and local wound dehiscence, PRINEO demonstrates clear advantages over traditional closure methods and dressings. In the era of Enhanced Recovery After Surgery (ERAS) programs, these results underscore the potential of PRINEO to optimize postoperative outcomes.

O33

Direct comparison of postoperative release dynamics of cardiac troponin T and I after coronary artery bypass grafting

Luca Koechlin, Islam Salikhanov[1], Ivo Strebel, Brigitta Gahl[1 2], Voehringer Luise[1], Oliver Reuthebuch[1], Philip Haaf[3], Michael Zellweger[3], Martin Siegemund[4], Christian Müller, Denis Berdajs[1]

[1]Department of Cardiac Surgery, University Hospital Basel, Basel, Switzerland, Basel, Switzerland, [2]Surgical Outcome Research Center Basel, University Hospital Basel, University Basel, Basel, Switzerland, Basel, Switzerland, [3]Cardiovascular Research Institute Basel (CRIB), Basel, Switzerland, [4]University Hospital Basel, Intensive Care Unit, Department of Acute Medicine, University Hospital Basel, Basel, Switzerland, Basel, Switzerland

Introduction: Current guidelines and clinical practice consider cardiac troponin T (cTnT) and I (cTnI) equivalent in the postoperative setting after cardiac surgery. This study aimed to challenge this assumption by assessing differences in the release kinetics of cTnT and cTnI after uneventful coronary artery bypass grafting (CABG).

Material and Methods: Patients aged >18 years undergoing isolated CABG surgery were included. cTnT and cTnI were measured from the same blood samples, collected perioperatively in a standardized manner. Patients with patent bypass grafts confirmed by postoperative computed tomography and without a ≥10% decrease in left ventricular ejection fraction, indicating an uneventful recovery, were included. A biphasic cTnT/I pattern was defined as a ≥20% increase in cTnT/I compared to the immediate antecedent value after an initial decrease.

Results: A total of 258 patients (median age 69 [IQR 62–75] years) were included. Preoperative cTnT and cTnI levels below the 99th percentile were observed in 68 (26%) and 150 (58%) patients, respectively. Median (IQR) postoperative peak values were 349 ng/L (206–547) for cTnT and 1517 ng/L (752–2897) for cTnI, corresponding to 25x and 58x the upper reference limit (URL), respectively. Peaks for both cTnT and cTnI were most frequently observed at the 6-hour postoperative time point (Figure 1). A biphasic release pattern was identified in 48 patients (19%, 95% CI 14–24%) for cTnT and 33 patients (13%, 95% CI 9–17%) for cTnI.

Conclusion: cTnT and cTnI exhibit distinct postoperative release dynamics after uneventful CABG, with cTnI showing higher peak values compared to cTnT. Biphasic release patterns occurred more frequently with cTnT. These findings highlight the need for further studies to evaluate their clinical and academic implications, informing daily clinical practice.

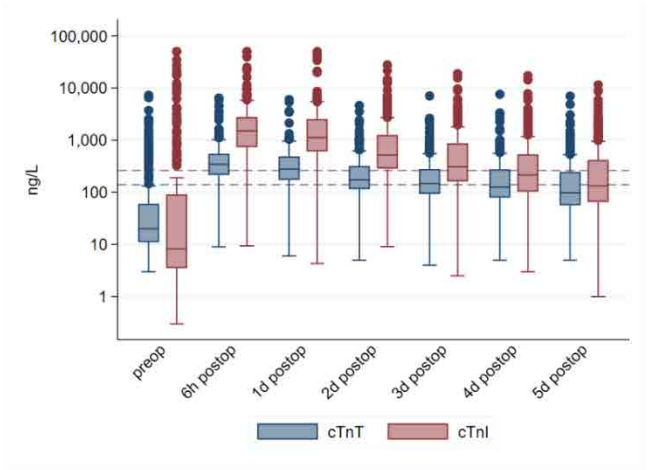

Figure 1.

Boxplots depicting perioperative concentrations of cardiac troponin T (cTnT) and cardiac troponin I (cTnI) (in ng/L) following coronary artery bypass grafting (CABG).

Dotted lines represent 10 times the upper reference limit (URL) for cTnT (blue) and cTnI (red)

cTn – cardiac troponin

O34

Feasibility and Short-Term Outcomes of Off-Pump Minimally Invasive Coronary Artery Bypass Grafting for Right Coronary Artery Revascularization

Márta Ambrus[1 2], Stak Dushaj[1 2], Dragan Odavic[1 2], Igor Tudorache[1 2], Héctor Rodríguez Cetina Biefer[1 2], Omer Dzemali[1 2]

[1]Universitätsspital Zürich, Zürich, Switzerland, [2]Stadtspital Zürich Triemli, Zürich, Switzerland

Introduction: In the past decade, minimally invasive direct coronary artery bypass grafting (MIDCAB) has become a popular method for revascularization of isolated proximal left anterior descending (LAD) stenosis. However, the use of minimally invasive off-pump CABG for right coronary artery (RCA) revascularization remains controversial in the cardiothoracic surgical community. This study aimed to evaluate the feasibility and short-term outcomes of off-pump multivessel minimally invasive coronary artery bypass grafting (MICS-CAB) through left anterior mini-thoracotomy for RCA revascularization using standard postoperative cardiac computed tomography angiography (CCTA) to assess procedural efficacy.

Material and Methods: This study analyzed 42 consecutive patients from a single center who underwent off-pump MICS-CAB for RCA stenosis between January 2023 and December 2024. Data were extracted from the medical records.

Results: Mean age at surgery was 66.33 years (±7.347). Of the participants, 36 (85.7%) were male and 6 (14.3%) female. Most patients, 30(71.4%), underwent elective surgery, 9 (21.4%) underwent expedited surgery, 2 (4.7%) underwent urgent surgery, and one(3.3%) underwent emergent surgery. Poor left ventricular function (LVEF ≤ 35%) was noted in 3 patients. One patient received off-pump Impella 5.5-assisted MICS-CAB. All surgeries were performed without cardiopulmonary bypass, averaging 282.38 minutes (±43). For bypass grafting, one patient underwent isolated RCA revascularization; 4 (9.52%) received double, 18 (42.86%) triple, 17 (40.48%) quadruple, and 2 (4.76%) quintuple grafts. The left radial artery was used in 38 (90.5%) cases for RCA revascularization, while 4 (9.5%) used the saphenous vein. Early graft occlusion of the RCA was documented once with CCTA, no revascularization done, and no in-hospital mortality cases.

Conclusion: Off-pump minimally invasive coronary surgery for the right coronary artery (RCA) is feasible and shows excellent short-term outcomes. These findings require validation using a larger cohort of patients. Routine postoperative CCTA scans effectively ensure early quality assurance; however, comprehensive long-term follow-up is still needed.

RAPID FIRE ABSTRACT SESSION "VALVULAR HEART DISEASE"

O35

Aortic arch morphology and cerebrovascular events after transfemoral transcatheter aortic valve implantation

Laura Baltruskeviciute[1], Federico Moccetti[1], Mathias Wolfrum[1], Stefan Toggweiler[1]

[1]Lucerne Cantonal Hospital, Department of Cardiology, Luzern, Switzerland

Introduction: Despite advances in transcatheter aortic valve implantation (TAVI), cerebrovascular events remain a major concern. The impact of aortic arch morphology on peri-procedural cerebrovascular events has not been investigated.

Material and Methods: We analysed consecutive patients who underwent transfemoral TAVI between March 2009 and January 2025 at the Heart Center Lucerne. Pre-procedural computed tomography scans were reviewed to assess aortic arch morphology, including measurements of arch angle, presence of calcification and soft plaques (Figure 1A-1D). Patients were classified as having an acutely angled (gothic, angle ≤ 138°) aortic arch or a round (romanesque, angle >138°) arch. The primary endpoint was the occurrence of cerebrovascular events within 30 days following TAVI, defined according to VARC-3 criteria.

Results: A total of 1248 patients with a mean age of 81 ± 6 years (44% female) were studied. Cerebrovascular events occurred in 38 patients (3.0%) within 30 days of the TAVI-

procedure. Patients who experienced cerebrovascular events had a significantly higher prevalence of a round arch (89% vs. 72%, p = 0.021) and soft plaques along the outer curvature (45% vs. 26%, p = 0.010) (Figure 2). Other predictors of cerebrovascular events included peripheral arterial disease (29% vs. 12%, p = 0.002) and implantation of more than one transcatheter heart valve (11% vs. 2%, p<0.001). The use of cerebral protection devices did not differ (47% vs. 50%, p = 0.7).

Conclusion: The presence of an acutely angled (gothic) arch was not associated with increased risk for cerebrovascular events within 30 days after TAVI. However, a round arch and soft plaques along the outer curvature were associated with more cerebrovascular events. Such patients may benefit from careful advancement of the valve catheter when crossing the aortic arch or an alternative (transapical, direct aortic) access route.

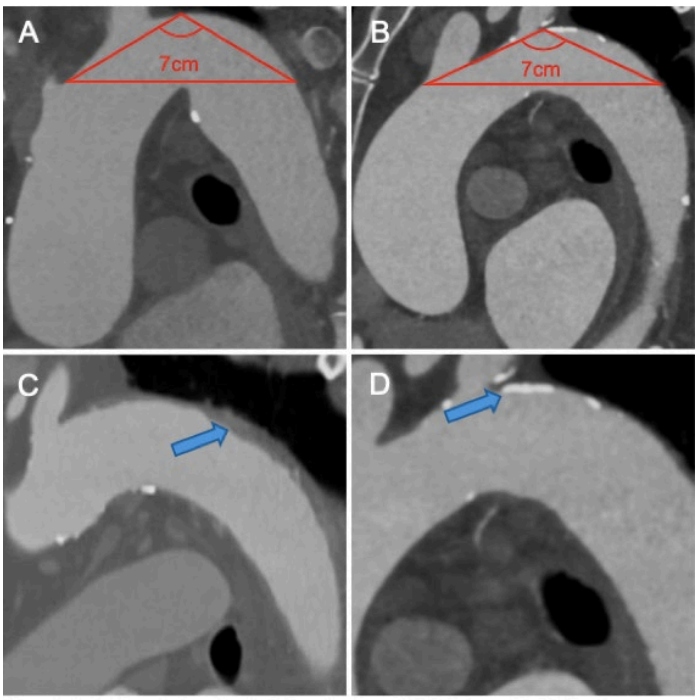

Figure 1: A) Acutely angled aortic arch B) Round aortic arch C) Soft plaques D) Calcification

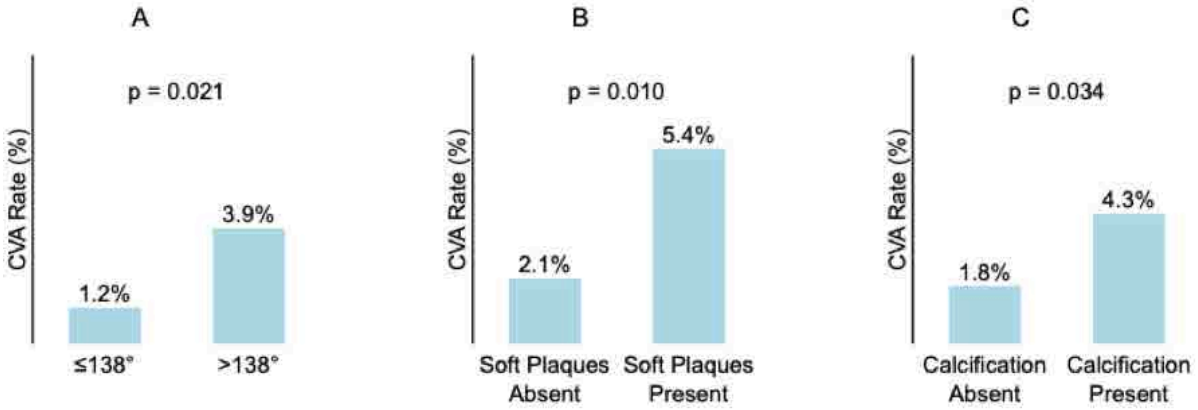

Figure 2: Panel A) CVA-Rates according to archtop angle B) CVA-Rates according to the presence of calcification C) CVA-Rates according to the presence of soft plaques. CVA: cerebrovascular accident

O36

Fully Automated Artificial Intelligence-Based Multi Sequences, Multi View, and Multi Label Cardiac Magnetic Resonance Image Quantification

Pooya Mohammadi Kazaj[1], Giovanni Baj[1], Giulin Tanner[1], Fabian Egli[1], Jonathan Schütze[1], Anselm Stark[1], Waldo Valenzuela[2], Moritz Hundertmark[1], Georgios Siontis[1], Christoph Gräni[1], Isaac Shiri[1]

[1]Department of Cardiology, Inselspital, Bern University Hospital, University of Bern, Switzerland, Bern, Switzerland, [2]University Institute for Diagnostic and Interventional Neuroradiology, Inselspital, Bern University Hospital, University of Bern, Freiburgstrasse, 3010, Bern, Switzerland, Bern, Switzerland

Introduction: Cardiac magnetic resonance (CMR) image analysis requires significant expertise and time and is subject to variability between and within observers. We developed and validated a fully automated artificial intelligence (AI)-based system for analysing CMR images, including short axis, 4-chamber cine and late gadolinium enhanced (LGE) image.

Material and Methods: Altogether 2,000 patients with diverse CMR images from different scanners with different settings as well as various diseases were enrolled. For cine images (short axis and 4-chamber), 500 CMR scans, along with corresponding segmentations of the left ventricular myocardium (LVM) and the left and right ventricles (LV and RV, respectively), were sourced from six centres and databases used for model development. The remaining images from two local registries were used to evaluate the model's performance. For cardiac substructure segmentation in LGE images (LV, RV, and LVM) and fat segmentation in 4-chamber images, a human-in-the-loop active learning approach was employed. A modified U-

Net network with deep supervision, enhanced by a range of image augmentation techniques, was developed for automatic segmentation. Cardiac functions were calculated in short axis cine images.

Results: In the test set, average Dice scores of 0.82, 0.91, and 0.92 were achieved for the RV, LV, and LVM, respectively, in short-axis, 4-chamber cine, and LGE images. For fat segmentation in 4-chamber images, an average Dice score of 0.60 was obtained across different chambers. In short-axis cine images, the stroke volumes for the LV and RV were calculated with mean percent errors of -2.52% and -8.43%, respectively. Additionally, mean percent errors of -3.22% for LV ejection fraction and -1.64% for RV ejection fraction were achieved in short-axis cine images.

Conclusion: The fully automated AI-based quantitative analysis of cardiac MR images developed in this study showed strong agreement with human expert reader ground truth measurements across various datasets which facilitate advanced quantifications across diverse CMR image types.

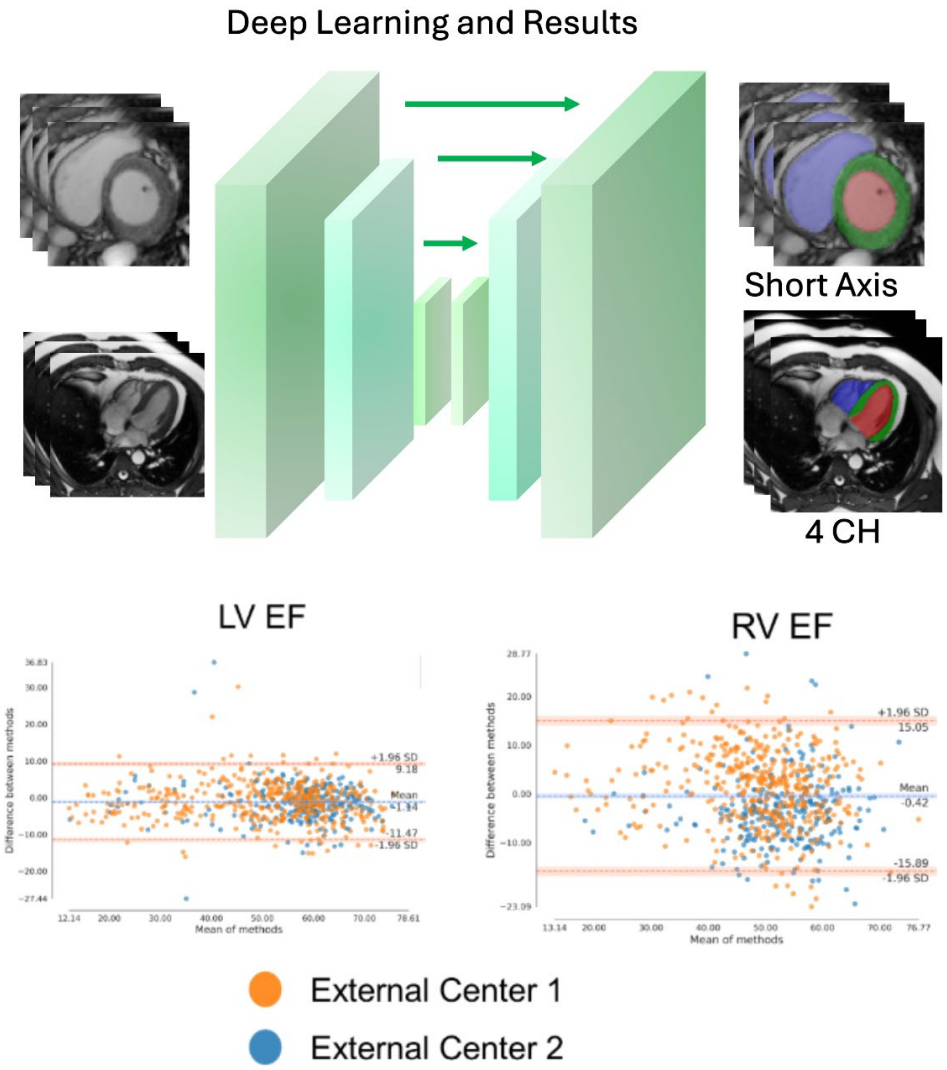

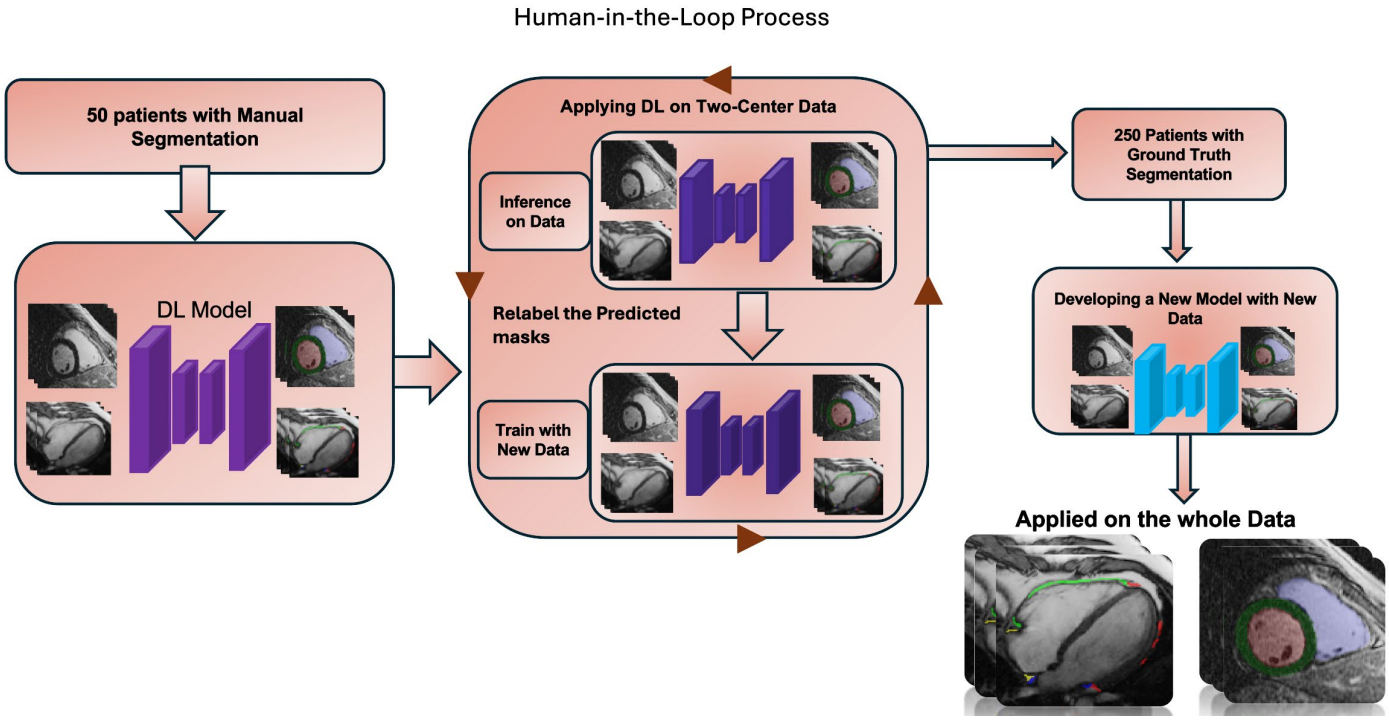

O37

Elevated stroke risk of underexpanded ACURATE neo and neo2 transcatheter aortic valves

Stefan Toggweiler[1], Thorald Stolte[2], Stephanie Brunner[1], Lucca Loretz[1], Federico Moccetti[1], Felix Mahfoud, Max Wagener[2], Christoph Kaiser, Mathias Wolfrum[1], Thomas Nestelberger[2]

[1]Luzerner Kantonsspital, Luzern, Switzerland, [2]University Hospital Basel, Basel, Switzerland

Introduction: A post-hoc analysis from a large randomized controlled trial has suggested that underexpansion of the ACURATE neo2 transcatheter aortic valve may be associated with an increased rate of stroke during follow-up between 30 days and 1 year. With this study, we aim to validate these findings, provide insights into long-term outcomes and the efficacy of postdilatation of underexpanded valves.

Material and Methods: Patients undergoing transcatheter aortic valve replacement with the ACURATE neo or neo2 were analyzed. Predilatation was routinely performed, but postdilatation only in the presence of a residual gradient or relevant PVL. Valve expansion was reviewed based on the final angiogram. Underexpansion was defined as at least one of the following: 1) non-parallel posts of the upper crown, 2) the inflow of the valve taller than wide or 3) the upper crown less expanded than the lower crown (for examples, see Figure, A).

Results: A total of 776 patients (mean age 82 ± 6 years, 55% women) were analyzed. Main results are summarized in the Figure A and B. Underexpansion was initially present in 34%. Postdilatation corrected underexpansion in most patients, but not all. During long-term follow-up, strokes occured more often in patients with underexpanded valves (HR 2.38, 95% CI 1.36 - 4.17, p = 0.002).

Conclusion: Postdilatation after ACURATE TAVR should be performed not only to correct paravalvular leaks or residual gradients, but also in the presence of underexpansion of the frame at leaflet insertion level. More research is needed to investigate the pathophysiology and clinical relevance of transcatheter heart valve underexpansion across different platforms.

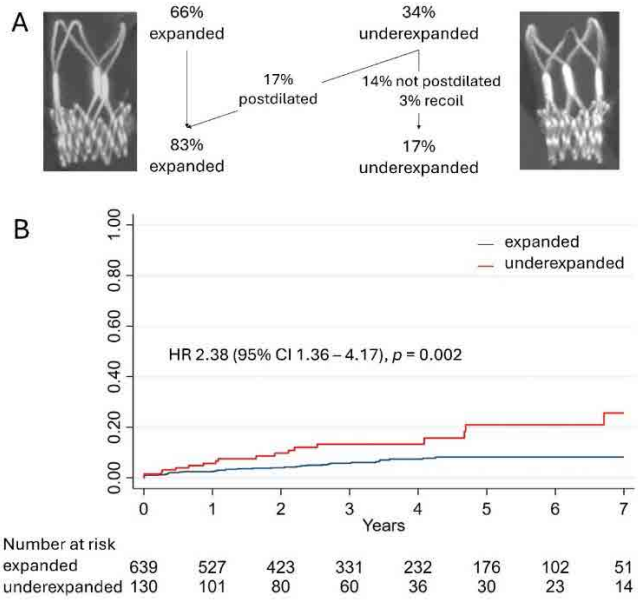

O38

Risk Stratification of Patients with Left Bundle Branch Block After Transcatheter Aortic Valve Implantation: An International Multicentric Comparative Study of a Novel, Simplified ECG Algorithm and Current ESC Criteria

Serban Teodor[1], Patrick Badertscher[2], Lena Rivard[3], Gregoire Massoullie[4], Ron Walksman[5], Valerie Pavlicek[6], Patrizio Pascale[7], Christian Reiter[8], Sven Knecht[2], Thomas Nestelberger[2], Christoph Kaiser, Andrea Papa[2], Felix Mahfoud, Christian Sticherling[2], Michael Kühne[2]

[1]Department of Cardiology, University Hospital Basel, Cardiovascular Research Institute Basel, Department of Internal Medicine, Cantonal Hospital Basel-Land, Basel, Switzerland, [2]Department of Cardiovascular Surgery, University Hospital Basel, Basel, Switzerland, [3]Montreal Heart Institute, Montreal, Canada, [4]University Hospital of Clermont-Ferrand, Clermont-Ferrand, France, [5]MedStar Washington Hospital Center, Washington DC, United States, [6]Saarland University Medical Center, Homburg, Germany, [7]Lausanne University Hospital, Lausanne, Switzerland, [8]Kepler University Clinic, Linz, Austria

Introduction: Managing left bundle branch block (LBBB) following transcatheter aortic valve implant (TAVI) is challenging. The European Society of Cardiology (ESC) guidelines recommend electrophysiological (EP) testing in LBBB patients meeting certain electrocardiographic (ECG) criteria. We aimed to develop a novel, simplified ECG algorithm for the prediction of infranodal conduction delay in LBBB patients after TAVI and compare it to current ESC criteria.

Material and Methods: We performed a multi-centric retrospective analysis of prospectively enrolled patients undergoing EP testing for LBBB after TAVI. A novel algorithm was developed by testing various combinations of the PR interval, QRS duration pre- and post-TAVI, as well as the changes in these parameters. Sensitivity, specificity, positive predictive value (PPV) and negative predictive value (NPV) were compared with the ESC guidelines for identification of patients with infranodal conduction delay, defined as His-to ventricular (HV) interval ≥ 70 ms.

Results: 769 patients with LBBB after TAVI underwent risk stratification using EP testing at seven institutions (mean age 82 ± 7 years, 55% women, 21% HV ≥ 70 ms). A novel, simplified ECG algorithm showed a sensitivity of 88% and an NPV of 92% for the rule-out of infranodal conduction delay (PR interval post-TAVI <190 ms OR QRS duration post-TAVI <160 ms) and a specificity and PPV of 85% and 41%, respectively, for the rule-in of infranodal conduction delay (PR interval post-TAVI ≥190 ms AND QRS duration post-TAVI ≥160 ms). In comparison, the ESC criteria had a sensitivity of 72%, NPV 88%, specificity of 53%, and PPV of 28%.

Conclusion: A novel, simplified ECG algorithm shows improved performance for the rule-out and rule-in of infranodal conduction delay compared to current ESC criteria.

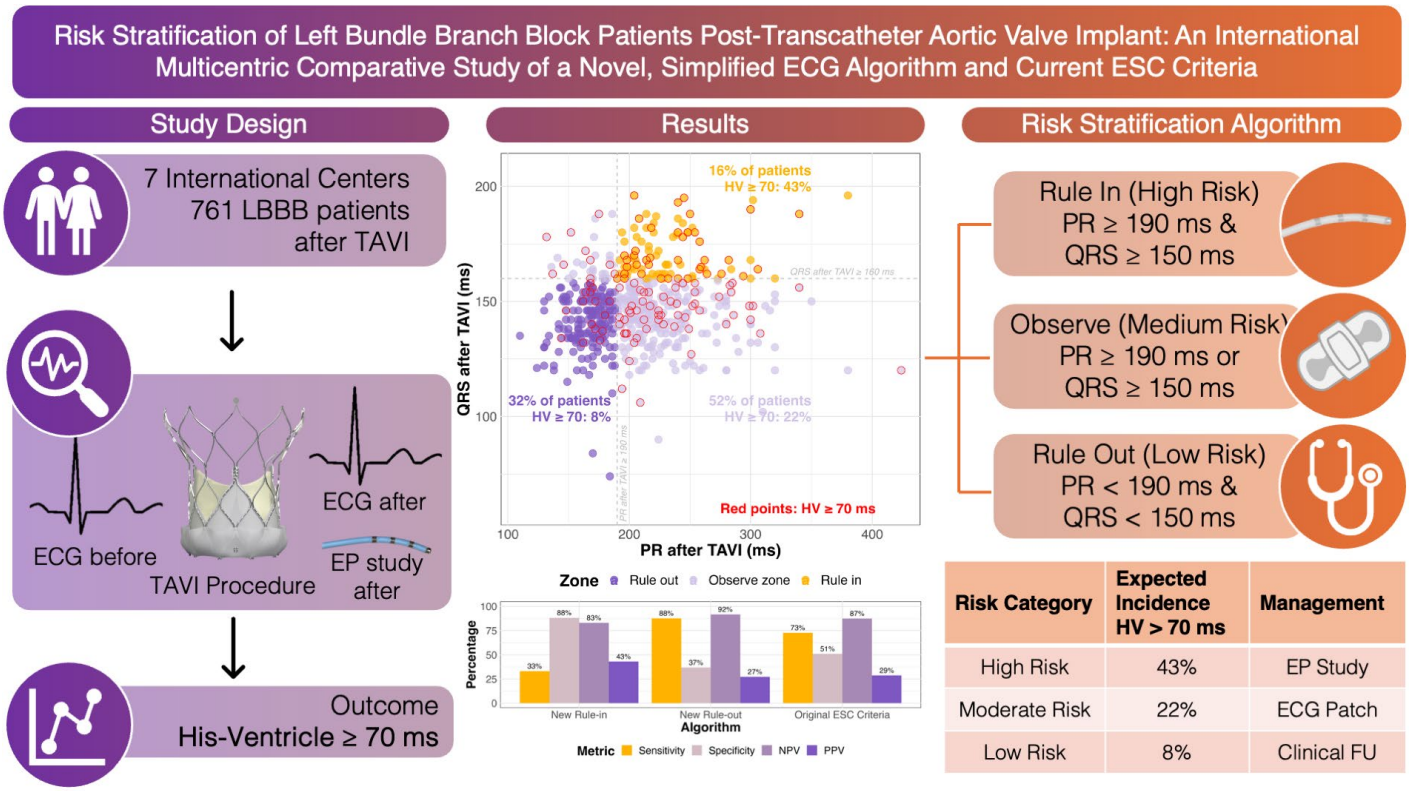

Risk Category	Expected Incidence HV > 70 ms	Management
High Risk	43%	EP Study
Moderate Risk	22%	ECG Patch
Low Risk	8%	Clinical FU

Graphical Abstract

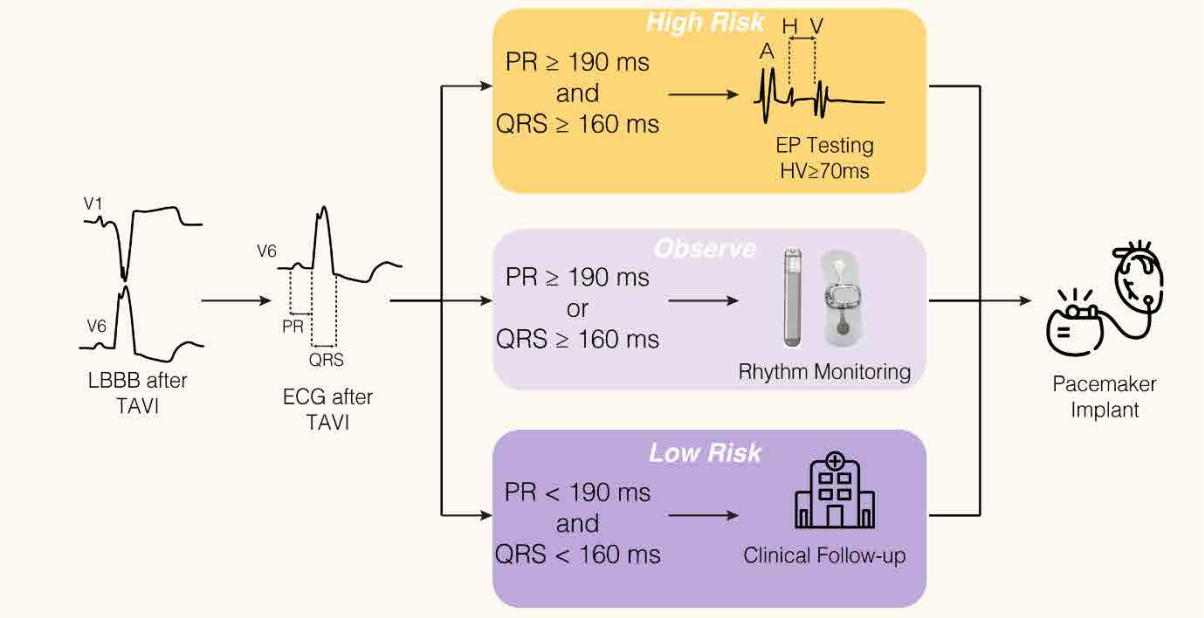

Proposed risk stratification of LBBB patients after TAVI based upon the post-procedural ECG. Abbreviations: LBBB – left bundle branch block, TAVI – transcatheter aortic valve implant

O39

Supra-annular implantation of transcatheter self-expanding valve in bicuspid aortic stenosis - a feasibility study

Federico Moccetti[1], Lucca Loretz[1], Mathias Wolfrum, Matthias Bossard[1], Adrian Attinger-Toller[1], Conrad Nina[1], Florim Cuculi[1], Stefan Toggweiler[1]

[1]Herzzentrum Luzerner Kantonsspital, Luzern, Switzerland

Introduction: In bicuspid aortic stenosis (BAV) the fused cusps are more rigid than in tricuspid stenosis and the leaflets often create a dome or funnel, so that the annulus may not be the narrowest structure. Accordingly, when implanting transcatheter heart valves (THVs) in BAV-patients, anchoring and sealing may occur at the level of the raphe rather than the annulus. Our hypothesis was that this peculiar anatomy allows for a higher (supra-annular) implantation with anchoring above the annulus (Panel A,B). We postulate that this strategy might decrease paravalvular leak (PVL) and interaction with the conduction system and thus reduce the need for pacemaker implantation.

Material and Methods: We analyzed 30 consecutive patients with BAV stenosis undergoing TAVR with self-expanding valves (Evolut Pro/Pro+/FX, Medtronic). Sizing was guided by the LIRA method (level of implantation at the raphe), and the cusp-overlap technique was employed to achieve high implantation. Echocardiographic and electrocardiographic outcomes were assessed pre-discharge, and patients were monitored for 30-day clinical outcomes.

Results: The cohort (mean age 79±6 years, 50% women) included predominantly Sievers type I BAV (90%). LIRA-guided sizing led to valve downsizing in 73% of cases (**Panel C,D,E**). Implantation was successful in all cases, with a median depth of 0mm (IQR -1mm to 0mm) meaning at or above the annulus level, with no valve migration. Paravalvular leak was none/trace in 54%, mild in 43%, and moderate in 3%. Permanent pacemaker implantation occurred in 6.6%, and new left bundle branch block in 23%. Mean transvalvular gradient was 11.1±6.8 mmHg. There were no strokes, coronary obstructions, or 30-day mortality **(Panel F).**

Conclusion: A supra-annular implantation strategy for BAV stenosis using the LIRA method and cusp-overlap technique is feasible and safe, achieving low paravalvular leak and conduction complications. Further studies in larger cohorts are needed to confirm these findings.

Implantation Strategy

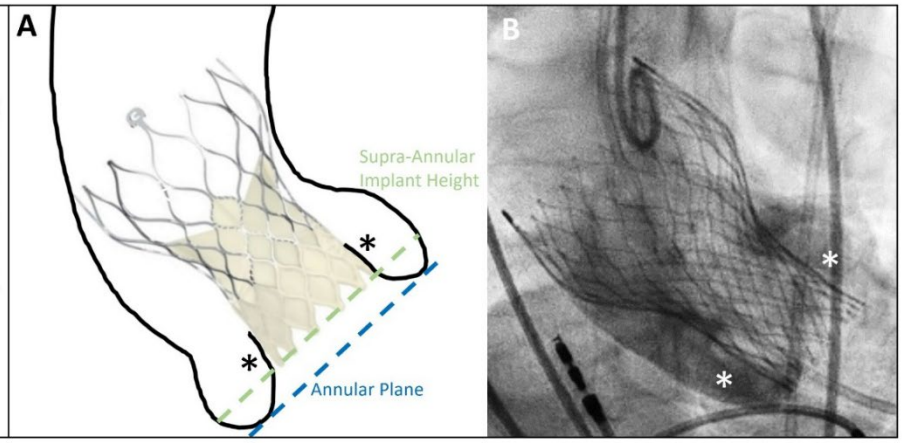

Sizing Strategy

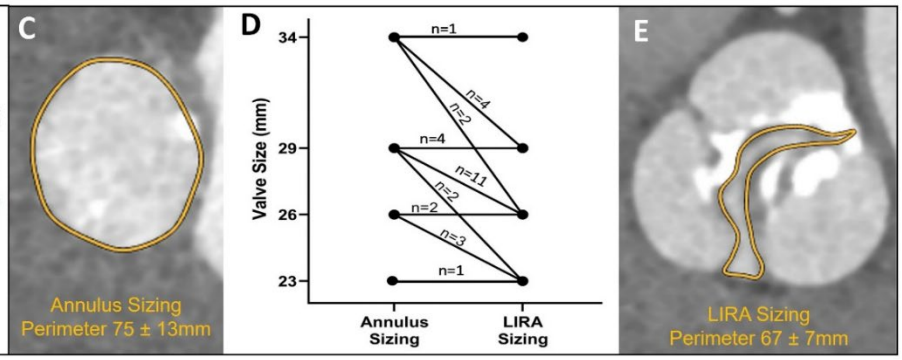

Results

F	**Implant depth, mm (IQR)**	**0 (-1, 0)**
	New permanent pacemaker	**6.6%**
	PVL none/trace	**54%**
	mild	**43%**
	moderate	**3%**
	severe	**0%**
	Mean gradient, mmHg	**11.1 ± 6.8 mmHg**
	Pop-outs	**0%**

O40

The relevance of right ventricular function and dimension in patients undergoing transcatheter tricuspid edge-to-edge repair

Stephanie Brunner[1], Lukas Stolz[2], Jörg Hausleiter[2], Stefan Toggweiler[1]

[1]Luzerner Kantonsspital, Lucerne, Switzerland, [2]LMU Klinikum München, Munich, Germany

Introduction: Patients with severe tricuspid regurgitation (TR) often present with abnormal right ventricular (RV) function and dimensions. The aim of this study was to investigate the impact of RV dysfunction and dilation on clinical outcomes in patients undergoing transcatheter tricuspid edge-to-edge repair (T-TEER).

Material and Methods: Patients from the international EuroTR registry undergoing T-TEER between 2016 and 2023 at 20 heart valve centers across Europe were included. RV dysfunction was defined as a TAPSE <17 mm, and RV dilation was defined as a RV mid-diameter >35 mm, as determined by baseline echocardiography.

Results: A total of 1,255 patients (mean age 78 ± 7 years, 53% female) were analyzed. TR was successfully reduced to a severity grade of ≤2 + in 997 patients (82%). In multivariable analysis, significant predictors of mortality after T-TEER included RV dysfunction (HR 1.05 per mm TAPSE decrease, 95% CI 1.01-1.08), RV dilation (HR 1.03 per mm RV mid-diameter increase, 95% CI 1.01-1.05), and residual TR after T-TEER (HR 1.25 per severity grade, 95% CI 1.06-1.46). These parameters were also significantly predictive for the combined endpoint of mortality and heart failure hospitalization. The worst prognosis was observed in patients exhibiting both RV dysfunction and dilation.

Conclusion: RV size and function, along with residual TR severity, were significant predictors of clinical outcomes, including all-cause mortality and heart failure hospitalization. Accordingly, early intervention to prevent RV dilation and dysfunction, as well as achieving maximal TR reduction, appears crucial for improving prognosis in patients undergoing T-TEER.

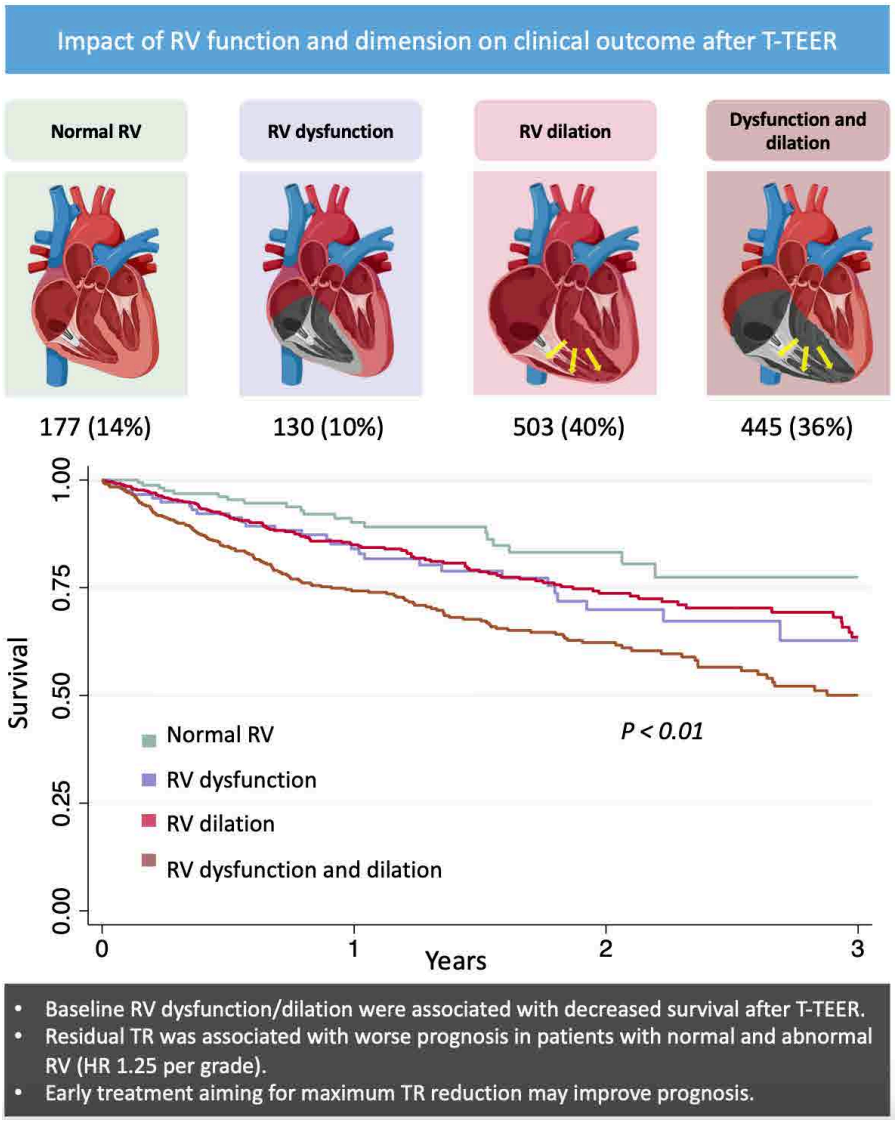

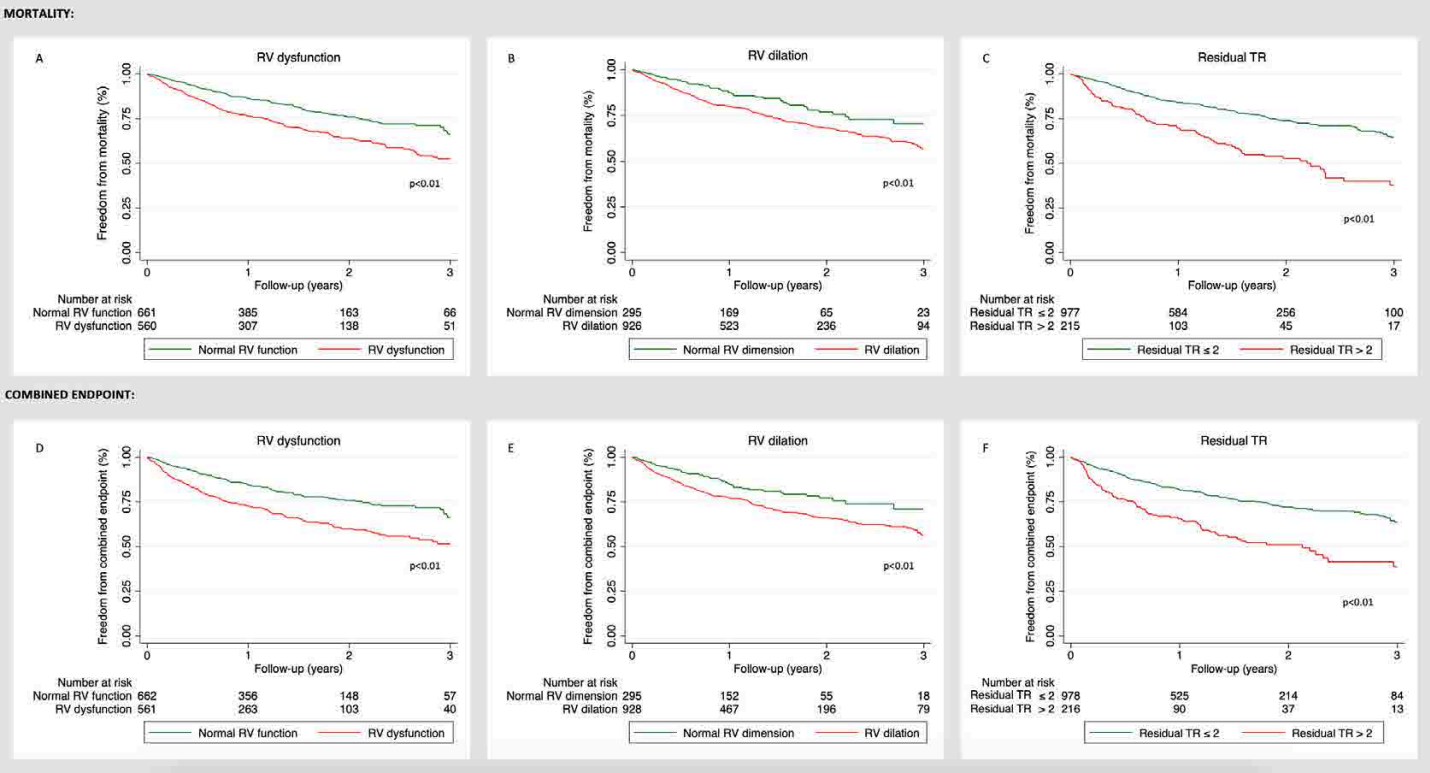

O41

2-Year Outcomes Following Transseptal Transcatheter Mitral Valve Replacement in the HighLife TransSeptal Mitral Valve Replacement (TSMVR) Feasibility Study: Durable Prosthesis Performance and Sustained Symptom Relief

Wolfgang Rottbauer[1]

[1]Ulm University Heart Center, Department of Cardiology, Ulm, Germany

Introduction: Many patients with severe mitral regurgitation (MR) are not suitable for surgical or transcatheter edge-to-edge repair because of high surgical risk and inappropriate mitral valve anatomy. 1-year outcomes have demonstrated high technical success, excellent MR reduction and good safety of the HighLife TransSeptal Mitral Valve Replacement (TSMVR) in patients with symptomatic MR (HighLife Feasibility Study (HL-2018-01) in Europe/Australia; NCT 04029363).

Material and Methods: This prospective, multicenter, non-randomized feasibility study evaluated TSMVR in 30 patients with at least moderate-to-severe symptomatic MR in a 2-year follow-up.

Results: Within the HighLife TSMVR Feasibility Study 30 patients (mean age 75.6 years, 27 % females, median STS 5.5%, mean LVEF 41%) with at least moderate-to-severe MR (90% secondary MR) were treated. In 90% technical success was achieved. No intraprocedural deaths, myocardial infarctions and strokes occurred. One patient experienced pericardial effusion and conversion to surgery. During the 2-year follow-up, all implanted patients had persistent excellent MR reduction ≤1+. Mean prosthesis gradient was stable at 4.8 mmHg 2 years after TSMVR (compared to 5.1 mmHg after 1 year of follow-up). Patients had sustained symptom relief indicated by NYHA class I/II in 82% after 2 years compared to NYHA class III/IV in 50% before TSMVR. After 2 years, 11 patients (37%) had died: 3 patients within the first month, 2 patients in the time up to 1 year and 6 patients in the second year.

In the second year after TSMVR, none of the implanted patients needed mitral-valve reintervention or surgery; none had severe bleedings or developed relevant paravalvular leaks requiring closure. Valve thrombosis or hemolysis did not occur within the 2-year follow-up. Left ventricular outflow tract obstruction was absent throughout the 2-year follow-up.

Conclusion: 2-year results from the HighLife TSMVR Feasibility Study demonstrate durable performance of the HighLife mitral valve prosthesis and sustained symptom relief.

O42

Left atrial appendage occlusion using the Amplatzer Amulet device in high-risk patients with atrial fibrillation undergoing transcatheter aortic valve replacement: A randomized pilot trial

Yiqi Gong[1], Priska Heinz[2], Mi Chen[1], Albert Markus Kasel[1], Ulrike Held[2], Francesco Paneni[1], Frank Ruschitzka[1], Marco Moccetti[3], Thomas Pilgrim[4], Barbara E Stähli[1], Fabian Nietlispach[5], Philipp Jakob[1]

[1]Department of Cardiology, University Heart Center, University Hospital Zurich and the Center for Translational and Experimental Cardiology (CTEC), University of Zurich, Zurich, Switzerland, [2]Department of Biostatistics at Epidemiology, Biostatistics and Prevention Institute, University of Zurich,, Zurich, Switzerland, [3]Cardiology Department, Cardiocentro Ticino, Lugano, Switzerland, [4]Department of Cardiology, Inselspital, University of Bern, Bern, Switzerland, [5]Heart Center im Park, Hirslanden Klinik im Park, Zurich, Switzerland

Introduction: This investigator-initiated, randomized, multicenter, non-blinded, all-comers pilot study assessed efficacy and safety of left atrial appendage occlusion (LAAO) with the Amplatzer Amulet LAA-device with early cessation of oral anticoagulation (OAC) as compared to standard medical therapy (SMT) in high-risk patients with atrial fibrillation (AF) undergoing transcatheter aortic valve replacement (TAVR).

Material and Methods: Patients with AF undergoing TAVR were randomly assigned to LAAO (TAVR+LAAO) or SMT

(TAVR+SMT). The primary endpoint was a composite of ischemic and hemorrhagic neurologic events, peripheral embolism, life-threatening/disabling and major bleeding, and cardiovascular death at 1 year. A sensitivity analyses was performed in the per-protocol population.

Results: This study included 81 patients, 40 with TAVR+LAAO and 41 with TAVR+SMT between May 2016 and May 2018 at 3 sites in Switzerland. Average age was 82.8 years. Mean STS score was 9.04% (5.42%), median CHA2DS2-VASc 4.00 [3.00,5.00] and median HAS-BLED 3.00 [2.00,3.00]. At discharge, 92% of TAVR+LAAO were on antiplatelet therapy only and 87% of TAVR+SMT on OAC. The primary endpoint occurred in 13 out of 40 patients (33%) in TAVR+LAAO and in 15 out of 41 patients (37%) in TAVR+SMT (OR, 0.83; 95%CI: 0.33-2.09, P = 0.70). Bleeding occurred in five patients (13%) in TAVR+LAAO and in seven patients (17%) in TAVR+SMT, with absent non-procedural bleeding in TAVR+LAAO and five gastrointestinal bleedings in TAVR+SMT. Four patients in the TAVR+LAAO (10%) and one patient (2.4%) in the TAVR+SMT had neurologic events. In the per-protocol analysis, the primary endpoint was similar (OR, 0.58; 95%CI, 0.21-1.53; P = 0.28). Two (5.6%) and one patient (2.4%) had neurologic events in TAVR+LAAO and TAVR+SMT, respectively. Bleeding rates were numerically lower in TAVR+LAAO (8.3%) as compared to TAVR+SMT (17%).

Conclusion: Among high-risk patients with AF undergoing TAVR, a strategy of a combined procedure with LAAO is an alternative to SMT with potential lower bleeding but higher neurological event rates. (NCT03088098)

RAPID FIRE ABSTRACT SESSION "BASIC SCIENCES"

O43

NCOR1 Regulates Macrophage-Driven Inflammation in Heart Failure with Preserved Ejection Fraction via the NLRP3-IL1b Pathway: A Translational Study

Era Gorica[1], Ludovica Di Venanzio[1], Iliana Papadopoulou[2], Shafeeq Mohammed[1], Natalia Atzemian[1], Alessandro Mengozzi[1], Hung-Wei Cheng[2], Valeria Masciovecchio[1], Marialucia Telesca[1], Alessia Mongelli[1], Burkhard Ludewig[2], Nazha Hamdani[3], Frank Ruschitzka[1], Sarah Costantino[1], Francesco Paneni[1]

[1]Center for Translational and Experimental Cardiology (CTEC), University of Zurich and University Hospital Zurich, Zürich, Switzerland, [2]Institute of Immunobiology,, Kantonsspital St. Gallen, St. Gallen, Switzerland, [3]Institute of Physiology, Ruhr University, Bochum, Germany

Introduction: Inflammatory response is a key player in heart failure with preserved ejection fraction (HFpEF) but the underlying mechanisms are poorly understood. Recent studies have shown a critical involvement of cardiac macrophage activation in myocardial remodeling thus contributing to HFpEF.

Material and Methods: Human and murine left ventricular (LV) myocardial tissue, FACS analysis of cardiac immune cells, and in vitro experiments were employed. RAW-264.7 cells exposed to palmitic acid (PA), bone marrow-derived macrophages from healthy and HFpEF mice, cardiomyocytes (H9c2), endothelial cells (HAECs), and ex vivo LV tissue analyses were used. ScRNA-seq of human failing hearts and LV myocardial samples assessed macrophage pro-inflammatory activity in HFpEF. HFpEF was induced in mice using a high-fat diet and L-NAME. Cardiac function was evaluated via ultrasound (Vevo3100), and LV samples analyzed macrophage inflammation. Myeloid-specific NCOR1 knockout (Ncor1-KO) mice were generated based on scRNA-seq findings identifying NCOR1 as key in macrophage-driven cardiac inflammation.

Results: The expression of macrophage markers in human LV specimens from HFpEF patients showed an increase in pro-inflammatory macrophages (M1) and a decrease in regulatory macrophages (M2) as compared to age-matched control donorsHFpEF mice showed increased vascular adhesion molecules (ICAM1, ICAM2, E-selectin) and M1 macrophage recruitment. Mice with macrophage NCOR1 deletion had reduced diastolic dysfunction and lung congestion, with improved exercise tolerance compared to WT littermates. These findings linked reduced myocardial inflammation (TNF-α, IL6, IL-1β) in Ncor1-KO mice to NCOR1's role in macrophage activation. In vitro, palmitic acid-induced stress upregulated NCOR1 and activated the NLRP3-IL1β pathway, while NCOR1 depletion mitigated harmful macrophage activation. NCOR1 silencing also reduced inflammation, oxidative stress, and cell death in cardiomyocytes and endothelial cells, highlighting dynamic crosstalk in HFpEF.

Conclusion: NCOR1 is a crucial regulator of immune response and inflammasome activation in cardiac macrophages. Our findings highlight its potential as a target for therapies aimed at preventing myocardial damage in HFpEF.

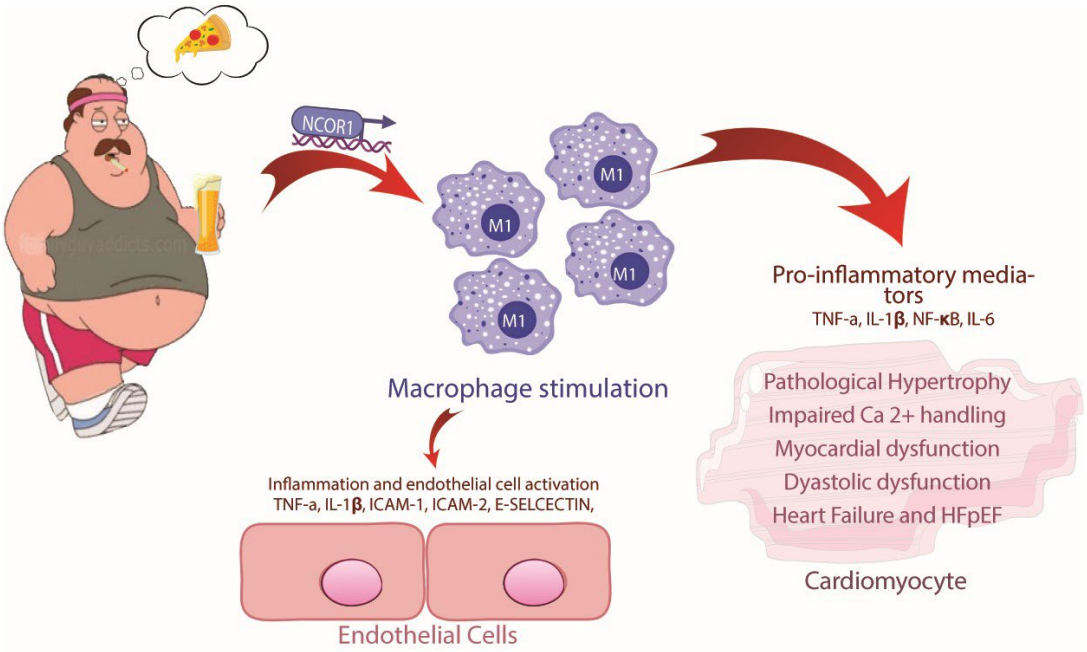

Figure 1. Macrophage polarization is regulated by Nuclear Receptor Corepressor 1 (NCOR1), which modulates the expression of pro- and anti-inflammatory cytokines. In response to this stimulus, macrophages can be polarized into the pro-inflammatory M1 phenotype. The sustained activation of M1 macrophages can lead to tissue damage, fibrosis, impaired cardiac function, and heart failure. Modulating macrophages polarization and their pro-inflammatory activity may represent a promising therapeutic strategy for the treatment of HFpEF.

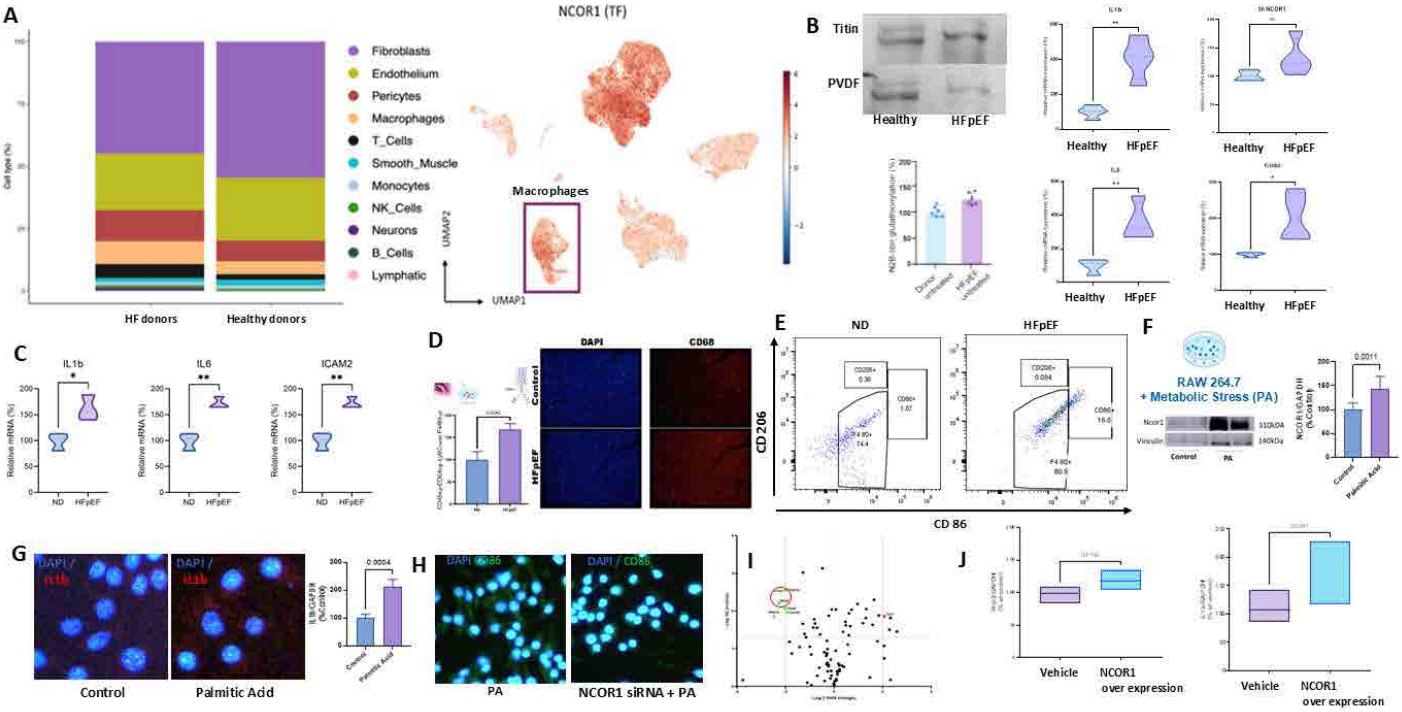

Figure 2. A)ScRNA sequencing of failing hearts reveals augmented macrophage population and NCOR1-TF being among the top regulated transcription factors in macrophage population. B-E)Disturbed macrophage polarization and pronounced inflammation confirmed in HFpEF patient's myocardium and left ventricle HFpEF mice specimens. F-G) Murine macrophage activation upon metabolic stress via Palmitic Acid (PA) induced NCOR1 and pro-inflammatory cytokines upregulation. H-J) NCOR1 silencing in vitro prevented macrophage NLRP3-IL1b axis activation.

O44

Long non-coding RNA PANDA drives diabetic vascular dysfunction by promoting endothelial senescence and oxidative damage

Alessia Mongelli[1], Alessandro Mengozzi[2], Shafeeq Mohammed[1], Era Gorica Hoxha[1], Marialucia Telesca[1], Frank Ruschitzka[3], Francesco Paneni[1 3], Sarah Costantino[1]

[1]Center for Translational and Experimental Cardiology (CTEC), Department of Cardiology, University Hospital Zurich, University of Zurich, Zürich, Switzerland, [2]Department of Clinical and Experimental Medicine, University of Pisa, Pisa, Italy, [3]Department of Cardiology, University Hospital Zurich, zürich, Switzerland

Introduction: LncRNAs are emerging as important players in the pathogenesis of cardiovascular disease as well lncRNAs have been found to trigger and modulate the diabetes. Clinically diabetic patients have 2-4 increased risk to develop cardiovascular disease with a higher rate of morbidity and mortality. Recent work has shown that PANDA, a newly identified lncRNA, is involved in cellular senescence, apoptosis and cell cycle progression, all features of diabetic vascular dysfunction

Material and Methods: Human aortic specimens were collected from diabetic and non-diabetic patients and underwent to RNAseq. *In vitro*, human aortic endothelial cells (HAECs) were exposed to high glucose concentrations (HG, 25 mM) and to 5 mM (normal glucose, NG). PANDA depletion in HG-treated HAECs is obtained by siRNA transfection. Real time PCR and western blot are used to detect RNA and protein levels, respectively. RNAs sequencing (RNA-seq) and bioinformatic analysis (network perturbation amplitude, NPA) were leveraged to unveil transcriptional changes. RNA immunoprecipitation (RIP) was performed to check PANDA binding to relevant transcriptional factors. ROS formation, senescence and angiogenesis are investigated through staining and cell proliferation assay

Results: PANDA is overexpressed in aorta of diabetic patiens as well in HAECs exposed to HG. Transcriptomic analysis revealed dysregulation of several genes upon PANDA silencing with the antioxidant gene. NPA shows the modulation of senescence, DNA damage, NRF2 signaling, hypoxic stress response and proliferation pathways in PANDA silenced cells. In particular in HG, PANDA binds the transcription factor NRF2 which in turn does not bind the promoter genes of anti-oxidative genes.The depletion of PANDA restores the detrimental effect of HG

Conclusion: The upregulation of PANDA drives endothelial senescence and impairing angiogenic properties. PANDA depletion in HG-treated HAECs rescued maladaptive transcriptional changes enhancing NRF2 pathway. These results indicate PANDA as a novel molecular target in the setting of diabetic vascular disease

Figure 1

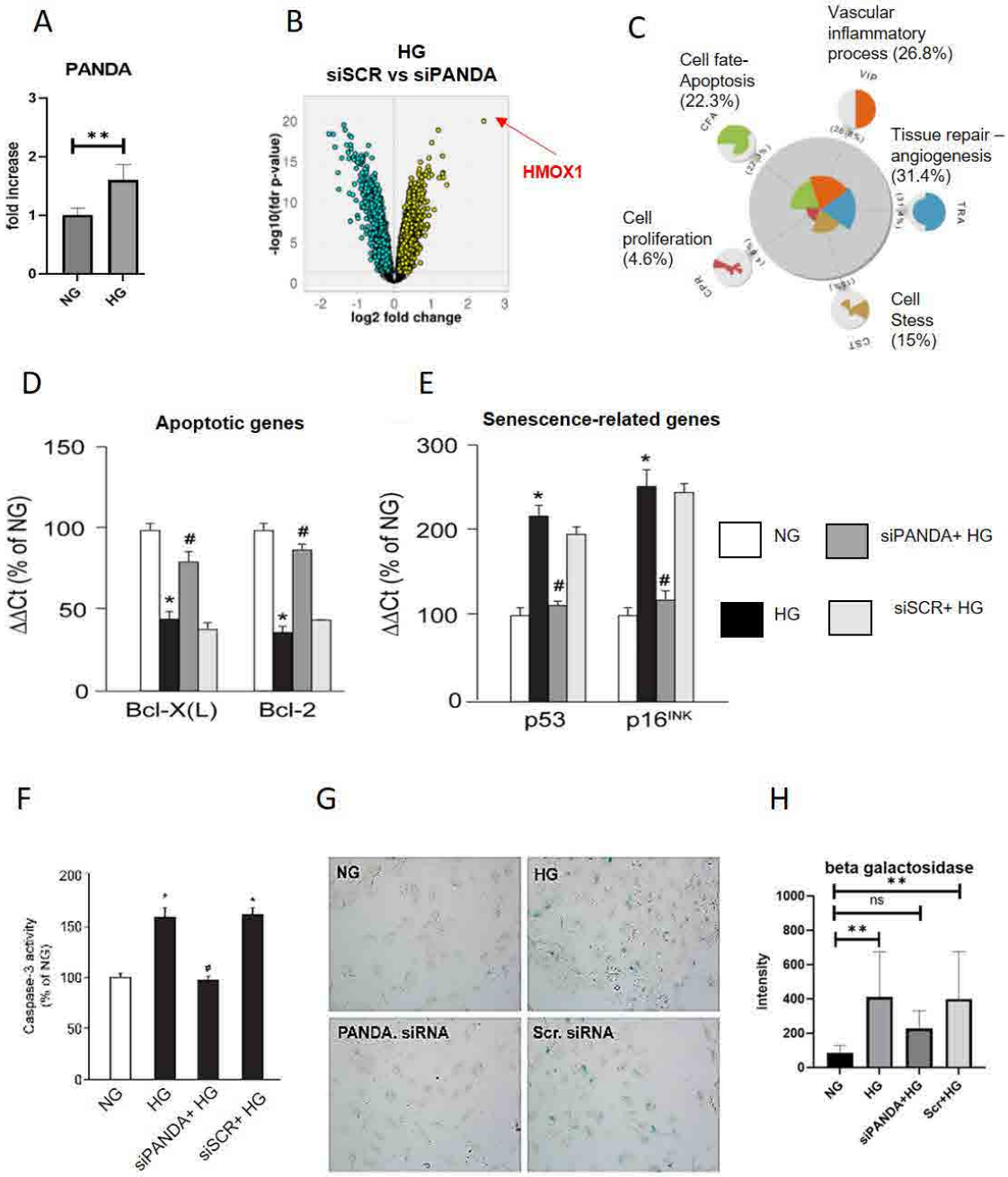

Figure 1. A) expression of PANDA in HAECs. PANDA is mostly expressed in HG. B) Transcriptomic analysis in PANDA-Silenced cells in HG. After the depltion of PANDA, the HMOX1 is the most up-regulated transcript. C) Pathway analysis reveals the modulation of apotosis, inflamation, cell stress, angiogenesis and proliferation. D) Real Time qPCR of anti-apotic genes. The depletion of PANDA increases the level of anti-apotoic genes in HG. E) Real Time qPCR on senescence-related gene. PANDA silencing reduce the expression of senescence-gene. F) Caspase 3 activity. In HG the activity is enhanced, the depletion of PANDA restore the level of activity. G) Beta-galactosidase staining. H) Quantification of beta-galactosidase staining. In PANDA-silenced cells the positivity of the beta-galactosidase is significantly reduced.

Figure 2

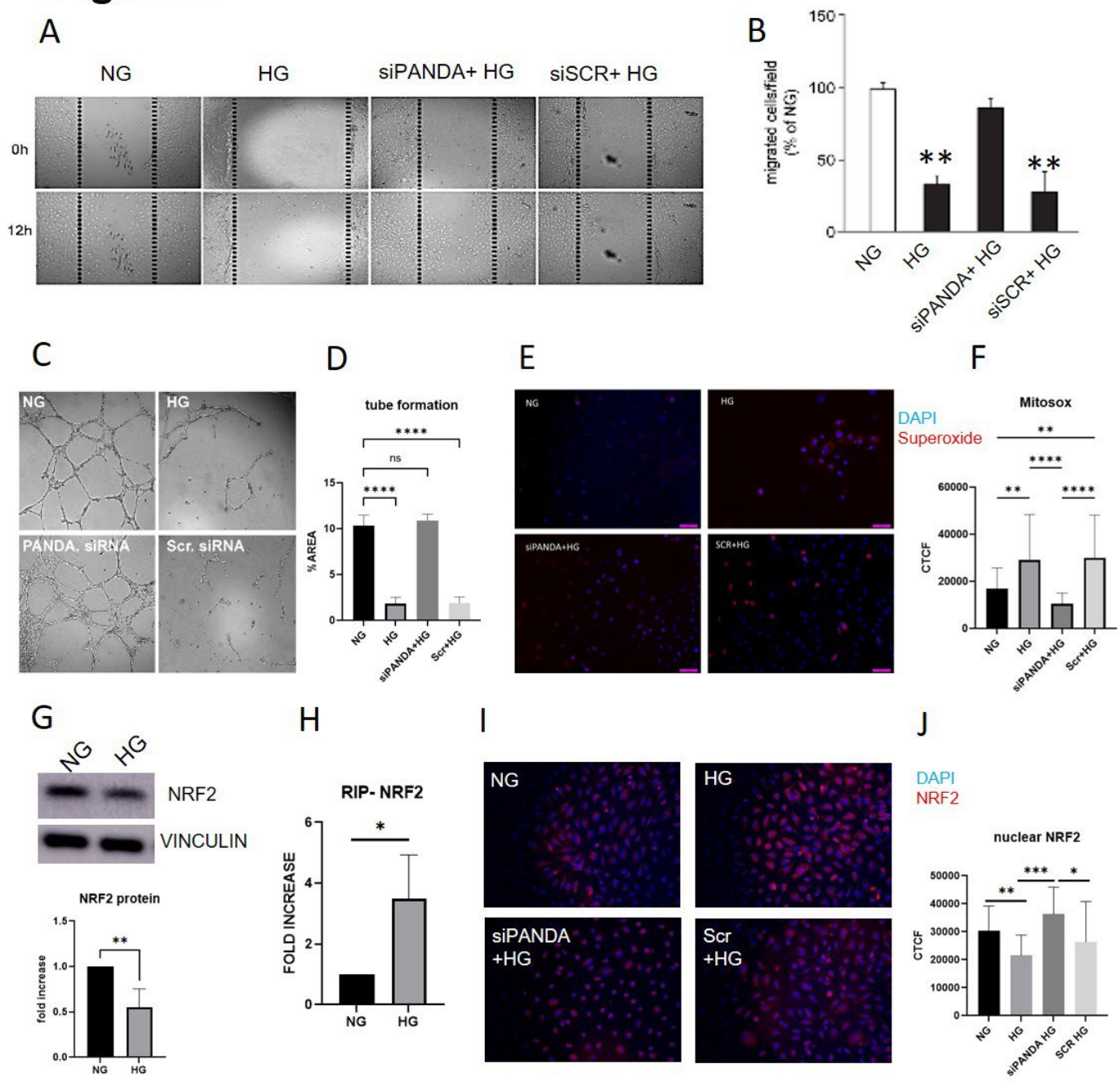

Figure 2. A-B) Migration assay during silencing of PANDA in HAECs. C-D) Tube-formation assays during silencing of PANDA in HAECs. E-F) Mitochondrial ROS assessed by MitoSOX in HAECs; G) Expression of NRF2 in HAECs during normal and high glucose conditions. H) RNA immunoprecicipation of NRF2 and PANDA; I-J) Immunofluorence of NRF2 in the four experimental conditions;

O45

Epigenetic and transcriptional landscape of the kidney in heart failure with preserved ejection fraction

Natalia Atzemian[1], Shafeeq Mohammed[1], Era Gorica[1], Ludovica Di Venanzio[1], Sarah Costantino[1], Frank Ruschitzka[1 2], Francesco Paneni[1 2]

[1]Center for Translational and Experimental Cardiology (CTEC), Department of Cardiology University Hospital Zurich, University of Zurich, Zurich, Switzerland, [2]Department of Cardiology, University Hospital Zurich, Zurich, Switzerland

Introduction: Heart failure with preserved ejection fraction (HFpEF) and chronic kidney disease (CKD) constitute a high-risk phenotype with significant morbidity and mortality and poor prognosis. Multiple proinflammatory comorbid conditions influence the pathogenesis of HFpEF and CKD. The understanding of the molecular mechanisms underpinning kidney damage cardio-renal interactions in HFpEF remains poorly understood. Unveiling new molecular targets could pave the way for new mechanism-based interventions to prevent HFpEF and CKD progression.

Material and Methods: A mouse model of HFpEF, characterized by the combination of high-fat diet (60 kcal% fat,) and L-NAME in the drinking water (0.5g/L) for 15 weeks was employed. Control mice received a control diet (10 kcal% fat,) and vehicle in the drinking water (Fig. A). Deep renal phenotyping in control and HFpEF mice was performed by: i) renal biomarker profiling; ii) histological analysis; iii) RNA-Sequencing; iv) proteomics; v) CUT&RUN assay to investigate chromatin accessibility (Fig. B).

Results: HFpEF mice displayed renal dysfunction as assessed by increased creatinine, cystatin C and galectin-3 levels (Fig. C), as well as alterations of tissue architecture as shown by Collagen 1A1 and PAS staining (Fig. D). Bulk RNA-seq and proteomic analyses unveiled three top-ranking signals in HFpEF vs control kidneys, namely Kynureninase (KYNU), Receptor Accessory Protein 6 (REEP6), and Retinol Dehydrogenase 16 family member 2 (RDH16F2) (Fig. E). Analysis of the chromatin landscape by CUT&RUN assays identified increased accessible loci in HFpEF vs control kidneys, with a prominent role of epigenetic readers (BET proteins) in regulating the transcription of target genes. Of interest, enhanced BET protein enrichment was associated with kidney inflammation and fibrosis in HFpEF mice.

Conclusion: HFpEF is associated with relevant epigenetic and transcriptional alterations in the kidney, eventually promoting organ dysfunction and structural remodeling. Our study sheds light on epigenome-environment interactions and new molecular targets potentially implicated in the progression of cardio-renal damage in HFpEF.

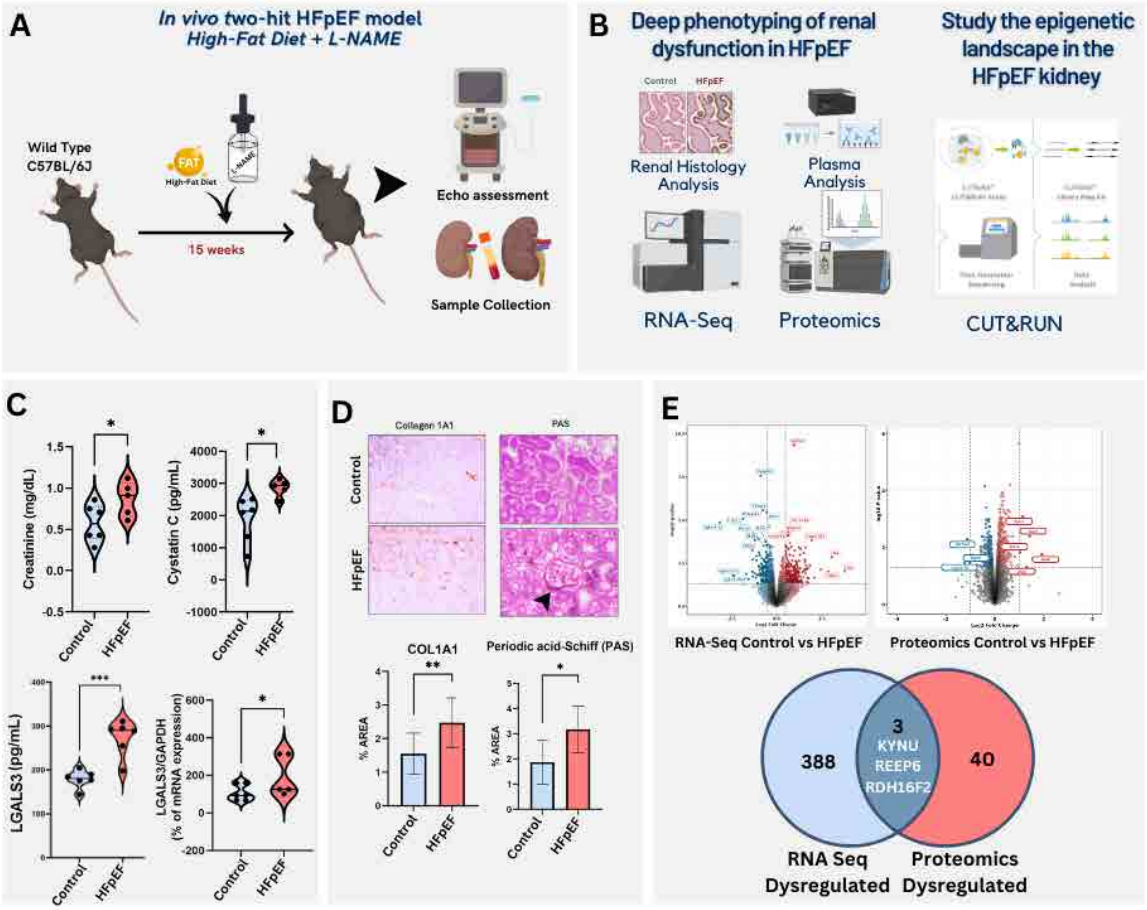

A) Schematic showing the mouse model of HFpEF; **B)** Multi-omic approach for deep phenotyping of the HFpEF kidney, incorporating plasma and histology renal function analyses, transcriptomics, proteomics and epigenomics; **C)** Markers of renal function; **D)** Periodic acid- Schiff and Collagen 1A1 stainings and quantification; **E)** Integration of RNA-seq and proteomic analysis showing convergence on 3 molecular targets, namely Kynureninase (KYNU), Receptor Accessory Protein 6 (REEP6), and Retinol Dehydrogenase 16 family member 2 (RDH16F2)

O46

Employing Epi-drugs to Rescue Lung Microenvironmental Changes in Heart Failure with Preserved Ejection Fraction

Marialucia Telesca[1], Valeria Masciovecchio[1], Papadopoulou Iliana[1], Shafeeq Ahmed Mohammed[1], Era Gorica[1], Jacopo Spezzini[1 2], Alessia Mongelli[1], Liberato Berrino[3], Ludewig Burkhard[1], Francesco Paneni[1], Frank Ruschitzka[1], Sarah Costantino[1]

[1]Center for Translational and Experimental Cardiology (CTEC), Department of Cardiology, University Hospital Zurich, University of Zurich., Schlieren, Switzerland, [2]University of Pisa · Department of Pharmacy, Pisa, Italy, [3]University of Campania "Luigi Vanvitelli", Naples, Italy

Introduction: Heart failure with preserved ejection fraction (HFpEF) is the most common form of heart failure and is frequently complicated by the development of pulmonary hypertension (PH). The prevalence of PH in HFpEF ranges from 30% to 80%, and it is a strong predictor of mortality. Understanding changes of the lung microenvironment, namely cell-cell communications among fibroblasts, immune and endothelial cells, could unveil new targets to tackle microvascular dysfunction and PH in this setting. Epigenetic changes, namely post-translational histone modifications, are emerging as pivotal modulators of gene expression in cardiovascular disease. Targeting these mechanisms with epi-drugs may restore vascular homeostasis

Material and Methods: HFpEF-PH was induced in mice via high-fat diet (HFD) and L-NAME for 15 weeks. Mice were treated with the BET-inhibitor Apabetalone (APA) for 14 days. Cardiac function and pulmonary pressure were assessed via ultrasound imaging. Single-nuclei RNA sequencing (snRNA-seq) was performed on lung specimens, and primary endothelial cells (mECs) and fibroblasts (mFs) were isolated and treated with APA.

Results: HFpEF mice displayed PH, as evidenced by elevated pulmonary artery pressure, increased pulmonary artery resistance, extended right ventricular wall thickness, and diminished pulmonary artery acceleration time. In vivo treatment with APA prevented PH development in HFpEF mice. SnRNA-seq revealed that mFs and mECs were the primary drivers of HFpEF-PH pathology and interactome analyses. Both mECs and mFs from obese mice exhibited an altered phenotype. Specifically, mFs exhibited a myo-fibroblast phenotype and altered bioenergetic profile, as shown by Seahorse experiments, whereas mECs displayed defective autophagy and up-regulation of NF-kB-related inflammatory genes, hypoxia-inducible factor (HIF1-α), and NADPH-oxidase-NOX4. Treatment with APA rescued mECs and mFs transcriptional alterations and cell dysfunction in HFpEF-PH mice.

Conclusion: BET inhibition restores lung microenvironmental homeostasis in HFpEF-PH, reducing inflammation and cellular dysfunction. Targeting epigenetic pathways may offer a novel therapeutic approach for PH in HFpEF.

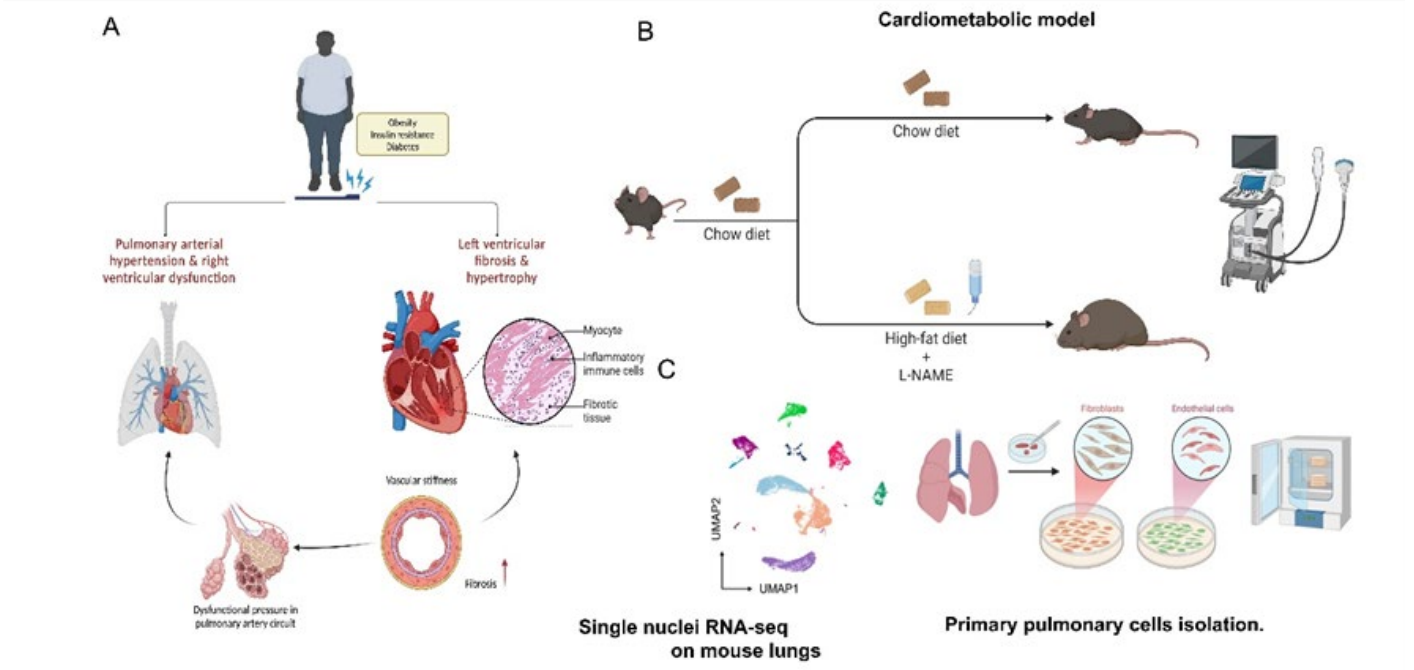

FIG.1 Obesity has been associated with a variety of health conditions, including diabetes, PH, and heart failure (HF). PH (group 2) is a prevalent complication of HFpEF, and fibrosis plays a substantial role in both conditions (A). To analyze the HFpEF-PH, a valid HFpEF model was used that combines metabolic and hemodynamic stress (B). Single-cell sequencing (scRNA-seq) was performed in lung specimens to analyze the transcriptional landscape in different cellular populations, and primary cells were isolated for molecular investigations (C).

1. Apabetalone improves cardiac function and fibrosis

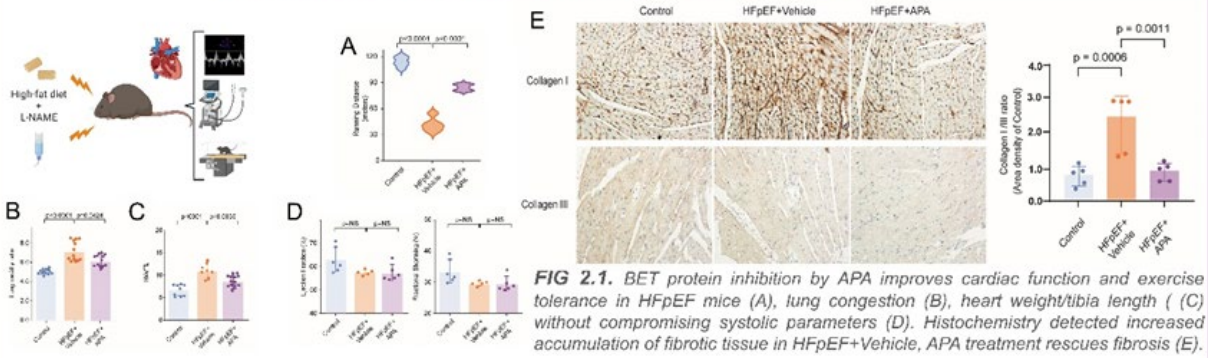

FIG 2.1. *BET protein inhibition by APA improves cardiac function and exercise tolerance in HFpEF mice (A), lung congestion (B), heart weight/tibia length ((C) without compromising systolic parameters (D). Histochemistry detected increased accumulation of fibrotic tissue in HFpEF+Vehicle, APA treatment rescues fibrosis (E).*

2. Apabetalone *rescues the PH phenotype*

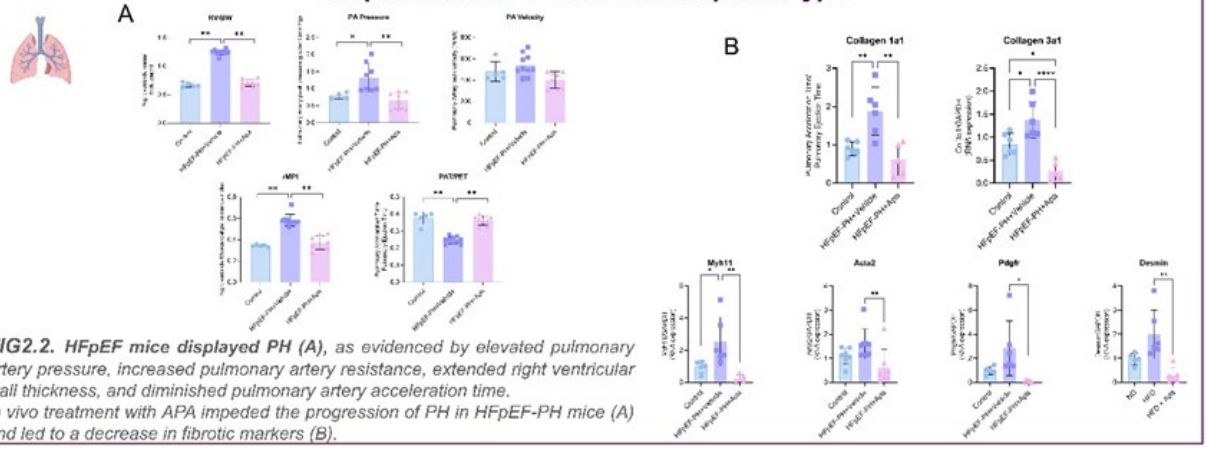

FIG2.2. ***HFpEF mice displayed PH (A),*** *as evidenced by elevated pulmonary artery pressure, increased pulmonary artery resistance, extended right ventricular wall thickness, and diminished pulmonary artery acceleration time.*
In vivo treatment with APA impeded the progression of PH in HFpEF-PH mice (A) and led to a decrease in fibrotic markers (B).

3. Murine Lung snRNA Analysis (CD vs HFpEF-PH)

Fibroblasts and aCap pulmonary ECs are increased in HFpEF-PH lung

Kantonsspital St.Gallen

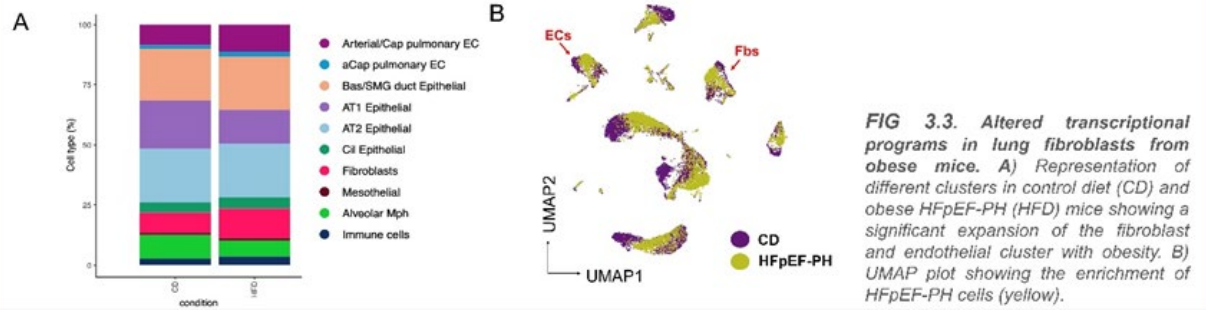

FIG 3.3. ***Altered transcriptional programs in lung fibroblasts from obese mice.*** ***A)*** *Representation of different clusters in control diet (CD) and obese HFpEF-PH (HFD) mice showing a significant expansion of the fibroblast and endothelial cluster with obesity. B) UMAP plot showing the enrichment of HFpEF-PH cells (yellow).*

O47

Ectoenzyme CD38: a novel determinant of age-associated vascular dysfunction

Yustina M Puspitasari[1], Kangmin Yang[1], Stefano Ministrini[1 2], Amedeo Tirandi[1 3], Susan Bengs[1], Luca Liberale[3 4], Fabrizio Montecucco[3 4], Tomasz J Guzik[5 6], Thomas F. Lüscher[1 7], Giovanni G. Camici[1 8]

[1]Center for Molecular Cardiology, Schlieren, Switzerland, [2]Cardiology department, Luzerner Kantonspital, Luzern, Switzerland, [3]First Clinic of Internal Medicine, Department of Internal Medicine, University of Genoa, Genoa, Italy, [4]IRCCS Ospedale Policlinico San Martino Genoa – Italian Cardiovascular Network, Genoa, Italy, [5]5Centre for Cardiovascular Science, Queens Medical Research Institute, University of Edinburgh, Edinburgh, United Kingdom, [6]Department of Medicine, Jagiellonian University Collegium Medicum, Cracow, Poland, [7]Department of Cardiology, Royal Brompton & Harefield Hospitals and National Heart & Cardiovascular Academic Group, King's College, London, United Kingdom, [8]Department of Research and Education, University Hospital Zurich, Zurich, Switzerland

Introduction: Aging is a major risk factor for cardiovascular diseases, marked by age-related vascular dysfunction. Recent studies highlight an important role of CD38 in the age-related declines of NAD levels, a key factor in the progression of age-associated diseases. Notably, CD38 inhibition significantly extends the lifespan of aged mice. However, its specific role in age-related vascular dysfunction remains unclear and warrants further investigation.

Material and Methods: CD38 plasma levels were measured in a cohort of hypertensive patients (40-80 years old) and correlated with macro- and microvascular function parameters. *Ex vivo* tension myograph experiments were performed on thoracic aortas of aged male C57Bl/6 mice following pre-incubation with the CD38-specific inhibitor, 78c. The effect of CD38 inhibition on senescent primary human aortic endothelial cells was also assessed.

Results: Circulating CD38 levels were negatively correlated with reactive hyperemia index – a readout of peripheral microvascular function. This correlation was independent of potential confounders, including body mass index and high-density lipoprotein levels. Interestingly, this association was modified by age and sex, showing a significant association in males or older individuals (Fig 1). CD38 expression was, indeed, upregulated in the aorta of aged mice and in senescent HAEC compared to the control. Meanwhile, *ex vivo* tension myograph experiments demonstrated that CD38 inhibition on aged vessels from male mice significantly increased endothelium-dependent relaxation responses to acetylcholine. This effect was abrogated in the presence of the endothelial nitric oxide synthase (eNOS) inhibitor, L-NAME, but not by the COXs inhibitor, indomethacin, indicating an involvement of the eNOS pathway. The notion was further supported by the observed increase in eNOS activation upon CD38 inhibition in 78c-treated senescent endothelial cells (Fig 2).

Conclusion: Data presented here demonstrate an association between CD38 and microvascular function, which is modified by both age and sex. Furthermore, CD38 inhibition alleviates age-dependent vascular dysfunction, at least in part, through enhanced eNOS activation.

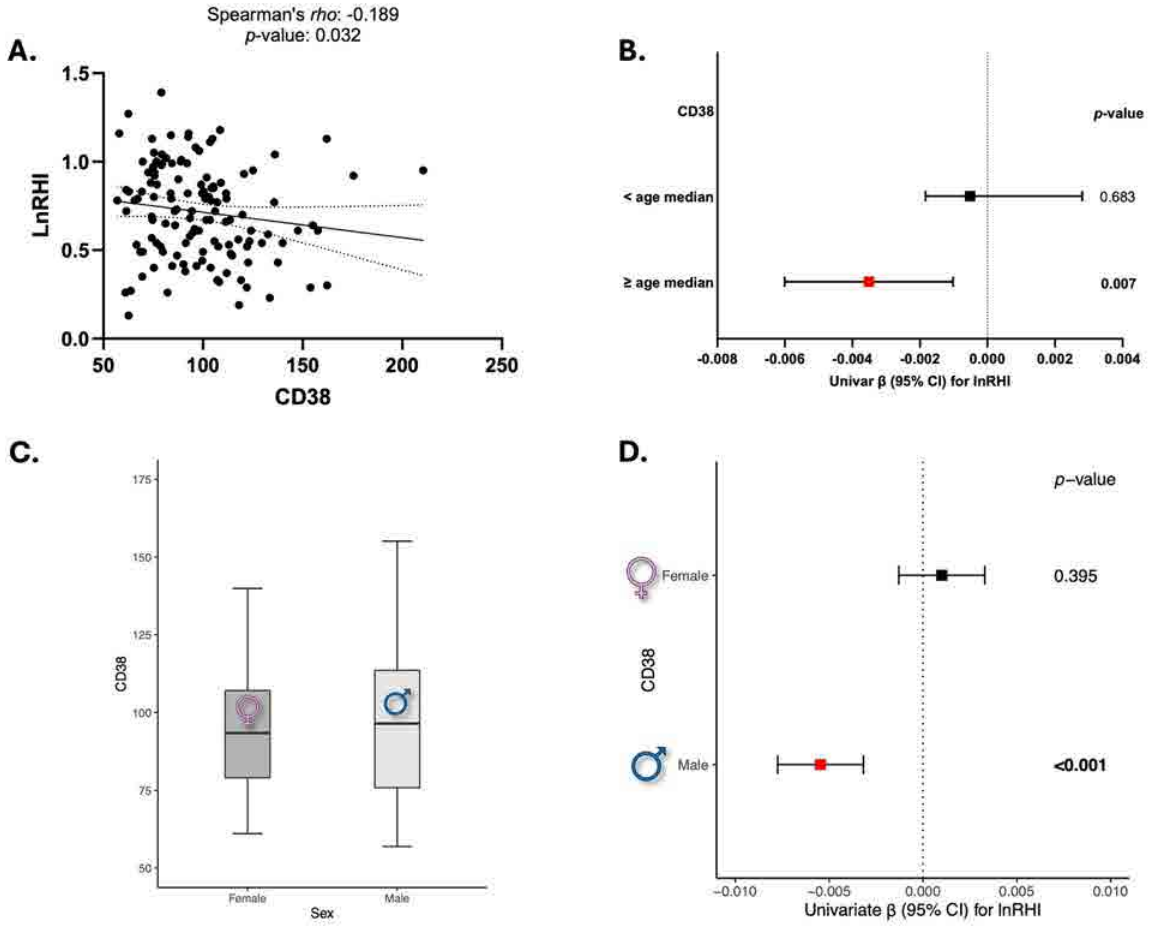

Figure 1. (A) Circulating CD38 levels were negatively correlated with the logarithmic scale of the reactive hyperemia index (lnRHI). (B) At the generalized linear model, this association was significant only in older individuals. (C) Circulating CD38 plasma levels were comparable between sexes. (D) The inverse association between plasma CD38 and lnRHI was significant in males but not in females.

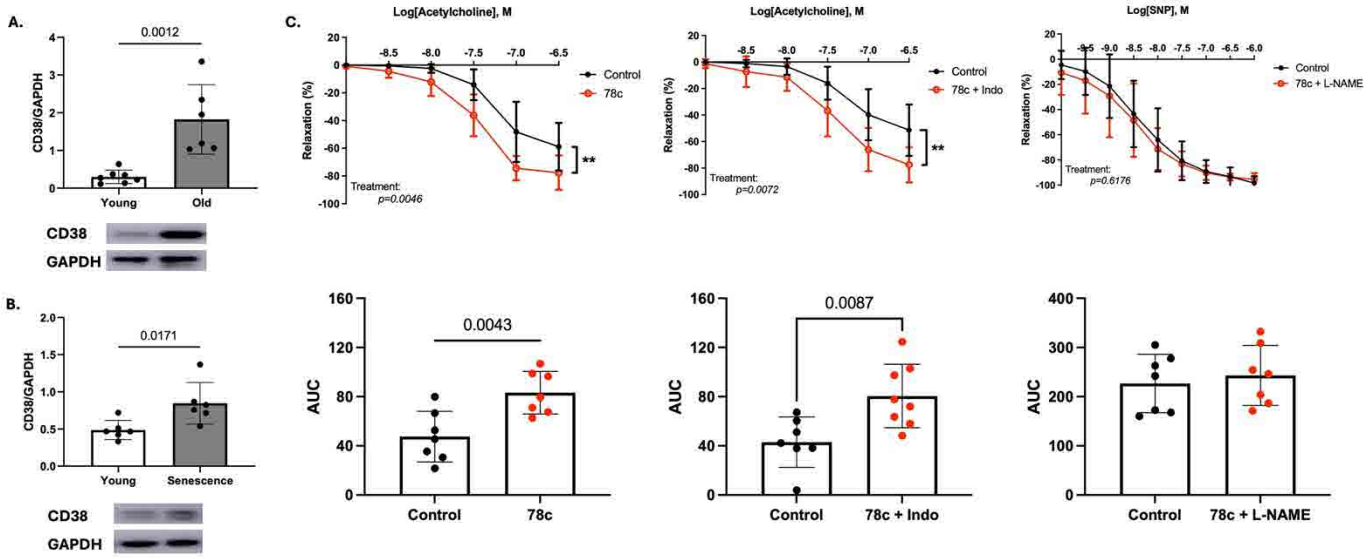

Figure 2. (A) Increased CD38 expression on aortas of aged mice and (B) senescent primary human aortic endothelial cells. (C) Effects of CD38 inhibition on aortic function. Concentration-dependent relaxations of intact thoracic aortic rings to acetylcholine (10^{-9}-$10^{-6.5}$M), with pre-incubation of indomethacin (10^{-5}M), and with pre-incubation of L-NAME (10^{-5}M), (n=8-6).

RAPID FIRE ABSTRACT SESSION "BASIC SCIENCES & RISK FACTORS"

O49

Metabolic Stress in Alveolar Macrophages Enhanced Inflammation and Pyroptosis

Valeria Masciovecchio[1], Era Gorica Hoxha[1], Jacopo Spezzini[1], Marialucia Telesca[1], Iliana Papadopoulou[2], Shafeeq Mohammed[1], Ludovica Di Venanzio[1], Francesco Paneni[1], Burkhard Ludewig[1], Frank Ruschitzka[1], Sarah Costantino[1]

[1]Center for Translational and Experimental Cardiology - CTEC, Schlieren, Switzerland, [2]Institute of Immunobiology, Kantonsspital St. Gallen, St. Gallen, Switzerland

Introduction: Heart failure with preserved ejection fraction (HFpEF) is a global public health issue associated with pulmonary hypertension (PH). PH is characterized by increased pulmonary resistance followed by right ventricular hypertrophy and failure. HFpEF exacerbates PH through systemic inflammation, metabolic dysregulation, and inflammatory mediators. This altered immune landscape, particularly the activation of alveolar macrophages, contributes to endothelial damage in the lungs, intensifying vascular remodeling. However, the exact mechanisms underlying PH remain unclear. We investigated the impact of cardiometabolic HFpEF-induced distress on alveolar macrophages and their role in endothelial damage in experimental PH.

Material and Methods: Mice were fed with high-fat diet and L-NAME for 15 weeks in order to recapitulate PH. At the end of treatment, echography, treadmill exhaustion tests, and lung congestion were obtained. Single nucleus RNA-Sequencing (snRNA-seq) was used for alveolar macrophage profiling. In vitro assays featured murine macrophages exposed to metabolic stress caused via palmitic acid (PA) were used.

Results: We demonstrated that murine HFpEF-induced PH (HFpEF-PH) leads to right ventricular remodeling and inflammation. SnRNA-seq identified upregulation of the Dusp1 gene in pulmonary macrophages of the HFpEF-PH group, emphasizing its regulatory role in modulating the alveolar macrophage response to metabolic and oxidative stress. In vitro metabolic stress in murine macrophages triggered oxidative stress, inflammation, and pyroptosis, with elevated markers such as IL-1β, TNF-α, and Caspase-1. Additionally, the autophagic machinery was disrupted, with genes like ATG14 and Beclin-1 upregulated and ATG7 downregulated. These changes promoted endothelial dysfunction through macrophage-derived secreted factors, linking metabolic stress to vascular pathology in HFpEF-PH.

Conclusion: SnRNA-seq of a murine model of PH induced by 15 weeks of a high-fat diet and L-NAME treatment revealed the impact of metabolic stress on alveolar macrophages. Our findings highlight the significant role of alveolar macrophages in PH and suggest new targets for PH treatment.

A

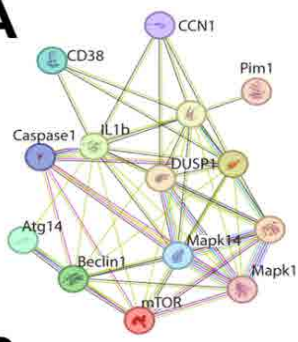

DUSP1		
Affected Pathway	Gene Count	FDR
MAP kinase activation, and Mitogen-activated protein	3 of 35	0.0021
Negative regulation of MAPK pathway	2 of 42	0.0142
Cytokine-mediated signaling pathway	3 of 371	0.0354
Negative regulation of catalytic activity	4 of 814	0.0331
Lysosome organization	2 of 87	0.0331
Negative regulation of cell cycle	3 of 353	0.0314
Cellular response to cytokine stimulus	7 of 810	3.28e-05
Regulation of apoptotic process	11 of 1652	3.19e-07

B

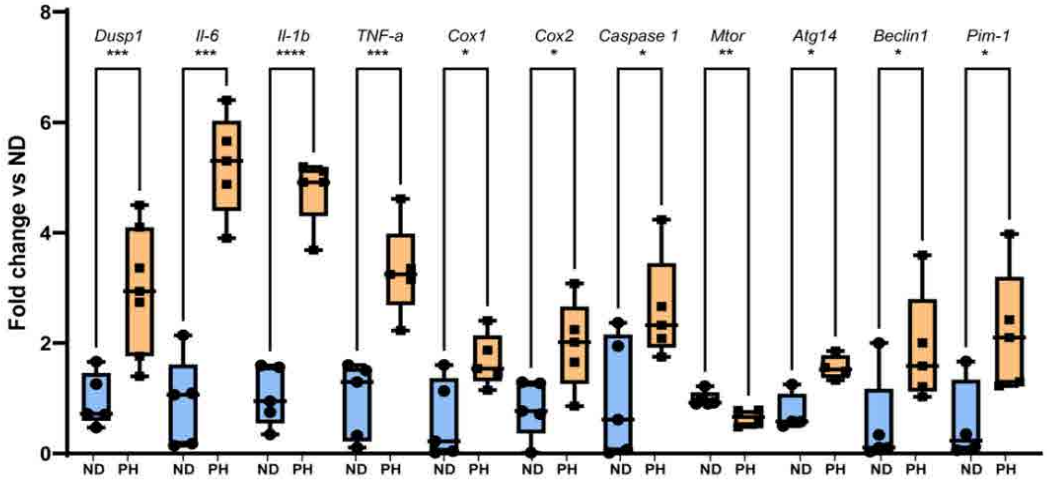

Figure 1: DUSP1-driven inflammation, disrupted autophagy, and pyroptosis in PH mice. **A)** Protein–protein interactions from the STRING database show top-ranking proteins interacting with DUSP1. DUSP1 displays strong interactions with several key proteins involved in various biological processes of macrophages, including those related to metabolism, inflammation, and cellular death. **B)** Molecular analysis of mice lung specimens reveals disrupted autophagy, pyroptosis, and inflammation in PH mice hearts compared to ND.

O50

Molecular damage patterns of cardiomyocytes during myocarditis and inflammatory cardiomyopathy revealed by spatial transcriptomics

Iliana Papadopoulou[1], Hung-Wei Cheng[1], Nadine Cadosch[1], Emily Payne[1 2], Christian Perez-Shibayama[1], Mechthild Lütge[1], Anna Joachimbauer[1 2], Frank Ruschitzka[2], Dörthe Schmidt[2], Cristina Gil-Cruz[1 2], Burkhard Ludewig[1 2]

[1]Institute of Immunobiology, Kantonsspital St. Gallen, St. Gallen, Switzerland, [2]Department of Cardiology, University Hospital Zurich, Zurich, Switzerland

Introduction: Immune cell infiltration and cardiomyocyte death represent the hallmarks of myocarditis. Acute myocarditis frequently triggers chronic inflammatory cardiomyopathy. Indeed, inflammatory stress drives cardiomyocytes towards apoptotic cell death leading to increased immune cell infiltration and activation, accelerated fibrosis, adverse remodeling, and, eventually, heart failure.

Material and Methods: We employed myosin heavy chain 6-specific T cell receptor transgenic mice (TCRM), which spontaneously develop CD4+ T cell-driven autoimmune myocarditis with subsequent inflammatory cardiomyopathy and heart failure. Single nucleus RNA-sequencing in combination with spatial transcriptomics analysis enabled us to characterize transcriptional, structural and interactome changes during disease progression. To generalize conclusions pertaining to human myocarditis, single nucleus RNA-sequencing data from human myocarditis and heart failure patients were analyzed.

Results: Our findings highlight the close interaction between cardiac fibroblasts, CD4 T cells and myeloid cells in inflammatory lesions. As the precise location of diverse cardiac cell types remains to be fully elucidated, we utilized a spatial resolution approach to examine the immunopathological alterations within the inflamed myocardium. The interplay among cardiac cells and the patterns of impaired cardiomyocytes were deciphered. Our analysis indicated discrete cellular neighborhoods in murine heart sections impacted by acute autoimmune myocarditis: (i) non-impaired regions underpinned by healthy cardiomyocytes (ii) highly inflamed regions homing activated fibroblasts, T cells, macrophages and damaged cardiomyocytes, (iii, iv) stressed and compensatory cardiomyocyte-speciifc regions, (v) and fibrotic niches populated by fibrotic fibroblasts and scarcely any stressed cardiomyocytes. Concurrently, we identified conservation of specific transcriptional profiles in murine and human cardiomyocytes.

Conclusion: Distinct cellular neighborhoods underpin the inflamed and failing heart. Spatial resolution of specific gene expression patterns in inflamed, stressed and fibrotic microenvironments of mouse and human hearts could bolster the identification of cardiomyocyte-preserving molecular circuits.

O51

Mechanisms of Aging associated Thrombus Formation: The dual-faced Role of Sphingosine-1-Phosphate.

Carolina Balbi[1], Evanthia Pavlidou[1], Pratintip Lee[1], Meret Allemann[1], Thomas F. Lüscher[1], Giovanni G. Camici[1], Jürg Beer[1]

[1]Center for Molecular Cardiology, University of Zürich, Schlieren, Switzerland

Introduction: Aging is linked to chronic inflammation ("inflammaging") and increased thrombus formation, contributing to cardiovascular events like stroke and heart attack. Platelets and megakaryocytes are central to these processes. Our single-cell RNA-seq analysis of aging bone marrow megakaryocytes (Mk) showed upregulation of the sphingosine-1-phosphate (S1P) transporter Mfsd2b. S1P is a lipid mediator involved in vascular integrity, inflammation, and thrombosis, and is increased in plasma upon platelet activation. Here, we investigate the role of S1P in thrombus formation in the aging, focusing on its molecular mechanisms and potential contributions to age-related cardiovascular risk.

Material and Methods: Bone marrow Mks were isolated from young (3 months) and old (24 months) mice for RNAseq. Tissue Factor (TF) expression was analyzed in TNFα-stimulated human aortic endothelial cells (hAECs) treated with different S1P concentrations. Platelet aggregation and thrombus formation were studied ex vivo in platelet-rich plasma (PRP) and whole blood from young donors treated with S1P.

Results: RNAseq revealed increased Mfsd2b expression and S1P plasma levels in aged mice. We found that high S1P levels (1μM) in TNFα-stimulated hAECs elevated TF expression and induced a pro-thrombotic phenotype. In sharp contrast, S1P levels at higher concentrations reduced platelet aggregation in PRP and thrombus formation in whole blood from young donors, with no effect at low concentrations.

Conclusion: Our data suggest an important dual role of S1P in thrombus formation: We propose that platelets from aged donors release increasingly more S1P, inducing a pro-thrombotic phenotype in endothelial cells. In contrast, platelets from young individuals store S1P effectively and counteract thrombus formation by promptly releasing higher amounts S1P upon activation (Figure1).

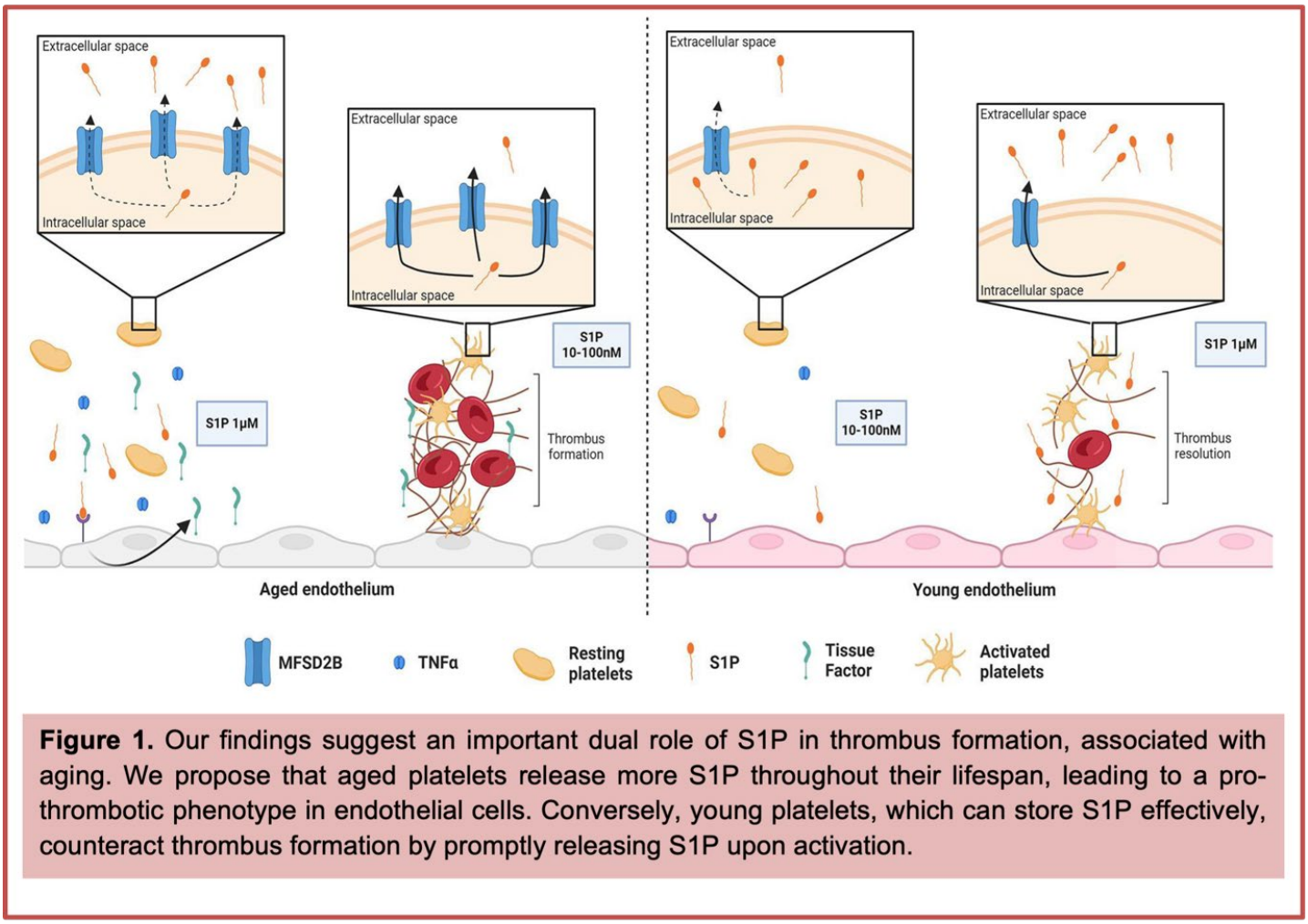

Figure 1. Our findings suggest an important dual role of S1P in thrombus formation, associated with aging. We propose that aged platelets release more S1P throughout their lifespan, leading to a pro-thrombotic phenotype in endothelial cells. Conversely, young platelets, which can store S1P effectively, counteract thrombus formation by promptly releasing S1P upon activation.

O52

Epigenetic Age of the Male and Female Heart: Insights into Cardiovascular Risk Assessment across Sexes

Alessia Mongelli[1], Antonella Farsetti[2], Nazha Hamdani[3], Frank Ruschitzka[4], Carlo Gaetano[5], Francesco Paneni[1]

[1]Center for Translational and Experimental Cardiology (CTEC), Department of Cardiology, University Hospital Zurich, University of Zurich, Zürich, Switzerland, [2]National Research Council (CNR)-IASI, Rome, Italy, [3]Department of cellular and translational Physiology, University of Bochum, Bochum, Germany, Bochum, Germany, [4]Department of Cardiology, University Hospital Zurich, zürich, Switzerland, [5]Laboratory of Epigenetics, ICS Salvatore Maugeri, Pavia, Italy

Introduction: Men and women show notable differences in symptoms/course and treatment of cardiovascular disease, suggesting the need for sex-specific biomarkers of cardiovascular damage. Chronological age is an established cardiovascular risk factor. However, people age differently, which matured the concept of "epi-genetic age determined by DNA metilation (DNAmAge)". The DNAmAge of a tissue provides information on its biological age and it can differ from the chronological age. Gathering information on the biological age of the heart could provide hints on premature cardiac aging and risk stratification. The discrepancy between chronological age and DNAmAge is defined as DeltaAge (= chronological years – DNAmAge years) and it has shown to predict mortality in humans. In this study, we assess sex-related differences in cardiac epigenetic age

Material and Methods: DNA was isolated from whole blood and heart specimens from women (N = 92) and men (N = 272) who underwent elective cardiac surgery for valve replacement or coronary artery bypass. After isolation, DNA was processed to convert the un-methylated cytosines to uracile. PCR reaction was used to amplify the target sequences followed by pyrosequencing to determine the methylation level of age-related CpGs

Results: Women were chronologically older than men (69.9±7 vs 64.6±9 years, $p<0.05$), while the 2 groups were comparable for cardiovascular risk factors. DeltaAge assessed in whole blood samples showed comparable values of chronological and epigenetic age in women and men (Figure1). BY contrast, DeltaAge assessed in cardiac specimens showed that 15.1% of women were biologically older (as compared to their chronological age) while a much higher rate (34.5%) was observed for men

Conclusion: We show that men's heart is at least 2 times older than the female heart. Our study could set the stage for larger studies leveraging the epigenetic clock as a molecular marker of premature aging and clinical outcome in men and women

Figure 1

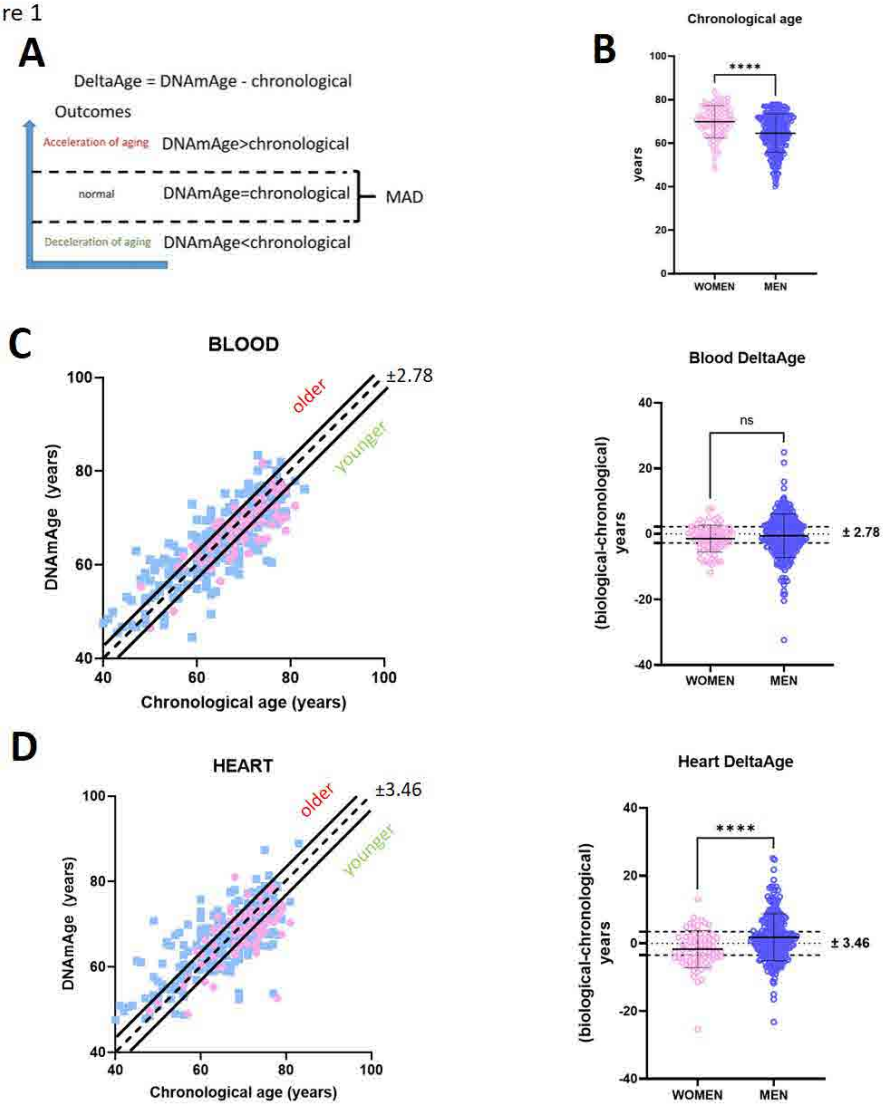

Cardiac-specific epigenetic clock of the male and female heart. A) Definition of DeltaAge: discrepancy between epigenetic age (DNAmAge) and chronological age. The DeltaAge defines three outcomes: biologically older; choeval (within the normal range) and biologically younger. **B**) Chronological age of male and female individuals. In the examined cohort, women were chronologically older than men . **C**) Blood DNAmAge and DeltaAge. Left: plot of chronological and DNAmAge estimated by a blood-specific formula; right: Whole blood DeltaAge in women and men (no differences). **D**) Heart DNAmAge and DeltaAge. Left: plot of chronological and DNAmAge estimated by the cardiac-specific formula; right: DeltaAge in heart specimens from men and women. Epigenetic age is higher in the male heart.

O53

NF-κB Interacting long non-coding RNA (NKILA) predicts major adverse cardiovascular events in the elderly: a prospective cohort study

Stefano Ministrini[1 2], Yustina M Puspitasari[1], Simon Kraler[1 3], Tetiana Lapikova-Bryhinska[1], Shafeeq Mohamed[4], Sarah Costantino[4], Francesco Paneni[4], Susan Bengs[1], Luca Liberale[5 6], Alexander Akhmedov[1], Margareta Hinterberger[7], Peter Riederer[8], Thomas F. Lüscher[1 9], Edna Grünblatt[10], Giovanni G. Camici[1 11]

[1]Center for Molecular Cardiology, University of Zurich, Schlieren, Switzerland, [2]Department of Cardiology, Luzerner Kantonspital, Luzern, Switzerland, [3]Department of Cardiology, Kantonspital Baden, Baden, Switzerland, [4]Center for Translational and Experimental Cardiology, Zurich University Hospital, Schlieren, Switzerland, [5]Department of Internal Medicine, University of Genoa, Genoa, Italy, [6]IRCCS Ospedale Policlinico San Martino, Genoa, Italy, [7]Department of Psychiatry, Danube Hospital Vienna, Vienna, Austria, [8]Clinic and Policlinic of Psychiatry, Psychosomatics and Psychotherapy, University Hospital of Würzburg, Würzburg, Germany, [9]Royal Brompton and Harefield Hospitals and Imperial College, London, United Kingdom, [10]Department of Child and Adolescent Psychiatry and Psychotherapy, Psychiatric University Hospital Zurich, Schlieren, Switzerland, [11]Department of Research and Education, Zurich University Hospital, Zürich, Switzerland

Introduction: NF-κB Interacting long non-coding RNA (NKILA) regulates the translocation of the transcription factor NF-κB and inhibits its transcriptional action, with divergent effects on vascular function. However, its predictive utility in the elderly remains unknown. We hypothesize that NKILA could be a novel predictor of major adverse cardiovascular events (MACE) in elderly patients depending on background cardiovascular risk.

Material and Methods: A total of 300 individuals aged 75 years old, prospectively recruited in the Vienna Transdanube Aging (VITA) cohort, were included. Plasma was collected at enrolment. Circulating lncRNA was detected using real-time quantitative polymerase chain reaction. The primary endpoint was MACE, defined as a composite measure of coronary artery disease, non-fatal myocardial infarction or stroke, and peripheral artery disease over a 7.5-year follow-up. The association between circulating NKILA and incident MACE was analyzed by the Kaplan-Meier method. Predictive performance was assessed by the area under receiver-operator characteristic curve (AUC).

Results: Subjects with circulating levels of NKILA in the upper tertiles had a higher MACE incidence compared to those in the lowest tertile (I tertile vs II tertile p = 0.026; I tertile vs III tertile p = 0.032; OR for II/III tertile = 9.49; Figure 1). The association between NKILA and incident MACE was independent potential confounder (adjusted OR = 15.45, p = 0.034). In sensitivity analyses, the discriminatory performance of NKILA was better in those with a history of MACE compared to subjects with previous MACE (AUC = 0.616 vs AUC = 0.759; Figure 2).

Conclusion: NKILA predicts the incidence of MACE in elderly subjects, with a better performance in those at high background risk. Hence, NKILA is a potential epigenetic regulator of cardiovascular ageing and age-related diseases. Independent studies are warranted to validate NKILA as a novel predictor of MACE in elderly subjects at high cardiovascular risk.

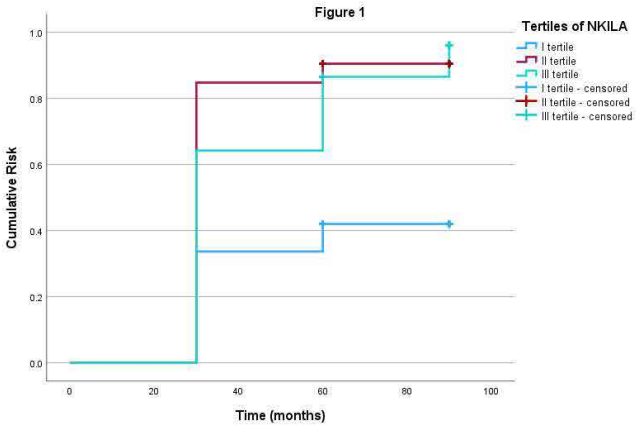

Figure 2

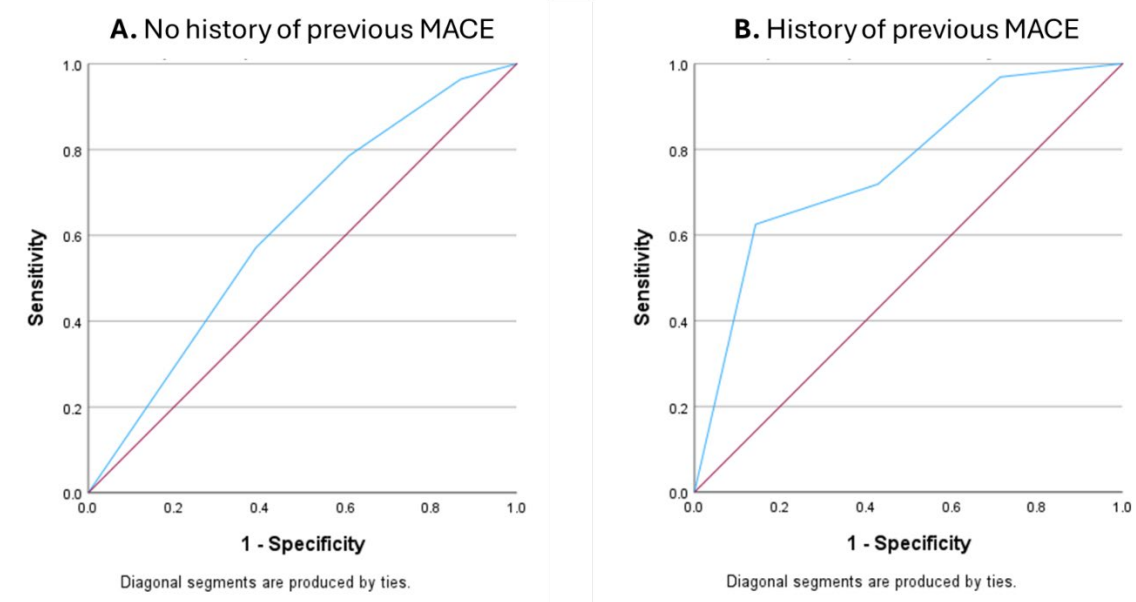

O54

Prognostic comparison of cTPA with coronary calcium for cardiovascular risk stratification

Michel Romanens[1], Ansgar Adams[2], Thomas D. Szucs[3], Nisha Arenja[4], Michel Wenger[5], Isabella Sudano[6]

[1]Vascular risk foundation, Varifo, Olten, Switzerland, [2]BAD Gesundheitsvorsorge und Sicherheitstechnik GmbH, Bonn, Germany, [3]European Centre of Pharmaceutical Medicine (ECPM), Basel, Switzerland, [4]Private practice, Grenchen, Switzerland, [5]Private practice, Binningen, Switzerland, [6]University Heart Centre, Cardiology, University Hospital, Zürich, Switzerland

Introduction: Evidence suggests carotid ultrasound has comparable prognostic information regarding cardiovascular events or death when compared to coronary calcium scoring derived from computed tomography.

Material and Methods: In this single-center study, we used standard imaging procedures for carotid total plaque area (cTPA) and coronary calcium Agatston scores (CCS) obtained between 2003 and 2024, performed a long-term follow-up in 472 cardiology patients (69% male, age 60 ± 9 years, 12% in secondary prevention) over 10 ± 7 years.

Results: We observed 63 events (15 PTCA, 4 CABG, 11 AMI, 5 STROKE/TIA, 28 deaths). Using COX multivariate forward regression with 7 clinical and 3 laboratory variables, the hazard ratio of cTPA>62 mm2 was 1.42 (95%CI 1.03 - 1.95, p = 0.03) and for CAC>100 was 1.74 (95%CI 1.39 - 2.19, p<0.0001). Using 3 categories of risk markers (low-intermediate, high, very high) in Cox regression, posttest risk of cTPA showed a hazard ratio of 1.56 (95%CI 1.14 - 2.13, p = 0.0053) and of CAC showed a hazard ratio of 2.26 (95%CI 1.61 - 3.16, p<0.0001), while SCORE2/-OP was excluded from the model. Net reclassification improvement was statistically not significant for cTPA (NRI 3% ± 12% p = 0.76), but was significant with CAC (NRI 29% ± 11%, p = 0.01). Area under the curve was statistically comparable for SCORE2/-OP, SCORE2TPA and SCORE2CAC (0.64, 0.63, 0.69 respectively, p = NS for the difference).

Conclusion: In cardiology patients with initial assessment of cardiovascular risk based upon SCORE2/-OP and two atherosclerosis imaging modalities, cTPA and CAC added significant and statistically comparable risk information. Given the lower cost and better environmentally friendliness, cTPA should be the initial imaging test to enhance risk prediction beyond cardiovascular risk factors.

Table 1: baseline characteristics of patients, with and without a clinical event

	ALL	EVENT	NO EVENT	p=
Patients	473	63	410	
Male	328	49	279	<0.0001
Male %	69	78	68	
Smoker	122	24	98	0.0166
Smoker %	26	38	24	
Diabetes Mellitus	50	11	39	0.0499
Diabetes Mellitus %	11	17	10	
Fam Hx ASCVD	90	12	78	0.9965
Fam Hx ASCVD %	19	19	19	
Statins and/or BP medication	202	32	170	0.1638
Statins and/or BP medication %	43	51	41	
Secondary Prevention	59	15	44	0.0035
Secondary Prevention %	12	24	11	
cTPA>62 mm^2	174	34	140	0.0024
cTPA>62 mm^2 %	37	54	34	
CCS> 100	135	46	89	0.0004
CCS> 100 %	29	73	22	
Age ± SD	60 ± 9	62 ± 9	60 ± 9	0.0602
BPs ± SD	131 ± 20	134 ± 20	131 ± 19	0.171
Cholesterol mmol/l ± SD	5.4 ± 1.0	5.4 ± 0.9	5.4 ± 1.1	0.7769
HDL mmol/l ± SD	1.4 ± 10.4	1.3 ± 0.2	1.4 ± 0.4	0.3388
SCORE2/-OP	6.4 ± 4.1	8.3 ± 4.9	6.2 ± 3.8	0.0002
SCORE2/-OP TPA	11.5 ± 10.2	15.8 ± 11.6	10.8 ± 9.8	0.0007
SCORE2/-OP CAC	10.5 ± 9.6	15.8 ± 10.0	9.7 ± 9.2	<0.0001
cTPA ± SD	62 ± 56	77 ± 59	58 ± 55	0.0082
CCS ± SD	158 ± 513	328 ± 679	155 ± 479	<0.0001
TIME years	10 ± 7	10 ± 6	10 ± 7	0.3847

Table 2: Hazard ratios, C-Statistics and Net Reclassification Improvement of cTPA, CAC, SCORE2/-OP and SCORE2/-OP posttest risk (based on CAC or cTPA)

N=473	HR (95% 95%-CI)	HR P value	C-Statistic	C-Statistic P value	NRI ± SE
CVD or DEATH (N=63)					
SCORE2/_OP alone	---	---	0.64	0.0003	---
+ CAC code	2.26 (1.61-3.16)	<0.0001	0.66	<0.0001	29% ± 11%
+ cTPA code	1.38 (1.01-1.89)	0.0427	0.60	0.0082	3% ± 11%

RAPID FIRE ABSTRACT SESSION "CLINICAL CASES 2"

O55

From ischemic stroke to diagnosis: Danon disease as rare genetic cause of cardiomyopathy in a young woman

Esther Scheirlynck[1], Laura Anna Leo[1], Giovanni Pedrazzini[1], Anna Giulia Pavon[1], Fabio Cattaneo[1], Manuela Averaimo[1], Francesca Romana Scopigni[1], Giulio Conte[1]

[1]Cardiocentro Ticino Institute, Ente Ospedaliero Cantonale, Lugano, Switzerland; Faculty of Biomedical Sciences, Università della Svizzera Italiana, Lugano, Switzerland

Introduction: This case outlines the challenging diagnosis of a young woman who presented with ischemic stroke and underlying cardiomyopathy. Despite the absence of typical clinical features, multimodal assessment revealed Danon disease, a rare genetic cause of cardiomyopathy in young patients.

Results: A 19-year-old girl with no significant medical history presented to the emergency department with left-sided hemiplegia, caused by an acute ischemic stroke. She was treated with systemic fibrinolysis and mechanical thrombectomy, achieving complete recanalization and neurological recovery.

The patient experienced mild muscle weakness over the last few months, had no visual impairment and normal intellectual development. The electrocardiogram showed sinus rhythm with low-voltage fragmented QRS complexes and diffuse T-wave inversions. Transthoracic echocardiography revealed a mixed hypertrophic and dilated cardiomyopathy with severe biventricular dysfunction. Cardiac MRI demonstrated extensive mid-myocardial late-enhancement and increased extracellular volume, affecting both ventricles. Endomyocardial biopsy revealed myocardial hypertrophy, interstitial fibrosis, and cytoplasmic vacuolization. Genetic testing, utilizing a cardiomyopathy gene panel, ultimately identified a pathogenic nonsense variant in LAMP2 (c.973del; p.Leu325TrpfsTer21), confirming the diagnosis of Danon disease. Neurological, ophthalmological, and hepatological evaluations are planned to assess extracardiac manifestations.

Heart failure therapy and oral anticoagulation were initiated. Episodes of non-sustained ventricular tachycardia led to the implantation of an implantable cardioverter defibrillator. She was subsequently referred to a cardiac transplantation centre and was listed for heart transplantation prior to discharge.

Conclusion: Danon disease is an X-linked dominant cardioskeletal myopathy caused by loss-of-function variants in LAMP2. The X-linked inheritance pattern complicates diagnosis in females, as clinical manifestations can vary widely. This case underscores the importance of genetic testing in the diagnostic evaluation of young patients with severe cardiomyopathy. The diagnosis of Danon disease impacted strongly on prognosis given the high incidence of sudden cardiac death and terminal heart failure. While no disease-specific treatment is currently available, an ongoing gene therapy trial holds promise.

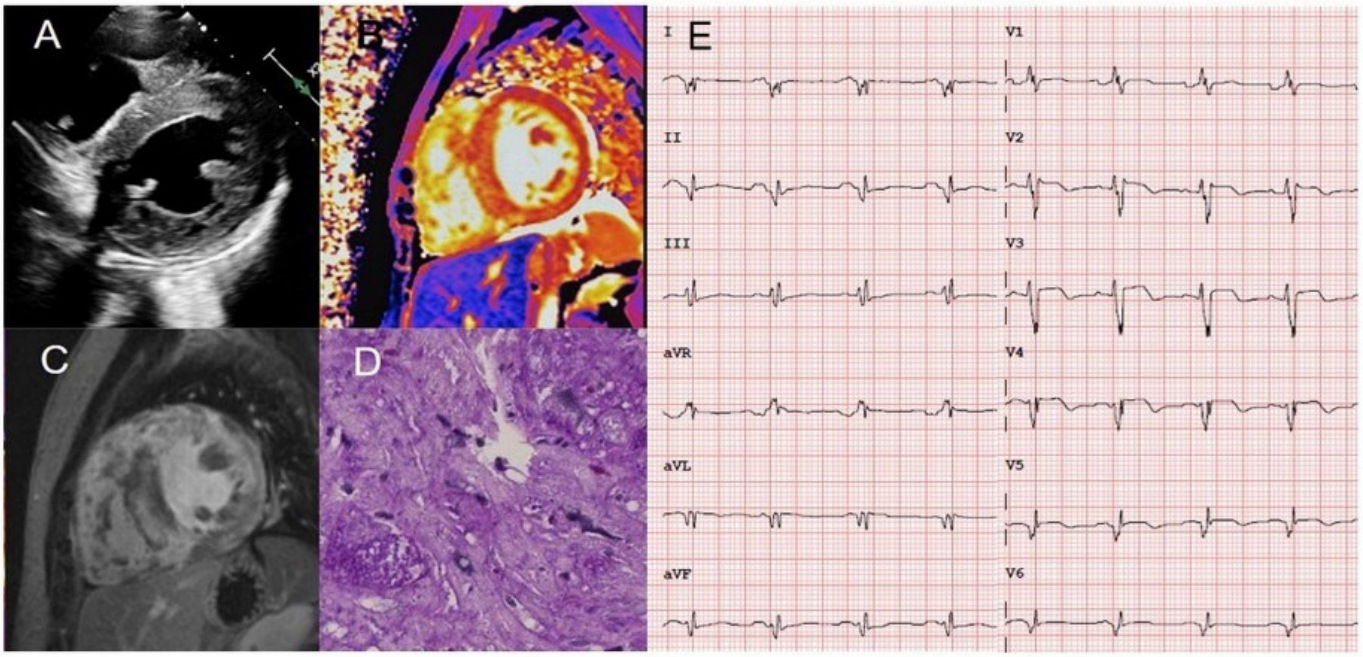

Fig. 1 Short axis (A) TTE, (B) T1 mapping CMR, (C) LGE CMR. (D) PAS staining endomyocardial biopsy. (E) ECG.

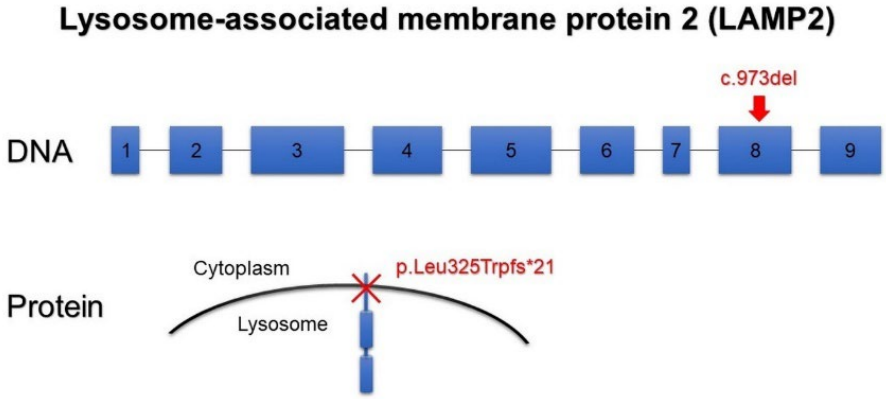

Fig. 2 Deletion of 1 base pair in exon 8 of the *LAMP2* gene, leading to a premature stop codon, and missing transmembrane and cytoplasmic domains of the protein.

O56

ECG with Anterior T-wave inversion in Caucasian Healthy Athletes: Cardiomyopathy or Athlete's Heart?

Patricia Lista[1], Riccardo Pin[1], Stefano Muzzarelli[2], Andrea Menafoglio[3], Marcello Di Valentino[1]

[1]Clinica Luganese Moncucco, Lugano, Switzerland, [2]Regional Hospital Locarno, La Carità, Locarno, Switzerland, [3]Regional Hospital of Bellinzona, Bellinzona, Switzerland

Introduction: A 39-year-old male referred to us for further investigation due to an abnormal ECG (Figure 1.). It emerged during a routine medical examination in a sports medicine center. The patient participates in amateur sports since the last 10 years and engaged before in competitive sports. He never complained any symptoms and, his family history is negative. Due to the ECG findings, any physical activity was restricted until undergoing a transthoracic echocardiography (TTE) and cardiac magnetic resonance imaging (CMR). The ECG performed in our ambulatory (Figure 3) showed a normal sinus rhythm with minimal alterations in repolarization. We recuperated the ECG from 15 years ago which was completely normal (Figure 2).

Material and Methods: The TTE showed normal size and function of both heart chambers making an Arrhythmogenic Cardiomyopathy (ACM) or Hypertrophic Cardiomyopathy (HCM) unlikely. The CMR, done at the patient's insistence due to anxiety, showed no abnormalities.

Results: Anterior (V1–V4) T-wave inversion (TWI) on an athlete's ECG is often considered abnormal, warranting evaluation to rule out conditions like ACM and HCM. The ECG in Figure 1 however shows anterior TWI preceded by J-point elevation, which is commonly seen in athletes due to a

physiological increase in vagal tone and physiological remodeling, representing a benign manifestation of intensive training (Figure 4). Their prevalence differs among ethnicities ranging from 2-28%. Whereas ST-segment elevation without J-point elevation preceding anterior TWI represent a cardiac pathology (Figure 5-6). Nevertheless, some features between athlete's heart, HCM and ARVC might overlap where a clear discrimination is challenging, needing further examination. The following flow chart (Figure 6) can be used to differentiate between normal and abnormal ECG in healthy athletes.

Conclusion: Careful ECG analysis in healthy athletes is crucial to avoid unnecessary exams and unnecessary anxiety.

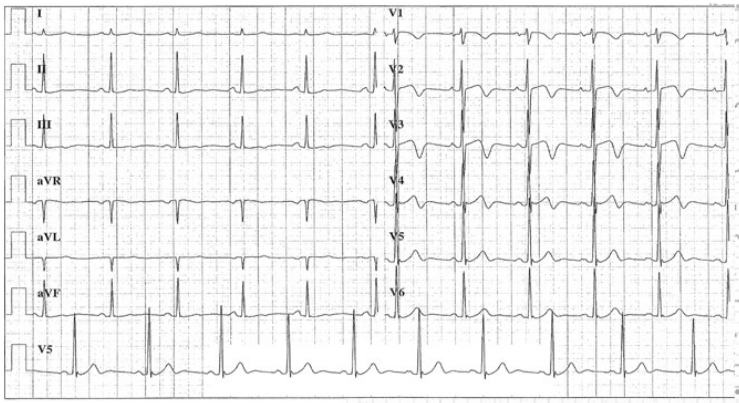

Figure 1

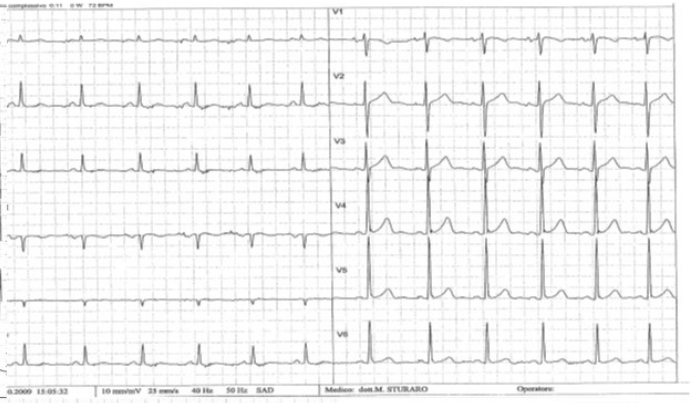

Figure 2

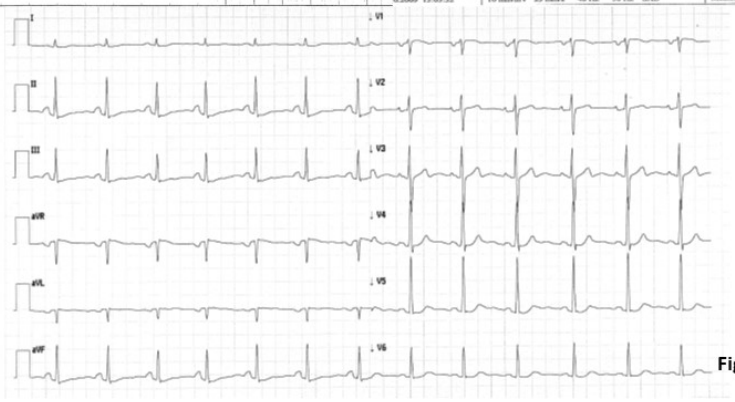

Figure 3

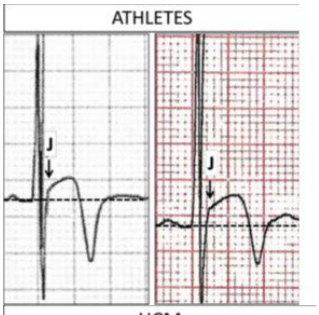

Figure 4

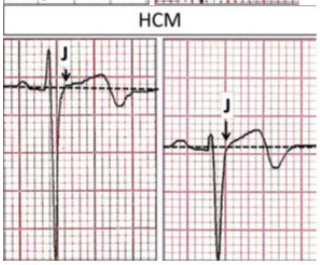

Figure 5

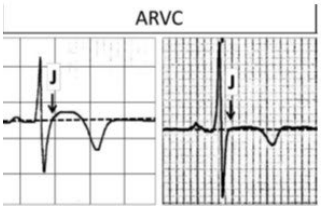

Figure 6

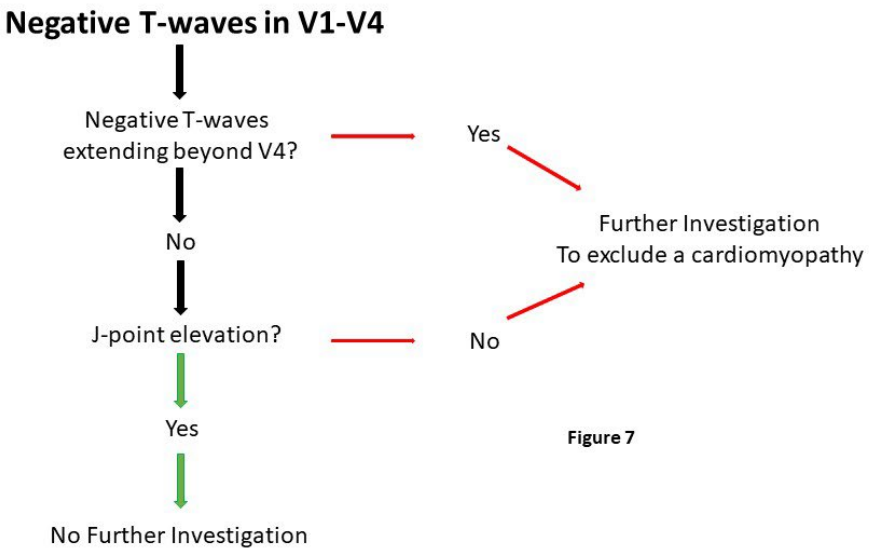

Figure 7

O57

Fully percutaneous treatment of LVOT-obstruction and severe mitral regurgitation in a patient with a history of acromegaly

Lucca Loretz[1], Stefan Toggweiler[1], Federico Moccetti[1], Mathias Wolfrum, Bart De Boeck[1], Matthias Bossard[1], Adrian Attinger-Toller[1], Yves Suter[2], Florim Cuculi[1], Simon Stämpfli[1]

[1]Herzzentrum Luzerner Kantonsspital, Luzern, Switzerland, [2]Luzerner Kantonsspital Wolhusen, Wolhusen, Switzerland

Introduction: We report a 79-year-old lady with congestive heart failure. The patient had a history of acromegaly due to a pituitary macroadenoma which had been surgically treated and the patient has since been in remission.

Material and Methods: ECG showed supraventricular tachycardia. Echocardiography revealed severe mitral regurgitation due to flail of the posterior leaflet as well as a peak pressure gradient in the left ventricular outflow tract of 107mmHg due to basal septal hypertrophy, although severe aortic stenosis could not be ruled out initially. Heart catheterization revealed coronary artery disease of the left anterior descending artery and elevated left atrial pressure of 41mmHg. Severe aortic stenosis could be ruled out by invasive pressure measurement.

Results: After successful Valsalva-maneuver to terminate the supraventricular tachycardia, the patient was administered to the ward and treated with i.v. diuretics. Laboratory analysis ruled out recurrence of hormone-active macroadenoma. After heart team decision, alcohol septal ablation and concomitant percutaneous coronary intervention was performed with subsequent mitral transcatheter edge-to-edge repair which resulted in a reduction of mitral regurgitation from severe to mild-to-moderate, reduction of LVOT gradient to 40mmHg and mean LAP to 8 mmHg. The patient was discharged home 2 days after mitral TEER.

Conclusion: In this complex scenario, we successfully performed PCI, TASH and mitral TEER. We are only aware of one other case of TASH in a patient with acromegaly. With todays advanced interventional techniques, elderly patients with complex pathologies may be successfully treated with a short recovery period and early discharge.

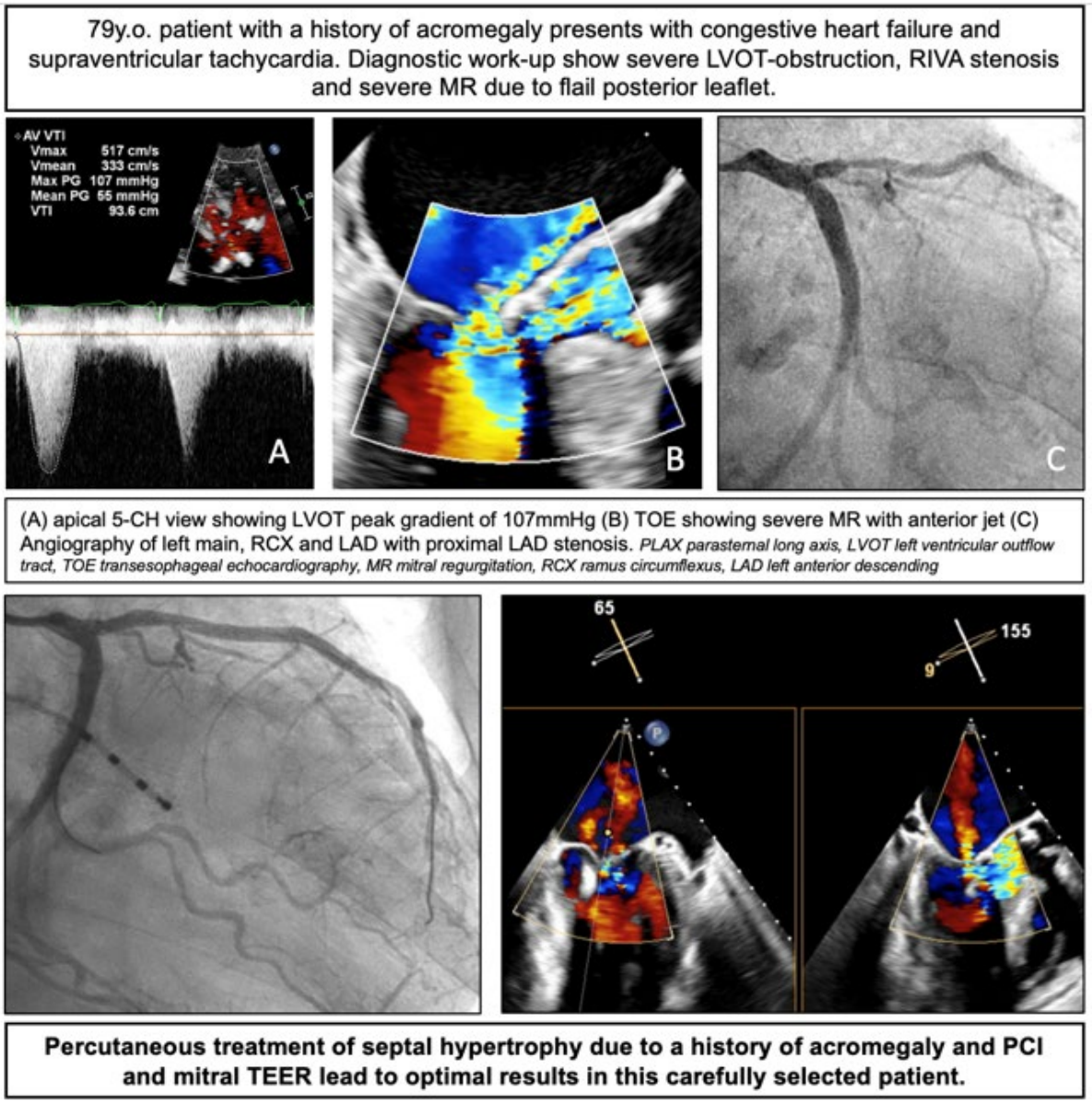

O58

Trans-baffle pulmonary vein isolation using a dual energy lattice tip catheter in a patient after mustard procedure

Salik Ur Rehman Iqbal[1], Tobias Reichlin[1], Laurent Roten[1]
[1]*Inselspital, University of Bern, Bern, Switzerland*

Introduction: A 26-year-old male with d-TGA post-Mustard procedure presented with symptomatic atrial flutter and rapid ventricular response. A 7-day ECG confirmed atrial flutter with 1: 1 AV conduction and heart rates up to 280 bpm. Echocardiography revealed a hypertrophic systemic right ventricle with reduced systolic function (RVEF 42%).

Material and Methods: Electrophysiological study induced intra-atrial reentry tachycardia (cycle length = 240 ms) , with transbaffle puncture performed at the inferior limb roof using a specialized 71-cm-NRG needle under 3D-Electroanatomical (EAM) guidance and TEE. A 9 mm diameter, lattice-tip catheter (Sphere-9, Affera, Inc.) was used for 3D-EAM. Mapping revealed scar tissue at the superior septum between the systemic venous baffle (SVB) and the right superior pulmonary vein. Phrenic nerve mapping was performed to avoid nerve damage. Ablation therapy utilized a dual-energy (radiofrequency and pulsed-field) lattice-tip catheter for precise mapping and ablation, enabling a seamless workflow without catheter exchanges.

Results: Radiofrequency ablation (RFA) at the superior end of the slow conduction zone terminated the arrhythmia into sinus rhythm. Right pulmonary vein isolation was achieved with combined RFA and pulsed-field ablation (PFA), while left pulmonary vein isolation was done exclusively with PFA. A cavotricuspid isthmus (CTI) line was created using RFA, achieving bidirectional conduction block. Re-evaluation confirmed pulmonary vein isolation and CTI block, with additional ablations completing the CTI line, Figures 1, A-D. The procedure, completed in 146 minutes with 8 minutes of fluoroscopy, successfully terminated atrial tachyarrhythmias. The patient was discharged in sinus rhythm with follow-up planned in 3 months.

Conclusion: This case demonstrates the first use of a dual-energy lattice-tip catheter in a post-Mustard repair patient, highlighting its versatility for safe, efficient mapping and ablation. The catheter integrates mapping and ablation, enabling accurate lesion delivery while minimizing risks. This case highlights significant benefits for managing arrhythmias in complex congenital heart disease patients.

Figure 1-A, Voltage map of the pulmonary venous baffle (PVB) (cranial view). Note the low voltage scar area indicated by the yellow arrow (insertion site of the SVB). 1-B, Local activation map of the intraatrial re-entry tachycardia (cranial view) of the PVB. Arrows (yellow) indicate the direction of propagation of wavefront. 1-C, RAO view showing the CTI ablation line (red dots) spanning both the SVB and PVB. 1-D, Right posterior oblique view demonstrating both WACA around the right and left pulmonary veins. The wide area circumferential ablation (WACA) around the right pulmonary veins was connected to the scar.

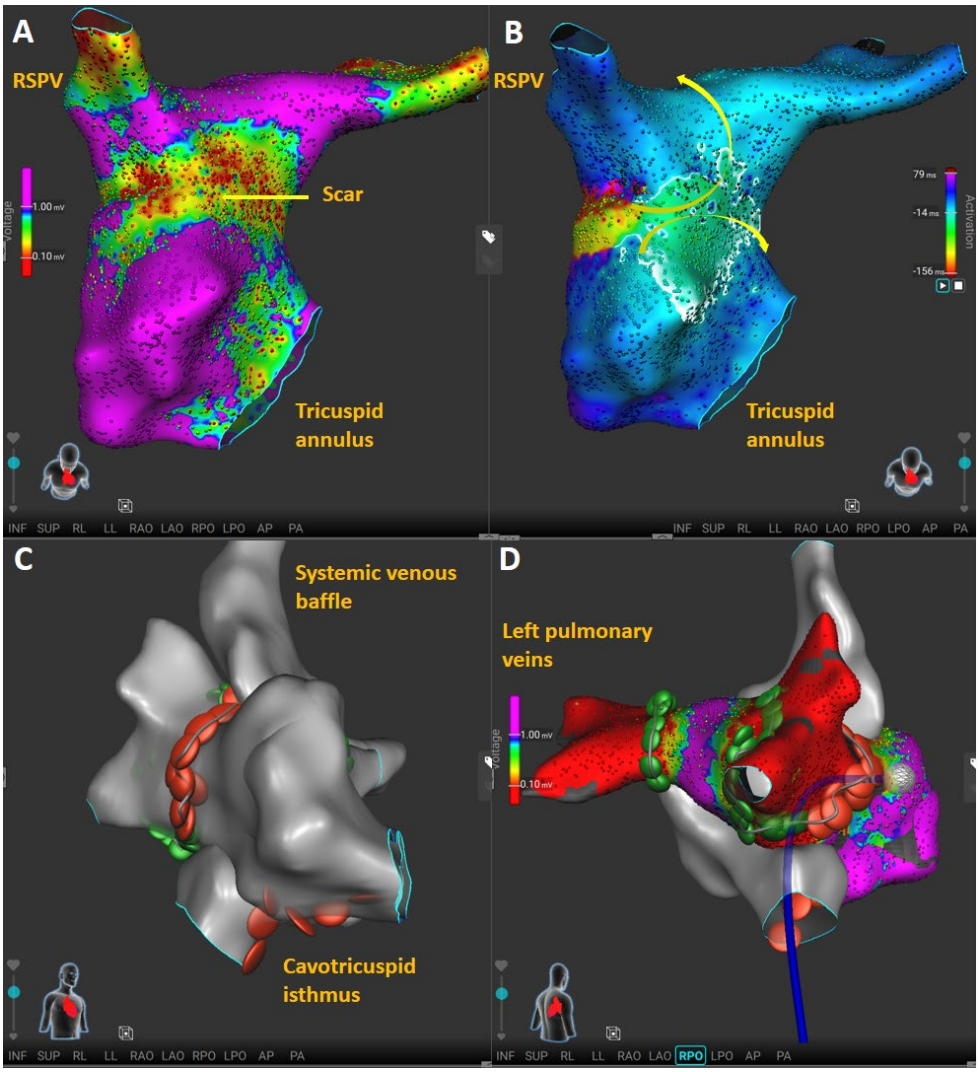

O59

Sudden Cardiac Death in a Young Athlete: A Novel Association of arrhythmogenic right ventricular cardiomyopathy with GJA1 and KCNQ1 Variants.

Lucas Tramèr[1], Ardan Saguner[2]

[1]Universitätsspital Zürich (USZ), Klinik für Kardiologie, Zürich, Switzerland, [2]Universitätsspital Zürich (USZ), Klinik für Kardiologie, Zürich, Switzerland

Introduction: A 31-year-old athletic Caucasian man without prior cardiac history experienced sudden cardiac death (SCD) during sleep. Autopsy revealed extensive fibrofatty infiltration of the right ventricle (RV), consistent with arrhythmogenic right ventricular cardiomyopathy (ARVC), and syndactyly. Genetic testing identified a previously described pathogenic heterozygous KCNQ1 missense variant (c.776G>A, p.(Arg259His) associated with the long QT syndrome type 1 and a previously described likely pathogenic heterozygous GJA1 missense variant (c.443G>A, p.(Arg148Gln) encoding connexin-43 (Cx43), a gap-junction protein involved in cardiac conduction and the pathophysiology of ARVC. GJA1 has been linked to cardiocutaneous syndromes, SCD, dilated cardiomyopathy, congenital heart malformations, syndactyly, oculodentodigital dysplasia and neurological disease, but not to ARVC.

Material and Methods: Cascade genetic screening revealed that the father carried the KCNQ1 variant and the mother the GJA1 variant. Syndactyly was present in the mother and brother, both GJA1-positive. One sister also carried this variant and had severe gait ataxia. The father and younger sister, both carrying the KCNQ1 variant, showed discrete ST-depressions at rest but a normal QTc and echocardiogram, remaining asymptomatic. None of the first-degree relatives showed an ARVC phenotype.

Results: Cx43 dysfunction, known to affect desmosomes in ARVC, may have disrupted connexome integrity, contributing to RV fibrofatty replacement and arrhythmogenicity. The absence of an ARVC phenotype in GJA1-positive relatives may be explained by the extensive endurance activity of the index patient, triggering the disease. The KCNQ1 variant, though not prolonging QTc in family members, may have contributed to arrhythmogenicity through subtle electrophysiological changes. This constellation of genetic and environmental factors likely culminated in SCD.

Conclusion: This is the first documented case linking GJA1 and KCNQ1 variants to ARVC, highlighting the interplay of multiple interacting genetic variants in SCD. It underscores the importance of thorough genetic and family screening in the diagnostic process and risk assessment in cardiomyopathies and channelopathies.

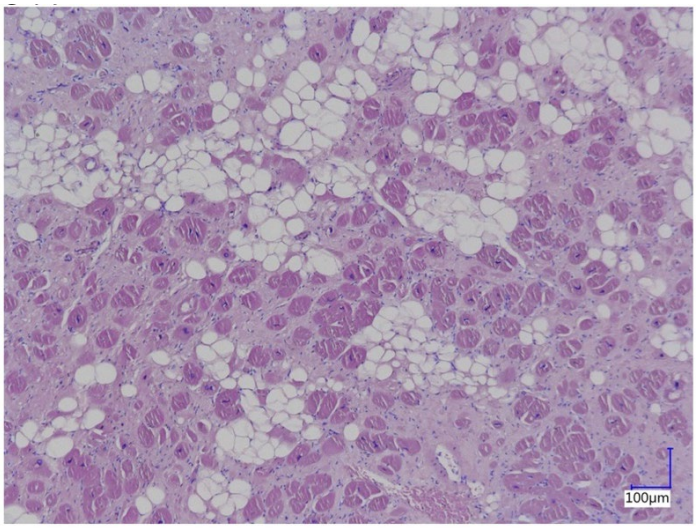

Figure 1: Histological section (200x) of the right ventricle obtained during autopsy. The section shows extensive fibrofatty replacement, consistent with ARVC.

RAPID FIRE ABSTRACT SESSION "RHYTHM DISORDERS 2"

O60

Pulsed field ablation for index pulmonary vein isolation: 3-year learning curve and the influence of adjunctive 3D mapping

Thomas Kueffer[1], Raphael King[1], Jens Maurhofer[1], Salik Ur Rehman Iqbal[1], Gregor Thalmann[1], Nikola Kozhuharov[1], Oskar Galuszka[1], Helge Servatus[1], Andreas Haeberlin[1], Fabian Noti[1], Hildegard Tanner[1], Laurent Roten[1], Tobias Reichlin[1]

[1]Department of Cardiology, Inselspital, Bern University Hospital, University of Bern, Bern, Switzerland

Introduction: The learning curve for pulmonary vein isolation (PVI) using "single-shot" pulsed-field ablation (PFA) is thought to be short. We analyze performance markers over time for PVI using PFA and 3D-EAM.

Material and Methods: Consecutive patients with AF undergoing a first PVI with PFA from May-2021-to-April-2024 were included. A learning curve was estimated using an exponential fit to procedure and fluoroscopy times of PVI-only procedures without the use of 3D-EAM. Patients were followed using 7d-Holter ECG at 3, 6, and 12 months. During clinically indicated repeat ablations, 3D mapping was used to assess PVI durability. Using procedure duration, fluoroscopy time, and PV-durability, two cutoffs are proposed to discern between learning curve, intermediate phase, and proficiency.

Results: A total of 1009 AF patients underwent a first PVI using PFA. In 458 (45%) cases, 3D-EAM was used, in 264/702 (37%) for PVI-only cases and 192/298 (64%) for cases involving additional lesions. Procedure and fluoroscopy time were steady after 18 and 8 procedures with a mean of 53 min and 15 min, respectively. Pulmonary vein durability increased from a median of 50% (2 veins) for the first 60 procedures per operator to a median of 75% (3 veins) thereafter (p = 0.02). Freedom from any atrial arrhythmia at 1 year was similar for patients treated during the learning curve and thereafter. Likewise, 3D-EAM had no significant effect on freedom from arrhythmia (with 3D-EAM 69%, without 3D EAM 65%, p = 0.40).

Conclusion: The learning curve for PFA procedures is brief in terms of procedure and fluoroscopy time. Nevertheless, fur-

ther improvements in PV durability can be expected with increasing experience. No difference in freedom from arrhythmia was observed during the learning curve or with the use of 3D-EAM.

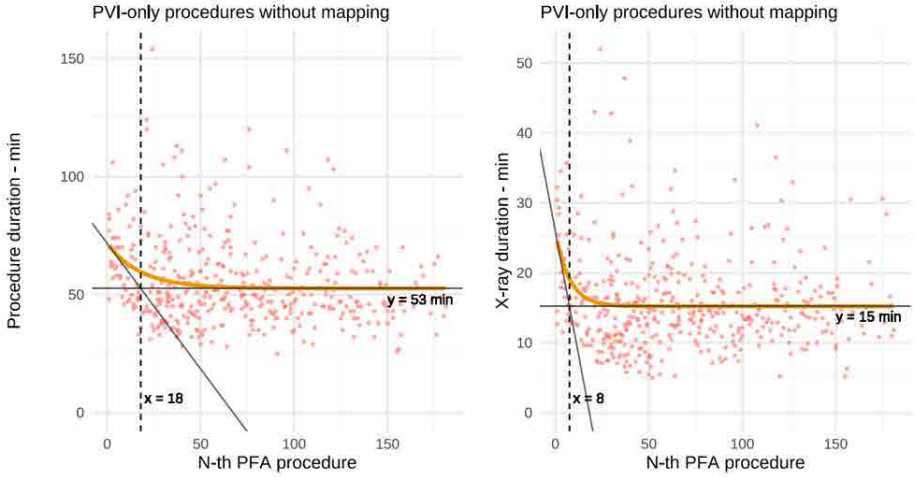

Learning curve of procedure and x-ray duration. Procedure time (Left Panel) and fluoroscopy time (Right Panel) in PVI-only procedures and without mapping to minimize bias. Least-square exponential fit with two linear functions asymptomatic to the initial decrease and the long-term stable operation. The intersection of these lines is used to quantify the learning curve.

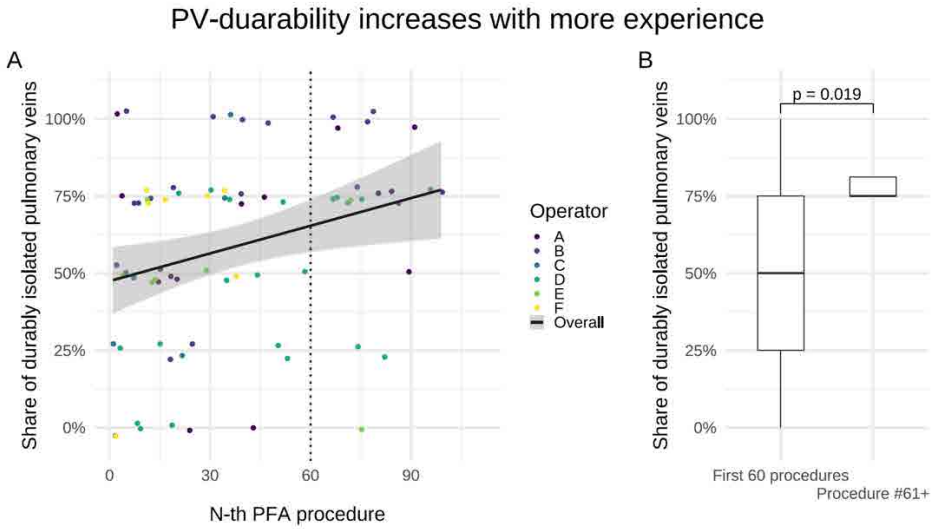

PV durability found during repeat procedures after a first pulsed-field ablation procedure. Overall PV durability increased from a median of 50% for the first 60 procedures of each operator to a median of 75% for PFA procedures #61 and more per operator.

O61

Comparison of acute lesion extent after pulsed field ablation and cryoballoon ablation – Insight from the randomized SINGLE-SHOT CHAMPION trial

Thomas Kueffer[1], Sven Knecht[2], David Spreen[2], Salik Ur Rehman Iqbal[1], Gregor Thalmann[1], Patrick Badertscher[2], Jens Maurhofer[1], Philipp Krisai[2], Corinne Jufer[1], Helge Servatius[1], Hildegard Tanner[1], Michael Kühne[2], Laurent Roten[1], Christian Sticherling[2], Tobias Reichlin[1]

[1]Department of Cardiology, Inselspital, Bern University Hospital, University of Bern, Bern, Switzerland, [2]Department of Cardiology, University Hospital Basel, University Basel, Basel, Switzerland

Introduction: The SINGLE SHOT CHAMPION multicenter trial compares pulsed-field ablation (PFA, FARAWAVE, Boston Scientific) versus cryoballoon ablation (CBA, Arctic Front, Medtronic) for pulmonary vein isolation (PVI) in patients with symptomatic paroxysmal atrial fibrillation (AF). We compare the acute lesion extent after fluoroscopy-guided single-shot PVI with PFA and CBA using adjunctive 3D-EAM at the end of the procedures in a subset of patients.

Material and Methods: Patients were enrolled and randomized 1: 1 to PVI using PFA CBA. 25 patients in each group underwent post-ablation 3D-EAM (Rhythmia, Boston Scientific). Data was collected on the PV isolation status and the minimal width of the posterior wall channel, defined as the shortest distance between low-voltage borders on bipolar voltage maps with thresholds set to 0.05 mV and 0.5 mV (Figure 1).

Results: 50 Post-ablation maps were available for analysis. LA size was not different between the groups. On post-ablation 3D-EAM, residual PV conduction was found in 4 pulmonary veins in 4 cases after CBA (16%, two right inferior, one left inferior, one left superior pulmonary vein). No residual PV conduction was found after PFA (p = .11). PFA led to wider PVI with lesions extending further into the posterior wall, resulting in narrower median width of the minimal posterior wall channel compared to CBA (14.0 mm, IQR 10.5-20.6 mm vs. 24.0 mm, IQR 19.1-26.9 mm, p<.001). Additionally, unintended posterior wall interruption by connecting lesions occurred in 3 (12%) PFA cases and no CBA cases (p = .23). Patients with inadvertent posterior wall interruption had smaller atria (median LAVI 18.5 ml/m^2, vs. 35.6 ml/m^2, p = .006).

Conclusion: In this randomized comparison, residual PV conduction was found in 16% after CBA and in 0% after PFA when using high-density 3D-EAM after ablation. The level of isolation was wider with PFA compared to CBA, and inadvertent posterior wall interruption occurred in some small atria after PFA.

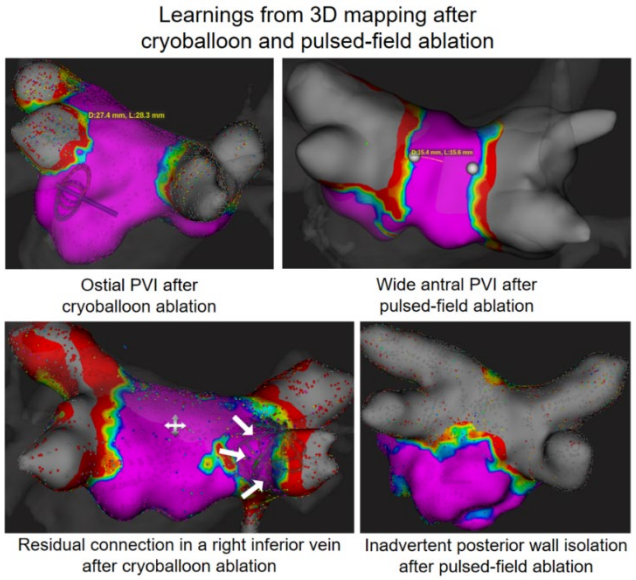

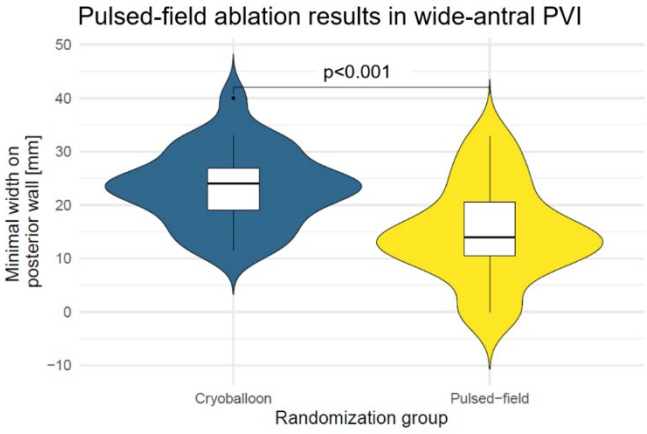

O62

Comparison of hemolysis induced by different pulsed-field ablation systems

Johannes Bruss[1], Thomas Kueffer[1], Gregor Thalmann[1], Nikola Kozhuharov[1], Andreas Häberlin[1], Fabian Noti[1], Claudia Herrera Siklódy[1], Boldizsar Kovacs[1], Valon Spahiu[1], Hildegard Tanner[1], Tobias Reichlin[1], Laurent Roten[1]

[1]Inselspital Bern, Bern, Switzerland

Introduction: Pulsed-Field Ablation (PFA) is a novel ablation technology that, as a side effect, causes dose-dependent hemolysis. Currently, three PFA systems are commercially available in Europe: the pentaspline catheter, the lattice-tip focal catheter, and the variable loop circular catheter. Previous studies examining hemolysis during PFA exclusively used the pentaspline catheter system. This study provides the first retrospective comparison of hemolysis levels among all available PFA systems and examines dose dependency across platforms.

Material and Methods: From our prospective atrial fibrillation ablation registry, we included all patients treated with the lattice-tip focal catheter (n = 18) or the variable loop circular catheter (n = 27). Additionally, 30 randomly selected patients treated with the pentaspline catheter during the same timeframe were included. Demographic and procedural data were collected, including the number of PFA applications,through chart review. Creatinine and hemolysis markers were measured pre-procedure and one day post-procedure. Statistical analyses was performed using Fisher's exact test, Kruskal-Wallis rank sum test, and pairwise Wilcoxon test.

Results: The median age of the 75 patients was 69 years; 34 (25%) were women. The median number of PFA applications was 46 for the lattice-tip focal catheter, 36 for the pentaspline catheter, and 21 for the variable loop circular catheter. Baseline creatinine and hemolysis markers were comparable across groups.

The decrease in haptoglobin was greater with the pentaspline and variable loop circular catheters than the lattice-tip focal catheter (-0.68 ± 0.37, -0.60 ± 0.29, -0.23 ± 0.21 g/l respectively; p <0.0005; Figure and Table). Per-application decreases also differed (-16.9 ± 8.5, -28.1 ± 13.6, -6.4 ± 8.7 mg/l; p <0.0001). LDH increases followed a similar pattern. No hemolysis-related complications occurred, and creatinine levels were unchanged.

Conclusion: Hemolysis levels vary significantly among PFA platforms, with focal catheters causing less hemolysis than large-footprint catheters.

	Lattice tip focal cath. (n = 18)	Pentaspline catheter (n = 30)	Variable loop circular cath. (n = 27)	p
Haptoglobin preinterventional (g/l)	1.19 ± 0.59	1.18 ± 0.53	1.19 ± 0.39	0.994
Haptoglobin postinterventional (g/l)	0.95 ± 0.48	0.50 ± 0.37	0.59 ± 0.32	< 0.005
Haptoglobin difference (g/l)	-0.23 ± 0.21	-0.68 ± 0.37	-0.60 ± 0.29	< 0.0005
Haptoglobin difference per application (mg/l)	-6.4 ± 8.7	-16.9 ± 8.5	-28.1 ± 12.6	< 0.0001
LDH preinterventional	207 ± 46	222 ± 51	203 ± 73	0.491
LDH postinterventional	232 ± 46	292 ±60	243 ± 42	< 0.0005
LDH difference	26 ± 36	66 ± 66	40 ± 64	0.030
Creatinine preinterventional	87.3 ± 15.0	85.1 ± 26.1	83.6 ± 20.9	0.484
Creatinine postinterventional	90.2 ± 15.0	85.8 ± 25.8	85.1 ± 21.1	0.404
Creatinine difference	2.9 ± 9.2	0.7 ± 11.6	1.5 ± 9.4	0.905

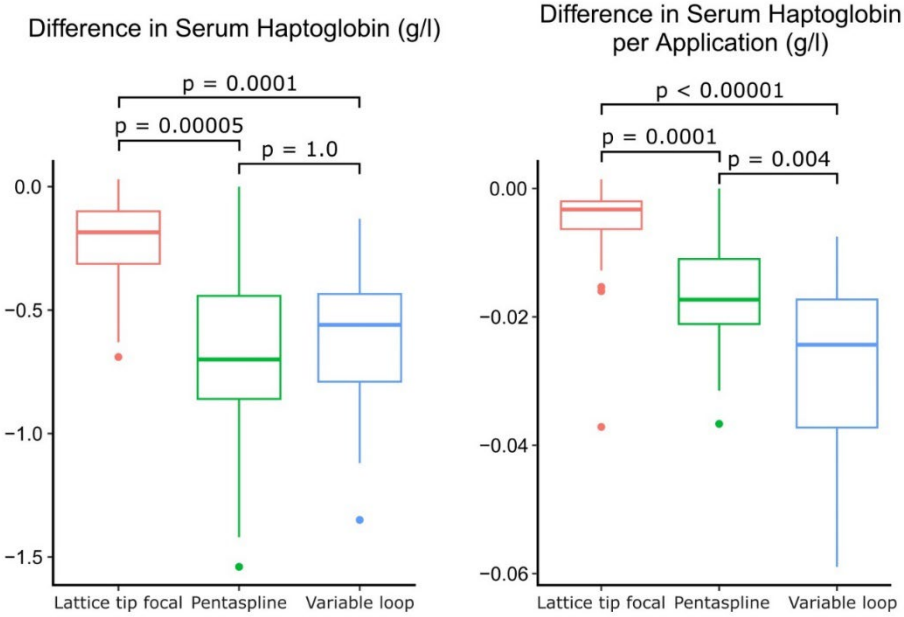

O63

NT-proBNP as a predictor of successful pulmonary vein isolation using pulsed-field, cryoballoon or radiofrequency ablation

Johannes Bruss[1], Thomas Kueffer[1], Gregor Thalmann[1], Nikola Kozhuharov[1], Andreas Haeberlin[1], Fabian Noti[1], Claudia Herrera Siklody[1], Boldizsar Kovacs[1], Valon Spahiu[1], Hildegard Tanner[1], Tobias Reichlin[1], Laurent Roten[1]

[1]*Inselspital Bern, Bern, Switzerland*

Introduction: B-Type natriuretic peptide (NT-proBNP) is a known biomarker for atrial disease and a predictor of pulmonary vein isolation (PVI) success. Pulsed-field ablation (PFA) has recently emerged as a novel technology for PVI. Previous studies have linked NT-proBNP levels to atrial fibrillation (AF) recurrence following PVI with radiofrequency ablation (RFA) and cryoballoon ablation (CBA). This study investigates whether NT-proBNP can also reliably predict successful PVI with PFA and evaluates its predictive strength.

Material and Methods: We included all patients from our prospective AF ablation registry who underwent primary PVI using RFA (n = 302), CBA (n = 399), or PFA (n = 527) between May 2018 and December 2023. Follow-up included 7-day Holter ECGs at 3, 6, and 12 months, with any additional AF recurrence data from clinical records. Baseline NT-proBNP was measured pre-procedure, using the 95th percentile (adjusted for age and sex) as the threshold. NT-proBNP values were standardized, log-transformed, and analyzed using log-rank tests, Mantel-Haenszel tests, and Cox proportional hazard models.

Results: Elevated NT-proBNP was observed in 576/1228 patients (47%). One-year recurrence-free survival, stratified by the NT-proBNP threshold, was similarly predictive across all technologies (RFA: 74% vs 55%, CBA: 81% vs 58%, PFA: 78% vs 57%; p <0.001; Figure 1). In a Cox model including NT-proBNP, age, sex, left atrial volume index (LAVI), and AF type, NT-proBNP (p <0.0005) and AF type (p <0.005) were the strongest predictors of recurrence-free survival compared to LAVI, Sex and Age. A second Cox proportional hazard model for recurrence-free survival, fitted only for converted NT-proBNP and type of atrial fibrillation, was used to develop a color-coded survival probability chart (Figure 2).

Conclusion: NT-proBNP is an independent, robust predictor of recurrence-free survival after primary PVI, regardless of ablation technology. A survival probability chart incorporating NT-proBNP and AF type may enhance shared decision-making.

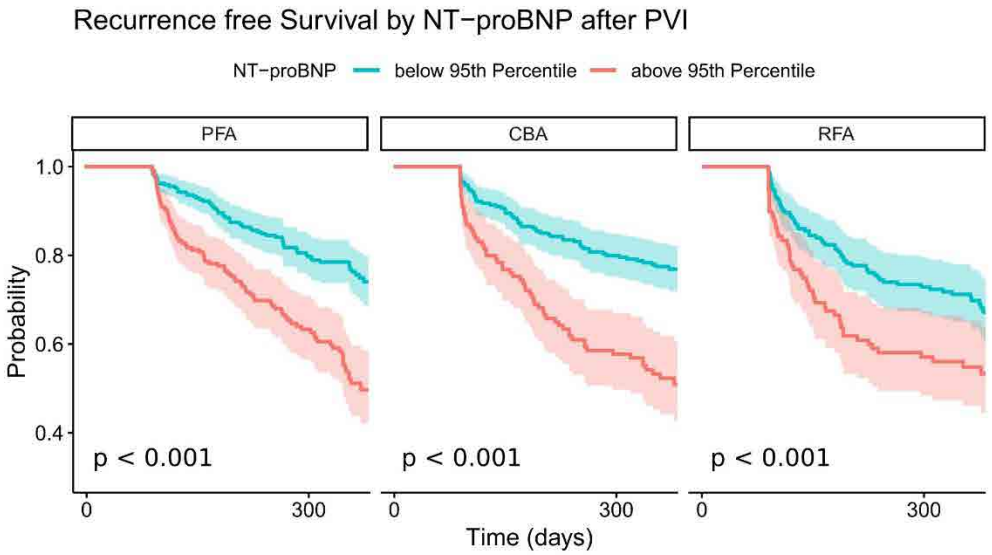

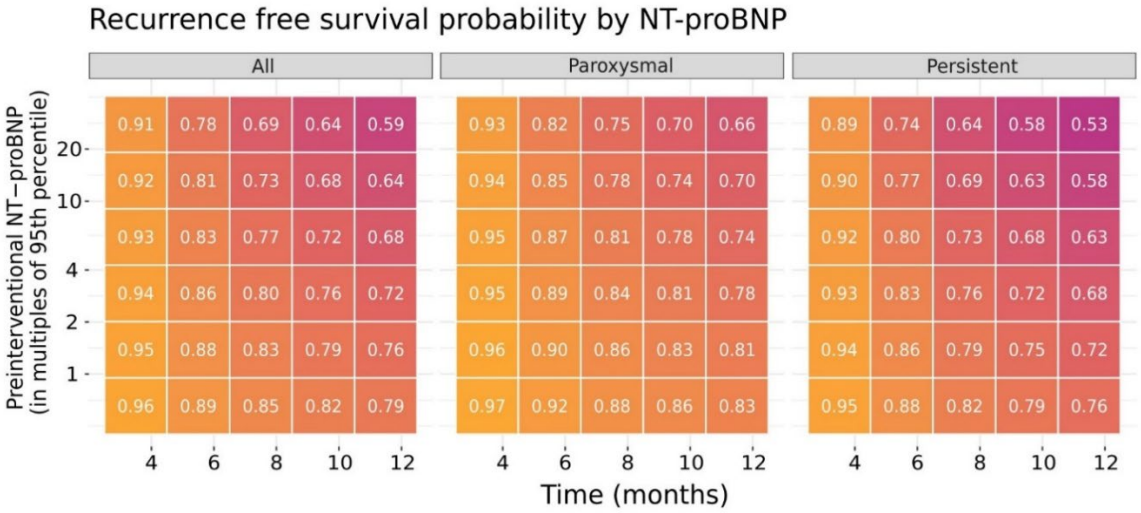

O64

First experience using a novel 3D enabled large-area focal pulsed field ablation catheter for ventricular ablation

Thomas Kueffer[1], Daniela Casoni[2], Christine Goepfert[3], Olgica Beslac[2], Chiara Parodi[2], David Ramirez[4], Kara Garrott[4], Brendan Koop[4], Sean Coe[4], Nathan Hagstrom[4], Guillaume Gilbert[4], Laurent Roten[1], Andreas Haeberlin[1], Tobias Reichlin[1]

[1]Department of Cardiology, Inselspital, Bern University Hospital, University of Bern, Bern, Switzerland, [2]Experimental Surgical Facility, Experimental Animal Center, University of Bern, Bern, Switzerland, [3]COMPATH, Institute of Animal Pathology, University of Bern, Bern, Switzerland, [4]Boston Scientific Corporation, St. Paul, MA, United States

Introduction: Pulsed-field ablation (PFA) has shown promising data in terms of safety and procedural efficiency for pulmonary vein isolation (PVI). Large-area focal PFA catheter designs might be suitable to deliver deep and durable lesions in ventricular myocardium. We investigate the dose-response of a novel large-area focal 3D-enabled map and ablate PFA catheter for ventricular ablation in a chronic preclinical swine model.

Material and Methods: An 8 F large-area focal catheter with a 9 mm hexaspline tip was used for 3D electroanatomical mapping of both ventricles in a porcine model. Using a PFA generator (FARASTAR, Boston Scientific), with a proprietary waveform optimized for the catheter, left- and right-ventricular lesions were placed with either a monopolar or bipolar ablation vector, and with 1, 2, or 4 applications per site (2.0 kV/application). Tissue contact was ensured using intracardiac echography and EGMs. The animals were survived for 1 week. Ablation lesions were assessed macroscopically after triphenyl tetrazolium chloride staining and using histopathology.

Results: A total of 69 chronic ventricular lesions (40, 58% monopolar and 29, 42% bipolar) from 7 pigs were available for analysis. By stacking 4 PFA applications rather than a single application, median chronic lesion depth 7 days after ablation increased from 4.8 mm (IQR 4.1-5.6) to 5.5 mm (IQR 5.0-6.2), p = 0.06 with bipolar ablation, and from 4.9 mm (IQR 4.4-5.2) to 6.5 mm (IQR 5.9-6.9), p = 0.002 with monopolar ablation. Lesion width ranged from a median of 20.6 mm (Range 11.5-41.6) for a monopolar ablation vector, to 21.9 mm (Range 13.1-39.8) for a bipolar ablation vector. On histology, lesion borders were clearly demarcated, and vessels and nerves preserved.

Conclusion: A novel large-area focal ablation catheter with the ability for high-density 3D mapping and pulsed-field ablation was able to create dose-dependent deep ventricular lesions durable 1 week after ablation.

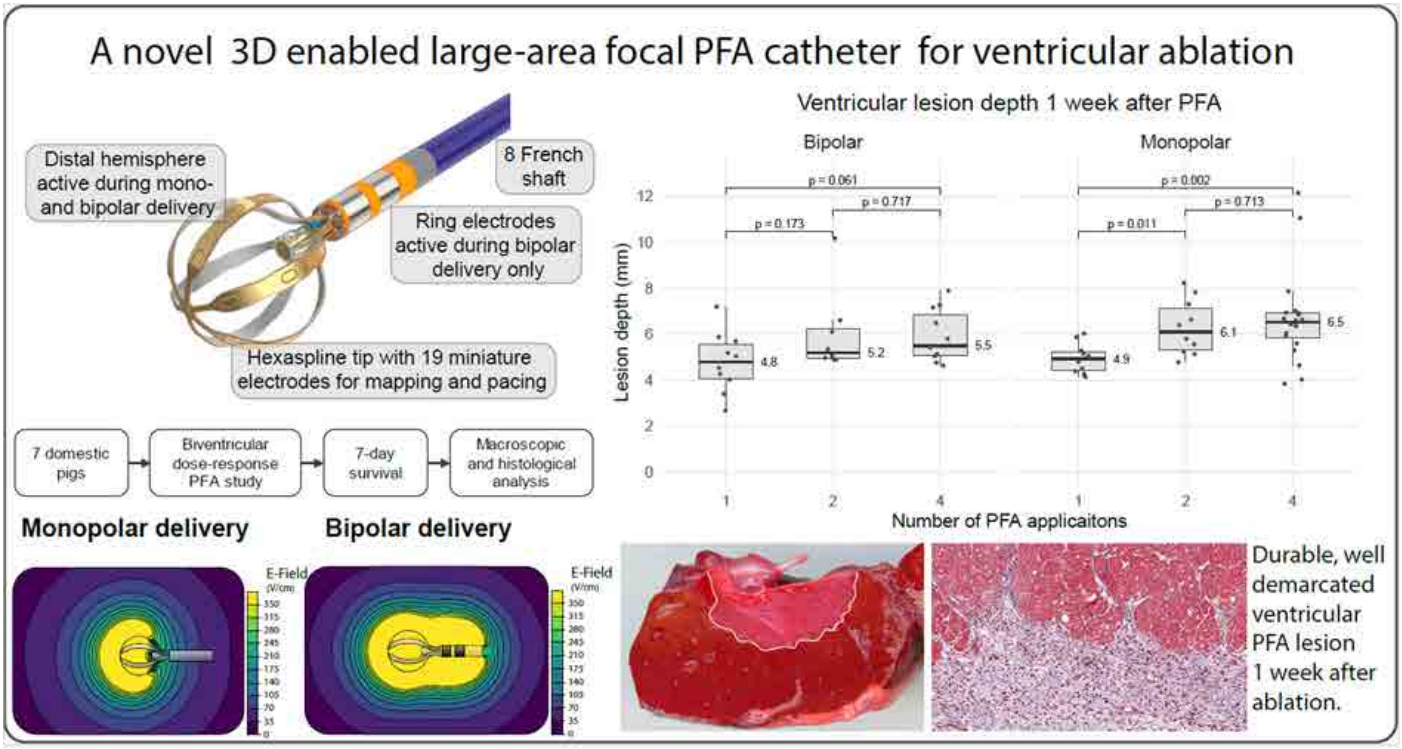

O65

Temporal Patterns of Atrial Fibrillation Recurrence after Catheter Ablation Using Pulsed-field Ablation

Fabian Jordan[1]*, Corinne Isenegger[1], Rebecca Arnet[1], Sven Knecht[1], Philipp Krisai[1], Nicolas Schärli[1], Gian Voellmin[1], David Spreen[1], Christian Sticherling[1], Michael Kühne[1], Patrick Badertscher[1]

[1]Cardiovascular Research Institute Basel (University Hospital Basel), Basel, Switzerland

Introduction: The prognostic implications of temporal patterns of atrial fibrillation (AF) recurrence after catheter ablation might differ between thermal and non-thermal energy sources such as pulsed-field ablation (PFA). While recurrence of AF during the blanking period after thermal ablation is not considered as a predictor for late recurrence, the impact of early recurrence after PFA ablation is incompletely understood.

Material and Methods: Consecutive patients undergoing PVI PFA were enrolled and prospectively followed up for at least 365 days. Early recurrence was defined as atrial arrhythmia lasting more than 30 seconds during a 90-day blanking period, while any recurrence occurring after 90 days was classified as late recurrence.

Results: A total of 233 patients underwent PFA for AF and had complete 365 days follow-up data available. The overall arrhythmia-free survival at 365 days was 72% (167 of 233 patients). Early recurrence was observed in 43 patients (19%). Of these, 49%, 21% and 30% were observed within the 1st , 2nd and 3rd month after the ablation procedure. Among patients with recurrence within the 1st, 2nd and 3rd month, no late recurrence was observed in 48%, 33% and 31% of patients, respectively, p<0.001. Among patients with early recurrence undergoing redo procedures (n = 82, 35%), the rate of durably isolated PV was 29%, 33% and 23% for early recurrence in the 1st , 2nd and 3rd month, p = 0.211, respectively (Figure1).

Conclusion: In this consecutive series of AF patients, early recurrence, especially during the 2nd or 3rd month after PVI, was strongly associated with an increased risk of late recurrence. While half of the early recurrences in the 1st month resolved, only a third of early recurrences in the 2nd and 3rd month resolved during 365 days of follow-up. The rate of durably isolated PV was similar among patients with early recurrence in the 1st, 2nd or 3rd month.

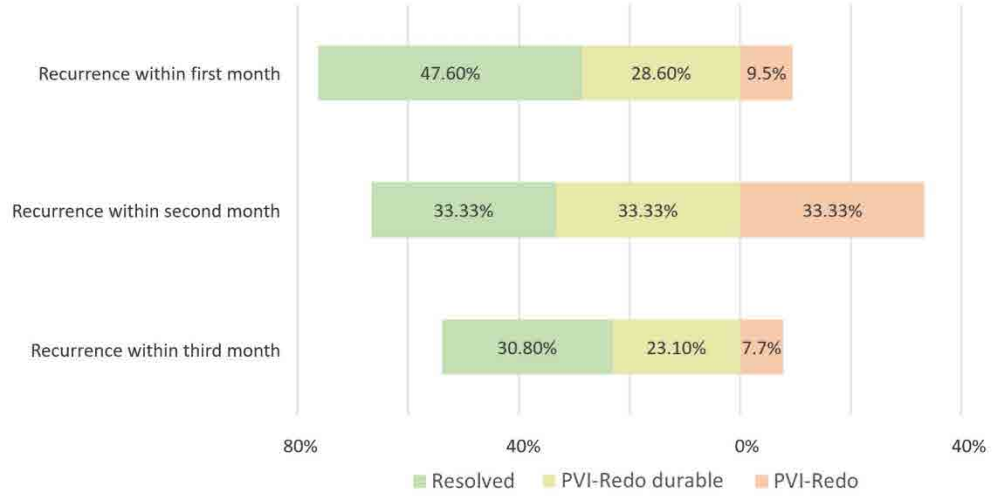

Figure1: Mirror Bar plot with percentages of groups on the x-axis. Resolved: no late recurrence detected. PVI-Redo durable: Late recurrence occurred, a redo-procedure was performed and the Pulmonary veins were durably isolated. PVI-Redo: Late recurrence occurred, a Redo-procedure was performed and the Pulmonary veins reconnected.

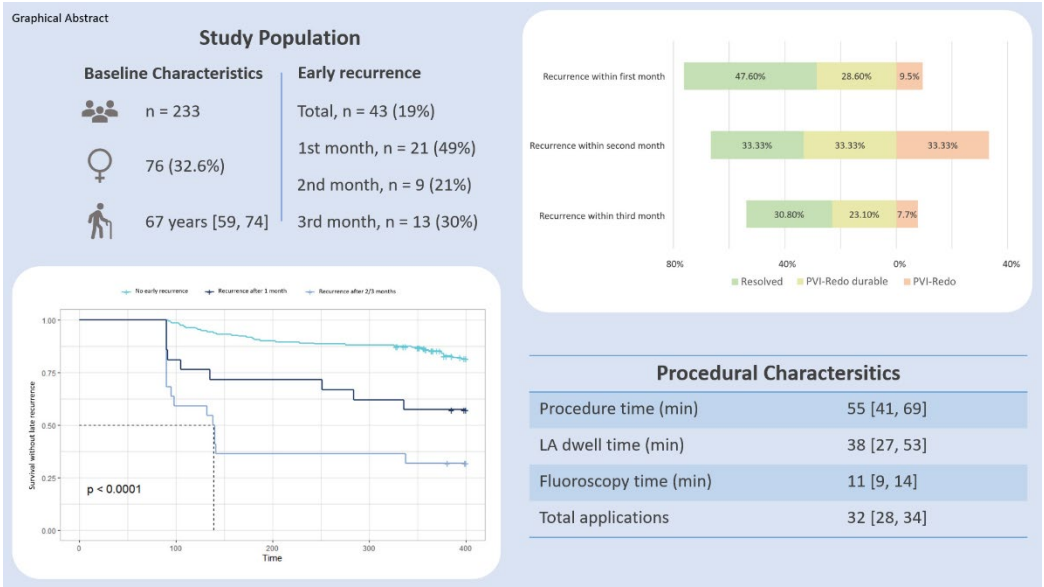

RAPID FIRE ABSTRACT SESSION "PREVENTION, REHABILITATION & SPORTS CARDIOLOGY"

O66

Relationship between time in systolic target range during 24-hour ambulatory blood pressure monitoring and mortality

Lucas Lauder[1], Igor Schwantke[2], Alejandro de la Sierra[3], Ernest Vinyoles[4], Manuel Gorostidi[5], Julián Segura[6], Bryan Williams[7], Natalie Staplin[8], Luis Ruilope[9], Michael Böhm[2], Felix Mahfoud

[1]University Hospital Basel, Cardiovascular Research Institute Basel, Basel, Switzerland, [2]Universitätsklinikum des Saarlandes, Saarland University, Homburg, Germany, [3]Hospital Mutua Terrassa, University of Barcelona, Barcelona, Spain, [4]University of Barcelona, Barcelona, Spain, [5]Hospital Universitario Central de Asturias, RedinRen, Oviedo, Spain, [6]Hospital Universitario 12 de Octubre, CIBER of Cardiovascular Disease, Madrid, Spain, [7]University College London, London, United Kingdom, [8]University of Oxford, Oxford, United Kingdom, [9]Hospital Universitario 12 de Octubre, Madrid, Spain

Introduction: Time in target range (TTR) reflects the proportion of time that blood pressure (BP) is within target range and therefore comprises information on BP variability and control. We examined the association of TTR for systolic BP (SBP) during 24-hour ambulatory BP monitoring (ABPM) with all-cause mortality.

Material and Methods: This analysis utilized data from the Spanish ABPM Registry, including patients from 223 primary care centres across Spain. Mortality data was obtained from a computerized search of the vital registry of the Spanish National Institute of Statistics. The 24h-TTR was calculated using linear interpolation between consecutive SBP recordings obtained from ABPM and determined the proportion of time spent in the TTR defined as a SBP of 120-134 mmHg during daytime and SBP of 110-119 mmHg during night-time. Association with all-cause mortality were assessed by Cox regression models adjusted for demographic and clinical.

Results: A total of 59,124 patients (47% female, mean age 58.7 years [standard deviation, SD 14.1]) were included in the Spanish ABPM Registry. The mean 24h-SBP was 128.8 mmHg (SD 13.7). The mean 24h-TTR was 30.7% (SD 16.8), ranging from 0% to 87.8% (34.3% [SD 19.9] during waking and 23.7% [SD 19.5] during sleeping periods). During a median follow-up of 9.7 years, 7,174 (12.1%) of 59,124 patients died. Increased 24h-TTR was associated with a lower risk of all-cause death (hazard ratio [HR] 0.83 per 1SD increment [95% CI 0.80-0.85). This association remained significant even after additionally adjusting for mean 24h-SBP (HR 0.89 per 1SD increment [95% CI (0.86-0.92)]. The association of 24h-TTR with all-cause death was not significant in patients with a mean 24h-SBP of <115 mmHg (p = 0.5205) but in those with 115-129 mmHg (p<0.0001), and ≥130 mmHg (p = 0.0001) (Figure).

Conclusion: Increased 24h-TTR was associated with a lower risk of all-cause death, particularly in patients with controlled and elevated mean 24h-SBP.

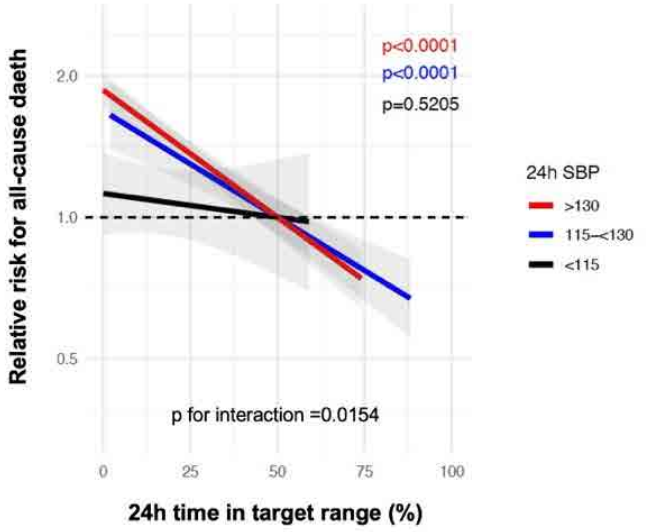

Figure. Association of time in target range for systolic blood pressure (SBP) during 24-hour ambulatory blood pressure monitoring and the relative risk for all-cause mortality according to mean SBP values

O67

Sex-Specific Neural and Cardiovascular Responses to Acute Mental Stress: A PET/MR Study

Nidaa Mikail[1], Alexia Rossi[1], Susan Bengs[2], Angela Portmann[2], Pimrapat Gebert[3], Achi Haider[1], Valerie Treyer[1], Antonio Gennari[1], Caroline Gebhard[4], Ronny Büchel[1], Giovanni G. Camici[2], Roland von Känel[1], Vera Regitz-Zagrosek[5], Philipp Kaufmann[1], Catherine Gebhard[6 7]

[1]University Hospital Zurich, Nuclear medicine, Zurich, Switzerland, [2]Center for Molecular Cardiology, Schlieren, Switzerland, [3]University of Zurich, Zurich, Switzerland, [4]University Hospital Basel, Basel, Switzerland, [5]Charité-Universitätsmedizin, Berlin, Germany, [6]Inselspital Bern, Bern, Switzerland, [7]University Hospital Zurich, Zurich, Switzerland

Introduction: Advances in cardiovascular disease (CVD) management have benefited men more than women, hinting at sex-specific mechanisms in CVD. Mental stress is increasingly recognized as a key factor in CVD, with fluor-18-fluorodeoxyglucose ([18F]FDG) uptake in the amygdala – indicative of stress-related neural activity (SNA) – linked to adverse cardiovascular outcomes. This study aimed to explore sex differences in (1) amygdala and myocardial responses and (2) hypothalamus-pituitary-adrenal (HPA) axis and sympathetic nervous system (SNS) responses to acute mental stress.

Material and Methods: Sixty-four healthy volunteers (50% women) aged 50–75 years were recruited at the University Hospital Zurich. Positron emission tomography/magnetic resonance (PET/MR) imaging used [18F]FDG for amygdala metabolism and [13N]ammonia ([13N]NH3) for amygdala and myocardial perfusion. Acute stress was induced by the Trier Social Stress Test (TSST) during [18F]FDG PET/MR and the Montreal Imaging Stress Task (MIST) during [13N]NH3 PET/MR. Primary endpoint: sex differences in SNA, assessed as the ratio of [18F]FDG uptake (SUVmean) in the amygdala

to the cerebellum. Secondary endpoints: differences in (i) amygdala perfusion ([13N]NH3), (ii) myocardial blood flow (MBF) and flow reserve (MFR), (iii) salivary cortisol (HPA activation), and (iv) heart rate response (HRR; SNS activation) to stress.

Results: The average age was 59.8 ± 5.8 years. Post-TSST, SNA was higher in women than men (0.7530 vs. 0.7173, p<0.001). MIST revealed significant amygdala perfusion reduction in women (Δ = -0.0181, p<0.001) and a non-significant trend in men (Δ = -0.0086, p = 0.064). Women had higher resting MBF (p = 0.019), but MFR showed no sex difference (p = 0.537). Men exhibited a significant cortisol increase (p = 0.034), while HRR was greater in women (p = 0.049).

Conclusion: Women exhibit a stronger amygdala response to acute mental stress, predominantly activating the SNS, while men engage the HPA axis more substantially.

O68

The influence of exercise modality and intensity on ventricular arrhythmia burden in patients with Arrhythmogenic Right Ventricular Cardiomyopathy with pathogenic plakophilin-2 variants

Fernando Beltrami[1], Kyle Boyle[1], Fu Guan[2], Corinna Brunckhorst[2], Firat Duru[2], Christina Spengler[1], Ardan Saguner[2]

[1]ETH Zürich, Zürich, Switzerland, [2]University Heart Center Zurich, Zurich, Switzerland

Introduction: Currently no prospective studies exist on the safety of physical activity for ARVC patients. We aimed to describe the average and peak ventricular arrhythmia burden – estimated from the prevalence of premature ventricular contractions (PVC) – measured during and after different exercise modalities and intensities.

Material and Methods: Twenty (8f/12m, age 48±15 years, BMI 24.1±2.9 kg/m^2, resting PVC burden 4.2 ±4.3%) ARVC patients with a pathogenic plakophilin-2 (PKP-2) variant performed two-legged squats and single arm biceps curls (each with 20 repetitions and 2 min duration), 5-min treadmill walking and 3-min cycling bouts aiming at heart rate (HR) of 80, 100 and 120 bpm. Each activity was followed by a 10-min recovery period. Blood lactate concentration [La$^-$] was assessed at the end of each cycling bouts, with 4mmol/L defined as a threshold to describe high-intensity exercise.

Results: Average PVC burden during activities (including 5 min recovery) was lower for biceps curls compared with all other activities (p <0.046, Fig1). Biceps curls elicited ~20 mmHg (p <0.001) lower systolic BP and ~40 bpm lower HR (p <0.001) compared with cycling at 120 bpm, despite similar perception of effort. Peak PVC burden ranged from 0–57% between participants and activities, and was higher during the recovery period (9±10%) compared with the active periods (5±8%, p = 0.005). No differences were detected between the peak PVC burden of the different activities. [La$^-$] when cycling at 120 bpm was 3.0±1.5 mmol/L (range 1.6-6.6 mmol/L), including five patients with >4.0 mmol/L.

Conclusion: Guidelines based on absolute HR, such as 120 bpm, might predispose a high number of patients to inadvertently perform high-intensity exercise, whereas exercises employing small muscle masses may allow long term training without inducing cardiac maladaptation. Since the PVC burden generally increases during recovery discontinuous exercise protocols might improve the prognostic values of ergospirometry and exercise prescription

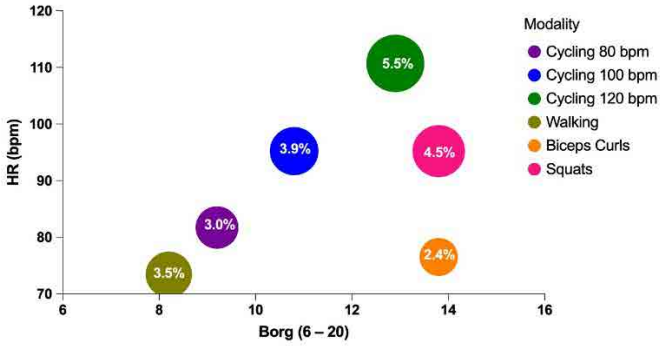

Figure 1: The size of the dots and numbers inside denote the ventricular ectopic burden (average over the activity plus 5 min of recovery) as a function of both heart rate (HR, y-axis) and perceived exertion (Borg 6-20 scale, x-axis) at the end of the bout for the different exercise modalities. Data are the average of n = 20 participants with definite ARVC harbouring a pathogenic/likely pathogenic plakophilin-2 variant.

O69

Pulmonary artery pressure in subjects having suffered from high altitude pulmonary edema and their offspring

Rodrigo Soria Maldonado[1], Theo Meister[1], Andrea Kieninger-Graefitsch[1], Claudio Sartori[2], Emrush Rexhaj[1]

[1]Inselspital, Bern, Switzerland, [2]CHUV, Lausanne, Switzerland

Introduction: High altitude pulmonary oedema (HAPE) is a life-threatening disease affecting otherwise healthy subjects exposed to altitudes >2500m. One of the main characteristics of HAPE is the presence of an exaggerated hypoxic pulmonary artery pressure (PAP). Despite advances in medicine, HAPE-aetiology remain unclear. Transgenerational inheritance was pointed out to increase HAPE susceptibility in offspring but this information is sparse. Therefore, the aim of this study was to assess if exaggerated hypoxic PAP observed in HAPE-prone is also present in their offspring.

Material and Methods: To address this issue, we assessed by echocardiography systolic (s) PAP at rest, after 20min of normobaric hypoxemia and during exercise (at 40 %; 60 % and 80% of maximal calculated exercise capacity) in HAPE-prone subjects and their offspring, and compared them to HAPE-resistant and their offspring. Normobaric hypoxemia was induced using an altitude simulator (AltiTrainer, SMTEC, Switzerland). At exercise end, comet tails were investigated to test for subclinical pulmonary interstitial water accumulation.

Results: Forty-eight participants (at least 10 per group) were enrolled. Estimated sPAP were similar in all groups at rest. From 40 % to 80% of exercise capacity, sPAP increased significantly higher between HAPE-prone and HAPE-resistant (p<0.001). More importantly, sPAP was higher also between the offspring of HAPE-prone and offspring of HAPE-resistant (p = 0.033). Comet tails were twofold increased in HAPE-prone compared to the other groups (p<0.01) and similar among HAPE-prone and HAPE-resistant offspring.

Conclusion: HAPE-prone and their offspring displayed an exaggerated increased pulmonary artery pressure under hypoxia and during exercise compared with their controls. Therefore, our data suggest that this problem could be transgenerational inherited.

O70

Evaluation of Guideline Adherence in Statin Therapy Among High Cardiovascular Risk Populations: A Comprehensive Analysis of the Zurich Aging Heart Cohort

Vera Graup[1], Shpend Tashi[2], Matthias Hermann[1]

[1]University of Zürich, Zürich, Switzerland, [2]University of Zurich, Zürich, Switzerland

Introduction: Cardiovascular disease remains the leading cause of morbidity and mortality in the elderly. Statin therapy has been established as an effective therapy in high-risk populations. This study aimed to evaluate adherence to LDL-C targets for elderly patients at very high cardiovascular risk.

Material and Methods: Retrospective analysis of patient data from the Aging Heart Zurich Cohort. Elderly patients hospitalized between 2015 and 2024 were categorized based on their ASCVD risk using the ESC SCORE2 criteria. Additionally, patients were divided into two age groups: those aged ≥80 years (very elderly) and those aged 65-79 years. The primary outcome was the degree of guideline-directed medical treatment, measured by LDL concentration.

Results: Our analysis included 3,237 patient datasets from the Zurich Aging Heart cohort with 67.2% men and 32.8% women, and average ages of 76.7 ±7.3 years for men and 78.5 ±7.3 years for women. A total of 82.7% of patients were classified as "very high risk" according to SCORE2/SCORE-OP. Statin therapy was administered to 66.7% of these patients. There was no significant difference in statin treatment rates between the two age groups (65-79 years: 67.9%; over 80 years: 65.1%; Chi-square = 0.09). There was no significant difference in LDL targets between very high-risk and non-very high-risk patients (very high risk: 2.2 ±1 mmol/L vs. non-very high risk: 2.2 ±0.9 mmol/L). However, a significant difference was observed in the achievement of an LDL target of <1.4 mmol/L between the two age groups of very high-risk patients (very elderly: 44.9%; elderly: 59.3%; p = 0.0001).

Conclusion: The achievement of LDL-C goals in patients at very high ASCVD risk was better than reported in previous studies. Both patients over and under 80 years were similarly likely to receive statin treatment. Notably, a significant disparity existed in the ability of very high-risk patients aged above and below 80 to reach LDL targets.

O71

Prevalence and Risk Factors of Orthostatic Hypotension in the population-based Swiss Longitudinal Cohort Study (SWICOS)

Renate Schoenenberger-Berzins[1], Stefanie Hess[1], Dragana Radovanovic[2], Franco Muggli[2], Augusto Gallino[3], Gianfranco Parati[4], Paolo Suter[5], Andreas Schoenenberger[6]

[1]Herzzentrum, Kantonsspital Luzern, Luzern, Switzerland, [2]Faculty of Biomedical Sciences, Università della Svizzera italiana, Lugano, Switzerland, [3]Cardiovascular Research Unit, Dep. Medicina Interna, San Giovanni Hospital, Bellinzona, Switzerland, [4]Istituto Auxologico Italiano, IRCCS, Cardiology Unit and Department of Medicine and Surgery, University of Milano-Bicocca, Milano, Italy, [5]University Hospital Zurich, Zurich, Switzerland, [6]Medizinische Klinik, Kantonsspital Münsterlingen, Münsterlingen, Switzerland

Introduction: The prevalence of orthostatic hypotension (OH) ranges from 5% to 30%. Most of these previous studies embraced highly selected study populations and were not truly population-based. Therefore, we examined characteristics of OH in the population-based SWICOS study.

Material and Methods: The 496 SWICOS participants underwent blood pressure (BP) measurements after rest and 1 and 3 minutes after standing up. OH was defined as a reduction of systolic BP ≥20 mmHg and/or diastolic BP ≥10 mmHg within 3 min of standing up from the sitting position. Associations between baseline characteristics and OH were examined using multivariate logistic regression models, adjusted for age, sex, and other potentially influential variables.

Results: Among 496 participants, 72 (14.5%) had OH. Participants with OH were significantly older than participants without [mean age 62y vs. 48y; p<0.001)]. Among the participants older than 60 years (n = 129), 38 individuals (30%) had OH. Participants with OH were more often affected by arterial hypertension (32% vs 13%; p<0.001), diabetes (10% vs 3%; p = 0.009), obesity (22% vs. 12%; p = 0.023), lower muscle mass (65% vs. 71%; p<0.001), or reduced walking distance (160m vs. 170m; p<0.001). Participants with OH had a higher seated systolic (148mmHg vs. 129mmHg) and diastolic BP (88mmHg vs. 80mmHg) (both p<0.001). From 28 participants with OH who were on a prescription for antihypertensive drugs, 12 (43%) were taking more than one antihypertensive drug and/or a diuretic. Independent predictors for OH were increased systolic BP (OR per mmHg increase 1.05 (95%CI 1.03-1.07; p<0.001), higher number of prescribed antihypertensive drugs (OR 3.35; 95%CI 1.17-9.56; p = 0.024) and reduced walking distance (OR 0.99; 95%CI 0.98-1.00; p = 0.037)

Conclusion: Higher systolic blood pressure, more intensive antihypertensive drug treatment and reduced walking distance were associated with OH. Adequate BP measurement, adequate selection of antihypertensive drug classes and regular physical activity may be effective preventive measures to reduce OH.

O72

Hourly Engagement Patterns with a Wearable Blood Pressure Monitor: Insights to Enhance Hypertension Management

Tiago Paggi de Almeida[1], David Perruchoud[1], Joachim Joachim[2], Josep Sola[1], Jay Shah[1], Grégoire Wuerzner[2]

[1]Aktiia SA, Neuchâtel, Switzerland, [2]Service de néphrologie et d'hypertension, CHUV, Neuchâtel, Switzerland

Introduction: Home blood pressure (BP) monitoring helps control hypertension. Their widespread use, however, is limited. Wearable devices using photoplethysmographic (PPG) signals enable cuffless, continuous BP monitoring and may boost engagement. This large-scale, population-based study is the first to investigate hourly user engagement with a wearable BP monitor.

Material and Methods: All users voluntarily purchased and wore a validated, CE-marked, cuffless wrist BP monitor (Aktiia SA, Neuchâtel, Switzerland). All users provided permission to use their anonymous and/or aggregated data for research purposes through the commercial agreement of usage for the Aktiia monitor. Every time the user accesses the smartphone application – *i.e.*, synchronisation – the data from the bracelet are transferred via Bluetooth and forwarded to Aktiia's cloud server, where they are stored. The smartphone application also displays the BP values measured by the Aktiia monitor and can be checked at any time by the user. The number of hourly App accesses for four weeks (01-28 September 2023) were retrospectively analysed (641,896 total synchronisations, median [IQR]: 24 [9-52] synchronisations per user). The hourly count was establish using a 1-hour centred rolling window with a 5-minute step.

Results: Data from 15,740 European residents (57.9±11.1 years, 21.8% women, BMI 27.9±4.9 kg/m²) were included in the investigation. Figure 1 illustrates the number of synchronisations by hour per user, superimposed by day of the week, highlighting changes in the attention windows according to each day of the week. A clear weekly pattern of interest was noticed from Sunday evening until Friday morning, with reduced interest in self-monitoring between Friday evening until Sunday morning. A noticeable lag of approximately 1-h on weekend mornings – suggesting users wake up later during weekends.

Conclusion: This study revealed distinct hourly BP engagement patterns, highlighting opportunities to enhance personalized healthcare. These insights pave the way for targeted, data-driven interventions to improve user engagement and hypertension management.

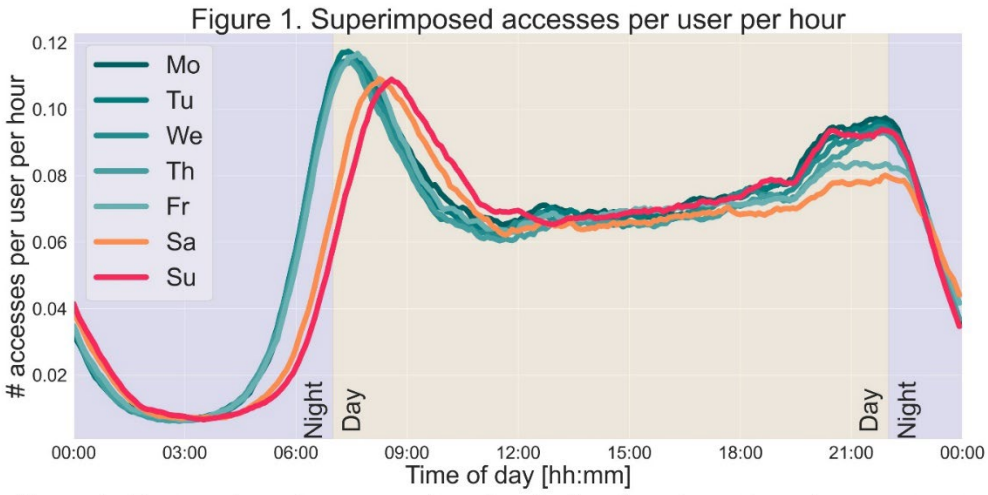

Figure 1. The number of accesses (synchronisations) performed per hour per user, superimposed by day of the week, considering the four weeks included in the study, highlighting changes in the attention windows according to each day of the week.

ORAL ABSTRACT SESSION "CONGENITAL & PAEDIATRIC CARDIOLOGY"

O73

Hemodynamic Relevance Analysis of Anomalous Aortic Origin of Coronary Artery Using CT-derived Fractional Flow Reserve: Impact of Anatomy and Atherosclerosis

Adriana Ferroni[1], Anselm Stark[1], Marius Bigler[1], Ryota Kakizaki[1], Andreas Haeberlin[1], Lorenz Räber[1], Isaac Shiri[1], Christoph Gräni[1]

[1]Department of Cardiology, Inselspital, Bern University Hospital, Bern, Switzerland

Introduction: Anomalous aortic origin of a coronary artery (AAOCA) with an interarterial course is a rare congenital condition that can cause ischemia. Stress-induced invasive testing is recommended due to potential dynamic compression of AAOCA, but it requires expertise and is uncomfortable for patients. A non-invasive alternative to assess the hemodynamic relevance of AAOCA is desirable, though the role of CT-FFR in this context remains unclear.

Material and Methods: In this study, patients with right-AAOCA were retrospectively included from the Coronary Artery Anomaly registry from Bern, Switzerland. All participants underwent CT-FFR analysis using cFFR software (Siemens Healthineers) alongside additional CCTA-based quantification of coronary artery disease (CAD), anatomical features, including intramural course length, degree of stenosis, ostial lumen area, and minimal lumen area. Patients' symptoms were clinically categorized as either anomaly-related or non-anomaly-related.

Results: A total of 116 patients were included in the final analysis, with a mean age of 58 ± 13 years. CAD was present in 70 (60%) patients, with 40 (34%) showing CAD (≥50% stenosis) in the anomalous vessel. CT-FFR was 0.93 ± 0.06 in all patients. Of the 20 (17%) patients with a pathological CT-FFR≤0.8, only 3 (15%) patients had no additional CAD in the anomalous vessel. CT-FFR correlated with ostial area ($r = 0.25$, $p = 0.019$) and intramural length ($r = -0.45$, $p<0.001$), but no AAOCA anatomical feature could predict CT-FFR ≤0.8. CAD was a significant predictor for pathological CT FFR with an odds ratio of 1.3 (95% CI 1.14-1.51, $p<0.001$).

Conclusion: In right-AAOCA cases on CCTA, CAD in the anomalous vessel impacts hemodynamic significance, while anatomical AAOCA features seem to have less impact on CT-FFR. However, as CT-FFR was validated against fixed stenosis in CAD and may not account for dynamic compression under stress in AAOCA, further comparison with the invasive gold standard and outcome analysis is needed for definitive conclusions.

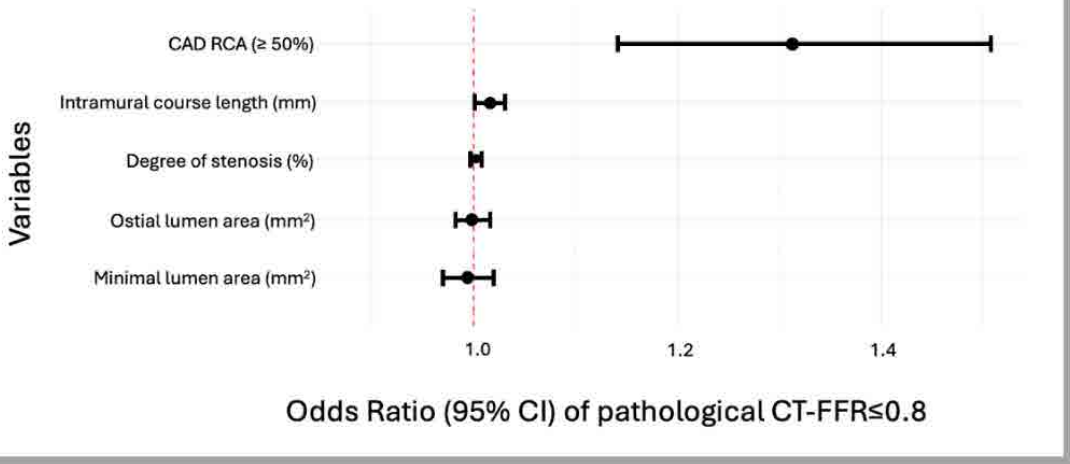

Figure 1: The odds ratio for having a pathological CT-FFR ≤0.8 is shown, with coronary artery disease (CAD) in the right coronary artery being the only statistically significant predictor when compared to the anatomical features.

BEST SURGICAL ABSTRACT

O31

Direct Comparison of Cardiac Troponin T and I: Impact on Definitions of Perioperative Myocardial Infarction after Coronary Artery Bypass Grafting

Luca Koechlin, Islam Salikhanov[1], Ivo Strebel, Brigitta Gahl[1 2], Philip Haaf[3], Michael Zellweger[3], Martin Siegemund[4], Christian Müller, Denis Berdajs[1]

[1]Department of Cardiac Surgery, University Hospital Basel, Basel, Switzerland, Basel, Switzerland, [2]Surgical Outcome Research Center Basel, University Hospital Basel, University Basel, Basel, Switzerland, Basel, Switzerland, [3]Cardiovascular Research Institute Basel (CRIB), Basel, Switzerland, [4]University Hospital Basel, Intensive Care Unit, Department of Acute Medicine, University Hospital Basel, Basel, Switzerland, Basel, Switzerland

Introduction: This study aimed to compare the postoperative release dynamics of cardiac troponin (cTn) T and I after uneventful coronary artery bypass grafting (CABG) surgery and its impact on biomarker thresholds for perioperative myocardial infarction (PMI) across various definitions.

Material and Methods: Patients aged >18 years undergoing isolated CABG surgery were included. cTnT and cTnI were measured from the same blood samples, collected perioperatively in a standardized manner. Patients with patent bypass grafts confirmed by postoperative computed tomography and without a ≥10% decrease in left ventricular ejection fraction, indicating an uneventful recovery, were included. PMI criteria were assessed according to current guidelines: the Universal Definition of Myocardial Infarction (UDMI), Academic Research Consortium-2 (ARC-2), and VISION trial.

Results: A total of 258 patients (median age 69 [IQR 62–75] years) were included. Median postoperative peak values were 349 ng/L (IQR 206–547) for cTnT and 1517 ng/L (IQR 752–2897) for cTnI. Biomarker cutoffs for PMI were exceeded more frequently with cTnI compared to cTnT across all definitions (e.g., UDMI: n = 150 [60%, CI 54–66%] for cTnT vs. n = 181 [72%, CI 67–78%] for cTnI; ARC-2: n = 75 [30%, CI 25–36%] for cTnT vs. n = 173 [69%, CI 63–75%] for cTnI; Figure 1). Differences persisted when echocardiogram and electrocardiogram data were included.

Conclusion: Our findings challenge current recommendations to equate cTnT and cTnI, as they reveal significant discrepancies in the definition of PMI, with a much higher occurrence when cTnI is used. This has major clinical and academic implications, as the choice of assay can influence the incidence of PMI by up to 300%.

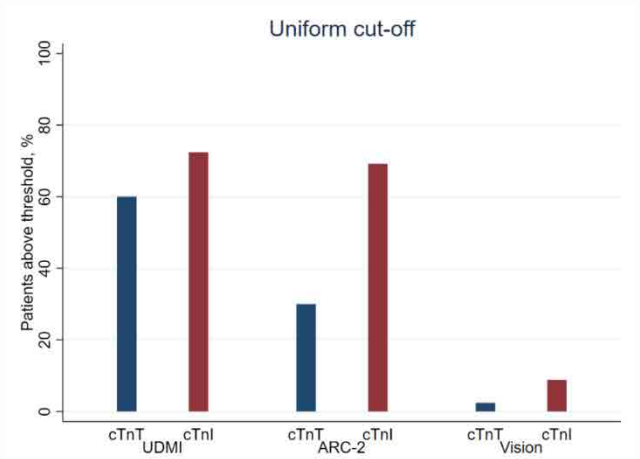

Figure 1.

Barchart showing the proportion of patients fulfilling the required cTn thresholds according to the various definitions of perioperative myocardial infarction when using cTnT (blue) and cTnI (red).

UDMI – Universal Definition of Myocardial Infarction

ARC-2 – Academic Research Consortium

cTn – cardiac troponin

BEST ORAL ABSTRACT – BASIC SCIENCE

O48

Unfolding the Link Between Protein Misfolding and Stroke-Heart Syndrome

Thamonwan Diteepeng[1], Yustina M Puspitasari[2], Stefano Ministrini[2 3], Marialucia Telesca[1], Daria Vdovenko[4], Alexander Akhmedov[2], Jürg Beer[2 5], Sarah Costantino[1 6], Frank Ruschitzka[1 6], Francesco Oaneni[1 6], Giovanni G. Camici[2 7], Marco Luciani[1 6]

[1]Center for Translational and Experimental Cardiology, Department of Cardiology, University Hospital Zurich, University of Zurich, Schlieren, Switzerland, [2]Center for Molecular Cardiology, University of Zurich, Schlieren, Switzerland, [3]Cardiology Department, Luzerner Kantonspital, Lucerne, Switzerland, [4]Maisonneuve-Rosemont Hospital Research Center, Department of Microbiology, Infectious disease and Immunology, University of Montreal, Quebec, Canada, [5]Department of Internal Medicine,, Cantonal Hospital of Baden, Baden, Switzerland, [6]Department of Cardiology, University Heart Center, University Hospital Zurich, Zurich, Switzerland, [7]Department of Research and Education, University Hospital Zurich, Zurich, Switzerland

Introduction: The brain-heart axis plays a key role in the post-stroke cardiovascular complications termed the stroke-heart syndrome (SHS). Alongside inflammatory and neurohormonal signals, protein misfolding has emerged as a potential contributor into this organ crosstalk due to the presence of ischemia-related misfolded toxic proteins (oligomers) and their propagation. However, their biological relevance in SHS remains elusive. This study investigates the involvement of protein misfolding in SHS by evaluating oligomer presence in the myocardium following an acute ischemic stroke (AIS) and its effects on cardiac function and proteostasis.

Material and Methods: AIS was induced via 45-minute left transient middle cerebral artery occlusion (tMCAO) in 3-4 months old wild-type C57BL/6J male and female mice, followed by 48 hours of reperfusion. Cardiac function was assessed using electro- and echocardiography at pre- and post-operative assessment. Oligomer localization and biological responses in proteostasis were examined.

Results: AIS induced cardiac dysfunction, including irregular heart rates consistent with supraventricular arrhythmias, reduced cardiac output and a tendency towards decreased stroke volume and fractional shortening. Elevated oligomer levels in the ipsilateral brain hemisphere was detected, confirming the localized ischemic insult. Notably, increased oligomers accumulation in the myocardium is correlated with disrupted cardiac proteostasis, evidenced by alterations in the chaperone (heat-shock protein 90) and the unfolded protein response marker (cleaved ATF6). Myocardial responses included activated autophagy and antioxidant defenses by protein kinase AKT dephosphorylation, increased expression of autophagosome protein LC3B-II and catalase, reflecting a complex systemic response.

Conclusion: AIS-induced oligomers accumulate in both the murine brain and heart indicating their systemic presence and correlation with disrupted cardiac resistance to proteotoxicity. These findings suggest oligomers as additional components of SHS pathophysiology with ongoing studies aimed at investigating the biological and clinical relevance of proteotoxicity in this adverse condition.

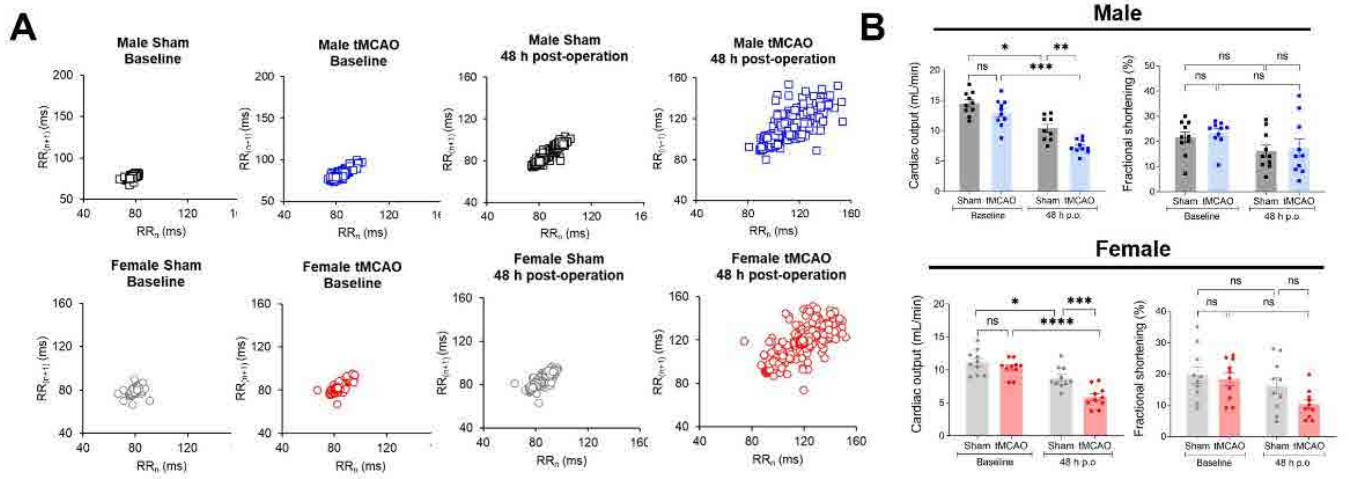

Figure 1 AIS induces cardiac dysfunctions (A) Poincaré plots of consecutive RR intervals time series in the heart of male and female subjected to tMCAO or sham surgery at before (baseline) and 48 h post-surgery. (B) Echocardiographic parameters: cardiac output and fractional shortening. (N=10 per group). Data are presented as mean ± SD. Two-group comparisons were performed using Student's two-tailed test. p.o.: post-operation.

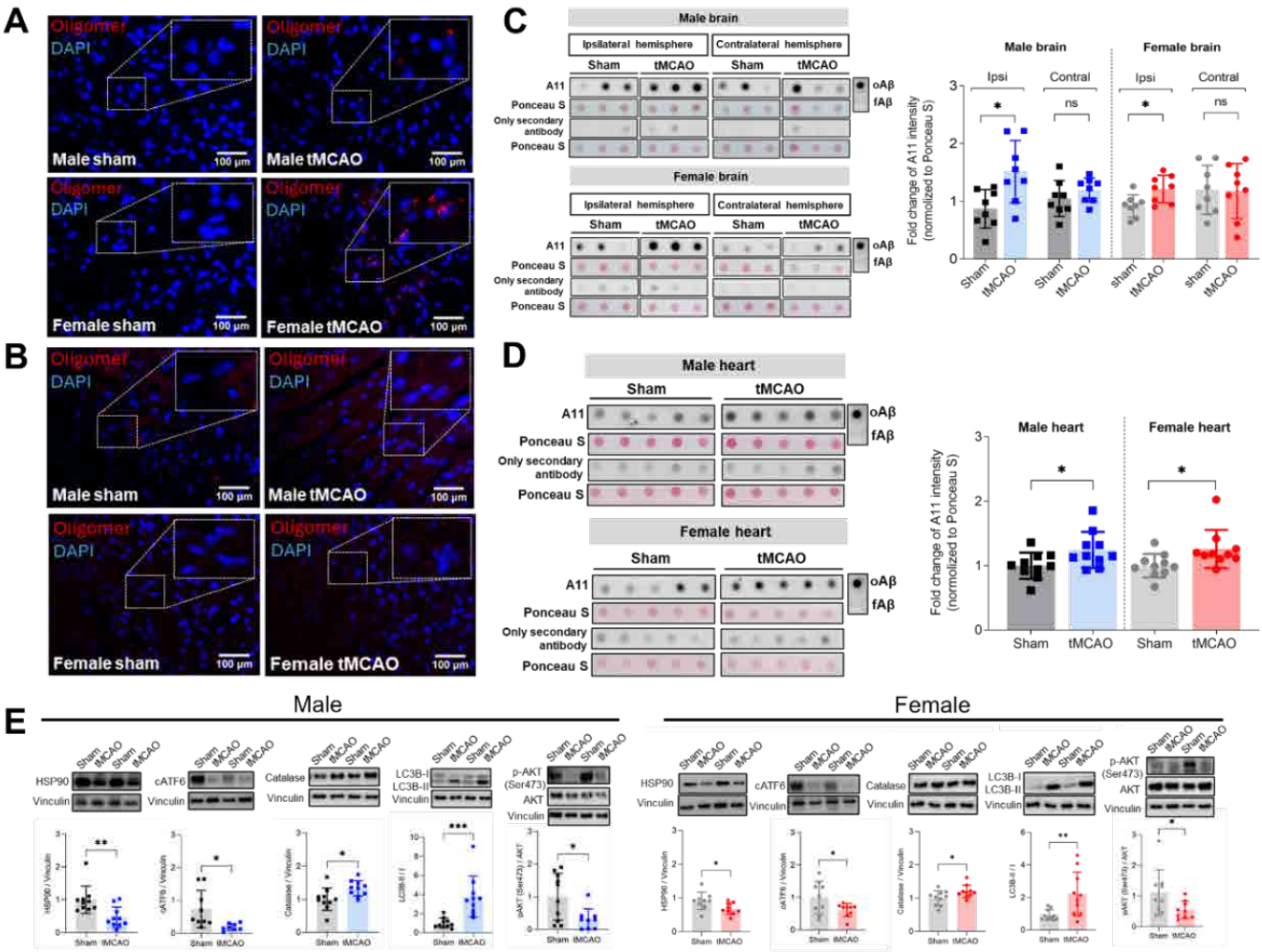

Figure 2 AIS triggers oligomer accumulation and altered cardiac proteostasis. (A) Immunofluorescence staining against oligomers with an oligomer-specific A11 antibody (red) and nuclei with DAPI (blue) of the injured ipsilateral brain hemisphere and (B) the heart from male and female mice mice. (C) Semi-quantification of oligomer levels in the brain and (D) the heart by dot blot assay. (E) Immunoblot analysis of proteotoxicity resistance markers in mouse hearts (N=10 per group). Data are presented as mean ± SD. Two-group comparisons were performed using Student's two-tailed test. *P = 0.05. Scale bar: 100 µm. oAβ: oligomeric amyloid-β, fAβ, fibrillar amyloid-β.

BEST ORAL ABSTRACTS – CONGENITAL / PEDIATRIC HEART DISEASE

O74

Comparison of free-running whole-heart 5D CMR to standard 2D volumetry in patients with left-sided congenital heart disease

Alissia Megalo[1], Christopher Roy[1], Eva Vögeli[1], Estelle Tenisch[1], Fabienne Dirbach[1], Milan Prsa[1], David Saraiva Rodrigues[1], Jerome Yerly[1], Judith Bouchardy[1], Magalie Ladouceur[1], Matthias Stuber[1], Jürg Schwitter[1], Tobias Rutz[1]

[1]Lausanne University Hospital and University of Lausanne, Lausanne, Switzerland., Lausanne, Switzerland

Introduction: Patients with left-sided congenital heart disease (CHD) require regular follow-up for evaluation of ventricular volumes and function. Although standard 2D cine sequences are well established, their need for repetitive breath-holds prolongs scan times and is challenging in poorly compliant patients. The new free-running whole-heart 5D imaging technique using a Gadolinium-enhanced fast interrupted steady state (FISS) sequence offers a potential solution by providing isotropic 3D volumes without the need for breath-holding or ECG triggering. This study compares the free-running 5D imaging to standard 2D cine.

Material and Methods: In patients with left-sided CHD a whole-heart free-running 3D radial FISS research sequence was acquired in addition to standard 2D cine images. All 5D images where reconstructed offline using a compressed-sensing based approach. 5D dataset were reformatted into short and long-axis images to match the same spatial orientation as that from standard 2D cine images. Right (RV) and left ventricular (LV) end-diastolic and end-systolic volumes as well as ejection fractions (EF) were compared between both techniques.

Results: Twenty-six CHD patients (38±16 y/o, 35% female, 8 bicuspid aortic valve, 5 coarctation, 9 aortic dilatation, 1 mitral regurgitation, 1 patent arterial duct, 1 Tirone-David and 1 Ross-procedure) were included. There were no significant differences between FISS and 2D cine volumes and ejection fractions exept for LV endsystolic and RV enddiastolic volumes (Table). Bland-Altman-analyses showed a trend to larger ventricular volumes (Table, Figure). There was an excellent correlation of 2D and FISS volumes and ejection fractions.

Conclusion: Preliminary data indicate that 5D imaging provides comparable results to standard 2D volumetry in left-sided CHD. Further studies are needed to fully establish the role of this innovative technology in clinical practice.

Table Comparison of absolute volumes and ejection fraction between 2D and FISS

Parameter	2D	FISS	p	bias	R	p*
LVEDV, ml	192 ± 12	197 ± 54	0.076	5.9 ± 15.3 (-24.3; 35.9)	0.963	< 0.001
LVESV, ml	83 ± 25	89 ± 27	0.024	6.1 ± 12.0 (-17.5, 29.6)	0.895	< 0.001
LVEF, %	56 ± 7	55 ± 5	0.204	-1.5 ± 5.4 (-12.0, 9.1)	0.611	0.002
RVEDV, ml	174 ± 51	183 ± 49	0.011	8.9 ± 15.4 (-21.3, 39.2)	0.953	< 0.001
RVESV, ml	79 ± 30	82 ± 29	0.438	3.1 ± 18.6 (-33.3, 39.5)	0.795	< 0.001
RVEF, %	55 ± 9	56 ± 6	0.661	-3.8 ± 8.2 (-12.3, 19.8)	0.321	0.136

Data shown are bias (ml) (95 % lower, upper limit of agreement), correlation coefficient.

p corresponds to 2D and FISS values, p* corresponds to correlation analyses.

Abbrevations: LVEDV = Left ventricular enddiastolic volume, LVESV = left ventricular endsystolic volume, LVEF = left ventricular ejection fraction, RVEDV = right ventricular enddiastolic volume, RVESV = right ventricular endsystolic volume, RVEF = right ventricular ejection fraction

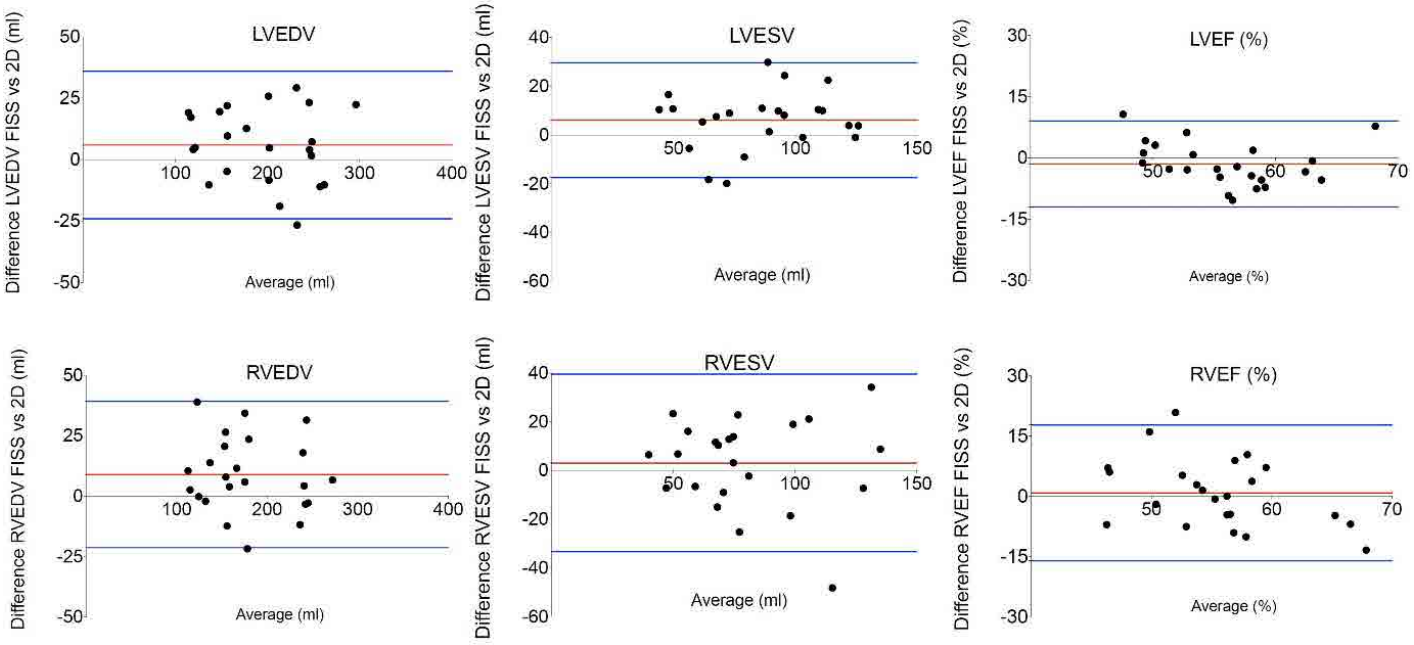

O75

Comparison of free-running whole-heart 5D CMR to standard 2D volumetry in patients with right-sided congenital heart disease

Eva Vögeli[1], Christopher Roy[2], Fabienne Dirbach[1], Alissia Megalo[1], Estelle Tenisch[2], Milan Prsa[3], David Rodrigues[2], Jerome Yerly[2 4], Judith Bouchardy[1], Magalie Ladouceur[1], Matthias Stuber[2], Jürg Schwitter[1], Tobias Rutz[1]

[1]Service of Cardiology, Lausanne University Hospital and University of Lausanne, Lausanne, Switzerland, [2]Department of Diagnostic and Interventional Radiology, Lausanne University Hospital and University of Lausanne, Lausanne, Switzerland, [3]Pediatric Cardiology Unit, Woman-Mother-Child Department, Lausanne University Hospital and University of Lausanne, Lausanne, Switzerland, [4]Center for Biomedical Imaging (CIBM), Lausanne, Switzerland

Introduction: Determination of cardiac volumes and ejection fraction in cardiac magnetic resonance (CMR) is important in right-sided congenital heart disease (CHD). Usually 2D cine sequences are acquired, however, precise prescription of image planes and repetitive breath-holds associated with long scan times can be difficult in patient-population with reduced compliance. Free-running whole-heart imaging may overcome these limitations by providing 3D volumes with isotropic resolutions and enabling the retrospective integration of arbitrary scan planes in free-breathing and without needing ECG-triggering (5D images). This study therefore compares free-running 5D imaging using a Gadolinium enhanced fast interrupted steady state (FISS) sequence to standard 2D cine acquisitions.

Material and Methods: In patients with right-sided CHD the FISS research sequence was acquired in addition to 2D standard cines a 1.5T scanner. 5D images where reconstructed offline using a compressed-sensing based approach. 5D dataset were reformatted into short and long-axis images to match the same spatial orientation as that from standard 2D cine images. Right (RV) and left ventricular (LV) end-diastolic and end-systolic volumes as well as ejection fraction (EF) were compared between both techniques.

Results: Thirty-one patients (age 36±14y, 17 women, 10 tetralogy of Fallot, 6 atrial switch operation for transposition of great arteries, 7 pulmonary stenosis, 5 atrial defect/shunt closure, 2 Ebstein disease, one pulmonary artery hypertension) were included. FISS derived ventricular volumes and ejection fraction differed significantly from those obtained by 2D cine (Table, Figure). Bland-Altman-analyses revealed a systematic mild overestimation of ventricular volumes and underestimation of ejection fraction by FISS (Table, Figure).

Conclusion: In this preliminary study, 5D imaging derived ventricular volumes and ejection fraction in complex right-sided CHD are comparable although associated with an apparently systematic overestimation of biventricular volumes and underestimation of ejection fraction. A larger study is on the way to provide more information on this new technology.

Table Comparison of absolute volumes, ejection fractions and bias between 2D and FISS cine sequences

Parameter	FISS	2D	p	bias	R	p*
LVEDV, ml	167 ± 43	157 ± 39	<0.001	9.5 ± 10.4 (-10.9; 30.0)	0.974	< 0.001
LVESV, ml	80 ± 32	70 ± 22	<0.001	10.5 ± 9.4 (-7.8, 28.9)	0.937	< 0.001
LVEF, %	52 ± 7	56 ± 5	0.001	-3.9 ± 6.2 (-16.1, 8.2)	0.432	0.015
RVEDV, ml	209 ± 62	201 ± 61	0.019	8.5 ± 19.0 (28.8, 45.9)	0.952	< 0.001
RVESV, ml	115 ± 42	104 ± 43	<0.001	11.3 ± 14.0 (-16.5, 39.1)	0.45	< 0.001
RVEF, %	46 ± 9	49 ±9	0.002	-3.7 ± 6.0 (-15.6, 8.3)	0.767	0.064

Data shown are bias (ml) (lower, upper limit of agreement), correlation coefficient

p corresponds to 2D and FISS values, p* corresponds to biais and correlation

Abbrevation: LVEDV = Left ventricular enddiastolic volume, LVESV = left ventricular endsystolic volume, LVEF = left ventricular ejection fraction, RVEDV = right ventricular enddiastolic volume, RVESV = rigth ventricular endsystolic volume, RVEF = right ventricular ejection fraction

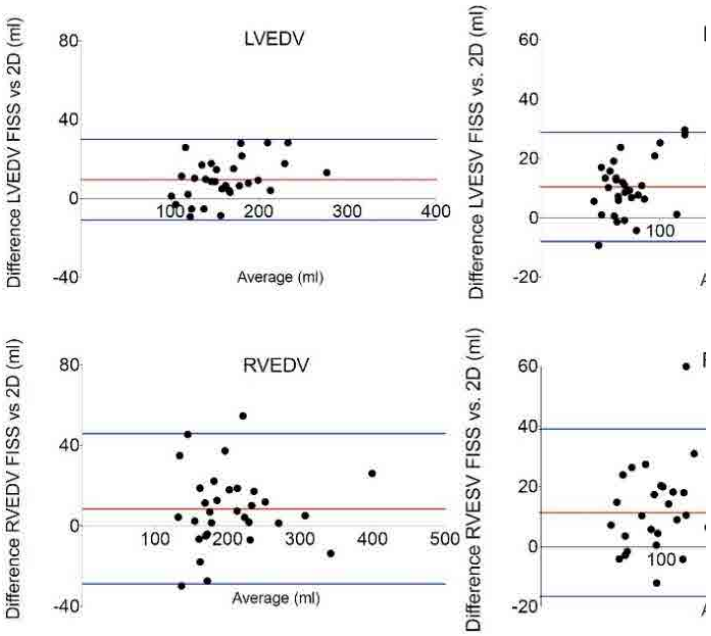

BEST ORAL ABSTRACT – HEART FAILURE

O76

Changes of amyloid burden in light chain amyloidosis on serial 18F-florbetapir PET/CT

Dominik C. Benz[1,2], Vasvi Singh[1], Olivier Clerc[1], Marie Foley Kijewski[1], Giada Bianchi[3], Andrew Yee[4], Frederick Ruberg[5], Michael Jerosch-Herold[1], Sarah Cuddy[1], Marcelo Di Carli[1], Ronglih Liao[6], Rodney Falk[1], Sharmila Dorbala[1]

[1]Cardiovascular Imaging and Amyloidosis Programs at Brigham and Women's Hospital, Harvard Medical School, Boston, United States, [2]University Hospital Zurich, Department of Cardiology, Zurich, Switzerland, [3]Amyloidosis Program, Division of Hematology, Brigham and Women's Hospital, Harvard Medical School, Boston, United States, [4]Massachusetts General Hospital, Harvard Medical School, Boston, United States, [5]Boston Medical Center, Boston University School of Medicine, Boston, United States, [6]Stanford University, Stanford, United States

Introduction: Monitoring organ response is key for the management of light chain (AL) amyloidosis. NT-proBNP and, more recently, extracellular volume (ECV) from cardiac magnetic resonance (CMR) imaging have been used to assess disease progression. However, neither of these markers is specific for cardiac amyloid burden. The aim of the present study is to compare longitudinal changes in cardiac uptake of 18F-florbetapir by PET with established biomarkers.

Material and Methods: This prospective study included 58 subjects with biopsy-proven AL amyloidosis; by conventional criteria, 40 subjects had AL cardiomyopathy (AL-CMP) and 18 subjects did not have cardiac involvement (AL-non-CMP). Subjects underwent serial 18F-florbetapir cardiac PET at baseline as well as 6 months (n = 52) and/or 12 months (n = 37) after initiation of plasma cell therapy. Each study visit included assessment of ECV, NT-proBNP, quality of life (Minnesota Living With Heart Failure Questionnaire) and functional capacity (6-min walk test). Myocardial amyloid burden was quantified as percentage injected dose (%ID). All comparisons were paired within subjects.

Results: In AL-CMP, %ID decreased from baseline to 6 months (median relative change: –12%, p = 0.002) and to 12 months (–14%, p = 0.003). In contrast, ECV trended to expand at 6 months (+4%, p = 0.088) and decreased from 6 months to 12 months (–6%, p = 0.004). Change in %ID correlated significantly with changes in NT-proBNP (rho = 0.531), quality of life (rho = 0.368) and functional capacity (rho = –0.459) at 12 months. Among responders in NT-proBNP, quality of life and functional capacity, %ID decreased significantly compared non-responders (Panel A-C). In contrast, change in ECV did not differ between responders and non-responders (Panel D-F). In AL-non-CMP, %ID remained unchanged (p = 0.523) while ECV increased (+6%, p = 0.011).

Conclusion: Serial 18F-florbetapir PET reveals temporal changes of amyloid burden in AL amyloidosis as early as 6 months after initiation of plasma cell therapy. These changes are associated with changes in established biomarkers of disease activity.

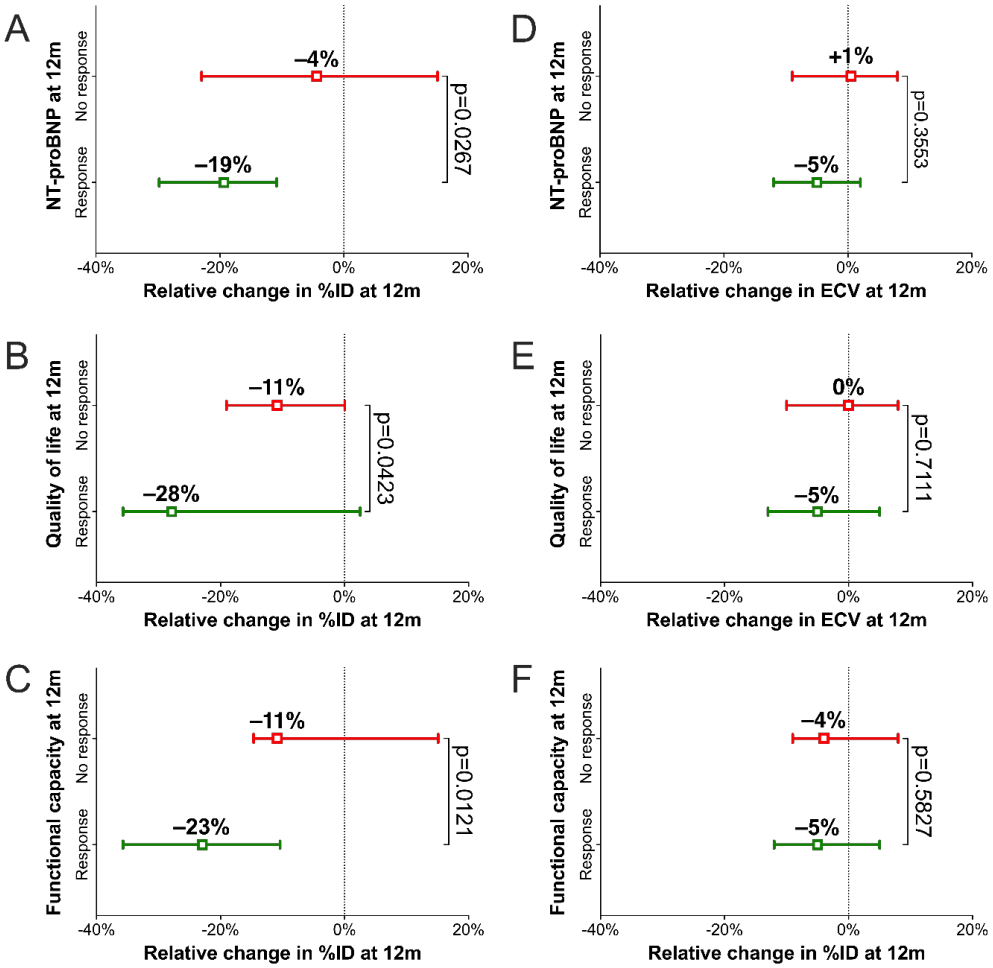

BEST ORAL ABSTRACT – CORONARY ARTERY DISEASE & ACUTE CARDIOVASCULAR CARE

O77

Gut-microbiota-derived imidazole propionate is a novel marker of cardiometabolic risk in patients with coronary artery disease

Florian A. Wenzl[1], Peizhi Wang[2], Katharina Beck[3], Slayman Obeid[4], Francesco Bruno[5], David Nanchen[6], Luca Liberale[7], Victor Schweiger[8], François MacH[9], Arnold von Eckardstein[10], Lorenz Räber[11], Arash Haghikia[12], Fredrik Bäckhed[13], Ulf Landmesser[14], Thomas F. Lüscher[15]

[1]Center for Molecular Cardiology, University of Zürich, Schlieren, Switzerland., National Disease Registration Service, NHS England, 10 South Colonnade, Canary Wharf, London, UK., Department of Clinical Sciences, Karolinska Institute, Stockholm, Sweden., Zurich, Switzerland, [2]Center for Molecular Cardiology, University of Zürich, Schlieren, Switzerland., Department of Cardiology, National Clinical Research Center for Cardiovascular Diseases, Fuwai Hospital, National Center for Cardiovascular Diseases, Chinese Academy of Medical Sciences and Peking Union Medical College, Beijing, China., Zurich, Switzerland, [3]Wallenberg Laboratory, Department of Molecular and Clinical Medicine and Sahlgrenska Center for Cardiovascular and Metabolic Research, University of Gothenburg, 413 45 Gothenburg, Sweden., Gothenburg, Sweden, [4]Division of Cardiology, Department of Medicine, Basel Cantonal Hospital, Basel, Switzerland., Basel, Switzerland, [5]Division of Cardiology, Cardiovascular and Thoracic Department, Molinette Hospital, Città della Salute e della Scienza, Corso Bramante 88, 10126 Turin, Italy., Heart Division, Royal Brompton and Harefield Hospitals, Sydney Street, London, UK., Turin, Italy, [6]Center for Primary Care and Public Health University of Lausanne., Lausanne, Switzerland, [7]First Clinic of Internal Medicine, Department of Internal Medicine, University of Genoa, 6 Viale Benedetto XV, 16132, Genoa, Italy., IRCCS Ospedale Policlinico San Martino, Genoa - Italian Cardiovascular Network, 10 Largo Benzi, 16132, Genoa, Italy., Genoa, Italy, [8]Department of Cardiology, University Hospital Zurich, Rämistrasse 100, 8091 Zurich Switzerland., Department of Cardiology, Angiology and Intensive Care Medicine, Deutsches Herzzentrum der Charité, Augustenburger Platz 1, 13353 Berlin, Germany., Berlin, Germany, [9]Department of Cardiology, Geneva University Hospital, Geneva, Switzerland., Geneva, Switzerland, [10]Institute of Clinical Chemistry, University Hospital Zurich and University of Zuich, Zurich, Switzerland., Zurich, Switzerland, [11]Department of Cardiology, Cardiovascular Center, University Hospital Bern, Bern, Switzerland., Bern, Switzerland, [12]University Hospital St Josef-Hospital Bochum, Cardiology and Rhythmology, Ruhr University Bochum, Bochum, Germany., Department of Cardiology, Angiology and Intensive Care, Deutsches Herzzentrum der Charité (DHZC), Campus Benjamin Franklin, Berlin, Germany., DZHK (German Centre for Cardiovascular Research), Partner site Berlin, Berlin, Germany., Bochum, Germany, [13]Wallenberg Laboratory, Department of Molecular and Clinical Medicine and Sahlgrenska Center for Cardiovascular and Metabolic Research, University of Gothenburg, 413 45 Gothenburg, Sweden., Region Västra Götaland, Sahlgrenska University Hospital, Department of Clinical Physiology, Gothenburg, Sweden., Gothenburg, Sweden, [14]Department of Cardiology, Angiology and Intensive Care, Deutsches Herzzentrum der Charité (DHZC), Campus Benjamin Franklin, Berlin, Germany., DZHK (German Centre for Cardiovascular Research), Partner site Berlin, Berlin, Germany., DZHK (German Centre for Cardiovascular Research), Partner site Berlin, Berlin, Germany., Berlin, Germany, [15]Center for Molecular Cardiology, University of Zürich, Schlieren, Switzerland., Heart Division, Royal Brompton and Harefield Hospitals, Sydney Street, London, UK., National Heart and Lung Institute, Imperial College, London, United Kingdom., Zurich, Switzerland

Introduction: Circulating imidazole propionate (ImP) is a gut-derived amino acid metabolite with adverse effects on glucometabolic function. This study examined the prognostic value of ImP in patients with coronary artery disease (CAD).

Material and Methods: Circulating ImP levels were measured in a prospective multicentre cohort of patients with acute coronary syndrome (ACS) from Switzerland (n = 4787), in a cohort of patients with chronic coronary syndrome (CCS, n = 883), and in individuals without CAD (n = 254) from Germany. All-cause mortality and major adverse cardiovascular events (MACE) defined as mortality, myocardial infraction, and cerebrovascular events were assessed at 1-year in patients with ACS and at a median follow-up of 2.95 years in patients with CCS. Multivariable-adjusted Cox models, accounting for established risk factors, were used to evaluate the incremental predictive value of ImP. In patients with ACS, we additionally adjusted for various gut-derived metabolites including trimethylaminoxid (TMAO).

Results: ImP levels were higher in patients with ACS and CCS compared to individuals without CAD. ImP was strongly associated with cardiometabolic traits including high HbA1C, presence of type 2 diabetes, impaired renal function, a higher number of affected coronary arteries, and decreased left ventricular function in both clinical entities. ImP was associated with increased mortality on crude (ACS HR per log2 increase: 1.68, 95% confidence interval [CI] 1.53–1.85; CCS HR: 1.46, 95%CI 1.23–1.74) and on multivariable-adjusted analysis (ACS HR: 1.28, 95%CI 1.12–1.48, CCS HR: 1.25, 95%CI 1.03–1.52) in both entities. Similar results were observed for MACE (ACS HR: 1.24, 95%CI 1.10–1.38; CCS HR: 1.21, 95%CI 1.09–1.36). In patients with ACS, ImP provided predictive value beyond TMAO (HR 1.64, 95%CI 1.18–2.28) and beyond the GRACE 2.0 score (HR 1.70, 95%CI 1.21–2.39).

Conclusion: Circulating ImP reflects the cardiometabolic risk of patients with CAD beyond established gut-derived metabolites. ImP may refine risk stratification for personalised secondary prevention strategies.

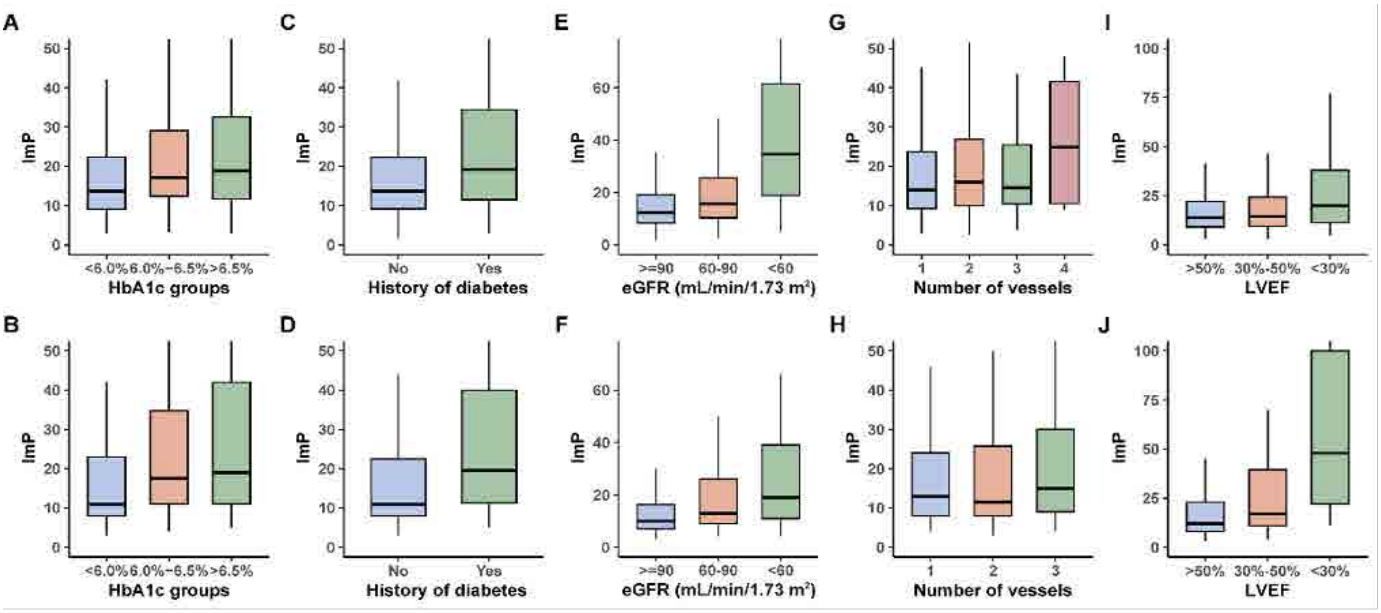

Figure 1: Box plots of ImP levels in patients with ACS (top) and CCS (bottom), stratified by HbA1c level (A and B), diabetes status (C and D), renal function (E and F), number of diseased vessels (G and H), and left ventricular function (I and J). ACS, acute coronary syndrome; CCS, chronic coronary syndrome; eGFR, estimated glomerular filtration rate; HbA1c, hemoglobin A1c; ImP, imidazole propionate; LVEF, left ventricular ejection fraction.

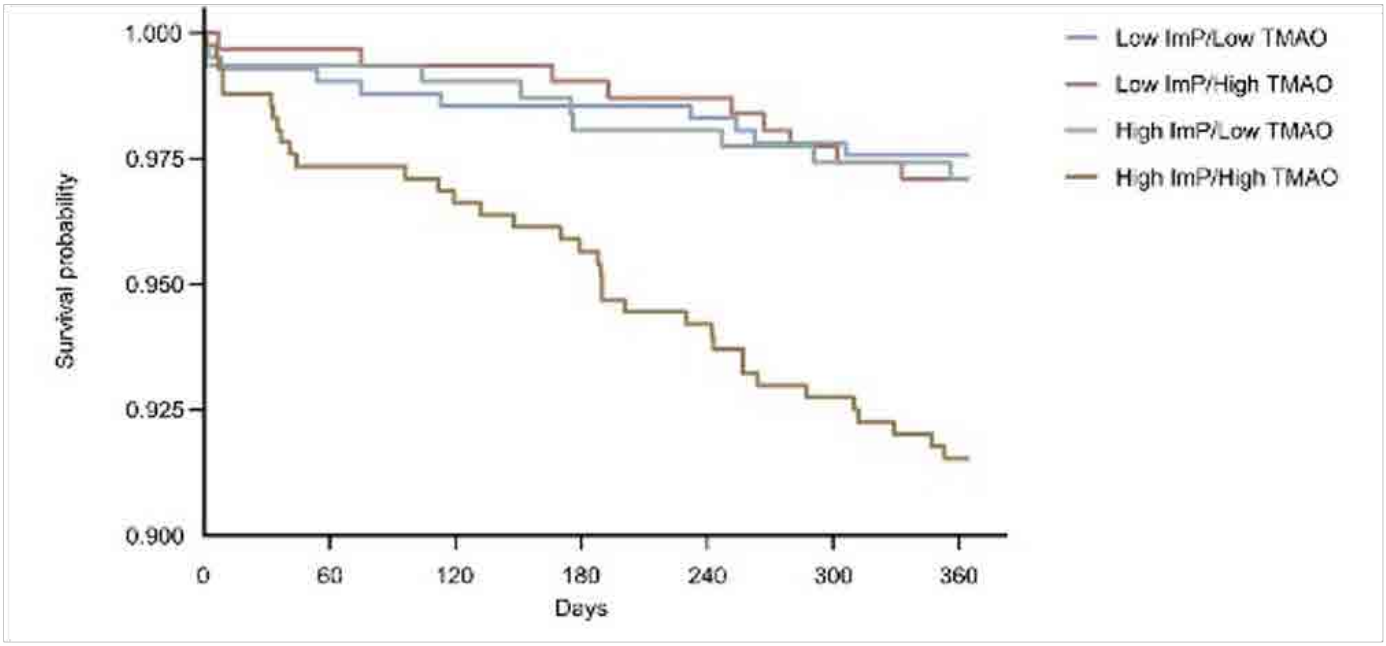

Figure 2: Kaplan-Meier plot of patients with ACS stratified according to TMAO levels and ImP levels. High and low levels refer to values above and below the median respectively.

BEST ORAL ABSTRACT – VALVULAR HEART DISEASE

O78

Long-Term Outcomes of Patients Requiring Pacemaker Implantation after Transcatheter Aortic Valve Implantation: Insights form the Nationwide SwissTAVI Registry

Serban Teodor[1], Patrick Badertscher[1], Stefan Stortecky[2], Sven Knecht[1], David Tueller[3], Raban Jeger[3], Oliver Reuthebuch[1], Oliver Muller[4], Stefan Toggweiler[5], Peter Wenaweser[6], Tobias Reichlin[2], Thomas Nestelberger[1], Felix Mahfoud, Michael Kühne[1], Christian Sticherling[1]

[1]Department of Cardiovascular Surgery, University Hospital Basel, Basel, Switzerland, [2]Inselspital, Bern University Hospital, Bern, Switzerland, [3]Triemli Hospital, Zürich, Switzerland, [4]Lausanne University Hospital - CHUV, Lausanne, Switzerland, [5]Cantonal Hospital Lucerne, Lucerne, Switzerland, [6]Hirslanden Clinic Zürich, Zürich, Switzerland

Introduction: The impact of pacemaker (PM) implantation on outcomes following transcatheter aortic valve replacement (TAVI) remains controversial, especially as TAVI indications expand to low-risk patients.

Material and Methods: In this prospective, observational, nationwide TAVI cohort study, the outcomes of patients undergoing permanent PM implantation were investigated. Patients were enrolled from 19 centers across Switzerland between February 2011 and June 2022.

Results: Among 13'360 patients enrolled (mean age 82±7 years, 47% female, self-expanding valves 48%), 2028 (15%) required PM within 30 days post-TAVI. Patients requiring post-TAVI PM implantation were older (82±6 vs. 81±7 years), predominantly male (58% vs. 50%), and more often had atrial fibrillation (34% vs. 29%). At one year follow-up, these patients had higher overall (HR 1.28, 95% CI 1.09-1.49, p = 0.002) and cardiovascular mortality (HR 1.4, 95% CI 1.15-1.69, p = 0.001). These trends persisted at five and ten year follow-up. After multivariable adjustments, significantly higher rates of cardiovascular mortality, LVEF decline ≥10% and NYHA III-IV at one year follow-up were observed (aHR 1.35, 95%CI 1.23-1.49, p<0.001)), along with higher all-cause and cardiovascular mortality rates at 5- and 10-year follow-up in patients requiring PM implantation following TAVI compared to those not needing a PM.

Conclusion: In this large nationwide registry, patients receiving PM implantation within 30 days after TAVI had significantly higher rates of overall and cardiovascular mortality up to 10-years. As TAVI indications expand to lower-risk patients, these findings highlight the need for future research to reduce the incidence and mitigate risks associated with PM implantation after TAVI.

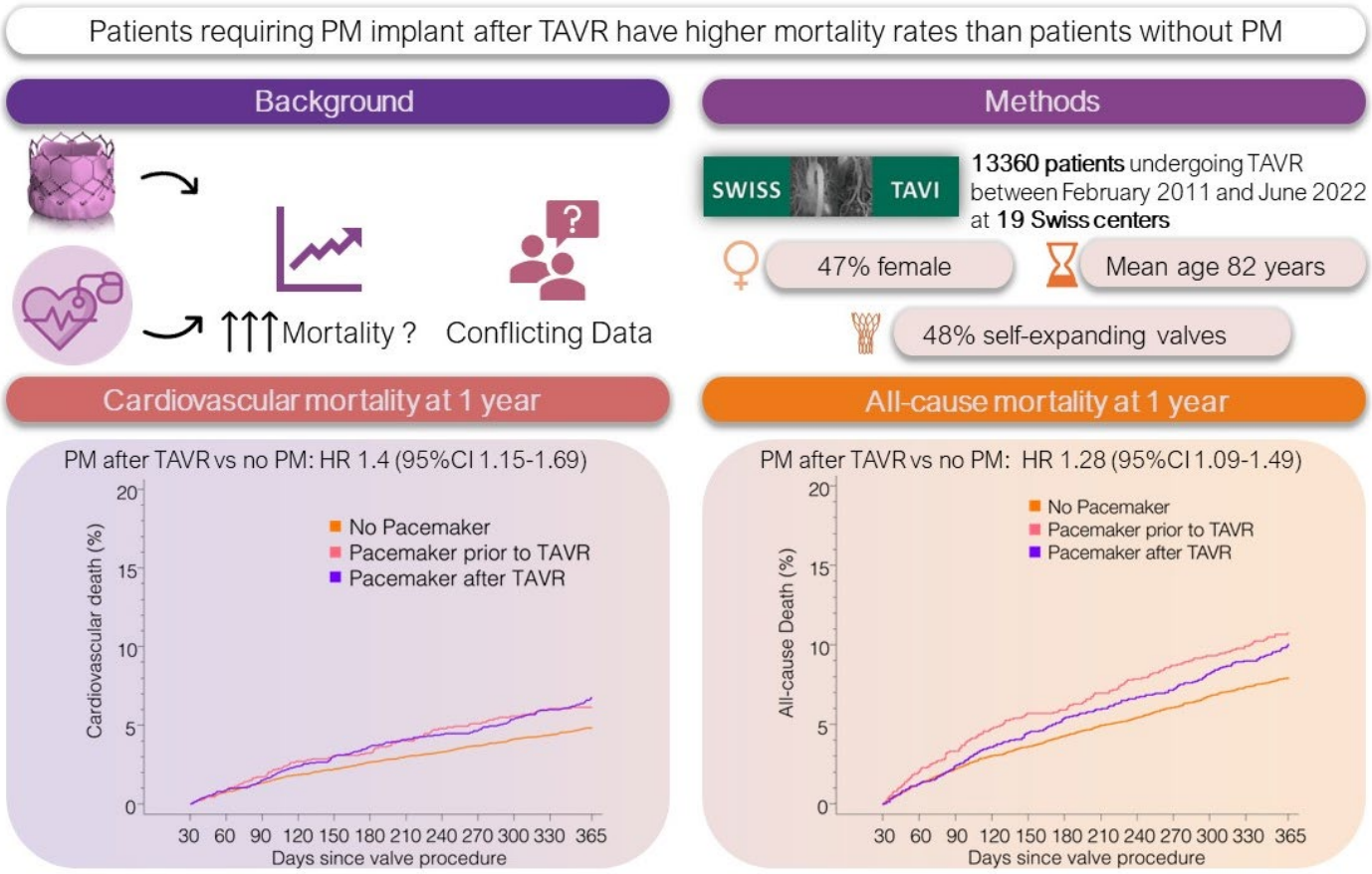

Central Illustration: Overview of background, methodology and main results. Abbreviations: HR – Hazard Ratios TAVR – transcatheter aortic valve replacement, PM – pacemaker

BEST ORAL ABSTRACT – CLINICAL CASE REPORTS

O79

Emergency management: Should global ischemia with typical acute chest pain go straight to the Cath Lab?

Ronja Dittrich[1], Stephan Schneiter[1], Ahmed Ouda[2], Philipp K. Haager[1]

[1]HEALTH Ostschweiz, Kantonsspital St. Gallen, department of cardiology, St. Gallen, Switzerland, [2]University Hospital of Zürich, department of cardiac surgery, Zürich, Switzerland

Introduction: A 55-year-old patient has been assigned to the emergency department with suspected Acute Coronary Syndrome. He had woken up 1 hour earlier that same morning with typical acute chest pain.

Material and Methods:

The ECG showed global ischemia with wide-spread ST depression maximally in leads V4-6 and ST elevation in lead AVR. Focused transthoracic echocardiographic findings in the emergency room showed preserved left ventricular ejection fraction with discrete hypokinesia of the anterior wall only, which didn't reflect the ECG findings as expected. At second glance, there was a relevant insufficiency of the aortic valve with dilation of the sinus of valsalva and the ascending aorta. The CT scan then confirmed a Type A aortic dissection (TAAD) with an intimal flap. The patient developed a cardiogenic shock and was urgently transferred to the cardiac surgery department at the University Hospital Zürich. Emergency replacement of aortic root, ascending aorta and hemiarch with reimplantation of native aortic valve was performed successfully. The patient was extubated 1 day after the operation and was discharged to rehab without any signs of infarction in the ECG.

Results: This case highlights the role of transthoracic echocardiography in emergency situations. On the one hand, echocardiography should not delay rapid percutaneous revascularization in patients with ST elevation myocardial infarction; on the other hand, it enables rapid clarification of the cause in the event of clinical evidence for cardiac decompensation or exclusion of mechanical complications in patients with acute coronary ischemia. High level of suspicion is required, especially in patients where ECG and echocardiographic findings of wall movement abnormalities don`t match like in this case. Main Reason is that TAAD may lead to coronary artery occlusion or dissection and can therefore mimic a STEMI.

Conclusion: TTE is useful to quickly identify and triage patients with acute aortic dissection causing coronary malperfusion as complication.

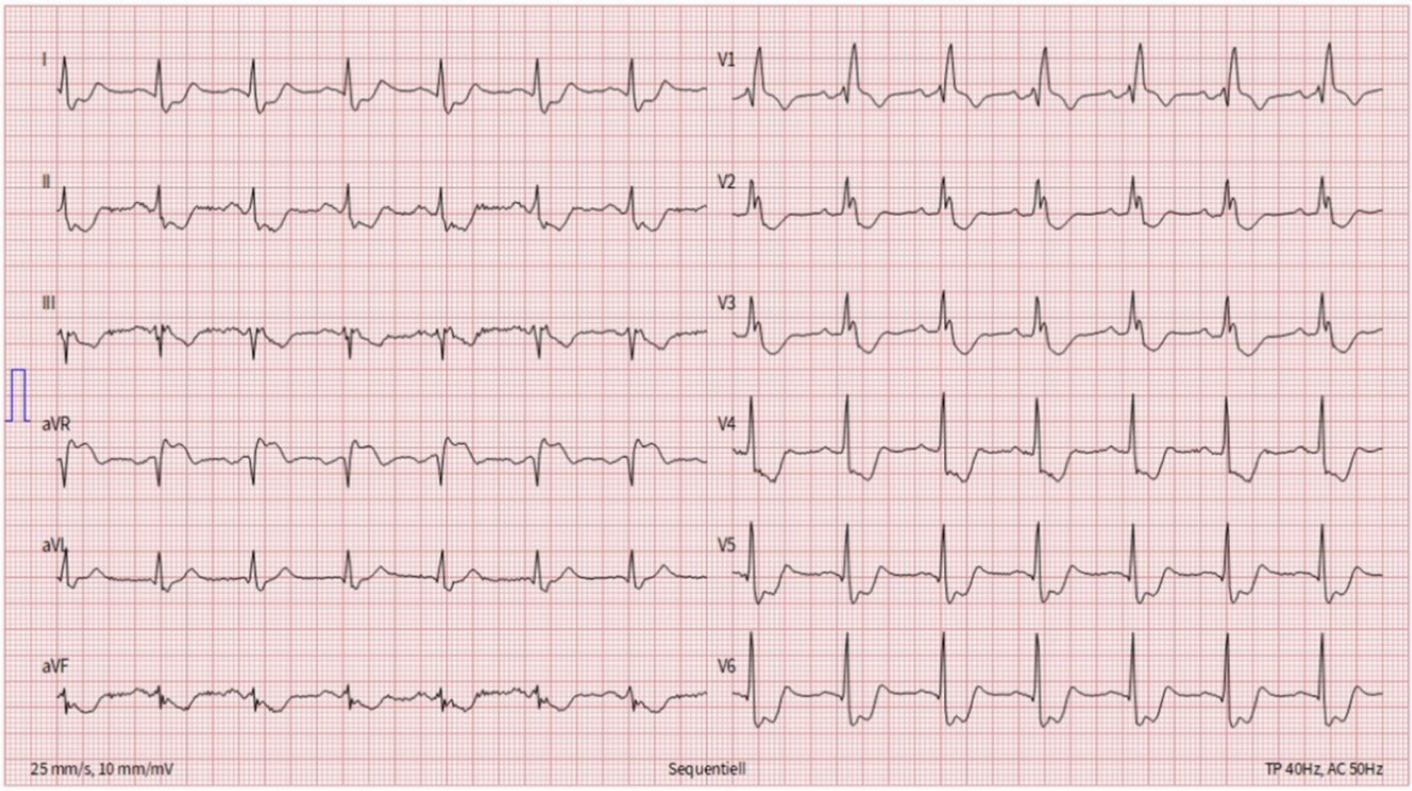

Figure 1: Initial 12-lead-ECG obtained in the emergency department

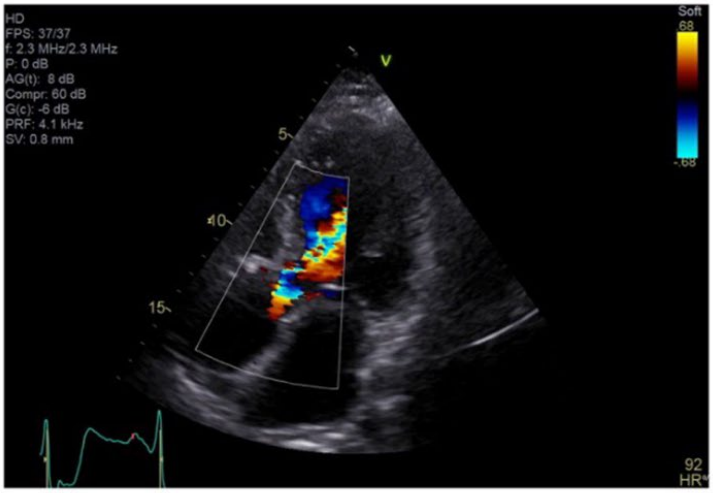

Figure 2: Bedside echocardiography showing 5-chamber view with relevant aortic insufficiency

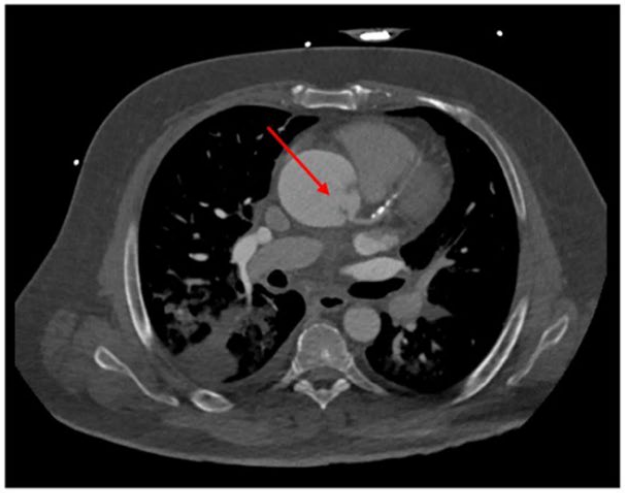

Figure 3: Chest CT scan showing a dilated ascending aorta (52 mm) with two intima flaps and mural hematoma. One intima flap close to the Left Main artery (red arrow).

BEST ORAL ABSTRACT – PREVENTION, REHABILITATION AND SPORTS CARDIOLOGY

O80

Endothelial dysfunction in patients with elevated lipoprotein(a) levels

Philip Sommer[1], Konstantinos Bitos[1], Natallia Laptseva[1], Frank Ruschitzka[1], Matthias Nägele[1], Andreas Flammer[1], Isabella Sudano[1]

[1]*University Heart Center, University Hospital Zurich, Zurich, Switzerland*

Introduction: Endothelial dysfunction is an early step in the pathogenesis of atherosclerosis. Epidemiological studies have identified lipoprotein (a) (Lp(a)) as a potential predictor of cardiovascular events. Retinal vessel analysis (RVA) is a novel approach for detecting and quantifying endothelial dysfunction, including dynamic measurements of retinal vascular dilation and static assessments of retinal vessels. However, the impact of elevated Lp(a) on retinal microvasculature remains unclear. This study includes preliminary data to examine the relationship between elevated Lp(a) levels and retinal microvascular function.

Material and Methods: This cross-sectional observational study enrolled 50 patients with at least one cardiovascular risk factor (mean age 57.6 ± 11.6 years; 39% female). Patients were classified into high Lp(a) and low Lp(a) groups using the European Atherosclerosis Society's rule-out value (<30 mg/dl). The Primary outcome was flicker-induced dilation of retinal arterioles (FIDart). Secondary outcomes included flicker-induced dilation of venules (FIDven), arteriovenous ratio and flow-mediated dilation. Multivariate regression was used to adjust for confounding factors.

Results: The low Lp(a) group included 34 patients (mean age 57.5±13.0; 41% female), whereas 16 patients belonged to the high Lp(a) group (mean age 57.7±7.9; 35% female). FIDart was significantly lower in high Lp(a) patients (mean FIDart: high Lp(a) 1.2 ± 1.3% vs low Lp(a) 2.4 ± 1.5%, P = 0.006). A negative correlation between FIDart and Lp(a) was found (r = -0.34, p = 0.02), indicating impaired microvascular function with higher Lp(a). This remained significant after adjusting for confounders (Lp(a) β-coefficient -0.41; p = 0.01). No significant differences were observed for FIDven, flow-mediated dilation, or arteriovenous ratio.

Conclusion: Elevated Lp(a) levels are associated with retinal microvascular dysfunction, as seen in reduced FIDart. Dynamic RVA could be a promising tool for studying microvascular dysfunction in high cardiovascular risk populations.

BEST ORAL ABSTRACT – RHYTHM DISORDERS

O81

How much atrial fibrillation is too much after ablation of paroxysmal atrial fibrillation? Insights from the COMPARE-CRYO study using continuous rhythm monitoring

Salik Ur Rehman Iqbal[1], Thomas Kueffer[1], Sven Knecht[1 2], Patrick Badertscher[2], Jens Maurhofer[1], Philipp Krisai[2], Corinne Jufer[1], Gregor Thalmann[1], Dik Heg[1], Helge Servatius[1], Hildegard Tanner[1], Michael Kühne[2], Laurent Roten[1], Christian Sticherling[2], Tobias Reichlin[1]

[1]Inselspital, University of Bern, Bern, Switzerland, [2]University of Basel Hospital, Basel, Switzerland

Introduction: Recurrence after pulmonary vein isolation (PVI) is currently defined as any atrial arrhythmia lasting >30s. Though widely used, this crietrion is suboptimal. The purpose of this study was evaluate the impact of alternative efficacy endpoints after PVI that might relate better to pateints' disease burden and metrics of healthcare utilization using continuous rhythm monitoring by means of implantable cardiac monitors (ICM).

Material and Methods: This is a prespecified sub study of the COMPARE-CRYO study, which enrolled patients with paroxysmal atrial fibrillation undergoing cryoballoon ablation. All patients underwent ICM implantation and the blanking period duration was 90 days. Patients were classified on the basis of AF burden, duration of the longest AF episode, and the number of AF episodes. Outcomes of redo procedures, AF-related hospitalizations (including cardioversions) and change in quality of life (EQ5D) score were assessed.

Results: For the 201 patients enrolled in the study, the primary endpoint of AF/AT recurrence occurred in 44% (89) patients. A total of 6104 arrhythmia episodes occurring between days 91 and 365 were analyzed. Rates of redo ablations and AF-related hospitalizations were lowest in patients with AF burden <0.1%, AF episode durations <1h or <6 AF episodes, respectively (Figure 1, Panel A-C). This increased for AF burden >0.1%, AF episode duration >1h, and >6 AF episodes and was highest for AF burden >1%, AF episode duration >24h, and >33 AF episodes (Figure 1, Panel A-C). Patients with their longest episode >24h had a reduced EQ-5D score at 12 months from baseline (p = 0.008).

Conclusion: Alternative efficacy endpoints based on AF burden, AF episode duration or number of AF episodes have a significant impact on healthcare utilization metrics. AF burden >0.1%, AF episode duration >1h and more than 6 AF episodes resulted in increased rates of redo procedures and AF-related hospitalizations.

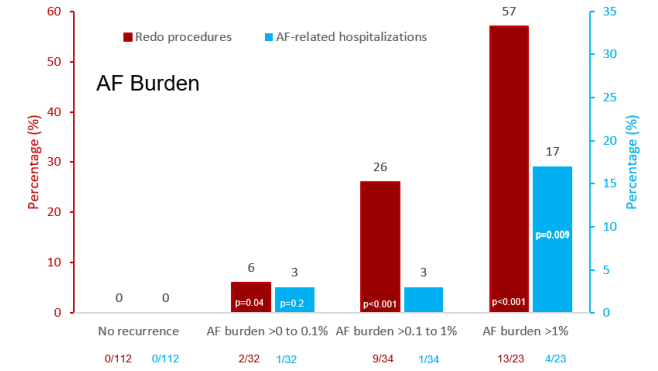

A

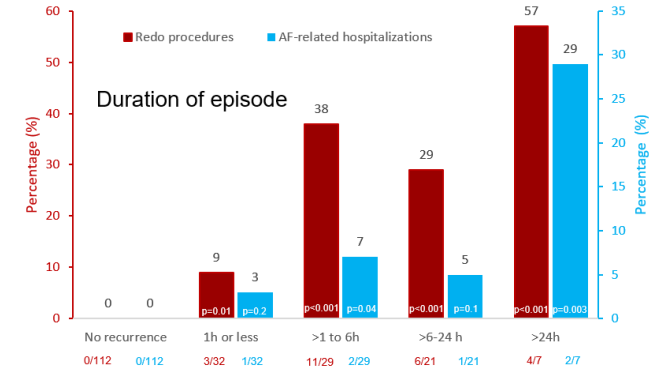

B

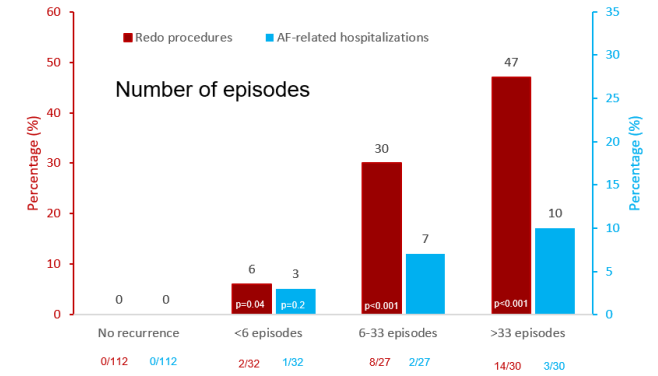

C

POSTER WALK "BASIC SCIENCE"

P002

Epigenetic editing of BET proteins restores autophagy and cardiac function in cardiometabolic heart failure with preserved ejection fraction

Ludovica Di Venanzio[1], Era Gorica[1], Shafeeq Mohammed[1], Natalia Atzemian[1], Sarah Costantino[1], Frank Ruschitzka[1], Francesco Paneni[1]

[1]CTEC- Center for Translational and Experimental Cardiology, Zürich, Switzerland

Introduction: Cardiometabolic heart failure with preserved ejection fraction (cHFpEF) is a prevalent disease whose underlying mechanisms are poorly understood. Autophagy appears to be involved in the pathophysiology of the disease. Epigenetic modulators, particularly BET (bromodomain and extraterminal) proteins, have emerged as potential therapeutic targets by influencing transcriptional regulation in response to environmental stressors. This study investigates whether BET proteins modulate autophagy in cHFpEF and whether their pharmacological inhibition by BET protein inhibitors can restore autophagic flux, rescuing cardiac damage.

Material and Methods: An established mouse model of cHFpEF combining metabolic and hemodynamic stress over 15 weeks was used. Mice were treated with either vehicle or the selective BET inhibitor RVX-208 for 14 days. Autophagic gene expression was assessed using a custom real-time PCR array and validated by immunoblotting. To examine chromatin changes, ChiP-seq assays was performed to study the enrichment of active chromatin marks and BET proteins gene loci in cardiac specimens from the different experimental groups.

Results: Autophagy was impaired in cHFpEF mice, evidenced by upregulation of mTOR signaling and decreased expression of autophagosome genes such as Atg7 and Atg13. Gene profiling revealed deregulation of key autophagy-related genes, including Atg5, TMEM74, and PS6K (an mTOR target). ChiP-seq revealed strong enrichment of BET proteins and active chromatin marks at the mTOR promoter, suggesting a direct role of BET proteins in regulating autophagy. Treatment with RVX-208 restored autophagic gene expression and improved both diastolic dysfunction and exercise tolerance.

Conclusion: Our study unveils a BET-driven epigenetic mechanism regulating autophagy in cHFpEF. Pharmacological inhibition of BET proteins restores autophagic flux while improving cardiac function in cHFpEF mice. Our results set the stage for preclinical studies testing FDA-approved BET inhibitors in the setting of HFpEF.

P003

Aging-Related Changes in Megakaryocyte Progenitors: A Single-Cell Transcriptomics Study Reveals the Upregulation of Prothrombotic and Proimmune-Related Mechanisms

Pratintip Lee[1], Aurelia Seeberger[1], Carolina Balbi[1], Meret Alleman[1], Adhideb Ghosh[2], Tongtong Wang[2], Giovanni Camici[1], Thomas Lüscher[1], Christian Wolfrum[2], Soheil Saeedi Saravi[3], Jürg Beer[1]

[1]Center for Molecular Cardiology, University of Zurich, Schlieren, Switzerland, [2]Department of Health Sciences and Technology, ETH Zurich, Zurich, Switzerland, [3]Center for Translational and Experimental Cardiology, Department of Cardiology, University Hospital Zurich, University of Zurich, Schlieren, Switzerland

Introduction: Platelet (Plt) reactivity increases with age and contributes to cardiovascular disease (CVD) and thromboembolism (TE). Despite the involvement of genetic and acquired risk factors, the mechanisms underlying age-related platelet dysfunction remain unclear.

Here, we studied the age-specific pro-thrombotic and pro-inflammatory characteristics of megakaryocytes (Mk) in an aging mouse model.

Material and Methods: Single-cell RNAseq was conducted on bone marrow (BM) samples obtained from femora and tibiae of young (3 months) and aged (>24 months) male and female mice. Sorting was employed to enrich Mk from the BM. Cells were processed and sequenced using the 10x Genomics single platform. Mk cells were defined transcriptionally by the expression of *Pf4, Vwf, Gp6, Gp1ba, Itgb3*, and *Mpl* genes. By functional pathway analyses, based on Gene Ontology (GO), we compared transcriptional signatures between aged and young mice using Seurat workflow and RStudio (v.2023.12.0).

Results: We identified 5 distinct Mk clusters (Mk1 to 5) (**fig. 1A**), with Mk3 and Mk4 subsets notably increased in aged mice consistently among male and female (**fig. 1B**). Pathway enrichment analyses revealed that Mk3 and Mk4 were enriched for procoagulant/pro-aggregatory as well as pro-immune-inflammatory genes respectively (**fig. 1C**). Interestingly, differential gene expression (DGE) analyses found that aged Mk displayed higher expression of platelet-related pathways including integrin signaling, aggregation, and platelet-leukocytes interactions. Additionally, we observed upregulated expressions of genes associated with both innate immunity (*Il1rapl2*, *Clec1a*, *B3galt1*) and adaptive immune responses mediated by T-cell (*Alcam*, *Tox) and* B-cell (*Igkv12-41*, *Ighm*) regulation. These findings highlight thromboinflammation as a potential mechanistic driver of age-related cardiovascular disease (CVD) and thromboembolic events (TE).

Conclusion: Aging is associated with the upregulation of immune-related and pro-thrombotic Mk subsets in BM. The findings suggest the innate and adaptive immune response as a mechanism for age-related CVD and TE may indicate future therapeutic targets.

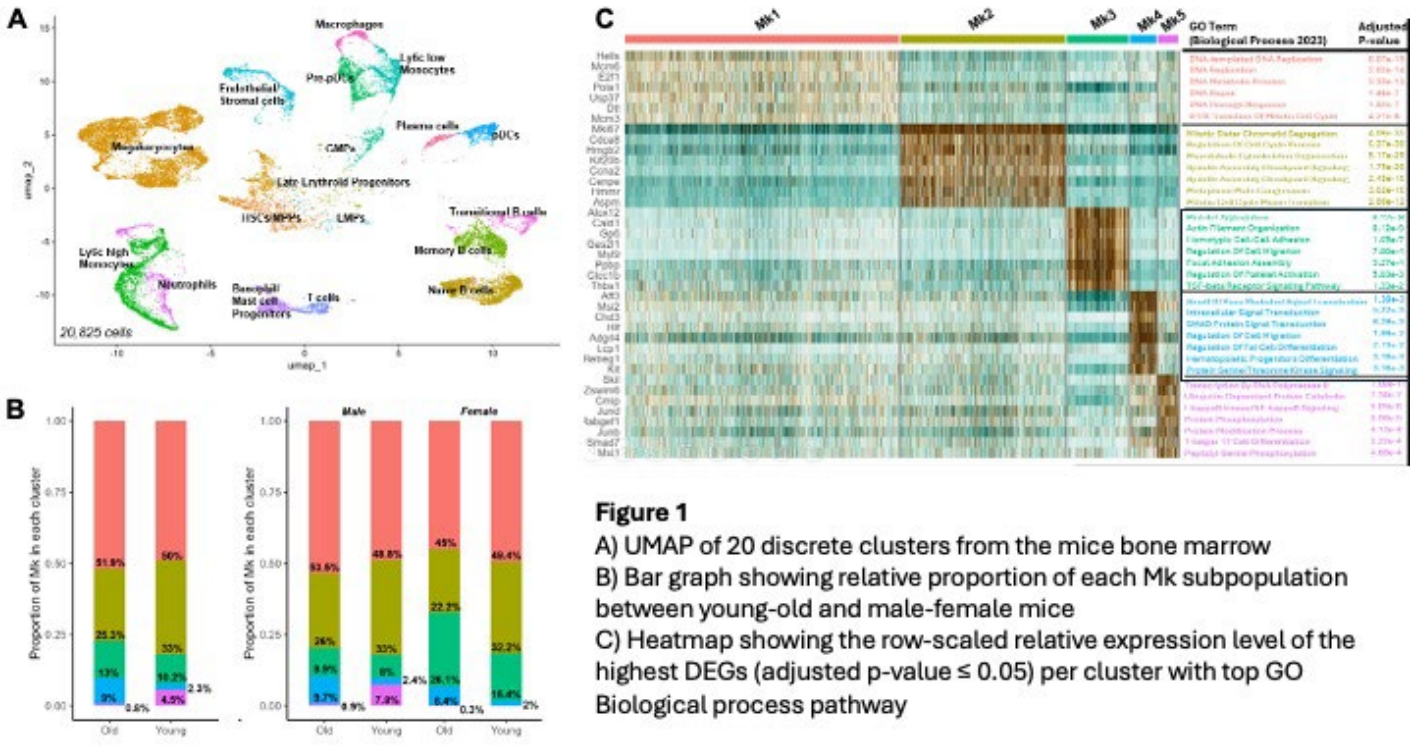

Figure 1
A) UMAP of 20 discrete clusters from the mice bone marrow
B) Bar graph showing relative proportion of each Mk subpopulation between young-old and male-female mice
C) Heatmap showing the row-scaled relative expression level of the highest DEGs (adjusted p-value ≤ 0.05) per cluster with top GO Biological process pathway

P004

The BET inhibitor Apabetalone Protects Against Heart Failure with Preserved Ejection Fraction by Suppressing Myocardial Inflammation

Era Gorica[1], Sarah Costantino[1], Shafeeq Mohammed[1], Marialucia Telesca[1], Alessia Mongelli[1], Valeria Masciovecchio[1], Alessandro Mengozzi[1], Frank Ruschitzka[1], Nazha Hamdani[2], Francesco Paneni[1]

[1]Center for Translational and Experimental Cardiology (CTEC), University of Zurich and University Hospital Zurich, Zürich, Switzerland, [2]Institute of Physiology, Ruhr University, Bochum, Germany

Introduction: Posttranslational histone modifications, play a major role in cardiac hypertrophy and dysfunction. Apabetalone (APA), a selective inhibitor of bromodomain and extraterminal containing protein family (BET) proteins, prevents BRD4 interactions with chromatin thus modulating transcriptional programs in different organs.

Material and Methods: Mice subjected to high fat diet and L-NAME treatment for 15 weeks to induce cHFpEF. Histology, mouse echocardiography (Vevo3100) and Treadmill exhaustion test were performed. Unbiased gene expression profiling by PCR array and proteomics was employed in left ventricular (LV) myocardial specimens from HFpEF and control animals. Cultured cardiomyocytes treated with palmitic acid (PA) were used as in vitro model of metabolic stress. cHFpEF mice were chronically treated with the BET inhibitor APA (150mg/kg/day) or vehicle (DMSO). To translate our findings to the human setting, passive stiffness of skinned CMs collected from cHFpEF patients was assessed before and after APA treatment.

Results: HFpEF mice displayed LV hypertrophy, diastolic dysfunction, myocardial fibrosis, lung congestion and impaired exercise toleranc, compared to controls. Diastolic dysfunction - assessed by E/A ratio and isovolumic relaxation time (IVRT) - and lung congestion were significantly reduced in APA-treated mice, while exercise tolerance was improved. Transcriptomic analysis in PA-treated CMs and LV specimens from cHFpEF mice showed a profound deregulation of genes controlling inflammation, namely IL-6, TNF-alpha, and IL-1beta. ChIP assays showed BRD4 occupancy on the promoter of several inflammatory genes, including IL6. Treatment with APA suppressed inflammatory genes, with a pronounced effect on IL6. Moreover, APA reduced circulating levels of several inflammatory chemokines. The beneficial effects of APA were explained by modulation of IL-6/CaMKII/STAT3 pathway both in cHFpEF hearts and PA-treated CMs. In skinned CMs from cHFpEF patients, both APA and IL6 blockade were able to attenuate passive stiffness.

Conclusion: Our findings set the stage for preclinical studies and exploratory clinical trials testing APA in patients with cHFpEF.

P005

Pericardial fat-associated lymphoid clusters control cardiopathogenic T-cell activation and differentiation in autoimmune myocarditis

Nadine Cadosch[1], Cristina Gil Cruz[1 2], Hung-Wei Cheng[1], Frank Ruschitzka[2 3], Dörthe Schmidt[2], Christian Perez Shibayama[1], Burkhard Ludewig[1 3]

[1]Institute of Immunobiology, Medical Research Center, HOCH Health Ostschweiz, Kantonsspital St. Gallen, St. Gallen, Switzerland, [2]University Heart Center, University Hospital Zurich and University of Zurich, Zurich, Switzerland, [3]Center for Translational and Experimental Cardiology, University Hospital Zurich and University of Zurich, Zurich, Switzerland

Introduction: The parietal pericardium contains fat-associated lymphoid clusters (FALCs), which monitor the pericardial cavity for immune signals before substances are reabsorbed into the circulation, thus acting as immune surveillance hubs of the cardiac cavity. However, surprisingly little is known about the involvement of these non-classical secondary lymphoid organs in cardiac inflammation.

Material and Methods: Here, we used a mouse model of spontaneous autoimmune myocarditis to study the activation and differentiation of cardiac-specific T cells in pericardial FALCs using a combination of high-dimensional flow cytometry, single-cell RNA sequencing and confocal microscopy.

Results: We found a close correlation between myocardial and pericardial inflammation, with cardiac myosin-specific memory $CD4^+$ T cells accumulating in pericardial FALCs after their initial activation in heart-draining lymph nodes. Single-cell transcriptomic analysis of immune and stromal cells isolated from pericardial FALCs indicated the presence of distinct cellular niches that serve as amplifiers of cardiopathogenic T cell responses. $CD4^+$ T cells in FALCs were underpinned by CCL19-expressing fibroblastic reticular cells (FRCs), which directed T cell recruitment and differentiation. Bioinformatics analysis identified FRCs as key T cell interaction partners that control T cell differentiation toward the Th17 pathway via IL-6. Indeed, antibody-mediated blockade of IL-6 reduced the infiltration of IL-17^+ T cells in both the pericardium and heart, thereby preventing progression to inflammatory cardiomyopathy and heart failure.

Conclusion: In conclusion, this study highlights the role of pericardial FALCs in cardiac inflammation and reveals key mechanisms regulating T cell behavior in this specific microenvironment.

P006

Role of paracardial fat in heart failure with preserved ejection fraction

Alessia Mongelli[1], Iliana Papadopoulou[2], Era Gorica Hoxha[1], Shafeeq Mohammed[1], Héctor Rodríguez Cetina Biefer[3], Omer Dzemali[3], Sarah Costantino[1], Burkhard Ludewig[2], Frank Ruschitzka[4], Francesco Paneni[1 4]

[1]Center for Translational and Experimental Cardiology (CTEC), Department of Cardiology, University Hospital Zurich, University of Zurich, Zürich, Switzerland, [2]Medical Research Center, Kantonsspital St. Gallen, St. Gallen, Switzerland, [3]Department of Cardiac Surgery, University Hospital Zurich, Zürich, Switzerland, [4]Department of Cardiology, University Hospital Zurich, zürich, Switzerland

Introduction: Cardiometabolic HFpEF (cHFpEF) is a multisystemic syndrome where biological signals generated in several organs contribute to adverse cardiac remodeling and high mortality rates. Paracardial fat (pCF) – largest fat depot that surrounds the heart - is emerging as a metabolically active tissue which could contribute to cardiac dysfunction in cHFpEF. We investigate the role of pCF in cHFpEF.

Material and Methods: A mouse model of cHFpEF, characterized by the combination of high-fat diet (60 kcal% fat,) and L-NAME in the drinking water (0.5 g/L) for 15 weeks,. Control mice received a control diet (10 kcal% fat,) and vehicle in the drinking water. Single-cell nuclei RNA sequencing (snRNAseq) was performed by using the 10x Chromium analyzer. Cell-cell communication analysis was performed by using *CellChat* software. The function of top-ranked genes was investigated in vitro, in human adipocyte cell line

Results: The transcriptional and cellular landscape of pCF was performed by high-resolution snRNAseq analysis and 20’397 cells from control and cHFpEF mice were captured. Several clusters were identified. At clustering resolution, the analysis revealed two different adipocyte groups: adipocyte1 (defined by Pparg/Nrg4 markers) and adipocyte2 (Ncam1/Itga7 markers). The adipocyte2 cluster was highly enriched in cells from cHFpEF mice and showed a significant dysregulation of several genes on top of them neuronatin (*NNAT, up-regulated)* and Acetyl-CoA Carboxylase Alpha (ACACA, down-regulated). Pathway analysis confirmed the activation immuno-metabolic signaling, integrin-mediated signaling, adipocyte catabolic processes and inflammation in pCF cHFpEF. Interactome analysis unveiled a strong link between adipocytes and immune cell activation; while molecules for endothelial and smooth muscle cells develop and homeostasis are depleted in HFpEF vs control pCF specimens

Conclusion: pCF is a dysfunctional fat depot in cHFpEF and could contribute to myocardial inflammation in this setting.

Figure1

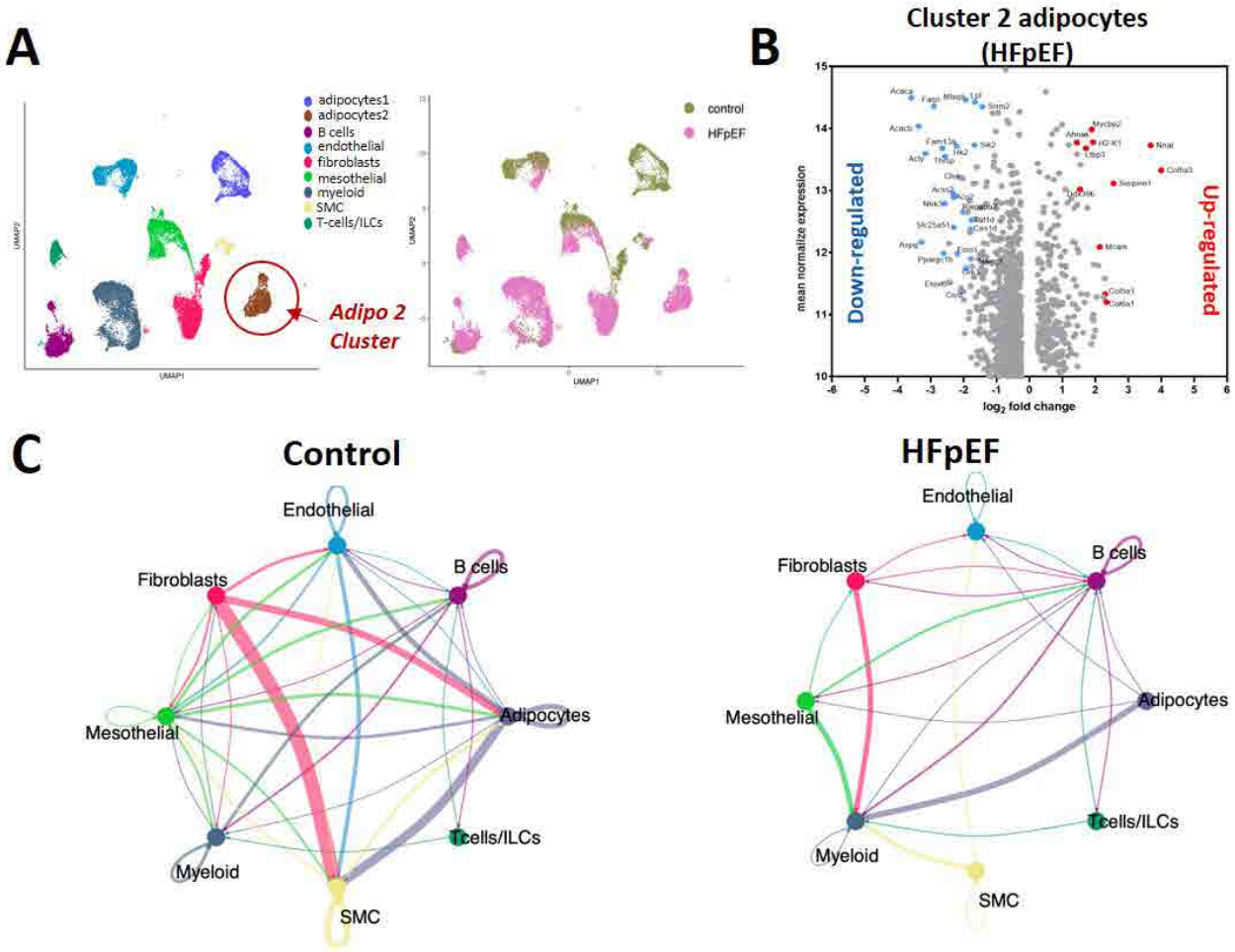

Altered transcriptional programs and adipocyte-immune cross-talk in pCF from cHFpEF mice. A) UMAP plot (snRNA-seq) of pCF cells colored by cluster (left panel); UMAP plot showing enrichment of HFpEF cells in the adipocyte2 cluster (right panel); **B)** scatter plot showing transcriptional changes in the adipocyte 2 cluster of pCF from HFpEF vs control mice; **C)** interactome analysis of snRNAseq showing disruption of pCF homestasis in HFpEF vs control mice. A strong connection between adipocytes and immune cells was observed in pCF from HFpEF mice (right panel). In HFpEF pCF, adipocytes are depicted as «signals senders» while immune cells are «signals receivers».

P007

BET Protein Inhibitor Apabetalone (RVX-208): A Novel Shield Against Doxorubicin-Induced Endothelial Senescence

Shafeeq Mohammed[1], Pascale Enz[1], Natalia Atzemian[1], Marialucia Telesca[1], Era Gorica[1], Grigorios Panteloglou[2], Alessia Mongelli[1], Alessandro Mengozzi[1], Ludovica Di Venanzio[1], Besa Emini Veseli[1], Frank Ruschitzka[3], Sarah Costantino[1], Francesco Paneni[1]

[1]Centre for Translational and Experimental Cardiology (CTEC), Department of Cardiology, University Hospital of Zurich, Zurich, Switzerland, [2]Institute of Clinical Chemistry, University Hospital of Zurich, Zurich, Switzerland, [3]University Heart Center, Department of Cardiology, University Hospital of Zurich, Zurich, Switzerland

Introduction: Accumulation of senescent endothelial cells (ECs) plays a pivotal role in cardiometabolic disorders and lifespan reduction. Yet, only a few senolytics are known to date. Bromo-and extraterminal domain (BET) proteins, known epigenetic reader proteins, recognize acetylated histone tails and regulate the gene transcription. RVX-208, an FDA-approved BET inhibitor, has shown to modulate transcriptional programs involved in inflammation, cancer, and renal disease. Yet, its potential role in EC senescence and cardio-oncology remains elusive. Our study aims to investigate whether pharmacological modulation of BET proteins by RVX-208 can mitigate doxorubicin-induced endothelial senescence.

Material and Methods: Human aortic endothelial cells (HAECs) were exposed to different concentrations of Doxo (50 nM-500 nM) in presence or absence of RVX-208 (5 μM-20 μM) for 48 hours. Cell morphology changes, cell cycle arrest, senescence associated secreted phenotype (SASP) release, upregulation of SA-β gal activity, DNA damage response (γH2AX) and expression of p21, p16 and p53 were used as molecular markers of cellular senescence.

Results: Doxo-treated ECs showed a dose-dependent increase in senescence markers (p16, p21 and p53) and DNA-damage response (γH2AX). Of interest, treatment with RVX-208 prevented the upregulation of senescent markers. RVX-208 prevented Doxo-induced upregulation of genes involved in inflammation, oxidative stress and mitochondrial dysfunction as shown by RNA-seq and proteomic analysis. Conditioned media from Doxo-treated ECs showed an enrichment of SASP-associated markers (IL6, CCL2, IL8, TIMP2 and PDGF-β) as shown by dot-blot arrays. Exposure of healthy ECs to conditioned media from senescent ECs recapitulated aging features. Notably, RVX-208 blunted the release of SASP markers (IL6, CCL2 and IL8) from Doxo-treated ECs. ChIP-seq analysis unveiled the BET protein occupancy (BRD4) with concomitant enrichment of activating chromatin marks (H3K27Ac and H3K4me) on the promoter of senescence genes P53 & P21

Conclusion: Targeting BET proteins with RVX-208 may offer a promising therapeutic strategy to prevent endothelial aging in cancer patients undergoing cardiotoxic therapies

.

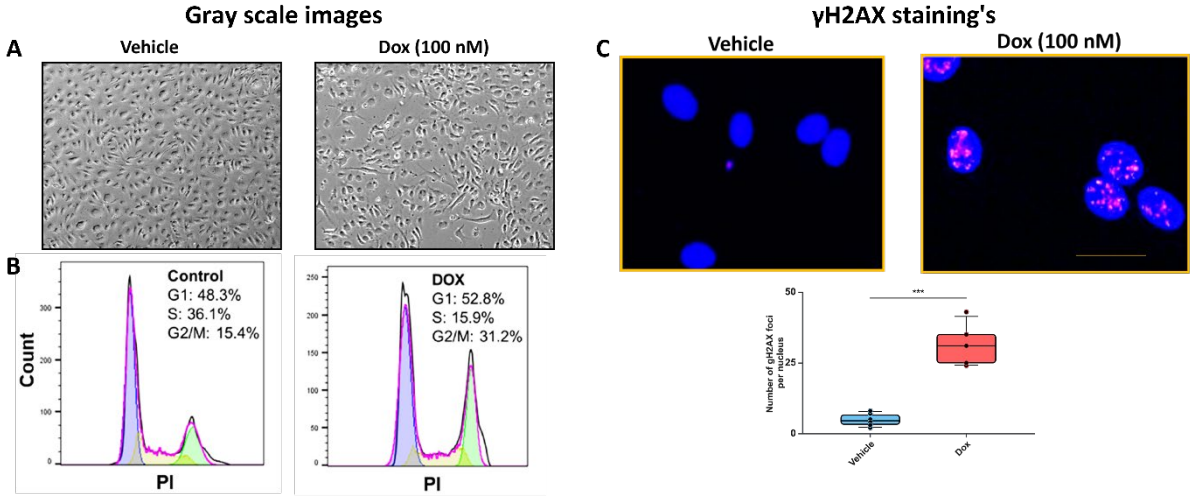

Fig 1: A. Doxorubicin (Dox; 100 nM) treatment for 48 hours leads to senescence in human aortic endothelial cells (HAECs) displayed by change in the morphology like long, cylindrical, and round shaped cells, whereas no morphological changes were found in HAECs treated with vehicle. **B.** Cell cycle analysis by flow cytometry after Dox treatment for 48 hours, showed the DOX-induced accumulation of cells in the G2/M-phase, a hallmark of the cell cycle effect of Dox treatment. **C.** HAECs treated with DOX (100 nM) showed a DNA damage response confirmed by γH2AX positive cells compared to Vehicle treatment. Boxplot graph showing the quantification of gH2AX staining.

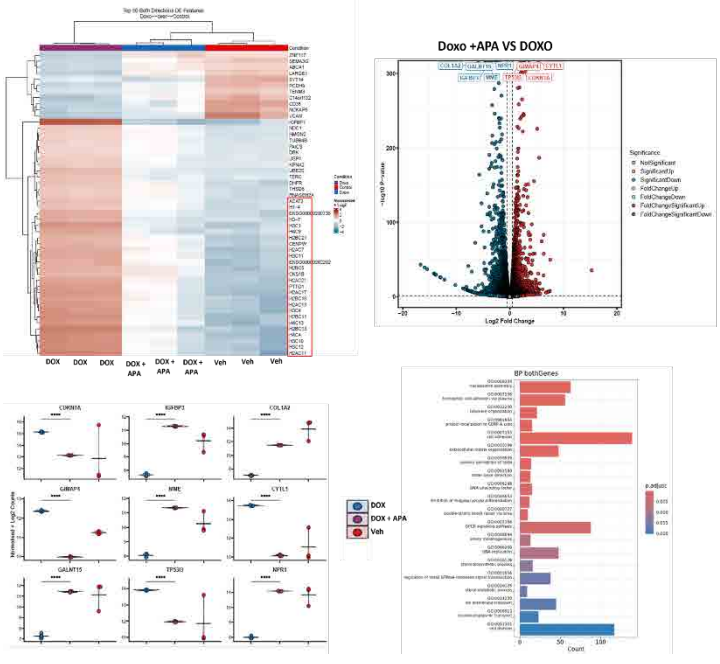

Fig 2. RNA-seq performed in HAECs exposed to Dox showed upregulation of genes that has a prominent role in epigenetic regulation (marked with red rectangle box in heat map graph), whereas HAECs treated with Dox in presence of apabetalone (20 uM) showed rescue in up regulation. Both volcano plot and dot plots, showing the deregulation of genes that are involved in regulation of senescence, reaction oxygen species, inflammation, and endothelial dysfunction, confirming the vascular toxicity. Whereas apabetalone able to rescue the deregulation of genes rescuing the vascular dysfunction. HAECs treated with Dox showed alteration in biological processes like cell adhesion, DNA unwinding factor, dsDNA break, extracellular matrix organization and artery morphogenesis.

P008

The contribution of bone marrow aged megakaryocytes/platelets to HFpEF

Carolina Balbi[1], Lee Pratintip[1], Meret Sarah Allemann[1], Soheil Saeedi Saravi[2], Thomas F. Luscher[1], Giovanni G. Camici[1], Jurg H. Beer[1]

[1]Center for Molecular Cardiology, University of Zurich, Schlieren, Switzerland, [2]CTEC, University of Zurich, Schlieren, Switzerland

Introduction:

Heart failure with preserved ejection fraction (HFpEF) is a major cause of hospitalizations and mortality in individuals aged 65 and older. HFpEF is a multifactorial and multisystemic syndrome, with a complex pathophysiology and phenotype. This necessitates individualized approaches that consider age-related changes and common comorbidities. Interestingly, megakaryocytes (Mk), the bone marrow cells responsible for platelet (Plt) production, undergo significant changes with aging, including alterations in function and gene expression, which may contribute to increased platelet reactivity, inflammation, and fibrosis, all of which are implicated in age-related cardiovascular diseases such as HFpEF.

Here we aim to investigate the link between Mk/Plt aging and cardiac dysfunction, focusing particularly on Plt-derived extracellular vesicles (EVs) and their role in HFpEF.

Material and Methods: We conducted comprehensive studies in young (4m) and old (18m) wild-type mice, including echocardiography, imaging, and biochemical analyses. Single-cell RNA sequencing (scRNAseq) was performed on Mk. Plt-derived circulating extracellular vesicles (Circ_EVs) were characterized.

Results: Despite preserved ejection fraction and fractional shortening in aged mice, indicating stable global left ventricular systolic function, significant age-related decline in diastolic function was observed. Aged mice exhibited reduced E/A ratios and prolonged IVRT. Additionally, aged mice demonstrated increased cardiac interstitial fibrosis, with upregulated expression of fibrosis markers. A significant increase in LV mass was also noted. Bone marrow scRNAseq analysis showed that aging Mk/Plt significantly upregulates TGF-β1, a key mediator in cardiac remodeling. Given that platelets are a primary source of EVs, we analyzed circulating Evs and found an increase in Circ_Evs in aged mice, suggesting heightened platelet reactivity with aging. Flow cytometry further confirmed elevated platelet reactivity in older mice.

Conclusion: Our findings indicate that aged mice develop a HFpEF-like phenotype together with elevated Plt reactivity, EVs and TGFβ1 production. The role of Plt-derived Circ_EVs in contributing to the cardiac phenotype warrants further investigation to establish a direct mechanistic link.

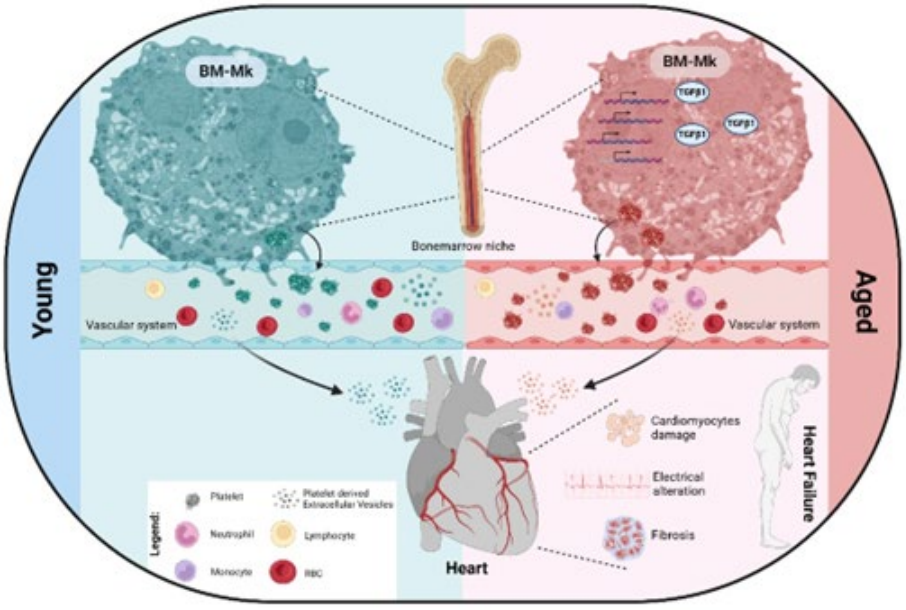

P009

Cardiac Health Status Shapes Therapeutic Bone Marrow Cell Repair Capacities

Shaista Ahmed[1], Ines Borrego[1], Aurelien Frobert[1], Stephan Cook[1], Marie-Noëlle Giraud[1]

[1]University of Fribourg, fribourg, Switzerland

Introduction: Clinical trials demonstrated beneficial outcomes following administration of Bone marrow cells (BMC), including improved quality of life and decreased infarct size. Harnessing the potential of cell-based therapeutics and their secretome requires a comprehensive understanding of their composition, functions, and mechanisms of action. The study investigates how the cardiac status -healthy versus infarcted- affects the therapeutic cell compositions and their properties.

Material and Methods: BMCs were isolated from healthy male rats (hBMC), and infarcted one (iBMC) obtained 2 weeks post MI, induced by coronary artery ligation, and cultured for 2 weeks. iBMC or hBMC were applied together with fibrin to infarcted rats post-MI. After 4 weeks, echocardiography, analysis of infarct size, and macrophage content were performed. Spectral flow cytometry characterized cell composition focusing on macrophage (CD68+) subsets, distinguishing M2 (CD206+, CD163+, Arg1+) from M1 (iNOS+, CCR7+, CD80+) macrophages. Metabolic (seahorse) assay, PCR, and MS proteomic characterized the cell's properties. Potency assays

were performed for immunomodulatory properties and pro-proliferative capacities.

Results: Infarcted rats treated with iBMCs exhibited significantly improved cardiac function than hBMC and reduced infarct expansion, accompanied by increased CD206+/M2 macrophages. Hematopoietic CD45+, CD68+ and M2 macrophage markers were upregulated in iBMCs. These cells showed increased metabolic activities compared to hBMCs and upregulation of the expression of genes involved in immune response, inflammation, angiogenesis, and ECM remodeling. Importantly, the secretome of iBMC showed an enhanced capacity to induce a phenotype switch of macrophages toward an anti-inflammatory profile. Furthermore, the secretome of iBMC-primed M2 macrophages demonstrated a higher capacity to foster cardiomyoblast proliferation.

Conclusion: The advanced therapeutic medical product (ATMP) obtained from cultured iBMC demonstrated increased reparative M2 content and higher therapeutic capacity than the hBMC. We highlight the importance of considering donor health status in developing reparative ATMP for cardiac repair and the need to incorporate potency assays.

Cardiac function, indicated by the ejection fraction (shown as a difference between pre and 4 weeks post-treatment), improved after iBMC administration compared to animals receiving no treatment (Sham). The expansion of fibrotic scars was significantly reduced only in animals receiving iBMC. The values are presented as mean ± STDEV.

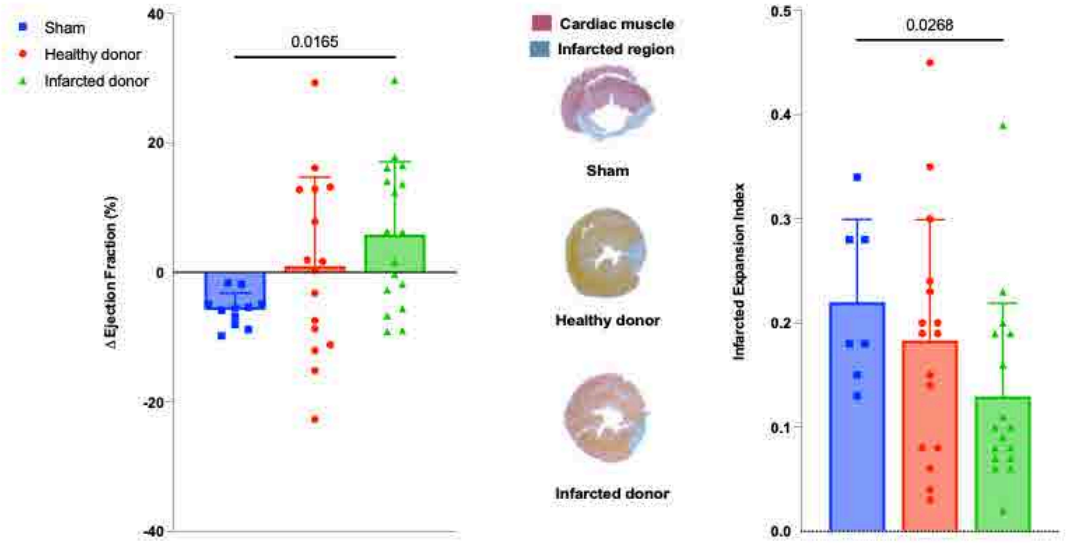

P010

The Inflammatory spectrum in Myocarditis

Anna Joachimbauer[1 2], Christian Perez-Shibayama[1], Emily Payne[1 2], Isabella Hanka[1 3], Hung Wei Cheng[1], Hans Rickli[3], Micha Mäder[3], Leslie Cooper[4], Oliver Borst[5], Ardan Saguner[2], Frank Ruschitzka[2], Burkhard Ludewig[1 2], Dörthe Schmidt[2], Cristina Gil Cruz[1 2]

[1]Institute of Immunobiology, Kantonsspital St. Gallen., St. Gallen, Switzerland, [2]University Heart Center, University Hospital Zurich, Zurich, Switzerland, [3]Cardiology Division, Kantonsspital St. Gallen St. Gallen, St. Gallen, Switzerland, [4]Department of Cardiovascular Medicine, Mayo Clinic., Jacksonville, FL, United States, [5]Universitätsklinikum und Medizinische Fakultät Tübingen, Tübingen, Germany

Introduction: Myocarditis is recognized as the prototypical inflammatory disease of the heart. However, its diagnosis remains challenging due to the heterogeneity of clinical manifestations, which can range from mild chest discomfort to life-threatening arrhythmias, heart failure, sudden cardiac arrest, and death. Currently, there are no reliable biomarkers to facilitate patient stratification for optimized therapeutic interventions, primarily due to the incomplete understanding of the molecular mechanisms underlying this severe condition.

Material and Methods: To elucidate these pathways, we conducted high-dimensional analyses on prospective patient cohorts. We utilized single-nucleus RNA sequencing (snRNA-seq) from endomyocardial biopsies (EMB) to directly assess inflammatory mechanisms within the myocardium. In parallel, we performed high-throughput profiling of inflammatory mediators in the serum of myocarditis patients.

Results: Our findings demonstrate dynamic alterations in the cardiac microenvironment, characterized by varying degrees of immune cell infiltration. Notably, T cell infiltration was strongly correlated with the pro-inflammatory reprogramming of both immune and non-immune cardiac cells, including macrophages, fibroblasts, endothelial cells, and cardiomyocytes. We identified upregulation of key cytokines and chemokines involved in immune cell recruitment and activation, such as CCL2, CXCL10, CXCL9, and IL-6. Serum analysis revealed distinct inflammatory patterns among patients with acute myocarditis, allowing stratification into inflammatory signatures characterized by T cell-related cytokines or by myeloid cell-related cytokines.

Conclusion: In conclusion, our results indicate that the heterogeneity observed in myocarditis is reflected both in tissue and systemic circulation, with a broad spectrum of inflammatory responses. Further investigations are ongoing to correlate these molecular signatures with distinct clinical phenotypes in acute myocarditis.

P011

The Molecular Signature of High-Intensity Interval Training associated with Cardiorespiratory Fitness in Individuals with Prediabetes

Candela Diaz Canestro[1], Kit Cheung[1], Yan Liu[2], Yao Wang[2], Michael Tse[3], Aimin Xu[2]

[1]Center for Molecular Cardiology, University of Zurich, Schlieren, Switzerland, [2]University of Hong Kong, Department of Medicine, Hong Kong, Hong Kong, [3]University of Hong Kong, Active Health Clinic, Centre for Sports and Exercise, Hong Kong, Hong Kong

Introduction: Patients with type 2 diabetes mellitus (T2DM) exhibit reduced cardiorespiratory fitness (CRF), determined as maximal oxygen consumption (VO2max), compared to healthy age-matched individuals. Exercise training (ET) substantially improves VO2max in T2DM patients, however, a wide interindividual variability seems indisputable. Therefore, additional research is required to elucidate the molecular mechanisms explaining the heterogenous response to ET in individuals with prediabetes.

Material and Methods: Longitudinal proteomics (Olink Proteomics AB, Uppsala, Sweden) in serum samples as well as fecal metagenomics and metabolomics (BGI, Hong Kong S.A.R., China) were performed in well-characterized medication-naïve overweight and obese Chinese men with prediabetes (n = 36, 24-62 years old), before and after 12-week high intensity ET intervention

Results: 12-Week ET reduced body weight, adiposity, improved insulin sensitivity, lipid profile and VO2max in individuals with prediabetes. In parallel, we detected significant changes in serum proteins at 4 weeks (12.9% of total proteins, false discovery rate (FDR)<0.05) and 12 weeks (35.9%, FDR <0.05) after ET. Moreover, abundance of bacteria with anti-inflammatory effects such as Fusicatenibacter as well as fecal metabolites with protective properties such as L-Arginine increased at the end of the intervention (p<0.05, Figure 1B and C). Notably, baseline levels of the erythropoiesis-stimulating hormone, i.e. erythropoietin (β = -279.03, P = 0.024), and Faecalibacterium (β = -96.79, P = 0.039), a bacterial genus that produces butyrate and other short-chain fatty acids, were negatively associated with changes in VO2max (Figure 1D and E).

Conclusion: The present findings provide a detailed map of the proteomic and gut microbiota changes in response to ET in individuals with prediabetes and identify potential mechanisms responsible for VO2max adaptations. In addition, the recognition of baseline proteomic and metagenomic signatures associated with VO2max trainability may facilitate the clinical implementation of personalized exercise interventions to improve CRF in individuals with prediabetes.

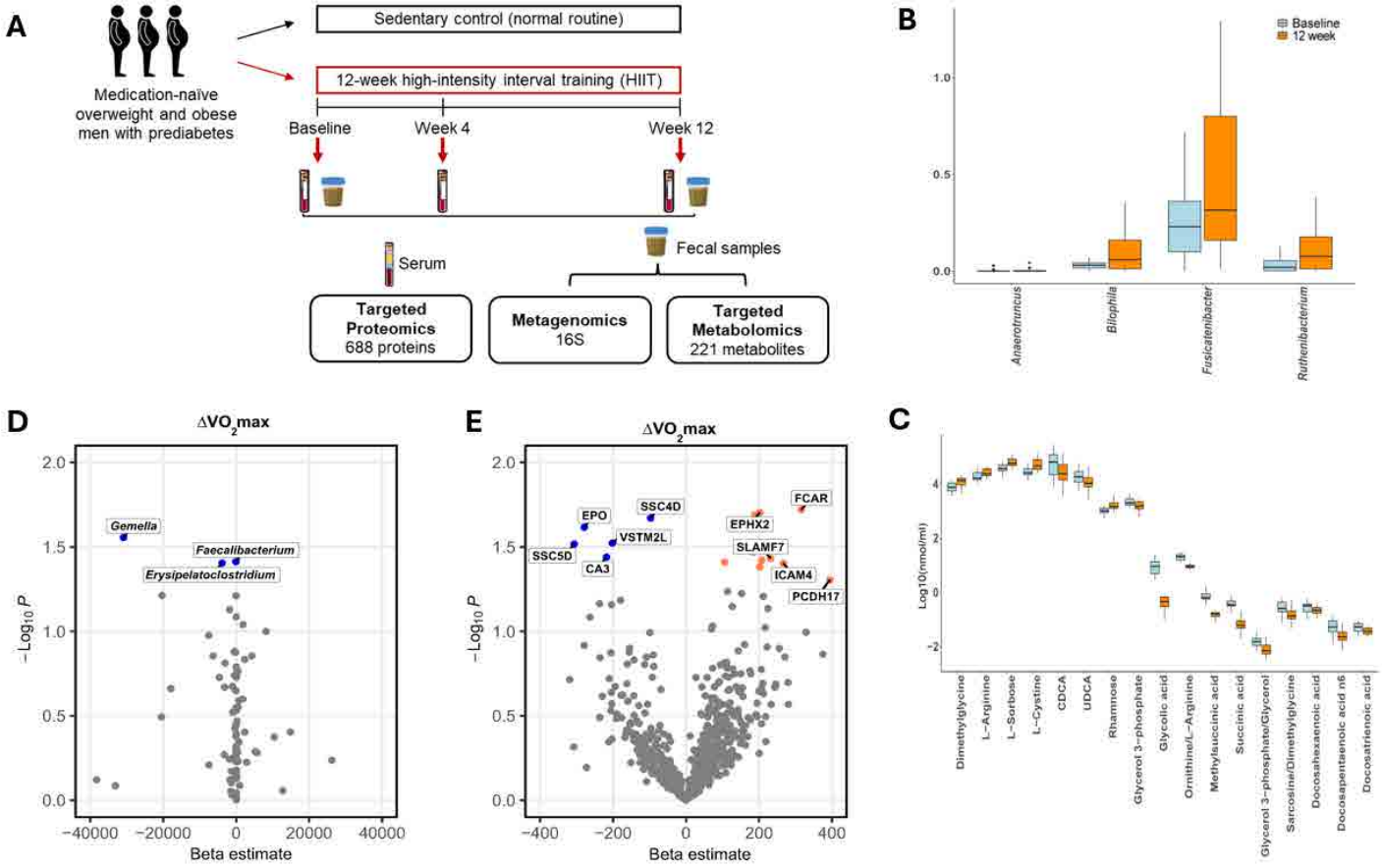

Figure 1. Proteomic and metagenomic signature associated with maximal aerobic capacity (VO_2max) in response to 12-week high-intensity interval training (HIIT). (A) Study design. (B) Baseline genus-level bacteria and (C) serum proteins associated with changes in VO2max. (D) genus-level genomic variations and (E) fecal metabolites before and after 12 week of HIIT.

P012

Deciphering the molecular mechanisms of drug-induced hidden cardiotoxicity by a multi-omics approach: the case of rofecoxib

Bennet Weber[1], Gábor Brenner[1], Barnabás Váradi[1], Bence Ágg[1], Csenger Kovácsházi[1], Olivér Balogh[1], Donagh Egan[2], Kieran Wynne[2], David Matallanas[2], Rainer Schulz[3], Péter Ferdinandy[1 4], Zoltán Giricz[1 4], Anikó Görbe[1 4]

[1]Center for Pharmacology and Drug Research & Development, Department of Pharmacology and Pharmacotherapy, Semmelweis University, Budapest, Hungary, [2]Systems Biology Ireland and School of Medicine, University College Dublin, Dublin, Ireland, [3]Institute of Physiology, Justus-Liebig University, Giessen, Germany, [4]Pharmahungary Group, Budapest, Hungary

Introduction: Drug-induced cardiotoxicity that becomes apparent only in the presence of comorbidities is defined as hidden cardiotoxicity. Currently, the most prominent candidate of this phenomenon is the Cyclooxygenase-2 inhibitor, rofecoxib, owing to clinical and preclinical observations. We previously reported increased acute mortality in rats due to the proarrhythmic effects of the drug on the ischemic heart. However, the underlying molecular background of hidden cardiotoxicity remained unknown. Hence, we aimed to identify the molecular mechanisms of hidden cardiotoxicity exemplified by rofecoxib.

Material and Methods: Rats received four weeks of treatment with rofecoxib or its vehicle. RNA sequencing and proteomic datasets of left ventricular tissue samples were used for an unbiased differential expression analysis followed by *in silico* molecular network analysis and pathway reconstruction analysis.

Results: Importantly, the transcriptomic analysis was unable to reveal the mechanism of hidden cardiotoxicity. By modelling posttranscriptional regulation in an *in silico* molecular correlation network, we found that the regulation exerted by microRNAs on mRNAs did not result in differential protein expression during experimental target validation by Western blot. Nonetheless, we identified conspicuous changes by mass-spectrometry-based proteomics, revealing 132 proteins that were dysregulated in expression or on phosphorylation sites. Moreover, bioinformatic means allowed us to identify two kinases that regulate key phosphorylation sites that may mediate cardiotoxicity. Finally, the pathway reconstruction analysis found a complex molecular network whose clustered proteins regulate processes involving cytoskeleton binding, $mRNA_3$ processing, proteolysis, translation, citrate acid cycle, and calcium ion signalling.

Conclusion: This is the first demonstration showing that a multi-omics characterization can reveal the molecular mechanisms of hidden cardiotoxicity. We demonstrate that transcriptomics gives limited information on rofecoxib's hidden cardiotoxic effects, which are primarily caused by posttranslational modifications and protein expression changes. Among other mechanisms, proteins relating to cardiac calcium handling are affected by rofecoxib, which could explain the fatal arrhythmias following ischemia/reperfusion.

POSTER WALK "CORONARY ARTERY DISEASE AND ACUTE CARDIAC CARE 1"

P013

Simplified Acute Physiology Score II to predict hospital mortality among ST-elevation myocardial infarction patients in Switzerland

Lara Berther[1], Hans Rickli[1], Jan Loosli[2], Marco Roffi[3], Giovanni Pedrazzini[4], Gian-Reto Kleger[1], Dragana Radovanovic[2]

[1]Kantonsspital St. Gallen, St. Gallen, Switzerland, [2]University of Zurich, AMIS Plus Data Center Epidemiology, Biostatistics and Prevention Institute, Zurich, Switzerland, [3]Hôpitaux universitaires de Genève, Geneva, Switzerland, [4]Istituto Cardiocentro Ticino, Lugano, Switzerland

Introduction: ST-elevation myocardial infarction (STEMI) is a prevalent diagnosis in Swiss intensive care units (ICU). Nevertheless, a validated scoring system to predict early mortality prediction among these patients is lacking. SAPS II (Simplified Acute Physiology Score II) is collected in each ICU patient on a mandatory base. However, this score was developed to predict mortality in critically ill patients, explicitly excluding cardiac patients in its original conception. Evidence about its predictive validity for hospital mortality in patients with STEMI is scarce.

Material and Methods: ICU patients with STEMI enrolled in the Acute Myocardial Infarction in Switzerland (AMIS) Plus registry between 2005 and 2024 were included. In-hospital mortality was analysed using a multivariate logistic regression model.

Results: Out of 6,124 patients included (mean age 64.4 (±12.6); men n = 4,695, 77%), 13% (n = 818) had a return of spontaneous circulation after cardiac arrest and 19% (n = 1,164) a Charlson Comorbidity Index >1. Complications during hospitalisation included cardiogenic shock (n = 362, 5.9%), sepsis (n = 175, 2.9%) and acute kidney injury (n = 191, 3.1%). The overall in-hospital mortality was 8.1% (n = 498), while the mean SAPS II score recorded was 28.3. Patients who died had markedly higher SAPS II scores (mean 61.2 (±23); median 63.0, IQR 43, 80) compared to survivors (mean 25.4 (±14); median 22.0 ±18.0, IQR 18, 29) ($p<0.001$). For SAPS II between 30 and 60 crude in-hospital mortality was higher than predicted by the score, whereas for scores exceeding 60, predictions overestimated observed mortality (Figure 1). After adjusting for age and sex, each one-point increase in SAPS II was associated with an 8% higher mortality (OR 1.08; 95%CI 1.08-1.09; $p<0.001$).

Conclusion: The SAPS II is associated with hospital mortality in STEMI patients hospitalised in Swiss ICUs. The higher observed mortality compared to the predicted mortality in STEMI patients with lower SAPS II suggests the existence of mortality-related confounders not captured by the SAPS II.

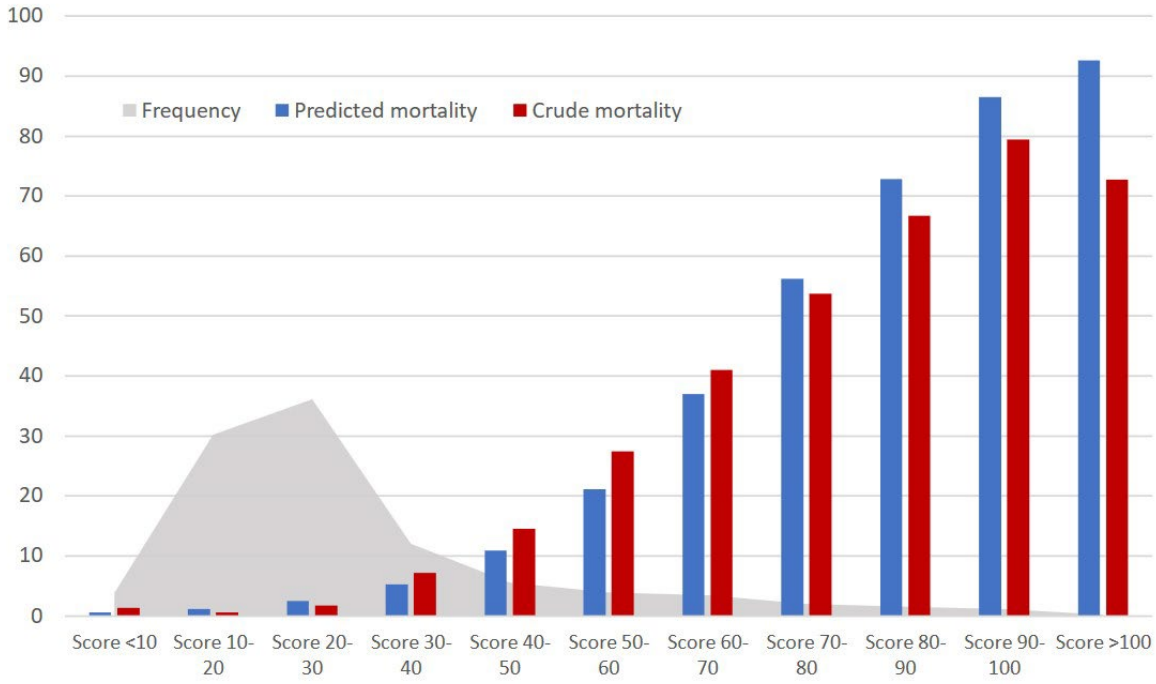

Figure 1: Crude and predicted mortality of STEMI patients according to SAPS II Scores and their recorded frequencies.

P014

Can Intraoperative Hyperoxia Induce Better Outcomes in Patients Undergoing Cardiac Surgery? A Systematic Review and Meta - Analysis

Victoria Zecchin Ferrara[1], David Downes[2], Jaivardhan A. Menon[3], Giang Son Arrighini[4]

[1]University of Padova, Padova, Italy, [2]The University of New England, Armidale, Australia, [3]Harvard Medical School, Boston, United States, [4]University of Bologna, Bologna, Italy

Introduction: While the use of high doses of supplementary oxygen during cardiac surgery is often considered beneficial, its necessity, safety, and efficacy remain subjects of ongoing debate.

Material and Methods: A meta-analysis adhering to PRISMA guidelines was conducted, systematically searching PubMed, Cochrane, and Embase from their inception to October 30th, 2024. The analysis included studies comparing hyperoxia and normoxia as interventional strategies in cardiac surgery. Results were reported using standardized mean differences (SMD), mean differences (MD), odds ratios (OR), and their respective 95% confidence intervals (95% CI).

Results: A total of 1188 patients from six studies met the inclusion criteria, with 592 assigned to the hyperoxia group and 596 to the normoxia group. Preoperative characteristics were comparable between the groups. Hyperoxia was associated with a significant increase in intraoperative arterial partial pressure of oxygen (PaO2) and a notable reduction in acute kidney injury (AKI) (Figure 1). However, no significant differences were found between the groups in terms of intraoperative oxygen saturation levels (SpO2%), postoperative delirium, stroke, atrial fibrillation (AF), surgical site infections (SSI), or hospital and ICU lengths of stay.

Conclusion: Although hyperoxia significantly increased intraoperative PaO2 and reduced postoperative AKI, these physiological effects did not yield clinical benefits, calling into question its presumed protective role in cardiac surgery. Larger, multicenter trials employing standardized methodologies are needed to clarify the long-term consequences and clinical implications of hyperoxia. Until then, a patient-centered approach to oxygen therapy remains essential for optimizing outcomes while minimizing potential risks.

P015

Adrenomedullin biomarkers enhance risk prediction for cardiogenic shock and mortality in acute coronary syndrome

Yifan Wang[1], Victor Schweiger[2], Luca Liberale[3 4], Lorenz Räber[5], Christian Templin[1 2], François MacH[6], Olivier Muller[7], Alexander Akhmedov[1], Giovanni G. Camici[1], Ilina Yulia[8], Kaufmann Paul[8], Andreas Bergmann[8], Florian A. Wenzl[1], Thomas F. Lüscher[1 9 10], Simon Kraler[1 11]

[1]Center for Molecular Cardiology, University of Zurich, Schlieren, Switzerland, [2]Department of Internal Medicine B, University Medicine Greifswald, Greifswald, Germany, [3]First Clinic of Internal Medicine, Department of Internal Medicine, University of Genoa, Genoa, Italy, [4]IRCCS Ospedale Policlinico San Martino Genoa - Italian Cardiovascular Network, Genova, Italy, [5]Department of Cardiology, Swiss Heart Center, Inselspital Bern, Bern, Switzerland, [6]Department of Cardiology, Geneva University Hospitals, Geneva, Switzerland, [7]Department of Cardiology, University Hospital of Lausanne, University of Lausanne, Lausanne, Switzerland, [8]PAM Theragnostics GmbH, Neuendorfstr. 15A, Hennigsdorf, Germany, [9]Royal Brompton and Harefield Hospitals and National Heart and Lung Institute, Imperial College, London, United Kingdom, [10]School of Cardiovascular Medicine and Sciences, Kings College London, London, United Kingdom, [11]Department of Internal Medicine and Cardiology, Cantonal Hospital Baden, Baden, Switzerland

Introduction: Cardiogenic shock (CS) remains a leading cause of mortality in acute coronary syndromes (ACS), with 1-year mortality plateauing at 50%. Vascular leakage contributes to CS initiation and progression, but management mainly relies on hemodynamic parameters. Adrenomedullin (ADM), a vasoactive peptide, regulates vascular permeability and conges-

tion. Nonetheless, the predictive value of ADM system components—glycine-extended adrenomedullin (ADM-gly; precursor) and biologically active adrenomedullin (bio-ADM)—for the prediction of CS and mortality remains unclear.

Material and Methods: We analysed 4,787 ACS patients (SPUM-ACS; NCT01000701), with plasma ADM-gly, and bio-ADM levels being assessed at presentation and post-angiography. The primary endpoint was in-hospital CS; the secondary endpoint was 1-year mortality. Logistic and Cox regression models were fit for CS and mortality prediction, respectively. Model performance was evaluated using receiver operating characteristic (ROC) curves, calibration plots, and reclassification metrics.

Results: ADM-gly and bio-ADM were independently linked to in-hospital CS (adjusted OR per $\log_2$ increase: ADM-gly, 1.65 [95% CI, 1.41–1.93]; bio-ADM, 1.64 [95% CI, 1.35–1.98]) and 1-year mortality risks (adjusted HR: ADM-gly, 1.34 [95% CI, 1.11–1.61]; bio-ADM, 1.49 [95% CI, 1.20–1.85]). Patients stratified by ADM system activation status (resting, initial, active, exhaustion) demonstrated distinct CS and mortality risks, with the active phase exhibiting the highest CS (8.1%) and 1-year mortality rates (5.7%) (Figure 1). The newly developed ADM-SHOCK score outperformed the ORBI risk score for CS prediction (AUC, 0.81 vs. 0.76, p<0.001) and effectively predicted 1-year mortality (Figure 2).

Conclusion: ADM system biomarkers refine risk prediction for in-hospital CS and 1-year mortality in patients with ACS. Incorporating ADM-gly and bioADM improves early risk assessment of ACS patients and underscores the role of vascular leakage in CS pathogenesis. The ADM-SHOCK score enhances the performance of established prediction tools for the personalized management of patients with ACS.

Figure 1

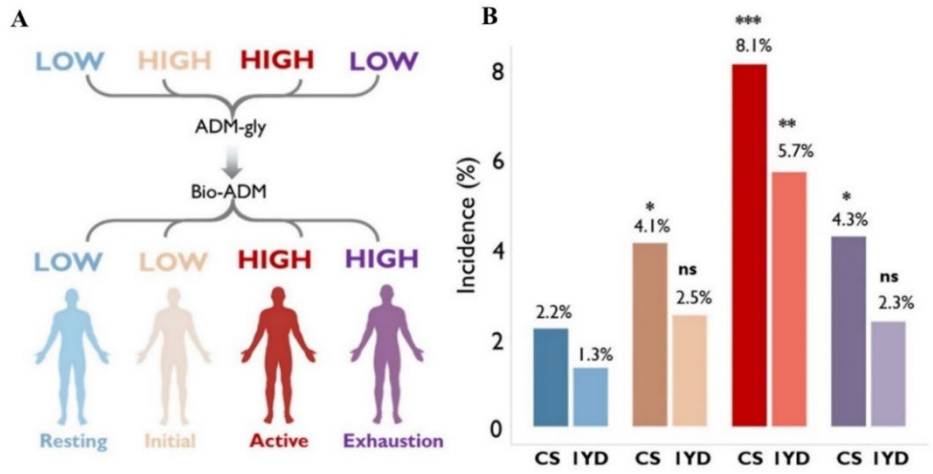

Figure 1. (**A**) ADM system activation status was defined by levels of ADM-gly and bio-ADM (> or ≤ median), respectively. Resting refers to low ADM-gly and low bio-ADM, initial to ADM-gly and low bio-ADM, active to high ADM-gly and high bio-ADM, and exhaustion to low ADM-gly and high bio-ADM. (**B**) Bar graph showing the relative incidence of cardiogenic shock (CS; darkened) and 1-year death (1YD; light-colored) depending on ADM activation status.

Figure 2

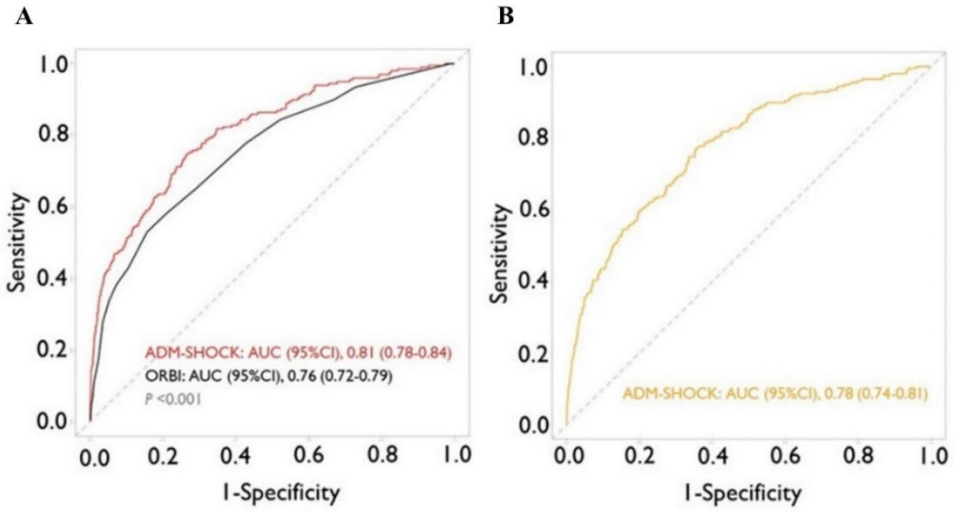

Figure 2. (**A**) ROC curves of the established ORBI (black) and the newly developed ADM-SHOCK score (red) in predicting in-hospital cardiogenic shock. ROC curves were compared using a paired DeLong test. (**B**) ROC curve for ADM-SHOCK to predict the secondary endpoint (i.e., 1-year mortality).

P016

Sex-specific differences in early occlusion rate after coronary artery bypass grafting

Luca Koechlin, Islam Salikhanov[1], Brigitta Gahl[1 2], Philip Haaf[3], Christian Müller, Denis Berdajs[1]

[1]Department of Cardiac Surgery, University Hospital Basel, Basel, Switzerland, Basel, Switzerland, [2]Surgical Outcome Research Center Basel, University Hospital Basel, University Basel, Basel, Switzerland, Basel, Switzerland, [3]Cardiovascular Research Institute Basel (CRIB), Basel, Switzerland

Introduction: Sex-specific differences in the early bypass graft occlusion rate following coronary artery bypass grafting (CABG) remain unclear.

Material and Methods: Consecutive adult patients undergoing isolated CABG surgery were included. Bypass graft patency was assessed using an ECG-gated coronary bypass computed tomography heart scan prior to discharge. Follow-up data included mortality, major adverse cardiac and cerebrovascular events, rehospitalizations, and cardiac reinterventions.

Results: A total of 562 patients (mean [SD] age 67 [9.5] years) were included, with 17% (n = 93) being female. Female patients had fewer distal anastomoses compared to male patients (median [IQR]: 3 [2–4] vs. 4 [3–4], p = 0.031), and were more likely to receive venous grafts and less likely to receive a second arterial graft. Bypass graft occlusion was detected in 40 out of 562 patients (7.1%), and occurred significantly more often in female patients compared to male patients (n = 12 [13%] vs. n = 28 [6.0%], p = 0.02). This resulted in 14 out of 283 (4.9%) and 32 out of 1607 (2%) occluded grafts in female and male patients, respectively (p<0.01). Female gender was significantly associated with higher odds of graft occlusion (OR = 2.33, 95% CI: 1.14–4.78, p = 0.020). During follow-up (median [IQR] 15 [13–20] months), no significant differences in major adverse events were observed between males and females during the follow-up period.

In general, overall mortality was 3%, with higher rates of rehospitalizations (19.2% vs. 4.9%, p = 0.01) and reinterventions (15.4% vs. 2.5%, p = 0.02) observed in patients with occluded grafts.

Conclusion: Early bypass graft occlusion, detected through standardized postoperative CT scans prior to discharge, occurred significantly more frequently in female patients compared to male patients after isolated CABG surgery. Potential underlying reasons may include differences in demographic data and intraoperative factors; however, these require evaluation in dedicated studies.

P017

A systematic analysis of female participation and gender-sensitive reporting in cardiovascular trials between 2017- 2024

Maximilian Bley[1 2], Susanne Menz[1 2], Linda Mathez[1 2], Vera Regitz-Zagrosek[3], Carolin Lerchenmueller[1 2]

[1]Chair for Gender Medicine, University of Zurich, 8006 Zurich, Switzerland, [2]Department of Cardiology, University Hospital Zurich, 8091 Zurich, Switzerland, [3]Institute for Gender in Medicine, Charité, 10115 Berlin, Germany

Introduction: The representation of different populations in clinical trials is crucial to ensure generalizability of the data. Previous studies have shown an underrepresentation of women as participants in cardiovascular clinical trials. In addition, global initiatives, including Sex and Gender Equity in Research (SAGER)-guidelines, aim to improve not only the number of women participants, but also the quality of the reporting with regards to gender. The representation of women in cardiovascular clinical trials has not been investigated for the recent years and the quality of the reporting has not been analyzed.

Material and Methods: We conducted a systematic analysis of clinical trials in the cardiovascular field published in PubMed between 2017 and 2024. We first analyzed female participation measured by the participation-prevalence-ratio (PPR), with a PPR of 0.8–1.2 reflecting the targeted balance. Second, we measured sex and gender-associated reporting of women as a subpopulation applying modified SAGER-guidelines. All analyses included comparisons between years and different disease entities.

Results: We identified 1,400 clinical trials with a total of 712,843 women participants (39.8 %) and a per-trial women-to-men ratio of 0.58 (IQR: 0.34-1.0). After adjusting to the prevalence, the median PPR of all trials remained suboptimal at 0.77 (IQR: 0.56-1.02) throughout the years with a small trend towards an increase in 2022 and 2023. The lowest PPR was found in clinical trials with a focus on ischemic heart disease, vascular diseases of the lower extremity, and stroke. The PPR was at target in trials with a focus on hypertension and pulmonary hypertension. We found that there is a lack of gender-sensitive reporting, especially for endpoints and discussions in the publications of these clinical trials.

Conclusion: Our results suggest an ongoing imbalance for the participation of women and a lack of gender-sensitive reporting in cardiovascular clinical trials, especially for ischemic heart diseases.

P018

The impact of insurance status on the therapy and outcome of STEMI patients in Switzerland

Jan Loosli[1], Fabienne Foster-Witassek[1], Hans Rickli[2], Marco Roffi[3], Giovanni Pedrazzini[4], Dragana Radovanovic[1]

[1]AMIS Plus Data Center, Epidemiology, Biostatistics and Prevention Institute, University of Zurich, Zurich, Switzerland, [2]Cantonal Hospital St. Gallen, Department of Cardiology, St. Gallen, Switzerland, [3]Geneva University Hospitals, Department of Cardiology, Geneva, Switzerland, [4]Cardiocentro Ticino, Department of Cardiology, Lugano, Switzerland

Introduction: Current literature reports large disparities in treatments and outcomes of ST-elevation myocardial infarction (STEMI) patients according to insurance status. Whether this applies to patients in Switzerland, where basic health insurance is mandatory, but individuals may purchase supplementary (private) insurance, is unknown.

Material and Methods: STEMI patients enrolled in the prospective, nationwide Acute Myocardial Infarction in Switzerland (AMIS) Plus registry between 2005 and 2023 were analyzed. We compared patients with basic and those with private insurance using descriptive statistics and assessed temporal trends of full guideline-recommended treatment (FGRT), consisting of optimal medical therapy (OMT) plus percutaneous coronary intervention, stratified by insurance type. Multivariate logistic mixed effects models were fitted to examine whether insurance type influenced treatments and outcomes.

Results: Among 16,463 patients, 13,023 (79.1%) had basic and 3,440 (20.9%) private health insurance. Patients with basic insurance were younger (64 vs. 69 years, p<0.001) and more likely male (74.9% vs. 72.0%, p<0.001). They also had higher rates of obesity (20.7% vs. 17.6%, p<0.001), diabetes (19.6% vs. 16.5%, p<0.001), were more often active smokers at time of STEMI (43.1% vs. 30.7%, p<0.001), but had lower rates of cancer (4.6% vs. 6.9%, p<0.001). Patients with basic

insurance more often received OMT (41.6% vs. 35.2%, p<0.001) and FGRT (39.7% vs. 33.9%, p<0.001; the Figure shows temporal trends according to insurance type). Nevertheless, they had higher rates of in-hospital mortality (8.6% vs. 5.7%, p<0.001) and major adverse cardiac and cerebrovascular events (MACCE) (9.7% vs. 6.9%, p<0.001). After adjusting for covariates, no significant association between insurance type (basic vs. supplementary) and OMT (adjusted odds ratio, 1.04; 95% confidence interval, 0.93-1.16; p = 0.53), FGRT (1.01; 0.90-1.13; p = 0.88), in-hospital mortality (1.32; 0.94-1.87; p = 0.11), or MACCE (1.32; 0.99-1.77; p = 0.06) remained.

Conclusion: In Switzerland, insurance status did not impact treatment or in-hospital outcomes of STEMI patients, suggesting a high level of equity in acute cardiac care.

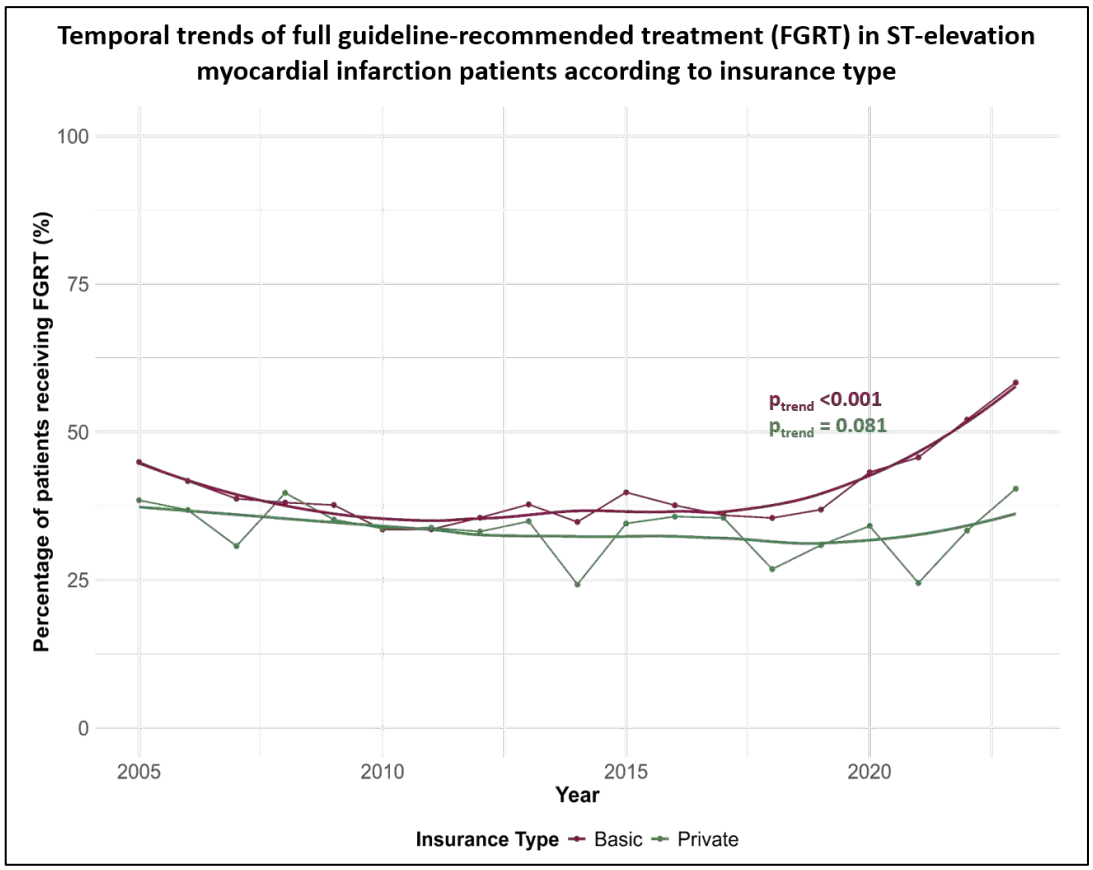

P019

TropoResp: Origin of cardiac troponin T/I in patients with chronic obstructive pulmonary disease: Heart or skeletal muscles?

Seunghyun Kim[1], Jeanne du Fay de Lavallaz[1 2], Danielle Gualandro[1 3], Ivo Strebel, Gabrielle Hure[2], Andrea Henneke[2], Franja Dugar[2], Vithushan Ratnarasa[2], Uliana Ivaniuk[2], Mark Wiese[4], Aljaz Hojski[4], Makhmudbek Mallaev[4], Nikolay Tsvetkov[4], Katharina Rentsch, Didier Lardinois[4], Christian Müller

[1]Department of Cardiology, University Hospital of Basel, University of Basel, Basel, Switzerland, [2]Cardiovascular Research Institute Basel, University Hospital of Basel, University of Basel, Basel, Switzerland, [3]Unidade de Medicina Interdisciplinar em Cardiologia, Instituto do Coração, Hospital das Clínicas HCFMUSP, Faculdade de Medicina, Universidade de São Paulo, São Paulo, Brazil, [4]Department of Thoracic Surgery, University Hospital of Basel, University of Basel, Basel, Switzerland

Introduction: High-sensitive cardiac troponin T and I (hs-cTnT/I) have been widely used for detecting myocardial injuries. However, recent studies reported evidence of increased cardiac troponins, especially cTnT, in patients with chronic obstructive pulmonary disease (COPD) without presence of known cardiac diseases, suggesting diagnostic challenges in true cardiac events. Our study aims to clarify the origin of cTnT/I either from cardiac or respiratory muscles, by focusing on COPD patients undergoing thoracic surgeries.

Material and Methods: 96 patients undergoing thoracic surgeries were recruited, 66 of which diagnosed with moderate to severe COPD, and 30 without COPD. Patients who had undergone acute cardiac conditions or cardiac surgeries/interventions shortly before the surgery were excluded. History taking was done preoperatively, and blood samples were collected at the moment of incision. Two muscle biopsies were taken intraoperatively, (intercostal or diaphragm) and differential gene expression (DGE) analysis was performed to assess the expression of cardiac troponin genes in respiratory muscles.

Results: Increased hs-cTnT was more prevalent in the COPD group than controls (52% vs. 32%, p = 0.05), while cTnT/I mismatch (increased hs-cTnT, normal hs-cTnI) was similar between groups (88% vs. 93%, p = 0.70). Among patients with cardiac history, the mismatch was significantly higher in the COPD group (81% vs. 20%, p = 0.04). Logistic regression identified age as a significant predictor of increased hs-cTnT (OR = 1.06, 95% CI: 1.01–1.12, p = 0.028) and cTnT/I mismatch (OR = 1.07, 95% CI: 1.01–1.13, p = 0.018). DGE analysis on the biopsy samples is ongoing, for the presence of cardiac troponin gene expression in respiratory muscles.

Conclusion: Elevated hs-cTnT concentration and cTnT/cTnI mismatch are common in patients with COPD, particularly those with known cardiac disease. Further studies need to

disentangle cardiac (increased sensitivity of cTnT versus cTnI for chronic cardiomyocyte injury) versus noncardiac (including respiratory muscle injury) causes for this phenomenon.

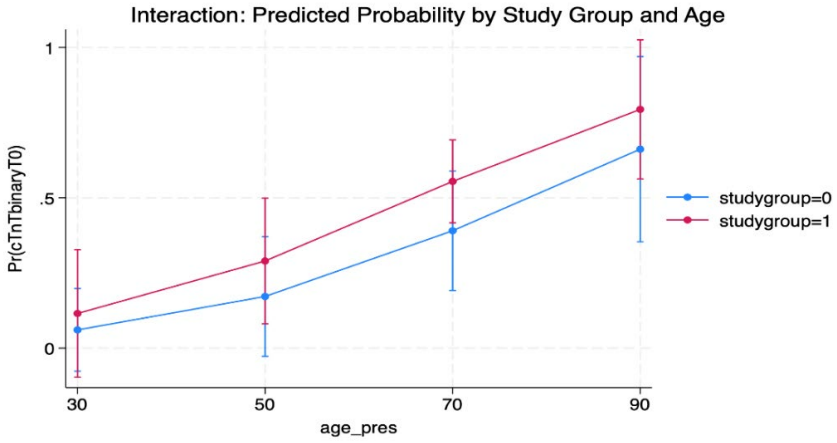

P020

Prognostic impact of left circumflex artery as the culprit lesion in STEMI: short- and long-term survival analysis

Dorian Garin[1], Nolan Grin[1], Wesley Bennar[1], Mario Togni[1], Pascal Meier[1], Peter Wenaweser[1], Puricel Serban[1], Stéphane Cook[1], Diego Arroyo[1]

[1]*University and Hospital Fribourg, Fribourg, Switzerland*

Introduction: The left circumflex artery (LCX) has been identified as a potential factor for elevated mortality and diagnostic delays in NSTEMI. However, whether these findings also apply to STEMI for short- and long-term outcomes, remains uncertain.

Material and Methods: We included all patients from the EVALFAST registry, which enrolls STEMI patients transferred directly to the catheterization laboratory at Fribourg Hospital since June 2008. The primary endpoint was cardiovascular (CV) and non-CV-death at 30 days, 90 days, 1 year, and 5 years using exact logistic regression adjusted for cofounders. Secondary endpoints included time from first medical contact (FMC) to diagnosis, LVEF, and peak CK-MB using generalized linear models.

Results: We included 1,205 patients, with similar baseline characteristics in LCX (n = 137) and non-LCX (n = 1,038) groups, except for more dyslipidaemia (p = 0.04) and reduced cardiac rehabilitation (23.4% vs. 33.4%, p = 0.009) in LCX. Although symptom-to-FMC intervals were similar (p = 0.96), LCX patients had longer FMC-to-diagnosis times (50.0 vs. 42.8 minutes, p = 0.009), higher peak CK-MB (261.8 vs. 212.9, p = 0.005), and paradoxically higher LVEF (52.5% vs. 46.0%, p<0.001). LCX was independently associated with early CV death (30-days adjusted odds ratio [OR] 4.64; p<0.001), though this effect partially diminished after adjusting for only for FMC-to-diagnosis (OR 2.51; p = 0.021). LCX remained predictive at 90 days (p = 0.008) and 1 year (p = 0.016) but lost significance after accounting for cardiac rehabilitation (p>0.06). By 5 years, LCX had no CV death impact, whereas rehabilitation remained protective (OR 0.53, p = 0.009) (Figure 1). Non-CV deaths were similar in both groups at all time points.

Conclusion: LCX culprit lesion was associated with prolonged diagnostic delays, elevated peak CK-MB, reduced cardiac rehabilitation, and increased early mortality, despite higher LVEF. Extended FMC-to-diagnosis intervals and lower rehabilitation participation emerged as key drivers of mortality, emphasizing the need for prompt recognition and comprehensive post-infarct care in LCX STEMI.

Figure 1

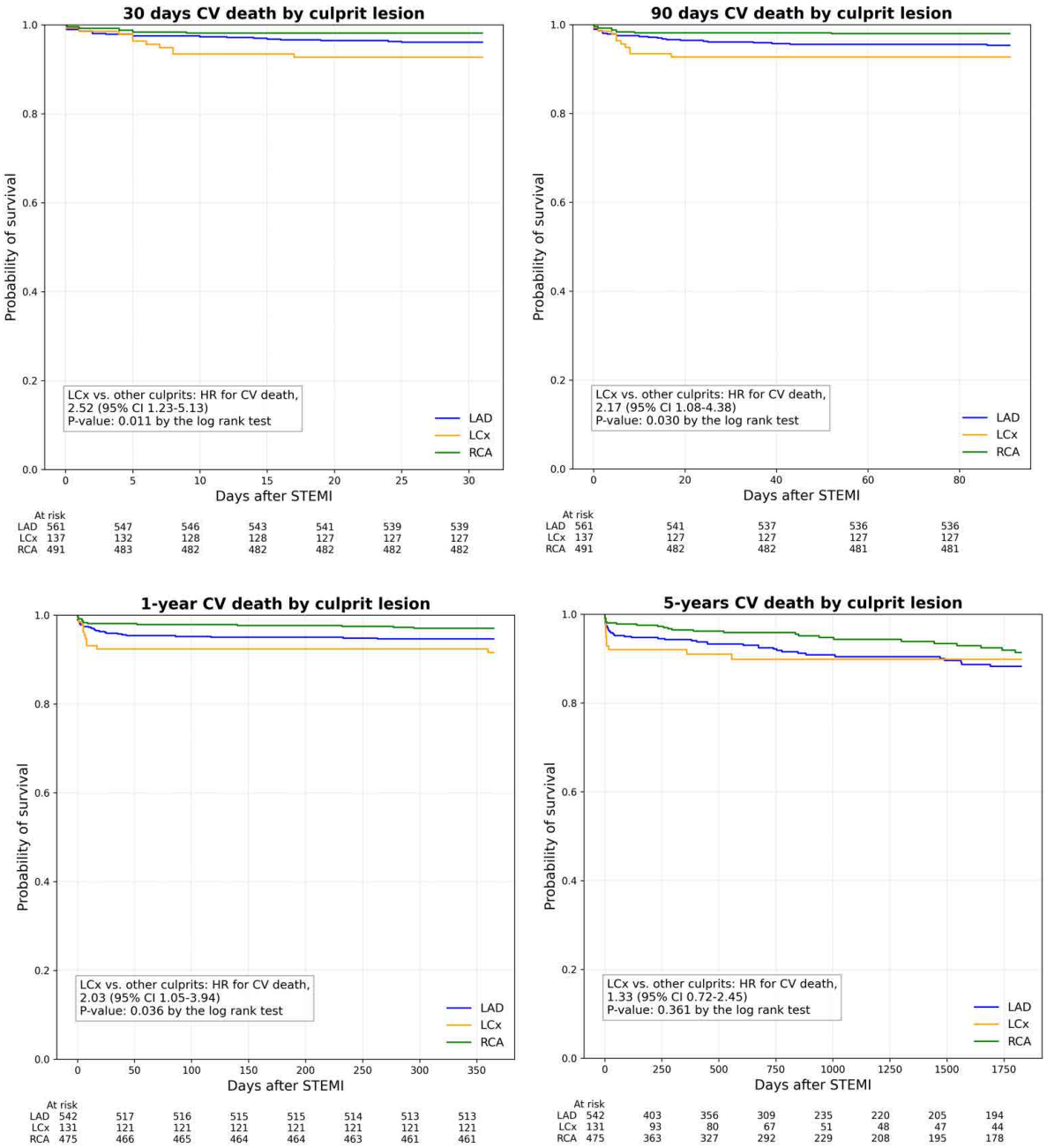

P021

Impact of left ventricular ejection fraction on the effect of beta-blocker therapy on one-year mortality in patients with acute myocardial infarction

Micha T. Maeder[1], Fabienne Foster[2], Dragana Radovanovic[2], Marco Roffi[3], Giovanni Pedrazzini[4], Hans Rickli[1]

[1]Health Ostschweiz (HOCH) Kantonsspital St. Gallen, St. Gallen, Switzerland, [2]AMIS Plus Data Center, Epidemiology, Biostatistics and Prevention Institute, University of Zürich, Zürich, Switzerland, [3]Department of Cardiology, Geneva University Hospitals,, Geneva, Switzerland, [4]Department of Cardiology, Cardiocentro Ticino, Lugano, Switzerland

Introduction: While the beneficial effect of long-term beta-blocker (BB) therapy for post-myocardial infarction (MI) patients with significant left ventricular systolic dysfunction [left ventricular ejection fraction (LVEF <40%)] and/or heart failure is well established, the role of BB therapy in patients with mildly reduced or preserved LVEF (LVEF >40%) in the reperfusion era is controversial. We aimed to assess whether there is a differential relationship between BB therapy and one-year mortality according to LVEF in a large contemporary cohort of MI patients.

Material and Methods: Patients included in the Acute Myocardial Infarction in Switzerland (AMIS plus) registry between 2005 and 2023 with information on BB status, LVEF by echocardiography, and one-year mortality were studied (n = 7820; 88% undergoing percutaneous coronary intervention). The association between BB status and one-year mortality and the interaction with LVEF (>40% versus ≤40%) were analyzed.

Results: In 1570/7820 (20.1%) patients LVEF was ≤40%. At hospital discharge, 6211/7820 (79.4%) patients were on BB therapy (LVEF >40%: 78.1%, LVEF ≤40%: 84.5%). Overall,

there were 253/7820 (3.2%) deaths after one year. As expected, one-year mortality was higher in patients with LVEF ≤40% compared to those with LVEF >40% 112/1570 (7.1%) versus 141/6250 (2.3%); p<0.001. In patients with LVEF >40%, mortality did not differ between patients with versus without BB 105/4884 (2.1%) versus 36/1366 (2.6%); p = 0.3. In contrast, among patients with LVEF ≤40% mortality was significantly lower in patients with BB compared to those without BB 78/1327 (5.9%) versus 34/243 (14%); p<0.001. An adjusted analysis with an interaction between BB therapy and LVEF revealed the same pattern of results (p = 0.02).

Conclusion: Data from our large, nationwide registry confirm a benefit from BB therapy on one-year mortality in MI patients with LVEF ≤40%. In contrast, in patients with LVEF >40% (representing 80% of the population), the benefit seems to be minimal or absent.

P022

Trends in early reperfusion therapy in non-ST-elevation myocardial infarction patients treated with PCI

Fabienne Foster-Witassek[1], Jan Loosli[1], Hans Rickli[2], Marco Roffi[3], Giovanni Pedrazzini[4], Dragana Radovanovic[1]

[1]AMIS Plus Data Center, Epidemiology, Biostatistics and Prevention Institute, University of Zurich, Zurich, Switzerland, [2]Cantonal Hospital St. Gallen, Department of Cardiology, St. Gallen, Switzerland, [3]Geneva University Hospitals, Department of Cardiology, Geneva, Switzerland, [4]Cardiocentro Ticino, Department of Cardiology, Lugano, Switzerland

Introduction: We aimed to analyse the proportion of non-ST-elevation myocardial infarction (NSTEMI) patients undergoing percutaneous coronary intervention (PCI) within 24h over the years, examine their risk profiles, and assess in-hospital mortality.

Material and Methods: We included all PCI-treated NSTEMI patients enrolled in the Swiss Acute Myocardial Infarction in Switzerland (AMIS) Plus registry between 2005 and 2024. Patients were grouped according to door-to-balloon times: early (<24h) and delayed intervention (>= 24h). In a subanalysis, we compared patients with immediate PCI (<2h) to those with PCI between 2-24h.

Results: From 9,364 patients, 7,825 (83.6%) received PCI within 24h. The proportion of delayed PCI dropped over time, albeit fluctuatingly (p_{trend} = 0.042, Figure). Patients with delayed PCI had lower crude in-hospital mortality than those treated early (1.8% vs. 2.8%, p = 0.034). After adjustment for admission year, age, sex, Charlson Comorbidity Index (CCI)>1, cardiac arrest preadmission, Killip class, heart rate and systolic blood pressure at admission, and creatinine, in-hospital mortality was similar in both groups (OR 0.79, 95%CI 0.47-1.26, p = 0.332).

Of early PCI patients, 1,824 (23.3% or 13.5% of the total population) had immediate PCI. Immediately treated patients were of similar age (64[56; 74] vs. 65[56; 75]; p = 0.057), less often women (19% vs. 23%; p<0.001), had a higher rate of cardiac arrest preadmission (15% vs. 1.6%; p<0.001) and Killip class 4 (8.1% vs. 1.2%; p<0.001), but a lower CCI>1 (17% vs. 21%; p<0.001). Unadjusted in-hospital mortality was higher (6.6% vs. 1.5%; p<0.001) but this difference also disappeared after adjustment (OR 1.40, 95%CI 0.91-2.13, p = 0.124).

Conclusion: Since 2005, the proportion of NSTEMI patients undergoing early PCI increased, but no clear trend was visible in the last decade. Adjusted in-hospital mortality did not differ between patients with early and delayed PCI. Patients with immediate PCI had worse cardiac function at admission but after adjustment for these high-risk characteristics, in-hospital mortality was similar to patients receiving PCI within 2-24h.

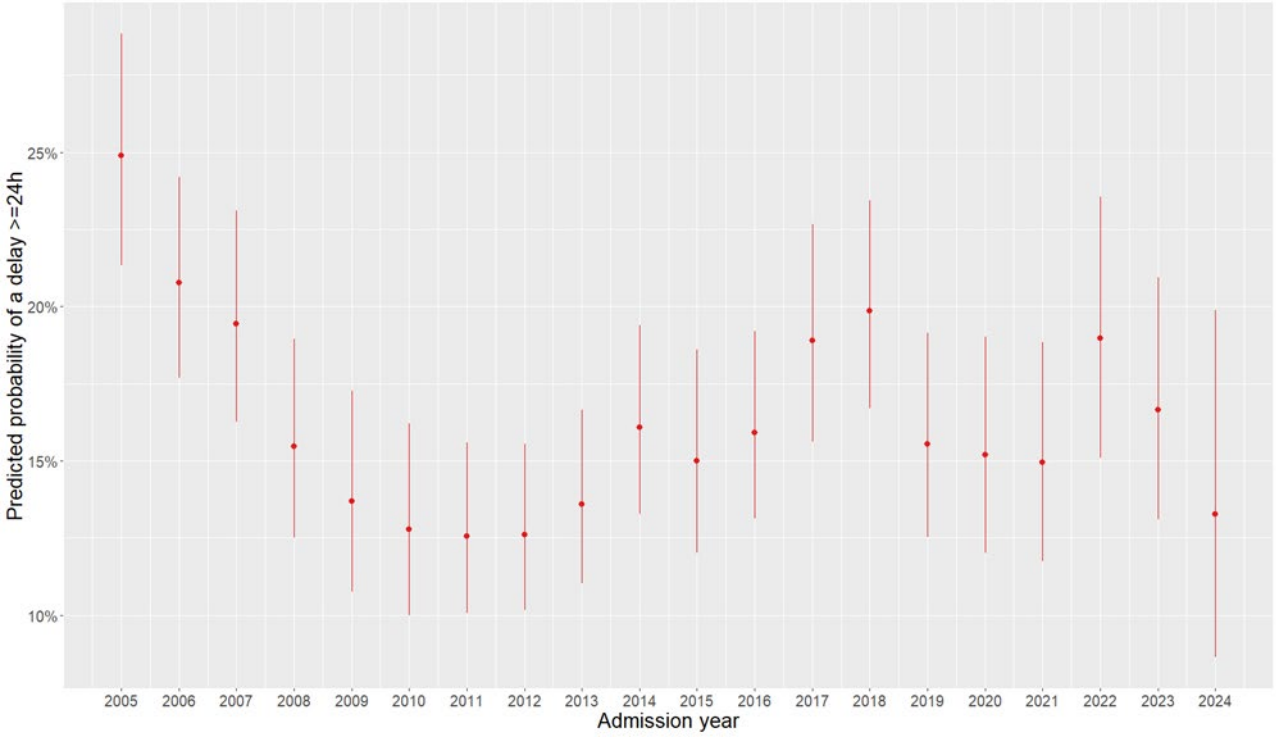

P023

Fasting Before Cardiac Catheterization: Still Necessary? A Systematic Review and Meta-Analysis of Randomized Clinical Trials

Adil Salihu[1], Stephane Fournier[1], Sarah Hugelshofer[1], Quentin Liabot[1], Victor Weerts[1], Georgios Tzimas[1], Valentina Rancati[2], Clemence Ferlay[1], Aurelia Zimmerli[1], Olivier Muller[1], Henri Lu[1], Panagiotis Antiochos[1], David Meier[1]

[1]Service of Cardiology, Lausanne University Hospital and University of Lausanne, Lausanne, Switzerland, [2]Service of Anesthesiology, Lausanne University Hospital and University of Lausanne, Lausanne, Switzerland

Introduction: Fasting prior to elective or non-urgent coronary angiography is commonly recommended to reduce the risk of adverse events, such as aspiration pneumonia. However, advancements in cardiac catheterization techniques and the use of mild sedation have led to questions about the necessity of this practice. This systematic review and meta-analysis aimed to evaluate the impact of fasting versus non-fasting protocols on patient outcomes and satisfaction.

Material and Methods: We systematically searched PubMed, Embase, and Cochrane Library databases for randomized clinical trials comparing fasting and non-fasting states before cardiac catheterization. Eight randomized trials, including a total of 3147 patients, were analyzed. The primary outcome was a composite of adverse events, including pneumonia, hypoglycemia, and nausea/vomiting. Secondary outcomes included individual adverse events and patient satisfaction.

Results: No significant difference was found in the incidence of composite adverse events between fasting and non-fasting groups (4.9% vs. 4.5%, OR, 1.07, 95%CI, 0.76, 1.50, p = 0.69). The incidence of hypoglycemia, pneumonia, and nausea/vomiting did not differ significantly between groups. Patient satisfaction was significantly higher in non-fasting protocols in four out of eight studies.

Conclusion: Our meta-analysis suggests that fasting prior to elective coronary angiography does not significantly reduce adverse events but may reduce patient satisfaction. These findings support reconsidering the necessity of fasting protocols in this context, although further studies are warranted to confirm these results.

Graphic abstract: Comparison of fasting vs non fasting protocol before cardiac catheterization

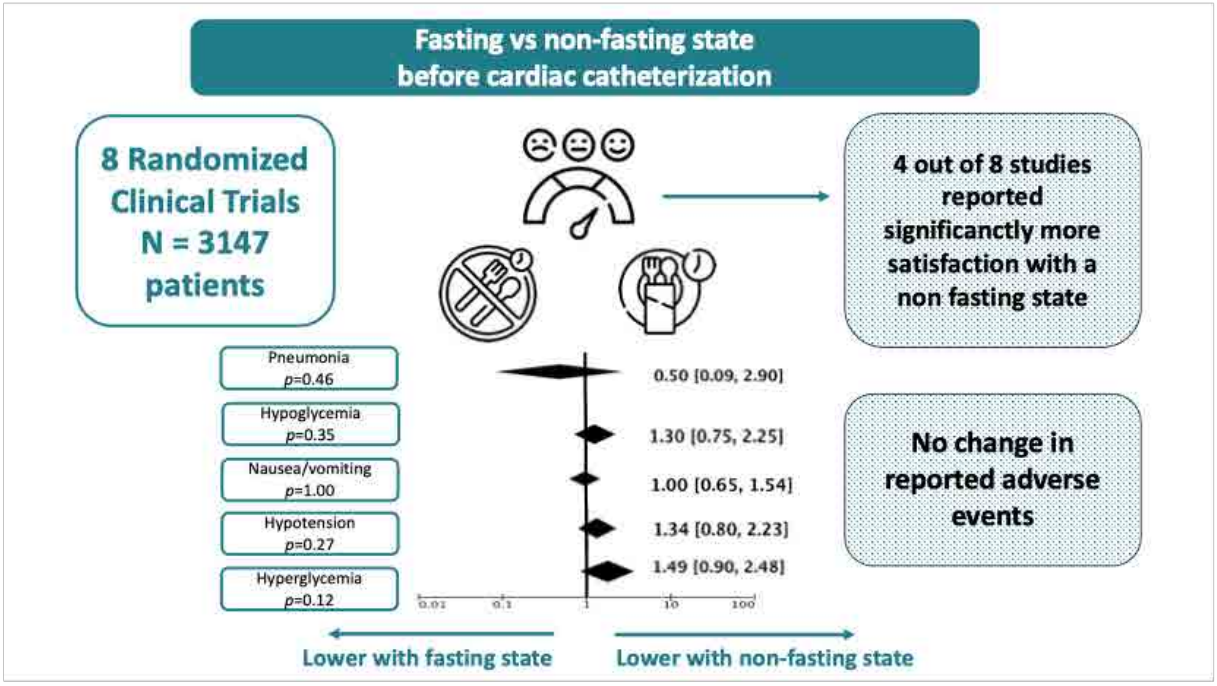

POSTER WALK "HEART FAILURE"

P024

Gene expression profiling for prediction of acute cellular rejection after heart transplantation

Roger Hullin[1], Marc Carminati[2], Costa Georgantas[3], Jonas Richiardi[4], Henri Lu[3], Piergiorgio Tozzi[3], Samuel Rotman[3], Ruud van Heeswijk[3]

[1]Lausanne University Hospital, Lausanne, Switzerland, [2]Medical School of the University Hospital Lausanne, Lausanne, Switzerland, [3]University Hospital Lausanne, Lausanne, Switzerland, [4]Radiology, Lausanne, Switzerland

Introduction: Histopathological grading of endomyocardial biopsies (EMB) is the standard for rejection surveillance after heart transplantation (acute cellular rejection (ACR): 0R = no; 1R = mild; 2R moderate). ISHLT consensus criteria for interpreting biopsies fail to predict future ACR. This study tested gene expression profiling (GEP) for prediction of future ACR.

Material and Methods: In the pilot study, 30 EMB were used including 10 EMB from patients with always 0R; 7 0R grade EMB preceding EMB with ACR; 4 EMB with 1R, 3 EMB with 2R, 6 EMB with 0R after ACR. GEP used Illumina RNA sequencing. 17 genes are differentially expressed between EMB with rejection (1R/2R) or without; 13 of these (CD40LG, HLA-DQB1, HLA-DOA, HLA-DOB, PRF1, HLA-DQA2, HLA-DRB1, TNF, HLA-G, HLA-DPB1, HLA-DPA1, HLA-DMB, HLA-DMA) were measured in the main study in a metagene summarizing the mean expression of these 13 genes with a cut-off chosen at the highest threshold to avoid false negative results.

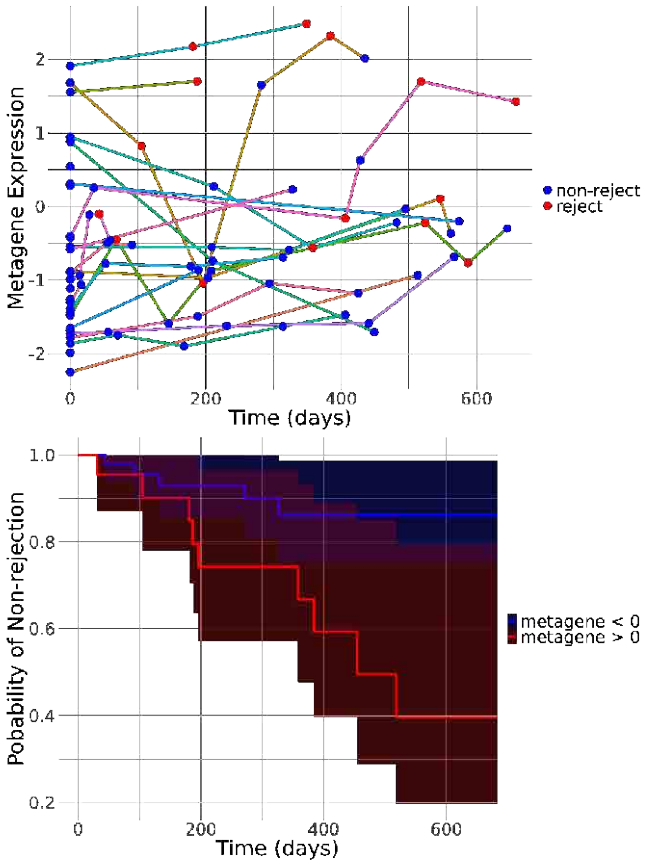

Figure 1: Top: Endomyocardial biopsy measurements with a corresponding metagene expression w.r.t time. Bottom: Kaplan-Meier survival curve illustrating the probability of non-rejection over time for two groups split by metagene expression at zero.

Results: First, the GEP was not different between EMB with 1R/2R; second, GEP was not different to the preceding or subsequent EMB even if their histophathology was negative or if time interval was longer (<10 months). The main study enrolled 29 HTx recipients (average follow-up time of 3.6±1.1 years) with 89/292 EMB having metagene assessment. The logistic mixed-effects regression model estimated the association between the metagene and graft rejection accounting for repeated measures within subjects over time; furthermore, age, sex, BMI, sex mismatch of donor/ receiver, and left ventricular ejection fraction were included as covariates. In this model, the metagene above the cut-off was significantly associated incident ACR (β = 0.96±0.36, p = 0.007) while other covariates were not related (p>0.1).

Conclusion: The results indicate that (a) the molecular phenotype in EMB does not reflect the current grading for ACR; (b) assessment of the metagene identifies patients at future risk for ACR.

P025

The pulmonary artery pulsatility index in patients with severe aortic stenosis undergoing valve replacement

Laura Rechsteiner[1], Lukas Weber[1], Philipp Haager[1], Johannes Rigger[1], Joannis Chronis[1], Peter Ammann[1], Roman Brenner[1], Martin Schmiady[2], Hans Rickli[1], Micha T. Maeder[1]

[1]Health Ostschweiz (HOCH) Kantonsspital St. Gallen, St. Gallen, Switzerland, [2]University Hospital Zürich, Zürich, Switzerland

Introduction: The pulmonary artery pulsatility index (PAPi), i.e. the pulmonary artery pulse pressure (PAPP) divided by the mean right atrial pressure (mRAP), is a novel invasive index of right ventricular function. We sought to assess the contributors and the prognostic impact of the PAPi in unselected patients with aortic stenosis (AS) undergoing aortic valve replacement (AVR)

Material and Methods: We studied consecutive patients with severe AS (n = 487, 74±10 years, 58% males, indexed aortic valve area 0.42±0.12 cm2/m2, left ventricular ejection fraction 57±12%) undergoing right heart catheterization prior to AVR (72% surgical, 28% transcatheter) with a post-AVR follow-up of several years.

Results: The mean PAPi was 4.7±3.3, and the mean values in the four PAPi quartiles were 2.1±0.5, 3.2±0.3, 4.5±0.5, and 8.9±4.2. Patients in the lowest PAPi quartile had similar AS severity, symptoms, B-type natriuretic peptide and surgical risk compared to patients in higher quartiles. Patients in the lowest PAPi quartile had the lowest PAPP and the highest mRAP and only a slightly reduced stroke volume index (SVI) but the highest pulmonary artery capacitance (PAC), i.e. the stroke volume dived by the PAPP. After a median post-AVR follow-up of 1361 days mortality did not differ across PAPi quartiles (log rank p = 0.50; Figure), which was independent of the AVR mode. However, all contributors of the PAPi equation, i.e. higher PAPP, lower PAC (i.e. stroke volume divided by PAPP), lower SVI, and higher mRAP were associated with increased mortality.

Conclusion: In unselected patients with severe AS, the low PAPP in those with low PAPi was mainly a reflection of a high PAC (indicating absence of relevant pulmonary vascular disease) rather than a low SVI. Accordingly, in the present cohort of unselected patients with AS, PAPi was not a marker of low (right ventricular) SVI, which may explain why the PAPi did not predict post-AVR mortality.

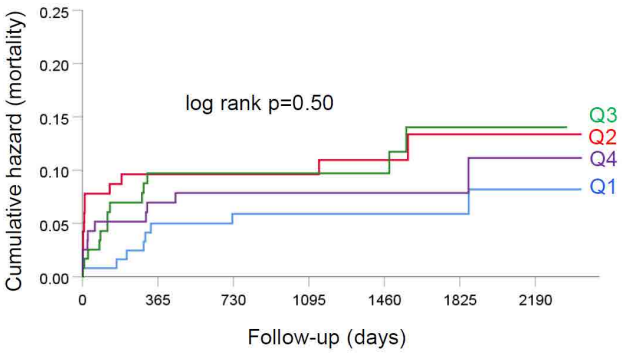

P026

The role of Erythroferrone on posttransplant adaptive immune response and 1-year acute cellular rejection

Barbara Pitta Gros[1], Angela Rocca[1], Henri Lu[1], Natallia Laptseva[2], Andreas Flammer[2], Michele Martinelli[3], Philippe Meyer[4], Martin Muller[3], Roger Hullin[1]

[1]CHUV, Lausanne, Switzerland, [2]Universitätsspital Zürich, Zurich, Switzerland, [3]Inselspital, Bern, Switzerland, [4]HUG, Geneve, Switzerland

Introduction: Iron metabolism dysfunction and anemia are common in patients awaiting heart transplantation (HTx). Hepcidin, erythroferrone, interleukin-6, hemoglobin and ferritin are central for iron homeostasis with erythroferrone and hepcidin being antagonists for the gene expression of hepcidin in the liver.

In a previous analysis of a multicenter cohort of 276 Swiss HTx recipients, we showed that high pretransplant erythroferrone levels >2.25 ug/l are predictive for the combined 1-year endpoint of all-cause mortality and ≥ acute cellular rejection while other regulators of iron homeostasis such as hepcidin, interleukin-6 or ferritin were not predictive.

Material and Methods: This study investigated in 237 survivors the 1-year posttransplant serum levels of iron homeostasis regulators (hepcidin, erythroferrone, interleukin-6, ferritin, hemoglobin) and the erythroferrone/interleukin-6 ratio in subgroups with ≤ or >2.25 ug/l erythroferrone further subdivided into HTx survivors with or without ACR.

Results: In HTx recipients without acute cellular rejection, levels of hemoglobin, hepcidin and ferritin were not different between HTx survivors with low or high erythroferrone levels while interleukin-6 levels were higher in the high erythroferrone subgroup. In HTx recipients with acute cellular rejection, levels of hepcidin, interleukin-6, and ferritin were not different between low and high erythroferrone levels whereas hemoglobin were higher in HTx recipients with ACR and high erythroferrone levels (Figure 1). The erythroferrone/interleukin-6 ratio was disproportionally higher in 1-year survivors with upper-quartile erythroferrone and incident ACR when compared to patients without ACR (1.18 vs 0.41; p = 0.016) (Figure2).

Conclusion: The disproportionally higher erythroferrone/interleukin-6 ratio in HTx recipients with acute cellular rejection and erythroferrone levels >2.25 ug/l suggests a role of erythroferrone in the adaptive immune response. Indeed, erythroferrone not only sequester bone-morphogenetic proteins (BMP) 2 and 6 which are master regulators of iron homeostasis but also BMP 7 which is important for maturation on T-lymphocytes.

Figure 1: Posttransplant levels of hemoglobin, IL-6, hepcidin and ferritin as a function of ERFE-levels ≤ 2.25 ug/l vs. >2.25 ug in patients with or without ACR

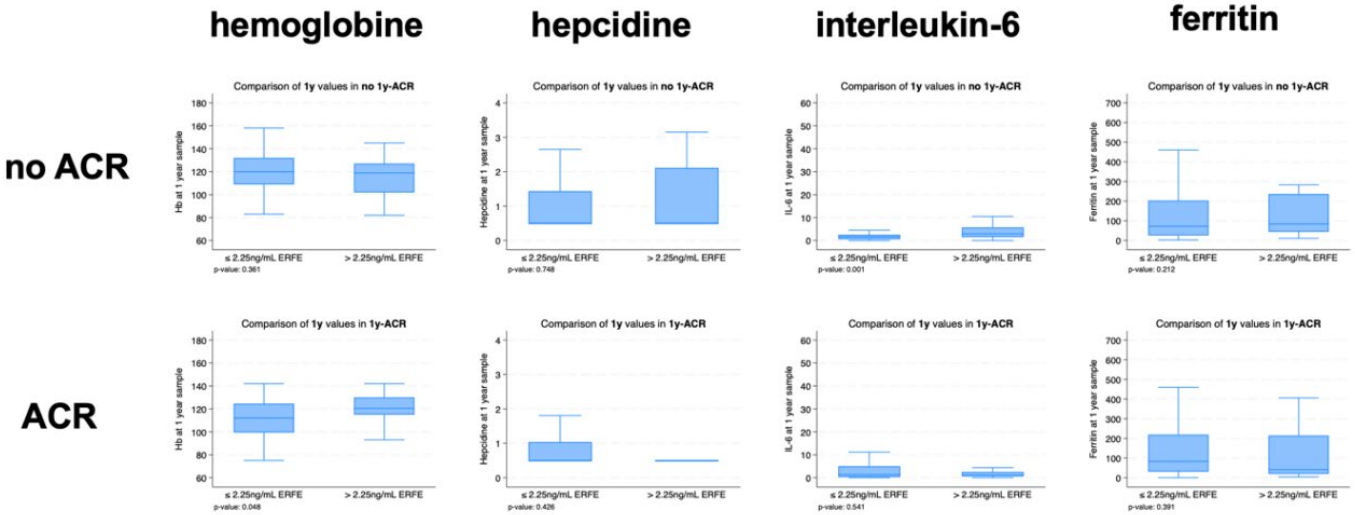

Figure 2: Comparison of the 1-year posttransplant erythroferrone / Interleukin-6 ratio in HTx recipients without and with ACR

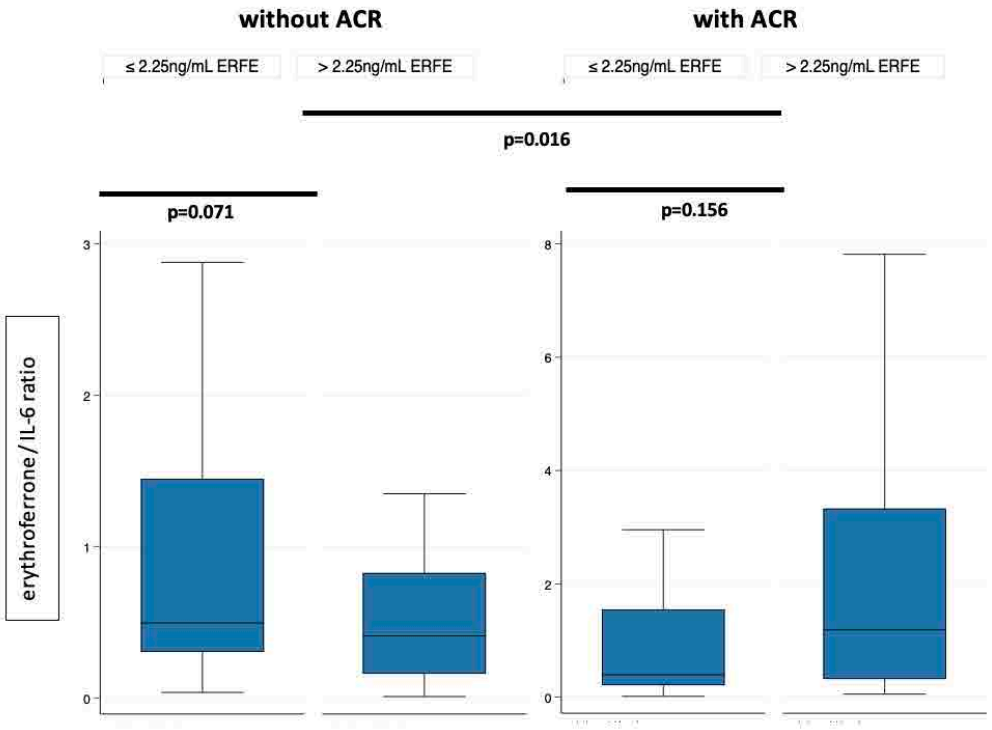

Patients without ACR: n=143, patients with ACR: n=72.

P027

Low Dose Apixaban in Heartmate 3 LVAD Patients, Interim Analysis of the Apixivad Trial, a Randomised Controlled Study

Bruno Schnegg[1], Ricardo Deveza[2], Sumita Barua[2], Lukas Capek[1], Jolie Bruno[1], Maryam Pavlicek-Bahlo[1], Elena Xourgia[1], Monika Fürholz[1], David Reineke[1], Lukas Hunziker[1], Michele Martinelli, Peter MacDonald[2], Critopher Hayward[2]

[1]Inselspital, Bern university hospital, Bern, Switzerland, [2]St-Vincent Hospital, Sydney, Australia

Introduction: Left ventricular assist devices (LVADs) improve outcomes in advanced heart failure but require anticoagulation. Vitamin K antagonists (VKA) are often limited by suboptimal 'Time in Therapeutic Range' (TTR), with associated increase in morbidity and mortality. There is emerging evidence on the use of Apixaban in HeartMate 3 (HM3) LVAD supported patients. We present the interim analysis of the ApixiVad study, evaluating reduced-dose apixaban in HM3 bridged to transplantation (BTT) and destination therapy (DT).

Material and Methods: ApixiVAD is an randomized, international, open-label study comparing the safety of reduced-dose apixaban (2.5 mg twice daily) with standard VKA (1: 1) for 2 years or until transplantation. Eligible patients were supported with the HM3 for at least 2-months, with TTR >60%. Primary outcomes included thromboembolic events, bleeding and death.

Results: Between 2022 and Januar 2025, 44 patients were randomised, 21 to apixaban and 23 to VKA. Median age was 55 years (50-63), 6 female (14%). Twenty four patients (55%) had underlying non-ischaemic heart disease and 37 (84%) received an LVAD as BTT. At interim analysis, patients were enrolled for a median 147 (86-226) days, 25 (58%) were transplanted, 5 (12%) had undergone a primary outcome and 13 (30%) remained active within the study. Two patients in the Apixaban group and one patient in the VKA group experienced bleeding, one patient in the VKA group suffered a stroke, one patient died of sepsis in the Apixiban group. There was no significant difference in the number of complications between groups (log rank test P = 0.6), haemolysis or peri-transplant transfusion requirement.

Conclusion: These results suggest reduced-dose Apixaban may provide a safe alternative to VKA in HM3 supported patients with similar hemocompatibility outcomes. Transplantation from apixaban is not associated with excess bleeding. Larger randomized-controlled trials are necessary to establish the long-term safety and efficacy of this approach.

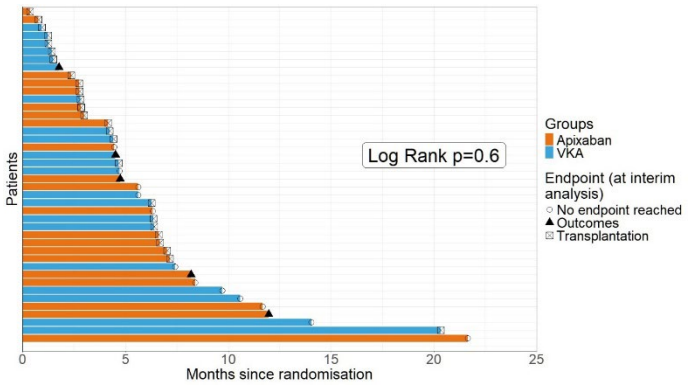

P028

Optimized carbon monoxide rebreathing technique: a novel tool to assess volume status in patients with heart failure.

Konstantinos Bitos[1], Thomas Haider[1], Natallia Laptseva[1], Valentina Rossi[1], Philip Sommer[1], Matthias Nägele[1], Frank Ruschitzka[1], Isabella Sudano[1], Andreas Flammer[1]

[1]Heart Failure and Heart Transplantation Unit, Department of Cardiology, University Heart Center Zurich, Zurich, Switzerland

Introduction: Assessment of volume overload in patients with heart failure (HF) remains very challenging in daily practice. The combination of clinical signs, biochemical and echocardiographic parameters is required to guide volume management in HF, often leading to inappropriate changes of diuretic therapy. Optimized carbon monoxide rebreathing technique (OpCOT) is a novel, easy feasible, investigator-independent, and safe method to assess blood volume profile and may be a helpful tool in HF volume management.

Material and Methods: In this observational study, we investigated the possible role of volume status estimation by OpCOT in HF patients. The volume profile, consisting of plasma volume (PV), red blood cell volume (RBCV) and blood volume (BV), was assessed via OpCOT in clinically compensated HF patients. Transthoracic echocardiography and biochemical analysis were also performed. Spearman's rank correlation was computed to assess the relationship between weight-adapted PV, RBCV and BV (PVw, RBCVw and BVw) and echocardiographic and laboratory parameters, known to be related to intravascular volume state.

Results: We included seventy-five HF patients, 14 females (19%), mean age±SD 62±13y, mean left ventricular ejection fraction (EF) 36±14%, NYHA class I-III. 52 out of 75 patients (69.4%) had reduced EF (HFrEF), 4/75 (5.3%) had mildly reduced EF (HFmrEF) and 19/75 (25.3%) had preserved EF (HFpEF). The median NT-proBNP was 964 ng/l (interquartile range 369-1630). The weight-adapted blood volume profile parameters were: PVw 42.5±13.2 ml/kg, RBCVw 33.6±11.9 ml/kg and BVw 76.1±23.3 ml/kg. There was a positive association between PVw and NT-proBNP (Spearman-Rho 0.419, p-value <0.001) as well as between PVw and left atrial volume index (LAVI) (Spearman-Rho 0.283, p-value 0.022).

Conclusion: Weight-adapted plasma volume, as measured by OpCOT was positively associated with NT-proBNP and LAVI in HF patients throughout the whole LVEF-range. It is a promising new marker which may be used to guide volume management more adequately in HF. Further prospective randomized trials are needed.

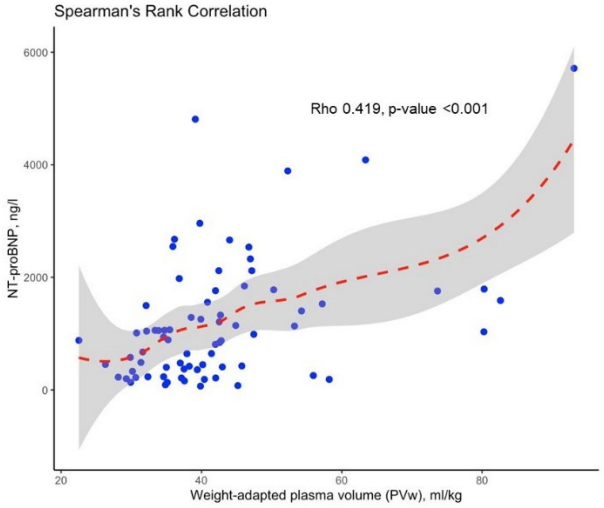

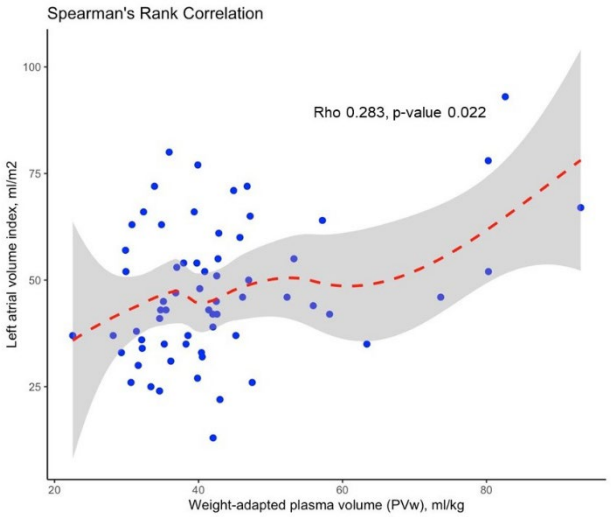

P029

Diagnostic and Prognostic Performance of IGFBP7 in patients with Acute Dyspnea in the Emergency Department

Codruta Popescu[1 2], Maria Belkin[1 2], Pedro Lopez-Ayala[1 2], Samyut Shrestha[1 2], Androniki Papachristou[1 2], Ivo Stebel[1 2], Christian Mueller[1 2]

[1]University of Basel, Basel, Switzerland, [2]Cardiovascular Research Institute Basel (CRIB) and Department of Cardiology, University Hospital Basel, University of Basel, Basel, Switzerland

Introduction: Acute Heart Failure (AHF) is a frequent reason for emergency department (ED) visits that require hospitalization. Despite progress in chronic heart failure therapy, AHF patients, especially the elderly, have substantial morbidity and mortality rates. High IGFBP7 levels cause collagen accumulation, which result in myocardial fibrosis and cardiac dysfunction. IGFBP7 was connected to disease progression and worse outcomes. The aim was to determine if IGFBP7 levels in ED patients with acute dyspnea could contribute to the diagnosis and risk evaluation of AHF.

Material and Methods: Patients presenting with acute dyspnea were enrolled in a prospective multicentre diagnostic study. IGFBP7 concentrations were measured in a blinded fashion. The final diagnosis was centrally adjudicated using all the individual patient information including cardiac imaging. Prognostic endpoints included all-cause mortality within 720 days and the combined outcome of all-cause mortality and AHF rehospitalizations.

Results: AHF was adjudicated in 52% of 966 patients. IGFBP7 levels were higher in AHF patients (150 [117.2-195.2] ng/mL vs. 91.3 [75.5-114.2] ng/mL, p<0.001). Patients in the highest IGFBP7 quartile were older, male, and more likely to have coronary artery disease, chronic heart failure, atrial fibrillation, and chronic renal disease. Participants had the lowest left ventricular ejection fraction (LVEF) and lowest estimated glomerular filtration rate (eGFR) before trial entry. The AUC of IGFBP7 was 0.85 (95% CI: 0.82 to 0.87), NT-proBNP was 0.92 (95% CI: 0.90 to 0.93), and hs-cTnT was 0.79 (p<0.001). Adding IGFBP7 to NT-proBNP increased the AUC to 0.93 (95% CI: 0.91 to 0.94). Patients with IGFBP7 plasma values above the median had a significantly greater mortality risk. AHF rehospitalization and all-cause death at 720 days were associated with IGFBP7 levels above the median.

Conclusion: IGFBP7 enhances the diagnostic and prognostic capabilities of NT-pro-BNP in patients presenting with acute dyspnea to the ED.

P030

Application of Perioperative CMR To Quantify Inducible Ischaemia During the Induction of Anaesthesia

Kady Fischer[1], Stephanie Keser[1], Yann Schwerzmann[1], Benedikt Türler[1], Thilo Schweizer[1], Leonard Grob[1], Adrian T Huber[2], Bernd Jung[2], Dominik P. Guensch[1 2]

[1]Department of Anaesthesiology and Pain Medicine, Inselspital, Bern University Hospital, University of Bern, Bern, Switzerland, [2]Department of Diagnostic, Interventional and Paediatric Radiology, Inselspital, Bern University Hospital, University of Bern, Bern, Switzerland

Introduction: Anaesthesia combined with surgery creates a complex perioperative pathophysiologic environment. Cardiovascular events account for 30-50% of perioperative complications, with most attributed to type-II myocardial ischaemia. Although patients with underlying coronary artery disease (CAD) are at higher risk, the temporal relationship with potential riggers for ischaemic events remain unclear. The induction of general anaesthesia bears many triggers as it is a complex sequence of events, including breathing pattern changes, intubation, ventilation and anaesthetics. Therefore, we applied novel cardiovascular magnetic resonance (CMR) techniques to image perturbations in myocardial oxygenation and function during general anaesthesia induction.

Material and Methods: Nine patients (no-CAD, n = 6, CAD n = 3) scheduled for elective surgery were prospectively recruited. Anaesthesia induction was performed inside an MRI (Figure 1) and oxygenation-sensitive CMR was acquired continuously from the awake stage, through induction, intubation, and for 10 minutes of maintenance. Myocardial oxygenation, peak strain and ventricular synchronicity were quantified.

Results: Prior to intubation, no-CAD patients exhibited fluctuations in cardiac function related to changes in breathing patterns and administration of sedatives led to a a reduction in systolic function but this was not temporally associated with oxygenation (Figure 2). In contrast, CAD patients showed coupled deoxygenation and systolic dysfunction in post-stenotic myocardial segments, indicating inducible ischaemia. After intubation, myocardial deoxygenation persisted for 8.7±0.8 minutes in no-CAD and 8.5±0.3 minutes in CAD patients. By 10min, myocardial oxygenation had normalized, but strain remained reduced, particularly in post-stenotic myocardium. Interestingly, mechanical dispersion as a marker of ventricular synchronicity, CAD patients exhibited worsening dyssynchrony (39±14ms, p<0.05) while no-CAD patients (8±13ms,p = 0.88) did not.

Conclusion: Novel application of perioperative CMR demonstrates that induction of anaesthesia triggers rapid fluctuations in myocardial oxygenation and function. Application of advanced imaging in a research setting provides new insights into how patients are vulnerable to perioperative myocardial ischaemia during cardiac and non-cardiac surgery.

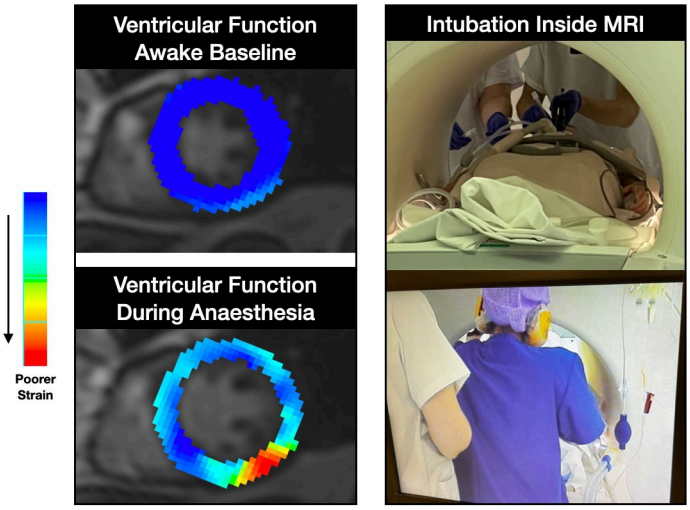

Fig 1: In a patient with an occlusion of the right coronary artery, systolic function drops during the induction of general anaesthesia, especially in the inferior wall (red)

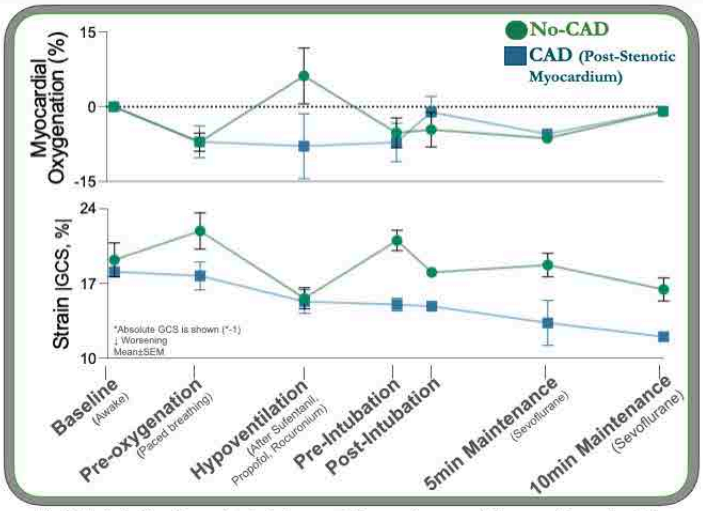

Fig 2: The induction of anaesthesia induces rapid changes in myocardial oxygenation and systolic function (global peak circumferential strain, GCS) in patients with no cardiac risk factors and patients with coronary artery disease (CAD). However, post-stenotic territory in particular presents with both deoxygenation and regional systolic function indicating inducible ischaemia.

P031

Moderate accuracy but high precision of artificial intelligence for automated echocardiographic measurements in ATTR cardiomyopathy

Amely Walser[1], Andreas Flammer[1], Rahel Schwotzer[2], Frank Ruschitzka[1], Felix C. Tanner[1], Dominik C. Benz[1]

[1]University Hospital Zurich, Department of Cardiology, Zurich, Switzerland, [2]University Hospital Zurich, Department of Hematology, Zurich, Switzerland

Introduction: Detection of disease progression is key to personalize treatment strategies in cardiac transthyretin (TTR) amyloidosis, particularly with emerging new therapies. Echocardiography can identify subtle changes in myocardial structure and function over time but is limited by operator dependence in clinical routine. This study evaluates the impact of automated measurements by artificial intelligence (AI) on agreement and precision.

Material and Methods: This retrospective longitudinal cohort study includes patients with ATTR cardiomyopathy who underwent serial echocardiograms. Septal thickness and end-diastolic volume (EDV) were assessed by an expert human

reader (cardiologist) and the AI-based solution US2AI (AI). Interrater variability was analysed by interclass correlation coefficient (ICC) and Bland-Altman analysis. Clinically meaningful changes were defined as absolute changes between consecutive 12-month intervals exceeding the mean difference ± 2×SD of intrarater variability, representing the maximum likely difference in repeated measurements.

Results: The study includes 62 patients (58 male, median age 73 years) and 178 echocardiograms (25 patients with multiple follow-ups). At baseline, median septal thickness was 16mm [interquartile range, 15-18] and 14mm [12-16], while EDV was 123ml [106-149] and 86mL [69-101] by cardiologist and AI, respectively. For septal thickness and EDV, AI showed moderate agreement with the cardiologist (ICC 0.65 and 0.49, respectively) with biases of -1.9mm (95% CI: -5.4 to 1.6mm) (**Panel A**) and -36 ml (95%: -74 to 3ml), respectively (**Panel B**). With regard to clinically meaningful differences (3.0 vs. 2.5mm and 43 vs. 21ml), no relevant differences were observed between cardiologist and AI for septal thickness (20% vs. 22%, p = 0.85; **Panel C**) or EDV (11% vs. 21%, p = 0.08; **Panel D**).

Conclusion: Automated measurements by AI have moderate agreement with a cardiologist but similar precision to measure changes over time. While the accuracy of AI may be limited, it could be useful to monitor disease progression in ATTR cardiomyopathy.

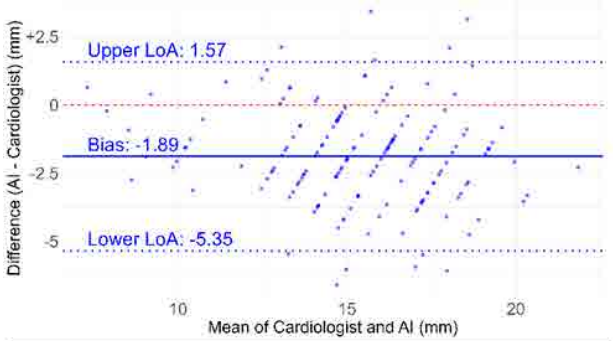

Panel A. Bland-Altman plot, cardiologist (red dotted line) vs. AI (blue) for septal thickness.

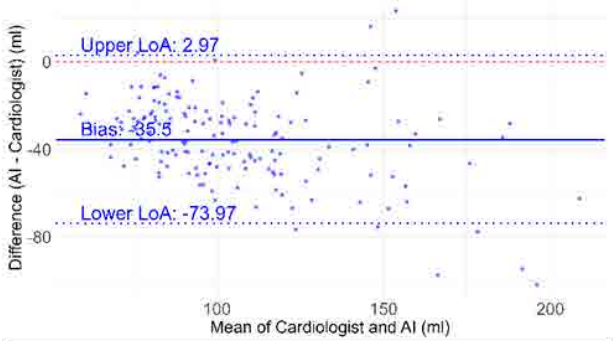

Panel B. Bland-Altman plot, cardiologist (red dotted line) vs. AI (blue) for EDV.

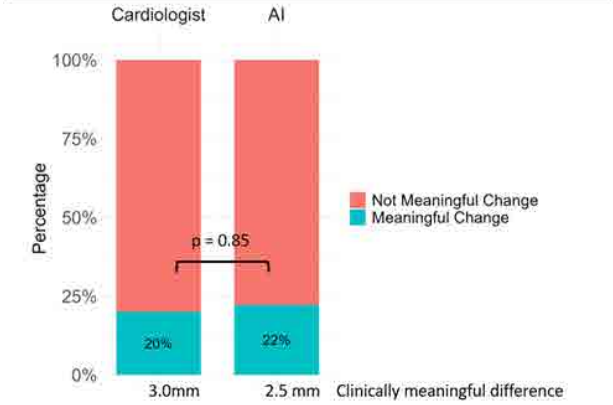

Panel C. Clinically meaningful changes in septal thickness over consecutive 12-month intervals.

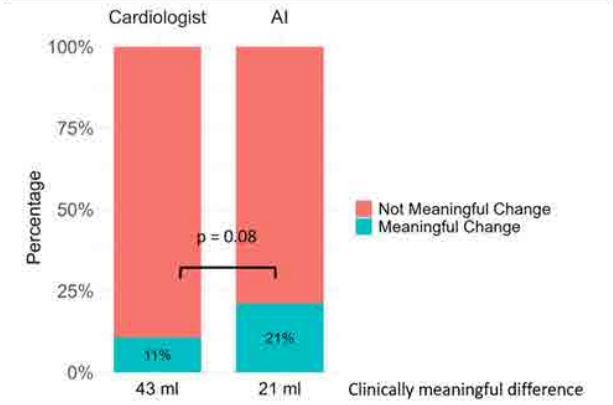

Panel D. Clinically meaningful changes in EDV over consecutive 12-month intervals.

P032

Impact of Digoxin Utilization on Gastrointestinal Bleeding in Patients With Continuous-Flow Left Ventricular Assist Devices: A Systematic Review and Meta-Analysis

Matteo Marchetti[1], Barbara Pitta Gros[1], Olivier Muller[1], Clémence Ferlay[2], Zied Ltaief[2], Matthias Kirsch[3], Patrizio Pascale[1], Philippe Meyer[4], Patrick Yerly[1], Panagiotis Antiochos[1], Roger Hullin[1], Henri Lu[1]

[1]Division of Cardiology, Lausanne University Hospital, University of Lausanne, Lausanne, Switzerland, Lausanne, Switzerland, [2]Intensive Care Unit, Lausanne University Hospital, University of Lausanne, Lausanne, Switzerland, Lausanne, Switzerland, [3]Division of Cardiac Surgery, Lausanne University Hospital, University of Lausanne, Lausanne, Switzerland, Lausanne, Switzerland, [4]Division of Cardiology, Geneva University Hospital, University of Geneva, Geneva, Switzerland, Geneva, Switzerland

Introduction: Continuous flow left ventricular assist device (CF-LVAD) improves quality of life and survival in patients with advanced heart failure, but is frequently complicated by gastrointestinal bleeding (GIB). Loss of pulsatile flow may lead to intestinal mucosal hypoxia, triggering neoangiogenesis via hypoxia-inducible factor 1-alpha (HIF-1a) and the formation of gastrointestinal angiodysplasias (GIAD), a common cause of GIB. Digoxin inhibits HIF-1a and may prevent GIAD development, though its impact on GIB remains uncertain. This systematic review and meta-analysis evaluated the association between digoxin use and GIB risk in CF-LVAD patients.

Material and Methods: This meta-analysis was registered in PROSPERO (CRD42024626222). The primary outcome was GIB occurrence. Research articles including adults with CF-LVAD support, comparing digoxin users versus non-users were included. Studies were identified using PubMed and EMBASE. Hazard ratios (HR) and their respective 95% confidence intervals (CIs) were pooled and meta-analyzed across studies. A random-effects model was used; heterogeneity was assessed using the Cochran Q test statistic and Higgins and Thompson I^2.

Results: A total of four studies were included, with 2'742 patients in the digoxin group and 12'175 in the no-digoxin group (mean age 55±13 years, 21% women). CF-LVAD support was axial (HeartMate II) in 78% and centrifugal (HeartMate III or HeartWare) in 22%. Digoxin use was associated with a non-significant reduction in GIB risk (HR: 0.70; 95%CI: 0.49-1.01; I^2: 70.7%; Figure 1A). However, for GIAD-related GIB risk, digoxin was associated with a lower risk (HR: 0.33; 95%CI: 0.13-0.82; I^2: 51.0%; Figure 1B).

Conclusion: Digoxin use was associated with a trend towards a lower risk of overall GIB, with a significantly lower risk observed for GIB likely caused by GIAD.

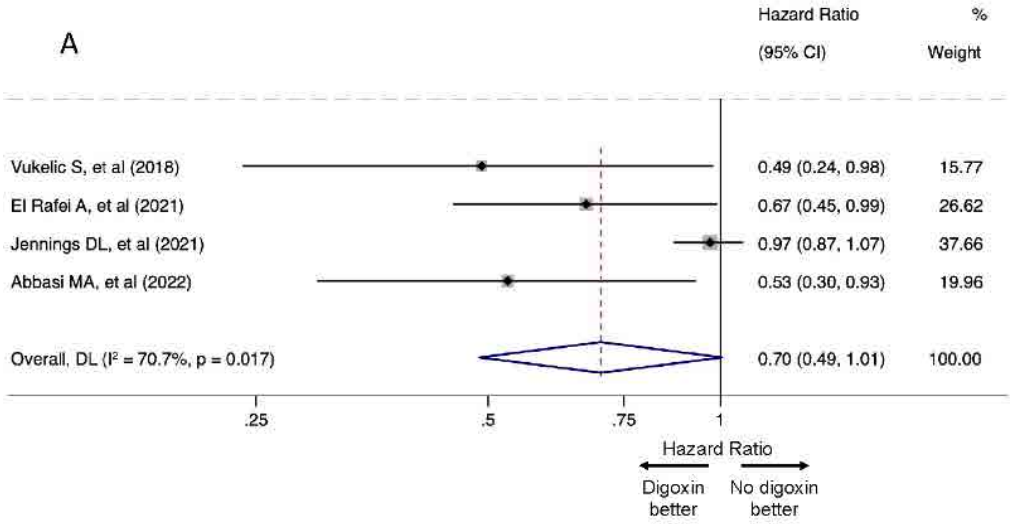

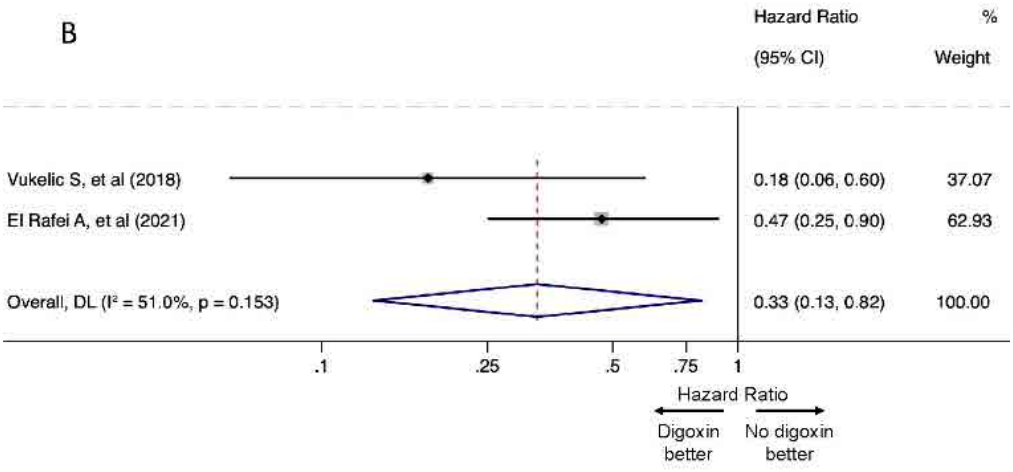

P033

Prognostic Impact of Systolic Blood Pressure Trajectory Among Patients Hospitalized in An Acute Heart Failure Setting: Insights From a Real-world Multicenter Cohort

Marc Carminati[1], Tamila Abdurashidova[1], Nisha Soborun[1], Barbara Pitta-Gros[1], Sara Schukraft[1], Georgios Tzimas[1], Pierre Monney[1], Roger Hullin[1], Henri Lu[1]

[1]*CHUV, Lausanne, Switzerland*

Introduction: Systolic blood pressure (SBP) is a prognostic marker in acute heart failure (AHF), but the prognostic implications of in-hospital changes in SBP are unclear. We aimed to assess the association between in-hospital SBP changes and outcomes in a real-world cohort of AHF patients enrolled in Kyrgyzstan and Switzerland.

Material and Methods: We analyzed consecutive patients hospitalized for AHF between 2005 and 2020 at two tertiary-care centers (Lausanne University Hospital, Switzerland; National Center of Cardiology, Kyrgyzstan) with available SBP measurements at admission (SBPa) and discharge (SBPd). Patients were classified into four SBP trajectory categories: *stable normal/low* (SBPa & SBPd <140 mmHg or SBPa <140 & SBPd≥140 mmHg, Δ <10), *increasing* (SBPa <140 & SBPd ≥140 mmHg, Δ ≥10), *decreasing* (SBPa ≥140 & SBPd <140 mmHg, Δ ≥10), *stable elevated* (SBPa & SBPd ≥140 mmHg or SBPa ≥140 & SBPd<140 mmHg, Δ <10. The association between categories and the primary outcome (first HF hospitalization or all-cause mortality) was assessed with Cox models. The relationship between the primary outcome rate and SBP change (SBPd – SBPa) was analyzed using restricted cubic splines.

Results: Among 1,490 patients (80% Swiss, 56% men, age 75±13 years), 621 experienced the primary outcome over a median 1-year follow-up. Compared to those with stable normal/low SBP, patients with decreasing SBP had a lower risk of the combined outcome (adjusted HR 0.81; 95%CI 0.66–0.99; P = 0.040; **Figure 1**). No significant differences were observed for other SBP trajectories. These results remained consistent regardless of sex ($P_{interaction}$ = 0.91), and LVEF ($P_{interaction}$ = 0.10). Among patients with a SBPa ≥140 mmHg, SBP decline was associated with a lower rate of the primary outcome (**Figure 2**).

Conclusion: In this real-world, bicenter cohort of 1,490 AHF patients, in-hospital decline in SBP emerged as an independent predictor of improved outcomes in those with elevated SBPa.

Figure 1. Cumulative Incidence of the Composite Outcome of First Heart Failure Hospitalization or All-Cause Death According to Categories of Systolic Blood Pressure Trajectory

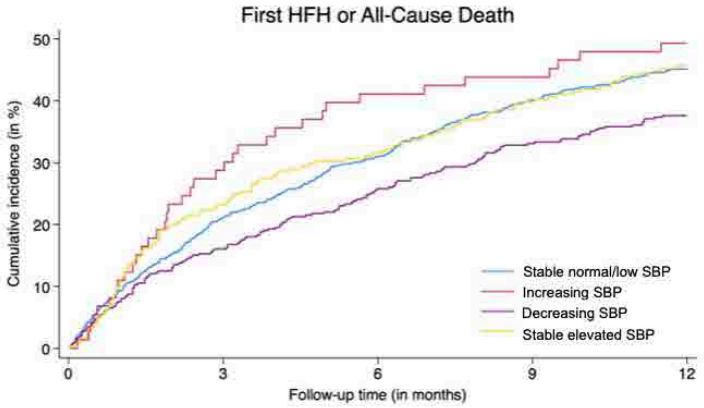

	Events, n (%)	Event rate (95% CI), per 100 py	Unadjusted HR (95% CI)	Adjusted HR (95% CI), Model*
First HFH or All-Cause Death				
- Stable normal/low SBP (n=757)	325 (42.9)	64.0 (57.5-71.4)	1 (reference)	1 (reference)
- Increasing SBP (n=77)	36 (46.8)	76.5 (55.2-106.0)	1.09 (0.77-1.54)	1.00 (0.70-1.43)
- Decreasing SBP (n=412)	150 (36.4)	49.4 (42.1-58.0)	0.78 (0.64-0.94)	0.81 (0.66-0.99)
- Stable elevated SBP (n=244)	110 (45.1)	65.5 (54.3-79.0)	0.97 (0.78-1.20)	0.96 (0.76-1.21)

*Adjusted for age, sex, BMI, prior MI, AFF, prior HFH, hypertension, diabetes, LVEF, eGFR, beta-blockers, ACEi, ARB, MRA.
All analyses are stratified by country (Switzerland or Kyrgyzstan).
Abbreviations : ACEi = angiotensin-converting enzyme inhibitor; AFF = atrial fibrillation or flutter; ARB = angiotensin receptor blocker; BMI = body mass index; CI = confidence interval; eGFR = estimated glomerular filtration rate; HFH = heart failure hospitalization; HR = hazard ratio; LVEF = left ventricular ejection fraction; MRA = mineralocorticoid receptor antagonist; py = patient-years; SBP = systolic blood pressure.

Figure 2. Rate of First HFH or All-Cause Death According to Mean Change in SBP (SBP at discharge – SBP at admission) Among Patients With a SBP ≥140 mmHg at Admission

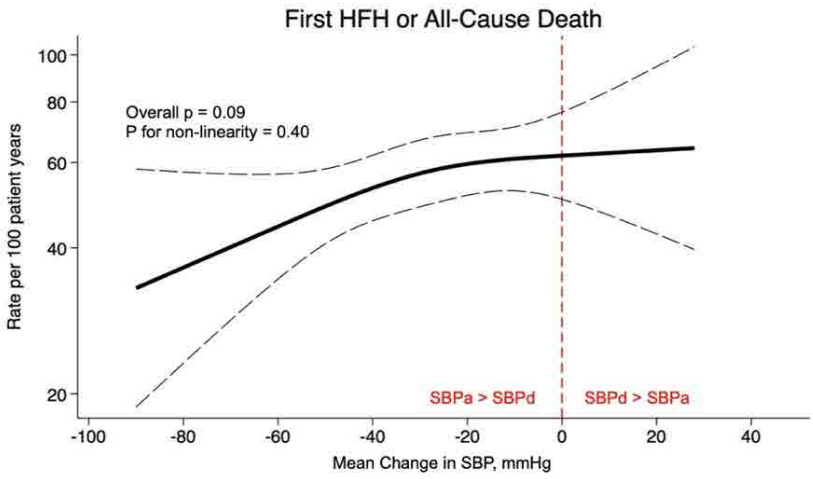

Abbreviations: HFH = heart failure hospitalization; SBP = systolic blood pressure; SBPa = systolic blood pressure at admission; SBPd = systolic blood pressure at discharge.

P034

Atrial function quantified by cardiovascular magnetic resonance imaging improves risk stratification in suspected myocarditis.

Delia Brändle[1 2], Kady Fischer[2], Benedikt Bernhard[1], Dominik P. Guensch[2], Raymond Y. Kwong[3], Christoph Gräni[1]

[1]Department of Cardiology, Inselspital, Bern University Hospital, University of Bern, Bern, Switzerland, [2]Department of Anaesthesiology and Pain Medicine, Inselspital, Bern University Hospital, University of Bern, Bern, Switzerland, [3]Non-invasive Cardiovascular Imaging, Cardiovascular Division, Department of Medicine, Brigham and Women's Hospital, Harvard Medical School, Boston, United States

Introduction: Myocarditis is characterized by inflammation and potential myocardial dysfunction. Although any cardiac tissue can be affected, current clinical evaluations primarily focus on the left ventricle. Novel cardiovascular magnetic resonance (CMR) based rapid four-chamber post-processing techniques allow for semi-automated measurements of long-axis shortening simultaneously in the atria and ventricles. We aimed to investigate the prognostic value of atrial function in patients with suspected myocarditis.

Material and Methods: Patients referred for a clinically indicated CMR with suspected myocarditis. Using a rapid analysis module, left- and right atrial and reservoir function as well as left ventricular systolic contractility were calculated with long-axis shortening techniques (CVI42®, Circle Cardiovascular Imaging). Right ventricular function was measured with tricuspid annular planar systolic excursion (TAPSE). These CMR functional measurements were associated with major adverse cardiac events (MACE), defined as sustained ventricular tachycardia, hospitalization for heart failure and death.

Results: A total of 195 patients (aged 15-80 years, 44% female) were identified. After a median follow-up of 6.4 years, 38 (20%) experienced a MACE. Atrial function assessment revealed that 129 (73%) patients had poor left atrial function (<29%) and 72 (41%) had abnormal right atrial function (<27%), and both atrial functions were associated with MACE (see Figure). In cases where left ventricular function was preserved, 28 (14.4%) patients with isolated atrial dysfunction were identified. Among these, 4 (14%) had a MACE. Multivariable analysis showed that including left atrial measurements to left ventricular function incrementally improved prognostication, with left atrial function remaining a significant independent predictor of outcome (chi-2 = 18.0 vs chi-2 = 26.4, p<0.01). The same was observed when adding right atrial findings to TAPSE (chi-2 = 21.5 vs chi-2 = 28.7, p<0.01).

Conclusion: CMR-based atrial analysis identifies atrial dysfunction and independently improves risk stratification in patients with suspected myocarditis, regardless of left ventricular function. Therefore, prognostication can be improved through comprehensive four-chamber functional assessment.

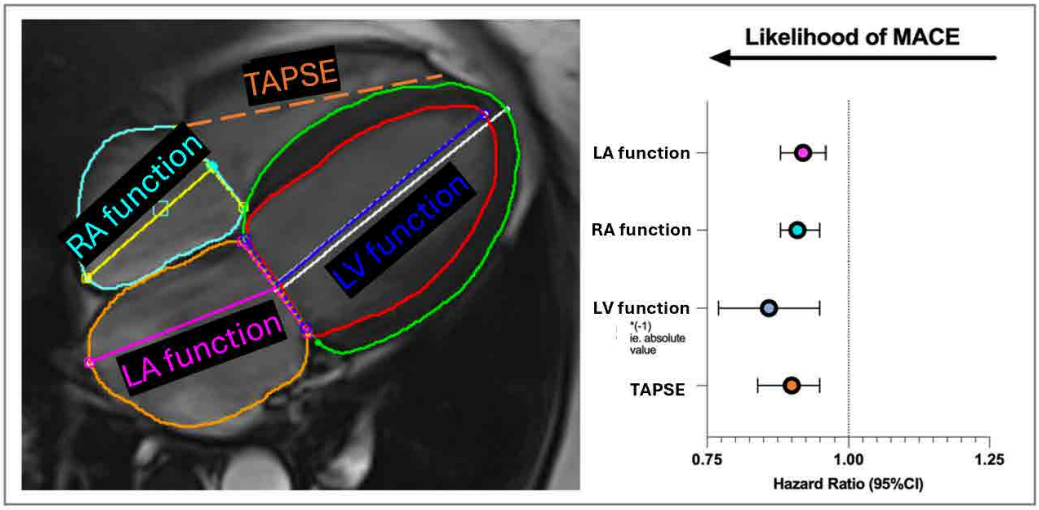

Example of atrial and ventricular 4-chamber analysis (left), and the forestplot (right) shows all measurements have a univariable association with major adverse cardiac events (MACE). LA: left atrial, LV: left ventricular, RA: right atrial, TAPSE: tricuspid annular plane systolic excursion.

P035

Anticoagulants for treatment of left ventricular thrombus: An updated systematic review and meta-analysis

Isabella Schmal[1], Thomas Seiler[2], Irena Majcen[1], Erika Nerdrum Aargaard[1], Luca Federico Vercelli[1], Adrian Attinger-Toller[1], Florim Cuculi[1 3], Matthias Bossard[1 3]

[1]Cardiology Division, Heart Center - Luzerner Kantonsspital, Luzern, Switzerland, [2]Department of Cardiology, Inselspital Bern, Bern, Switzerland, [3]Faculty of Health Sciences and Medicine, University of Lucerne, Luzern, Switzerland

Introduction: The management of left ventricular thrombus (LVT) with anticoagulants has evolved from traditional vitamin K antagonists (VKAs) to direct oral anticoagulants (DOACs). Despite emerging recommendations for DOACs, evidence remains conflicting. This systematic review and meta-analysis sought to evaluate the comparative safety and efficacy of DOACs versus VKAs in LVT treatment.

Material and Methods: Searches of MEDLINE, Cochrane Database, Embase, conference abstracts, and ClinicalTrials.gov were conducted up to December 1, 2024. Randomized clinical trials (RCTs) and observational cohort studies comparing outcomes in patients with LVT treated with DOACs versus VKAs were considered. Three reviewers independently extracted data and assessed study quality. Risk of bias was determined using the ROBINS-I and ROB-2 tools. Random-effects models were used for comparison. The safety endpoint of interest comprised any clinically relevant bleeding. The primary efficacy outcome was the occurrence of stroke and/or systemic embolism. Additionally, thrombus resolution rate and all-cause mortality were compared.

Results: We included finally 35 studies (4 RCTs and 31 observational) involving 5049 patients (30.7% DOAC, 69.3% VKA). No significant differences were found between DOACs and VKAs for: Stroke/systemic embolism: 11.3% versus 17.4%, OR 0.80 (95% CI 0.60–1.08), p = 0.5, I^2 = 0%; bleeding events: 6.9% versus 8.4%, OR 0.81 (95% CI 0.63–1.05, p = 0.81, I^2 0%); and thrombus resolution rate: 69.2% versus 68.3%, OR 1.07 (95% CI 0.88–1.29, p = 0.6 , I^2 0%) (Figure below). All-cause mortality may slightly favor DOACs (15.4% versus 17.9%, OR 0.93 (95% CI 0.65–1.35), p = 0.02). Of note, 16 studies had a relevant risk of bias due to their retrospective observational design and/or small sample size.

Conclusion: Based on primarily observational data, outcomes for patients with LVTs appear similar when treated with DOACs compared to VKAs. Although DOACs seem non-inferior to VKAs in LVT management, randomized trial data supporting the unrestricted prescription of DOACs in this context are lacking.

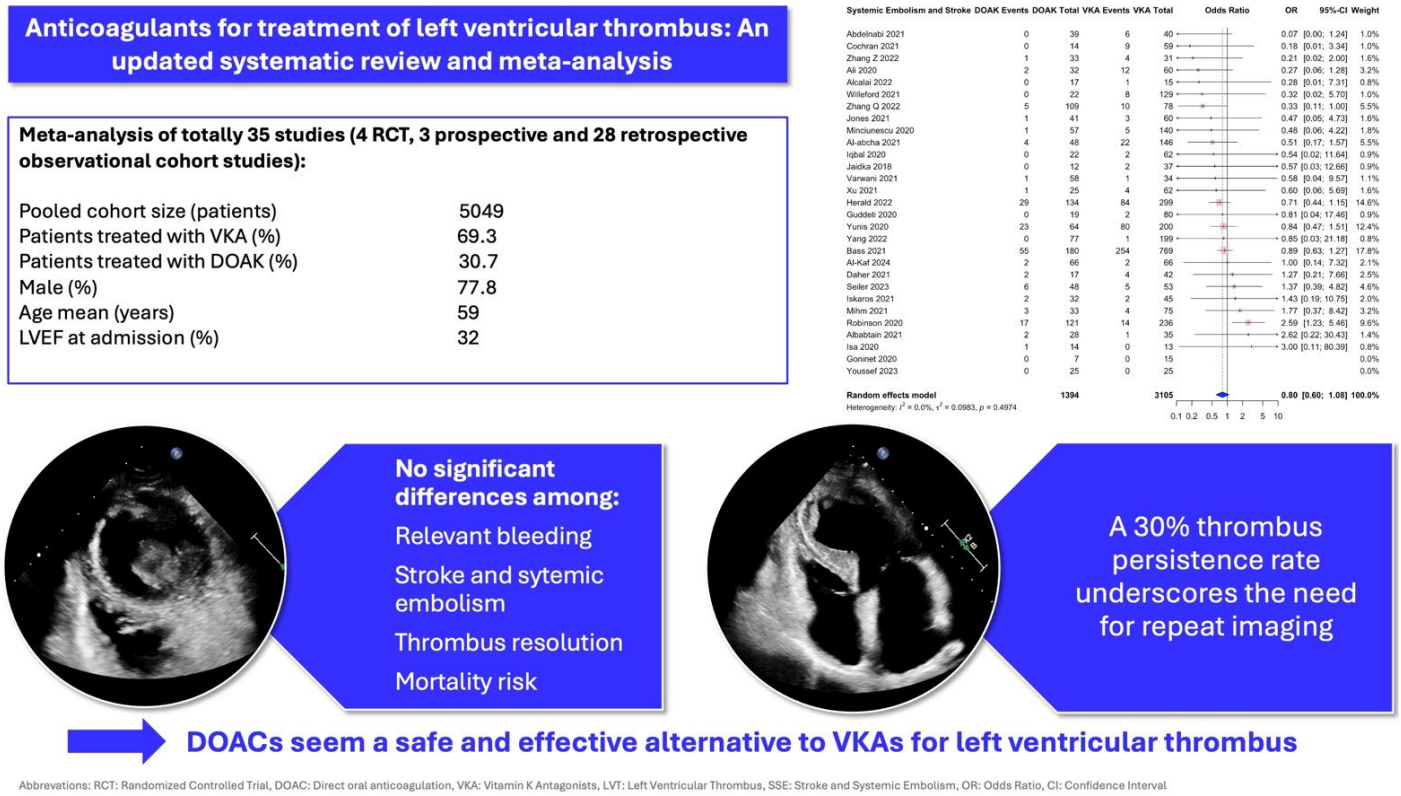

POSTER WALK "RHYTHM DISORDERS 1"

P036

Catheter ablation for atrial fibrillation in patients with tricuspid regurgitation

Jonas Brügger[1], Corinne Isenegger[1], Fabian Jordan[1], Sven Knecht[1], Philipp Krisai[1], Gian Völlmin[1], David Spreen[1], Nicolas Schaerli[1], Beat Schär[1], Felix Mahfoud[1], Christian Sticherling[1], Michael Kühne[1], Patrick Badertscher[1]

[1]Department of Cardiology, University Hospital Basel, Cardiovascular Research Institute Basel (CRIB), Basel, Switzerland

Introduction: Contemporary guidelines recommend rhythm control strategies including catheter ablation (CA) for patients with symptomatic atrial fibrillation (AF). The impact of coexisting tricuspid regurgitation (TR) on procedural characteristics and efficacy of patients undergoing CA for AF remains unclear. We aimed to assess procedural characteristics and efficacy of patients with moderate/severe TR undergoing CA for AF.

Material and Methods: This retrospective analysis included patients with moderate/severe TR undergoing CA for AF of the SWISS-AF-PVI-Registry. All patients received a transesophageal echocardiography before CA. Patient characteristics, procedural characteristics and long-term follow-up data including serial echocardiograms were obtained.

Results: 133 patients were included, 127 patients (95%) with moderate TR and 6 patients (5%) with severe TR (median age 72 years, 55% female). Paroxysmal AF was present in 43% and persistent AF in 57%. LA diameter, LVEF, RV/RA gradient and RA area were 43 [39-48] mm, 56 [45-63] %, 27 [21-35] mmHg and 25 [20-32] cm2, respectively. The used ablation modalities were radiofrequency (51%), pulsed-field-ablation (38%) and cryoballoon-ablation (11%). The median procedural duration was 68 [54 - 84] min, the left atrial dwell time 49 [36-63] min and the fluoroscopy time was 8 [4-13] min. Two complications (2%) were observed. The median follow-up was 310 [105-526] days, and the 1-year Kaplan-Meier estimate for atrial arrhythmia recurrence-free survival was 60%. 63% of patients showed a TR improvement after CA during follow-up. When comparing TR improvement in patients with/without recurrence, a higher proportion of patients without recurrence showed TR improvement: 79% vs 51%, p = 0.017. Among the 6 patients with severe TR, 2 patients (33%) underwent interventional tricuspid valve reconstruction.

Conclusion: Despite the high AF recurrence rates of 60% in patients undergoing CA with significant TR, CA resulting in maintenance of sinus rhythm appeared to improve the severity of TR, suggesting a possible induction of reverse positive atrial and tricuspid annular remodeling.

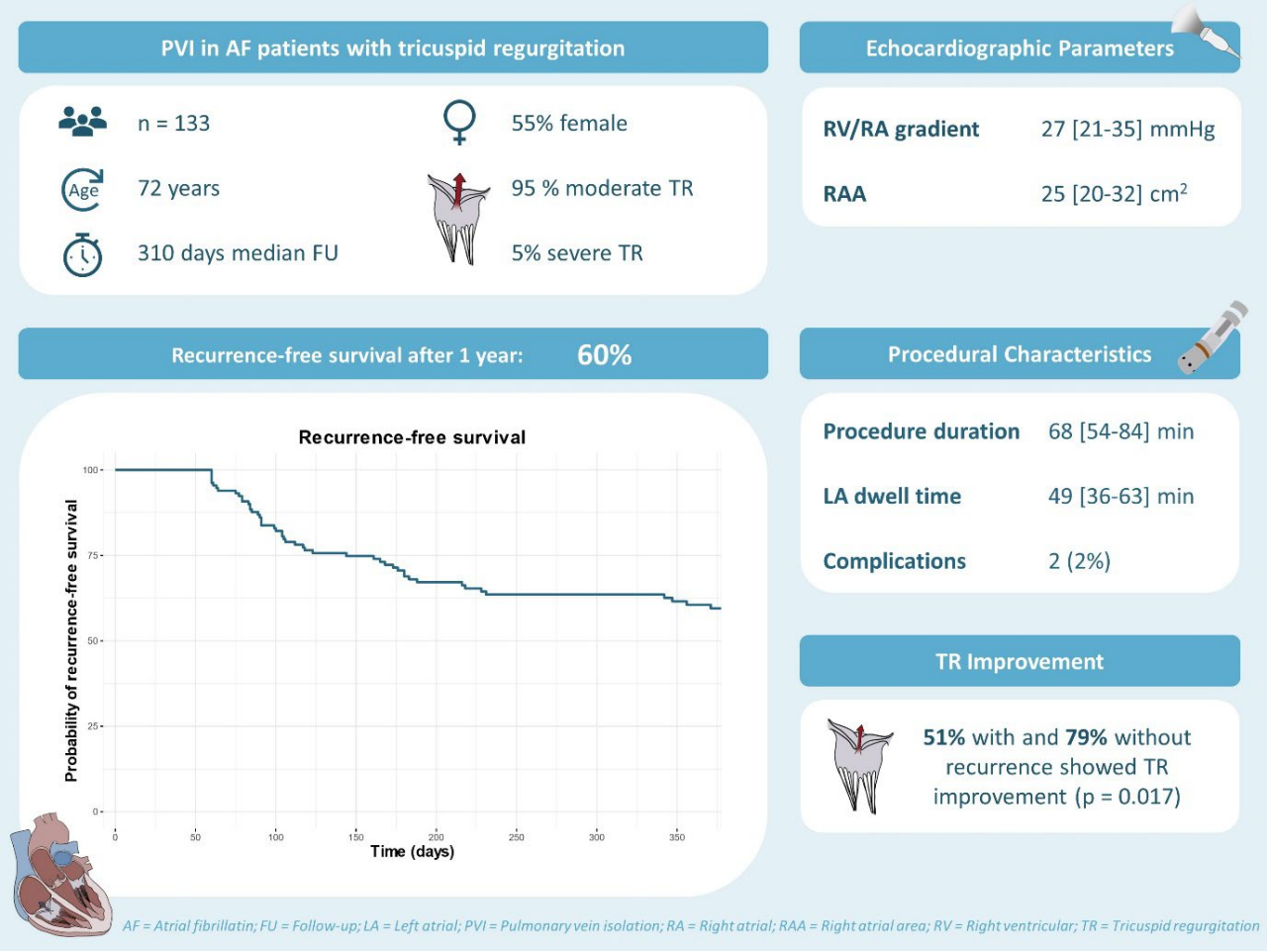

P037

Stellate Ganglion Blockade for Treatment of Ventricular Electrical Storm: An updated meta-analysis

Stefanos Zafeiropoulos[1], Ioannis Doundoulakis[2], Ardan Saguner[1], Marat Fudim[3]

[1]Department of Cardiology, University Hospital of Zurich, Center of Translational and Experimental Cardiology, Zürich, Switzerland, Zurich, Switzerland, [2]Heart Rhythm Management Centre, UZ Brussels, Brussels, Belgium, [3]Division of Cardiology, Duke University Medical Center, Durham, United States

Introduction: Ventricular electrical storm (ES) significantly increases the risk of heart failure hospitalization, heart transplantation and mortality. Standard treatment options include antiarrhythmic drugs and catheter ablation. The autonomic nervous system plays a role in arrhythmogenesis, and autonomic modulation techniques, such as stellate ganglion blockade (SGB), have shown promise in drug-refractory ES. This meta-analysis aims to evaluate the efficacy and safety of SGB in patients with drug-refractory ES.

Material and Methods: We conducted a systematic search of MEDLINE, CENTRAL, and Scopus databases to identify trials using SGB in ES patients, following PRISMA guidelines. The primary outcome was the percentage of patients free from ventricular arrhythmias (VA) at 24 and 72 hours post-SGB; the secondary outcome was the incidence rate ratio (IRR) of VA episodes before and after SGB. A random-effects meta-analysis was performed using R.

Results: Out of 932 screened articles, 9 studies with 418 patients met the inclusion criteria. The mean age was 63.6 ± 12.3 years, 84.4% were male, with a mean left ventricular ejection fraction of 27.4 ± 11.3%, and 56.9% had ischemic cardiomyopathy. Pharmacological SGB was performed in 8 studies, with one study using transcutaneous magnetic stimulation. The pooled proportion of VA-free patients was 75% (95% CI 62%-84%) at 24 hours and 59% (95% CI 45%-72%) at 72 hours (Figure 1). The incidence of VA episodes decreased from 15.64 to 0.62 episodes per 24 hours, with an IRR of 0.067, indicating a 93.7% reduction in the incidence rate of VA episodes post-intervention (Figure 2). No serious adverse events were reported; in-hospital mortality was 27.3%.

Conclusion: SGB is an effective and safe intervention for stabilizing patients with drug-refractory ES, with substantial VA suppression at 72 hours and a 94% reduction in episodes. This minimally invasive, accessible technique may be viable for hospitals lacking catheter ablation resources. Further randomized trials are warranted to confirm these findings.

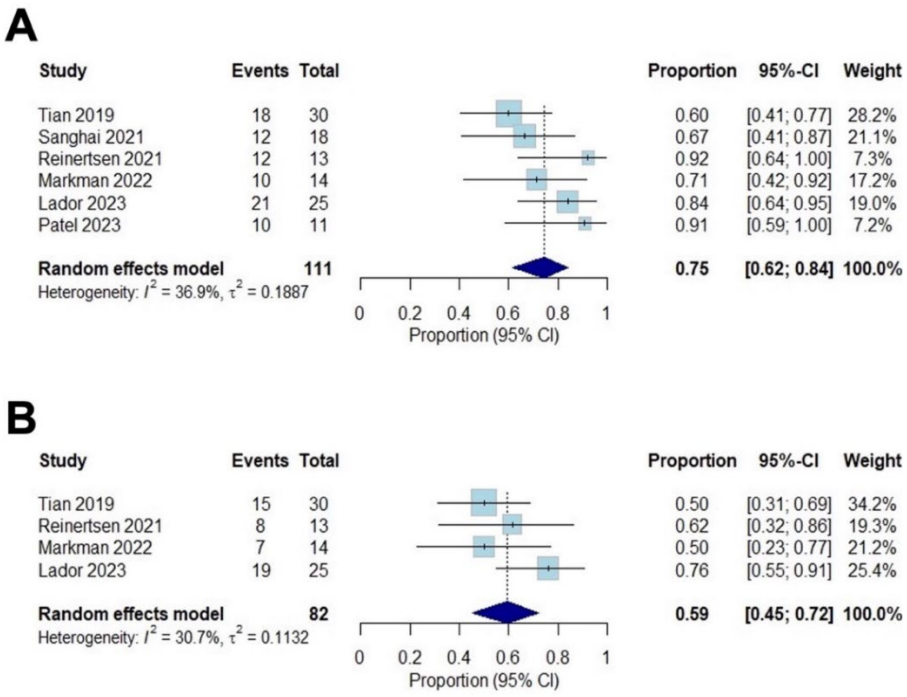

Figure 1. Proportions of patients free from VA recurrences after (A) 24 hours and (B) 72 hours post SGB.

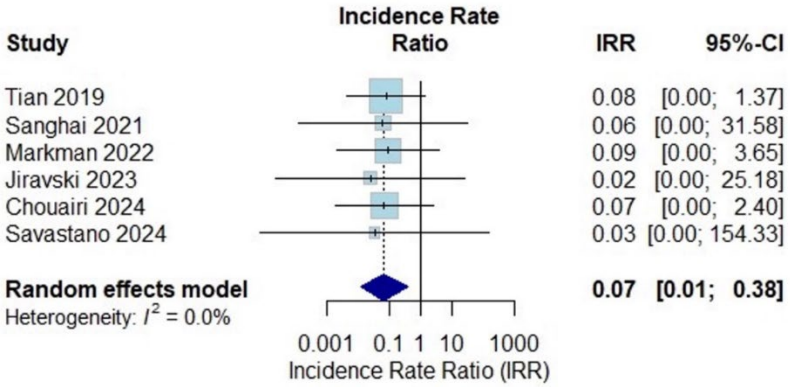

Figure 2. Incidence rate ratio of VA episodes pre- and post-SGB

P038

Pulsed-Field Versus Cryoballoon Versus Radiofrequency Ablation in Young Patients with Atrial Fibrillation Undergoing Pulmonary Vein Isolation

Matea Liskij[1,2], Corinne Isenegger[1,2], Jonas Brügger[1,2], Ruben Kerler[1,2], Fabian Jordan, Sven Knecht[1,2], Philipp Krisai[1,2], Nicolas Schärli[1,2], Beat Schär[1,2], Felix Mahfoud, Laurent Roten[3], Tobias Reichlin[3], Christian Sticherling[1,2], Patrick Badertscher[1,2], Michael Kühne[1,2]

[1]Department of Cardiology, University Hospital Basel, University of Basel, Basel, Switzerland, [2]Cardiovascular Research Institute Basel, University Hospital Basel, University of Basel, Basel, Switzerland, [3]Department of Cardiology, Inselspital Bern, University of Bern, Bern, Switzerland

Introduction: Little is known about the effects of different energy sources for ablation of atrial fibrillation (AF) in young patients. This study aimed to compare the procedural characteristics, safety, and effectiveness of cryoballoon ablation (Cryo), pulsed-field ablation (PFA), and radiofrequency ablation (RFA) in patients ≤ 50 years undergoing pulmonary vein isolation (PVI).

Material and Methods: Patients aged ≤ 50 years with AF who underwent their first PVI using either Cryo, PFA, or RFA were consecutively enrolled at two tertiary referral centers.

Results: A total of 355 patients (median age 46 [41-49] years, 18% female) were included out of which 95 patients (27%) underwent Cryo, 102 patients (29%) PFA and 158 patients (44%) RFA. Median procedure duration was 63 [51–81] min for Cryo, 67 [47–101] min for PFA, and 94 [75–130] min for RFA (p <0.001). Similarly, left atrial dwell time was 44 [34–57] min for Cryo, 43 [27–74] min for PFA, and 76 [57–97] min for RFA (p <0.001). Fluoroscopy time was significantly lower in the RFA group (5 [3–8] min), compared to Cryo (14 [11–20] min) and PFA (15 [10–25] min, p <0.001). Overall, there were 3 complications (1%), 1 (1%) in the Cryo and 2 (1%) in the RFA group.

The 1-year Kaplan-Meier estimate for recurrence-free survival was 60% in the Cryo group, 69% in the PFA group, and 71% in the RFA group (pLog-rank = 0.021).

Conclusion: In young patients with AF undergoing PVI, there are energy source-dependent differences in procedural characteristics and efficacy. These findings warrant further investigation in larger data sets.

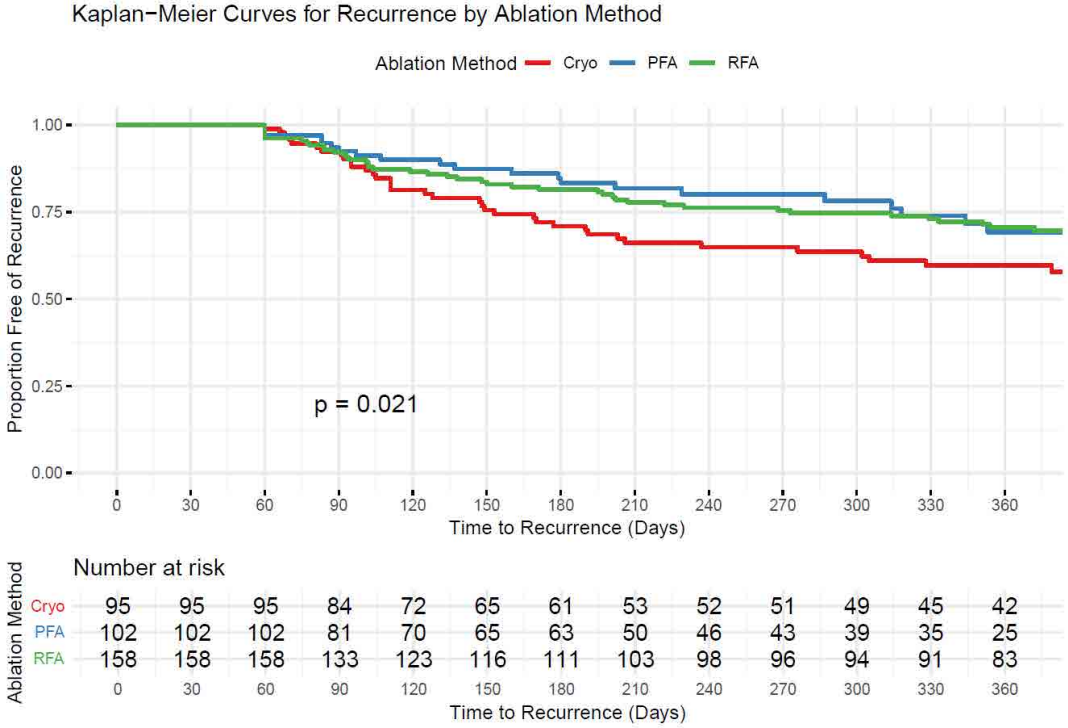

P039

What is special in de-novo left atrial flutter patients? A comparison to post-ablation left atrial flutter cases

Valon Spahiu[1], Thomas Kueffer[1], Rubèn Fuentes Artiles[1], Berat Gerguri[2], Salik Ur Rehman Iqbal[1], Gregor Thalmann[1], Claudia Herrera Siklody[1], Nikola Kozhuharov[1], Helge Servatius[1], Andreas Haeberlin[1], Fabian Noti[1], Hildegard Tanner[1], Laurent Roten[1], Tobias Reichlin[1]

[1]Inselspital, Bern, Switzerland, [2]Spitalriggisberg, Riggisberg, Switzerland

Introduction: Left atrial flutter (LAF) can arise following pulmonary vein isolation (PVI) or following PVI+ (lines), both approaches may create arrhythmogenic substrates. In a minority of patients, LAF presents as a de-novo arrhythmia without preceding left atrial ablations or interventions.

Material and Methods: We included patients undergoing LAF ablation between Jan 2021 and Jun 2023 at our institution. Baseline and procedural data were collected, and patients were followed with 7-day Holter ECG at 3, 6, and 12 months. The primary endpoint was recurrence of any atrial arrhythmia lasting longer than 30 seconds.

Results: 147 patients with LAF were analyzed (median age 71 years, IQR 65-75 years, 65% male). Of those, 32 (22%) presented with deNovo LAF, and 115 (78%) with post-ablation LAF (54 patients post PVI, 61 patients post PVI+). Patients in the deNovo group were older (74 years vs. 70 years, p = 0.037), more often female (50% vs. 30%, p = 0.058) and had a lower BMI (26.0 vs. 27.1, p = 0.025). In 28% of the patients in the deNovo group, no AF had been diagnosed before. The most prevalent dominant arrhythmia mechanisms in the deNovo group was localized septal micro-reentry (47%), followed by perimitral flutter (31%), roof dependent flutter (16%) and unmappable (6%). In the post-ablation group, the most prevalent dominant arrhythmia mechanism was perimitral flutter (40%), followed by localized septal micro-reentry (32%), roof dependent flutter (24%), and unmappable (4%). Freedom from any atrial arrhythmia at 12 months was similar for the two groups (deNovo 46%, Post Ablation 51%, p = 0.42.

Conclusion: deNovo LAF Patients represent a patient cohort that is older, more often female, with lower BMI. Septal micro-reentry was the most common arrhythmia mechanism in this cohort and an anterior isthmus line was performed in 72% of the patients. Arrhythmia-free survival was similar when compared to patients referred for LAF after prior left atrial ablation.

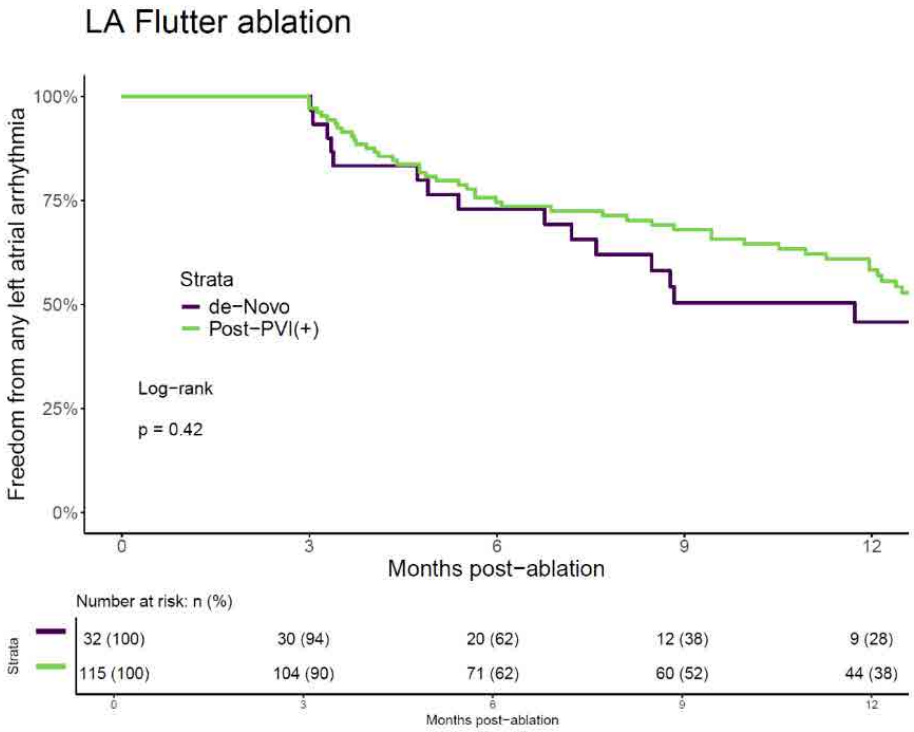

P040

Multi-Level Omics Analysis Identifies Fibrosis Markers as Predictors of Adverse Outcomes in Arrhythmogenic CardiomyopathyArrhythmogenic

Deniz Akdis[1 2], Verena Wilzeck[1], Sarah Costa[1], Christian Matter[1], Urs Eriksson[1 2], Stephan Winnik[1 2], Corinna Brunckhorst[1], Ardan Saguner[1], Firat Duru[1]

[1]University Heart Center Zurich, University Hospital Zurich, Zurich, Switzerland, [2]GZO Zurich Regional Health Center Wetzikon,, Wetzikon, Switzerland

Introduction: Arrhythmogenic cardiomyopathy (ACM) is an inherited cardiac disorder characterized by progressive fibrofatty replacement of the myocardium, predominantly affecting the right ventricle, leading to life-threatening ventricular arrhythmias and progressive cardiac dysfunction. The clinical heterogeneity of ACM and its variable genetic penetrance complicates management. In this study, we employ a multi-level strategy integrating myocardial transcriptomics and plasma proteomics to identify fibrosis-associated biomarkers that predict adverse outcomes in ACM.

Material and Methods: RNA sequencing of myocardial tissue samples from patients with definite ACM (n = 10, 80% with desmosomal mutation), dilated cardiomyopathy (DCM, n = 10), and healthy controls (n = 10) identified dysregulated genes between these age and gender matched groups. Proteomic profiling was conducted to quantify 360 proteins in definite ACM patients (n = 38) and controls (n = 24). Key proteomic findings were validated using enzyme-linked immunosorbent assay. The occurrence of major adverse cardiac events (MACE) were prospectively analyzed for all patients.

Results: RNA sequencing identified over 3,500, differentially expressed genes in ACM compared to controls, and over 400 genes compared to DCM. Pathway enrichment analysis revealed significant upregulation of fibrosis-related (e.g., extracellular matrix organization, collagen synthesis) and immune regulatory pathways (e.g., chemokine signaling). Fibulin-3, CXCL10 and endostatin were significantly elevated in ACM patients compared to controls. Over a median follow-up of 36 months, 23 of 38 ACM patients experienced MACE. Baseline plasma levels of fibulin-3 and endostatin were significantly higher in patients who developed MACE compared to those who remained event-free.

Conclusion: This integrative multiomics study highlights fibulin-3, CXCL10, and endostatin as promising novel biomarkers in ACM. Their association with fibrotic and inflammatory pathways underscores their potential utility for risk stratification. An external validation of these findings is needed to test their clinical value.

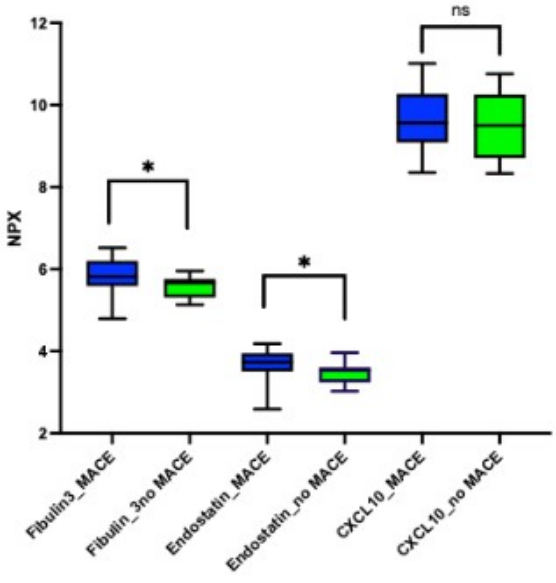

Figure 1. Higher fibulin-3 and endostatin levels are associated with adverse outcomes in ACM patients.

P041

Comprehensive electrophysiological study including ajmaline challenge to guide pacemaker implantation after transcatheter aortic valve replacement

Mattia Pagnoni[1], Cheryl Teres[1], Ciro Ascione[1], David Meier[1], Stephane Fournier[1], Giulia Domenichini[1], Mathieu Le Bloa[1], Adrian Luca[1], Etienne Pruvot[1], Olivier Muller[1], Patrizio Pascale[1]

[1]Service de Cardiologie, CHUV (Centre Hospitalier Universitaire Vaudois), Lausanne, Switzerland

Introduction: An electrophysiological study (EPS)-guided approach to predict high-grade atrioventricular block (HAVB) risk after TAVR is recommended by guidelines but remains debated due to conflicting data. The value of pharmacological challenge in this setting is unclear. This study evaluates the utility of routine EPS with Ajmaline challenge for risk stratification in patients with new-onset conduction disturbances post-TAVR.

Material and Methods: The EPS-based strategy was as follows: i) permanent pacemaker (PM) implantation for HV interval≥70ms, ii) Implantable loop recorder implantation for 55<HV<70ms, iii) In a subgroup of patients (with basal HV<70ms), systematic Ajmaline challenge was performed with PM implantation for post-Ajmaline HV≥120ms or a 100% increase, and ILR implantation for intermediate values. The primary outcome was HAVB persisting beyond 24 hours post-TAVR or the need for ventricular pacing in prophylactic PM patients.

Results: Among 101 patients, 18 with HV≥70ms received a PM. Of 83 patients with HV<70ms, 48 (58%) underwent Ajmaline challenge. The primary outcome occurred in 10 (55%) versus 17 (20%) of patients with HV≥70ms and <70ms, respectively. ROC analysis identified an optimal basal HV cutoff of 60ms (AUC = 0.779). Post-Ajmaline HV provided similar accuracy (AUC = 0.817) with an optimal cutoff of 83ms (Figure1), but did not significantly reclassify patients (Figure2). Post-Ajmaline delta HV was less predictive (AUC = 0.585). The optimized strategy using basal HV alone showed sensitivity = 78%, specificity = 74, NPV = 70%, and PPV = 53%, though 6 (22%) of the 27 at-risk patients were missed.

Conclusion: In patients with new-onset conduction disturbances post-TAVR, an EPS-based risk strategy based on the basal HV is predictive of the risk of HAVB with half of the identified patients who actually benefited from PM implantation. However, strategy aiming at reducing the 30% false negative rate should be pursued. In that respect, the adjunct of an ajmaline challenge to the EPS evaluation does not provide a meaningful added value.

Figure 1

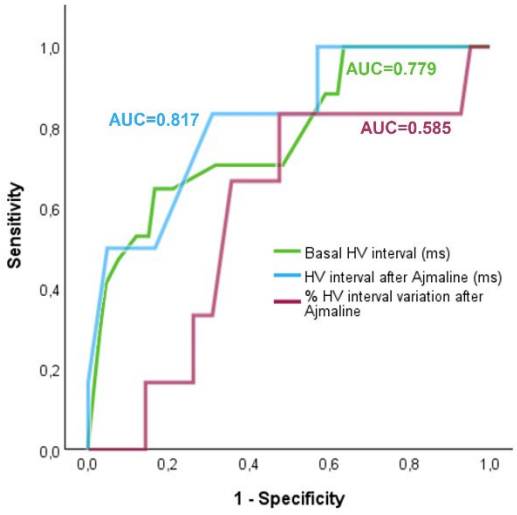

Figure 2

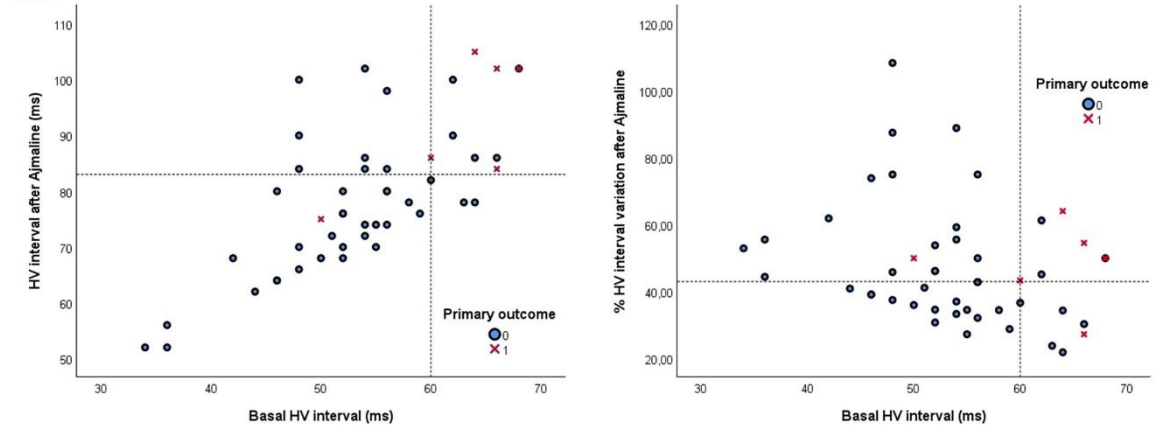

P042

Late Enhancement Myocardial Scar Characterization With Photon-Counting Detector CT Correlates with Invasive Electroanatomical Mapping in Patients with Structural Heart Disease

Martin F. Reiner[1], Victor Mergen[2], Konstantin Klambauer[2], Lukas Moser[2], Fu Guan[1], Corinna Brunckhorst[1], Firat Duru[3], Frank Ruschitzka[4], Robert Manka[5], Matthias Eberhard[2], Hatem Alkadhi[2], Ardan Saguner[4]

[1]Department of Cardiology, University Heart Center, University Hospital Zurich, Zurich, Switzerland, [2]Diagnostic and Interventional Radiology, University Hospital Zurich, University of Zurich, Zurich, Switzerland, [3]Department of Cardiology, University Heart Center, University Hospital Zurich, Center for Integrative Human Physiology, University of Zurich, Zurich, Switzerland, [4]Department of Cardiology, University Heart Center, University Hospital Zurich, Center for Translational and Experimental Cardiology (CTEC), Department of Cardiology, Zurich University Hospital, University of Zurich, Zurich and Schlieren, Switzerland, [5]Diagnostic and Interventional Radiology, University Hospital Zurich, University of Zurich, Department of Cardiology, University Heart Center, University Hospital Zurich, Zurich, Switzerland

Introduction: Myocardial scar visualization from late enhancement (LE) imaging using photon-counting detector computed tomography (PCD-CT), may complement electroanatomical mapping (EAM) in patients with structural heart disease and guide radiofrequency catheter ablation (RFCA) for ventricular arrhythmias. Here we compare myocardial scar detected by LE PCD-CT imaging with invasive endocardial EAM.

Material and Methods: This single-center retrospective observational study included 20 patients (12 [60%], ischemic cardiomyopathy; 8 [40%] non-ischemic cardiomyopathy) who underwent PCD-CT with LE imaging prior to EAM and RFCA for ventricular arrhythmias between May 2022 and February 2024. Myocardial scar was defined by low voltage electrograms <5 mV in unipolar and <0.5 mV in bipolar maps. Myocardial segments with scar identified on polar and atlas maps from cardiac LE scans were compared with low voltage segments detected by EAM.

Results: Mean age was 64±8 years, 4 (20%) patients were female and 16 (70%) had cardiac implantable electronic devices. In patients with ischemic cardiomyopathy, concordance of abnormal segments on CT was very good with unipolar EAM (κ = 0.655 ± 0.249), and good with bipolar EAM (κ = 0.547 ± 0.267). In patients with non-ischemic cardiomyopathy, concordance of abnormal segments on CT was moderate compared with unipolar (κ = 0.455 ± 0.356) and bipolar (κ = 0.255 ± 0.260) EAM. In 13 patients with additional non-invasive imaging including cardiac magnetic resonance (CMR) and nuclear imaging, concordance with LE PCD-CT was very good in patients with ischemic cardiomyopathy (n = 9, κ = 0.761 ± 0.210), excellent in 31% (5/16) segments and fair for all other segments in patients with non-ischemic cardiomyopathy (n = 4, κ = 0.336 ± 0.552).

Conclusion: Myocardial scar visualization on LE images from PCD-CT scans yields a high concordance with endocardial EAM, particularly with unipolar EAM in patients with ischemic heart disease. Therefore, PCD-CT may be an alternative for pre-procedural imaging if CMR imaging is not feasible.

P043

Predicting atrial fibrillation and ventricular tachycardia from normal sinus rhythm: model explainability and the influence of daily activities

Martin Camenzind[1], Gil Sharvit[1], Filippo Parisi[1], Patric Eberle[1]

[1]Hochschule Luzern - Technik & Architektur, Horw, Switzerland

Introduction: Atrial fibrillation (AF) and ventricular tachycardia (VT) are life-threatening cardiac arrhythmias that are challenging to detect due to their transient and paroxysmal nature. Brief episodes often evade identification even in 24-hour recordings, particularly in asymptomatic patients. Existing diagnostic approaches lack both sensitivity and interpretability, limiting their clinical utility. This study presents an improved explainable machine learning (ML) framework capable of predicting AF and VT from normal sinus rhythm (NSR) ECG recordings while aiding clinical interpretability by visualizing the underlying ECG features driving these predictions. This study has the potential to improve AI-based early detection of arrhythmia by enhancing transparency of AI-powered tools, thus, facilitating clinical implementation.

Material and Methods: Our two-phase ML framework combines self-supervised learning on a huge corpus of 9 public datasets including 269 million 10-second ECG segments with fine-tuning, trained on our internal dataset of 24-hour single-lead Holter ECG recordings (N = 1348). A robust preprocessing pipeline ensured clean NSR windows. Time synchronized accelerometer data enabled estimation of activity levels during recordings. Model interpretability was enabled through visualizing the attention-weights, identifying key ECG features contributing to predictions.

Results: The model achieved state-of-the-art performance, with an area under the ROC curve (AUC-ROC) of 0.91 for AF and 0.85 for VT. Calibrated thresholds resulted in a mean sensitivity of 0.82 for AF and 0.82 for VT, with corresponding specificities of 0.85 and 0.76. Explainability analyses identified critical ECG segments associated with a higher arrhythmia risk, enabling clinicians to assess such ECG segments to increase precision of diagnosis and tailor interventions.

Conclusion: This study advances arrhythmia prediction by addressing the gap between AI-driven models and clinical decision-making. With explainable predictions in combination with simple and easy to understand visualization, our framework provides cardiologists with the insights needed supporting early interventions and personalized patient care.

P044

Pulse Field Ablation for Atrial Fibrillation at Lausanne University Hospital: Initial Experience with Farawave and Varipulse Catheters Using Distinct Workflows

Jorge Solana Muñoz[1], Adrian Luca[1], Mathieu Le Bloa[1], Cheryl Teres[1], Ciro Ascione[1], Mattia Pagnoni[1], Patrizio Pascale[1], Etienne Pruvot[1]

[1]University Hospital of Lausanne (CHUV), Lausanne, Switzerland

Introduction: Pulse Field Ablation (PFA) is an emerging technology for atrial fibrillation (AF). Our center implemented three workflows for pulmonary vein isolation (PVI) using Farawave (Boston Scientific) and Varipulse (Biosense Webster) catheters, including CT-guided fluoroscopy and integration with the Carto3 electroanatomical 3D-mapping (EAM) system. We evaluated the feasibility, procedural efficiency and costs of PFA across workflows.

Material and Methods: A total of 157 PVI-only de novo procedures were included and divided into three groups: Fara-Carto (n = 121, Farawave with Carto3), Fara-CT (n = 24, Farawave with cardiac-CT segmentation merged with fluoroscopy), and Vari-Carto (n = 12, Varipulse fully integrated into Carto3). Total procedural time (TPT), left-sided dwelling time (LT), dose-area product (DAP) and acute PVI success rates were analyzed. Additionally, cost variations were assessed based on consumables and workflow-specific exams, excluding common costs.

Results: Acute PVI was achieved in all cases except one in Vari-Carto. Fara-CT showed a significant reduction in TPT compared to Fara-Carto (62.6 vs 83.4 min, Δ25%, $p<0.01$) and Vari-Carto (73.5 min, Δ15%, $p<0.05$). Similarly, Fara-CT demonstrated significantly shorter LT ($p<0.05$) compared to both groups using the EAM system. Differences were attributed to workflow steps such as pre- and post-ablation 3D-mapping. DAP did not differ significantly between Fara-Carto and Fara-CT but was significantly ($p<0.001$) reduced in Vari-Carto. The Fara-CT workflow was the most cost-effective, totaling 8.65k CHF including CT scan, followed by Vari-Carto at 9.8k CHF. Fara-Carto exceeded 10k CHF (11.1k CHF) due to the additional mapping catheter requirement (Table 1).

Conclusion: CT-guided PFA was the shortest and most cost-effective workflow, improving procedural efficiency while reducing expenses. Fully integrated catheters with EAM systems enabled near zero-radiation procedures but at a higher cost and longer procedural time. Semi-integrated PFA workflows (Fara-Carto) inherit limitations from fully integrated and CT-guided approaches. We present tailored options for PFA therapy based on equipment constraints and clinical priorities.

Group	FaraCarto (Boston Scientific & Carto3)	FaraCT (Boston Scientific & cardiac-CT)	VariCarto (Varipulse & Carto3)
Especific costs per workflow	Farawave (PFA Cath)	Farawave (PFA Cath)	Varipulse (PFA & EAM Cath)
	Faradrive (sheat)	Faradrive (sheat)	Vizigo (sheat)
	Cable Farawave	Cable Farawave	Cable Varipulse
	Patchs EAM		Patchs EAM
	Lasso or Pentarray (EAM Cath)	Cardiac CT	Cable Vizigo
	Cable Lasso		
	Quadri Xtrem	Quadri Xtrem	CS Webster Auto-ID
	Cable Xtrem	Cable Xtrem	Cable CS
Total	**11 088.18 CHF**	**8 648.00 CHF**	**9 798.28 CHF**

Table 1. Comparison of specific costs across different PFA workflows.

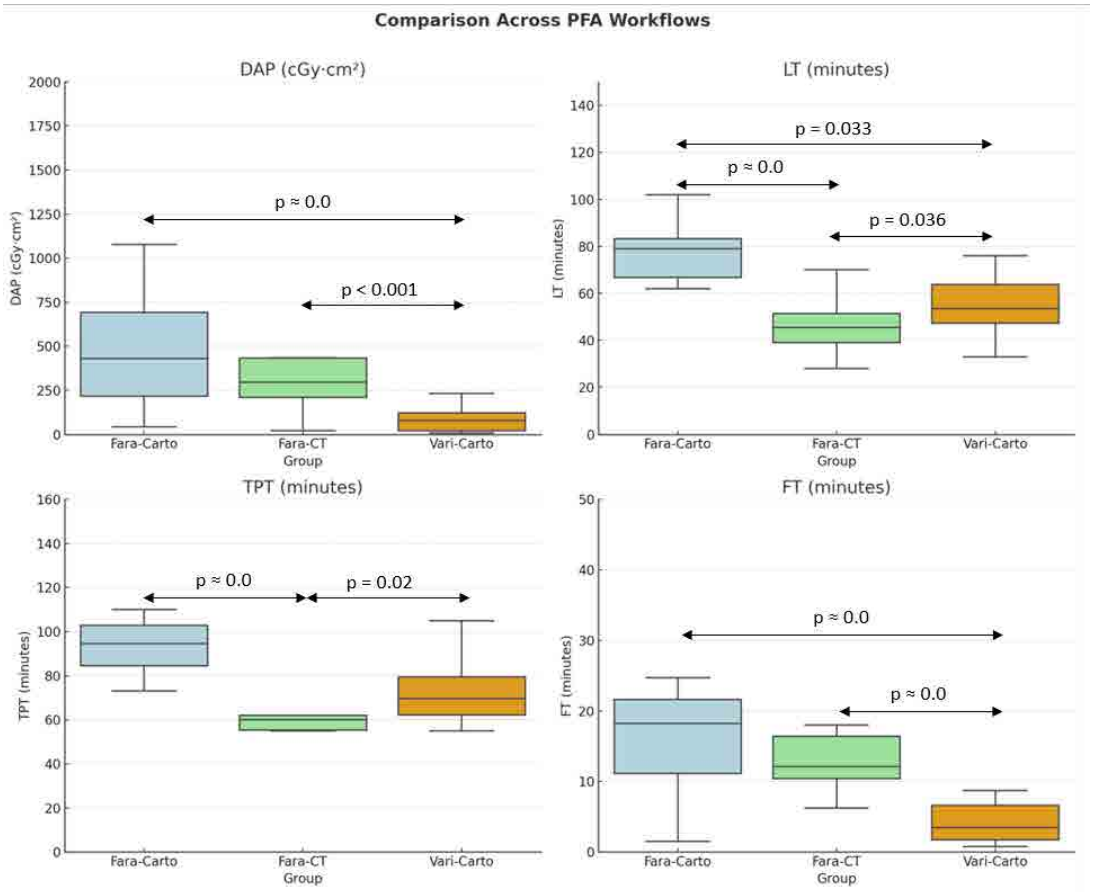

Figure 1. Comparison of procedural parameters across PFA workflows.

P045

A Novel 12-Lead ECG Algorithm for Accurate Prediction of Atrial Tachycardia Origin to Guide Electrophysiology Procedures

Ann-Kathrin Gamer[1], Anne Aimee Bernand[2], Stefanie Hess[1], Florim Cuculi[1], Amir Jadidi[1]

[1]Luzerner Kantonsspital, Luzern, Switzerland, [2]Johnson & Johnson, Zug, Switzerland

Introduction: Noninvasive prediction of atrial tachycardia (AT) origin based on P-wave patterns in the 12-lead ECG has been reported. Determining the origin is critical for planning electrophysiological (EP) procedures, including the need for a right-sided or an additional left-sided transseptal approach for mapping and ablation. Precise localization further optimizes procedural success.

Material and Methods: We analyzed P-wave patterns in precordial leads V1–V6 in 64 patients undergoing AT mapping and ablation. The AT mechanism was identified using activation and/or entrainment mapping, with acute termination at the arrhythmia's critical isthmus or origin. Specific P-wave patterns were assessed to distinguish right- from left-sided AT.

Results: A total of 64 cases were included (mean age 66.7 ± 13.5 years; 40.6% female). Prior left atrial (LA) ablation had been performed in 34.4% of patients. LA-AT occurred in 36 (56.3%), comprising 19 (52.8%) macro-reentrant and 17 (47.2%) localized or focal ATs. Right atrial AT (RA-AT) was identified in 28 (43.8%), including 10 (35.7%) cavo-tricuspid isthmus (CTI) –dependent flutters and 18 (64.3%) RA-AT not dependent on CTI. Analysis showed that positive concordance of P-wave polarity in V1–V6 was associated with LA-AT in 91.2%, while P-wave discordance (a polarity change from positive to negative or vice versa) in V1–V6 was seen in 83.3% of RA-AT cases.

Conclusion: This novel 12-lead ECG algorithm reliably predicts AT origin. Positive P-wave concordance in V1–V6 strongly correlates with LA-AT, whereas P-wave discordance indicates RA-AT. By providing a noninvasive tool for prediction of atrium of origin, this algorithm can help electrophysiologists optimize mapping and ablation strategies to maximize procedural success.

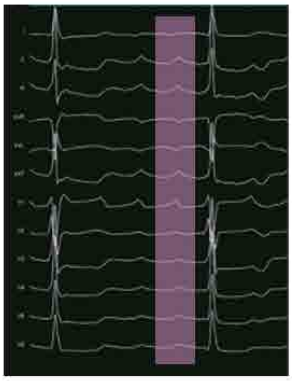
LA-AT: Perimitralflutter

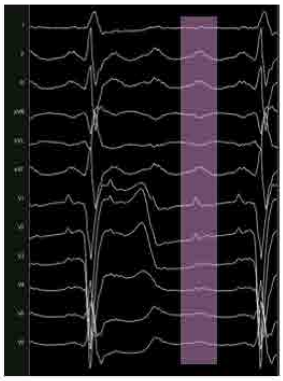
LA-AT: Roof dependant flutter

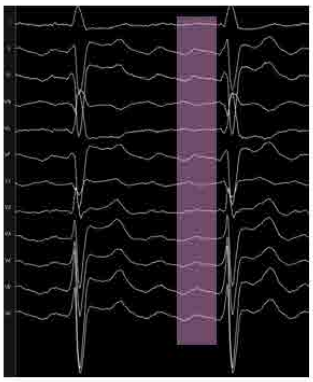
RA-AT: CTI dependant CCW

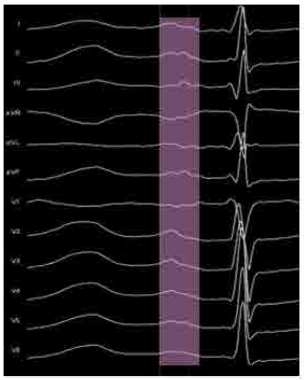
RA AT: Crista terminalis

POSTER WALK "VALVULAR HEART DISEASE"

P046

A Prospective Cohort Based Preprocedural Prediction Model for One-year Survival After Transcatheter Aortic Valve Implantation

Qi Chen[1], Thierry Donati[1], Monika Hebeisen[2], Neria E. Winkler[1], Jonathan Michel[1], Barbara Staehli, Albert Markus Kasel[1], Felix C. Tanner[1]

[1]Department of Cardiology, University Heart Center, University Hospital Zurich and University of Zurich, Zürich, Switzerland, [2]Department of Biostatistics, Epidemiology, Biostatistics and Prevention Institute, University of Zurich, Zürich, Switzerland

Introduction: In patients with severe aortic stenosis who are not candidates for surgery, transcatheter aortic valve implantation (TAVI) reduces all-cause mortality. However, registry data have reported a one-year mortality rate after TAVI ranging from 10% to 25%. Accurate prediction models are needed to identify patients at high mortality risk after TAVI to prevent futile interventions. This study aimed to develop and validate a pre-procedural prediction model to assess the risk of early death after TAVI.

Material and Methods: Patients undergoing TAVI due to severe aortic stenosis were prospectively recruited into a cohort. Eligible patients were divided into derivation and validation cohorts in a temporal manner. Four experienced cardiologists selected potential clinical and echocardiographic predictors from the baseline characteristics. A prediction model was developed using multiple logistic regression after imputing missing data. The performance of prediction model was assessed through receiver operating characteristic (ROC) curves and calibration plots to evaluate discrimination and calibration.

Results: A total of 1,702 patients were enrolled in the study, with 1,278 patients used to develop the prediction model and 424 patients assigned to the validation cohort (Figure 1). Twelve potential predictors were incorporated into the final model. The area under the ROC curve was 0.74 (95%CI 0.70-0.78) for the derivation cohort and 0.72 (95%CI 0.64-0.81) for the validation cohort (Figure 2). Using a threshold of 0.2 to define high risk, 30% of patients classified as high risk in the validation cohort died within one year following TAVI.

Conclusion: Our prediction model demonstrated acceptable performance in predicting one-year mortality after TAVI in a real world European modern cohort, highlighting its potential for integration in routine clinical practice. Specifically, it may help evaluate the necessity of TAVI when anticipated benefits are uncertain.

Figure 1: The flowchart of patient determation

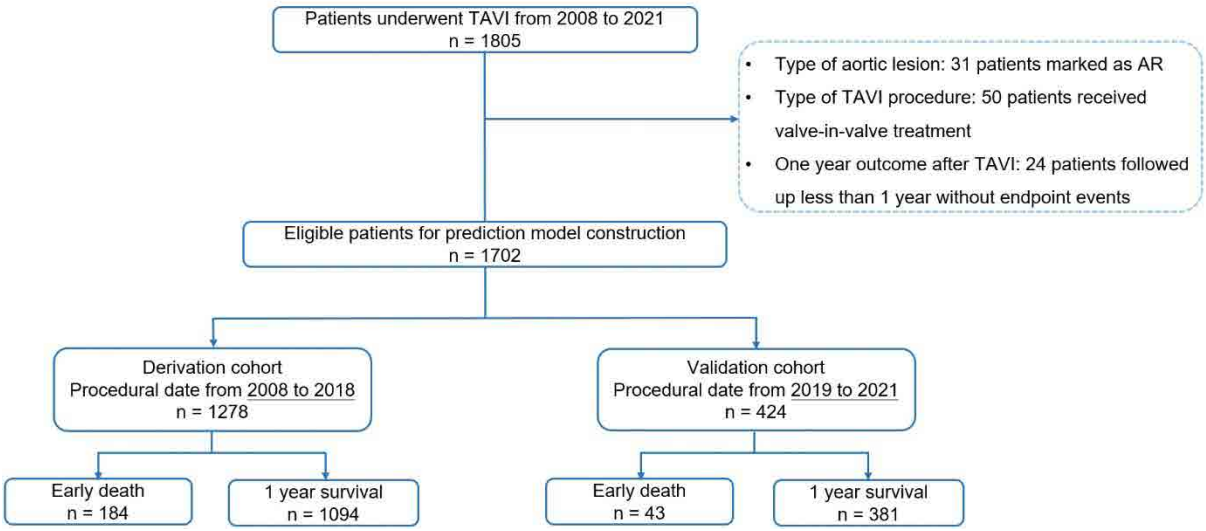

Figure 2: Discrimination and calibration of the prediction model among validation population

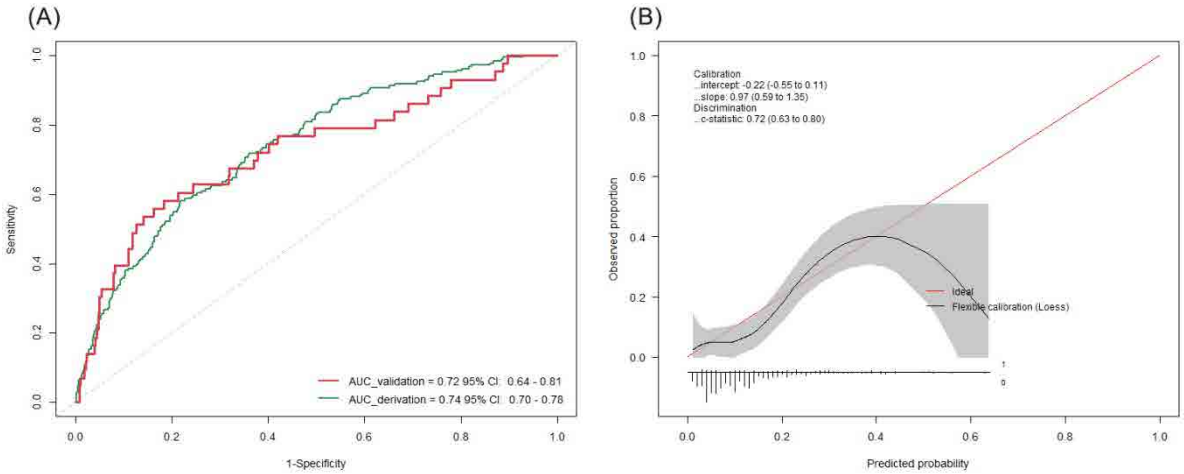

P047

Association of Body Mass Index with Procedural Success and Outcomes in Patients undergoing Transcatheter Aortic Valve Replacement

Jakob Reichl[1], Adisa Poljo[2], Thorald Stolte[1], Ramona Schmitt[3], Jasper Boeddinghaus, Max Wagener[1], Gregor Leibundgut[1], Christoph Kaiser, Dirk Westermann[3], Tau Hartikainen[3], Felix Mahfoud, Philipp Breitbart[3], Philipp Ruile[3], Thomas Nestelberger[1]

[1]Department of Cardiology and Cardiovascular Research Institute Basel (CRIB), Basel, Switzerland, [2]Department of Visceral Surgery, Clarunis, University Digestive Health Care Center Basel, St. Clara Hospital and University Hospital Basel, Basel, Switzerland, [3]Department of Cardiology and Angiology, Medical Center – University of Freiburg, Faculty of Medicine, Bad Krozingen, Germany

Introduction: Obesity is an escalating public health concern and is associated with adverse outcomes in cardiovascular disease (CVD). Recent studies have reported a paradoxical association between obesity and improved outcomes after transcatheter aortic valve implantation (TAVI), with lower mortality observed in obese patients.

Material and Methods: Patients undergoing TAVI at two large, high volume multinational centers were included in a combined registry. Using the recent World Health Organization (WHO) classifications, patients were categorized into four BMI groups: underweight (BMI <18.5 kg/m2), normal weight (BMI 18.5-24.9 kg/m2), overweight (BMI 25.0-29.9 kg/m2), and obese (BMI ≥30.0 kg/m2). The primary outcome was technical success and safety, including 30-day rates of all-cause-mortality, stroke, and overall bleeding. Secondary outcomes included all-cause mortality at one and five years.

Results: A total of 6,156 patients were included in this analysis: 114 (1.8%) underweight, 2393 (38.8%) normal weight, 2380 (38.6%) overweight, and 1269 (20.6%) obese. No significant differences were observed between BMI groups for 30-day all-cause mortality, stroke, overall bleeding or technical success rates. However, underweight patients had significantly higher all-cause mortality compared to normal-weight patients at one year (23.7 vs. 13.2%, adjusted Hazard Ratio 1.89, 95% CI 0.35-0.78, p = 0.001) and five years (53.2% vs. 44.0%, aHR 1.4, 95% CI 1.0-2.0, p = 0.048). Obese patients had similar mortality rates to normal-weight patients at one year (11.4 vs. 13.2%, aHR 0.85, 95% CI 0.70-1.04, p = 0.120) and five years (41.0 vs. 44.0%, aHR 1.09, 95% CI 0.91-0.95, p = 0.200).

Conclusion: While obesity was not associated with improved short- or long-term outcomes compared to normal-weight patients, underweight at baseline was an independent predictor of higher all-cause mortality after TAVI. These findings challenge the obesity paradox in the context of TAVI.

P048

AI-guided aortic stenosis risk stratification using a guideline-integrated large language model

Dorian Garin[1], Stéphane Cook[1], Wesley Bennar[1], Mario Togni[1], Pascal Meier[1], Peter Wenaweser[1], Puricel Serban[1], Diego Arroyo[1]

[1]*University and Hospital Fribourg, Fribourg, Switzerland*

Introduction: Traditional risk calculators like EuroSCORE II may inadequately classify severe aortic stenosis (AS) patients by overlooking key comorbidities and anatomical variables, limiting their utility in guiding transcatheter aortic valve implantation (TAVI) versus surgical aortic valve replacement (SAVR). We developed a guidelines-integrated large language model (LLM) based on the 2021 ESC guidelines for valvular heart disease to improve risk stratification compared to EuroSCORE II.

Material and Methods: We retrospectively studied 231 AS patients evaluated by a Heart Team for procedural risk (low vs. high) from January 2022 to December 2024. Clinical vignettes were created to simulate Heart Team discussions. The guidelines-integrated LLM (GPT-4o, version 2024-08-06) classified risk using a Forest-of-Thought prompting method. Its performance was compared to a EuroSCORE II-based approach (low risk: EuroSCORE II < 4% and age < 75; high risk: EuroSCORE II > 8%), assessing accuracy, sensitivity, specificity, and ROC area. Subanalyses evaluated LLM performance with and without EuroSCORE II input.

Results: In identifying high-risk patients, the guidelines-integrated LLM achieved 90.05% accuracy (95% CI, 86.07 to 94.02), notably surpassing the EuroSCORE II-based method at 50.23% (95% CI, 43.58 to 56.87) (p<0.0001). For low-risk stratification, it again outperformed the EuroSCORE II-based model (90.05% vs. 85.97%; p = 0.039) (Figure 1). Comparing LLM variants with and without EuroSCORE II information showed a +7.69% mean accuracy gain (p = 0.002) when EuroSCORE II was omitted. Logistic regression indicated that the LLM with EuroSCORE II input overemphasized variables like pulmonary artery pressure (p = 0.007) and kidney disease (p = 0.032), while the LLM balanced multiple predictors, enhancing risk stratification.

Conclusion: A guidelines-integrated LLM strategy leveraging ESC guidelines provided superior high and low-procedural risk stratification of patients with severe aortic stenosis compared to a EuroSCORE II-based approach. By encompassing a wider range of clinically relevant factors this approach may enhance both clinical decision-making and individualized patient management, potentially better identifying candidate for TAVI.

Figure 1

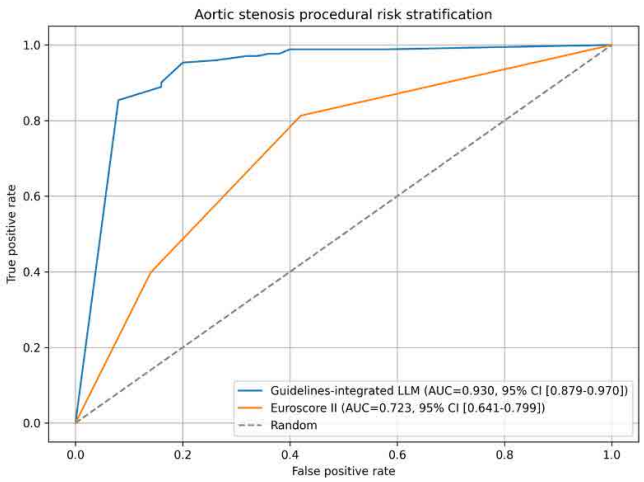

P049

Importance of right heart catheterization in patients with mitral regurgitation undergoing valve repair/replacement for the prediction of persistent pulmonary hypertension

Mark Güpfert[1], Lukas Weber[1], Philipp Haager[1], Philipp Baier[1], Sebastian Kopp[1], Johannes Rigger[1], Joannis Chronis[1], Marc Gerhard[1], Hans Rickli[1], Micha T. Maeder[1]

[1]*Health Ostschweiz (HOCH) Kantonsspital St. Gallen, St. Gallen, Switzerland*

Introduction: In mitral regurgitation (MR), valve procedures are performed to reduce left atrial pressure and thereby pulmonary pressures. We evaluated the value of right heart catheterization (RHC) prior to a mitral valve procedure for the prediction of persistent PH several months thereafter.

Material and Methods: We studied 274 consecutive patients (mean age 68±11 years) with at least moderate MR (84% degenerative, 11% functional, 5% combined) undergoing RHC followed by surgical (70%) or transcatheter (30%) valve repair/replacement who had an echocardiogram with valid information on PH after a median follow-up of 6 months. PH (mean pulmonary artery pressure >20 mmHg) was classified by mean pulmonary artery wedge pressure (mPAWP) and pulmonary vascular resistance (PVR) according to 2022 ESC/ERS guidelines. The probability of PH at follow-up was assessed by peak tricuspid regurgitant velocity and indirect PH signs.

Results: At baseline, 143/274 (52%) had any PH: 40 with isolated post-capillary, 65 with combined pre- and post-capillary, 27 with pre-capillary, 11 with unclassified PH. Follow-up PH probability was low, intermediate, or high, in 149, 73, and 42 patients. There was a progressive increase in baseline mPAP (21±10 vs. 24±9 vs. 30±9 mmHg; p<0.001), mPAWP (13±8 vs. 15±8 vs. 18±7 mmHg; p<0.001), and PVR (1.8±1.1 vs. 2.1±1.4 vs. 3.1±1.8 WU; p<0.001) in patients with low, intermediate or high PH probability at follow-up. Patients with combined pre- and post-capillary PH at baseline had a nearly 11-fold higher risk (odds ratio 10.7) for a high follow-up PH probability compared to those with no PH, while the risk for isolated post-capillary and pre-capillary PH was intermediate (odds ratios 4.4 and 6.0; p<0.05 for all) and not significant for unclassified PH (odds ratio 2.1).

Conclusion: In MR, the presence and invasive hemodynamic constellation of PH provides important information regarding the likelihood of persistent PH several months after a mitral valve procedure.

P050

Improving large language models' accuracy for aortic stenosis treatment via Heart Team simulation: a prompt design analysis

Dorian Garin[1], Wesley Bennar[1], Stéphane Cook[1], Charlie Ferry[1], Mario Togni[1], Pascal Meier[1], Peter Wenaweser[1], Puricel Serban[1], Diego Arroyo[1]

[1]*University and Hospital Fribourg, Fribourg, Switzerland*

Introduction: Large language models (LLMs) have shown potential in clinical decision support, but the influence of prompt design on their performance, particularly in complex cardiology decision-making, is not well understood.

Material and Methods: We developed two novel prompts based on the Tree-of-Thought (ToT) framework, designed to encourage a LLM to emulate a Heart Team (HT) discussion for patients with severe aortic stenosis, named Forest-of-Thought (FoT) and few-shot FoT (fs-FoT). These prompts

were compared against three established prompting approaches: zero-shot (0-shot), Chain-of-Thought (CoT), and few-shot CoT (fs-CoT). We included 231 patients, each with a local HT recommendation for TAVI, SAVR, or medical management. For each patient, the LLM (GPT-4o version 2024-05-13) generated treatment recommendations 40 times under every prompt, resulting in 46,200 total queries. The final recommendation for each scenario was defined by the most frequently chosen treatment. We then compared each prompt's recommendations to the local HT decisions, using the mean correct response rate as the primary outcome. Secondary outcomes included treatment invasiveness and the weight of cardiac and non-cardiac variables on treatment recommendations.

Results: The FoT prompt achieved the highest mean correct response rate of 94.04%, significantly outperforming all other prompting techniques (fs-FoT 87.16%, fs-CoT 85.32%, CoT 78.89%, 0-shot 73.40%; p<0.001) (Figure 2). FoT also demonstrated the highest AUC values (0.96–0.97). Overall, the LLM made significantly less invasive decisions compared to the HT (mean invasiveness score, -0.0884; p<0.001). Non-cardiac variables carried significantly more weight than cardiac variables in influencing LLM decisions (Cliff's delta -0.231; p = 0.04), whereas the HT showed no such preference (Cliff's delta +0.12; p = 0.75).

Conclusion: Prompt design significantly impacts LLM performance in clinical decision-making for severe aortic stenosis, with the FoT prompt markedly improving accuracy and aligning recommendations with expert decisions. The LLM tended to favour conservative treatment, being more influenced by non-cardiac comorbidities.

Figure 1

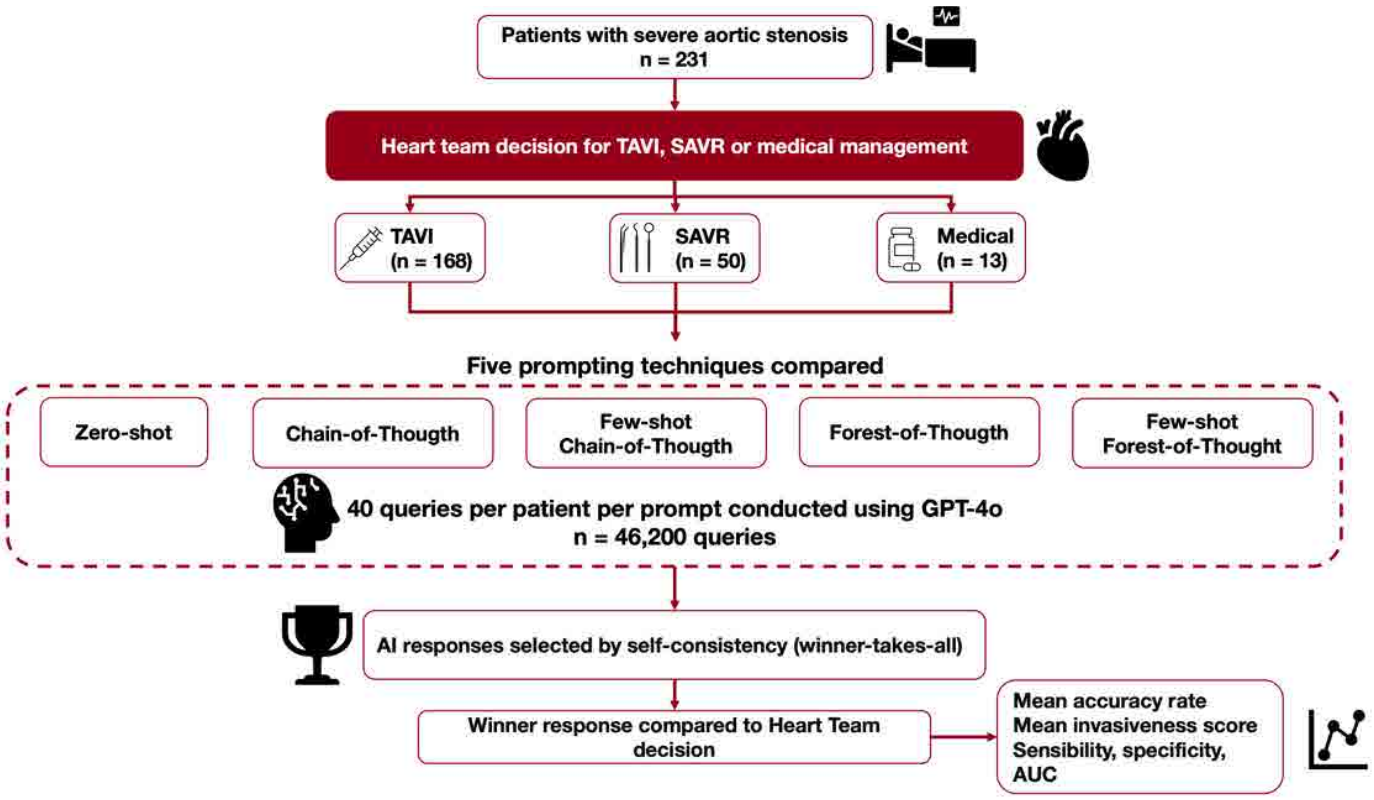

Figure 2

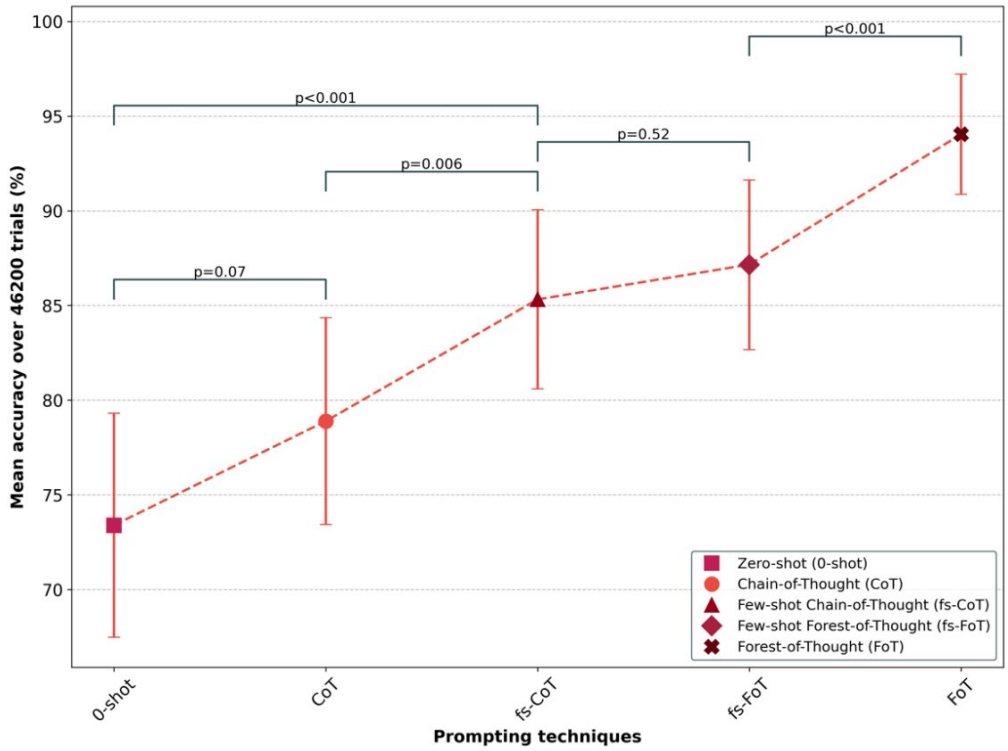

P051

Prognostic impact of atrial fibrillation in patients undergoing transcatheter aortic valve implantation

Jakob Reichl[1], Thorald Stolte[1], Jasper Boeddinghaus, Max Wagener[1], Gregor Leibundgut[1], Patrick Badertscher[1], Christian Sticherling[1], Michael Kühne[1], Christoph Kaiser, Felix Mahfoud, Thomas Nestelberger[1]

[1]Department of Cardiology and Cardiovascular Research Institute Basel (CRIB), Basel, Switzerland

Introduction: Atrial fibrillation (AF) is the most common arrhythmia and an important risk factor for adverse cardiac outcomes, including heart failure and stroke. Moreover, AF has been linked to worse outcomes following transcatheter aortic valve implantation (TAVI). Real-world data on the impact of AF on outcomes after TAVI remain limited.

Material and Methods: Patients undergoing TAVI at a tertiary center were consecutively included in a prospective registry. Cardiac rhythm at baseline was assessed using 12-lead ECGs. The primary outcome was all-cause mortality at 30 days. Secondary outcomes included all-cause mortality at one year, stroke at 30 days and one year, and procedural success, defined as freedom from periprocedural mortality, surgical re-interventions, re-interventions of the aortic valve, major access site complications, and periprocedural bleedings until discharge.

Results: Among 1655 patients undergoing TAVI, 428 patients (25.6%) had pre-existing AF, while 77 patients (4.6%) were diagnosed with new-onset AF. AF was not associated with higher mortality at 30 days (3.7% vs. 2.0%, p = 0.054, aHR 1.8 (95%CI 0.9-3.4)), but at one year (13.8% vs. 8.4%, p = 0.001, aHR 1.6 (95%CI 1.2–2.2)). The stroke rate was higher in patients with AF at 30 days (5.9% vs. 2.7%, p = 0.003, aHR 2.1 (95%CI 1.2–3.5)) and at one year (7.1% vs. 3.8%, p = 0.005, aHR 1.8 (95%CI 1.2–2.9)). At discharge, 452 patients (89.5%) with AF received oral anticoagulation. After adjusting for anticoagulant therapy, the difference in stroke risk at 30 days (5.7% vs. 2.3%, p = 0.058) and one year (6.8% vs. 4.2%, p = 0.165) was no longer significant. Patients with AF experienced more major or life-threatening bleeding complications (14.2% vs. 10.6%, p = 0.043). There were no differences in procedural success between patients with and without AF (78.8% vs. 78.3%, p = 0.886).

Conclusion: AF was associated with increased mortality at one year and higher rates of stroke and major bleeding at 30 days and one year after TAVI.

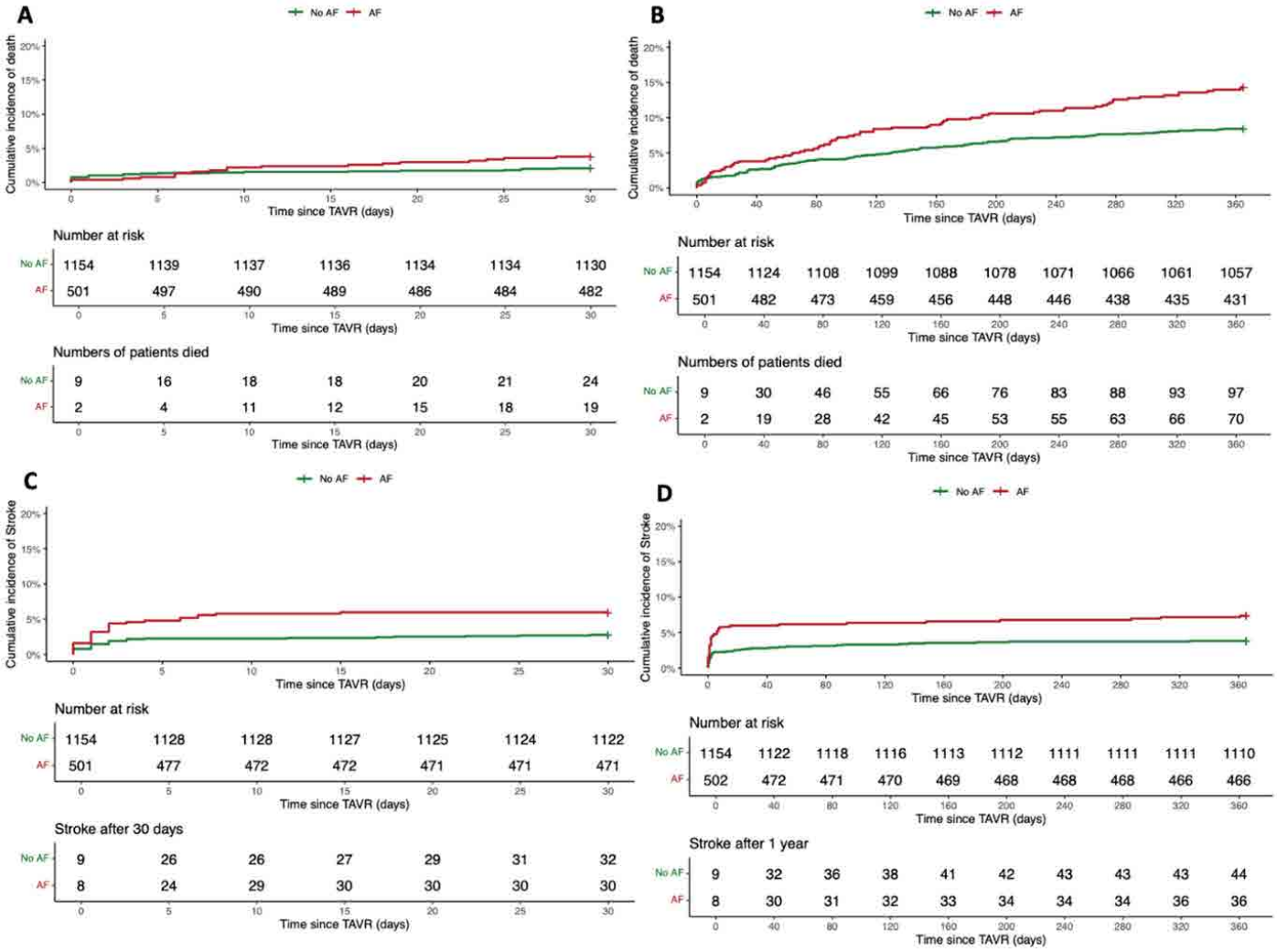

P052

Performance of three predictive scores of embolic events in patients with infective endocarditis

Nicoleta Ianculescu[1], Georgios Tzimas[1], Matthaios Papadimitriou-Olivgeris[2], Piergiorgio Tozzi[3], Matthias Kirsch[3], Benoit Guery[2], Pierre Monney[1]

[1]Lausanne University Hospital (CHUV), Department of Cardiology, Lausanne, Switzerland, [2]Lausanne University Hospital (CHUV), Department of Infectious Diseases, Lausanne, Switzerland, [3]Lausanne University Hospital (CHUV), Department of Cardiac Surgery, Lausanne, Switzerland

Introduction: Peripheral embolization is one of the most frequent complications of infective endocarditis (IE). To date, three scores were developed for the prediction of embolic events. The Embolic Risk French Calculator (*Staphylococcus aureus*, vegetation size, age, diabetes mellitus, atrial fibrillation, prior embolism)[1] and the Italian Study on Endocarditis (*S. aureus*, vegetation size)[2] were created to predict embolic events after the initiation of antimicrobial treatment, whereas the Naples score (*S. aureus*, vegetation size, d-dimers, CRP, splenomegaly)[3] to predict all embolic events (prior or after antimicrobial treatment initiation). The aim of the study was to evaluate the performance of each score in predicting the occurrence of embolic events.

Material and Methods: The retrospective study was conducted at Lausanne University Hospital (2014-2024). Sensitivity, specificity, positive and negative predictive values (PPV, NPV) and accuracy were calculated.

Results: In total 735 IE episodes were included; 491 (67%) associated with native valve, 196 (27%) with prosthetic valve and 31 (4%) with cardiac implantable electronic devices. Embolic events were present in 396 (54%) episodes; 293 (40%) before antimicrobial treatment initiation and 215 (29%) after (Table 1). The sensitivity of the French, Italian and Naples scores for their intended population was 45% (95% CI 38-52%), 70% (63-76%), and 58% (53-63%), respectively, while specificity was 74% (70-78%), 45% (41-49%), and 67% (62-72%), respectively (Table 2).

Conclusion: All three scores performance for the detection of embolic events was suboptimal for use in clinical practice.

References

- Hubert S *et al.* JACC. 2013 Oct. DOI: 10.1016/j.jacc.2013. 07.029
- Rizzi M *et al.* BMC Infectious Diseases. 2014 Dec. DOI: 10.1186/1471-2334-14-230
- Bertolino L *et al.* Infection. 2024 Dec. DOI: 10.1007/s15010-024-02444-1

	No embolic event	Embolic event	P
Embolic Risk French Calculator (after antimicrobial treatment initiation)	**N=520**	**N=215**	
Age (years)	69 (55-80)	67 (55-76)	0.078
Diabetes mellitus	115 (22%)	64 (30%)	0.030
Embolic events prior to antimicrobial treatment initiation	181 (35%)	112 (52%)	<0.001
Atrial fibrillation	150 (29%)	60 (28%)	0.858
Vegetation			
0-10mm	151 (29%)	57 (26%)	
>10mm	148 (29%)	98 (46%)	<0.001
Staphylococcus aureus	195 (38%)	103 (48%)	0.010
Final score (cumulative incidence at 14 days)	4 (3-8)	6 (3-12)	<0.001
High risk (>7% cumulative incidence at 14 days)	135 (26%)	97 (45%)	<0.001
Italian Study on Endocarditis (after antimicrobial treatment initiation)	**N=520**	**N=215**	
Staphylococcus aureus	195 (38%)	103 (48%)	0.010
Vegetation ≥13mm	122 (24%)	82 (38%)	<0.001
Final score	1 (0-1)	1 (0-1)	<0.001
Intermediate or high risk (≥1 points)	286 (55%)	150 (70%)	<0.001
Naples score (all embolic events)	**N=339**	**N=396**	
Staphylococcus aureus	120 (35%)	178 (45%)	0.010
D-dimer>747 ng/dl	10 (3%)	30 (8%)	0.008
CRP>67 mg/l	210 (62%)	296 (75%)	<0.001
Vegetation ≥14mm	42 (12%)	147 (37%)	<0.001
Splenomegaly	12 (4%)	58 (15%)	<0.001
Final score	2 (1-4)	3 (2-4)	<0.001
Intermediate or high risk (≥1 points)	111 (33%)	230 (58%)	<0.001

Data are depicted as number (%) or median (interquartile range)

	Sensitivity % (95% CI)	Specificity % (95% CI)	PPV % (95% CI)	NPV % (95% CI)	Accuracy % (95% CI)
Embolic Risk French Calculator (high risk)[a]	45 (38-52)	74 (70-78)	42 (37-47)	77 (74-79)	66 (62-69)
Italian Study on Endocarditis (intermediate or high risk)[a]	70 (63-76)	45 (41-49)	34 (32-37)	78 (74-82)	52 (49-56)
Naples score (intermediate or high risk)[b]	58 (53-63)	67 (62-72)	67 (64-71)	58 (54-61)	62 (59-66)

[a]prediction of embolic events after antimicrobial treatment initiation

[b]prediction of overall embolic events (before or after antimicrobial treatment initiation)

P053

Right ventricular to pulmonary artery coupling in patients with degenerative mitral regurgitation undergoing valve repair/replacement

Mark Güpfert[1], Lukas Weber[1], Sebastian Kopp[1], Philipp Haager[1], Philipp Baier[1], Johannes Rigger[1], Joannis Chronis[1], Marc Gerhard[1], Hans Rickli[1], Micha T. Maeder[1]

[1]Health Ostschweiz (HOCH) Kantonsspital St. Gallen, St. Gallen, Switzerland

Introduction: In degenerative mitral regurgitation (MR), a low ratio of tricuspid annular plane systolic excursion (TAPSE) to systolic pulmonary artery pressure (sPAP), a simplified measure of right ventricular (RV) to pulmonary artery coupling, predicts poor outcome after mitral valve repair. We assessed invasive hemodynamics and the likelihood of pulmonary hypertension (PH) recovery after mitral valve repair/replacement of patients with low TAPSE/sPAP ratio.

Material and Methods: We studied 169 patients (mean age 67±11 years, 26% females) with at least moderate degenerative MR undergoing right heart catheterization followed by surgical (81%) or transcatheter (19%) valve repair/replacement. The TAPSE/sPAP ratio was calculated from echocardiography (TAPSE) and invasive (sPAP) data. An echocardiogram with valid information on PH (PH probability by peak tricuspid regurgitant velocity and indirect signs) was available in 91% of patients after a median follow-up of 6 months.

Results: The median (interquartile range) TAPSE/sPAP ratio was 0.74 (0.50-1.07) mm/mmHg. Patients with inframedian TAPSE/sPAP ratio had similar MR severity but larger left atrial volume index (70±23 vs. 61±21 ml/m2) compared to those with supramedian TAPSE/sPAP ratio and had lower stroke volume index (33±11 vs. 41±9 ml/m2) and pulmonary capacitance (2.4±1.0 vs. 5.6±2.5 ml/mmHg) and higher mean right atrial pressure (6±3 vs. 3±2 mmHg), mean pulmonary artery pressure (29±9 vs. 15±4 mmHg), mean pulmonary artery wedge pressure (19±7 vs. 9±3 mmHg), and pulmonary vascular resistance (2.6±1.7 vs. 1.3±0.5 WU; p<0.05 for all). The TAPSE/sPAP ratio as a dichotomized (odds ratio 10.62 if inframedian; p = 0.002) or continuous (odds ratio 0.65 per 10 mm/mmHg increase; p<0.001) variable was associated with a high PH probability at follow-up.

Conclusion: In patients with degenerative MR, a low TAPSE/sPAP ratio is a marker of a poor hemodynamic constellation including left atrial hypertension, pulmonary vascular disease and RV dysfunction and a predictor of incomplete PH reversal six months after a mitral valve procedure.

P054

Cardiac MRI predictors of reverse remodeling in patients with severe ventricular secondary mitral valve regurgitation undergoing M-TEER: PRE-MITRA preliminary results

Ciocca Nicola[1], Jonathan Schütze[1], Lukas Eugster[1], Nicolas Brugger[1], Yasaman Safarkhanlo[1], David Tueller[2], Annina Studer[2], Christoph Kaiser[3], Michael Zellweger[3], Giovanni Pedrazzini[4], Anna Giulia Pavon[4], Isaac Shiri[1], Stephan Windecker[1], Thomas Pilgrim[1], Fabien Praz[1], Christoph Gräni[1]

[1]Inselspital Bern, Bern, Switzerland, [2]Stadtspital Zürich Triemli, Zürich, Switzerland, [3]Unispital Basel, Basel, Switzerland, [4]EOC, Cardiocentro Lugano, Lugano, Switzerland

Introduction: Ventricular secondary mitral regurgitation (SMR) in heart failure patients worsens prognosis, and while combining M-TEER with GDMT shows promise, identifying the best candidates for intervention remains challenging. We aimed to evaluate whether Cardiac Magnetic Resonance (CMR) is able to predict reverse remodeling and better identify responders to the intervention.

Material and Methods: Prospective multicenter observational study of patients with echocardiographic severe ventricular SMR (regurgitant volume ≥ 30 mL/beat or EROA ≥ 20 mm²) and symptomatic heart failure (LVEF 15-50%), despite receiving optimal GDMT undergoing M-TEER. CMR and echocardiography were performed at baseline, followed by clinical and echocardiography follow-up at 6- and 12- month. The primary endpoint was echocardiographic reverse remodeling (≥10% reduction in LVEDV) in patients with successful SMR reduction at 12 months.

Results: A total of 39 patients, mean age of 75±10years, 29 (74%) male, in 4 Swiss hospitals were included. In this preliminary analysis, 34 patients completed the 6-month follow-up, and 17 the 12-month follow-up. Considering the latest available follow-up, reverse remodeling was achieved in 14 out of 34 patients (41%). In univariate logistic regression, reverse remodeling showed association to higher LGE in the mid-anterolateral segment (p = 0.048), elevated native T1 in basal inferior/lateral segments (p = 0.11), lower 2D peak radial strain, and higher 2D peak circumferential strain in the mid-inferolateral segments (p = 0.06, p = 0.03). During follow-up, three patients (7.7%) died, and MACEs occurred in six patients (15.4%), trending with higher LVEDV [ml] and lower LVEF [%] (p = 0.09 and p = 0.12).

Conclusion: In the preliminary results of Pre-MITRA, 41% of the patients showed reverse remodeling at 6 or 12 months. CMR tissue characterization and strain showed a significant association between fibrosis in specific myocardial segments (mid-inferolateral/anterolateral) and reverse remodeling. Whether patients with ventricular SMR and fibrosis of the mitral valve pillar are those who best benefit from M-TEER needs to be evaluated with longer follow-up.

P055

Efficacy of a Novel Protocol for Eliminating Mycobacterium chimaera in Heater-Cooler Units: Single Center Clinical Study

Lilly Ilcheva[1], Alexej Janenko[2], Tobias Aigner[1], Dragan Odavic[2], Nestoras Papadopoulos[1], Héctor Rodríguez Cetina Biefer[1], Omer Dzemali[1]

[1]University Hospital Zurich, Herzallianz Zurich, Zurich, Switzerland, [2]CIty Hospital Triemli, Herzallianz Zurich, Herzallianz Zurich, Zurich, Switzerland

Introduction: Mycobacterium chimaera, a non-tuberculous mycobacterium, has become a significant concern in cardiothoracic surgery, particularly open-heart procedures. This slow-growing pathogen causes severe disseminated infections through bioaerosols from contaminated heater-cooler units (HCUs) during cardiopulmonary bypass. Since the first documented outbreak in 2013, M. chimera infection has been recognized as a global health issue. Current disinfection methods have proven to be largely ineffective. This study evaluated a novel protocol using a stable hypochlorous acid solution (Hydroliq) to eliminate M. chimera from infected HCUs and maintain M. chimera-free devices.

Material and Methods: This study was conducted from March 2023 to August 2024 in two phases. Phase I explored different amounts of Hydroliq and water change intervals in three HCUs using redox potential (ORP ≥500 mV), pH, chloride ion levels, and mycobacterial cultures as outcome measures. Phase II implemented the optimized protocol during cardiopulmonary bypass surgery, with regular M. chimera microbiological testing, redox potential, chloride ion levels, and pH values

Results: In the first phase, different concentrations and frequencies of water changes were tested, leading to an optimal decontamination regime by adding 200 ml Hydroliq with twice-weekly water changes. In the second phase, 337 cardiac surgeries were performed over 7 months using treated HCUs. This achieved optimal results, maintaining a redox potential above 500 mV (median 598 mV) (Figure 1), median pH value of 7.39 (Figure 2), and median chloride anion concentration of 1.33. No M. chimera infections were detected during this period, demonstrating the effectiveness of this protocol in clinical practice.

Conclusion: This novel decontamination protocol effectively eliminated M. chimera from HCUs and reduced postoperative infections in patients undergoing cardiac surgery. These findings support the implementation of this method as a safe and effective strategy to prevent HCU-related infections. Further investigation with a larger dataset is required to prove or reject this approach.

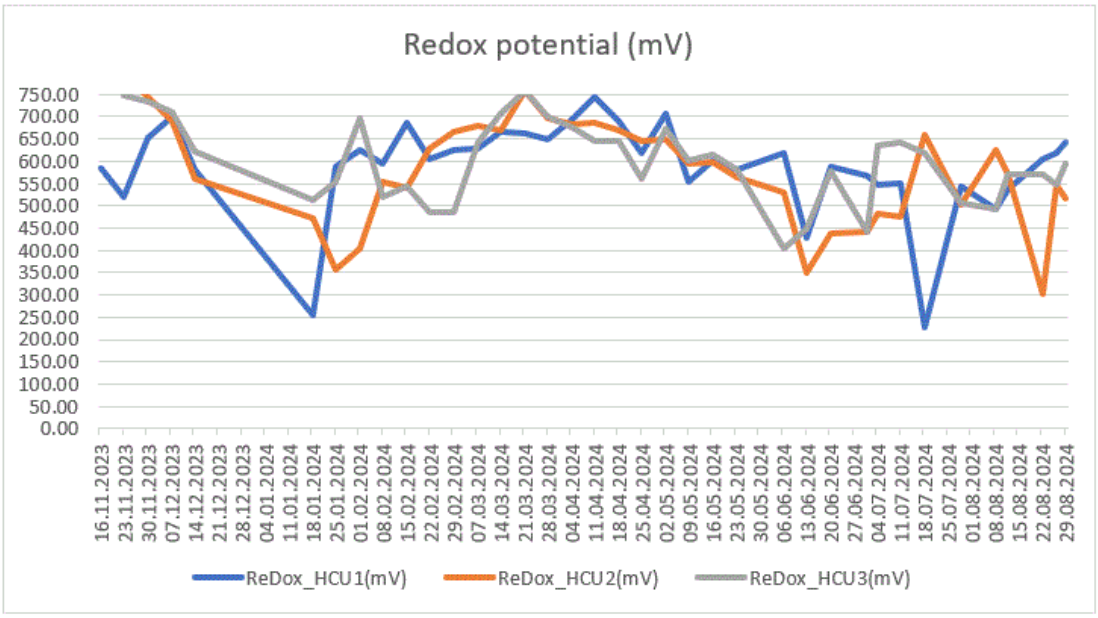

Figure 1. Redox potential (ORP) in mV during second phase of the study

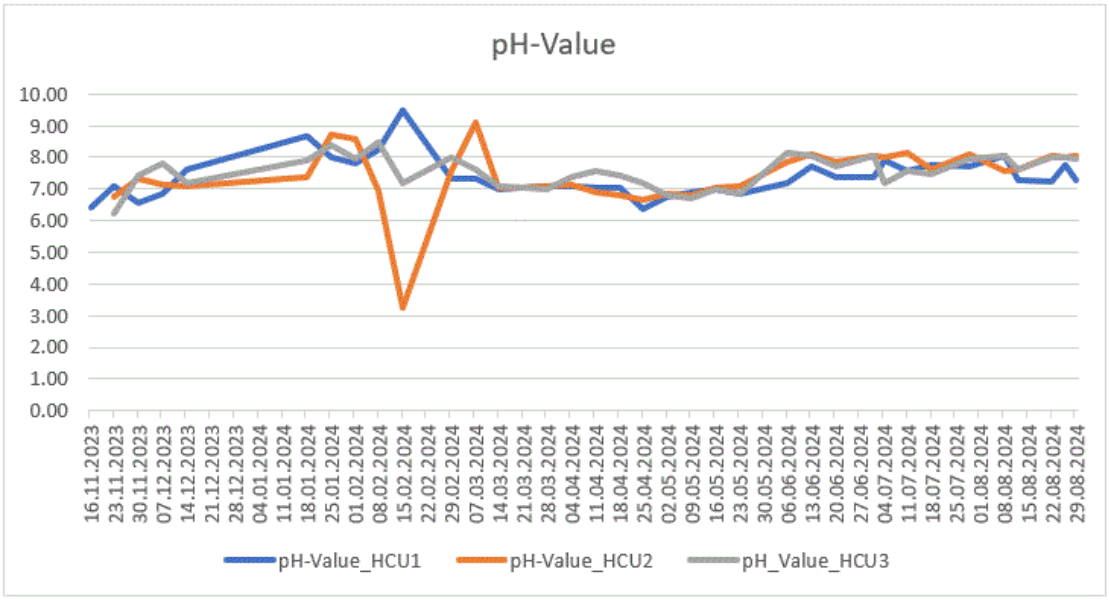

Figure 2. pH values during second phase of the study

P056

Functional and morphological predictors of left ventricular fibrosis in patients with mitral annular disjunction in cardiac magnetic resonance imaging

Martin F. Reiner[1], Daniel Escribano-García[2], Federica Guidetti[3], Verena Wilzeck[4], Rabea Schlenker[1], Andrea Biondo[5], Firat Duru[1], Frank Ruschitzka[6], Gianluigi Savarese[3], Hatem Alkadhi[5], Robert Manka[7]

[1]Department of Cardiology, University Heart Center, University Hospital Zurich, Zurich, Switzerland, [2]Hospital Universitario Puerta de Hierro-Majadahonda, Cardiology Department, Madrid, Spain, [3]Division of Cardiology, Department of Medicine, Karolinska Institutet, Stockholm, Sweden, [4]Department of Cardiology, University Heart Center, University Hospital Zurich, Diagnostic and Interventional Radiology, University Hospital Zurich, University of Zurich, Zurich, Switzerland, [5]Diagnostic and Interventional Radiology, University Hospital Zurich, University of Zurich, Zurich, Switzerland, [6]Department of Cardiology, University Heart Center, University Hospital Zurich, Center for Translational and Experimental Cardiology (CTEC), Department of Cardiology, Zurich University Hospital, University of Zurich, Zurich and Schlieren, Switzerland, [7]Diagnostic and Interventional Radiology, University Hospital Zurich, University of Zurich, Department of Cardiology, University Heart Center, University Hospital Zurich, Institute for Biomedical Engineering, University and ETH Zurich, Zurich, Switzerland

Introduction: Mitral annular disjunction (MAD) is characterized by a separation of the mitral valve hinge point and the left ventricular (LV) myocardium and significantly increases the risk of ventricular arrhythmias through the combination of LV fibrosis and increased mechanical stretch. We investigated functional and morphological predictors of LV fibrosis by cardiac magnetic resonance (CMR) imaging.

Material and Methods: 111 patients with inferolateral MAD were included; MAD distance, presence and size of mitral valve prolapse (MVP), midmyocardial replacement fibrosis of the basal inferolateral LV segment as well as the movement pattern of this segment were analyzed. Longitudinal and radial systolic displacement of the basal inferolateral LV wall was judged as homogeneous or accelerated by visual impression by two independent investigators.

Results: Median age was 52 years (IQR36-69) and 47% were female. Midmyocardial replacement fibrosis of the basal inferolateral LV wall was present in 27 (24%) patients. Patients with fibrosis were older (63.0 years [IQR53.0-70.0] vs. 47.5years [IQR 34.0-67.5], p = 0.011), more likely to have MVP (24 [89%] vs. 58 [69%], p = 0.041), had larger median MAD distance (6.0mm [IQR 5.0-9.0] vs. 5.0mm [IQR3.0-8.0], p = 0.018) and were more likely to exhibit an accelerated longitudinal motion of the basal inferolateral LV wall (20 [74%] vs. 26 [31%], p<0.001) (Table 1). Multivariable logistic regression revealed that age (OR 1.06, CI 1.03-1.10, p = 0.001) and accelerated longitudinal motion of the basal inferolateral LV wall (OR 10.59, CI 2.84-39.49, p<0.001) were the only significant predictors of replacement fibrosis (Table 2). Posterior MVP distance (OR 1.29, CI 1.02-1.62, p = 0.032) and MAD size (OR 1.28, CI 1.05-1.56, p = 0.017) were associated with an accelerated motion of the basal inferolateral LV segment.

Conclusion: Age and accelerated longitudinal motion of the basal inferolateral LV segment predict replacement fibrosis of the inferolateral wall in MAD patients. MAD size and posterior MVP size are associated with this accelerated movement pattern.

Table 1. Baseline characteristics of patients with inferolateral MAD. IQR = interquartile range, LV = left ventricular, LVED = left ventricular end-diastolic, MAD = mitral annular disjunction, MVP = mitral valve prolapse, SD = standard deviation.

Baseline characteristics	Total N = 111	No fibrosis N = 84	Fibrosis N = 27	P-value
Age [years], median (IQR)	52.0 (36.0-69.0)	47.5 (34.0-67.5)	63.0 (53.0-70.0)	0.011
Female [%]	52 (47%)	42 (50%)	10 (37%)	0.24
Height [m], mean ± SD	1.73 ± 0.09	1.74 ± 0.10	1.71 ± 0.08	0.082
Weight [kg], median (IQR)	66.0 (58.0-76.0)	64.0 (57.0-78.0)	68.0 (60.0-74.0)	0.45
Body mass index [kg/m^2], median (IQR)	22.5 (19.7-25.2)	22.0 (19.3-24.7)	22.9 (21.3-26.1)	0.063
LVED volume [ml/m^2], median (IQR)	86.0 (77.0-107.0)	86.0 (77.5-100.5)	91.0 (73.0-118.0)	0.48
LV ejection fraction [%], mean ± SD	55.6 ± 6.5	56.1 ± 6.6	54.3 ± 6.1	0.20
LV mass [g/m^2], median (IQR)	44.0 (36.0-50.0)	43.0 (36.0-50.0)	46.0 (36.0-55.0)	0.38
MVP [%]	82 (74%)	58 (69%)	24 (89%)	0.041
Anterior MVP [%]	50 (45%)	31 (37%)	19 (70%)	0.002
Anterior MVP distance [mm], median (IQR)	0.0 (0.0, 4.0)	0.0 (0.0, 3.0)	3.0 (0.0, 4.0)	0.010
Posterior MVP [%]	79 (71%)	57 (68%)	22 (81%)	0.17
Posterior MVP distance [mm], median (IQR)	3.0 (1.0, 5.0)	2.5 (0.0, 4.5)	4.0 (2.0, 7.0)	0.016
Bileaflet MVP [%]	47 (42%)	30 (36%)	17 (63%)	0.013
MAD distance [mm], median (IQR)	6.0 (4.0-8.0)	5.0 (3.0-8.0)	6.0 (5.0-9.0)	0.018
Accelerated longitudinal motion of the basal inferolateral LV segment [%]	46 (41%)	26 (31%)	20 (74%)	<0.001
Accelerated radial motion of the basal inferolateral LV segment [%]	27 (24%)	19 (23%)	8 (30%)	0.46

Table 2. Odds ratio for replacement fibrosis of the basal inferolateral left ventricular wall. CI = confidence interval, LV = left ventricular, LVED = left ventricular end-diastolic, MAD = mitral annular disjunction, MVP = mitral valve prolapse. *Variables included in multivariable logistic regression.

Predictors of basal inferolateral LV fibrosis		
Univariable logistic regression	**Odds ratio (95% CI)**	**P-Value**
Age*	1.04 (1.01-1.06)	0.008
LVED volume index	1.01 (0.99-1.03)	0.355
LV ejection fraction	0.96 (0.89-1.02)	0.201
MVP	3.59 (0.99-12.98)	0.052
Anterior MVP	4.06 (1.59-10.37)	0.003
Anterior MVP distance*	1.19 (1.01-1.39)	0.034
Posterior MVP	2.08 (0.71-6.10)	0.180
Posterior MVP distance*	1.20 (1.01-1.41)	0.034
Bileaflet MVP	3.06 (1.24-7.52)	0.015
MAD distance	1.11 (0.97-1.26)	0.128
Accelerated longitudinal displacement*	6.37 (2.40-16.93)	<0.001
Accelerated radial displacement	1.44 (0.55-3.81)	0.462
Multivariable logistic regression	**Odds ratio (95% CI)**	**P-Value**
Age	1.06 (1.03-1.10)	0.001
Anterior MVP distance	1.00 (0.79-1.27)	0.985
Posterior MVP distance	1.12 (0.86-1.46)	0.390
Accelerated longitudinal displacement	10.59 (2.84-39.49)	<0.001

P057

Characteristics and outcomes of patients with degenerative mitral regurgitation and severe pulmonary hypertension undergoing valve repair/replacement

Mark Güpfert[1], Lukas Weber[1], Johannes Rigger[1], Joannis Chronis[1], Philipp Haager[1], Philipp Baier[1], Sebastian Kopp[1], Marc Gerhard[1], Hans Rickli[1], Micha T. Maeder[1]

[1]Health Ostschweiz (HOCH) Kantonsspital St. Gallen, St. Gallen, Switzerland

Introduction: In patients with degenerative mitral regurgitation (MR), a systolic pulmonary artery pressure (sPAP; assessed by right heart catheterization [RHC]) >50 mmHg represents an indication for valve surgery regardless of symptoms or any other criteria by current ESC guidelines. We aimed to describe detailed invasive hemodynamics of such patients and to assess their likelihood of PH recovery after mitral valve repair/replacement.

Material and Methods: We studied 251 patients (mean age 67±11 years, 25% females, left ventricular ejection fraction [LVEF] 62±8%) with at least moderate degenerative MR undergoing RHC followed by surgical (83%) or transcatheter (17%) valve repair/replacement. An echocardiogram with valid information on PH was available in 90% of patients after a median follow-up of 6 months. The probability of PH at follow-up was assessed by peak tricuspid regurgitant velocity and indirect PH signs according to 2022 ESC/ERS guidelines.

Results: 30/251 (12%) patients had an sPAP >50 mmHg. Patients with sPAP >50 mmHg had similar MR severity and LVEF as compared to those with sPAP ≤50 mmHg but had lower tricuspid annular plane systolic excursion (20±6 vs. 24±5 mm) and cardiac index (2.2±0.5 vs. 2.6±0.5 l/min/m2) and higher mean right atrial pressure (8±4 vs. 4±2 mmHg), mean pulmonary artery pressure (40±7 vs. 19±6 mmHg), mean pulmonary artery wedge pressure (26±7 vs. 12±5 mmHg), and pulmonary vascular resistance (4.0±2.4 vs. 1.6±0.8 WU; p<0.05 for all). An sPAP >50 mmHg was strongly associated with a high probability of PH at the follow-up echocardiogram (odds ratio 6.35 [95%confidence interval 2.51-16.09]; p<0.001).

Conclusion: In patients with degenerative MR, presence of an sPAP >50 mmHg identifies a population in a very advanced stage of MR-related cardiac damage including left atrial disease, pulmonary vascular remodeling and right ventricular dysfunction. Mechanical correction of MR cannot not fully revert PH in these patients within the first months after the procedure.

POSTER WALK "CLINICAL CASES"

P058

Takotsubo and severe aortic stenosis, a deadly combination

Nerea Lopez Perez*[1], Sebastien Colombier[1], Manon Ollagnon[1], Sandra Bommeli[1], Dominique Delay[1]

[1]Hôpital du Valais, Sion, Switzerland

Introduction: Takotsubo cardiomyopathy, also known as stress-induced cardiomyopathy or "broken heart syndrome," is a transient left ventricular dysfunction often triggered by emotional or physical stress. It typically presents with apical ballooning and impaired left ventricular wall motion. The combination of Takotsubo cardiomyopathy with pre-existing severe aortic stenosis poses a complex and life-threatening challenge.

Material and Methods: We report the case of a 64-year-old woman with a history of severe aortic stenosis, hypertrophic obstructive cardiomyopathy and a 55mm ascending aorta aneurysm who developed Takotsubo cardiomyopathy following a major emotional stress. The patient was admitted for acute heart failure which required emergency intubation and mechanical ventilation. Echocardiography revealed left ventricular dysfunction, typical signs of Takotsubo cardiomyopathy associated with left ventricular outflow tract obstruction and systolic anterior motion of the mitral valve with significant regurgitation. She then developed refractory cardiorespiratory arrest following ventricular fibrillation. Femoro-femoral veno-arterial extracorporeal membrane oxygenation (ECMO) was implanted under mechanical cardio-pulmonary resuscitation. After hemodynamic stabilization, she underwent emergent aortic valve and ascending aorta replacement, with septal myectomy.

Results: The postoperative course was marked by a transient vasoplegic and hemorrhagic shock. ECMO was successfully weaned after 3 days and extubation could be carried out on day-5. Left ventricular function returned to normal and mitral regurgitation disappeared. This case highlights the deadly association of a severe aortic stenosis and a Takotsubo cardiomyopathy. In this particular situation, presence of septal hypertrophy further increased the obstructive effect to left ventricle ejection, already severly dimished by the apical ballooning. Furthermore, blood acceleration in the outflow tract triggered significant mitral regurgitation precipitating pulmonary oedema and cardiac arrest.

Conclusion: Prompt institution of ECMO support followed by emergency surgery aiming at correcting the two causes of obstruction proved to be the winning therapeutic strategy facing this critical combination

P059

Unruptured Sinus of Valsalva Aneurysm Causing Right Ventricular Outflow Tract Obstruction

Linus Wildt*[1], Neza Pristov[2], Se-Il Yoon[3], David Schibilsky[1], Robert Von Wattenwyl[1], Bart De Boeck[2], Stefan Toggweiler[2], Peter Matt[1], Simon Stämpfli[2, 4]

[1]Division of Cardiac Surgery, Lucerne, Switzerland, [2]Division of Cardiology, Heart Center Lucerne, Luzerner Kantonsspital, Lucerne, Switzerland, [3]Herzpraxis Sursee, Sursee, Switzerland, [4]Center for Molecular Cardiology, University of Zurich, Zurich, Switzerland

Introduction: A sinus of Valsalva aneurysm (SOVA) is a rare cardiac anomaly that typically remains asymptomatic but carries risk of life-threatening complications, particularly rupture. In rare cases, unruptured SOVA may cause symptoms due to compression of adjacent structures. We report a case of an unruptured right coronary sinus aneurysm causing right ventricular outflow tract (RVOT) obstruction, successfully managed with aortic root reconstruction.

Case Description: A 59-year-old female patient presented with three-month history of reduced exercise tolerance, exertional dyspnea (NYHA class III), and chest discomfort. Physical examination revealed a grade 2/6 systolic murmur and arterial hypertension. Transthoracic echocardiography (TEE) identified a 45×48×48 mm aneurysm originating f rom the right coronary sinus, resulting in significant RVOT obstruction and elevated right ventricular pressures. Cardiac MRI and CT angiography confirmed the diagnosis and provided detailed anatomic visualisation (Figure 1). Given signs of mildly impaired RV function, preoperative optimization with levosimendan was initiated. Intraoperatively, the aortic annulus, sinotubular junction and aortic valve leaflets appeared intact. The right coronary sinus was massively dilated with a thinned wall protruding into the RVOT. Unexpectedly, the non-coronary sinus was also found to be thinned and enlarged, an unexpected finding not evident on preoperative imaging. Both sinuses were completely resected, and a modified Yacoub aortic root reconstruction was performed using bovine pericardial patch to restore geometry of the aortic root while preserving the native valve (Figure 2 A, B). Intraoperative TEE confirmed excellent aortic valve competence. Postoperative recovery was uncomplicated aside from a transient neurological episode, which resolved without residual deficits. Follow-up imaging demonstrated normalized aortic root dimensions (Figure 2 C), preserved valve function, and complete resolution of RVOT obstruction.

Conclusion: This case underscores a rare manifestation of unruptured SOVA. Early diagnosis including multimodal imaging and timely surgical intervention are critical. Aortic root reconstruction with preservation of the native valve can offer excellent anatomical and functional outcomes.

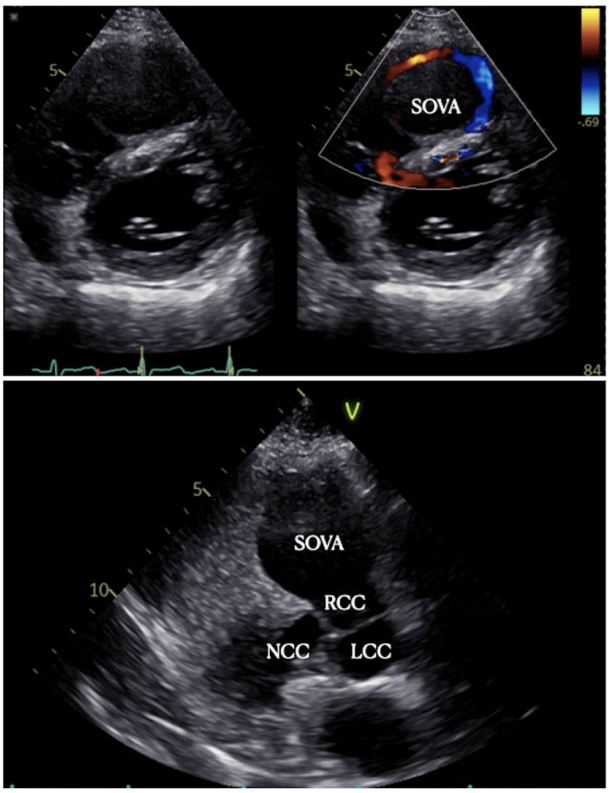

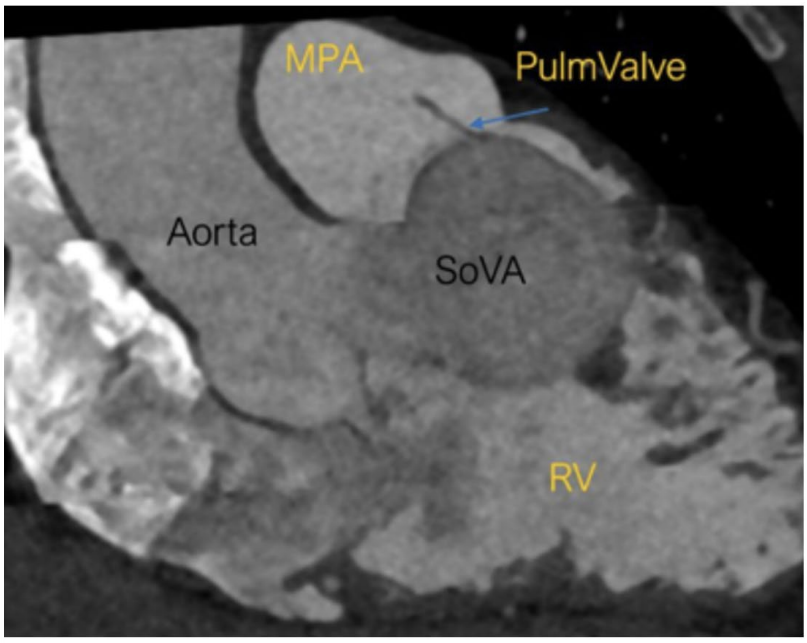

SOVA: Sinus of Valsalva Aneurysm, LCC: Left coronary cusp of the aorta, RCC: right coronary cusp of the aorta, NCC: non-coronary cusp of the aorta, MPA: Main Pulmonary Artery, RV: right ventricle, PulmValve: pulmonary valve,

P060

Atropine use in unstable monomorphic ventricular tachycardia: a case report.

Mattia Pagnoni[1], Cheryl Teres[1], Ciro Ascione[1], Mathieu Le Bloa[1]

[1]Service de Cardiologie, CHUV (Centre Hospitalier Universitaire Vaudois), Lausanne, Switzerland

Introduction: Hemodynamic (HD) tolerance during monomorphic ventricular tachycardia (VT) is poorly understood. An abnormal parasympathetic reflex, failing to augment sinus rhythm (SR), predicts HD instability. Atropine, a vagolytic agent, shows promise in raising blood pressure (BP) during VT, although it is currently recommended only for bradycardia. We report a case of VT with hypotension successfully treated with Atropine

Material and Methods: A 68-year-old man with no cardiac disease presented with palpitations, dizziness, and sweating during exercise. Initial ECG showed a wide QRS tachycardia indicating VT. He had low BP (70/58 mmHg) but no hypoperfusion signs. Following the ACLS algorithm, Adenosine was administered by the ER team, without any effect. The patient then received IV Metoprolol (3 mg in total) and IV Amiodarone, mildly reducing the ventricular rate but causing a BP drop to 45/12 mmHg with hypoperfusion symptoms (dizziness and sweats). Intravenous Atropine (1 mg) increased BP to 85/55 mmHg, normalizing neurological status. Persistent VT required sedation and synchronized cardioversion (200 J). Post-cardioversion ECG revealed diffuse ST-segment depression; coronary angiography showed no significant stenosis. Echocardiography indicated mild RV dysfunction and suspected RV apical wall hypo-akinesis. MRI revealed a fibrotic aneurysm in the basolateral RV wall, suggesting arrhythmogenic RV cardiomyopathy (ARVC). FDG PET-CT showed no myocardial uptake.

Results: HD instability during VT is linked to abnormal autonomic responses, mediated by the Bezold-Jarisch reflex, causing bradycardia, vasodilation, and hypotension. Antiarrhythmics like Amiodarone can worsen this instability. Atropine, by counteracting vagal activity, has shown promise in improving HD tolerance. In this case, Atropine stabilized BP, enabling safer cardioversion. Prior studies have demonstrated Atropine's potential to enhance tolerance in unstable VT, suggesting a role for vagolytic therapy in emergency VT management.

Conclusion: Abnormal parasympathetic responses affect VT tolerance. Atropine may improve HD stability during unstable VT, offering a potential adjunct in emergency treatment strategies.

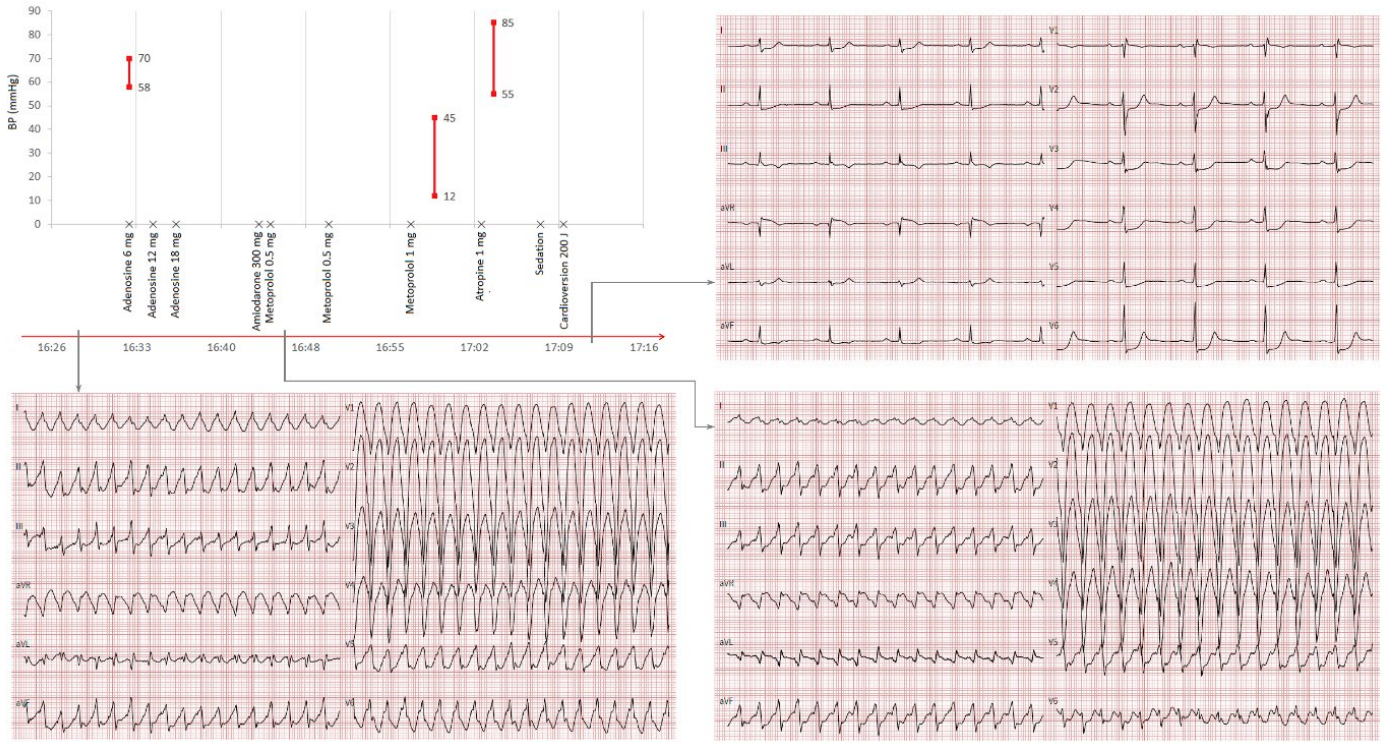

P061

Severe tricuspid regurgitation in the elderly: to clip or not to clip?

Micha T. Maeder[1], Philipp Baier[1], Sebastian Hasslacher[1], Hans Rickli[1], Philipp Haager[1]

[1]Health Ostschweiz (HOCH) Kantonsspital St. Gallen, St. Gallen, Switzerland

Introduction: Percutaneous tricuspid valve repair is an increasingly performed procedure, which improves quality of life in selected patients with severe tricuspid regurgitation (TR). However, for the evaluation of the appropriateness of an intervention identification of the exact mechanism(s) underlying TR is mandatory.

Results: A 80-year-old male presented with shortness of breath. He had permanent atrial fibrillation and a pacemaker for recurrent syncope. Echocardiography showed a left ventricular ejection fraction (LVEF) of 55-60%, diastolic LV dysfunction, dilated atria, mild mitral regurgitation, and a dilated right ventricle (RV) with impaired function (tricuspid annular plane systolic excursion 14 mm). There were severe functional TR and a high probability of significant pulmonary hypertension (PH). Right heart catheterization revealed a systolic/diastolic/mean pulmonary artery (PA) pressure of 74/13/34 mmHg and a mean pulmonary artery wedge pressure (mPAWP) of 18 mmHg. However, the PA oxygen saturation was 79% (Figure, A). There was an anomalous vessel draining into the superior vena cava (SVC) with an oxygen saturation of 97% (Figure, B). Thus, the patient had partial anomalous pulmonary venous return [one right pulmonary vein (PV) draining into the SVC] with a left-to-right shunt with a pulmonary flow of 7.1 l/min and a ratio of pulmonary to systemic blood flow of 1.8: 1.0. The increased pulmonary flow (high RV stroke volume, very large PA pressure amplitude) and the mildly elevated pulmonary vascular resistance of 2.3 WU resulted in a transpulmonary gradient of 16 mmHg, which added to an elevated mPAWP [heart failure with preserved LVEF (HFpEF)] led to substantial combined pre- and post-capillary PH.

Conclusion: This case highlights the importance of combined non-invasive and invasive imaging in patients with severe TR. Here, TR is the result of substantial right ventricular volume and pressure overload with very limited treatment options (congenital defect and HFpEF), and percutaneous repair is not appropriate.

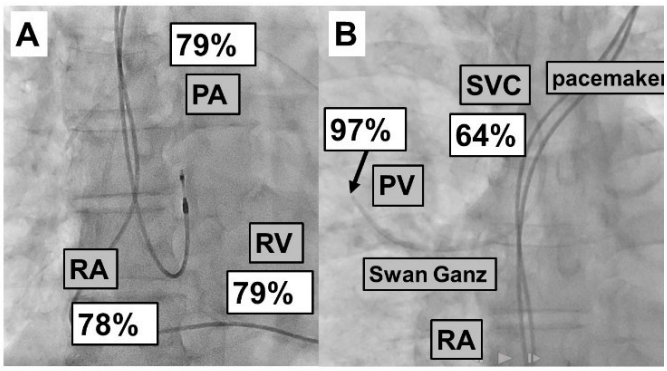

P062

X-ray guided conduction system pacing lead implantation in LBBAP after transcatheter tricuspid valve replacement is feasible and safe

Thomas Seiler[1], Andreas Häberlin[1], Gregor Thalmann[1], Nikolas Kozhuharov[1], Claudia Herrera Siklody[1], Boldizsar Kovacs[1], Thomas Küffer[1], Hildegard Tanner[1], Laurent Roten[1], Valon Spahiu[1], Daryoush Samim[1], Fabien Praz[1], Tobias Reichlin[1], Fabian Noti[1]

[1]*Inselspital Bern, Bern, Switzerland*

Introduction: We describe a case series of conduction system pacemaker (CSP) implantation following transcatheter tricuspid valve implantation (TTVI).

Material and Methods: Pacemaker implantation was performed according to the EHRA guidelines and the EHRA clinical consensus statement on CSP implantation. Details are displayed in Figure 1.

Results: Patient 1 (82 years, male) suffering from advanced cardiac amyloidosis underwent TTVI due to severe symptomatic secondary tricuspid regurgitation (TR). Months later he developed poorly tolerated atrial fibrillation (AF) and a pace and ablate strategy with a left optimized cardiac resynchronization (LOT-CRT) pacemaker was pursued. The patient died due to progressive heart failure 2 years later without tricuspid valve or lead dysfunction.

Patient 2 (81 years, male) with permanent AF and mildly reduced left ventricular function underwent single-chamber CSP implantation due to complete heart block following combined trans catheter aortic valve implantation (TAVI) and TTVI. CSP lead performance was stable with proper function of the tricuspid valve prosthesis at 3 months follow-up.

Patient 3 (61 years, female) with post-actinic valvular cardiomyopathy underwent surgical aortic and mitral valve replacement and primary prevention ICD-implantation 5 years ago. LVEF improved to 45%, but a progressive symptomatic TR was treated with TTVI after ICD-extraction. Due to a post-interventional complete AV-block a CSP pacemaker implanted. Valvular function as well as CSP lead performance was favorable after 3 months.

Patient 4 (85 years, female) with permanent AF and preserved ejection fraction underwent TTVI due to symptomatic severe secondary TR. A complete AV-block following TTVI triggered an implantation of a CSP. Both, the tricuspid valve and CSP lead showed stable function at short-term follow up.

Conclusion: X-ray guided CSP lead implantation in LBBAP after TTVI seems feasible. Short-term follow up is promising in respect of valve prosthesis function as well as effective physiological pacing, but needs to be confirmed in larger studies with long-term follow-up.

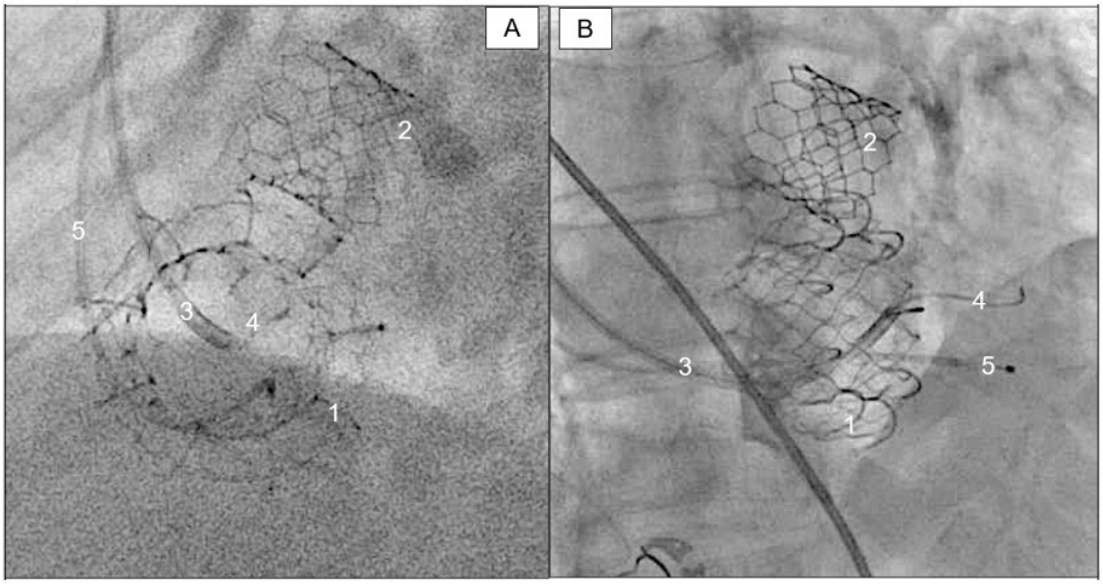

Figure 1: Peri-interventional X-ray images in LAO 40° (depicted in A) and RAO 30° (depicted in B). 1 = tricuspid valve prosthesis, 2 = aortic valve prosthesis, 3 = conduction system pacing sheath, 4 = guide wire, 5 = temporary pacemaker lead.

To cross the valve, a central position of the dedicated 3-dimensional CSP sheath and guide wire at the atrial site of the valve prosthesis was confirmed by x-ray in 2 planes (RAO ~30° and LAO ~40°) in order to obtain proper longitudinal and axial alignment with the valve prosthesis (Figure 1). Advancing the CSP sheath over the guide wire allowed atraumatic crossing of the valve prosthesis and prevented entanglement in the metallic struts. Left bundle branch area lead (LBBAP) implantation was aimed at least 5mm distal to the ventricular valve prosthesis cage. To avoid leaflet restriction final lead slack was judged in RAO ~30°.

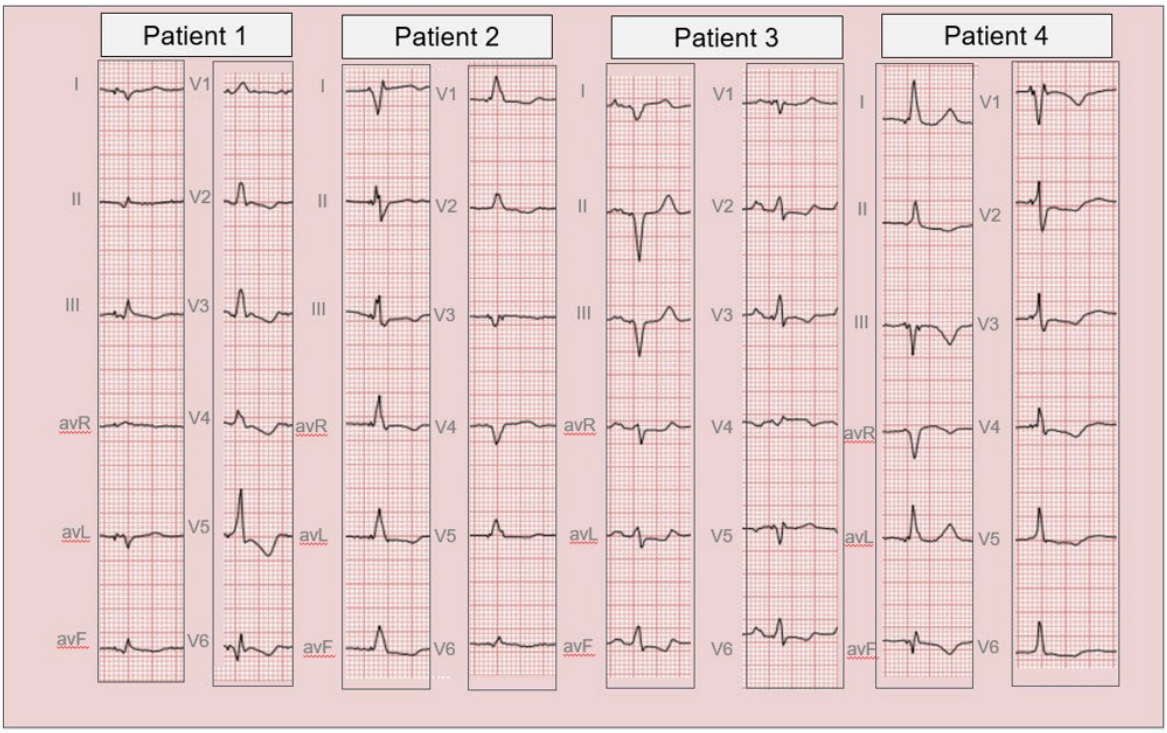

Figure 2: Presented are the post-interventional paced QRS complexes after optimizing the programming (paper speed is 25mm/second).

P063

Acquired tumoral coronary artery fistulas: a case report

Adel Younes[1], Stefano Caselli[1], Silvan Vesenbach[1], Marco Giacchi[1]

[1]*Hirslanden Klinik im Park, Zürich, Switzerland*

Introduction: Coronary artery fistulas (CAFs) are rare congenital or acquired malformation defects in the coronary system.

Material and Methods: 79-year-old patient, with a history clear cells renal carcinoma (ccRCC) and total nephrectomy in 2015, presented in 2022 with out-of-hospital cardiac arrest (OHCA) caused by subocclusive ostial left anterior descending artery (LAD) stenosis, which was treated with primary percutaneus coronary intervention (PCI). During cardiological follow-up cardiac-MRI and chest-CT scans revealed incidental findings of enlarged mediastinal lymph nodes and multifocal lung lesions. Further diagnostic workup was recomended, but denied by the patient.In early 2024 the patient developed dyspnea NYHA II. A follow-up coronary angiogram showed a patent stent in the LAD. However, by late 2024, with worsening dyspnea and evidence of lateral ischaemia on stress echocardiography, a repeat angiogram was performed. While the coronary anatomy remained stable, newly developed CAFs were incidentally detected from the circumflex and right coronary arteries draining into the left lung. Retrospective analysis of the early 2024 angiogram revealed the CAFs were already present but minimally visible.

Results: Thorax CT and biopsy confirmed the histological diagnosis of a large ccRCC-metastasis, prompting initiation of a tyrosine kinase inhibitor therapy (Axitinib). The CAFs were determined to be part of the angiogenic tumoral development. Treatment of the tumor could potentially involved coiling of the fistulas, which may offer a dual benefit by reducing tumor growth and mitigating the “steal phenomenon” under exertion, thereby alleviating ischemic effects on the coronary arteries.

Conclusion: Coiling of tumoral CAFs could potentially provide significant prognostic and symptomatic benefits.

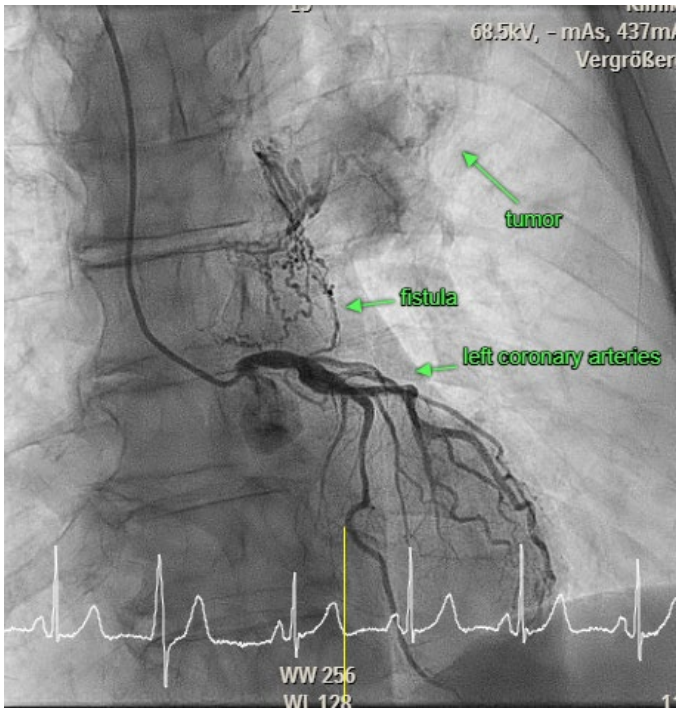

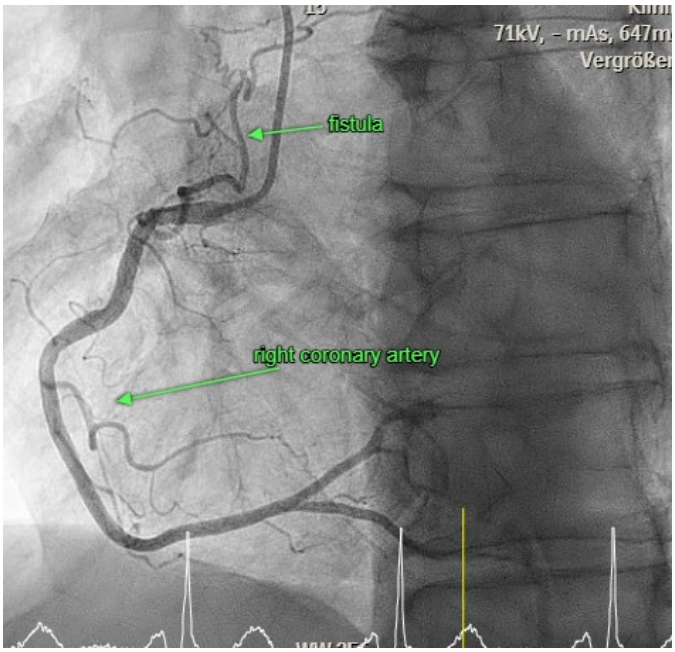

P064

The myocardial bridge: a rare cause of effort angina treated surgically

Filip Dulguerov[1], Samuel Khatchatourov[1], Dilan Lemarchal[1], Lucian Ion[1], Matthias Kirsch[1]

[1]CHUV, Lausanne, Switzerland

Introduction: Intramyocardial left anterior descending arteries (LAD) are rare vascular anomalies where the LAD penetrates the myocardium, potentially causing ischemia and leading to symptoms like effort angina. Diagnosing this condition can be challenging, particularly in the absence of electrocardiographic changes. This case report discusses a 50-year-old healthy male patient with effort angina diagnosed with an intramyocardial LAD, and treated with surgical release of the myocardial bridge.

Material and Methods: A 50-year-old male presented with recurrent effort-induced angina but had no associated electrocardiographic abnormalities or troponin elevation. A comprehensive diagnostic workup, including transthoracic echocardiography, cardiac MRI, and coronary angiography, was performed. These imaging modalities were used to identify the intramyocardial LAD and to assess its role in the patient's symptoms. Given the rare nature of the condition and the patient's young age, surgical intervention was chosen. The surgical technique for the release of the myocardial bridge was video-documented.

Results: Cardiac imaging confirmed the presence of an intramyocardial LAD, with the artery coursing through the myocardium, likely causing localized ischemia during exertion. Coronary angiography showed no performed, with no immediate complications. The patient experienced significant symptom relief post-operatively and remained asymptomatic during follow-up, with no recurrence of angina.

Conclusion: Intramyocardial left anterior descending arteries are a rare but important cause of effort angina, especially in young, otherwise healthy individuals. Advanced imaging is crucial for diagnosis, and surgical release of the myocardial bridge can provide effective treatment. This case, illustrated by a detailed surgical video, highlights the importance of recognizing this rare condition and the efficacy of surgical intervention in relieving symptoms.

P065

Aorto-left ventricular tunnel or coronary cameral fistula, that is the question.

Giulia Scopetani[1], Cristiana Voicu[2], Nawal Dakka[2], Milan Prsa[2], René Prêtre[1]

[1]Department of Cardiovascular Surgery, CHUV, Centre Hospitalier Universitaire Vaudois and University of Lausanne (UNIL), Lausanne, Switzerland, [2]Division of Pediatric Cardiology, Department of Women, Mother and Child, Lausanne University Hospital, Lausanne, Switzerland

Introduction: Aorto-left ventricular tunnel (ALVT) and coronary cameral fistula (CCF) are rare congenital cardiac malformations that can be challenging to differentiate. ALVT is an extracardiac channel connecting the ascending aorta to the left ventricular cavity, bypassing the semilunar hinge. CCF, on the other hand, is an abnormal connection between a coronary artery branch and a cardiac chamber.

Material and Methods: We present a case of a male newborn at 38 weeks gestation. Initial postnatal echocardiography and cardiac CT revealed an ambiguous diagnosis between ALVT and CCF, associated with critical valvar aortic stenosis. He underwent urgent surgical intervention.

Results: Surgical exploration confirmed an aneurysm emerging beneath the aortic annulus, displacing the right ventricular infundibulum. A commissurotomy and shaving of the right coronary (RC) and non-coronary leaflets were performed to improve valve function. The aortic side of the communication presented a large orifice that displaced the RC ostium, which originated from the tunnel without tortuosity. The ventricular opening was identified in the fibrous triangle beneath the left-right coronary commissure, lacking an intramyocardial course. This finding excluded CCF. The ventricular component was closed using a xenopericardium patch. Closure of the aortic orifice required cutting the RC ostium and sinus reconstruction using tunnel tissue. Moderate residual aortic stenosis and mild regurgitation were deemed acceptable postoperatively.

Conclusion: ALVT and CCF are rare congenital cardiac lesions that require prompt surgical intervention to prevent heart failure and associated complications. ALVT repair is technically more challenging. The absence of coronary tortuosity and intramyocardial tracts rather than CCF.

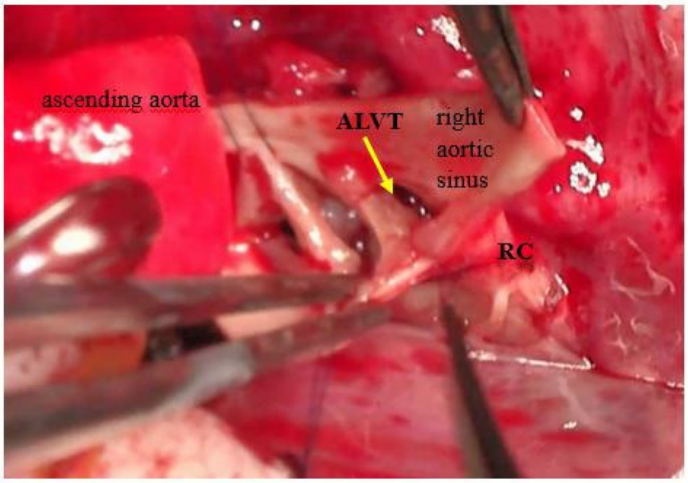

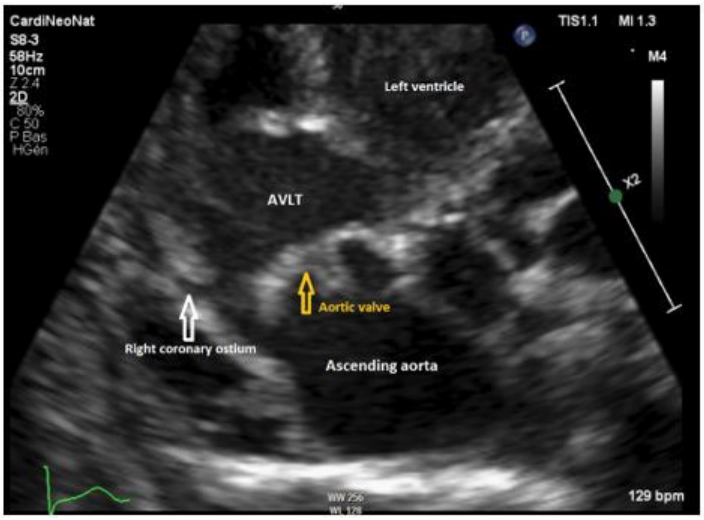

P066

Pyoderma Gangrenosum after Aortic Dissection repair: a challenging case

Christian-Jean Sordet[1], Sebastien Colombier[1], Sandra Bommeli[1], Nicolas Balagué[2], Laurent Parmentier[3], Dominique Delay[1]

[1]Service de Chirurgie cardiaque, Hôpital du Valais, Sion, Switzerland, [2]Service de Chirurgie Plastique, Hôpital du Valais, Sion, Switzerland, [3]Service de Dermatologie, Hôpital du Valais, Sion, Switzerland

Introduction: Pyoderma gangrenosum (PG) is a rare non-infectious inflammatory neutrophilic dermatosis characterized by destructive, necrotizing skin ulcers. PG is observed in association with immune disease and can appear on the wounds after surgery.

Material and Methods: We present the case of a 57-year-old male patient, admitted in the emergency department for acute chest pain. CT-scan revealed a Stanford type A De Bakey type I aortic dissection. Patient underwent an emergent ascending and hemi-arch aortic replacement with a hybrid AMDS stent, under mild hypothermia and semi-selective brain perfusion through subclavian and femoral cannulation. Surgery and immediate post-operative course were uneventful. On post-operative day-6, the patient developed cutaneous vesicles on the femoral cannulation site, followed few days later, by appearance of the same lesions on sternal and right subclavian wounds. Since the patient was very thin sternal bone was rapidly exposed. Infective complication was suspected. Sternal wires were extracted followed by implantation of vacuum-assisted closure dressings (VAC) for each wound. Since all microbiological samples remained sterile, immune disease was incriminated and Pyoderma gangrenosum diagnosis confirmed by cutaneous biopsy analyses.

Results: Methylprednisolone was introduced under antibiotical protection and VAC dressings were replaced twice a week. Clinical improvement of the wounds was observed. After 2 weeks, the sternum was closed with double musculocutaneous pectoralis major flap and two large cutaneous flaps to reduce skin tension. However, the patient subsequently experienced recurrent sternal wound dehiscence and partial necrosis of the skin graft, necessitating additional surgical interventions. Large antibiotical coverage, prednisone and ciclosporine were administrated. After several debridements of the sternal wound and a prolonged VAC dressing therapy, the surgical site showed gradual improvement allowing the patient to leave the hospital 2 months postoperatively.

Conclusion: Mimicking skin infection, PG is frequently misdiagnosed after surgery, with the result of correct immunosuppressive therapy introduction often being delayed.

P067

Case Report of Pickering Syndrome secondary to Seronegative Immune Mediated Necrotizing Myopathy

Theo Meister[1], Julija Bienz[1], Rodrigo Soria Maldonado[1], Martina Boscolo[1], Emrush Rexhaj[1]

[1]Department of Cardiology and BioMedical Research, University Hospital of Bern, Bern, Switzerland

Introduction: Immune-mediated necrotizing myopathies (IMNM) are rare types of idiopathic inflammatory myopathies (IIM) characterized by severe proximal muscle weakness and muscle fiber necrosis with a paucity of inflammatory cells in skeletal muscular biopsy. Serologically, IMNM are further classified into 3 subtypes based on the presence or absence of two specific autoantibodies: the anti-3-hydroxy-3-methylglutaryl coenzyme A reductase (HMGCR) and the anti-signal recognition particle (SRP). Especially the seronegative form in which both HMGCR and SRP autoantibodies are undetectable, exhibits a higher risk of various extra skeletal muscle involvement, including cardio-myositis. Nevertheless, severe cardiac involvement remains an extremely rare yet potentially life-threatening clinical manifestation of seronegative IMNM with only three adult cases described previously (Tab. 1).

Material and Methods: A 59-year-old male previously diagnosed with seronegative IMNM presented with severe hypertension and acute cardiac decompensation. On initial echocardiography, cardiac function was globally reduced with signs of eccentric left ventricular hypertrophy. Coronary angiography was normal, but cardiac magnetic resonance scan found diffuse intra-myocardial edema (Fig. 1). The patient was suspected of having IMNM associated cardio-myositis and was started on RAAS inhibitors, Beta blockers, diuretics and SGLT2i. In parallel, his immunosuppressive treatment with corticosteroids and azathioprine was increased. Under this new regiment, the patient rapidly developed acute renal failure caused by bilateral renal artery stenosis

Results: After successful stenting of the stenotic arteries, cardiac and renal function significantly improved, and at one-year follow-up, no more signs of myocardial edema or inflammation were found in the magnetic resonance study

Conclusion: Here, we describe a new case of acute congestive heart failure facilitated by severe reno-vascular hypertension in a patient with seronegative IMNM. This case highlights the importance of early recognition and treatment of elevated blood pressure in IMNM patients to avoid major adverse cardiac events

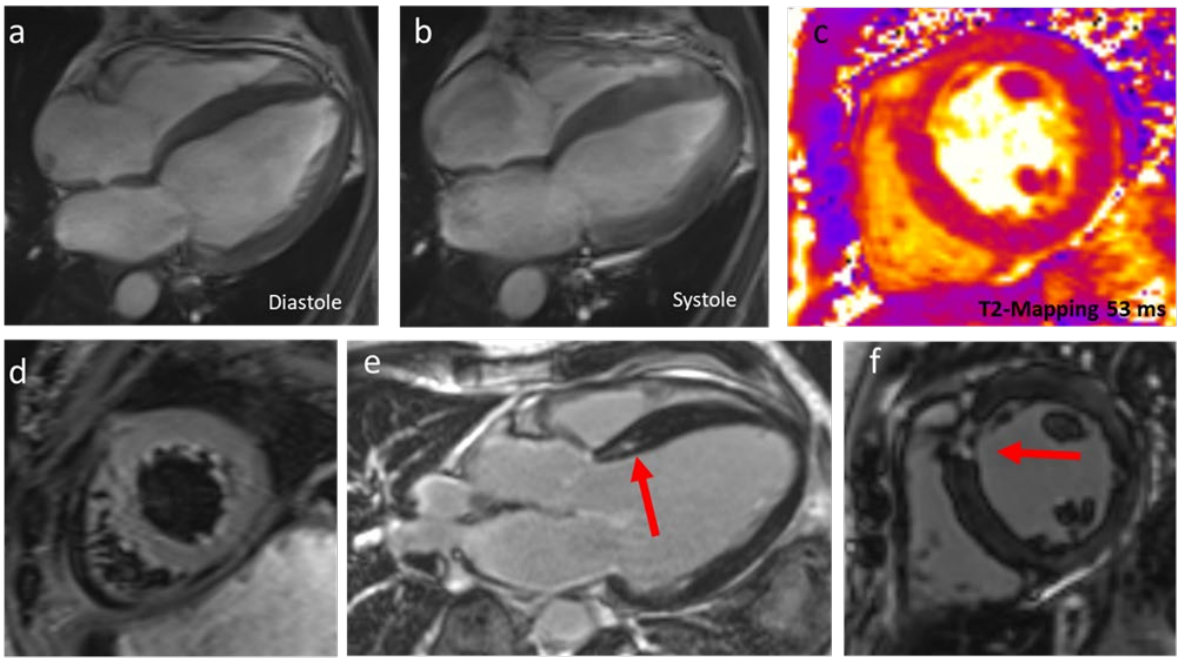

Figure 1. Cardiac magnetic resonance sequences at baseline: cine-sequence of the four chambers view in end-diastole and end-systole (panel a and b) show a dilatation of the left ventricle with reduced systolic function, EF 39%, end diastolic volume 266 ml. Increased native T2-signal (panel c) and hyperintense signal in Short Tau Inversion Recovery - STIR (panel d) to be ascribed and interpreted as diffuse myocardial edema and myocardial inflammation. Late gadolinium enhancement sequences – LGE show mid-wall fibrosis in the basal anteroseptum (red arrow) visible in the three chambers long-axis (panel e) and short-axis view (panel f).

Table 1. Characteristic of patients with seronegative IMNM and cardiac involvement

Case-Report	Age	Sex	Symptoms	Blood pressure	Echocardiography	Cardiac magnetic resonance	Cardiac biopsy
(Glenn-Cox et al., 2020)	74	Man	General malaise with chest pain, shortness of breath and peripheral edema	Not reported	EF was normal, abnormal septal motion consistent with left bundle branch block	Dis-coordinated right ventricle contraction with septal regional wall motion abnormality and small pericardial effusion. No LGE	Not reported
(Tsang et al., 2022)	30	Woman	Persistent chest pain, fatigue and diffuse myalgias	Not reported	EF 32% with global hypokinesis	Diffuse patchy LGE of the midwall of left ventricle	Mononuclear myocarditis with active myocyte injury and patchy fibrosis replacing myocytes
(Srivatsav et al., 2023)	46	Man	Fatigue, myalgias, palpitations	164/97 mmHg	EF 45-50%, hypokinesis of the basal inferolateral wall	LGE of the basal inferolateral wall of left ventricle, left ventricle mid-myocardial scarring EF 44% with mild global hypokinesis.	Not performed

EF= ejection fraction; LGE=left gadolinium enhancement

POSTER WALK "CORONARY ARTERY DISEASE AND ACUTE CARDIAC CARE 2"

P068

Can Artificial Intelligence outperform Humans in Detecting Coronary Occlusions in real life challenging ECGs ?

Aurelia Zimmerli[1], Marion Dupre[1], C-Yasmine Sellah[1], David Meier[1], Adil Salihu[1], Quentin Liabot[1], Victor Weerts[1], Vladimir Rubimbura[1], Olivier Roux[2], Olivier Muller[1], Pierre-Nicolas Carron[3], Olivier Hugli[3], Stephane Fournier[1]

[1]Department of Cardiology, Lausanne University Hospital and University of Lausanne, Lausanne, Switzerland, [2]Herzzentrum im Park, Hirslanden Klinik im Park, Zurich, Switzerland, [3]Department of Emergency, Lausanne University Hospital and University of Lausanne, Lausanne, Switzerland

Introduction: Occlusion myocardial infarction (OMI) on the ECG can present as STEMI, NSTEMI, ST depression, or other patterns (e.g., de Winter T-waves, hyperacute T waves), posing a diagnostic challenge. Even experienced physicians may overlook OMI on ECG, leading to delays in catheterization laboratory activation. Recently, smartphone applications utilizing artificial intelligence (AI) have been shown to exhibit a promising accuracy in ECG interpretation in large datasets. The aim of our study was to retrospectively compare the diagnostic performance of an AI-based application (PMCardio®) with that of interventional cardiologists in interpreting non-pathognomonic ECGs that generated debates about diagnosis.

Material and Methods: In total, 33 ECGs that were diagnostically challenging upon patient admission to the emergency department were included. A group of 3 interventional cardiologists, blinded to the final diagnosis, independently assessed whether the ECG suggested CO requiring immediate invasive coronary angiography. The diagnostic performance of the cardiologists was compared to that of the AI application, with the final diagnoses as gold standard.

Results: Overall, 88% of patients had a final diagnosis of cardiac origin for their chest pain, including 23 acute coronary syndromes, of which 13 (57%) involved complete vessel occlusion (Figure 1). The 3 cardiologists achieved sensitivities of 62-85-62%, negative predictive values (NPVs) of 74-83-69%, specificities of 70-50-55%, and positive predictive values (PPVs) of 57-52-47%, respectively. Their overall misclassification rates were 33-36-42%. In contrast, AI analysis demonstrated a sensitivity and NPV of 100%, a specificity of 60%, a PPV of 62%, and an overall misclassification rate of 24%, outperforming interventional cardiologists (Figure 2).

Conclusion: In this retrospective study based only on challenging ECGs, an AI application demonstrated a sensitivity and NPV of 100% in identifying ECGs indicative of OMI, underscoring its reliability for clinical use. These findings highlight the potential of AI to enhance diagnostic accuracy and support clinical decision-making.

Figure 1.

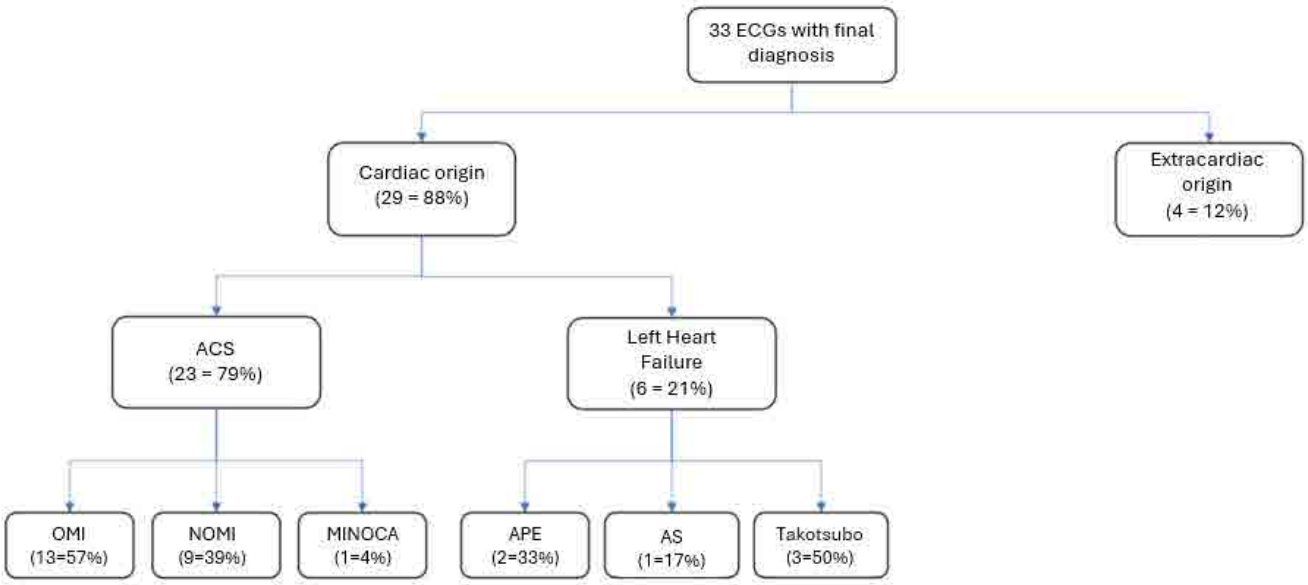

Figure 2.

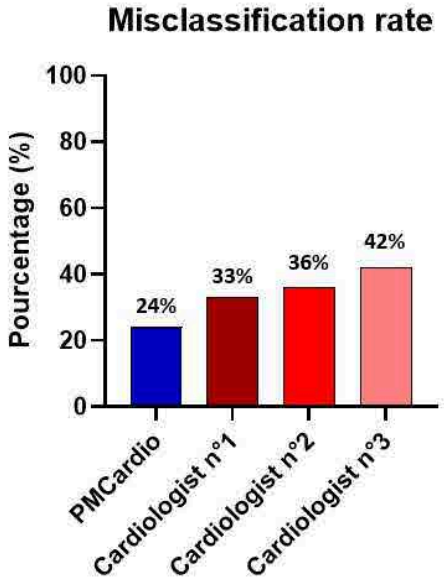

P069

Characterizing silent plaque ruptures in non-infarct related vessels of patients with AMI: a pooled, multimodality, serial intracoronary imaging study

Ryota Kakizaki[1], Flavio Biccirè[1], Yasushi Ueki[1], Sylvain Losdat[2], Georgios Siontis[1], Stefan Stortecky[1], Jonas Häner[1], Thomas Engstrøm[3], Irene Lang[4], Konstantinos Koskinas[1], Lorenz Räber[1]

[1]Bern University Hospital, Inselspital, University of Bern, Bern, Switzerland, [2]CTU Bern, University of Bern, Bern, Switzerland, [3]Rigshospitalet, Copenhagen University Hospital, Copenhagen, Denmark, [4]Medical University of Vienna, Vienna, Austria

Introduction: Plaque rupture is the predominant etiology of acute myocardial infarction (AMI) and may also occur at non-obstructive lesions in non-infarct related coronary arteries (non-IRAs) without inducing acute ischemia (i.e. silent plaque rupture). The purpose of this study was to (1) assess the frequency and characteristics of lesions with plaque rupture in non-IRAs among AMI patients, (2) evaluate morphological changes of plaque rupture in 52 weeks, and (3) investigate the baseline plaque morphology of new-onset silent plaque ruptures at 52 weeks.

Material and Methods: The present study analyzed pooled data from the IBIS-4 (NCT00962416) and PACMAN-AMI trial (NCT03067844). Patients presenting with AMI and non-obstructive lesions in non-IRAs underwent optical coherence tomography (OCT) and intravascular ultrasound (IVUS) imaging at baseline and after 52 weeks. Plaque rupture was defined as intimal disruption with cavity in OCT. An IVUS-derived lesion was defined as plaque burden ≥40% with longitudinal extension of ≥3 mm.

Results: Among 783 lesions from 323 patients evaluated by OCT at baseline, 46 rupture sites were identified in 41 lesions (5.2%) of 40 patients (11.9%). Lesions with plaque rupture had larger percent atheroma volume as assessed by IVUS (53.3±6.4% vs. 49.5±5.8%, P<0.001) and thinner minimum fibrous cap thickness in OCT (69±49 µm vs. 116±84 µm, P = 0.010) compared to those without (Figure). Among 41 rupture sites in 38 lesions with serial intracoronary imaging, 21 (51.2%) healed at 52 weeks. At 52 weeks, 10 rupture sites in 10 lesions were newly detected, and thin-cap fibroatheroma (TCFA) was the most frequent baseline plaque morphology of new-onset plaque rupture.

Conclusion: OCT-detected plaque ruptures in non-IRAs were observed in one out of 10 AMI patients at the index event. Lesions with plaque rupture had larger plaque burden and thinner fibrous cap. TCFA was the most frequent underlying plaque morphology of new-onset silent plaque rupture during one-year follow-up.

Comparison of the intracoronary imaging findings between lesions with versus without plaque rupture

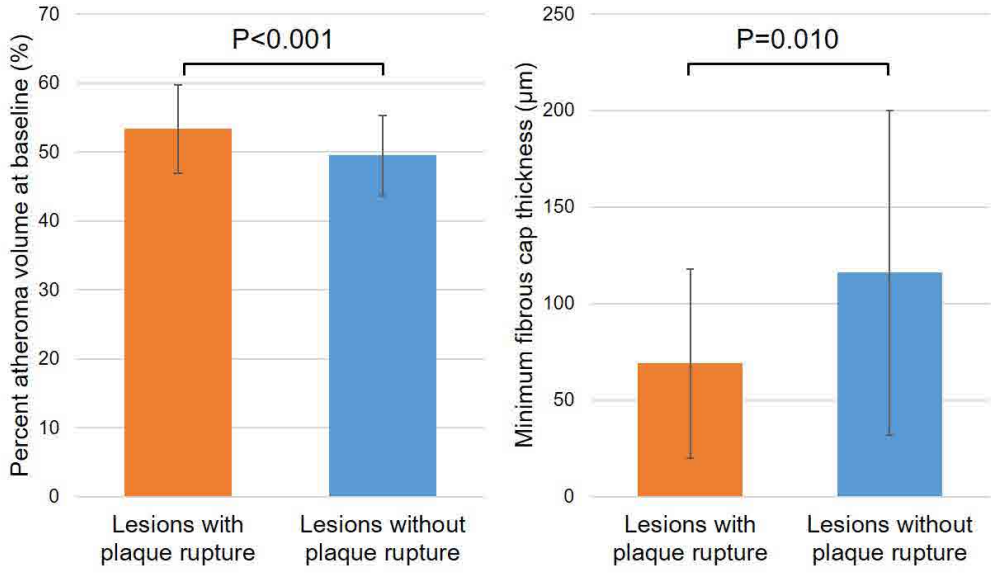

P070

Diagnostic Accuracy of Angiography-Derived Murray Law-Based Quantitative Flow Ratio (μQFR) Versus Pressure-Derived Fractional Flow Reserve (FFR) in Moderate to Severe Calcified Coronary Lesions – The DIAMOND Study

Wesley Bennar[1], Diego Arroyo[1], Charline Oppe[1], Dorian Garin[1], Laure Allemann[1], Thais Pittet[1], Pascal Meier[1], Puricel Serban[1], Mario Togni[1 2], Stéphane Cook[1 2]

[1]Hôpital Fribourgeois, Fribourg, Switzerland, [2]Clinique CECIL, Lausanne, Switzerland

Introduction: Murray law-based Quantitative Flow Ratio (μQFR) is a novel AI-assisted two-dimensional modality for physiological lesion evaluation based on contrast flow velocity estimates. This approach enables physiological assessment of coronary lesions, without requiring a pressure wire or hyperemia induction. However, the accuracy of μQFR compared to Fractional Flow Reserve (FFR) for evaluating calcified lesions (ACC/AHA classification type B2 or C) has not been adequately studied to date. This study aimed to determine the accuracy of μQFR in detecting hemodynamically significant calcified coronary stenosis, defined as FFR ≤ 0.80.

Material and Methods: This two-center, investigator-initiated trial included patients with at least one calcified lesion (type B2 or C) with 30% to 90% diameter stenosis and FFR assessment performed during coronary angiography. μQFR was computed for all eligible lesions by a trained nurse blinded to FFR results. The study compared the sensitivity and specificity of μQFR with FFR as the gold-standard.

Results: A total of 125 patients were enrolled, and paired assessments of μQFR and FFR were available for 107 patients and 120 lesions. The mean FFR, μQFR, and percent diameter stenosis were 0.775 (95% CI: 0.757–0.793), 0.788 (95% CI: 0.772–0.805), and 56.75% (±10.14%), respectively. Among the lesions, 84 (70%) had an FFR ≤ 0.80. The sensitivity of μQFR for detecting hemodynamically significant stenosis was 75% (95% CI: 65.6%–84.6%), and its specificity was 77.8% (95% CI: 63.5%–92.0%). Diagnostic precision was 75.8% (95% CI: 68.1%–83.6%), with an area under the receiver operating characteristic curve of 0.80 (95% CI: 0.720–0.886). The positive predictive value was 88.7%, and the negative predictive value was 57.1%. Positive and negative likelihood ratios were 3.38 and 0.32, respectively.

Conclusion: μQFR is simple to compute and offers moderate sensitivity, specificity, and accuracy for detecting significant calcified coronary stenosis. It provides an alternative when FFR is unavailable or challenging to perform.

Table 1:

Diagnostic Consistency Between FFR and μQFR for Identifying Hemodynamically Significant Stenosis:		
	FFR > 0.8	**FFR ≤ 0.8**
QFR > 0.8	28/120 (23.3%)	21/120 (17.5%)
QFR ≤ 0.8	8/120 (6.7%)	63/120 (52.5%)
Difference between μQFR and FFR:		
>0.05	48/120 (40%)	
>0.10	25/120 (20.8%)	
Diagnostic Performance of μQFR With FFR as a Reference:		
Accuracy	75.83% (68.06% – 83.60%)	
Sensitivity	75.00% (65.55% – 84.55%)	
Specificity	77.78% (63.51% – 92.04%)	
Positive Predictive Value (PPV)	88.73% (81.19% – 96.27%)	
Negative Predictive Value (NPV)	57.14% (42.78% – 71.50%)	
Positive Likelihood Ratio (+LR)	3.38 (1.80 – 10.62)	
Negative Likelihood Ratio (–LR)	0.32 (0.17 – 0.54)	

Figure 1: Representative images of Murray law-based quantitative flow ratio (μQFR) and FFR analysis in coronary lesions.

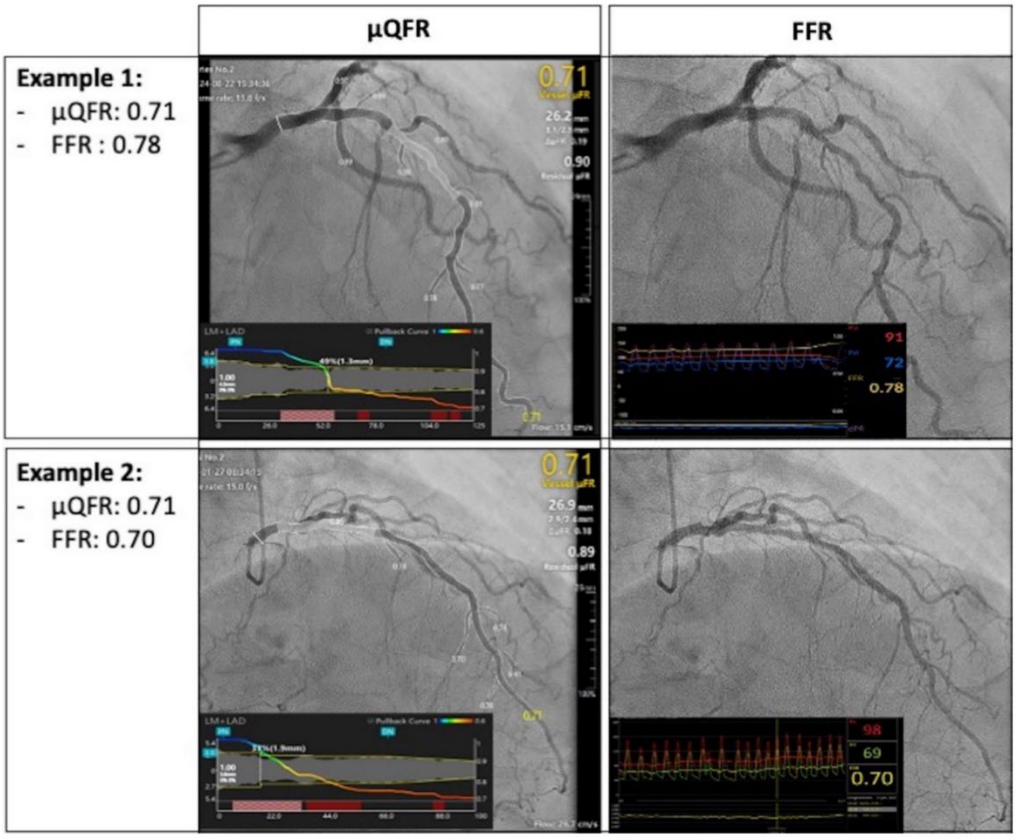

P071

Rationale and Development of the Computed Tomography Simulated Pressure Loss Index (CTSPLI) for non-invasive phenotyping of coronary atherosclerosis

Andreas Giannopoulos[1], Dimitrios Moysidis[1], Dominik C. Benz[1], Aju Pazhenkottil[1], Philipp Kaufmann[1], Ronny Büchel[1]

[1]Clinic of Nuclear Medicine, Department of Cardiac Imaging, University Hospital of Zurich, Zurich, Switzerland

Introduction: Combining coronary CT angiography (CCTA) and computational fluid dynamics offers promising non-invasive alternatives for functional assessment of coronary artery disease (CAD). We describe the rationale and development of the Computer Tomography Simulated Pressure Loss Index (CT_{SPLI}), a non-invasive computational metric based on CT_{FFR} that can objectively phenotype CAD at the coronary artery level.

Material and Methods: CT_{SPLI} was developed in 15 healthy individuals who underwent CCTA and PET-myocardial perfusion imaging and were characterized by lack of atherosclerotic plaques, normal endothelium-dependent-(cold pressor test-induced hyperemia), and endothelium independent-(adenosine-induced hyperemia) vasodilatation and hence normal epicardial coronaries and microvasculature. In these individuals, CT_{FFR} analysis identified functional disease as regions with FFR drop of ≥0.0015/mm. CT_{SPLI} was then calculated by combining the length of functional disease with the magnitude of pressure loss along the artery. CT_{SPLI} provides a quantitative assessment of the flow resistance distribution in epicardial coronaries, where lower values (approaching 0) indicate diffuse CAD and higher values (approaching 1) focal CAD.

A second cohort of 29 patients undergoing CCTA and CT_{FFR} due to suspected obstructive CAD was retrospectively enrolled for the clinical investigation of CT_{SPLI}. Coronaries were phenotyped as having focal, diffuse of mixed CAD patterns based on a. visual assessment of the distribution of plaques and CT-FFR pullback patterns and b. using CT_{SPLI}.

Results: A total of 76 arteries (LAD: 36, LCX: 19, RCA: 21) from 29 patients were analyzed. Expert visual assessment based on anatomy and CT-FFR classified 21 arteries as focally diseased, 46 as diffusely diseased and 9 with mixed pattern. CT_{SPLI}-derived physiology led to reclassification of a total of 46 arteries (57.8%) with 42% of focal disease reclassified to a diffuse or mixed pattern, whereas 24% of diffuse disease was reclassified as functional focal CAD.

Conclusion: CT_{SPLI} can effectively and objectively phenotype CAD patterns, potentially enabling non-invasive personalization of management and revascularization strategies.

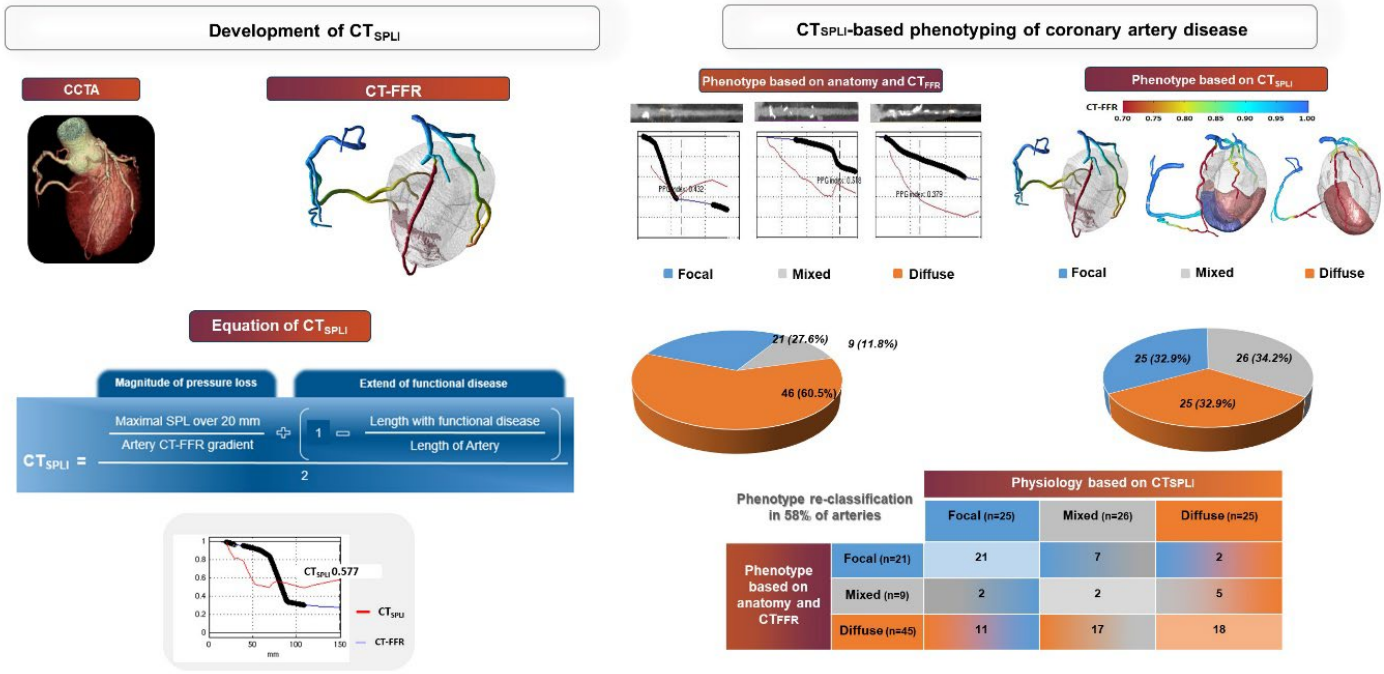

P072

Comparison of the 2024 European Society of Cardiology risk-factor clinical likelihood model and an artificial intelligence-based tool for ischemia detection in patients with suspected chronic coronary syndrome referred for 82Rb-PET

Simon Frey[1 2], Igor Schneider[1 2], Ann-Sophie Otto[1 2], Florian Geiser[1 2], Damian Wild[3], Andrew Tsirkin[4], Caroline György[4], Peter Ruff[4], Philip Haaf[1 2], Felix Mahfoud, Christian Müller, Michael Zellweger[1 2]

[1]University Heart Center, University Hospital Basel, Basel, Switzerland, [2]Cardiovascular Research Institute Basel (CRIB), Basel, Switzerland, [3]Division of Nuclear Medicine, University Hospital Basel, Basel, Switzerland, [4]Exploris Health, Wallisellen, Switzerland

Introduction: Patients are referred to coronary artery disease (CAD) testing based on their pre-test probability (PTP). The novel risk factor-weighted clinical likelihood (RF-CL) proposed by the 2024 ESC guidelines on chronic coronary syndromes (CCS) uses symptoms, age, sex and risk factors. Artificial intelligence-based (AI) tools can incorporate many more variables, and could therefore improve PTP assessment. Study aim was to compare a novel AI tool with the RF-CL model.

Material and Methods: RF-CL and a memetic pattern-based algorithm (MPA) were applied to 1657 consecutive patients with suspected CCS referred for ^{82}Rb-Positron Emission Tomography (PET). Distribution across risk groups, receiver operator curve and test characteristics were calculated. Endpoints were defined as small ischemia (Summed Difference Score ≥2) and relevant ischemia (≥10% of myocardium).

Results: Mean age of the patients was 65±11 years; 43% were female. Median RF-CL was 11% [6, 19], respectively. Typical and atypical angina were present in 20% and 25%, respectively. Small ischemia was observed in 19%, relevant ischemia in 9%. Distribution of patients across risk categories is shown in figure 1. For small ischemia, AUC was similar (RF-CL: 0.689 (0.658–0.720) vs. MPA 0.706 (0.676–0.736), p = 0.227). For relevant ischemia, AUC was significantly higher for the MPA: 0.698 (0.654–0.742) vs. 0.757 (0.721–0.793), p = 0.004. As shown in table 1, sensitivity and negative predictive value (NPV) were higher for the MPA model.

Conclusion: The MPA model showed a significantly better discriminatory power for detection of relevant ischemia in patients with suspected CCS compared to the proposed RF-CL model. In addition, relevant ischemia could be excluded with a very high degree of certainty. Tools using artificial intelligence should be used more frequently in daily routine for assessment of PTP.

Figure 1: Distribution across risk groups

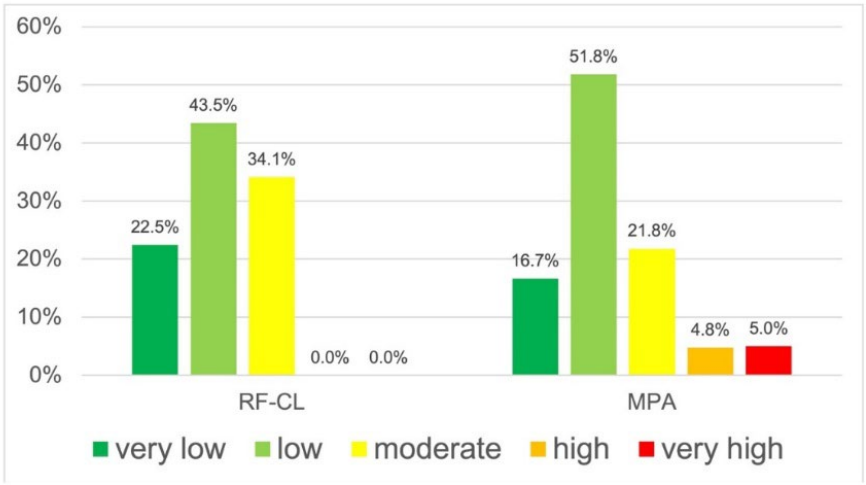

The bar chart indicates the distribution of patients across the different risk categories. Both, RF-CL and the memetic pattern-based algorithm (MPA), allocate the majority of patients in the low-risk category. RF-CL: risk factor-weighted clinical model.

Table 1: Test characteristics

		Sensitivity	NPV
Small ischemia	RF-CL	0.921 (0.886 - 0.946)	0.933 (0.903 - 0.954)
	MPA	0.962 (0.935 - 0.978)	0.957 (0.926 - 0.975)
Relevant ischemia	RF-CL	0.925 (0.870 - 0.957)	0.970 (0.948 - 0.983)
	MPA	0.993 (0.962 - 0.999)	0.996 (0.98 - 0.999)

Test characteristics to detect or exclude a small (SDS ≥2) or relevant (SDS ≥7) ischemia. NPV: negative predictive value. RF-CL: risk factor-weighted clinical model. SDS: summed difference score.

P073

Artificial Intelligence-Based Major Adverse Cardiovascular Events Prediction Using Multimodal Information: Time-to-Event Prognostic Modeling in Suspected Myocarditis Patients

Giovanni Baj[1], Pooya Mohammadi[1], Jonathan Schütze[1], Benedikt Bernhard[1], Georgios Siontis[1], Raymond Kwong[2], Isaac Shiri[1], Christoph Gräni[1]

[1]Inselspital, Department of Cardiology, Bern, Switzerland, [2]Noninvasive Cardiovascular Imaging Section, Cardiovascular Division, Department of Medicine and Department of Radiology, Brigham and Women's Hospital, Harvard Medical School, Boston, United States

Introduction: Myocarditis, marked by inflammation of the myocardium, varies widely in clinical phenotypes and outcomes. Yet, predicting patient outcomes remains challenging, as current methods and subjective assessments often fail to offer clear prognostic indicators. This study introduces a novel approach to predicting Major Adverse Cardiovascular Events (MACE) in myocarditis patients using multimodal data and artificial intelligence.

Material and Methods: A total of 665 patients diagnosed with suspected myocarditis based on current ESC criteria, recruited from two major registries (CMRMyo, FlamBeR) were included. We collected multimodal data such as CMR images, ECGs, clinical information, and lab tests from each patient at baseline. 1597 features were extracted and analyzed using a time-to-event machine learning (ML) pipeline for predicting the time to first MACE (i.e., death, sustained ventricular arrhythmia, heart failure hospitalization, and recurrent myocarditis). After applying z-score normalization, we removed features with high correlation. Various feature selection methods and survival time-to-event models were utilized. The development phase, including pre-processing, feature selection, and hyperparameter optimization, used 70% of the dataset, with the evaluation conducted on the remaining 30% hold-out test set. We assessed model performance using the c-index and cumulative AUC (C-ACU).

Results: The best-performing feature in univariate analysis achieved a C-index of 0.59. The conventional multivariate Cox-PH model reached a C-index of 0.72 and a C-AUC of 0.74. Key features selected during feature selection were primarily derived from CMR images, ECG, and clinical data. The top-performing model, ML survival support vector machine with a 90% variance threshold, achieved a C-index of 0.79 and a C-AUC of 0.83. This was closely followed by the Cox-Lasso model, which recorded a C-index of 0.78 and a C-AUC of 0.81.

Conclusion: Leveraging multimodal data, including imaging, signal, laboratory, and clinical information, with ML algorithms allows more accurate prediction of MACE in suspected myocarditis patients comparwed to single features and conventional models.

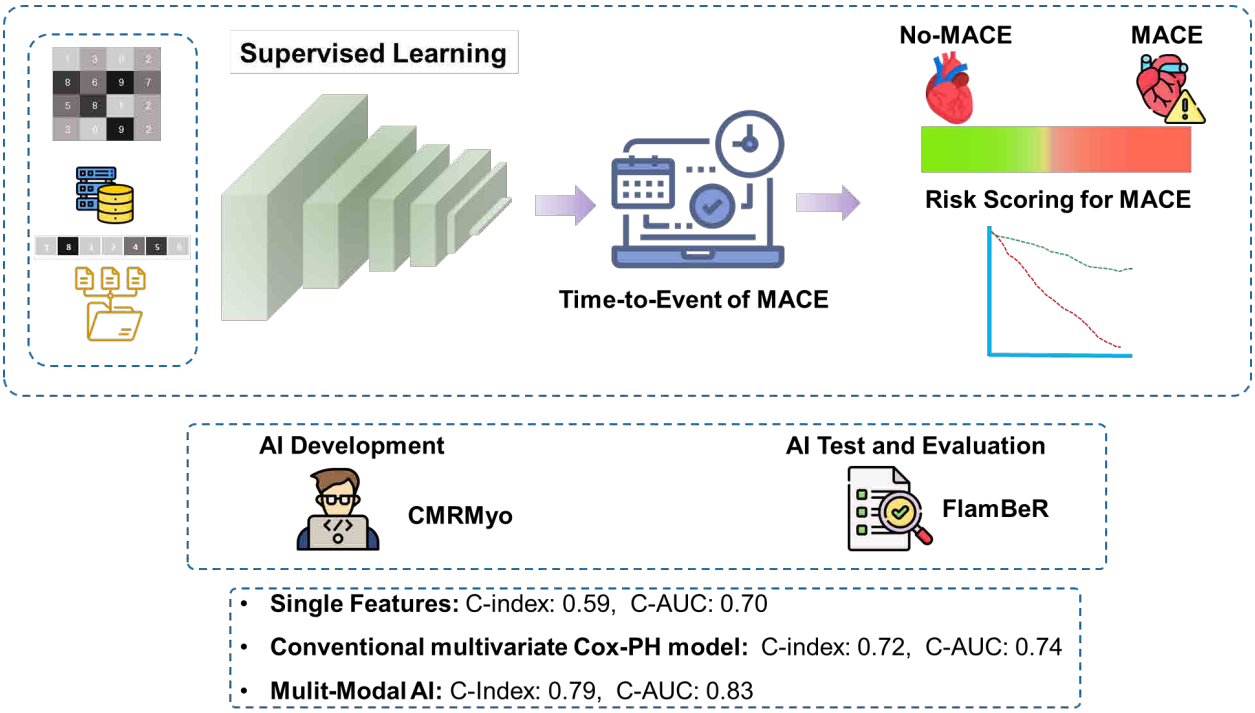

P074

Impact of FFR-CT before coronary angiography on the management of non-culprit lesions among high-risk NSTE-ACS patients

Aurelia Zimmerli[1], David Meier[1], Adil Salihu[1], Daniele Andreini[2], Thabo Mahendiran[1], David Rotzinger[1], Georgios Tzimas[1], Bernard De Bruyne[3], Carlos Collet[3], Olivier Muller[1], Stephane Fournier[1]

[1]Department of Cardiology, Lausanne University Hospital and University of Lausanne, Lausanne, Switzerland, [2]Department of Clinical and Biomedical Sciences, IRCCS Ospedale Galeazzi Sant'Ambrogio, University of Milan, Milan, Italy, [3]Cardiovascular Center Aalst, OLV Clinic, Aalst, Belgium

Introduction: This prespecified secondary analysis of a multicenter, single-arm, double-blinded, core-lab adjudicated study, evaluates the potential role of fractional flow reserve derived from coronary computed tomography (FFR-CT) in managing non-culprit lesions in high-risk non-ST-elevation acute coronary syndrome (NSTE-ACS) patients. The management of intermediate lesions remains challenging. This study investigates the diagnostic accuracy of FFR-CT compared with invasive FFR as the gold standard.

Material and Methods: Patients with an identified culprit lesion and at least one additional stenosis ≥30% in another vessel were eligible. This study included 49 patients with 67 non-culprit lesions from the initial cohort of 168 patients. These patients presented with chest pain and elevated high-sensitivity troponin (hs-Tn) levels, underwent coronary computed tomography angiography (CCTA), and subsequently ICA. For both FFR-CT and ICA, hemodynamically significant lesions were defined as having an FFR value of ≤0.8. The primary endpoint was the negative predictive value (NPV) of FFR-CT in ruling out hemodynamically significant lesions in non-culprit vessels. Secondary endpoints included sensitivity, specificity, positive predictive value (PPV), and overall diagnostic accuracy of FFR-CT.

Results: Of the 67 non-culprit lesions assessed, FFR-CT classified 33 (49%) as non-significant and 34 (51%) as significant. The NPV of FFR-CT was 94%, with 31 out of 33 lesions classified as non-significant by FFR-CT and confirmed as non-significant by invasive FFR. For the 34 lesions deemed significant by FFR-CT, 26 were confirmed as positive by invasive FFR, yielding a PPV of 76%. FFR-CT demonstrated a sensitivity of 93% and specificity of 79%, resulting in an overall diagnostic accuracy of 85% (Figure 1).

Conclusion: This analysis highlights the potential of FFR-CT in supporting early decision-making for the treatment of non-culprit lesions in high-risk NSTE-ACS patients. The high negative predictive value of 94% underscores the ability of FFR-CT to rule out hemodynamically significant lesions, potentially reducing Unnecessary invasive coronary angiographies and procedures.

Figure 1. Diagnostic performance of FFR-CT as compared to invasive FFR for the evaluation of non-culprit lesions.

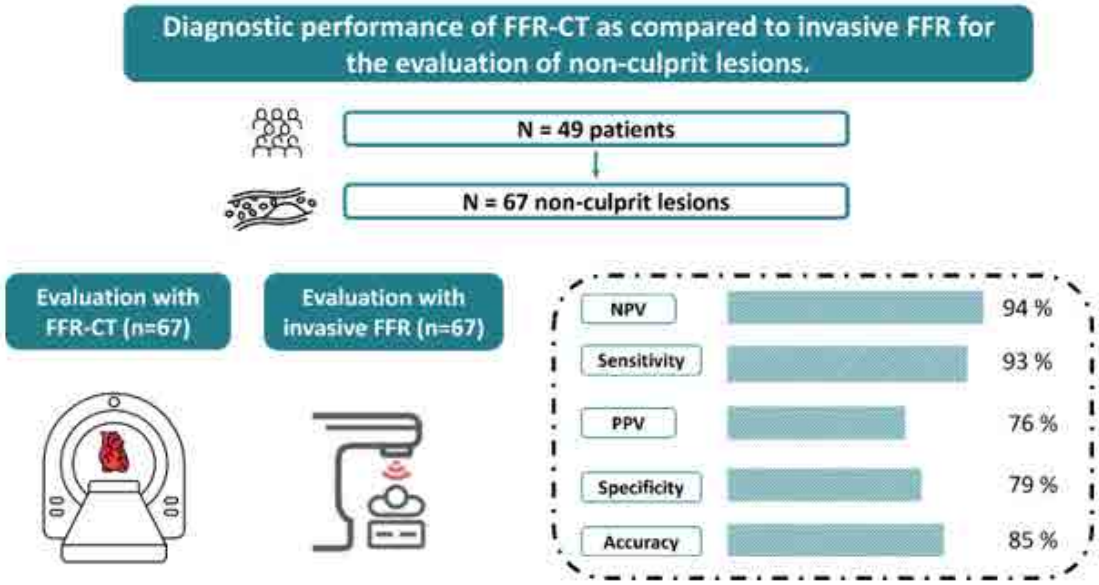

P075

A contemporary look into spontaneous coronary artery dissection: the SwissSCAD registry

Sophie Degrauwe[1], Gregor Fahrni[2], Christoph Kaiser[3], Marion Dupre[4], Stéphane Cook[5], Thomas Gillhofer[6], Marco Roffi[1], Franz Eberli[2], Daniel Weilenmann[7], Matthias Bossard[8], Dik Heg[9], Hans Rickli[7]

[1]Geneva University Hospitals, Geneva, Switzerland, [2]Triemli Hospital, Zurich, Switzerland, [3]Basel University Hospitals, Basel, Switzerland, [4]CHUV, Lausanne, Switzerland, [5]Fribourg Cantonal Hospital, Fribourg, Switzerland, [6]Kantonsspital Winterthur, Winterthur, Switzerland, [7]Kantonsspital St. Gallen, St. Gallen, Switzerland, [8]Heart Center – Luzerner Kantonsspital, Luzern, Switzerland, [9]University of Bern, Bern, Switzerland

Introduction: The primary objective of the SwissSCAD registry is to address contemporary characteristics, management and in-hospital major adverse cardiac events (MACE; defined as a composite of stroke/transient ischemic attack, reinfarction, repeat revascularization and in-hospital death) of patients presenting with spontaneous coronary artery dissection (SCAD) in Switzerland.

Material and Methods: We performed an investigator initiated, multicentre, retrospective and prospective observational study including patients with non-atherosclerotic SCAD in 8 centres in Switzerland. Institutional ethics approval and patient consents were obtained. We recorded baseline demographics, precipitating/predisposing conditions, angiographic features, baseline characteristics, as well as in-hospital treatment and MACE.

Results: From August 2020 to March 2024, 264 patients were enrolled. Mean age was 53.4±10.7 years, 85% were women. Cardiovascular risk factors included hypertension (32%), familial history of coronary artery disease (31%), hypercholesterolemia (25%), active smoking (23%), and diabetes mellitus (3%). Patients presented with STEMI in 35% and with NSTACS in 59% of cases. While all patients had coronary angiography, treatment was conservative in 97% of patients. Percutaneous coronary intervention was performed in 3% of patients, coronary artery bypass grafting was limited to 1 patient. In-hospital MACE occurred in 11% of patients with following distribution: stroke/TIA (4%), re-infarction (3%), repeat revascularization (2%), in-hospital death (2%). Dual antiplatelet therapy (DAPT) was prescribed in 55% of patients at discharge.

Conclusion: Contemporary SCAD patients are treated almost exclusively conservatively. In-hospital MACE rates are sizable, though in-hospital mortality is low.

P076

AI-enhanced fluoroscopy significantly reduces radiation doses in diagnostic coronary angiography

Lukas Altwegg[1], Christoph Kohler[1], Andreas Patz[2], Michael Zierler[1]

[1]St. Claraspital, Basel, Switzerland, [2]Canon Medical System Europe, Amstelveen, Netherlands

Introduction: Conventional cineangiography during diagnostic coronary angiography (DCA) and PCI provides high-resolution imaging at the cost of radiation dose exposure. AI-enhanced fluoroscopy may reduce reliance on cineangiography, thus lowering radiation exposure while maintaining diagnostic accuracy. This study evaluates deep learning-based AI fluoroscopy developed by Canon Medical Systems (αEvolve) in reducing the need for cine-acquisitions and hereby lowering radiation exposure in DCA.

Material and Methods: From December 2023 until October 2024 AI-enhanced fluoroscopy was evaluated in a prospec-

tive study comprising a total of n = 540 patients being referred to the cathlab at St. Claraspital, Basel. Out of this cohort we selected a group of patients with DCA solely (AI-cohort; n = 49) based on specific criteria allowing for comparison with a group of patients having had DCA in the year before AI was installed (PreAI-cohort; n = 58). As indicators of radiation exposure, we assessed radiographic frame counts and the dose area product (DAP).

Results: In this analysis of 107 patients, 55 % were male, the mean BMI was 27.4±5.6 kg/m² and median fluoroscopy time was 3.5min (IQR, 2.0 to 5.3). There were no significant differences in baseline characteristics between patients imaged with or without AI. For patients in the AI-group there were significantly fewer cine-runs (median frame count 220; IQR 170 to 330) compared with the PreAI-cohort (median frame count 441; IQR 369 to 544; p<0.0001). Similarly, the median DAP was significantly lower in patients with AI-imaging (1085.9 Gy/m²; IQR, 637.5 to 2344.6 vs. 1495.6 Gy/m²; IQR, 1058.3 to 2593.7; p<0.05). Besides BMI, gender and fluoroscopy time, AI-enhanced fluoroscopy was the main predictor of DAP (p<0.0001).

Conclusion: AI-enhanced fluoroscopy during SCA clearly reduced the need for cine-acquisition, resulting in significantly lower radiation doses compared to conventional imaging. This study highlights the potential of AI-based image enhancement in reducing radiation exposure in X-ray guided procedures.

POSTER WALK "PREVENTION, REHABILITATION & SPORTS CARDIOLOGY"

P077

Cannabis Use and Cardiac Structure and Function Assessed by Echocardiography: The Coronary Artery Risk Development in Young Adults Study (CARDIA)

Xeno Grunder[1], Allison Carroll[2], Chike Nwabuo[3], Baris Gencer[1 4], Joao Lima[3], Jamal Rana[5], Stéphanie Baggio[1 6], Stephen Sidney[7], Kali Tal[1], Reto Auer[1 8], Julian Jakob[1 9]

[1]University of Bern, Institute of Primary Health Care (BIHAM), Bern, Switzerland, [2]Northwestern University Feinberg School of Medicine, Chicago, Illinois, United States, [3]John Hopkins University, Baltimore, United States, [4]Cardiology Department, Lausanne University Hospital, Lausanne, Switzerland, [5]Kaiser Permanente Northern California, Department of Cardiology and Division of Research, Oakland, United States, [6]University of Fribourg, Laboratory of Population Health (#PopHealthLab), Fribourg, Switzerland, [7]Kaiser Permanente Northern California, Division of Research, Oakland, United States, [8]University of Lausanne, Center for Primary Care and Public Health (Unisanté), Lausanne, Switzerland, [9]University Hospital Bern, Inselspital, Department of Paediatrics, Bern, Switzerland

Introduction: Cannabis use is a rising public health issue. Given the impact of smoke exposure on cardiovascular health, it is pertinent to assess associations between cannabis use (current and cumulative) and clinical and subclinical cardiovascular disease (structure and function).

Material and Methods: We included 5,115 adults aged 18-30 years at baseline from the Coronary Artery Risk Development in Young Adults (CARDIA) Study, followed 30 years and with echocardiography at visit years 5, 25 and 30. We computed 4 categories of self-reported cannabis exposure: never users (index group), past users with <1 “cannabis year” exposure (1 cannabis-year = 365 days of use), past users with ≥1 cannabis year, and current users. We studied echocardiographic markers of cardiac structure: indexed to body surface area left ventricular mass (LVMi), left ventricular end-diastolic volume (LVEDVi), left ventricular end-systolic volume (LVESVi), left atrial area (LAAi); cardiac function: left ventricular ejection fraction (LVEF), longitudinal peak strain (EII), ratio of early diastolic mitral inflow velocity to early diastolic mitral annulus velocity (E/e’-ratio), and right ventricular systolic pressure (RVSP). We performed multivariable mixed models, adjusted for demographics, physical activity, cardiovascular risk factors, anti-hypertensive medication, alcohol, tobacco and illicit drugs use, with weights to account for informative censoring.

Results: 5,115 participants contributed to 8,783 individual echocardiography exams. At year 30 of the 3,046 participants undergoing echocardiography, median age was 56 years, 57% (1,817) were women, 48% (1,535) were black, 85% (2,731) reported ever using cannabis. The cannabis use groups differed on nearly all characteristics, especially sex, physical activity and other substance use. In multivariable adjusted models, we found no association between cannabis use and cardiac structure (LVMi, LVEDVi, LVESVi, LAAi) or function (LVEF, EII, E/e’, RVSP).

Conclusion: In the CARDIA study population, cannabis use, either current or cumulative, was not associated with structural and functional heart disease as measured by echocardiography.

P078

Early repolarization in pediatric and adolescent athletes: analysis of a single-center prospective cohort

Birane Kane[1], Albane Maggio[2], Cecilia Craviari[3], Aurélie Schneider-Paccot[3], Mehdi Namdar[3], Maclej Albinski[4], Vincent Gabus[4], Aaron Baggish[5], Philippe Meyer[3]

[1]University of Geneva, faculty of medicine, Geneva, Switzerland, [2]University Hospital of Geneva, Department of Pediatrics, Geneva, Switzerland, [3]University Hospital of Geneva, Division of Cardiology, Geneva, Switzerland, [4]Hôpital Riviera-Chablais, Rennaz, Switzerland, [5]Centre Hospitalier Universitaire Vaudois (CHUV), Lausanne, Switzerland

Introduction: Early repolarization (ERP) is an electrocardiographic finding linked to arrhythmic risk in adults, yet often deemed benign in athletes. Its prevalence and characteristics remain underexplored in pediatric populations. We prospectively screened healthy athletes aged 8–17 years participating in “The Escalade race” in Geneva from 2018 to 2024. This study describes the prevalence of ERP, its ECG features, and associated covariates.

Material and Methods: We enrolled athletes who trained ≥6 hours per week with no known heart disease. Data included demographics, anthropometrics, sports discipline, medical history, blood pressure, heart rate, cardiac auscultation, and 12-lead resting digital ECG performed at least one hour before or after the race. ECGs were interpreted using the 2017 international recommendations and categorized as normal variants, borderline, or abnormal. ERP was identified based on a published consensus (Macfarlane 2015), assessing terminal QRS slurring or notching, location, amplitude, and slur angle. Each ECG was reviewed by a medical student and an experienced cardiologist.

Results: Among 425 athletes (242 males; mean age 12.7 ± 2.6 years), 77.2% demonstrated normal variants, 6.4% borderline findings, and 1.6% abnormal findings. ERP was present in

14.5%, with no overall sex difference. However, among athletes with ERP, females more frequently exhibited slurred patterns (10.6% vs. 7.0%, p = 0.009), while males had more notched patterns (5.6% vs. 0.6%, p = 0.019). ERP prevalence did not vary by sports discipline or weekly training hours. It correlated with shorter QRS duration (p = 0.018), shorter QTc interval (p = 0.002), a lower P axis (p = 0.01), and left ventricular hypertrophy (p<0.001). It was also associated with the overall presence of normal ECG findings but not with borderline or abnormal findings.

Conclusion: ERP occurred in about one in seven pediatric athletes and clustered with other normal ECG adaptations, reinforcing its benign nature in this population.

P079

Definitions for Hypertensive Response to Exercise – A Systematic Review

Gloria Petrasch[1], Elisa Alba Schmidt[1], Hadassa Brito Da Silva[1], Valeria Heller[1], Nina Schmidt[1], Gioia Bebi[1], Laura Spormann[1], Céline Ghidoni[2], Greta Hametner[1], Jan Riess[1 3], Jan Vontobel[1], Mark Haykowsky[4], David Niederseer[1 5 6]

[1]Hochgebirgsklinik, Medicine Campus Davos, Davos, Switzerland, Davos, Switzerland, [2]University Hospital Zurich, University Heart Center Zurich, Department of Cardiology, Zurich, Switzerland, [3]Department of Cardiology, University Heart and Vascular Center Hamburg, University Medical Center Hamburg-Eppendorf, Hamburg, Germany, [4]Integrated Cardiovascular Exercise Physiology and Rehabilitation (iCARE) laboratory, College of Health Sciences, Faculty of Nursing, Edmonton, Alberta, Canada, [5]Center of Translational and Experimental Cardiology (CTEC), Department of Cardiology, University Heart Center Zurich, University Hospital Zurich, University of Zurich, Zurich, Switzerland, [6]Christine Kühne-Center for Allergy Research and Education (CK-CARE), Medicine Campus Davos, Davos, Switzerland

Introduction: Hypertension is a modifiable risk factor for cardiovascular disease, yet resting blood pressure (BP) often fails to detect hypertensive episodes during daily activities, affecting 10–15% of adults. A hypertensive response to exercise (HRE), characterized by abnormally high systolic BP (SBP) rises, is associated with future hypertension and cardiovascular events, even in normotensive individuals and athletes. However, inconsistent definitions of HRE lead to varying incidence estimates. This study aimed to collect available HRE values and investigate definitions for HRE.

Material and Methods: Following PRISMA guidelines, a comprehensive search of MEDLINE and Embase (1974–2024) identified studies on normotensive adults and athletes with or without HRE. Studies reporting BP cutoffs during various exercise modalities and intensities were included, encompassing original research designs.

Results: Twenty-five studies with 15,391 participants (mean age 50 years, 28.3% female, 5.4% athletes) were analyzed (*Fig. 1*). Exercise protocols included treadmill (14 studies), bicycle ergometry (7), shuttle/runs (3), and hand-grip strength (1), mostly using peak intensities with automated BP measurements. SBP thresholds for HRE varied, commonly ≥210 mmHg for men and ≥190 mmHg for women, though some studies proposed higher cut-offs or included diastolic BP criteria (*Fig. 2*). HRE definitions and methodologies were highly variable.

Conclusion: Age, sex, fitness level, and test protocols significantly affect BP response but are often excluded from HRE definitions. Older adults and postmenopausal women exhibit exaggerated responses, while athletes demonstrate higher peak SBP due to increased cardiac output and strength, yet thresholds remain the same as for non-athletes. Variability in protocols, measurement methods, and outdated thresholds further complicates standardization. Standardized, phenotype-specific criteria are critical to improving diagnostic accuracy and clinical recommendations for HRE.

Reference (year)	Proposed/Used BP Cut-offs for MEN	Proposed/Used BP Cut-offs for WOMEN	Cut-off Definition According to Previous Studies	Study Participants	(n)	Gender, male (%)	Mean Age (years)	Exercise Test Modality	Intensity at BP measurement	Resting BP Measurement Method	Exercise BP Measurement Method	Study Type
Bassett Jr. et al. (1998)	Peak SBP ≥ 220 mmHg	NA		Healthy normotensives	68	100	24.0	Bicycle	Peak	Automated	Automated	Cross-sectional
Côté et al. (2018)	Peak SBP ≥ 210 mmHg DBP ≥ 90 mmHg	Peak SBP ≥ 190 mmHg DBP ≥ 90 mmHg	*yes*	Normotensives, elevated BP and hypertensives with and without EBPR	3913	66.7	43.1	Treadmill	Submaximal	Automated	Automated	Cross-sectional
Dimitriadis et al. (2017)	Peak SBP ≥ 210 mmHg	Peak SBP ≥ 190 mmHg		High normotensives (130-139 SBP/85-89 DBP)	20	60	52.0	Treadmill	Peak	NR	NR	Cross-sectional
Duyuler et al. (2017)	Peak SBP ≥ 210 mmHg	Peak SBP ≥ 190 mmHg	*yes*	Normotensive apparently healthy with and without EBPR	44	64	48.0	Treadmill	Peak	NR	NR	Cross-sectional
Mariampillai et al. (2020)	Peak SBP ≥180-200 mmHg at 100 W	NA		Appearently healthy white men	1999	100	56.5	Bicycle	Submaximal	Manual (supine)	Manual	Cohort-Study
Fitzgerald et al. (2019)	Peak SBP ≥ 210 mmHg	Peak SBP ≥ 200 mmHg	*yes*	Apparently healthy individuals	3200	65	58.0	Treadmill	Peak	Manual	Manual	Cross-Sectional
Janssens et al. 2024	Peak SBP ≥ 210 mmHg	Peak SBP ≥ 190 mmHg	*yes*	Predominately endurancetrained athletes (77%) (mostly cycling and rowing)	589	81	52.0	Bicycle	Peak	Automated	Automated	Cross-Sectional
González et al. (2008)	Peak SBP ≥ 230 mmHg; ≥ 150 mmHg DBP Peak SBP ≥200 mmHg; ≥ 100 mmHg DBP	NA		Normotensive, apparently healthy adolescents	2	100	15.0	Run/shuttle-run	Peak	Automated	Automated	Case Series
Grossman et al. (2013)	Peak SBP ≥ 200 mmHg	Peak SBP ≥ 200 mmHg		Normotensive, apparently healthy individuals	69	87	54.0	Treadmill	Peak	Automated (24h)	NR	Case Series
Jin et al. (2020)	Peak SBP ≥ 210mmHg	Peak SBP ≥ 190mmHg		Normotensive and white-coat-hypertensive individuals	295	51.3	52.7	Treadmill	Peak	Automated	Automated	Case-Control
Kalos et al. (2017)	Peak SBP ≥ 210mmHg	Peak SBP ≥ 190mmHg		Individuals with high-normal office BP (130-139 SBP/85-89 DBP), but normal 24h-BP (114 SBP/72 DBP) with and without EBPR	42	69	53.0	Treadmill	Peak	Automated	NR	Cross-Sectional
Esefeld et al. (2013)	Peak SBP ≥ 220 mmHg	Peak SBP ≥ 220 mmHg		Normotensives with and without HRE Untreated hypertensives	10	80	39.0	Treadmill	Peak	NR	NR	Case-Control
Karavelioglu et al (2013)	Peak SBP ≥210 mmHg ≥ 105 mmHg DBP	Peak SBP≥190mmHg ≥105 mmHg DBP		Normotensives with or without type 2 diabetes mellitus	67	42	52.0	Treadmill	Peak	Automated	Automated	Case-Control
Koletsos (2018)	Peak SBP ≥220 mmHg ≥ 120 mmHg DBP	Peak SBP ≥ 220 mmHg SBP		Normotensive individuals Masked Hypertensives Hypertensives	28	56	46.0	Handgrip	30% MVC	Automated	Automated	Cross-Sectional
Kumagai et al. (2002)	SBP at double product breaking point - resting SBP	NA		Men with and without Type 2 Diabetes Mellitus	*63*	100	49.3	Bicycle	Submaximal	Manual	Automated	Cross-Sectional
Leiba et al. (2013)	1. absolute SBP threshold: SBP ≥ 200mmHg 2. formula = (max. SBP-resting SBP)/(max. workload achieved)	NA		Normotensive, apparently healthy firefighters	720	100	38.0	Treadmill	Peak	NR	NR	Cross-Sectional
Lu et al. (2023)	Peak SBP ≥ 210 mmHg DBP ≥ 90 mmHg or increase in DBP ≥ 10 mmHg during exercise	Peak SBP ≥ 190 mmHg DBP ≥ 90 mmHg or increase in DBP ≥10 mmHg during exercise	*yes*	Normotensives with and without hypertrophic cardiomyopathy	333	67	46.0	Treadmill	Peak	NR	NR	Longitudinal study
Michishit et al. (2017)	NA	Peak SBP ≥190 mmHg	*yes*	Normotensives with and without EBPR	78	0	50.2	Bicycle	Submaximal	Automated	Automated	Case-Control
Pincomb et al (1991)	Peak SBP≥230 DBP≥100 mmHg	NA		Healthy men with and without EBPR	34	100	28.5	Bicycle (supine)	Submaximal and maximal	Automated	Automated	Case-Control
Riaz et al. (2018)	Peak SBP >220 mmHg	Peak SBP >220 mmHg		Normotensive individuals	3401	76	50.0	Treadmill	NR	NR	NR	Cross-Sectional
Tsioufs et al. (2018)	Peak SBP≥210 mm Hg	Peak SBP≥190 mm Hg	*yes*	Normotensive individuals with and without EBPR	42	69	53.0	Treadmill	Peak	NR	NR	Cross-Sectional
Yang et al. (2014)	Peak SBP≥200 mm Hg	Peak SBP≥190 mm Hg		Normotensive individuals with and without EBPR	171	57	48.0	Treadmill	Peak	Automated	Automated	Cohort-Study
Cruz (2016)	Peak SBP ≥ 210 mmHg	Peak SBP ≥ 190 mmHg	*yes*	Normotensive badminton athletes	*16*	50	*19.0*	Run/shuttle-run	Peak	Automated	Automated	Cross-Sectional
Sless et al. (2015)	Peak SBP ≥210mmHg	Peak SBP ≥190mmHg		Endurance trained normotensive individuals (≥10 years of endurance activity)	68	71	*53.0*	Bicycle	Peak	Automated	Automted	Cross-Sectional
Trachsel et al. (2015)	Peak SBP ≥200 mmHg	Peak SBP ≥190 mmHg		Normotensive amateur athletes with and without EBPR	119	51	45.0	Run/shuttle-run	Peak	Automated	Automated	Case-Control

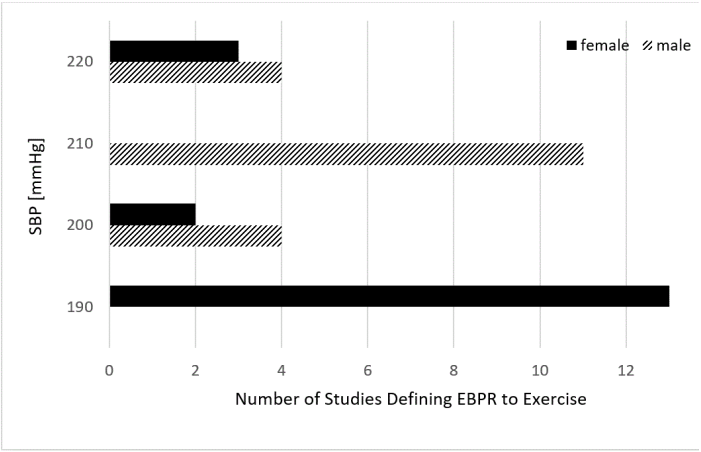

Figure 2. Summary of systolic blood pressure (SBP) thresholds used to identify Hypertensive Response to Exercise (HRE).

P080

Comparison of patient characteristics and health outcomes between self-selected centre-based cardiac rehabilitation and hybrid cardiac telerehabilitation - a prospective cohort study

Prisca Eser[1], Matteo Pini[1], Thomas Vetsch[1], Thimo Marcin[1], Seraina Berni[1], Regula Burri[1], Flurina Casanova[1], Sarina Huber[1], Franziska Gurschler[1], Claudia Böni[1], Michael Hubli[1], Nico Herwegh[1], Andreas Zimmermann[1], Laura Hess[1], Sven Schmutz[1], Matthias Wilhelm[1]

[1]*Inselspital, University hospital Bern, Bern, Switzerland*

Introduction: Data on self-selected modes of delivery of cardiac rehabilitation (CR) are limited. This study compared centre-based CR (cbCR) with hybrid cardiac telerehabilitation (hCTR) in terms of patient characteristics, change in physical and mental functioning, and achievement of guideline-directed treatment targets.

Material and Methods: From May 2022 to December 2023, consecutive patients with cardiovascular diseases were enrolled at a tertiary centre into a 3-month cbCR or hCTR programme based on shared decision-making. Changes in exercise capacity, anxiety, depression, and health-related quality of life (hrQoL) scores from admission to the discharge visit were compared between CR modalities. The achievement of two-step blood pressure and LDL-cholesterol (LDL-C) goals, as well as the HbA1c goal in patients with diabetes at the discharge visit was compared between CR modalities.

Results: Out of 1292 patients screened, 406 (21% females, age 60.4 ± 12.7 years) were eligible and completed the study. Of those, 72% chose cbCR and 28% chose hCTR. Patients in hCTR were three years younger, exhibited higher baseline peak VO2 (91% vs. 80% of predicted), better hrQoL, and lower depression and anxiety scores (Figure 1). No significant differences were found in improvements in physical or mental functioning, or in meeting blood pressure and HbA1c targets between the two groups. A smaller proportion of hCTR participants achieved the LDL-C step I target (56% vs. 69% in cbCR).

Conclusion: Overall, hCTR attracted slightly younger patients with better baseline health, but both modalities showed similar effects on most health outcomes. CbCR was associated with tighter lipid control, which could be related to more intense counselling or patient preference.

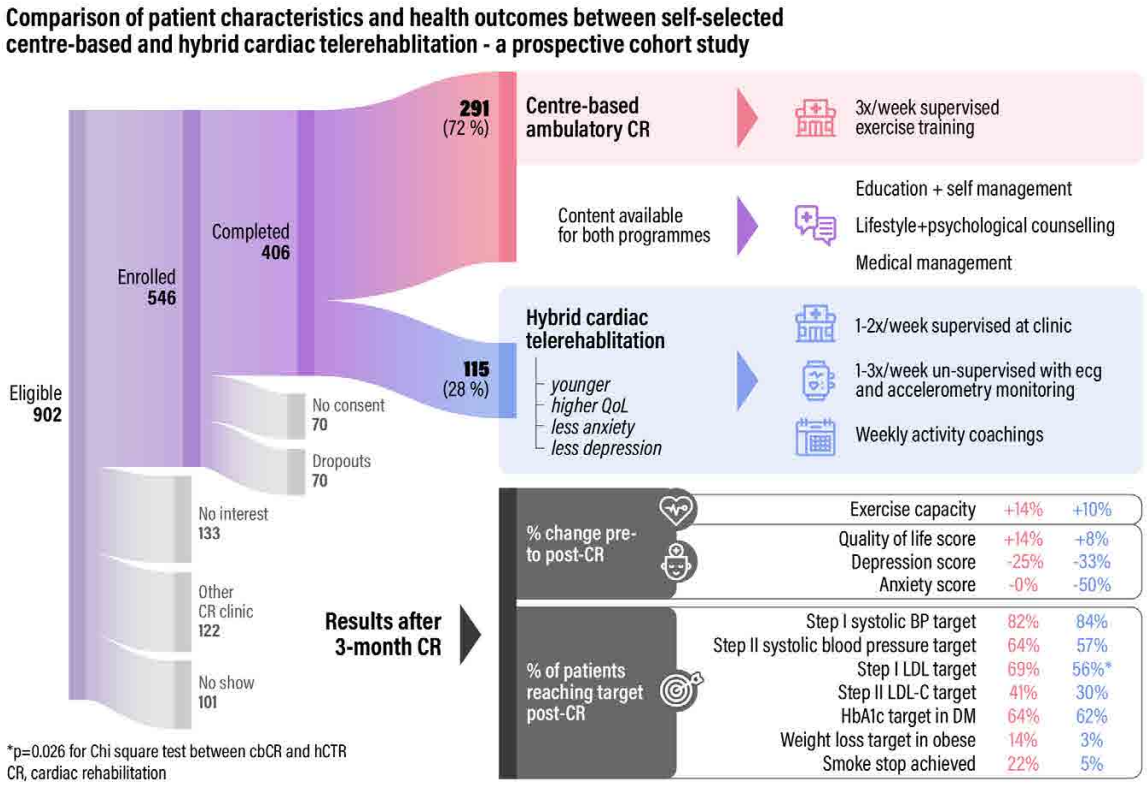

Figure 1: Graphical abstract.

P081

Impact of an education program on adherence to direct oral anticoaglants, treatment satisfaction and quality of life in stroke patients with atrial fibrillation

Caroline Kleinecke[1], Armela Nuhu[2], Petra Burkardt[3], Steffen Gloekler[4], Stefan Schwab[3], Bernd Kallmuenzer[3]

[1]Kantonsspital Aarau, Aarau, Switzerland, [2]Klinikum Hochrhein, Waldshut-Tiengen, Germany, [3]Friedrich-Alexander University Erlangen-Nuernberg, Erlangen, Germany, [4]Hirslanden Klinik im Park, Zurich, Switzerland

Introduction: A structured and intensified patient education program in stroke patients with atrial fibrillation (AF) may improve adherence to direct oral anticoagulants (DOACs), satisfaction with this therapy, as well as quality of life.

Material and Methods: In this prospective, bicentric clinical trial patients with AF who were hospitalized for suspected ischemic stroke were randomly assigned (1: 1) to an intensified patient education on DOACs or to standard of care at two stroke units (University Hospital Erlangen and Hochrhein clinic, Germany). The education program included two personalized tutorials provided by trained professionals during hospital stay and six weeks after discharge, respectively. Primary endpoint was adherence to treatment after three months, measured on the Morisky Medication Adherence Scale. Secondary endpoints were satisfaction with treatment (Anti-Clot Treatment scale, ACTS), as well as quality of life (EQ-5D-3L VAS).

Results: Of 200 participants (77.4 ± 9.1 years, 46.0% females, NIHSS on admission 3.7 ± 4.9, CHA2DS2-VASc score: 5.6±1.5, HAS-BLED score: 3.2±0.9, final diagnosis of ischemic stroke 72.0%, TIA 16.0%, naïve to DOACs: 43.0%) 100 were assigned to the intervention and 100 to standard of care. At 3-months follow-up both groups reported equally good (education vs standard group: 82/95 [86.3%] vs 76/93 [81.7%], p = 0.39) and moderate (13/95 [13.7%] vs 16/93 [17.2%], p = 0.50) adherence to DOACs. Satisfaction with DOACs (ACTS: 70.7 ± 5.5 vs 69.7 ± 7.0, p = 0.23) was high and did not differ between the groups. Quality of life after stroke was overall reduced, but not affected by the intervention (no differences in the measurements for mobility, self-care, usual activities, pain/discomfort and anxiety/depression).

Conclusion: In this cohort of stroke survivors with AF, both adherence and satisfaction with DOACs were high and quality of life after stroke was reduced. After 3 months a structured patient education program on DOACs was not superior to standard of care.

P082

Changes in blood pressure over a 6-years period in the population-based Swiss Longitudinal Cohort Study (SWICOS)

Renate Schoenenberger-Berzins[1], Dragana Radovanovic[2], Franco Muggli[2], Augusto Gallino[3], Gianfranco Parati[4], Paolo Suter[5], Andreas Schoenenberger[6]

[1]Herzzentrum, Kantonsspital Luzern, Luzern, Switzerland, [2]Faculty of Biomedical Sciences, Università della Svizzera italiana, Lugano, Switzerland, [3]Cardiovascular Research Unit, Dep. Medicina Interna, San Giovanni Hospital, Bellinzona, Switzerland, [4]Istituto Auxologico Italiano, IRCCS, Cardiology Unit and Department of Medicine and Surgery, University of Milano-Bicocca, Milano, Italy, [5]University Hospital Zurich, Zurich, Switzerland, [6]Medizinische Klinik, Kantonsspital Münsterlingen, Münsterlingen, Switzerland

Introduction: Previous studies reported an increasing burden of cardiovascular risk factors in developed countries over the years. In particular, an increasing prevalence of obesity is a cause of concern. Therefore, we analyzed changes in blood pressure (BP) and other cardiovascular risk factors in the population-based Swiss Longitudinal Cohort (SWICOS) over a 6-years period.

Material and Methods: This analysis comprised 366 SWICOS participants who underwent follow-up 6 years after the initial baseline examination until October 31, 2024. BP, other cardiovascular risk factors and further potentially influential variables were descriptively compared between baseline and follow-up.

Results: Of the 366 SWICOS participants, 158 (43.2%) were males and 208 (56.8%) females. The mean follow-up duration was 6.56±0.6 years, and mean age of the participants significantly (p<0.001) increased by the same amount. The prevalence of obesity, defined as body mass index >30kg/m2, significantly (p<0.001) increased from 13.2% at baseline to 17.9% at follow-up. This was also reflected by the significant (p<0.001) increase of mean relative body fat mass from 26.9±0.3% to28.6±7.9%. The median time spent watching television increased from 420 to 540 minutes per week (p<0.001), at the same time mean relative body muscle mass decreased significantly (p<0.001) from 69.1±8.5% to 51.7±10.8%. This decrease in muscle mass was also reflected by less force (e.g., decrease of measured handgrip strength from 35.9±12.2kg to 33.2±12.3kg, p<0.001). At the same time, mean systolic BP remained unchanged (133.5±18.6mmHg at baseline vs. 132.2±17.8mmHg at follow-up, p = 0.091), whereas mean diastolic BP significantly increased from 80.9±9.6mmHg at baseline to 83.6±10.3mmHg at follow-up (p<0.001). LDL non-significantly decreased from 3.4±1.0mmol/l to 3.3±1.0mmol/l (p = 0.063).

Conclusion: This analysis suggests that despite an ageing population with increasing weight and increasingly sedentary lifestyle, it was possible to keep BP and LDL values in the same range over a 6-years period in a country with unlimited access to healthcare.

P083

Real-World Comparison Uncovers Variability and Precision Gaps in Validated Home Blood Pressure Devices

Brian Thompson[1], Joachim Joachim[1], Patrick Taffé[2], Grégoire Wuerzner[1]

[1]Service de néphrologie et d'hypertension, CHUV, Neuchâtel, Switzerland, [2]Center for Primary Care and Public Health (unisanté), Division of Biostatistics, University of Lausanne, Lausanne, Switzerland

Introduction: Home blood pressure monitoring (HBPM) provides valuable long-term data for patients and clinicians. However, little is known about difference across validated devices and precision in a real-life setting. In this study, we compared the performance of two validated, cuff-based oscillometric HBPM devices in a home-like setting without clinical supervision.

Material and Methods: In this monocentric study, participants self-positioned the cuffs following the user manuals without assistance (wrist monitor: Omron BP 6100, Omron Healthcare Co. Ltd, Japan; upper-arm monitor: MicroLife WatchBP Home, MicroLife, Switzerland), simulating real-world use but otherwise standard conditions. Manuals were available one week prior and throughout the visit. Data collection occurred in two sessions approximately one hour apart. During each session, BP was measured simultaneously with the monitors were placed on opposite arms, and then swapped after the first measurement. Participants with ≥15 mmHg or ≥10 mmHg interarm difference in systolic or diastolic BP (SBP, DBP), respectively, were excluded from the analysis. Differences and

precision between the readings were analysed using the Bland-Altman Limits of Agreement (LoA) and Taffé Biasplot methods.

Results: A total of 121 participants were included in the analysis (48.5±15.9 y.o., 51.5% women, BMI 28.1±5.5 kg/m²). The differences between the two devices were (mean [LoA]) 9.8 [-25, 44] mmHg for SBP and 8.4 [-11, 28] mmHg for DBP. Bias increased and precision decreased with higher values for both SBP and DBP (Figure 1). The upper-arm monitor demonstrated greater precision compared to the wrist monitor.

Conclusion: Our study reveals significant differences (exceeded generally accepted thresholds) between two validated HBPM devices in real-life settings. The SBP discrepancies of up to 44 mmHg pose a risk of inaccurate BP diagnosis and management. These findings underscore the importance of revising validation protocols to better align with real-world performance and support accurate clinical decision-making.

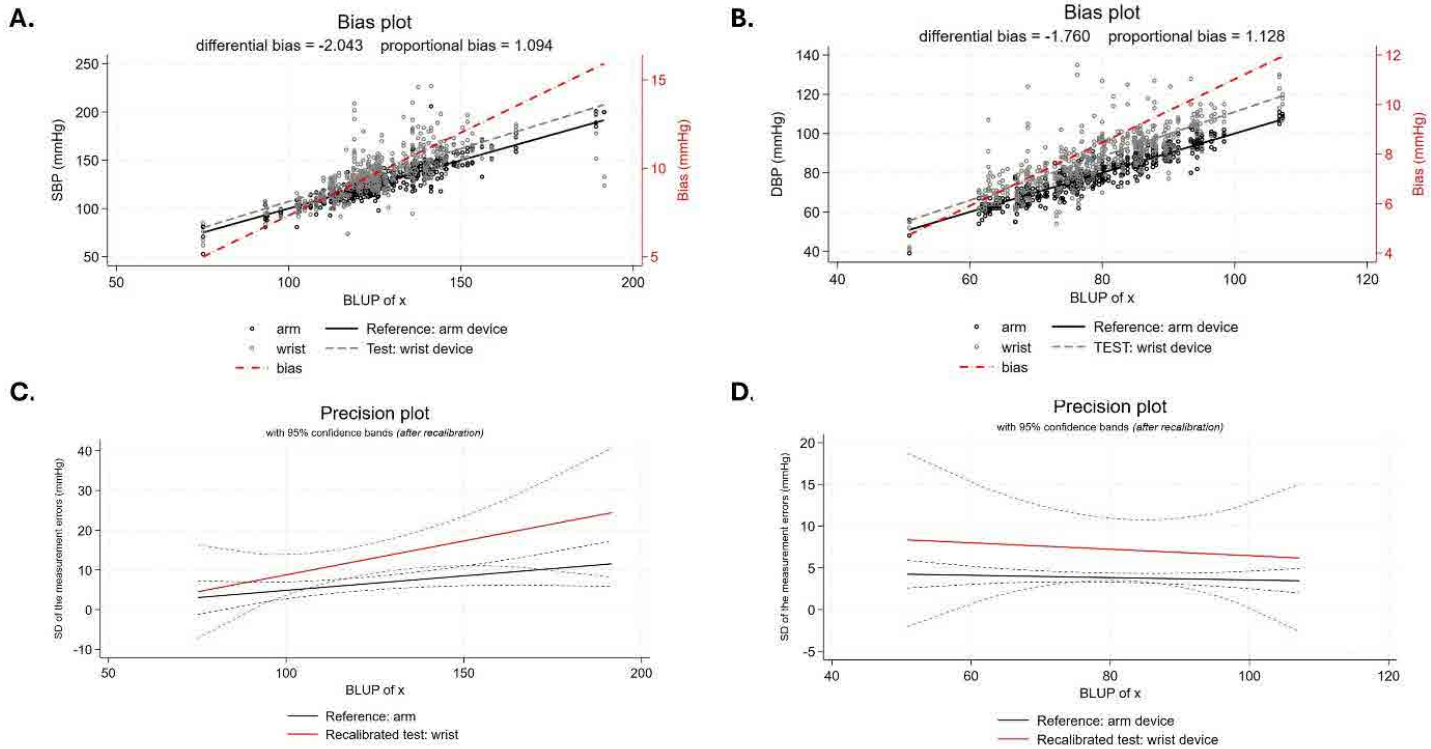

Figure 1. Bias plots (A: SBP, B: DBP) and Precision plots (C: SBP, D: DBP) comparing simultaneous BP measurements from wrist and upper-arm oscillometric monitors. The x-axis shows the Best Linear Unbiased Prediction (BLUP) of x, an estimate of the true BP of the study participants given the two noisy measured values by the oscillometric devices. Bias plots reveal larger biases at higher BPs, and Precision plots show greater measurement error variability for wrist devices.

P084

"Fantastic Four" application in heart failure patients with reduced ejection fraction in an Exercise-Based Cardiac Rehabilitation setting

Elisa Alba Schmidt[1], Greta Hametner[1], Hadassa Brito Da Silva[1], Gloria Petrasch[1], Miriam Albus[1], Sarah Sichler[1], Jan Riess[1 2], Matthias Klimek[3], Pietro Sartori[3], Jan Vontobel[1], Andreas Ziegler[2 3 4], David Niederseer[1 5 6]

[1]Hochgebirgsklinik, Medicine Campus Davos, Davos, Switzerland, Davos, Switzerland, [2]Department of Cardiology, University Heart and Vascular Center Hamburg, University Medical Center Hamburg-Eppendorf, Hamburg, Germany, [3]Cardio-CARE, Medizincampus Davos, Davos, Switzerland, [4]Centre for Population Health Innovation (POINT), University Heart and Vascular Center Hamburg, University Medical Center Hamburg-Eppendorf, Hamburg, Germany, [5]Center of Translational and Experimental Cardiology (CTEC), Department of Cardiology, University Heart Center Zurich, University Hospital Zurich, University of Zurich, Zurich, Switzerland, [6]Christine Kühne-Center for Allergy Research and Education (CK-CARE), Medicine Campus Davos, Davos, Switzerland

Introduction: Heart failure with reduced ejection fraction (HFrEF) is linked to high morbidity and mortality, requiring multifaceted management strategies. Exercise-based cardiac rehabilitation (EBCR) improves compensation status, functional capacity, quality of life, and reduces hospital readmissions in HFrEF-patients. Guideline-directed medical therapy (GDMT) is essential to lower mortality, mitigate symptoms, and prevent disease progression. Up-titrating medication can be challenging during acute episodes, due to factors like volume status, kidney function, and post-operative effects. This study aims to characterize GDMT prescription during EBCR.

Material and Methods: This monocentric retrospective cohort includes patients undergoing inpatient EBCR at a specialized center. Descriptive statistics were performed to assess the characteristics of the cohort, using the Chi-square test for categorical variables and Cochran's Q test to evaluate changes in medication prescription from admission to discharge.

Results: Data from 869 patients were analyzed between December 2022 and June 2024. The mean age of the population was 65 years, with 77.8 % being male. In this analysis, we specifically examined data from 100 HFrEF-patients. The proportion of patients receiving all "fantastic four" GDMT at discharge rose from 21% at admission to 56% (P <0.001). In the

group of 44 HFrEF-patients that could not receive all "fantastic four" medications, beta blockers (BB) and mineralocorticoid receptor antagonists (MRA) were used in 90.9 % and 86.4 % of the patients, respectively. Sodium glucose transporter 2 inhibitors (SGLT2i) were prescribed to 81.8 %, and angiotensin receptor neprilysin inhibitors (ARNI) to 75.0 % of patients.

Conclusion: Inpatient EBCR effectively increased GDMT prescription to more than 50 percent. These results underscore the role of EBCR in optimizing medication up-titration and overcoming barriers to optimal GDMT. This study provides a foundation for refining treatment protocols and inform strategies for better implementation of evidence-based therapies in this population.

P085

Real-world Use of Oral Semaglutide in Adults with Type 2 Diabetes: the PIONEER REAL Switzerland Multicentre, Prospective, Observational Study

Flavio Acquistapace[1], Davide Girola[1]

[1]CardiocareSCA: Primary Care Cardiological Practice, Lugano, Switzerland, Lugano, Switzerland

Introduction: Real-world data provide insight into how medications perform in clinical practice. PIONEER REAL Switzerland aimed to understand clinical outcomes with oral semaglutide in adults with type 2 diabetes (T2D).

Material and Methods: 34–44-week, multicentre, prospective, non-interventional, single-arm study of adults with T2D naïve to injectable glucose-lowering medication who were initiated on oral semaglutide in routine clinical practice. The primary endpoint was change in HbA_{1c} from baseline (BL) to end of study (EOS); secondary endpoints included change in body weight (BW) from BL to EOS and the proportion of participants achieving HbA_{1c} <7.0% and the composite endpoints HbA_{1c} reduction ≥1% with BW reduction ≥3% or ≥5% at EOS. Safety was assessed in participants who received ≥1 dose of oral semaglutide.

Results: Of 185 participants (female/male, n = 67/118) initiating oral semaglutide, 168 (90.8%) completed the study and 143 (77.3%) remained on treatment with oral semaglutide at EOS. At BL, participants had a mean age of 62 years, diabetes duration of 6.4 years, HbA_{1c} of 7.7%, BW of 95.6 kg and body mass index of 33.2 kg/m^2; 56.2% of participants were receiving glucose-lowering medications. Significant reductions were observed for HbA_{1c} (estimated change [95% confidence interval (CI)] −0.91% [−1.10, −0.71]; p <0.0001), as well as BW (estimated change [95% CI] −4.85% [−5.70, −4.00]; p <0.0001). In total, 139 adverse events (AEs) were reported in 65 (35.1%) participants; most were mild or moderate. The most frequent were gastrointestinal disorders (27.0%), and 31 AEs in 20 (10.8%) participants led to discontinuation of oral semaglutide. Six serious AEs were reported; all were considered unlikely to be related to oral semaglutide.

Conclusion: People living with T2D treated with oral semaglutide in Switzerland achieved clinically significant reductions in HbA_{1c} and BW, no new safety signals. *CTR* NCT04537624

P086

Cardiovascular complications and thromboembolic disease in men with testosterone or anabolic therapy

Adel Younes[1], Stefano Caselli[1], Marco Giacchi[1], Keiko Yonekawa[1], Helene Hammer[1], Christian Schmied[1], Christine Attenhofer Jost[1]

[1]Hirslanden Klinik im Park, Zürich, Switzerland

Introduction: Testosterone replacement therapy (TRT) or anabolic androgenic steroid (AAS) use has been associated with various cardiovascular and thromboembolic disorders as well as secondary erythrocytosis. We analyzed our patients with TRT and AAS accordingly.

Material and Methods: We analyzed clinical findings, complications, echocardiographic findings and laboratory tests in men on TRT or AAS.

Results: There were 25 men (age 51.9years, 29-82y), TRT 15, ASA 11 patients. LVH was observed in 12 patients (pts) (48%), average LV ejection fraction was 56%, less than 50% in only 12%. Hypertension (HTN) was present in 56%. LV hypertrophy was more pronounced than expected in hypertensive heart disease, sometimes resembling noncompaction/hypertrabeculation cardiomyopathy or other cardiomyopathy (see Figure, Panels A-C). In 50% of pts, left ventricular global longitudinal strain (GLS) was <16%. Diastolic dysfunction was frequent (56%). Criteria of HFpEF were fulfilled in 52%. A high hematocrit was observed in 53%. Acute coronary syndrome ever was reported in no patients, acute cerebrovascular incident in 12%. Atrial fibrillation was seen in 20%. A thromboembolic event was reported in 3 pts (highest hemoglobin 198g/l). Free testosterone levels were frequently elevated when measured.

Conclusion: In both groups with both TRT and AAS, signs of impressive LV cardiomyopathy are frequently observed. Especially in the setting of a high hematocrit, LV cardiomyopathy due to TRT or AAS has to be considered.

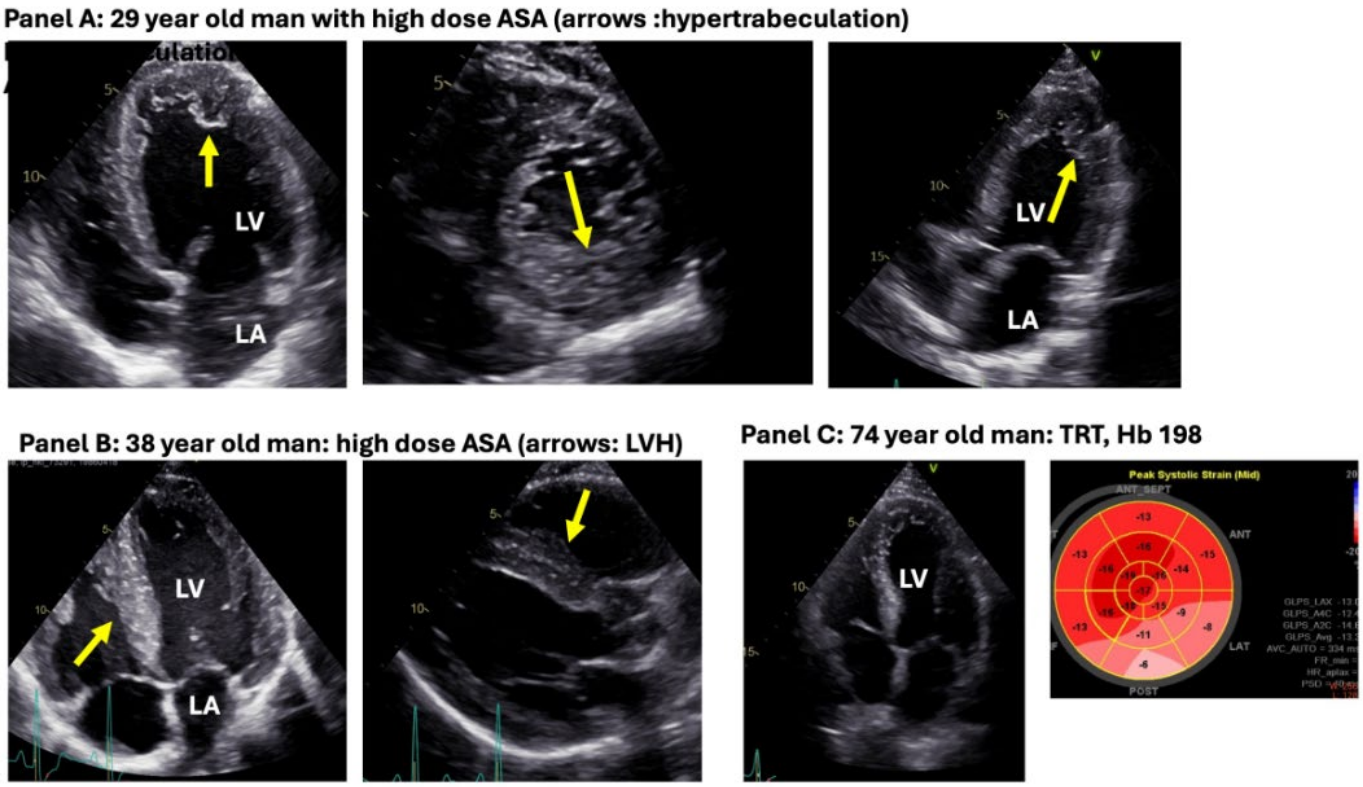

P087

A qualitative Interview Study on the Implementation of Entrustable Professional Activities in Swiss Cardiology Training Sites as perceived by Cardiology Trainees

Vera Bissig[1], Eva Hennel[1], Monika Brodmann-Maeder[1], Fabienne Schwitz[1 2]

[1]Schweizerisches Institut für ärztliche Weiter- und Fortbildung SIWF, Bern, Switzerland, [2]Department of Cardiology, Inselspital, Bern, Switzerland

Introduction: Recently, the implementation of Entrustable Professional Activities (EPAs) has gained attention. In 2022, an EPA-based curriculum for cardiology was introduced in Switzerland. EPAs represent an integral component of Competency-Based Medical Education (CBME), providing a practical framework for assessing a trainee's readiness to perform clinical tasks independently. Using the Consolidated Framework for Implementation Research (CFIR 2.0) , this study examines the perception of cardiology trainees of the implementation of EPAs in their training in Switzerland, the benefits and obstacles they experience and the changes in the feedback culture and perception of responsibility discerned.

Material and Methods: We conducted a qualitative interview study. The CFIR 2.0 was applied to analyze the implementation process, identifying key influencing factors. Eight semi-structured interviews were conducted with cardiology trainees from five different training sites to explore their perceptions and challenges related to EPAs. A purposeful sampling strategy was employed to ensure diversity across hospital types, geographic regions, and trainee demographics. Interview data were transcribed and systematically analyzed to identify barriers and facilitators in the adoption of EPAs. The framework method was used for data analysis, ensuring a structured approach to thematic identification.

Results: Ten themes were identified with the most important ones being 'Impact of time constraints on EPA assessment' and 'Attitude of trainees towards EPAs'. For details see figure 1. Key findings are shown in table 1.

Conclusion: This study underscores the complexity of implementing EPAs. Trainees appreciated the increased feedback, but uncertainties remain regarding the qualitative improvement of feedback. Key obstacles were time constraints and integration of EPAs into the clinical workflow. These findings provide

valuable insights from trainees for refining EPA implementation to enhance CBME.

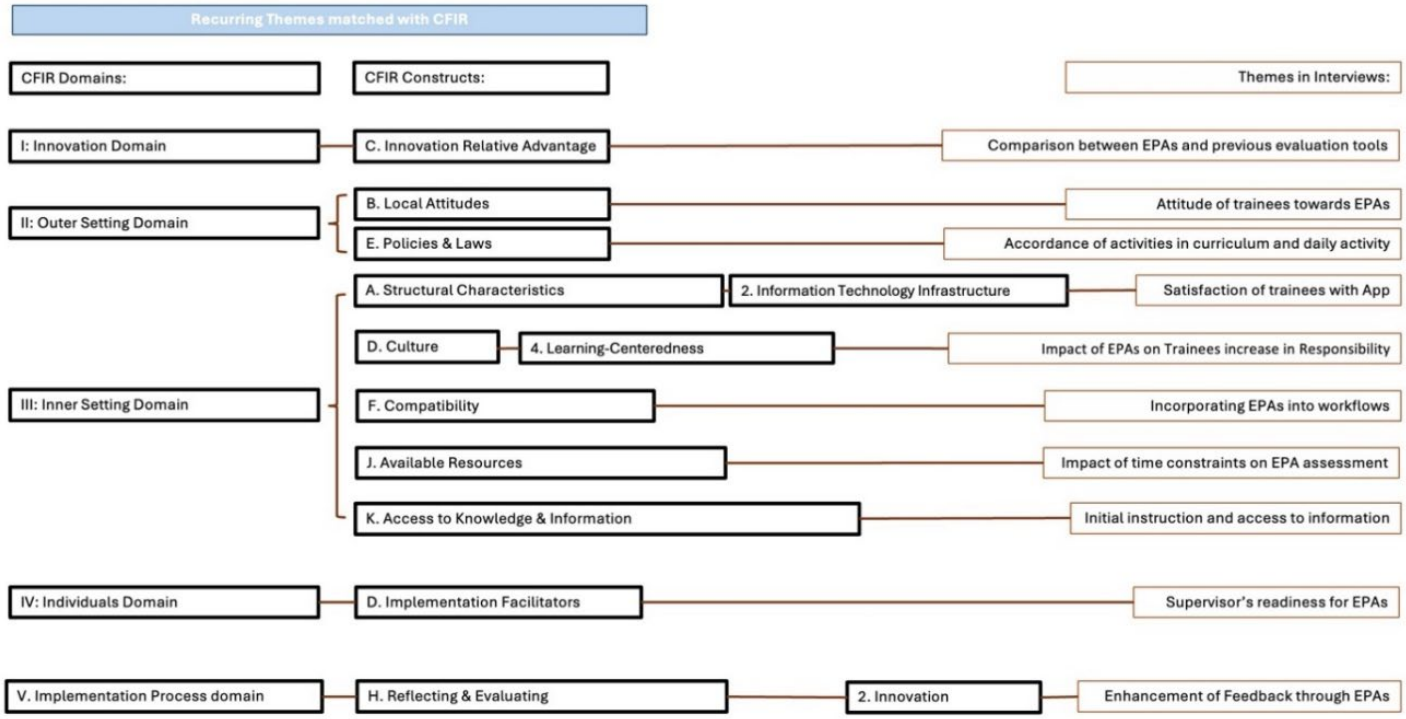

Figure 1
Recurring Themes in interviews matched with CFIR1

Table 1
Themes identified in the interviews and their description

Themes	Description of Themes
Comparison between EPAs and previous assessment tools	Subjective comparison of trainees between EPAs and previous assessment tools such as DOPS and Mini-CEX.
Attitude of trainees towards EPAs	The advantages the trainees perceive of the EPAs, what they like about them, the concerns they have and the struggles they have with their implementation.
Accordance of activities in curriculum and daily activity	Whether assessments cover activities that are regularly performed and if the levels requested seem feasible. Also, whether there are assessments missing in the EPA based curriculum.
Satisfaction of trainees with App	Handling and reception of the app.
Impact of EPAs on Trainees increase in Responsibility	Whether EPAs affect the responsibility the trainees have in the everyday practice. If the increase of responsibility is more gradual thanks to EPAs.
Incorporating EPAs into workflows	The workflows where EPAs are implemented into and how shift work and different areas in the hospital are obstacles or facilitators in the implementation of EPAs.
Impact of time constraints on EPA assessment	The obstacles the trainees face with finding enough time to assess the EPAs, the reasons behind this, the ideas on how to improve upon that and the advantages of EPAs regarding time.
Initial instruction and access to information	The initial instruction the trainees received, how they can access information on the EPAs and their role during the implementation.
Supervisor's readiness for EPAs	The willingness of supervisors to assess the EPAs, their motivation and quality of feedback they share when assessing an EPA.
Enhancement of Feedback through EPAs	Explores the feedback quality and quantity created by the assessments of EPAs.

P088

Diagnostic utility of electrocardiographic criteria for identifying left ventricular hypertrophy defined by electrocardiography in adults with uncomplicated hypertension in rural Africa

Valeriya Nemtsova[1], Annina Vischer[1], Blaise Lukau[2], Martin Rohacek[3], Jonathan MacKo[1], Herry Mapesi[3], Fiona Vanobberghen[4], Andrew Katende[5], Ravi Gupta[2], Niklaus Labhardt[6], Maja Weisser[7], Thilo Burkard[1]

[1]Medical Outpatient Department and University Center for Hypertension, University Hospital Basel, Basel, Switzerland, [2]SolidarMed Partnerships for Health, Maseru, Lesotho, [3]Ifakara Health Institute, Ifakara branch, Ifakara, Tanzania, [4]Swiss Tropical and Public Health Institute, Basel, Switzerland, [5]St. Francis Regional Referral Hospital, Ifakara, Tanzania, [6]Division of Clinical Epidemiology, Department of Clinical Research, University Hospital Basel, Basel, Switzerland, [7]Infectious Diseases & Hospital Epidemiology, University Hospital Basel, Swiss Tropical & Public Health Institute (Swiss TPH), Basel, Switzerland

Introduction: Traditional electrocardiographic (ECG) criteria for detecting left ventricular hypertrophy (LVH) have mainly been evaluated in European and American cohorts with underrepresentation of persons with African descent. This study tested the applicability of these criteria in a large cohort of black African adults with untreated, uncomplicated hypertension, comparing ECG findings with left ventricular (LV) mass measured by echocardiography.

Material and Methods: In the CoArtHA trial (Identifying most effective Treatment Strategies to control Arterial Hypertension in sub-Saharan Africa, NCT04129840), 1268 hypertensives from Tanzania and Lesotho were assessed. We evaluated traditional ECG criteria against echocardiographic measures of LVH. LVH was defined as LV mass indexed to body surface area (LVMI) >95 g/m² in women and >115 g/m² in men. Spearman correlations were used for continuous data, and discriminative performance was measured by area under the curve (AUC).

Results: Complete baseline ECG and echocardiographic data were available for 1125 participants (median age 53.4 years, 72% women). The median (IQR) systolic/diastolic blood pressure were 149 (141–163)/99 (93–106) mmHg, respectively. LVH was detected in 56 (5%) participants. The strongest correlations were observed for the Cornell Voltage Product, Cornell Voltage Criteria, and R amplitude in aVL (r = 0.373, r = 0.327, r = 0.304, respectively; p <0.001, Figure1). The highest specificity was found for strain pattern, Cornell Voltage Product, and R amplitude in aVL (0.970, 0.923, and 0.844, respectively). The highest positive predictive value was for strain pattern, Cornell Voltage Product, and Sokolow-Lyon voltage product (0.272, 0.204, and 0.140, respectively). The best discriminative performance was observed with Cornell Voltage Product, R amplitude in aVL, and Cornell Voltage Criteria (AUC: 0.738, 0.708, and 0.704, respectively, Figure 2)

Conclusion: In this cohort, the Cornell Voltage Product demonstrated the highest diagnostic accuracy for detecting LVH, although the overall correlation and discriminative performance were weak to moderate.

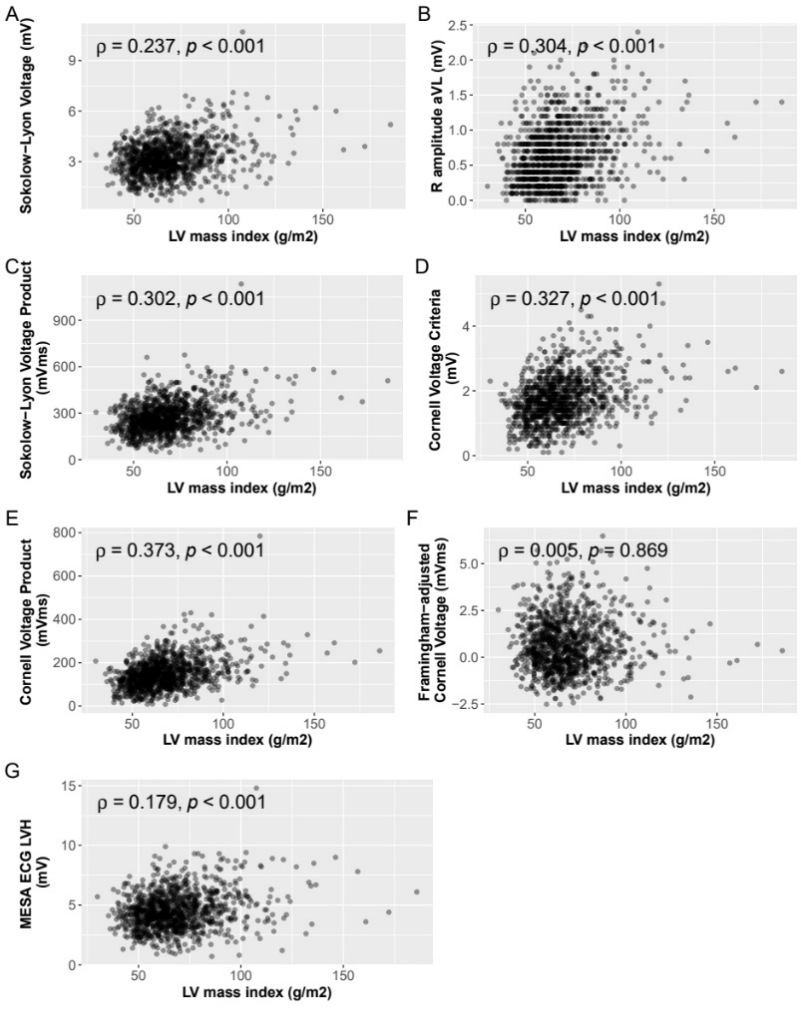

Figure 1. Scatter plots showing correlation (Wilcoxon) between continuous ECG parameters and continuous Left Ventricular Mass Index (LVMI) g/m2 defined by echocardiography.

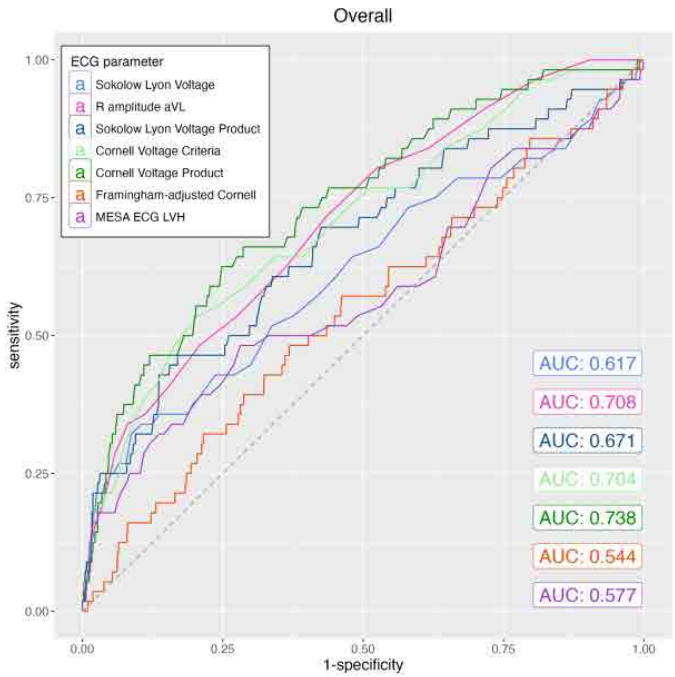

Figure. Receiver operator curve analysis for different ECG parameters for the detection of left ventricular hypertrophy defined by echocardiography.

P089

Sex differences in the changes of emotional health, independence, quality of life and exercise capacity after cardiac rehabilitation

Sarah Sichler[1], Miriam Albus[1], Jan Riess[1 2], Gloria Petrasch[1], Elisa Alba Schmidt[1], Hadassa Brito Da Silva[1], Matthias Klimek[3], Pietro Satori[3], Greta Hametner[1], Jan Vontobel[1], Andreas Ziegler[3 4 5], David Niederseer[1 6 7]

[1]Hochgebirgsklinik, Medicine Campus Davos, Davos, Switzerland, [2]Department of Cardiology, University Heart and Vascular Center Hamburg, Hamburg, Germany, [3]Cardio-CARE, Medizincampus, Davos, Switzerland, [4]Department of Cardiology, University Heart and Vascular Center Hamburg, University Medical Center Hamburg-Eppendorf, Hamburg, Germany, [5]Centre for Population Health Innovation (POINT), University Heart and Vascular Center Hamburg, University Medical Center Hamburg-Eppendorf, Hamburg, Germany, [6]Center of Translational and Experimental Cardiology (CTEC), Department of Cardiology, University Heart Center Zurich, University Hospital Zurich, University of Zurich, Zurich, Switzerland, [7]Christine Kühne-Center for Allergy Research and Education (CK-CARE), Medicine Campus Davos, Davos, Switzerland

Introduction: Sex differences in hormones, body composition, and behavior are known to influence performance and adherence in exercise-based cardiac rehabilitation (EBCR) programs. The quality and quantity of participation in EBCR programs can in turn have an impact on the outcomes of EBCR. Therefore, this study analyzes sex differences in the changes of exercise capacity (six-minute walk test (6MWT)), Health related Quality of Life (MacNewHeart (MNH)), independence (functional independence measure (FIM)), and emotional health (hospital anxiety depression scale (HADS)) after EBCR.

Material and Methods: Data of patients referred for inpatient EBCR in Switzerland between December 2022 and June 2024 were examined in a monocentric retrospective cohort study. For this analysis we included all patients who had at least one of the four assessments (6MWT, FIM, HADS, MNH) for admission and discharge. The median differences with 95% Confidence Intervals (CI95%) between men and women were calculated using the Hodges-Lehmann estimator. P-values were determined using the Wilcoxon signed rank-sum test.

Results: The cohort consisted of 673 men and 192 women who performed a median course of 20 days of EBCR-program, with median age of 65 years [quartiles 57–72]. Between men and women there were no significant differences in the changes for 6MWT (median difference = -5m [CI95% -19 to 9], p = 0.584) and HADS (median difference = -0.5 points, [CI95% -1.9 to 0.9], p = 0.694). For MNH (median difference = 4.5 points, [CI95% 0.4 to 8.6], p = 0.013) and FIM (median difference = 3 points, [CI95% 0.3 to 5.7], p = 0.014) there were significant differences in the changes for men and women.

Conclusion: Women left EBCR with higher scores for independence and health related quality of life than men. Regarding emotional health (HADS) and physical capacity (6MWT) no significant sex-specific differences were found.

P090

Impact of beta-blocker therapy on post-exercise heart rate recovery

Elija Oeschger[1], Hans Rickli[1], Marc Buser[1], Roman Brenner[1], Peter Ammann[1], Niklas Ehl[1], Florian Franzeck[1], Micha T. Maeder[1]

[1]Health Ostschweiz (HOCH) Kantonsspital St. Gallen, St. Gallen, Switzerland

Introduction: Post-exercise heart rate (HR) recovery (HRR), i.e. the difference in HR between peak exercise and a certain time point during recovery [typically minute (M) 1], is a simple clinical parameter. HRR is thought to reflect the sympathico-vagal balance and is a strong predictor of mortality. Beta-blocker therapy reduces the peak exercise HR and may also impact on HRR. We aimed to assess the impact of beta-blocker therapy on HRR.

Material and Methods: We studied 271 patients in sinus rhythm with (n = 157) or without (n = 134) beta-blocker therapy undergoing a clinically indicated cycle exercise stress test. HR during exercise and recovery was recorded in a prospective manner by a research assistant. HRR from M1 to 5 was assessed in absolute [peak HR minus HR at M1 to 5 (in bpm)] and relative [(peak HR minus HR at M1 to 5) / peak HR (in %)] terms.

Results: Resting (72±12 versus 78±16 bpm) and peak (126±20 versus 147±26 bpm; p<0.001 for both) HR were lower in patients with versus without beta-blocker therapy. HRR in absolute terms was lower from M1 to 5 in patients with versus without beta-blocker therapy (M1: 21±9 versus 24±13 bpm, M2: 31±13 versus 37±16 bpm, M3: 37±14 versus 45±83 bpm, M4: 40±16 versus 49±18 bpm, M5: 42±16 versus 51±20 bpm; p<0.05 for all). In contrast, there was no difference in relative HRR between patients with versus without beta-blocker (M1: 17±6 versus 16±7%, M2: 24±6 versus 25±9%, M3: 29±9 versus 30±10%, M4: 31±10 versus 33±9%, M5: 32±10 versus 34±10%; p>0.05 for all).

Conclusion: By the reduction of peak HR beta-blocker therapy also reduces HRR expressed in absolute terms (bpm). In contrast, relative HHR (% reduction), i.e. the slope of the HR/time relationship, is not affected by beta-blocker therapy. This should be considered when interpreting HHR data in patients on beta-blocker therapy.

P091

Estimated glomerular filtration rate dynamics in cardiac rehabilitation patients

Elisa Alba Schmidt[1], Gloria Petrasch[1], Miriam Albus[1], Sarah Sichler[1], Jan Riess[1 2], Eleonora Di Carluccio[3], Pietro Sartori[3], Greta Hametner[1], Hadassa Brito Da Silva[1], Jan Vontobel[1], Andreas Ziegler[2 3 4], David Niederseer[1 5 6]

[1]Hochgebirgsklinik, Medicine Campus Davos, Davos, Switzerland, Davos, Switzerland, [2]Department of Cardiology, University Heart and Vascular Center Hamburg, University Medical Center Hamburg-Eppendorf, Hamburg, Germany, [3]Cardio-CARE, Medizincampus Davos, Davos, Switzerland, [4]Centre for Population Health Innovation (POINT), University Heart and Vascular Center Hamburg, University Medical Center Hamburg-Eppendorf, Hamburg, Germany, [5]Center of Translational and Experimental Cardiology (CTEC), Department of Cardiology, University Heart Center Zurich, University Hospital Zurich, University of Zurich, Zurich, Switzerland, [6]Christine Kühne-Center for Allergy Research and Education (CK-CARE), Medicine Campus Davos, Davos, Switzerland

Introduction: Kidney dysfunction is a known risk factor for cardiovascular disease (CVD) progression, with impaired renal function accelerating cardiac health deterioration. In patients undergoing exercised-based cardiac rehabilitation (EBCR), the relationship between kidney dysfunction and CVD progression is crucial but underexplored. Acute kidney injury after cardiac surgery can lead to acute kidney disease and potentially progress to chronic kidney disease (CKD). This study emphasizes the importance of monitoring kidney function during EBCR to improve patient outcomes and guide interventions.

Material and Methods: This retrospective monocentric cohort study examined patients referred to a specialized rehabilitation center in Switzerland between December 2022 and June 2024 for inpatient EBCR. Kidney function was assessed by creatinine measurements and eGFR calculations (CKD-EPI formula) at admission and discharge. Functional capacity was measured using the six-minute walking distance (6MWD).

Results: The cohort of 869 patients was predominantly male (77.8%) with a median age of 65 years [quartiles 57–72]. Comorbidities included hypertension (60.0%), type 2 diabetes (17.8%) and CKD (9.1%). The median EBCR duration was 20 days [quartiles 20–27]. Functional capacity testing measured through 6MWD increased from 384 meters [quartiles 291–465] at admission to 519 meters [quartiles 483–600] at discharge. eGFR calculation showed a median of 77 ml/min/1.73m² [quartiles 62– 90] at admission and 76 ml/min/1.73m² [quartiles 61– 89] at discharge, resulting in a Hodges-Lehmann analysis shift of 0.5 [95%CI -1.16 to 2.16]. 19.2% of patients had an eGFR <60 ml/min/1.73m² at admission, 19.7 % at discharge.

Conclusion: While 6MWD improved in our EBCR patients, eGFR did not improve during EBCR in our cohort, almost 1/5 of patients remained at high risk for CKD. This might be contrary to common assumptions of rapid kidney function recovery after acute injury. Future studies should include eGFR measurements and albuminuria screening to guide therapy.

POSTER WALK "RHYTHM DISORDERS 2"

P092

Premature explantation of implantable cardiac monitors

Laurent Roten[1], Elena Blumenthal[1], Thomas Kueffer[1], Aline Mühl[1], Barbara Steinhauer[1], Jasmin Steiner[1], Sarah Aerschmann[1], Gregor Thalmann[1], Nikola Kozhuharov[1], Andreas Haeberlin[1], Fabian Noti[1], Claudia Herrera Siklody[1], Boldizsar Kovacs, Hildegard Tanner[1], Tobias Reichlin[1]

[1]Inselspital, Bern University Hospital, Bern, Switzerland

Introduction: Implantable cardiac monitors (ICMs) are utilized for a variety of clinical indications. This study aims to assess the incidence of premature ICM explantation, identify the reasons for premature explantation, and compare these outcomes across different manufacturers.

Material and Methods: Data on all ICM implantations performed at our center since January 2020 were collected within a prospective registry. Follow-up of the status of each ICM was evaluated for all patients. The primary endpoint was defined as premature explantation due to ICM malfunction, early battery depletion, ICM infection or patient discomfort. Early battery depletion was defined as depletion occurring within the first two years post-implant. Patients who died, transferred remote monitoring to an external site, discontinued monitoring after diagnosis or upon physician decision, or were lost to follow-up were censored.

Results: A total of 923 patients were included (mean age 64.4 years; 31.5% women). The indications for ICM implantation were cryptogenic ischemic stroke in 307 patients (33.4%), syncope in 127 (13.8%), follow-up after atrial fibrillation ablation in 2 (0.2%), palpitations in 8 (0.9%), enrollment in a study protocol in 431 (46.8%), and other indications in 45 (4.9%). The ICMs used were manufactured by Medtronic in 572 patients (62%), Biotronik in 100 (10.8%), Boston Scientific in 184 (19.9%), and Abbott in 67 (7.3%). The mean follow-up duration was 23 months. Premature explantation occurred in 40 patients (4.3%). The table provides a breakdown of the reasons for premature explantation overall and by manufacturer. The Figure shows survival free from premature explantation by manufacturer, with statistical comparison using the Log-rank test.

Conclusion: Premature explantation occurs in approximately one out of every twenty-five patients with an ICM, with one device showing a higher rate of premature explantation compared to the others. The main reason for premature explantation is patient discomfort. Device malfunction, early battery depletion, and infections are rare occurrences.

Table. Reason for premature explantation of implantable cardiac monitors

Variable	Overall 40/923	Abbott 2/67	Biotronik 17/100	Boston Sc. 6/184	Medtronic 15/572
ICM malfunction	1 (2.5)	0 (0.0)	0 (0.0)	0 (0.0)	1 (6.7)
Early battery depletion (<2 years after implant)	2 (5.0)	0 (0.0)	1 (5.9)	1 (16.7)	0 (0.0)
ICM infection	4 (10.0)	1 (50.0)	1 (5.9)	1 (16.7)	1 (6.7)
Patient discomfort	33 (82.5)	1 (50.0)	15 (88.2)	4 (66.7)	13 (86.7)

Numbers are no. (%)

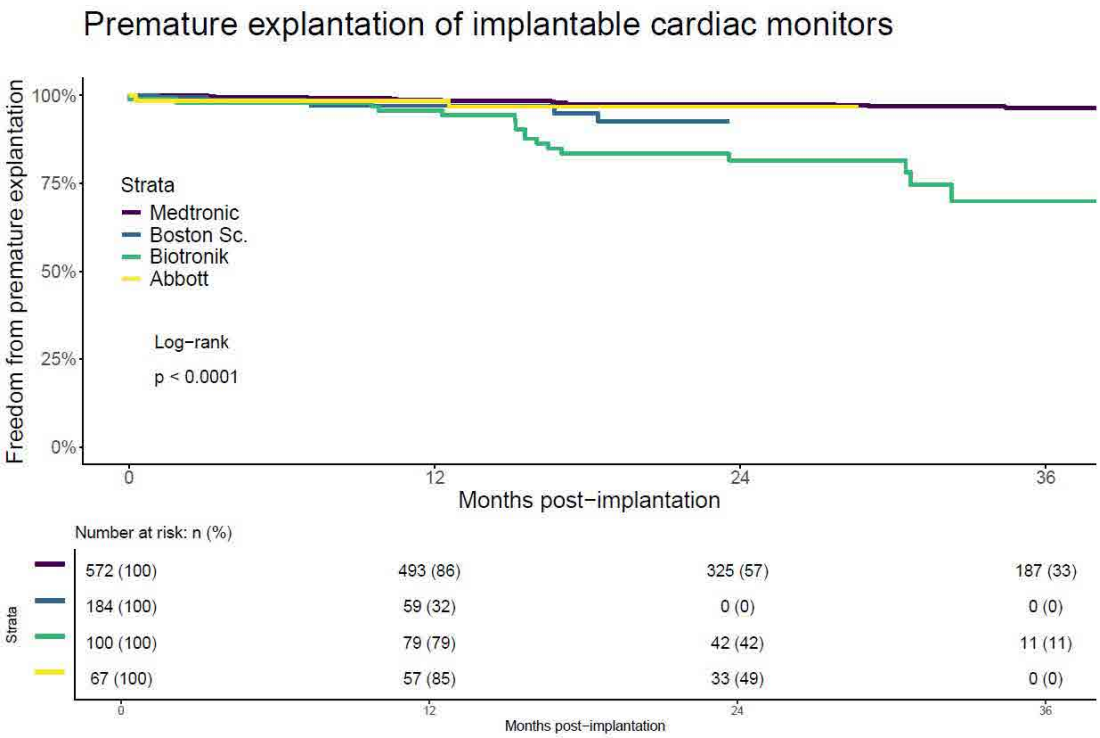

P093

Dual AV Node Physiology in Patients undergoing Pulmonary Vein Isolation for Atrial Fibrillation

Fu Guan[1], Stephan Winnik[1], Deniz Akdis[1], Zihao Zhang[2], Firat Duru[1], Urs Eriksson[2]

[1]University Hospital Zurich, Zurich, Switzerland, [2]University of Zurich, Zurich, Switzerland

Introduction: In patients with atrial fibrillation (AF), dual AV-node physiology (DAVP) may contribute to arrhythmogenesis. However, the coexistence of AF and DAVP remains underexplored, and the impact of slow pathway (SP) ablation on AF recurrence is unclear. This study investigates the prevalence of DAVP in AF patients undergoing pulmonary vein isolation (PVI) and its potential role in AF recurrence.

Material and Methods: Between 1. April and 31. August 2024, AF patients referred for ablation with informed consent were enrolled. PVI procedures were performed using radiofrequency ablation using standardized ablation protocols by the same intervention team. After PVI, electrophysiological (EP) studies were performed to classify patients based on DAVP presence. If AV-nodal reentry tachycardia (AVNRT) was induced, additional SP ablation was performed. A three-month follow-up assessed procedural outcomes.

Results: Among 83 patients (mean age 68±17 years, 68.2% male), PVI was acutely successful in all cases with confirmed entrance and exit block. The presence of DAVP could be identified in 25 of these patients (30.1%). In five patients (6.0%) with additional confirmed AVNRT, SP ablation was performed. Patients with DAVP exhibited significantly higher His bundle signal amplitudes and durations than those without (19.28±7.6 mV vs. 16.41±4.9 mV, P<0.05, and 0.26±0.09 ms vs. 0.19±0.04 ms, P<0.05) (Figure 1). At three-month follow-up, AF recurrence occurred in 12.1% of patients. AF recurrence was associated with older age, higher CHA2DS2-VA scores and larger LA volumes. The patients with DAVP had a higher tendency for AF recurrence, than those without, albeit without reaching significance (15.0% vs 12.1%, P = 0.66). Notably, no AF recurrence was observed in patients who underwent SP ablation (Figure 2).

Conclusion: DAVP is highly prevalent in AF patients undergoing PVI and is associated with prominent His bundle potentials. SP ablation may have a potential role in reducing AF recurrence following PVI.

Figure 1 A. Comparison of His bundle amplitudes (mV) between AF patients in the DAVP group and no-DAVP group

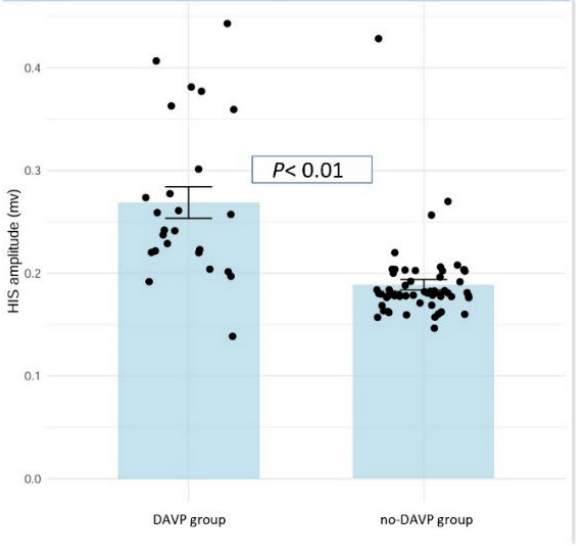

Figure 1 B. Comparison of His bundle durations (ms) between AF patients in the DAVP group and no-DAVP group

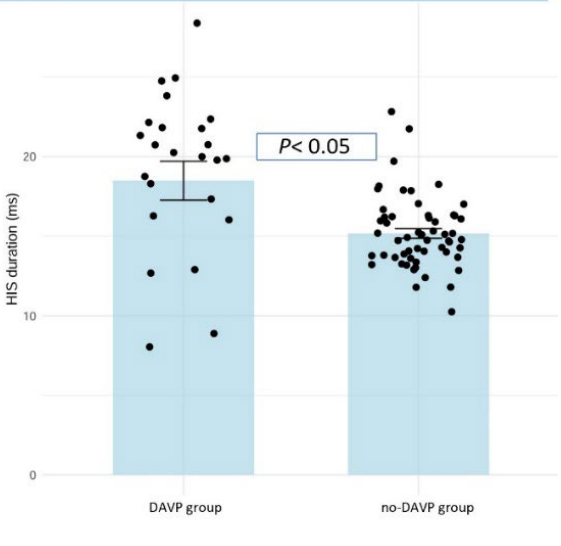

Figure 2. Kaplan–Meier curves for AF-free survival rates. Group 1: Patients who underwent PVI and simultaneous SP ablation for inducible AVNRT; Group 2: Patients who underwent PVI and have no DAVP during EP study; Group 3: Patients who underwent PVI and have DAVP during EP study; no SP ablation due to non-induction of AVNRT.

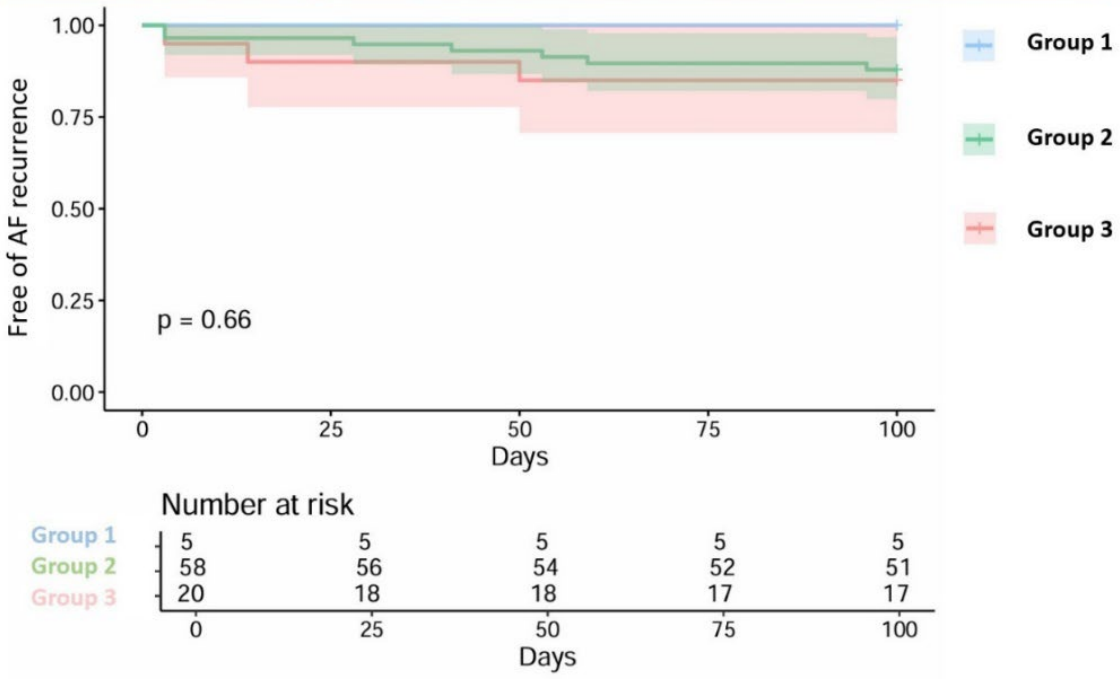

P094

Automated Analysis of Unipolar Electrograms During Pulsed Field Ablation for Atrial Fibrillation

Olivier Leonard[1], Adrian Oraei[1], Martin Valvik[1], Jorge Solana Muñoz[2], Cheryl Teres[2], Mathieu Le Bloa[2], Ciro Ascione[2], Patrizio Pascale[2], Etienne Pruvot[2], Adrian Luca[2]

[1]CathVision ApS, Copenhagen, Denmark, [2]Lausanne University Hospital, Lausanne, Switzerland

Introduction: Accurate dose titration during pulsed field ablation (PFA) for pulmonary vein isolation (PVI) in atrial fibrillation (AF) is essential to prevent reversible electroporation and to optimize tissue response. We sought to evaluate the utility of automated analysis of unipolar electrograms (EGMs) in assessing tissue response during PFA.

Material and Methods: Unfiltered unipolar EGMs were acquired using a proprietary pentaspline basket catheter (BSCI, USA) before and after PFA applications. Data from nine patients with paroxysmal AF undergoing PVI were retrospectively analyzed. Each vein was treated with paired PFA in flower and basket configurations. The EGMs were processed through an algorithm (PFA Analyzer) developed by CathVision, Denmark. The algorithm decomposed single-beat unipolar EGMs to isolate near-filed (NF) potential, removing far-field potentials as well as the injury current induced by PFA delivery. A peak-to-peak threshold of 0.1mV was used to identify absence of residual NFs following PFA (Panel A).

Results: 386 unipolar EGMs from nine procedures were analyzed: 193 prior to each paired PFA application and 193 after the first application of each pair. Before each paired PFA application, NF potentials were observed with an average amplitude of 0.205mV. Residual NFs were detected in 51.8% (100 of 193) of recordings after the first PFA application of each pair, with an average amplitude of 0.1mV (Panel B). Panel C shows that on average the intra-vein EGM amplitude decreased from 0.453mV before the initial PFA application to 0.06mV after the final PFA application within a vein.

Conclusion: Residual NF potentials following PFA can be automatically identified in unipolar EGMs. While pulmonary vein NFs before PFA confirm effective tissue contact, the presence of residual NFs after PFA may indicate incomplete isolation. A complete EGM amplitude reduction (below 0.1mV) after the final PFA confirms the residual nature of detected potentials after first PFA application.

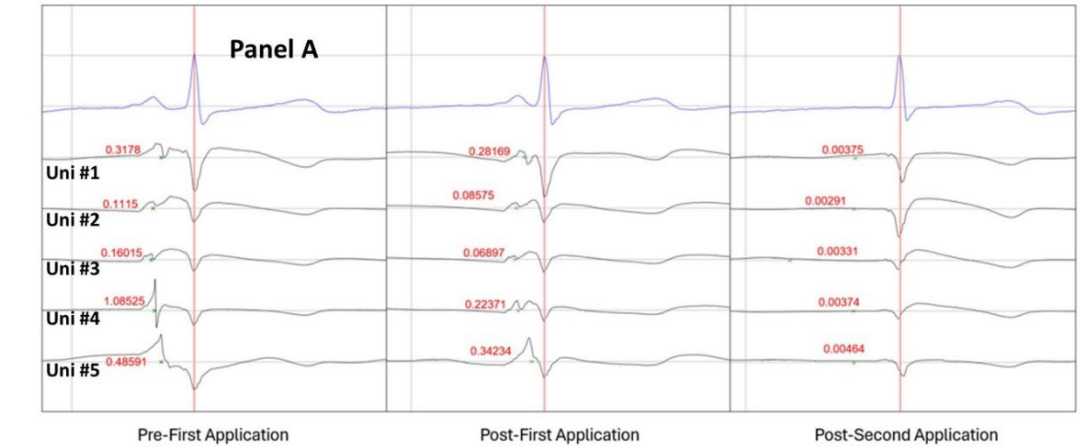

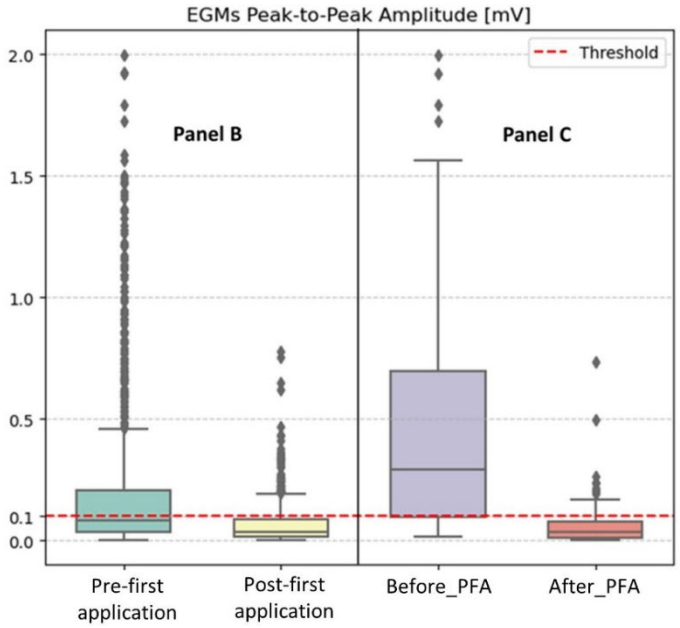

***Panel A**: Example of unipolar EGMs recorded during paired PFA applications.*

***Panel B**: Boxplot showing the amplitude of near-field potentials detected before and after the first application of paired applications.*

***Panel C**: Boxplot comparing the amplitude of unipolar EGMs before the first and after the last PFA application within a vein.*

P095

Non-antiarrhythmic pharmacological interventions to reduce atrial fibrillation recurrences after electrical cardioversion - a scoping review

Kseniya Bulatova[1], William McIntyre[2], Stefan Hohnloser[3], Mate Vamos[4], David Conen[2], Jeff Healey[2], Alexander P. Benz[2], Philipp Krisai[1]

[1]University Hospital Basel, Basel, Switzerland, [2]Population Health Research Institute, Hamilton, Canada, [3]Johann Wolfgang Goethe University Frankfurt am Main, Frankfurt am Main, Germany, [4]University of Szeged, Szeged, Hungary

Introduction: While the use of anti-arrhythmic drugs (AADs) following electrical cardioversion (ECV) for atrial fibrillation (AF) reduces AF recurrence rate, about half of patients treated with AADs still have AF recurrences within 6 months. Thus, there is a need for non-AAD pharmacological interventions to improve sinus rhythm maintenance after ECV.

Material and Methods: We performed a scoping review according to the PRISMA-ScR extension and the framework by Arksey and O-Mailey. MEDLINE and EMBASE were searched for randomized control trials (RCTs) that included patients undergoing ECV for AF or AFlu with any pharmacological intervention other than a class I, III or IV AAD within 24 hours pre-/post-ECV and reported AF recurrence.

Results: From the 5078 articles identified, 65 RCTs were accessed for eligibility, and 22 were selected for final review (Figure 1). Non-AAD pharmacological interventions were categorised as statin (n = 6), fish oil (n = 2), anti-inflammatory (n = 2), anti-diabetic (n = 1), beta-blocker (n = 3), renin-angiotensin aldosterone system (RAAS) inhibition (n = 4), or other (n = 3). Findings suggest that some non-AADs may enhance ECV success rates, particularly metoprolol, statins and RAAS inhibitors (Table 1). For example, both rosuvastatin (relative risk [RR] 0.35, 95% confidence interval [CI] 0.12-0.96, p <0.05) and atorvastatin (predictor-adjusted RR 0.19, 95% CI 0.052-0.72, p = 0.01) reduced AF recurrence within 3 months post-ECV. Metoprolol reduced AF recurrence within 6 months post-ECV compared to placebo in two trials (Kühlkamp, 50.6% vs. 60.0%, p = 0.002; Nergårdh, 54% vs. 74%, p <0.01). Conclusory evidence on the optimal dosing, timing and duration of non-AAD interventions remains insufficient.

Conclusion: Several non-AAD pharmacological treatments may improve ECV outcomes in patients with AF/AFlu. Factors diminishing the validity of the observed studies include absence of placebo, simultaneous amiodarone treatment, and short follow-up period. Moreover, some RCTs showed a questionably large reduction in AF recurrence, possibly due to small sample sizing leading to overestimation of the effect.

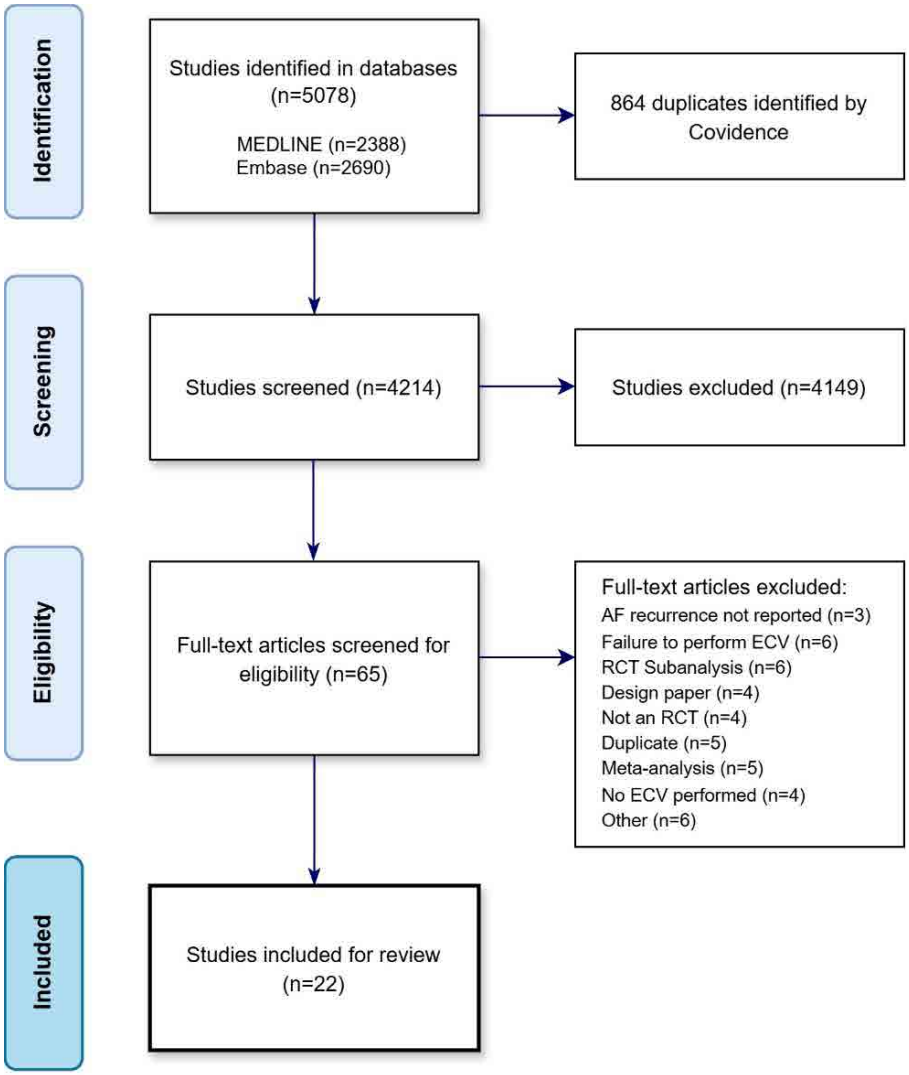

Figure 1
PRISMA flow diagram of study selection process. AF = atrial fibrillation, ECV = electrical cardioversion.

Study (Author, Year)	Period Given	All Patients on AAD Therapy	Intervention	Control	N Total (analysed)	N Intervention (analysed)	Intervention Recurrence	N Control (analysed)	Control Recurrence	Follow-Up Time	Conclusion
Statin											
Almroth et al.[1], 2009	Pre, post	No	Atorvastatin 80 mg	Placebo	234 (222)	118 (111)	70	118 (111)	68	6 months	No effect
Demir et al.[2], 2011	Pre, post	Yes (>90% amiodarone)	Atorvastatin 40 mg	None	48 (44)	24 (22)	6	24 (22)	3	3 months	No effect
Negi et al.[3], 2011	Pre, post	No	Atorvastatin 80 mg	Placebo	64 (64)	33 (33)	22	31 (31)	26	12 months	No effect
Tveit et al.[4], 2004	Pre, post	No	Pravastatin 40 mg	None	114	57 (40)	29 (18)	57 (40)	28 (17)	1.5 months	No effect
Xia et al.[5], 2009	Pre, post	No	Rosuvastatin 10 mg	None	64	32	5	32	13	3 months	+
Ozaydin et al.[6], 2006	Pre, post	No	Atorvastatin 10 mg	None	48	24	3	24	11	3 months	+
Fish oil											
Bianconi et al.[7], 2011	Pre, post	No	n-3 PUFA (3g/d pre, 2g/d post)	Placebo	214 (187)	111 (95)	56	103 (92)	47	6 months	No effect
Kumar et al.[8], 2012	Pre, post	No	6g fish oil (1.08 g EPA, 0.72 g DHA)	None	182 (178)	92 (91)	43	90 (87)	75	12 months	+
Ozaydin et al.[9], 2011	Post	Yes (amiodarone)	n-3 PUFA 2g/d	None	47	23	9	24	9	12 months	No effect
Anti-inflammatory											
Krisai et al.[10], 2020	Post	No	Canakinumab 150 mg (single dose within 60 min)	Placebo	24 (24)	11 (11)	4	13 (13)	10	6 months	No effect
Korantzopoulos et al.[11], 2005	Pre, post	Yes (amiodarone)	Vitamin C (2 g loading dose, then 500 mg BID)	None	50 (44)	N/A (22)	1	N/A (22)	8	1 week	+
Anti-diabetic											
Gu et al.[12], 2017	Pre, post	Yes (amiodarone)	Pioglitazone 30 mg OD	None	100 (97)	50 (48)	22	50 (49)	24	3 months	No effect
Beta blocker											
Katritsis et al.[13], 2003 *	Post	No	Bisoprolol 10 mg OD (5 mg for LVEF <40%)	Carvedilol 25 mg	90 (34)	47 (19)	8	43 (15)	5	12 months	No effect
Kühlkamp et al.[14], 2000	Post	No	Metoprolol (target dose 200 mg)	Placebo	394 (325)	197 (162)	82	197 (163)	106	6 months	+
Nergårdh et al.[15], 2007	Pre, post	No	Metoprolol CR (target dose 200 mg OD)	Placebo	168 (160)	83 (79)	45	85 (81)	63	6 months	+
RAAS Inhibition											
Madrid et al.[16], 2002 †	Pre, post	Yes (amiodarone)	Irbesartan 150 mg OD (up to 300 mg, if tolerated)	None	154 (88)	79 (41)	9 (N/A)	75 (37)	22 (N/A)	8.5 months (median)	+
Madrid et al.[17], 2004	Pre, post	Yes (amiodarone)	Irbesartan 150 mg OD	None	90 (56)	30 (19)	8 (N/A)	30 (18)	14 (N/A)	7.5 months (median)	No effect
			Irbesartan 300 mg OD			30 (19)	11 (N/A)				
Tveit et al.[18] 2007	Pre, post	No	Candesartan (8 mg OD pre, 16 mg OD post)	Placebo	171 (137)	86 (68)	N/A (48)	85 (69)	N/A (45)	6 months	No effect
Ueng et al.[19], 2003	Pre, post	Yes (amiodarone)	Enalapril 10 mg BID (20 mg BID post, if tolerated)	None	159 (125)	79 (64)	N/A (18)	80 (61)	N/A (32)	9 months (median)	+
Other											
Frick et al.[20], 2000	Pre, post	Yes (sotalol)	Magnesium 10.3 mmol BID	Placebo	131 (114)	67 (57)	40	64 (57)	36	18 months (mean)	No effect
Frick et al.[20], 2000	Pre, post	No	Magnesium 10.3 mmol BID	Placebo	170 (131)	85 (64)	52	85 (67)	57	21 months (mean)	No effect
De Ferrari et al.[21], 2015	Post	No	Ranolazine 375 mg BID	Placebo	241 (238)	N/A (65)	37	N/A (55)	31	4 months	No effect
			Ranolazine 500 mg BID			N/A (60)	25				No effect
			Ranolazine 750 mg BID			N/A (58)	23				No effect

Table 1

Effect of non-antiarrhythmic pharmacological interventions to improve electrical cardioversion success. * Pharmacologic cardioversion with oral Propafenone or intravenous Ibutilide, and only if this failed, patients underwent electrical cardioversion. † At the time of the scheduled electrical cardioversion, pharmacological conversion was documented in 62 patients, of whom 29 (38.6%) were in the amiodarone-only group and 33 (42%) were in the amiodarone-irbesartan group. Trials showing reduction in AF recurrence in the intervention group compared to control have been highlighted in blue. Abbreviations: *AAD* anti-arrhythmic drug, *BID* twice daily, *DHA* docosahexaenoic acid, *EPA* eicosapentaenoic acid, *LVEF* left ventricular ejection fraction, *N/A* not available, *OD* once daily, *n-3 PUFA* n-3 polyunsaturated fatty acid, *RAAS* Renin-angiotensin aldosterone system.

P096

Pulsed-Field Ablation versus Cryoballoon Ablation in Patients with Persistent Atrial Fibrillation Undergoing First Catheter Ablation

Jonas Brügger[1], Corinne Isenegger[1], Fabian Jordan[1], Sven Knecht[1], Philipp Krisai[1], Gian Völlmin[1], David Spreen[1], Nicolas Schaerli[1], Beat Schär[1], Felix Mahfoud[1], Christian Sticherling[1], Michael Kühne[1], Patrick Badertscher[1]

[1]Department of Cardiology, University Hospital Basel, Cardiovascular Research Institute Basel (CRIB), Basel, Switzerland

Introduction: Catheter ablation (CA) for persistent atrial fibrillation (AF) is more challenging and associated with less favorable outcomes. While early studies showed similar outcomes for pulsed-field ablation (PFA) and cryoballoon ablation in all-comers, the impact of the used ablation modality on clinical outcomes in patients with persistent AF remains unclear. This study aims to compare PFA and cryoablation in terms of procedural characteristics, safety, and efficacy in patients undergoing CA for persistent AF.

Material and Methods: Patients with persistent AF who underwent their first CA at a tertiary referral center using either PFA or Cryo between January 2018 and June 2024 were enrolled.

Results: 220 patients (median age 66 [60–72] years, 24% female) were included. 113 patients (51%) underwent PFA and 107 patients (49%) cryoablation. Median procedure duration, LA dwell time and fluoroscopy time were shorter in the PFA group: 49 [39–61] min vs 60 [49–75] min (p <0.001), 34 [25–43] min vs 37 [31–53] min (p <0.001), and 9 [8–13] min vs 11 [8–16] min (p = 0.008). Overall, there were 5 complications (2%), 3 (3%) in the PFA and 2 (2%) in the Cryo group. 21% of the PFA group received additional posterior wall ablation (PWI). During a median follow-up of 365 days, recurrence-free survival was 72% in the PFA group and 60% in the Cryo group (pLog-rank = 0.079).

Conclusion: In patients with persistent AF undergoing CA, PFA results in increased efficiency, but similar safety and recurrence-free survival rates. Future studies are warranted assessing the role of extended ablation strategies when using PFA such as PWI in patients undergoing CA for persistent AF.

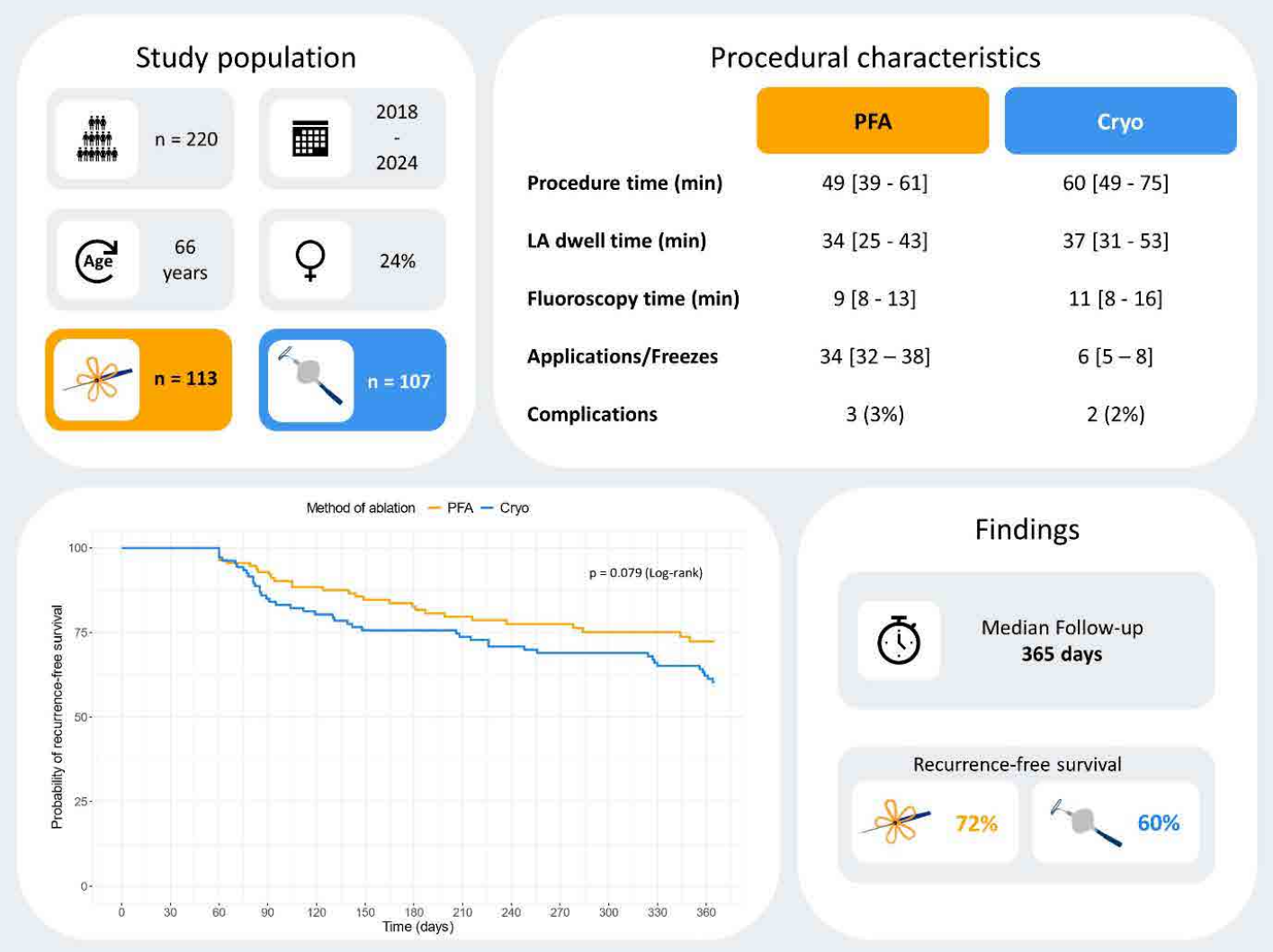

P097

Validation of a variable loop circular pulsed field ablation catheter for assessment of pulmonary vein isolation by 3D mapping

Thomas Kueffer[1], Ajay Panakal[2], Claudia Herrera[1], Hildegard Tanner[1], Helge Servatius[1], Laurent Roten[1], Tobias Reichlin[1]

[1]Department of Cardiology, Inselspital, Bern University Hospital, University of Bern, Bern, Switzerland, [2]Johnson&Johnson MedTech, Zug, Switzerland

Introduction: In pulmonary vein isolation (PVI) procedures, acute ablation effectiveness is usually assessed with dedicated mapping catheters with closely spaced and small electrodes. With catheter designs optimized for pulsed-field ablation (PFA), 3D mapping capabilities are limited due to fewer, larger and more widely spaced electrodes, all affecting EGM recordings. We validate the performance of a novel variable loop circular (VLC) PFA catheter for endpoint assessment of PVI compared to a dedicated octaspline high-density mapping.

Material and Methods: Patients undergoing a PVI procedure using the VLC-PFA catheter were included. PVI was performed using the recommended ablation protocol of at least four applications per vein. Maps were acquired twice, once with the VLC-PFA catheter and once using a dedicated octaspline high-density mapping catheter. PV isolation status was assessed for each vein within a wide-antral PV area. Additional PFA applications were delivered only after confirmation of residual PV connection by both catheters.

Results: In 30 patients (median age 73 years, IQR 56-78 years, 70% male, 19 de novo procedures, 11 repeat procedures), acute PVI was achieved in 100% with a median of 21 (IQR 18-24) PFA applications. 38 maps were available for both catheters, resulting in 148 PVs available for analysis. The accuracy of PV assessment with the VLC-PFA catheter was 98% (145/148 veins). In 2/158 (1.4%) PVs, the VLC incorrectly indicated PV-isolation, with a mismatch close to the carina. In 1/158 (0.7%), the VLC incorrectly indicated residual PV-conduction. In 12 cases, posterior wall ablation was performed using the LVC-PFA catheter. Both catheters agreed in the assessment of the posterior wall in 11/12 (92%) of these cases. In the remaining case, the VLC-PFA catheter did not record small fragmented signals on the posterior wall.

Conclusion: Despite fewer, larger and more widely spaced electrodes, endpoint assessment for PVI can be reliably performed with a novel 3D mapping-enabled VLC PFA catheter.

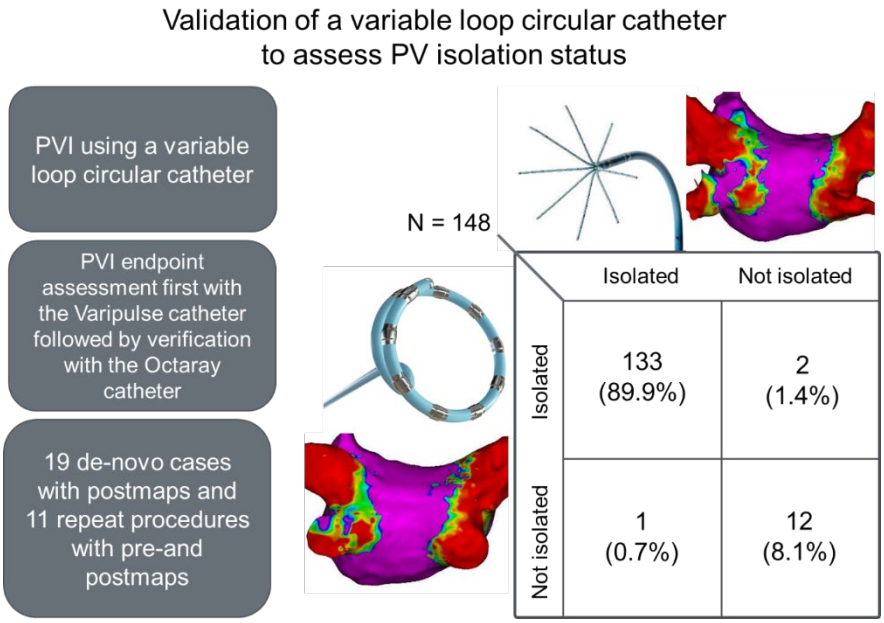

P098

Predicting outcomes in ICD patients with dilated cardiomyopathy: mortality and ventricular arrhythmia based on CHA2DS2-VA Score

Benjamin Vögeli[1], Patrick Badertscher[1], Philipp Krisai[1], Michael Kühne[1], Christian Sticherling[1], Beat Schär[1]

[1]Department of Cardiology, University Hospital of Basel, Basel, Switzerland

Introduction: Current guidelines recommend the use of the CHA2DS2-VA-score (CVS) for evaluating stroke risk in atrial fibrillation (AF) patients. Several studies have shown that the CVS was a reliable predictor for cardiovascular outcomes among patients with cardiovascular disease, beyond the AF population. Today, it is still largely undetermined, which patients with dilated cardiomyopathy (DCM) should receive an ICD for primary prevention. We hypothesized that the CVS might be a reliable predictor of ventricular arrhythmias (VA).

Material and Methods: Between March 1994 and August 2024, 401 patients with DCM undergoing ICD implantation were included in a prospective ICD registry. Comorbidities, CVS at implant, and mortality and VA during follow-up were assessed in all patients. DCM patients were stratified into low or high CVS, with the cutoff determined by the median score within the cohort. Mortality outcomes and VA according to the CVS by plotting Kaplan-Meier curves were observed.

Results: Mean age was 62 (± 13) years and 24% were female. Mean left ventricular ejection fraction was 26% (± 8). Median CVS was 2. Median follow-up was 6.5 years. The most frequent device type was cardiac resynchronization therapy-ICD (50%). All-cause mortality was 39% and cardiovascular mortality 20%. We observed 233 VA (Ventricular tachycardia (VT) n = 117, fast ventricular tachycardia (FVT) n = 81, ventricular fibrillation (VF) n = 35). A higher CVS (3-8) was associated with higher all-cause (Figure 1) and cardiovascular mortality compared to a lower CVS (0-2) (log rank p <0.01). CVS was

not predictive for overall VA (AUC 0.54) or any type of VT (i.e. VT, FVT and VF, AUC 0.52, 0.58 and 0.53, respectively).

Conclusion: In this large cohort of DCM patients undergoing ICD implantation for primary prevention, all-cause mortality was high. While the CVS is a reliable tool for identifying patients at increased risk for mortality, it has little predictive accuracy for the occurrence of VA.

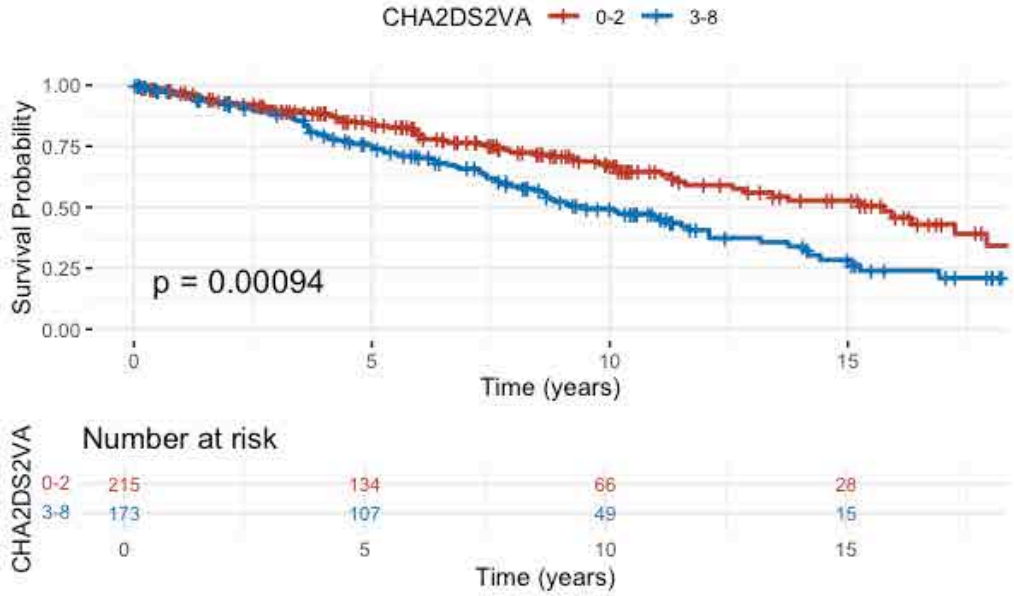

P099

Simplifying Atrial Tachycardia Ablation: High Density Mapping of Slow Conduction Sites during Sinus Rhythm Identifies Critical Isthmuses of Atrial Tachycardia

Stefanie Hess[1], Amir Sherwan Jadidi[1], Anne-Aimée Bernard[2]

[1]Luzerner Kantonsspital, Luzern, Switzerland, [2]Johnson and Johnson MedTech, Zug, Switzerland

Introduction: Identifying critical isthmuses (CIs) for atrial tachycardia (AT) typically requires mapping during tachycardia. This study evaluates whether sinus rhythm (SR) mapping can reliably identify and eliminate slow conduction zones predisposing to AT.

Material and Methods: Patients with a history of AT (focal or reentrant) undergoing catheter ablation with 3D high-density mapping were enrolled. Activation and voltage mapping was performed during AT, with SR restored by overdrive pacing or cardioversion when necessary. SR voltage maps (n = 16) and paced maps from the crista terminalis (n = 4) were obtained (cutoff: 0.05–0.5 mV) and compared to AT maps to identify CIs, defined by electrograms with diastolic potentials and prolonged, fragmented morphology at slow conduction sites with optimal PPI. Ablation targeted these slow conduction areas during SR, with procedural success confirmed by acute AT non-inducibility.

Results: Nineteen patients (mean age: 70.9 ± 10, 47.37% female, 10 redo procedures) presented with 20 ATs. Voltage mapping during AT revealed a mean value of bipolar voltage (near-field and far-field component), near-field and far-field EGM duration of 0.25 ± 0.24 mV and 93.5 ± 39.0 ms at CI. The mean value of bipolar voltage (near-field and far-field component), near-field and far-field EGM duration during SR corresponding to CI in AT were 0.35 ± 0.26 mV and 80.81 ± 33.67 ms, respectively. SR voltage maps reliably identified CIs, showing prolonged, fractionated EGMs with low bipolar voltage. Ablation during SR achieved AT non-inducibility in all cases, with arrhythmia freedom

in 16/19 (84%) patients.

Conclusion: The findings demonstrate that targeting conduction abnormalities during SR is sufficient for procedural success, eliminating the need for successive tachycardia induction, mapping and ablation.

Figure 1: Critical Isthmus in AT (left) and Sinus rhythm (right)

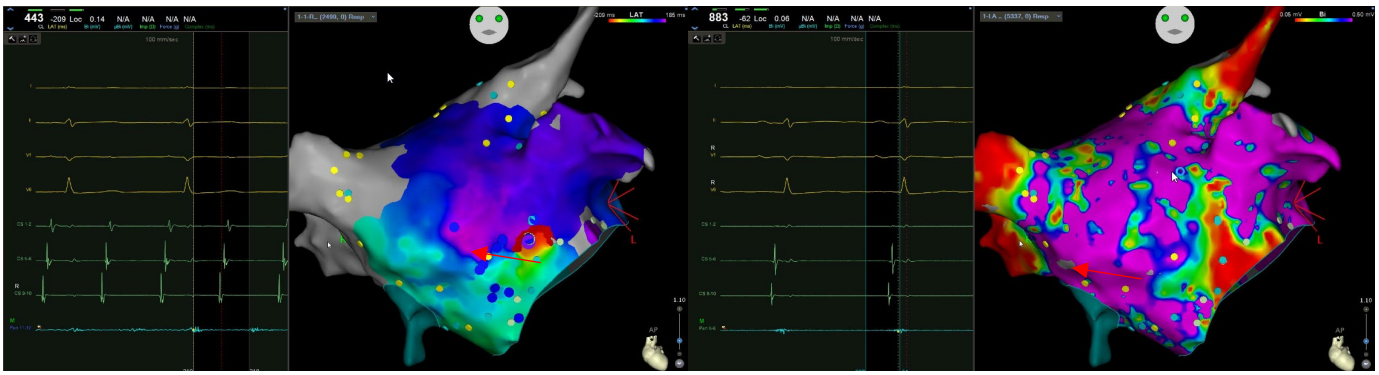

P100

Leadless Atrial Pacing: First Swiss Implantation Experience And Early Follow-up

Elia von Felten[1], Alexander Breitenstein[2], Andreas Müller[1], Caroline Wiederkehr[1], Theresa Brix[1], Daniel Hofer[1 2]

[1]Stadtspital Zürich Triemli, Klinik für Kardiologie, Zürich, Switzerland, [2]Universitätsspital Zürich, Klinik für Kardiologie, Zürich, Switzerland

Introduction: Leadless pacemakers are associated with a lower incidence of long-term complications compared to conventional devices. However, before the recent introduction of an active-fixation atrial leadless pacemaker, only ventricular devices were available. We describe our first real-world Swiss implantation and short-term follow-up experience with this new technology.

Material and Methods: This study is a retrospective, single-center, single-operator analysis. Consecutive patients undergoing implantation of an active-fixation atrial leadless pacemaker, either as standalone therapy or as part of a dual-chamber leadless pacemaker system, were included.

Results: Among the 23 included patients (mean age 73 years, 52% male), the indications for device therapy were sinus node disease in eight patients (35%), AV block in thirteen (57%), and binodal disease in two (9%). All 14 de novo dual-chamber and nine atrial single-chamber implantations were successful. The mean procedure time for atrial single-chamber implantation was 29 minutes (±11), and for dual-chamber, 34 minutes (±9). The mean fluoroscopy time was 3 minutes (±1.5) for the atrial pacemaker (AR) and 3.2 minutes (±1.5) for the dual-chamber system (DR). One patient (4%) experienced a complication (small pericardial effusion). Median sensing, pacing threshold, and impedance were 1.5 mV (IQR 1–2.4), 1.8 V/0.4 ms (IQR 1.5–3), and 340 Ω (IQR 310–375) at implantation, and 4 mV (IQR 3–4.9), 0.5 V/0.4ms (IQR 0.5–0.5), and 320 Ω (IQR 310–360) after a mean follow-up of 22 days (IQR 21–27).

Conclusion: With the recently introduced active-fixation atrial leadless pacemaker, we observed an efficient and safe implantation procedure and recorded acceptable and stable parameters during follow-up.

Table 1: Patient characteristics (all patients n=23)

Age (years)	73 ±11
Male	12 (52%)
BMI (kg/m2)	27 ±4
Sinus node disease	8 (34.8%)
AV-block	13 (56.5%)
Binodal disease	2 (8.7%)
Chronic kidney disease	10 (43.5%)
Arterial hypertension	16 (69.6%)
Diabetes	7 (30.4%)
Atrial fibrilation	8 (34.8%)
Heart failure	1 (4.3%)
Coronary artery disease	4 (17.4%)
Malignancy	3 (13.0%)
COPD	2 (8.7%)
Obstructive sleep apnea	2 (8.7%)
Cerebrovascular disease	4 (17.4%)
Implantation time (min)	32 ±10
Atrial single chamber, n=9	29 ±11
Dual chamber, n=14	34 ±10
X-ray (min)	3.1 ±1.4
Atrial single chamber, n=9	2.8 ±1.4
Dual chamber, n=14	3.2 ±1.4
Complications	1 (4%)
Atrial single chamber, n=9	1 (11%)
Dual chamber, n=14	0 (0%)

The values given are mean or absolute numbers and (in parenthesis) standard deviations or percentages, respectively.

Figure 1: Outcome (all patients n=23) – Atrial measurements of impedance (A), pacing threshold at 0.4ms (B) and sensing (C) at implantation, 1 day post-implantation and at follow-up (median 22 days, IQR 21-27).

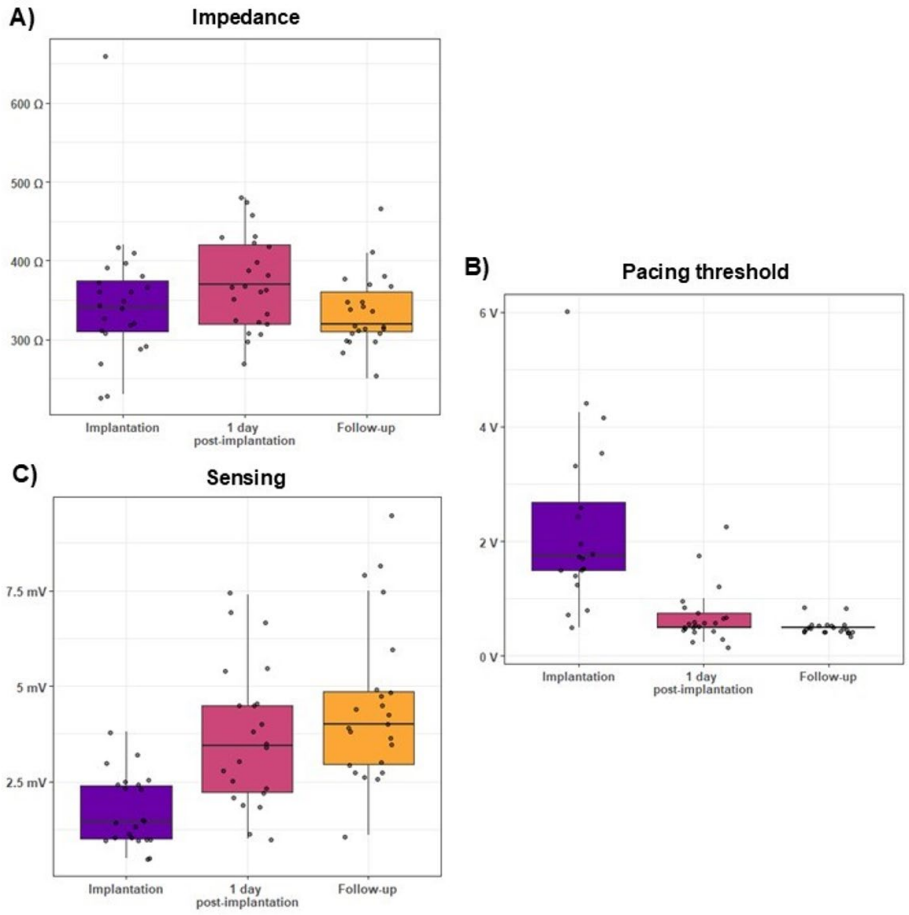

POSTER WALK "CONGENITAL & PAEDIATRIC CARDIOLOGY & GENETICS"

P101

Modelling and simulation as a tool for efficient repurposing in rare diseases: A case study describing the dose rationale for empagliflozin in paediatric heart failure

Sebastiano Lava[1], Alessandro Di Deo[2], Oscar Della Pasqua[2]

[1]Pediatric Cardiology Unit, Department of Pediatrics, Centre Hospitalier Universitaire Vaudois and University of Lausanne, Lausanne, Switzerland, Heart Failure and Transplantation, Department of Paediatric Cardiology, Great Ormond Street Hospital, London, United Kingdom, Clinical Pharmacology and Therapeutics Group, University College London, London, United Kingdom, Lausanne, Switzerland, [2]Clinical Pharmacology and Therapeutics Group, University College London, London, United Kingdom, London, United Kingdom

Introduction: Current therapy for paediatric heart failure is unsatisfactory, 5-year mortality being 30-50%. Trials in this population have often failed, mainly because of sample size issues, suboptimal dose, inappropriate formulations, and inadequately performing endpoints. We developed a bridging study protocol to assess pharmacokinetics, pharmacodynamics, and safety of empagliflozin in children with heart failure.

Material and Methods: A modelling, extrapolation and simulation approach was used to characterize empagliflozin pharmacokinetics in children and optimize the study design. Protocol elements of interest were dose, sample size and sampling schedule. The study design was evaluated based on an optimization algorithm and a simulation re-estimation procedure. Given the importance of characterizing interindividual differences, a large virtual paediatric cohort was simulated (n = 16,929). Regimens were considered that ensure comparable exposure to adults (area-under-the-concentration-time-curve, AUC, between 1864-8338 nmol·h/L) under the assumption of a similar pharmacokinetic-pharmacodynamic relationship in adults and children.

Results: We identified a lowest safe weight of 15kg as inclusion criterion for the prospective trial, achieving, with the lowest commercially available tablet of 10mg, a median AUC ratio of 1.03 (interquartile range 0.82-1.30) relative to a 50kg adult receiving the 25mg dose (median 7163, IQR 6115-8338 nmol·h/L). The developed, optimized sampling scheme with 12 patients, providing 7 samples each, based on a sampling matrix with four different groups, allows precise estimates of PK parameters.

Conclusion: In a first phase 2.a trial among children 6-18 years with Duchenne muscular dystrophy-associated heart failure, followed for 6 months, on top of PK, ease-of-swallow and safety, several efficacy endpoints will be explored (NCT06643442). This simulation exercise identified the lowest safe weight for inclusion, and developed a sampling matrix able to maximize the reliability of the delivered PK information whilst minimizing the number of patients and samples, reducing patient burden, improving trial feasibility and allowing an efficient progression towards evidence-based empagliflozin use in children.

P102

Rheumatic Heart Disease in Sub-saharan Africa: Prevalence and Factors in a group of Cameroonian Schoolchildren

Chris Nadège Nganou-Gnindjio[1], Sandrine Ngambono[1], Joel Obama[1], Anicet Ladibe Gakdang[1], David Chelo[1]

[1]Faculty of Medicine and Biomedical Sciences, University of Yaoundé I, Cardiology department, Yaoundé Teaching Hospital, Yaoundé, Cameroon

Introduction: Rheumatic heart disease (RHD) remains the predominant cause of acquired heart disease among children and adolescents in developing countries. This study aimed to evaluate the prevalence of rheumatic heart disease through echocardiographic screening and identify associated factors in a cohort of schoolchildren living in Yaoundé, Cameroon.

Material and Methods: A cross-sectional study was conducted from February to May 2023 involving students aged 5 to 19 years from three primary and three secondary schools in Yaoundé. Participants who presented with rheumatic valve anomalies on ultrasound, with informed parental consent, were included. Data were entered and analyzed using SPSS statistics software version 23.0. The association between qualitative variables was examined using odds ratios with a 95% confidence interval and a significance level of 5%.

Results: Out of 1,020 children recruited, 133 (13.03%) were diagnosed with RHD. The mean age was 11.69±4.09 years, from 5 to 19 years. The sex ratio (M/F) was 0.56. Notably, 19 (14.3%) of the affected children were from impoverished families. Cardiac auscultation revealed murmurs in 23 (17.3%) participants, predominantly at the mitral focus in 78.3% of cases. Monovalvular lesions were prevalent in 126 (94.8%) cases, exclusively affecting the mitral valve. Bivalvular lesions were identified in 6 (4.4%) patients, and trivalvular lesions were observed in 1 (0.8%) student. Independent risk factors for rheumatic heart disease included residence in an urban slum (adjusted OR: 2.5[1.70-3.74]; adjusted p<0.001), at least one episode of angina (adjusted OR: 1.65 [1.08-2.54]; adjusted p<0.001), or fever (adjusted OR: 2.53[1.58-4.06]; adjusted p = 0.021) within the past 12 months.

Conclusion: The prevalence of RHD among schoolchildren in Yaoundé is significant. Emphasizing preventive measures, such as early detection through echocardiographic screening and addressing associated risk factors, is crucial. Implementing prevention strategies at multiple levels can help reduce the incidence and long-term impact of this disease in our country.

P103

Automated IntraVascular UltraSound Image Processing and Quantification in Coronary Artery Anomalies: The AIVUS-CAA software

Anselm Stark, Sebastian Balzer[1], Pooya Mohammadi Kazaj[1], Marc Ilic[1], Ryota Kakizaki[1], Andreas Giannopoulos[2], Andreas Haeberlin[1], Lorenz Räber[1], Isaac Shiri[1], Christoph Gräni[1]

[1]Department of Cardiology, Inselspital, Bern University Hospital, Bern, Switzerland, [2]Department of Cardiology, Zurich University Hospital, University of Zurich, Zurich, Switzerland

Introduction: Coronary artery anomalies (CAA) with an intramural course are associated with elevated risks of ischemia and sudden cardiac death under stress. Intravascular ultrasound (IVUS) is essential for assessing coronary vessel dynamics in these patients. However, the rarity of such anomalies, along with unique geometric changes in the intramural course and ostium, complicates image analysis, leading to inconsistencies and time-consuming evaluations. Our developed executable zero/low-code software addresses these limitations by providing automated lumen segmentation and cardiac phase identification in IVUS images acquired during rest and stress protocols.

Material and Methods: The software was developed to enable: (1) automated segmentation of lumen contours, trained and validated on 7,627 IVUS frames from 15 patients with right CAA, using a human-in-the-loop active learning process with a modified U2-Net deep learning model; (2) extraction of systolic and diastolic frames through a dual-gating approach that combines image- and contour-based methods; and (3) a graphical user interface for manual correction of results. The gating module was validated using a custom 3D printed-flow-loop simulating patient-specific hemodynamics, while segmentation accuracy was assessed via intraclass correlation coefficient (ICC) analysis comparing AI-generated contours with those delineated by experienced readers.

Results: The deep learning model achieved a mean Dice score of 0.96 (SD: 0.02), sensitivity of 0.96 (SD: 0.03), and specificity of 0.997 (SD: 0.003). ICC values for lumen area measurements were 0.92 (95%CI: 0.88-0.95) for rest and 0.98 (95%CI: 0.97-0.99) for stress conditions (all p <0.001. The gating module demonstrated excellent reproducibility for identifying systolic and diastolic frames under both conditions (ICC = 1.00, p <0.001).

Conclusion: AIVUS-CAA offers a reliable, automated tool for precise IVUS analysis at rest and during stress, enhancing the evaluation of geometrical changes of coronary vessels in CAA patients and enabling efficient clinical decision-making in a streamlined workflow.

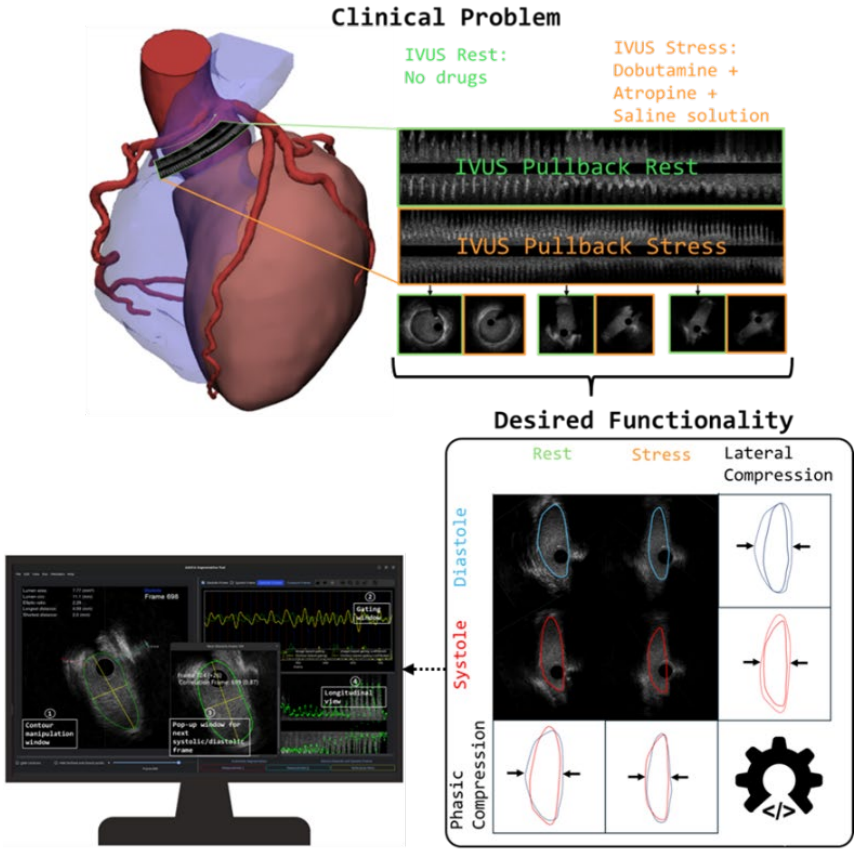

Figure 1: Illustration of the clinical problem using one intravascular ultrasound (IVUS) pullback during rest and another during dobutamine-atropine and volume challenge (stress). The objective is to demonstrate the compression of the intramural course (the area inside the aortic wall) between systole and diastole (i.e., phasic compression) as well as between rest and stress (i.e., lateral compression). The bottom left shows a representation of the graphical user interface that integrates all of these functionalities.

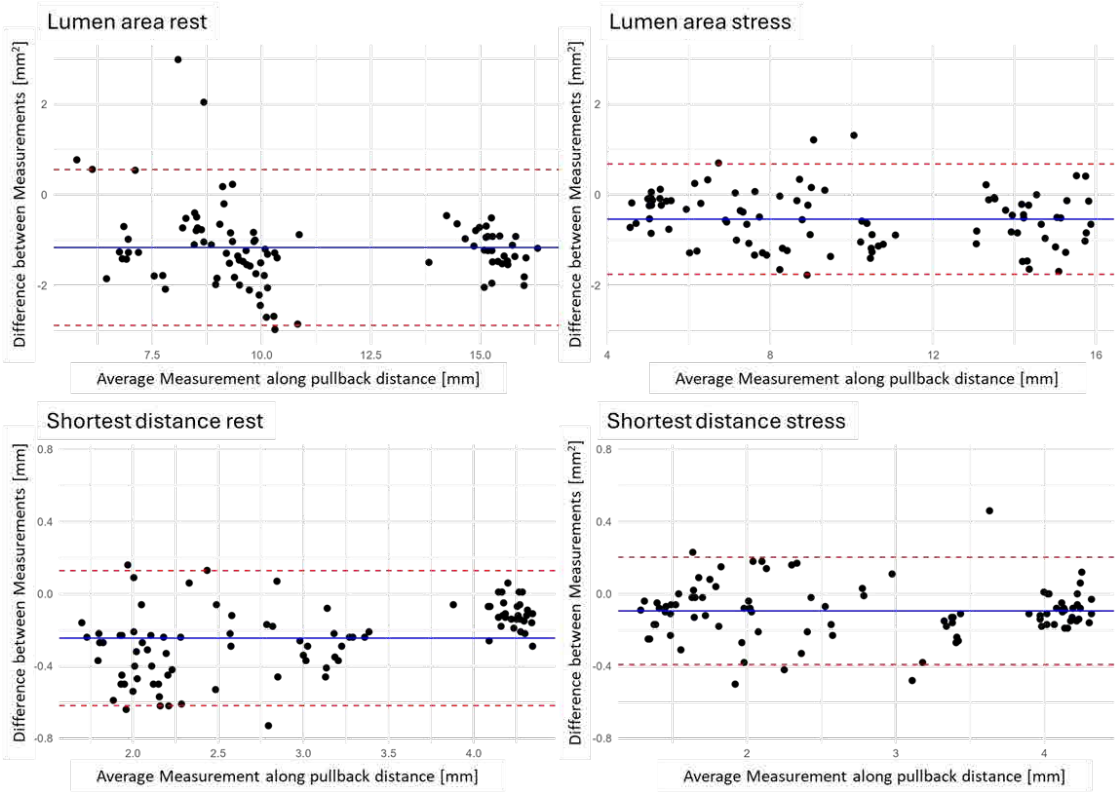

Figure 2: (top row) Bland-Altman plots comparing lumen area of automatically segmented IVUSimages and user-contoured frames. (bottom row) Bland-Altman plots comparing shortest distance of automatically segmented IVUSimages and user-contoured frames.

P104

Diagnostic Performance of Noninvasive Functional- and Anatomical Imaging for Hemodynamic Relevance in Right Coronary Artery Anomalies

Marius Bigler[1], Anselm Stark[1], Frederico Caobelli[2], Axel Rominger[2], Ryota Kakizaki[1], Flavio Biccirè[1], Isaac Shiri[1], Matthias Siepe[3], Stephan Windecker[1], Lorenz Räber[1], Christoph Gräni[1]

[1]Department of Cardiology, Inselspital, Bern University Hospital, University of Bern, Bern, Switzerland, [2]University Clinic of Nuclear Medicine, Inselspital, Bern University Hospital, Bern, Switzerland, [3]Centre for Congenital Heart Disease, Department of Cardiovascular Surgery, Inselspital, Bern, Switzerland

Introduction: Right anomalous aortic origin of a coronary artery(R-AAOCA) is a rare congenital condition increasingly diagnosed with the growing use of cardiac imaging. Due to dynamic lateral compression of the anomalous vessel,invasive stress testing with dobutamine fractional flow reserve(FFR-Dobutamine)is considered the reference standard.However,a reliable alternative method is needed to overcome extensive invasive testing,and it remains uncertain whether noninvasive imaging can accurately assess hemodynamic relevance in R-AAOCA.The aim of this study was to evaluate the diagnostic performance of noninvasive functional- and anatomical cardiac imaging in determining the hemodynamic relevance of R-AAOCA, compared to FFRDobutamine reference standard.

Material and Methods: Consecutive R-AAOCA patients with an interarterial and intramural course were prospectively included between 06/2020 and 10/2024.All patients underwent coronary computed tomography angiography(CCTA),nuclear cardiac imaging and invasive FFRDobutamine.Hemodynamic relevance of the anomalous vessel was defined as FFRDobutamine≤0.8.

Results: Fifty-one patients(age 51±12, 29% female) with newly detected R-AAOCA and right coronary dominance and no stenotic atherosclerotic plaques in the anomalous vessel at functional testing were assessed.Median FFRDobutamine was 0.88(0.80-0.91) and 14(27%) were hemodynamic relevant(i.e. FFRDobutamine≤0.8).Functional nuclear imaging detected ischemia in 4(8%) cases,(i.e. 29% of hemodynamically relevant cases,all of which were correctly identified),leading to a sensitivity of 29%,a specificity of 100%,and an accuracy of 80% in predicting FFRDobutamine≤0.8.Anatomical CCTA assessment showed a high negative predictive value with an area under the ROC-curve of 0.82-0.90,100% sensitivity,and 41-68% specificity for different CCTA features(i.e.,CCTA-minimal lumen area; CCTA-ostial lumen area; and CCTA-ostial and minimal lumen minor axis),leading to rule-out 41-68% hemodynamic relevant cases.

Conclusion: In adults with R-AAOCA,functional nuclear imaging demonstrates a high positive predictive value,identifying correctly one-third of cases with hemodynamic relevance,while CCTA offers a high negative predictive value.This combined noninvasive approach enables functional imaging to rule-in,and CCTA to rule-out hemodynamic relevant R-AAOCA patients,reducing the need for extensive invasive testing to a small subset.

P105

Inferolateral T-Wave Inversions in a Young Athlete: A Marker of Pathology Beyond the Athlete's Heart

Michael Stiefel[1 2], Christian Schmied[1 2 3], David Niederseer[2 4]

[1]Klinik für Kardiologie, UniversitätsSpital Zürich, Zürich, Switzerland, [2]Translational and Experimental Cardiology (CTEC), Departement Kardiologie, UniversitätsSpital Zürich, Zurich, Switzerland, [3]Herzgefaesszentrum im Park, Hirslanden Klinik im Park, Zürich, Zürich, Switzerland, [4]Hochgebirgsklinik Davos, Medizin Campus Davos, Davos, Switzerland

Introduction: Anterior T-wave inversions are typical in juvenile ECGs and black athletes, often reflecting physiological changes. However, inferolateral T-wave inversions are pathological and strongly associated with structural cardiac abnormalities such as apical hypertrophic cardiomyopathy.

Material and Methods: We report the case of a 23-year-old asymptomatic professional soccer player of West-African descent, referred for evaluation after routine ECG screening revealed inferolateral T-wave inversions. The athlete's medical history and family background were unremarkable.

Results: Echocardiography revealed apical cavum obliteration with a resting gradient of 35 mmHg, apical displacement of the posteromedial papillary muscle, mild hypertrophy with a maximum myocardial thickness of 11 mm, and hyper-trabecularization of the apex. Other parameters, including biventricular systolic and diastolic function, left ventricular (LV) dimensions, and mass, were within normal ranges. Cardiac magnetic resonance (CMR) imaging demonstrated focal epicardial late gadolinium enhancement (LGE) at the apex and confirmed the apical displacement of the posteromedial papillary muscle. No evidence of hypertrophic cardiomyopathy was found, with the LV appearing normal in both size and thickness. The systolic cavum obliteration was attributed to the displaced papillary muscle and a congenitally narrow ventricular apex. The athlete showed no arrhythmias during 48-hour monitoring and exhibited above-average performance on the exercise test.

Conclusion: Inferolateral T-wave inversions, apical flow acceleration, an apically displaced posteromedial papillary muscle, and epicardial apical fibrosis could indicate an early form of apical hypertrophic cardiomyopathy (HCM) or, alternatively, healed myocarditis as a potential cause of the subepicardial fibrosis and associated ECG abnormalities. Papillary muscle abnormalities alone, which can be linked to lateral T-wave inversions, were identified as a benign variation with favorable outcomes in athletes. Shared decision-making allowed the athlete to continue professional sports under strict cardiological monitoring, with recommendations for annual follow-ups, family screening, and a loop recorder for risk stratification. No arrhythmias were detected during the initial follow-up..

P106

Brothers of the world: a case report of Genetic Dilated Cardiomyopathy in a patient with a positive unknown familiarity for Heart Failure and Bicuspid Aortic Valve

Simone Sarzilla[1], Laura Anna Leo[1], Giorgio Moschovitis[1], Francesca Romana Scopigni[1], Elia Rigamonti[1]

[1]Istituto Cardiocentro Ticino, Lugano, Switzerland

Introduction:

Non-ischemic dilated cardiomyopathies present diagnostic and therapeutic challenges. Prognosis, response to heart failure medications and arrhythmia risk depend on the underlying etiology. Comprehensive phenotype assessment, including family history and genetic testing, is crucial in managing these patients.

Material and Methods: A 49-year-old male presented with acute heart failure with severe systolic dysfunction and left ventriculr thrombosis. Genetic testing identified a Likely Pathogenic TTN gene mutation[1]. His family history included a brother with severe left ventricular dysfunction supposedly secondary to aortic insufficiency due to bicuspid valve disease and early death after a complicated surgical replacement of the degenerated aortic valve bio-prothesis[2-3]. The patient improved significantly with guideline-directed medical therapy (GDMT) and did not require an ICD despite a single episode of monomorphic Non-Sustained Ventricular Tachycardia. Anticoagulation therapy with NOAC was discontinued after six months thanks to the low thromboembolic risk profile[4-6]. The screening of relatives showed no pathlogical findings.

Results: Genetic testing confirmed Titin-related dilated cardiomyopathy, which responded favorably to GDMT. TTN mutations are the leading cause of inherited dilated cardiomyopathy (DCM), presenting a low arrhythmia risk initially[7-9]. This supports the decision not to implant an ICD but to continue monitoring rhythm with an implantable loop recorder due to potential long-term arrhythmia risk.

Conclusion: This case underscores the critical role of genetic testing and family history in dilated cardiomyopathy: the TTN mutation guided therapeutic decisions and an earlier recognition of this genetic condition could benefits both the patient and his relatives, demonstrating the importance of precision medicine and familial screening in improving outcomes for inherited cardiomyopathies.

Table 1 - Day of Hospitalisation with Diagnostic Examinations, Clinical events, Evolution of Sympthoms and Laboratory Analysis

		05.jan	26.jan	26.jan	26.jan	26.jan	26.jan	26.jan	01.feb	02.feb	03.feb	04.feb	05.feb	19.feb	05.mar	11.apr	28.jun	22.jul	12.nov
Investigations:																			
TT-E, EF	%		20			26									33			46	
LV-Thrombus						x													
Coronary Angiography						x													
Cardiac MRI								"Mid-line sign"											
Physical stress test														x			x		
Watts	W													119			160		
Double Product	bpm x mmHg													14840			19300		
Tratement:																			
Aspirin 100 mg	cpr		x	x	x	x	x	x											
LMWH - Enoxaparin	U		100, bid	100, bid	100	100, bid	100, bid	100											
Rivaroxaban 20mg	cpr							x	x	x	x	x	x						
Furosemide (IV)	mg		40, bid	40, bid															
Torasemide (os)	mg				20, bid	20, bid	20, bid	20	20	10	10	10							
SGLT2-i (Dapaglifozin 10mg)	cpr			x	x	x		x	x	x	x	x	x		x	x	x	x	
ARN-i (Sacubitril-Valsartan)	mg			50, bid	50, bid	100, bid	150, bid	150, bid	150, bid	150, bid	200, 150	200, 150	150, bid		200, bid	200, bid	200, bid	200, bid	
Beta Blockers (Metoprolol)	mg				25, bid	25, bid	50, bid	75, bid	75, bid	100 bid	100, bid	100, bid	100, bid		100, bid	100, bid	100, bid	100, bid	
MRA (Spironolactone)	mg			25	25	25	25	50	50	25	25	25	25		25	25	25	25	
Ferric Carboxymaltose	mg						500												
Wearable Life Vest												x	x		x	x	x		
Laboratory testing:																			
NT-proBNP	(<173 ng/L)		5144				1252						379		805	312	73	144	
Hs Troponin-T	(<14 ng/L)		90	75		56	44												
CK	(< 190 U/L)		431	340		443	465												
ALAT	(<50 U/L)		99	81									54		21		18	19	
y-GT	(<71 U/L)		101	96											55		61	51	
Creatinine	(<126 umol/L)		94	83	91	97	95		96				104		99	84	76	96	
Transferrin Saturation	(>20 %)		14																
Ferritin	(30-300 ug/L)		131																
NYHA class, HF signs and Arrhythmia		NYHA I-II	NYHA III, peripheral congestion						NSVT									NYHA II	NVST
Wheight	Kg	101	110	107,8	105	101,5	99,6	98,2	97,7	97,5	97,8	97,5	97,5	101	99,5	100	101,5	102,5	

"x" indicates that a procedure was performed, values shown in parenthesis are normal values

TT-E = Trans-thoracic Echocardiography, EF = Ejection fraction, MRI = Magnetic Resonance Imaging, LMWH = Low Molecular Wheight Heparin, SGLT2-i = Sodium-Glucose Transport Protein inhibitors, ARN-i = angiotensin receptor/neprilysin inhibitor, MRA = mineralcorticoid receptor antagonist, CK = Creatine Kinase, ALAT = Alanin-Aminotransferase, y-GT=Gamma Glutamyl Transferase, NYHA = New York Heart Association Functional Classification, NSVT = Non-sustained Ventricular Tachycardia

Figure 1 - Echocardiography evaluation at the admission (A-B) and at the follow-up (C-D): A and C show EF analysis by 3D Dynamic Heart model; B and D show Global Longitudinal Strain analysis; CMR short axis view: (E) SSFP; (F) LGE image showing the fibrosis; (G) T1 mapping.

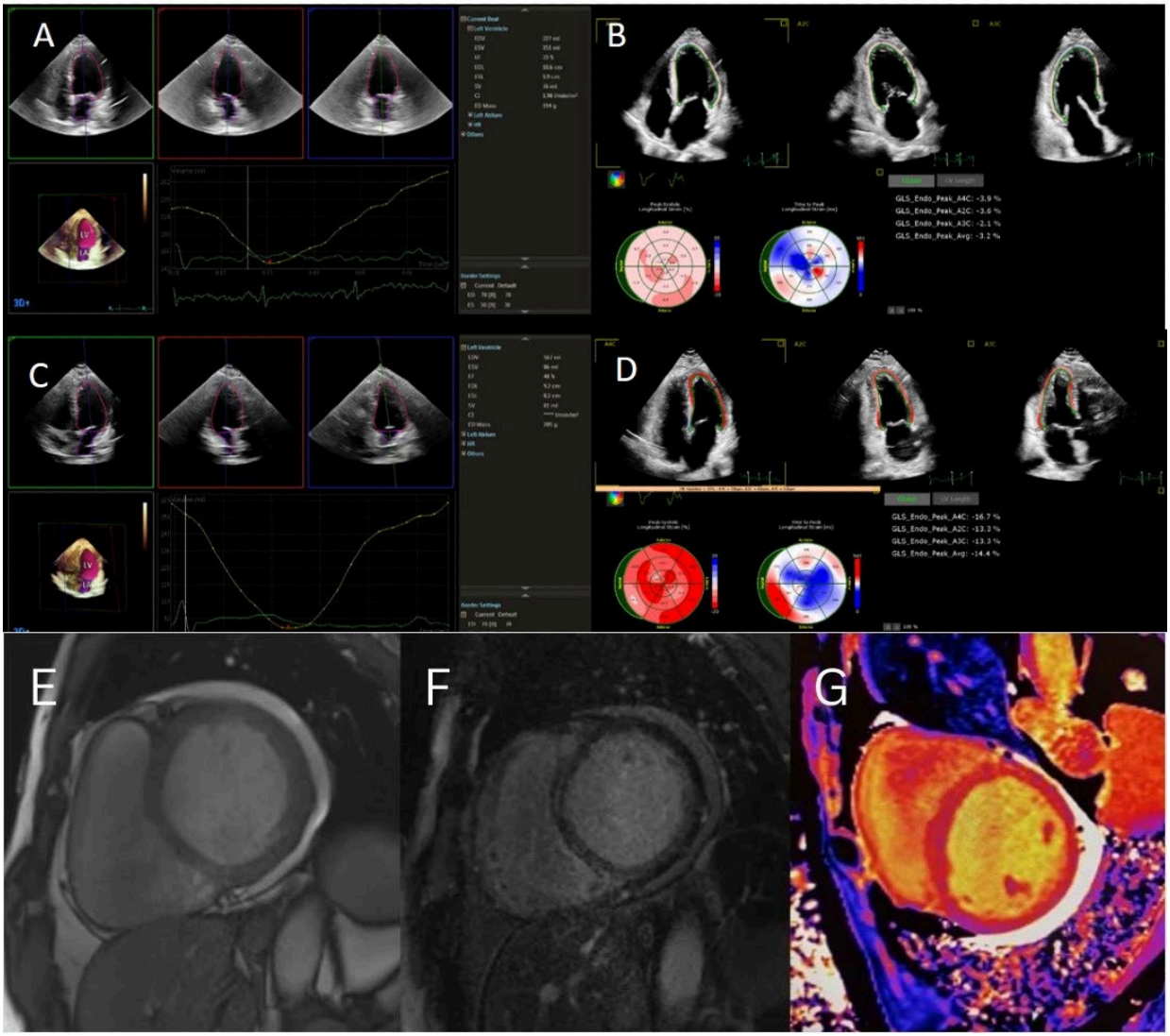

1	McNally EM, Mestroni L. Dilated Cardiomyopathy. *Circ Res*. 2017;121(7):731-748. doi:10.1161/CIRCRESAHA.116.309396
2	Jeong H, Shim CY, Kim D, et al. Prevalence, Characteristics, and Clinical Significance of Concomitant Cardiomyopathies in Subjects with Bicuspid Aortic Valves. *Yonsei Med J*. 2019;60(9):816-823. https://doi.org/10.3349/ymj.2019.60.9.816
3	Zhang D, Lu YT, Zhou ZM, et al. Clinical characteristics and management of coexistent cardiomyopathy in patients with bicuspid aortic valve. Journal of Geriatric Cardiology. 2023;20(3):205-213. doi:10.26599/1671-5411.2023.03.005
4	Wu HS, Dong JZ, Du X, et al. Risk Factors for Left Ventricular Thrombus Formation in Patients with Dilated Cardiomyopathy. *Semin Thromb Hemost*. 2022;49. doi:10.1055/s-0042-1756197
5	Huang L, Zhao X, Wang J, et al. Clinical Profile, Treatment, and Prognosis of Left Ventricular Thrombus in Dilated Cardiomyopathy. Clin Appl Thromb Hemost. 2023;29. doi:10.1177/10760296231179683
6	Bozkurt B, Colvin M, Cook J, et al. Current Diagnostic and Treatment Strategies for Specific Dilated Cardiomyopathies: A Scientific Statement From the American Heart Association. *Circulation*. 2016;134(23):e579-e646. doi:10.1161/CIR.0000000000000455
7	Arbelo E, Protonotarios A, Gimeno JR, et al. 2023 ESC Guidelines for the management of cardiomyopathies: Developed by the task force on the management of cardiomyopathies of the European Society of Cardiology (ESC). Eur Heart J. 2023;44(37):3503-3626. doi:10.1093/eurheartj/ehad194
8	Chmielewski P, Truszkowska G, Kowalik I, et al. Titin-Related Dilated Cardiomyopathy: The Clinical Trajectory and the Role of Circulating Biomarkers in the Clinical Assessment. Diagnostics. 2022;12(1). doi:10.3390/diagnostics12010013
9	Gigli M, Stolfo D, Merlo M, Sinagra G, Taylor MRG, Mestroni L. Pathophysiology of dilated cardiomyopathy: from mechanisms to precision medicine. Nat Rev Cardiol. Published online 2024. doi:10.1038/s41569-024-01074-2

P107

Late-Onset Hereditary Transthyretin Amyloid Cardiomyopathy: First Case of a p.Val142Ile mutation in Switzerland

Vanessa Logaritsch[1], Violeta Mihaylova[2], Martin Meyer[3], Stefan Toggweiler[1], Simon Stämpfli[1 4]

[1]Heart Center Lucerne, Luzerner Kantonsspital, Lucerne, Switzerland, [2]Neurocenter, Luzerner Kantonsspital, Lucerne, Switzerland, [3]Heart Clinic Lucerne, Lucerne, Switzerland, [4]Center for Molecular Cardiology, University of Zurich, Schlieren, Switzerland

Introduction: The p.Val142Ile mutation is the most common transthyretin (TTR) variant leading to TTR-amyloid (ATTR) cardiomyopathy (CM), typically found in people of African descent and extremely rare in European populations. This case describes the first Swiss patient with this mutation.

Material and Methods: An 82-year-old Swiss female of Caucasian descent with a history of coronary artery disease, paroxysmal atrial fibrillation, and arterial hypertension was hospitalized for acute decompensated heart failure. Echocardiography showed moderately reduced ejection fraction and reduced longitudinal strain with apical sparing. 99mTc-DPD scintigraphy revealed Perugini grade 3 cardiac radiotracer uptake. Serum and urine protein electrophoresis, as well as immunofixation, excluded AL amyloidosis, confirming the diagnosis of ATTR-CM. Genetic testing surprisingly identified the p.Val142Ile TTR variant, which is extremely rare in European populations but common in patients of African descent. Neurological examination revealed predominantly sensory and primary axonal polyneuropathy. However, the neurological findings were considered more likely due to hypothyroidism and chronic kidney disease than ATTR. Tafamidis therapy was initiated, and the patient's condition remained stable with standard heart failure management. Family screening identified one brother and one son carrying the mutation, but neither exhibited a phenotype consistent with ATTR-CM (Figure).

Conclusion: This case – the first description of a p.Val142Ile mutation in a patient of Swiss origin – highlights the importance of including genetic testing in the workup of ATTR-CM. Such testing may reveal unexpected findings that can impact patient management and guide family screening.

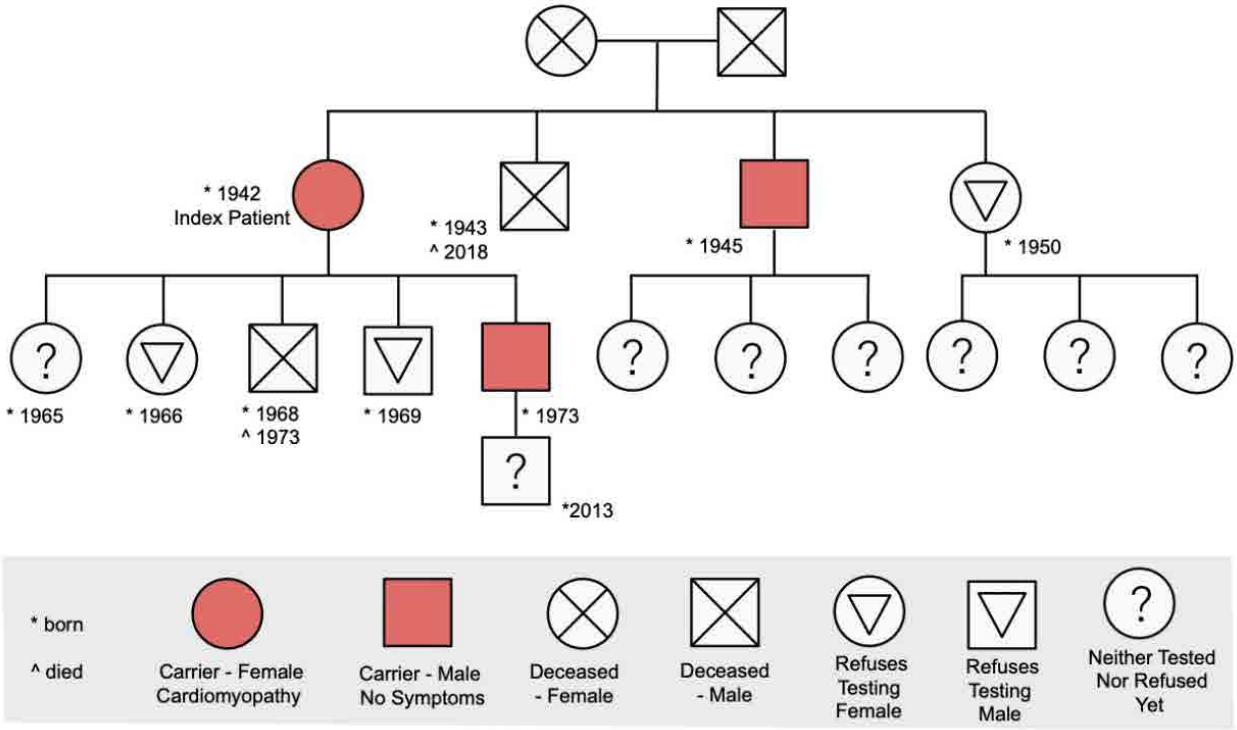

Figure: Pedigree

P108

When Pacing Goes Off Track: Macrodislocation of a Leadless Pacemaker

Vanessa Logaritsch[1], Christian Grebmer[1], Florim Cuculi[1]

[1]Heart Center Lucerne, Luzerner Kantonsspital, Lucerne, Switzerland

Introduction: The number of implanted leadless pacemakers is steadily increasing, not only due to new technologies enabling atrial communication. Up to this point, there are only a handful of case reports on complications, particularly (macro-) dislocations, resulting in the subsequent need for device explantation. This case report describes an uncommon instance of peripheral device migration and the subsequent interventional management strategy.

Case Summary: We report on a 26-year-old patient with symptomatic asystoles during epileptic seizures and pauses up to 17 seconds, who was referred for implantation of a leadless pacemaker for syncope protection. After multiple intraprocedural repositionings due to reduced sensing and lack of injury potential, the leadless pacemaker (Aveir VR, Abbott) was successfully implanted. The following day, the patient presented with twitching of the right leg at a rate of 60/min, prompting immediate X-ray control and device check. Radiologically, a macro-dislocation of the pacemaker into the venous pelvic-leg axis was found (Figure 1). After deactivating the device, the leadless pacemaker was successfully explanted using a catheter-based approach (snaring technique, Figure 2 and 3). Subsequently, a new femoral puncture was performed with implantation of a leadless pacemaker from a different manufacturer.

Discussion: In this case, we report the first instance described in the literature of a leadless pacemaker dislocation into the region of the right common iliac vein. Leadless pacemakers are playinan increasingly important role in pacemaker therapy. They are particularly attractive due to their low complication rate. While complications such as device dislocation are rare, they must nevertheless be considered when choosing the device and call for a dynamic problem-solving approach.

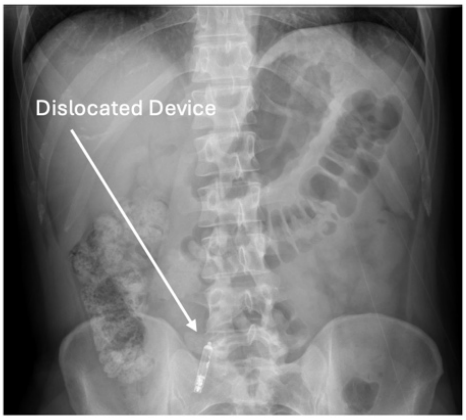

Figure 1: Dislocation of the AVEIR leadless pacemaker into the venous pelvic-leg axis

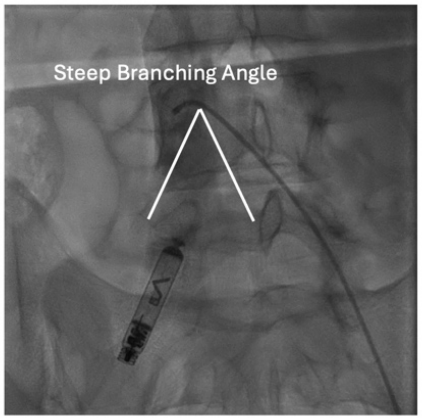

Figure 2: Due to the steep branching angle, removal of the device from the left femoral approach (cross-over) was not possible.

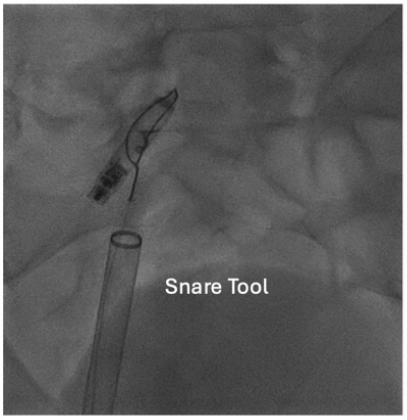

Figure 3: Snaring of the AVEIR from the right femoral approach.

AUTHOR INDEX

The numbers refer to the numbers of the abstracts.

Bold numbers = presenting author

SWISS MEDICAL WEEKLY

Editor in chief:
Prof. Gérard Waeber

Deputy editor in chief:
Prof. Stefan Weiler

Academic editors: see www.smw.ch

Managing editors:
Natalie Marty, MD
Jan Roth, MD

doi: https: //doi.org/10.57187/s.4706
ISSN online supplement: 2504-1622

Guidelines for authors and online submission:
www.smw.ch

Cover image: © minnystock | Dreamstime.com